Simulation and Optimisation of the Interior High Pressure (IHP) manufacturing process using the Finite Element Method (FEA)

Wolfgang Rimkus
Dipl.Ing. Mphil.

A Thesis submitted in fulfilment of the requirements of the University of Wolverhampton for the Degree of Doctor of Philosophy

This research programme was carried out in collaboration with the Fachhochschule Aalen, Germany

March 2000

UNIVERSITY OF WOLVERHAMPTON
School of Engineering and The Built Environment (SEBE)

Signature ..... Wolfgang Rimkus .....

Date ..... 12/01/2001 .....

ABSTRACT

Today, the market for metal working industry is characterised by an increase in parts varieties, a decrease in batch sizes, and an increase in quality requirements. To remain competitive, companies are forced to ensure that their production output complies with the increasing demand for higher productivity, flexibility and safety. Only new production methods and use of simulation techniques can help to achieve this goal.

Prototyping tools for the Interior High Pressure (IHP) forming technique are relatively expensive in comparison to conventional sheet metal forming. Prototyping using the trial and error approach ("Real Prototyping") is time consuming, and hence very costly. Simulation of the manufacturing processes within the production engineering ("Digital Prototyping") can help to reduce production time and therefore reduce this considerable cost. Simulation of the IHP forming process helps to replace the classical prototyping method. Today the product development time can be reduced by around 30%, and using the simulation technique will reduce the development time even further. With a further development of the simulation technique, which is the main tasks of this work, a further significant reduction of development time is expected.

The aim of the presented work is to improve the integration of the hydroforming simulation into the simultaneous engineering process chain. Today the available simulation software packages are difficult to use and implement. The motivation of this work is to develop tools and methodologies for a fast and easy simulation of the IHP forming process. The target group of the work will be small and medium sized companies (SMEs), because of the difficulty and costs involved for such companies to employ a specialist for the simulation of hydroforming processes. A further aim of the work is to identify the limitations of the process and of the simulation (if there is a difference).

The work was subdivided into four main topics. The first covered a thorough investigation to identify and select the best and most suitable material model to use in the hydroforming simulation, which included the best geometric configurations for tools and punches.

The second topic covered the development of knowledge about the design of load-curves. This knowledge is then used to create diagrams and formulas with which the load-curves are then applied easily and quickly.

The third topic was the development of a graphical user interface (GUI) for the hydroforming simulation. This GUI was integrated into the FE software package ANSYS, and hence, enables the user to create the input files of the IHP forming process simulation easily and quickly. The user is only required to define the major parameters, most of these parameters are available for the user to select through menus. The developed software automatically defines all other necessary parameters. Furthermore a software program to post the simulation results back into the CAD system was developed. This tool creates a link between the initial design process and the final output stage of virtual prototyping, and hence, allows the comparison of various stages within the forming process, as well as the ability to adjust the process parameters as part of the optimisation process.

The last topic was the validation of the developed methodology and software. The capability of the developed system by applying it to two concrete applications. The results of the real forming process were compared to the virtual forming results. Within this chapter the different material models offered by the simulation program LS-DYNA and the influence of an anisotropic material (tube) properties were also compared. 1/9/01

Table of Contents

List of Tables

List of Figures

Abbreviations

ASE	Aufblasen, Stauchen, Expandieren (blow-up, compression, expansion)
CAD	Computer Aided Design
CAE	Computer Aided Engineering
CAM	Computer Aided Manufacturing
CAQ	Computer Aided Quality
CAx	Computer Aided Domain
CIM	Computer Integrated Manufacturing
CPS	Computer Processing Simulation
CPU	Central Processing Unit
CSCW	Computer Supported Co-operative Work
CVP	Collaborative Virtual Prototyping
DIN	Deutsche Industrie Norm (German Industrial Standard)
DMU	Digital Mock-up
EDM	Engineering Data Management
FE	Finite Element
FEA	Finite Element Analysis
FEM	Finite Element Method
FLC	Forming Limit Curve
FLD	Forming Limit Diagram
GDR	German Democratic Republic
HF	High Frequency
IGES	Initial Graphics Exchange Specification
IHP	Interior High Pressure
ISO	International Standard Organisation
PDM	Product Data Management
RAM	Random Access Memory
RPD	Rapid Product Development
SAE	Society of Automotive Engineers
SE	Simultaneous Engineering
VDA	Society of the German Automotive Industries (Verband der Deutschen Automobilindustrie)
VR	Virtual Reality
WIG	Wolfram Inertgas

Acknowledgements

This thesis was done in co-operation with the Aalen University for Applied Sciences and the University of Wolverhampton. The project took place over the period of September 1996 to September 1999.

I would like to thank the following people for their support and assistance without which this project would not have been possible.

Professor Dr. Musa Mihsein, my director of study for his considerable motivation, guidance, advice and assistance throughout. I would also like to thank Dr. Richard Hall for his valuable ideas and inspirations during this period.

Professor Dr.-Ing. Herbert Bauer for making it possible for me to do this project, for his intense care, the interesting discussions and the good pieces of advice.

The co-workers and the diploma candidates at the Aalen University and the University of Wolverhampton, in particular

Dipl. Ing. Harald Edling
Dipl. Ing. Andreas Haas
Dipl. Ing. Iohan Lerch
Dipl. Ing. Stefan Scholze
Dr. Ilias Oraifige

Finally, I must thank all my family, my wife Agnes and my children Maria, Anna, Sarah and Lisa who have been a constant source of support and encouragement and the missing borne during the creation of this work.

Formula symbols

ρ	[kg/mm^3]	Density
ν	[-]	Poisson's ratio
μ	[-]	Friction coefficient
ε	[-]	Elongation
φ	[-]	Strain
τ_B	[N/mm^2]	Shear strengthen
τ_F	[N/mm^2]	Shear stress
τ_N	[N/mm^2]	Friction shear stress
σ_N	[N/mm^2]	Normal stress
$\sigma_1, \sigma_2, \sigma_3$	[N/mm^2]	Principal stresses
Δt	[s]	Time step
A	[mm^2]	Area
b	[mm]	Width
C_T	[Nm/°]	Torsion stiffness
E	[N/mm^2]	Young's modulus
F	[N]	Force
f(t)	[-]	Function vs. Time
F_a	[N]	Axial force
F_g	[N]	Counter-holder force
F_N	[N]	Normal force
F_R	[N]	Friction force
h	[mm]	Height
k_f	[N/mm^2]	Yield stress
l	[mm]	Length
n	[-]	Strain hardening coefficient
p_i	[bar]	Interior pressure (internal)
R_{eH}	[N/mm^2]	Upper yield stress
R_m	[N/mm^2]	Tensile stress
S	[mm^2]	Actual cross-section area
s	[mm]	Wall thickness
S_0	[mm^2]	Starting cross-section area
s_{al}	[mm]	Movement axial piston - left
s_{ar}	[mm]	Movement axial piston - right
t	[s]	Time
V	[mm^3]	Volume

Research Objectives and Organization of Thesis

This research project was initiated by the Universities of Wolverhampton, England and the University of Aalen, Germany to improve the applications of the finite element (FE) simulation techniques in the field of the interior high pressure forming (IHP). The main objectives of the research are to:

- improve the integration of the hydroforming simulation into the simultaneous engineering process chain.

- identify the limitations of the process and of the simulation (if there is a difference).

For the improvement of the development of hydroformed products, i.e. a reduction of the time needed, a better product quality and reduced production material, the simulation techniques must be used. It is well known that small and medium sized companies have difficulties in using the simulation techniques as there are no efficient tools. One of the objectives of this work is to improve the process chain within this area.

The thesis is organized in the following manner:

Chapter one gives an overview of the method of the Interior High Pressure (IHP) Forming Technique. It describes how the process works and which variants of the process are available today. Furthermore this chapter shows some typical applications of the IHP techniques in the automotive and sanitary industries. It also discusses the advantages of the IHP techniques and looks at the economical aspect of the method including some real examples. Finally this chapter gives a brief overview of machines used for IHP forming.

Chapter two gives a critical literature review on previous work carried out in the field of sheet metal forming process simulation using FE techniques with a special focus at the IHP process simulation.

Chapter three gives an overview of the FE program systems which can be used for the simulation of IHP forming processes. Furthermore the question „why simulation“ is discussed. It also describes the theoretical background of the FE program systems and discusses the differences between the explicit and implicit procedures. Finally upcoming developments and future tendencies are shown and discussed.

Chapter four describes the results of the basic examinations concerning IHP forming especially the modelling of the IHP forming simulation process. First of all the background of the material behaviour theory would be displayed in general.

Chapter five shows how the load-curves for axial force and interior pressure can be created and develops some diagrams for the easy and fast design of these curves. Beside this some basic

investigations about the influence of the friction to the forming process and the effects appearing by using thick tubes are investigated.

Chapter six describes the development of a fast and user-friendly FE-interface program to simulate an hydroforming operation using the interior high pressure (IHP) process. The interface program has been integrated within the FE code ANSYS and is using the explicit code LS-DYNA for the simulation.

Chapter seven introduces a method for leading back the simulation results into the CAD system for further processing. For multi-stage forming processes this procedure can also be used to lead back the geometry of the intermediate states into the CAD system, e.g. for the construction of special shaped punches.

Chapter eight validates the use of the FE techniques by comparison with two fullscale IHP applications. The results of the real forming process will be compared with the simulated forming results. Within this chapter the different material models offered by the simulation program LS-DYNA are compared and the influence of the anisotropic material (tube) properties are investigated.

Chapter nine discussed the work carried out in the whole research program and outlines proposed future work to be carried out.

CHAPTER 1

Principle of Interior High Pressure Forming (IHP) Technique

This chapter gives an overview of the methods of the Interior High Pressure Forming Technique. It describes how the process works and which variants of the process are available today. Furthermore this chapter shows some typical applications of the IHP technique in the automotive and sanitary industries. It also discusses the advantages of the IHP technique and looks at the economical aspect of the method including some real examples. Finally this chapter gives a brief overview about machines used for IHP forming.

1 Introduction

Interior high pressure forming (IHP, hydroforming, hydrostatic-aided forming, bulge forming) has become an increasingly attractive manufacturing process for the production of hollow bodies. Due to environmental pressures to produce non-polluting products, the use of the IHP technique has become more popular. In order to produce new complex lightweight automobile parts, it is necessary to develop new production technique. The IHP technique offers a high innovation potential for the forming of tubes, sheets, tailored tubes and tailored blanks.

The IHP forming technique has been known since the beginning of the 20th century (Geckeler, 1928) and it was mentioned for the first time in the 19th century (Wang, 1994). There is a patent from the year 1850 (**Mücke, 1995**) for the manufacturing of a wind instrument with water-pressure. The goal of this technique is to form metal similar to glass-blowing. Publications on the production of wavy tubes in 1902 (**Sauer, 1978**) and hollow aircraft propellers in 1929 (**Sauer, 1978**) using this technique are present.

During and after the second world war the development of this technology stopped. Then technique called IHP resumed in the 50's. First papers about IHP forming were from Japan and the USA (**Ekholm, 1958; Ogura, 1966; Ogura, 1968**). The technology was developed further in the 60's. The IHP technique was used in industry for about 30 years. At the beginning parts with a simple geometry and shape like connection elements for pipe systems (fittings) and bearings for bicycles as well as taps for the sanitary industries are produced. The IHP technique was originally developed for the production of tube connection elements like t-pieces (**Figure 1-1**) and taps and grips (**Figure 1-2**) for sanitary use and wavy tubes (**Figure 1-3**) for stream heaters. Using such technique it is possible to produce 25 and more t-pieces in one cycle stream.

In the following years publications came from eastern European countries and the former GDR **(Bogojavlenskij, 1972; Tscheckel, 1977; Eberlein, 1978; Bogojavlenskij, 1978)**. A fast spread of the IHP method was not possible because there were problems with the valve- and machine technique, especially the inaccurate control technique which posed a great problem. Today it is possible to realise and control high pressures greater than 10000 bar, and for this reason interior high pressure forming technique have spread especially in the automotive industry, as well as in the bicycle and sanitary industries **(Ebbinghaus, 1990; Klaas, 1994)**. Well-known automotive applications include exhaust manifolds, exhaust pipes and parts of the space-frame **(Figure 1-4)**.

The main application at which the IHP technique was used successfully was the automotive chassis, the framework that holds together the basic parts of a car. While chassis' designs vary, all are driven by the same fundamental design criteria which is to provide maximum stiffness, dimensional stability, fatigue life, and crashworthiness with minimum mass and cost.

Automotive chassis' engineers embraced the IHP technique because it allowed them to make their designs more effective. Consequently, the demand for IHP formed components has grown dramatically. This increased demand forced hydroform equipment producers and chassis system suppliers to accelerate development efforts as they competed for market shares.

1.1 The IHP Technique

The principle of the IHP technique is to place a tube into a mostly horizontal divided die and load them with internal pressure and axial force at both ends of the tube. The axial force is necessary to push material into the forming region. The material of the tube reaches yield point and flows into the tool cavities, hence it the part is formed **(Figure 1-5)**. The internal pressure of a low pressure IHP forming generally reaches a maximum of 800 bar, while for a high pressure IHP forming it can be as high as 7000 bar. The IHP-process is divided into two phases, in the first phase the tube is expanded inside the tool. In the second phase, the calibration phase, radiuses on the workpiece are being completely formed. The problem of the IHP process is the design of the interior pressure and axial force diagram, under certain circumstances vs. counter-holder force, called load-curve **(Figure 1-6)**.

With load-curves the process is steered in a manner that the tube does not burst or fold. If the axial force is too great in comparison to the interior pressure the tube folds or wrinkles. If the interior pressure is too great in comparison to the axial force, the tube bursts. **Figure 1-7** shows the limitations of the forming possibilities for t-pieces.

The fluid used for the IHP process is normally an oil and water mixture. The composition of the fluid has no great influence on the process. However, oil reduces the friction during the forming process. **Figure 1-8** shows the different IHP stages arranged according to their tension condition.

The exact definition of the IHP is :

„IHP is the forming of a part up to the shape of a tool through a fluid with direct contact to the part. Out of the force of the fluid other forces can act to support the forming process“ (Roll, 1988)

1.2 Applications of the of IHP technique

The interior high pressure forming technique is mostly used for tubular parts. The tubes can be used straight or bent, and materials used for IHP parts are steel, copper and aluminium. For the aluminium parts, rope-casting profiles are often used. A typical example of a part out of IHP formed rope-casting profiles is the space-frame for the Audi A8 (**Figure 1-9, 1-10**). IHP manufactured workpieces have diameters which range from a few millimetres to one meter, with filling volumes of up to 800 litres. For some parts the punching of holes are integrated into the IHP process, e.g. the punching of the blocked up section of a t-piece. **Table 1-1** shows an overview of the current automotive IHP applications (see also **Figure 1-4**).

Body Systems	Chassis Systems	Steering &Suspension	Engine & Drive Line
Instrument Panel Beams	Front Engine Cradles	Control Arms	Exhaust Manifolds
Radiator Enclosures	Rear Cradles	Trailing Links	Cam Shafts
Seat Frames	Ladder Frames	Steering Columns	Driven Axle Housing
Side Roof Rails	Hitch Bars		
Roof Bows	Bumper Beams		
Body Side Rails			
Roll Over bars			

Table 1-1 Current Automotive IHP Applications

The interior high pressure forming can be subdivided into two different manufacturing procedures: free expansion and expansion in a closed tool in which the tool can be divided transversely or vertically (**Figure 1-11**). For free expansion there is no real technical application known, because it is only possible to produce spherical shapes. This report therefore looks only at the second case.

The IHP technique makes it possible to create parts which have less weight, and configurations which cannot be produced with conventional methods. Furthermore, the IHP technique can save time and money because complex configurations can be produced in one step. Therefor it is possible to save manufacturing steps like welding and other manufacturing operations. IHP

products can be classified into three groups :

- **Leading components** (fittings, exhaust systems, taps)

  Leading components are parts with a thin wall thickness and a complex longitudinal axis. Limited through the high forming degree, parts can be produced which consist of several single parts within one forming step. Optimised cross-sections can be produced using the IHP technique.

- **Power leading waves** (hollow waves, camshafts, build camshafts)

  Power leading waves are parts with a thick wall and some diameter turnover. It is possible to get a weight reduction of up to 50% in contrast to conventional parts.

- **Structural parts in cars** (undercarriage parts, body, space-frame-nodes, tank)

  Structural parts in cars are long and curved with different, not rotationally symmetrical cross-sections. Conventionally these parts are produced out of two half shells welded on a boot plate. IHP products need no boot plate, so the weight can be saved. The hardening within the material of the component produced by the IHP process improves the stiffness. A typical application for this is an engine cradle (**Figure 1-12**).

Figure 1-13 presents three typical IHP products, an engine cradle for cars, a camshaft expanded completely out of a tube, and a t-piece with a slanting dome.

1.3 Advantages and Disadvantages of the IHP Technique

Workpieces produced using the IHP technique have the following advantages over conventional manufacturing technique.

- Reduction in material used
- Lower weight, conventional parts : hollow shaft 10-20%, IHP 40-50% (partly up to 75%)
- Reduction in number of parts
- Higher lifetime
- Low power consumption during production
- Good flow design
- No welding seam
- Reduction in production steps, therefore shorter time for processing
- Integration of punching is possible
- Increased limit drawing ratio in comparison with traditional deep-drawing

Deep drawing, using the Hydroform method, requires only a draw ring (blank holder) and a male punch. No die maker's fit is necessary. Set-ups are quick and simple. The tooling is self-centred and self-aligning. The flexible diaphragm minimises and often eliminates shock lines and draw marks normally created by matched die forming.

As pressures can be controlled over the entire blank, a higher percentage of reduction is possible and material thin-out can be kept to a minimum. Less material is used (tube forms are both, smaller in diameter and light in gage) because the process expands a smaller tube into a larger size. Hydroforming allows more complex parts to be made as a single unit, resulting in fewer small pieces which have to be assembled. Fewer components means fewer welds; less welding material contributes to lighter part weight, and better fit allows smaller diameter weld wire.

Other advantages include many parts that requires two or three operations on conventional presses can be formed in one hydroforming operation. Increased part strength, uniform wall thickness and reduced thinning with virtually no "springback" because the process forms material in its plastic state. Improved tolerance control delivers 90% reduction in true position tolerance of part features; provides 0.1 mm tolerances, and maximum part uniformity results from higher repeatability and the parts includes fewer joints and assembly points. Material savings due to less components and waste reduction, as well as smaller tube forms and fewer welds, and labour savings through eliminating other forming operations and assembly processes and exotic forming capability allows greater design flexibility.

Table 1-2 shows a typical comparison of conventional and hydroforming production for an exhaust manifold (**Figure 1-14**).

	Conventional production	Hydroforming production
number of individual parts	17	9
service life	700 – 1,000 h	> 1,500 h
manufacturing costs	100 %	85 %
development time	100 %	33 %
flange type	varies	same
weight	100 %	100 %
scrap		< 0.5 %

Table 1-2 Comparison of Conventional and Hydroforming Production for the Exhaust Manifold Illustrated

Disadvantages of the IHP process are:

- long process times (approximately between 20 and 60 seconds per part)
- only applicable for mass production
- process control needs a lot of experience
- presses with high clamping forces necessary
- coating of the tube (sheet) is necessary

1.4 Types of IHP

Recently, the IHP technology has been used not only for tubes but for deep drawing with fluid instead of a stamp.

The tools for the expansion in a closed tool (**Figure 1-15**) can be divided crosswise or lengthwise. Lengthwise divided tools have the disadvantage that the interior pressure acts contrary to the tool closing force. In this case greater closing forces are necessary. An advantage of crosswise divided tools is the easier fabrication by turning and dragging.

For the tool-bound expansion (**Figure 1-16**) the tool is divided crosswise. Tool and stamp are the same. The forming tool is opened at the beginning of the process. The size of the gap is equal to the length difference between the original tube and the finished product. During the forming process the tool is closed. In comparison to the forming in a closed tool, the risk of folding is greater, due to the missing friction the material can flow better.

In both cases a tube will be expanded up into a tool with mechanical load and hydrostatic pressure. The IHP technique for the expansion in a closed tool can again be subdivided into three procedures :

- interior pressure in combination with axial force - **expansion**
- interior pressure with a crosswise and under circumstances axial force - **transverse forming**
- only interior pressure - **calibration or expansion** (without axial force)

Expansion means that tubes are stretched up to the surface of the tool (**Figure 1-17**). This can be done with or without force in the axial direction. With force in the axial direction it is possible to reach much greater forming degrees. However, for long parts it is not possible to pull material into the forming region because of the friction between the tube and the tools due to the interior pressure. Furthermore, it is difficult to subsequently push material in if the tube is bend. The expansion can be fully or partly rotational-symmetric. For partly expanded parts a counter-holder prevents the tube from bursting. The counter-holder is normally force steered.

Transverse forming (**Figure 1-18**) is a partial movement of the middle axis with a stamp, the tube cross section can be retained or modified and it is possible to bend and expand parts in one step, as well as applying axial force.

Calibration (**Figure 1-19**) is the simplest definition of an IHP process. Calibration or post-stamping means that the tube is stretched up to the surface of the tool. The forming process results often only from the interior pressure, in some cases it is possible, to a certain degree, to bring material back with axial forging. The growth of the expansion depends on the strain rate of the material. Calibration is necessary to correct shape errors from the pre-form process which takes place through bending.

In nearly all cases the workpiece calibration is not an isolated process with the calibration follows the expansion process. During the calibration it is not normally possible to push material

back with axial force, because the friction is too high. Calibration as an isolated process, is used to correct errors resulting from bending by tubes or rope-casting profiles.

The rear axle of the BMW 5er series (**Figure 1-20**) is a typical example for an IHP product which has undergone bending, expansion and calibration processes. The rear axle consists of 4 IHP parts, two side members and two cross members. This construction produces a weight reduction of 30 %. The starting point for this part is 4 aluminium tubes. **Figure 1-21** shows the three forming steps necessary for the production of this BMW rear axle side member.

The **Figures 1-22, 1-23, 1-24** show, once again, the typical shapes of IHP parts.

1.5 Cross Sections and Semi-Finished Products Used for IHP Applications

Most common cross-sections used for IHP products are shown in **Figure 1-25**. The initial cross-section is normally a circle, with the exception of pre-formed tubes, which are calibrated. Tubular work in process parts are widely used as starting materials for IHP products, lengthwise welded tubes are mostly applied because they are cheaper and have smaller wall-thickness tolerance than seamless stretched precision tubes. The geometric quality has a significant influence on the result of the IHP forming process. Already slight groove, dents and wall-thickness variation affects the forming possibility, tubes welded with the WIG procedure or with laser are more suitable for IHP forming than HF welded tubes, the welding seam has normally no influence on the result of the IHP forming process.

Figure 1-26 shows various semi-finished product shapes used for IHP applications. The spectrum of semi-finished products vary from a simple single-walled or welded tube up to extruded sections for space-frame parts or double-walled (tailored) tubes.

1.6 Major Parameter of the Forming Process

Various parameters have a significant influence on the quality of products produced using the IHP forming process. The following are parameters which can have an influence on the IHP forming process. The **geometric shape** determines above all the forming, in the range of the free expansion. Due to the interior pressure there are stretching and bending effects, the growth of the radiuses and wall-thickness depends on the starting wall-thickness and the hardening exponent. **The tool parameters** depend on the process parameters and the geometric shape of the part and the case of the IHP forming. The shape of the part and the tool configuration must be adjusted during the process and in some cases a geometric configuration for the part can only be reached with a multi-sage process. These **process parameters** are the interior pressure, axial force, friction and the counter-holder force and the relationship of all these parameters to each other. Finally, the **raw material** have a great influence on the forming process, especially for expansion with axial forging and transverse forming. In this case the surface finish and lubricant have a significant influence on the result of the forming process and it is important that the lubricant is compatible with the fluid used for the expansion. For IHP forming the following lubricants are used : oil, aft, lack, wax and soap. The main IHP forming pro-

cess parameters are given in **Table 1-3.**

Part Configuration	**Process Parameter**	**Tool Configuration**	**Manufacturing Supplies**	**Failure Case**
dimensions	axial force	tool shape	lubricant	burst
wall-thickness	interior pressure	length- or cross-wise divided tool		wrinkle
material	friction			fold
	counter-holder			

Table 1-3 Significant IHP-parameters

1.7 Economic Aspects of Interior High Pressure Forming

To evaluate the use of the IHP technique it is necessary to consider other issues beside the initial cost. The two major disadvantages of the IHP process are the long process time and low production rate, however, it is possible to produce more than one part per cycle, and the long process time can then be justified. The process cycle time for an IHP process is normally between 25 and 400 seconds. For calibration the cycles are slightly shorter, for transverse forming they are slightly longer. Normally, it is not possible to reduce the pure process time, but the time used for filling and handling can be optimised.

The use of the IHP technique, is considered economical for a middle or high production demand. The costs for the tools and the optimisation of the process are high. Therefore the technique is normally non-economical for a single piece or a low rate production demand. It is also not economical for simple configurations, which can be produced by deep drawing, but if the technical advantages of IHP products are compared to products produced with other procedures it is then possible to simplify the used IHP process to produce products in small batches.

As mentioned above, the advantages of the IHP technology are the possibility to produce very complex configurations in a single part, better flow design and no welding seam. A further advantage of the IHP technique is that different process steps can be integrated into the IHP process, for example punching or joining parts together. The amount of pieces produced per year are about 25,000 to 300,000. In particular IHP technique are particularly economical for more complicated components. There are only a few publications available describing the lower costs of IHP components as compared to the cost of conventionally produced components. The problem is that companies are not interested in publishing the result of costs savings, because their customers would demand a reduction of prices. **Drapela, Vlasak and Tomas (1996)** discovered saving in costs of approximately 438.000 DM per year for the production of t-pieces. The cost reduction stands in comparison to the production of 100,000 t-pieces with conventional methods like welding or forging.

Schuler SMG, a German company which produces IHP parts, compares the costs of conventionally produced parts and IHP parts in its prospectus. The comparison of the costs relates to shell-shaped components. Schuler SMG gives a comparison of the costs for prototypes and for serial production (**Figure 1-27, 1-28**). The IHP technique is known under various different names. For instance, Schaefer uses the title ASE (Aufweit-Stauch-Expandier).

A main cost factor of IHP products are the tools. First attempts to reduce these costs have been made by the University of Paderborn, Laboratory for Transforming Manufacturing Procedures. Researchers developed a flexible multible split tool which avoids the cost consuming production of a special tool for each part.

The company Simpelkamp Press Systems (SPS), Aalen, put the idea into action and built a first tool in accordance with the specifications of the University of Paderborn (**Figure 1-29**). As the tool was only used for a few weeks only, it was not possible to reach a conclusion on the reduction of costs.

Simulation of the IHP forming process using FE technique is the second major tool applied for cost reduction. This report investigates the limitations of these FE technique in the field of the IHP simulation and develops a basic knowledge about the different parameters which have an influence on the process.

The following cost studies (**Seifert, 1999**) present some general hints about the financial aspects of IHP:

- IHP reduces the number of components for engine cradles and cross members.
- IHP reduces the component weight when using steel material by 10 to 20 %
- The tool costs of IHP in comparison to conventional stamping are 20 to 30 % less.
- The production costs of IHP are about 15% less than conventional stamping.

Normal hydroforming is used here to present high pressure forming. Most European engineers do not divide hydroforming into high- or low-pressure forming because the height of any physical size is relative. Most important is the necessary internal pressure which can be calculated by different methods depending on the boundary conditions of the hydroform process.

Using aluminium as the tube material leads to a reduction of weight by more than 30% but an increase of production costs by nearly the same amount as shown in **Tables 1-4, 1-5, 1-6**.

Production by means of hydroforming can, for instance, appear uneconomical for small quantities if only the component costs are considered, as the cycle times required are relatively long. Cycle time for different components is shown in **Table 1-7**.

Type	Number of Parts	Weigh t (kg)	Tool Costs (US-$)	Part Cost (US-$)
Conventionally manufac-tured	34	24,56	$ 5.359.090	$ 51,00
Hydroforming: Steel Engine Cradle	30	20,50	$ 3.712.636	$ 42,83
Hydroforming: Aluminium Engine Cradle	30	14,41	$ 3.891.727	$ 73,17

Table 1-4 Cost Study Engine Cradle (Seifert, 1999)

Description	Part Con-tent	Net weight	Tool cost	Piece cost
Stamped Steel Assembly	34	54.031 lbs.	$ 5.895.000	$ 56,10
Hydroforming: Steel Assembly (IHP)	30	45.095 lbs.	$ 4.083.900	$ 47,11
Hydroforming: Aluminium Assembly (IHP)	30	31.710 lbs.	$ 4.280.900	$ 80,48

Table 1-5 Cost Study: Engine Cradle (Seifert, 1999)

Description	Part Con-tent	Deflection per mm	Net weight	Tool cost	Piece cost
Stamped Steel Assembly	8	0.2658	28.9 lbs.	$ 3.666.600	$ 28.36
Hydroforming Steel Assembly	5	0.2382	21.72 lbs.	$ 2.007.350	$ 23.67
Hydroforming Aluminium Assembly	5	0.2583	14.72 lbs.	$ 2.007.350	$ 39.71

Table 1-6 Cost Study Cross Member (Seifert, 1999)

Component	Automation	Components per stroke	Cycle time
exhaust manifold with dome	No	2	15 ... 25 s
exhaust manifold tube	Yes	2... 4	15 ... 20 s
side member for pick-up	yes	2	40 s
instrument panel rail	yes	1	35 s
T-fittings	yes	up to 25	13 s

Table 1-7 Cycle Times for Different Parts (Schuler, 1998)

1.8 Materials, Lubricants and Machines used for Interior High Pressure Forming

As a matter of principle, all metallic materials with a sufficient forming property can be formed using the IHP method. All existing forming materials which are also used for pressure extrusion and deep drawing are suitable. The materials need the following properties :

- low flow-stress
- high forming possibility
- fine-grained structure

The austenitic high-quality steels are especially suitable for interior high pressure forming. The following table shows the materials often used for parts produced with the IHP technique. The IHP forming process produces a cold hardening of the whole part. The degree of hardening depends on the forming degree. For all steels an increase of hardness, tensile strength and the stretch limit simultaneous with a reduction of the breaking strain can be noticed. Non-iron metals are often used in the sanitary industries. Brass is often used due to the high strain possibility. Aluminium, which has a low strain possibility, is normally only calibrated with the IHP technique. For this reason, aluminium has a relatively small share in the field of IHP.

Material	**Material standard**	**Example**
Steel		
unalloyed steel for sheet metal	DIN 1623	St14
unalloyed steel for tubes	DIN 1626 - 1630, 17121	St32 -St52
case hardening steel	DIN 17210	C15, 20MnCr5, 20MoCr4, 21NiCrMo2
tempered steel	DIN 17210	C22 - C55, 32Cr2 - 42CrMo4
creep-resistant steel	DIN 17175	St35.8 - X20CrMoV12
non-rust steel	DIN 17440, 17455 - 17458	X6Cr13 - X20Cr13, X5CrNi1810 - X2CrNiMoN 17 13 5
non-iron metal, alloy		
Al, Al - alloy for sheet metal	DIN 1745 T1, DIN59606	Al 99,5; Al 99,99; AlMg 0,5; AlMgSi 0,5; AlZn
Al, Al - alloy for tubes	DIN 1746 T1	Al 99,5; Al 99,99; AlMg 0,5; AlMgSi 0,5; AlZn
Ti, Ti - alloy	DIN 17851	Ti Al 6 V 4
Cu, Cu - alloy for tubes	DIN 17671	E-Cu 58; CF-Cu; SE-Cu; CuZn5; CuZn 37; CuSn 8; CuNi 12 Zn 24
Cu, Cu - alloy for sheet metal	DIN 17670	E-Cu 58; CF-Cu; SE-Cu; CuZn5; CuZn 37; CuSn 4; CuSn 8; CuNi 12 Zn 24; CuNi 9 Sn 2
Ni, Ni - alloy		Ni 99,2; Ni 99,6

Table 1-8 Materials for IHP Parts

1.8.1 Lubricants

Lubricants are very important factors in the IHP process, because they minimize the friction between tool and workpiece during their relative motion. Many components can only be produced in the required shape with the help of lubricants. The lubricants relieve the forming of tubular branches, reduces partial stretching and make it possible to produce an even wall thickness. A number of different lubricants can be considered for use in IHP forming, depending on their composition, these can be classified into the following groups:

- solid lubricants, generally on a graphite or MoS_2 basis
- polymer dispersion based-lubricants
- waxes, oils
- emulsions

The lubricants are generally applied by spraying or immersion. The required thickness of the lubricant is determined by trial and error.

1.8.2 Machines

Machines developed for IHP forming must be categorised as special-machines, due to the simultaneous effects of the interior pressure and the axial forces the machines for IHP forming must be able to withstand the forces and pressures which are present. For parts with partial expansions (e.g. t-piece) additional tools for the counter-holder must be present. **Figure 1-30** and **1-31** shows a typical IHP press.

For IHP processes hydraulic presses are used to keep the IHP tools closed. Machines for the production of IHP components are, in principal, normal presses, which can be also used for conventional deep-drawing. The IHP press has an additional pressure transmitter for the hydroforming process. Recently particular presses for IHP forming have been developed. The difference to a deep-drawing press is that the pressure frame is very stiff to be able to keep the tool closed during the hydroforming process. This is especially important for large IHP applications like an engine cradle. Today, a wide spectrum of applications are known, from a small t-piece to automated handling systems for the mass production of automotive components.

The requirements of an IHP machine are a precise process control and the possibility of a flexible tooling system. Until today, the IHP procedure is characterised by high capital expenditure and long cycle times, however, a closer look at the whole production process reveals that the number of production steps and the number of component parts can be significantly reduced. For this reason the time for the whole production process is also less than conventional methods.

In order to optimise the process cycle times the following parameters are relevant (**Böhm, 1997**):

- Reduction of the filling time
- Integration of pre-forming operations with high velocity
- Quick transition form filling to forming
- Increase of the forming velocity
- Reduction of the times which are not process relevant

Furthermore a double ram press system shown in **Figure 1-32** can be used for the reduction of the cycle times. The principle of the double ram press system is to have two separate rams integrated into one press frame of a hydraulic press. Only one hydraulic and high-pressure system is installed. One or more tools can be installed on each ram side. While the first side is hydroforming, the second side is unloading, loading, filling and sealing, then the high pressure system switches from the first to the second side and hydroforming starts on the second ram side. Hydroforming of different parts with different process parameters on each ram is generally possible and hence the cycle time is reduced from 20 ... 30 seconds to about 15 seconds per part including loading and unloading. The double ram press system has further advantage that the two rams can be coupled for the manufacturing of large parts.

1.9 Conclusion

The calculations necessary to obtain the specifications of the forming parameters for IHP processes are achieved empirically. Therefor large number of trials are necessary. Today it is more and more clear that the simulation of the IHP forming processes with the help of the finite element method (FEM), represents a relevant support.

The task of the process simulation is to execute general feasibility studies for industrial applications of hydroforming technology by using the Finite Element Analysis (FEA) in order to obtain a reduction of the production development phase (time to market) or a reduction of the development costs (brake even point).

Crucial starting points for the optimisation of time, costs and quality of the configuration of the procedure are present in the first stage of the hydroform component development, where the modification of the process-influencing parameters is still possible without time-consuming and expensive cost, e.g. tool modifications.

Today, the FEM permits to represent the forming steps coherently for the production of a component. Thus, it offers a potential for predicting the feasibilities, component quality and the process integrity (security), which can be expected.

Figure 1-1 T-Piece

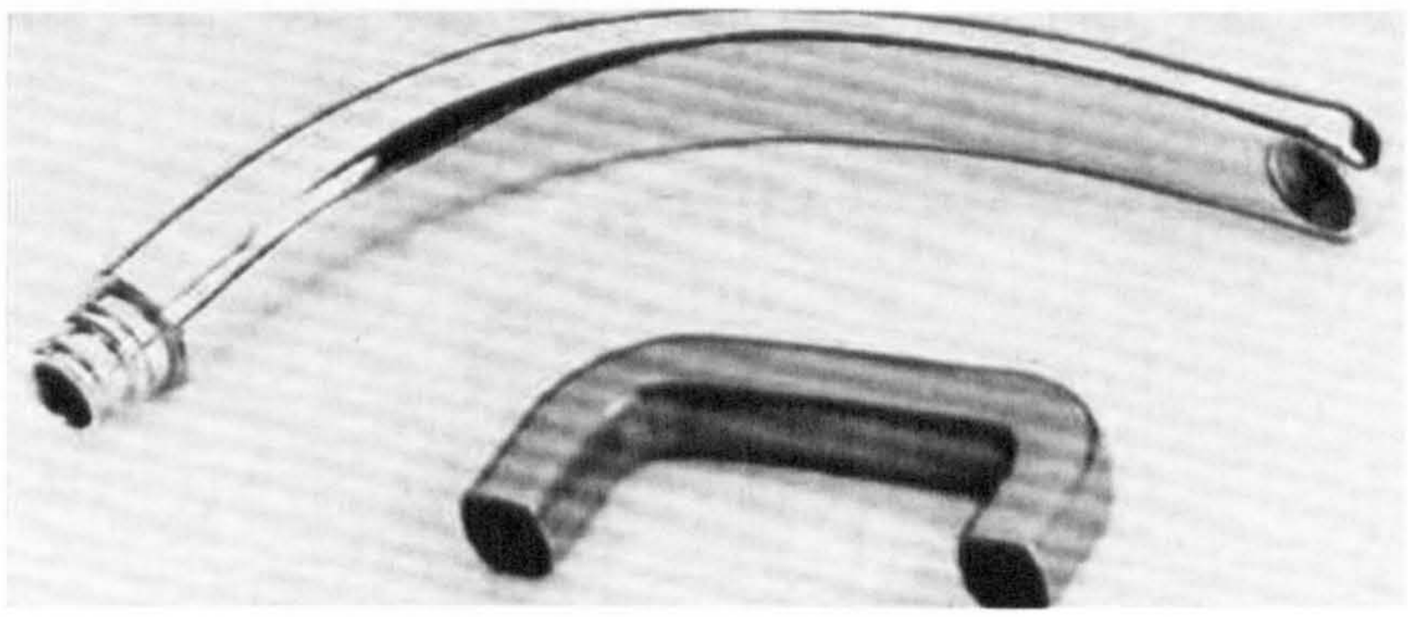

Figure 1-2 Tap, Grip

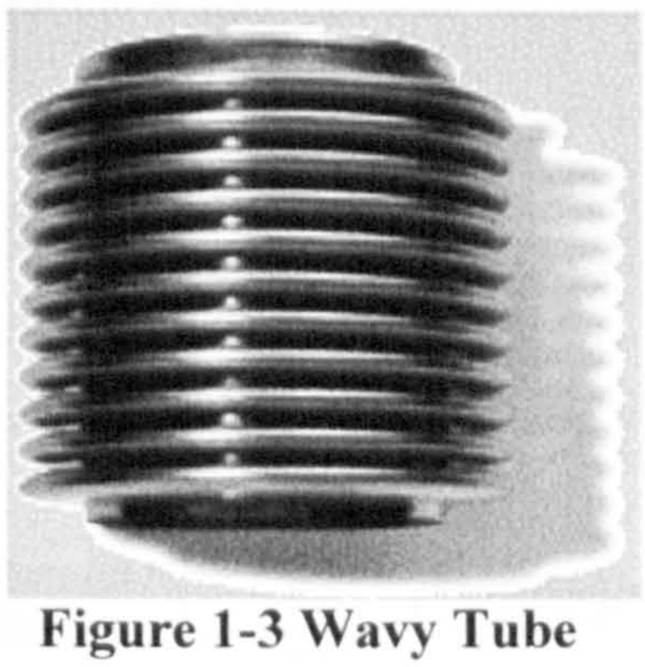

Figure 1-3 Wavy Tube

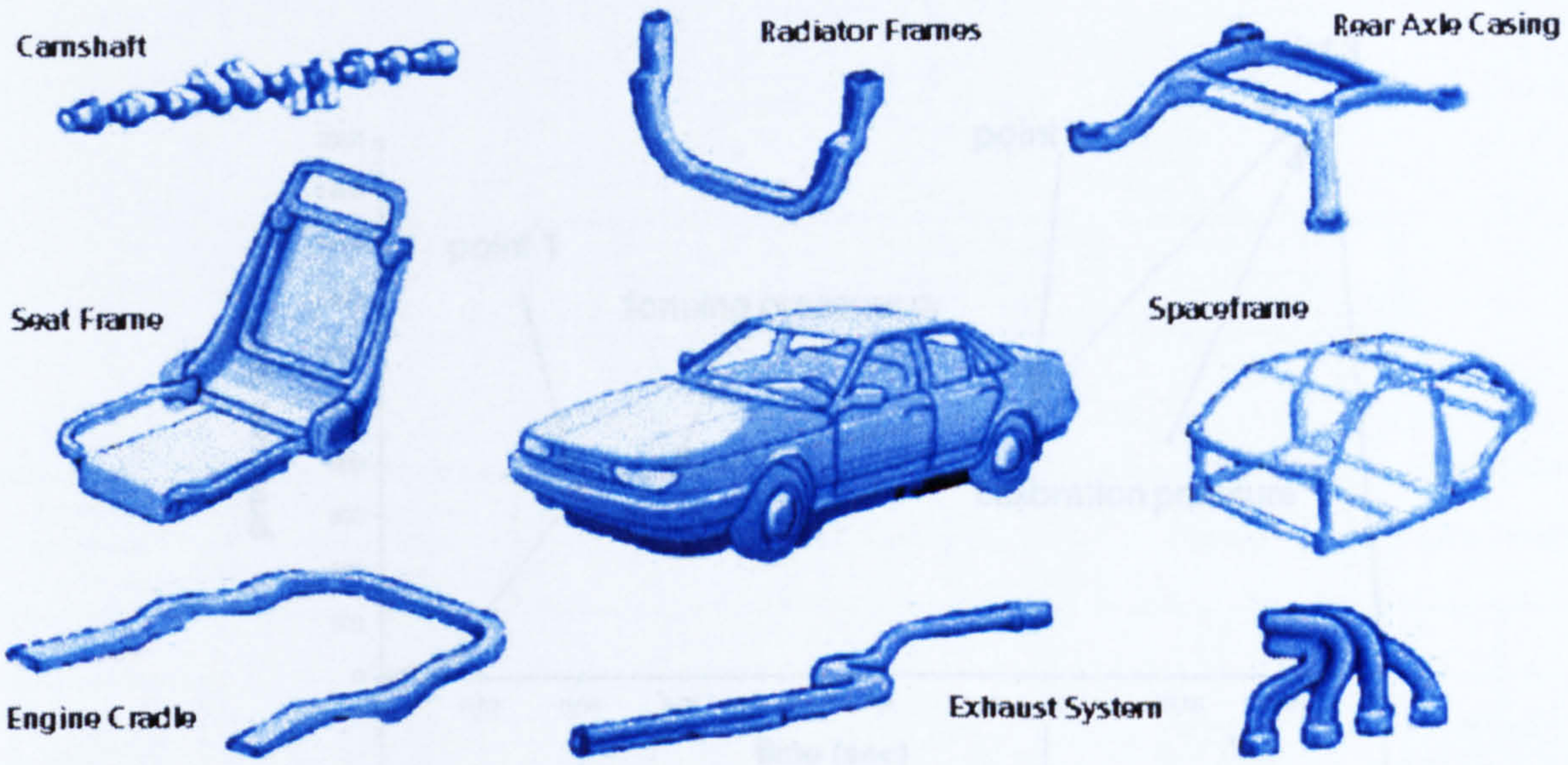

Figure 1-4 Hydroforming Applications in the Automotive Industries

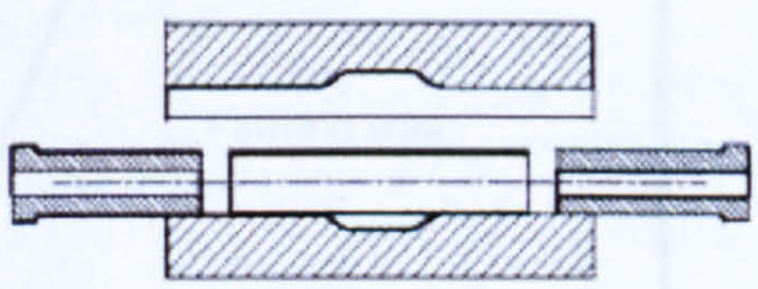

Figure 1-5 Interior High Pressure Forming (IHP) - Process Principle

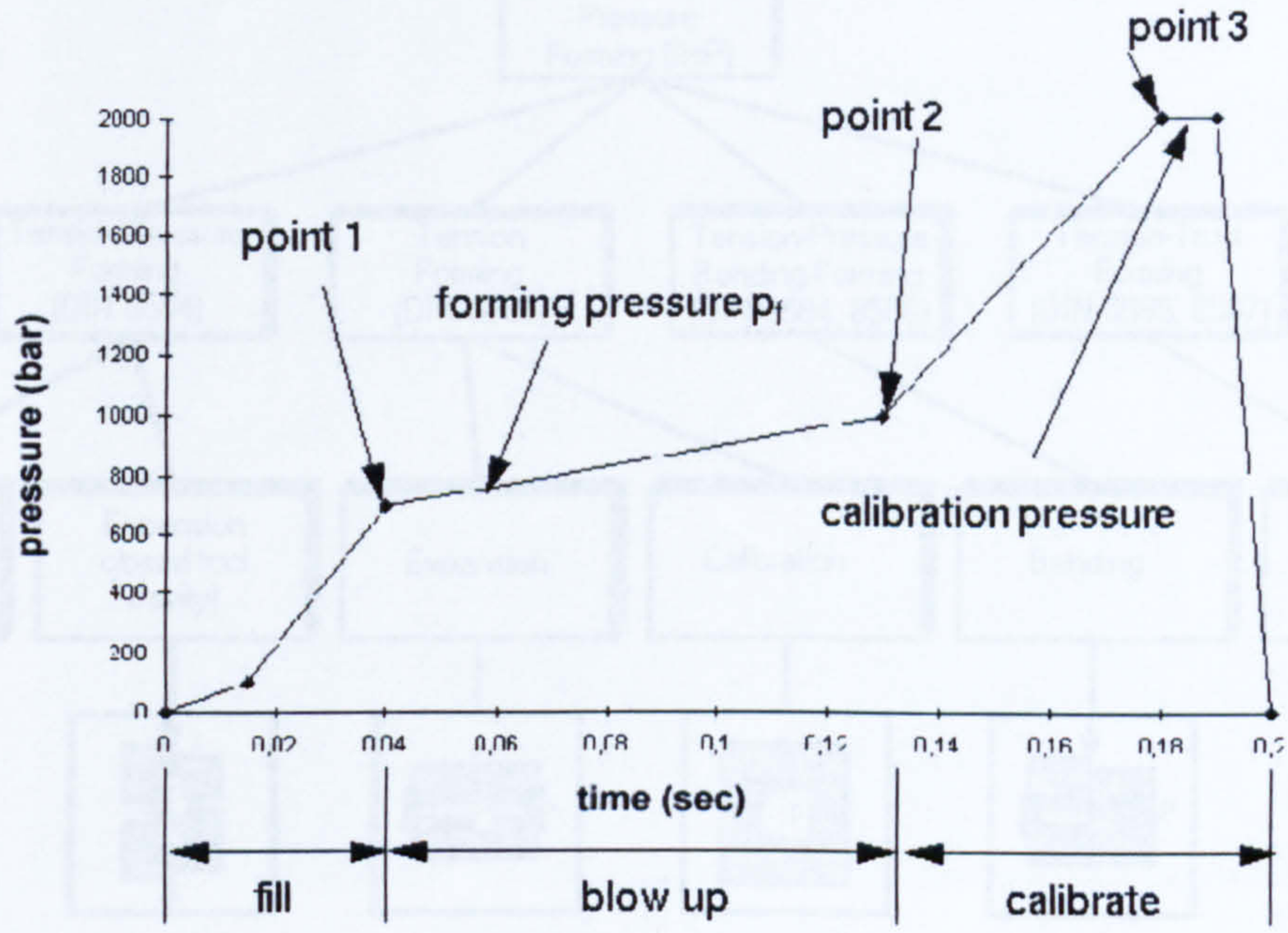

Figure 1-6 Load-Curve for Interior Pressure

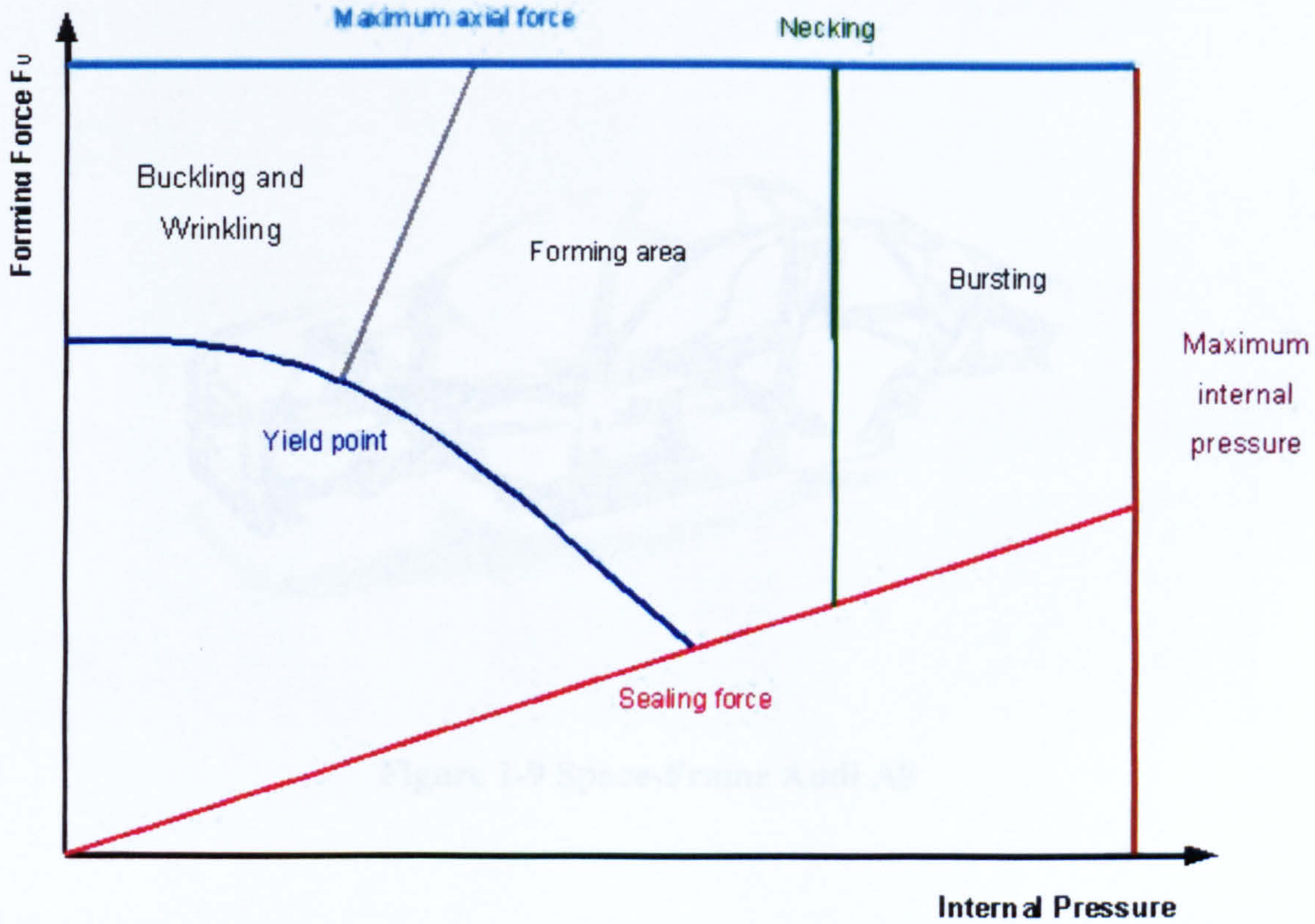

Figure 1-7 Limitations of the Forming Possibilities for T-Pieces (Klaas, 1987; Böhm, 1994; Dudziak, 1995)

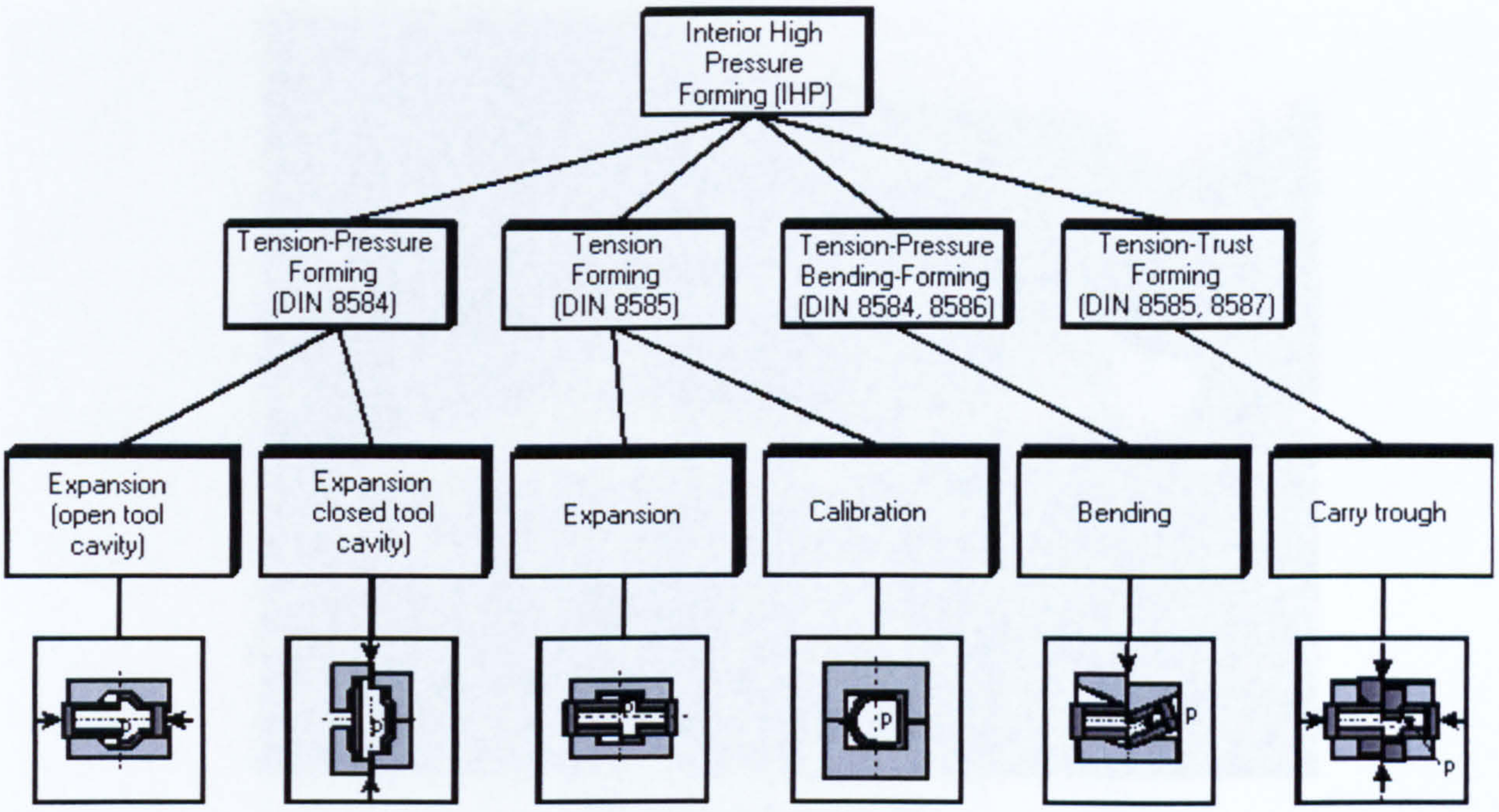

Figure 1-8 Regulations of the IHP Proceedings According to Effective Tensile Stresses

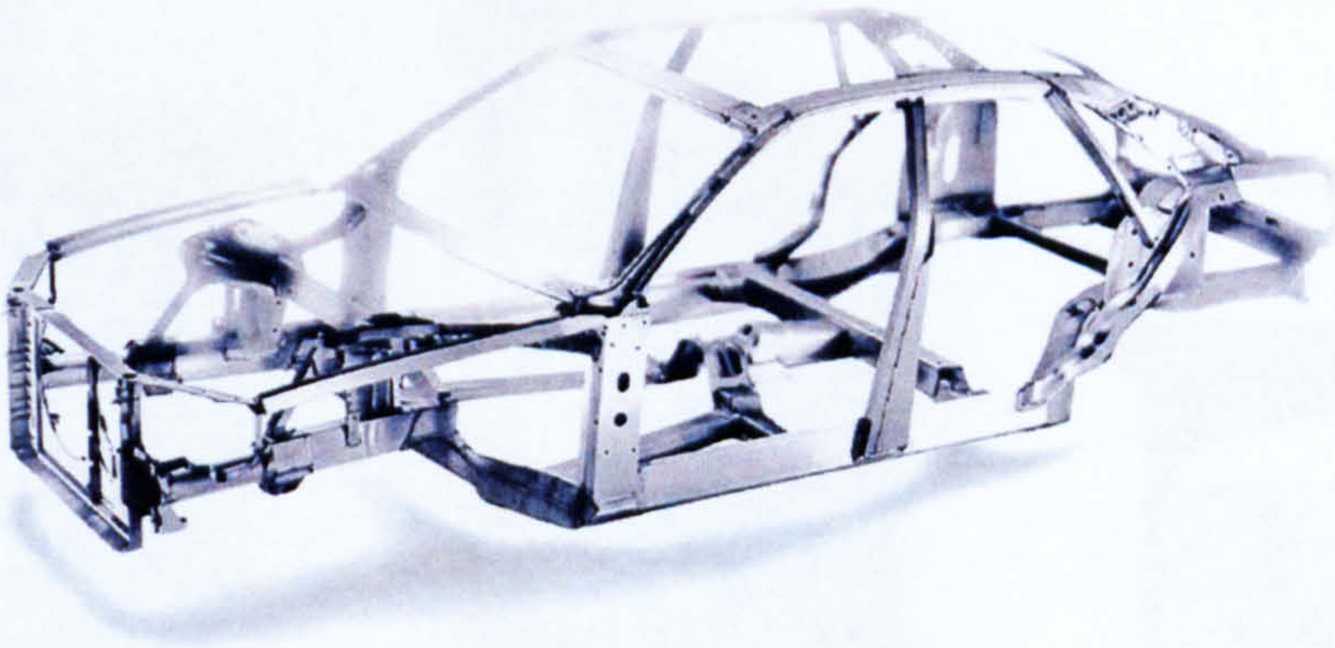

Figure 1-9 Space-Frame Audi A8

Figure 1-10 Audi A8

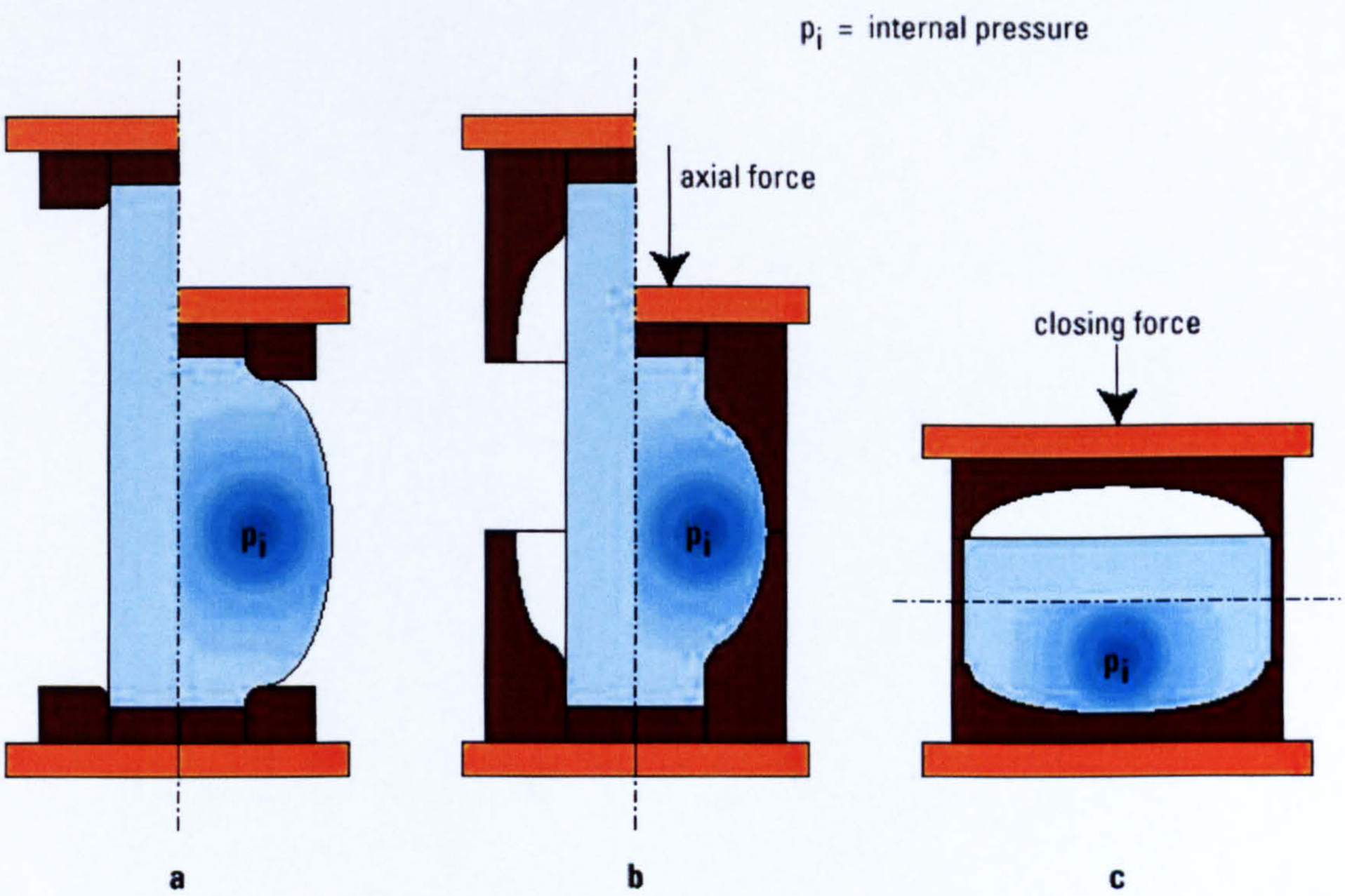

Figure 1-11 Process Variants of IHP Forming – a Free Expansion; b Tool-dependent IHP, Transversely Divided Tool; c Tool-dependent IHP, Longitudinal Divided Tool

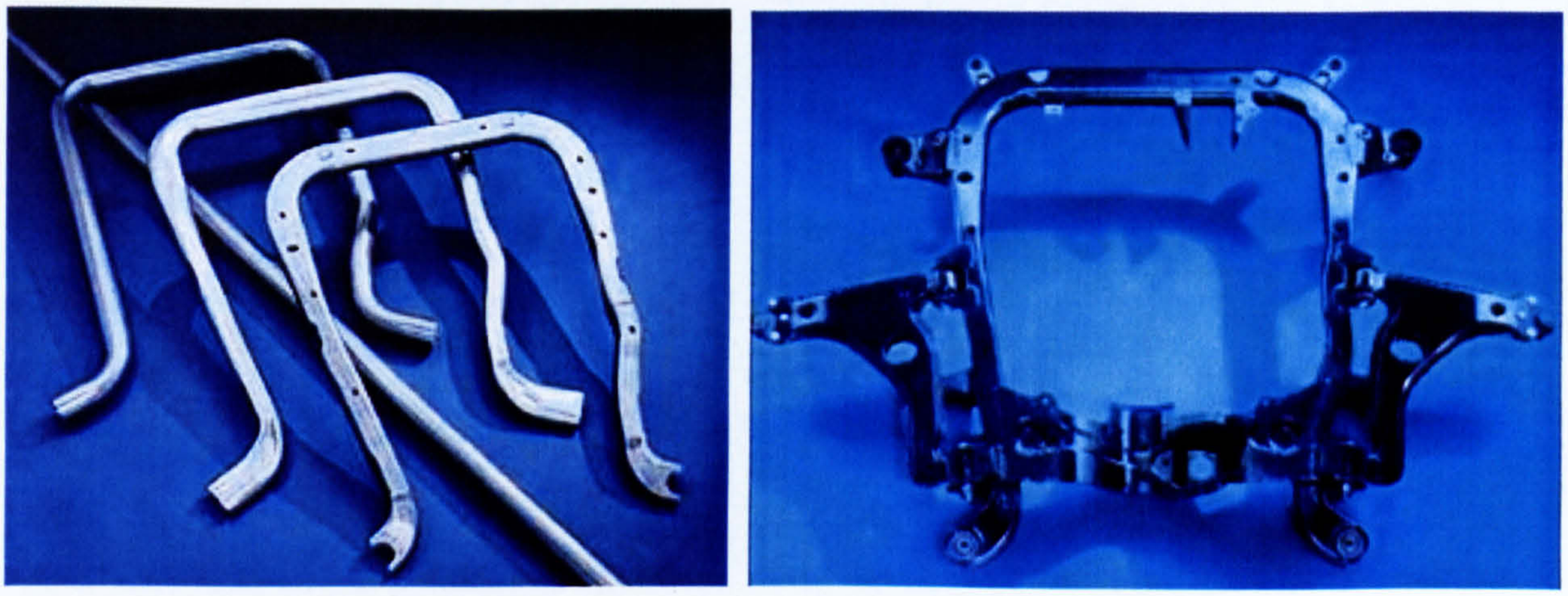

Figure 1-12 Engine Cradle Opel Astra

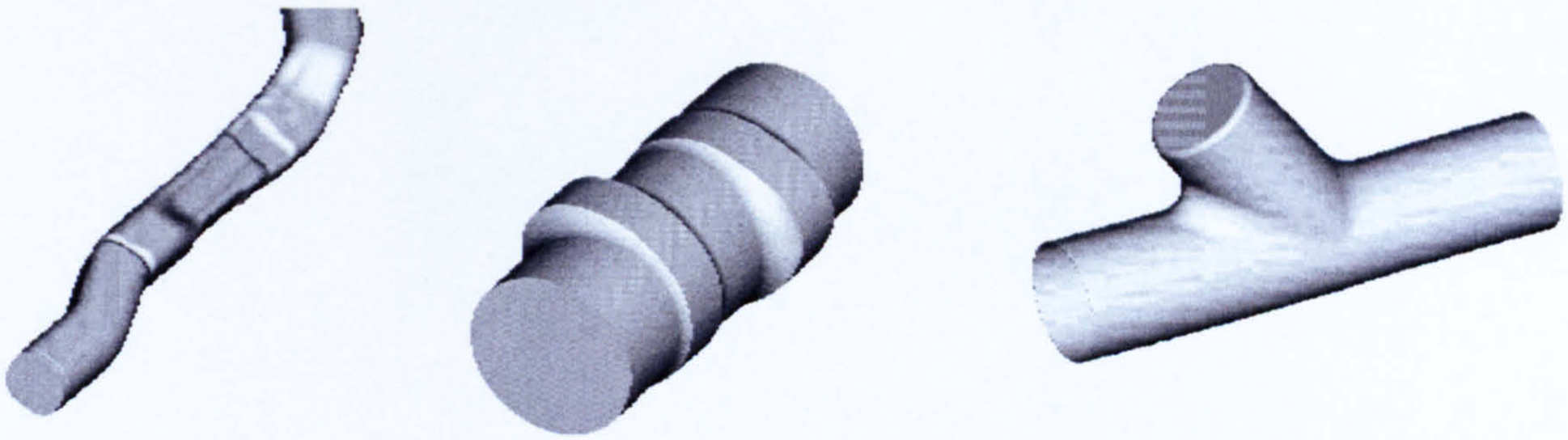

Figure 1-13 Typical IHP - Products - Carrier, Cam-shaft, T-Piece

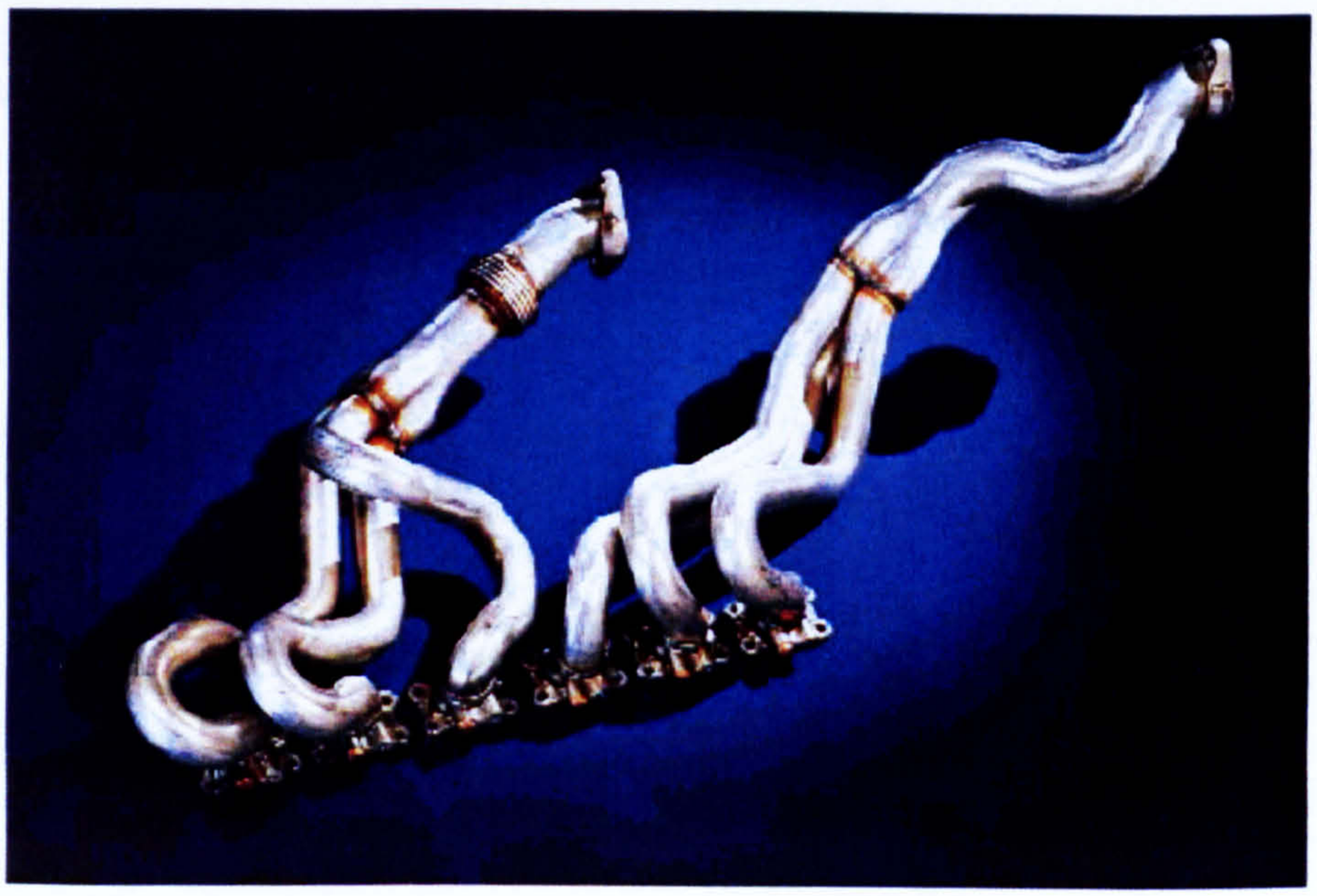

Figure 1-14 Exhaust Manifold

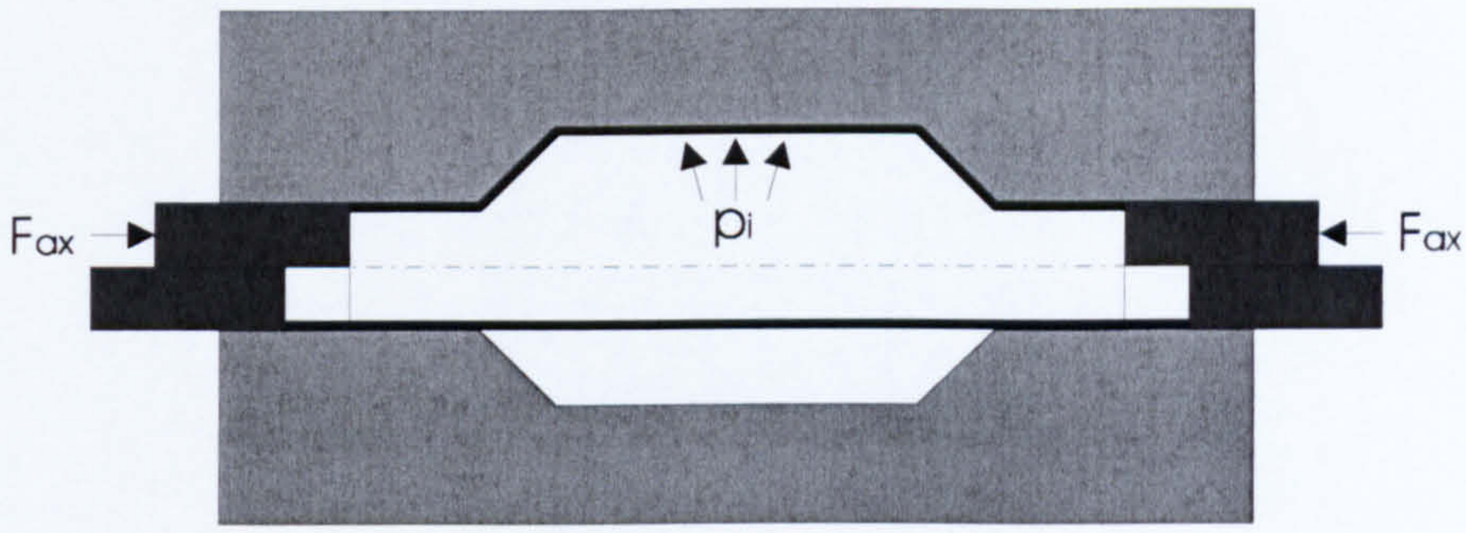

Figure 1-15 Expansion in a Closed Tool

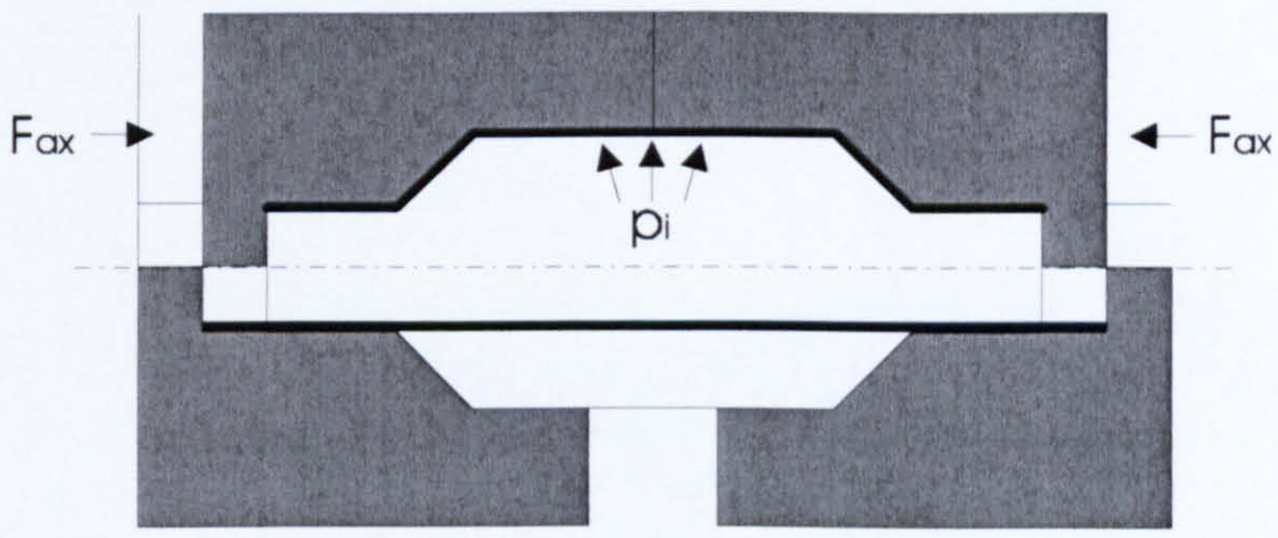

Figure 1-16 Tool-bounded Expansion

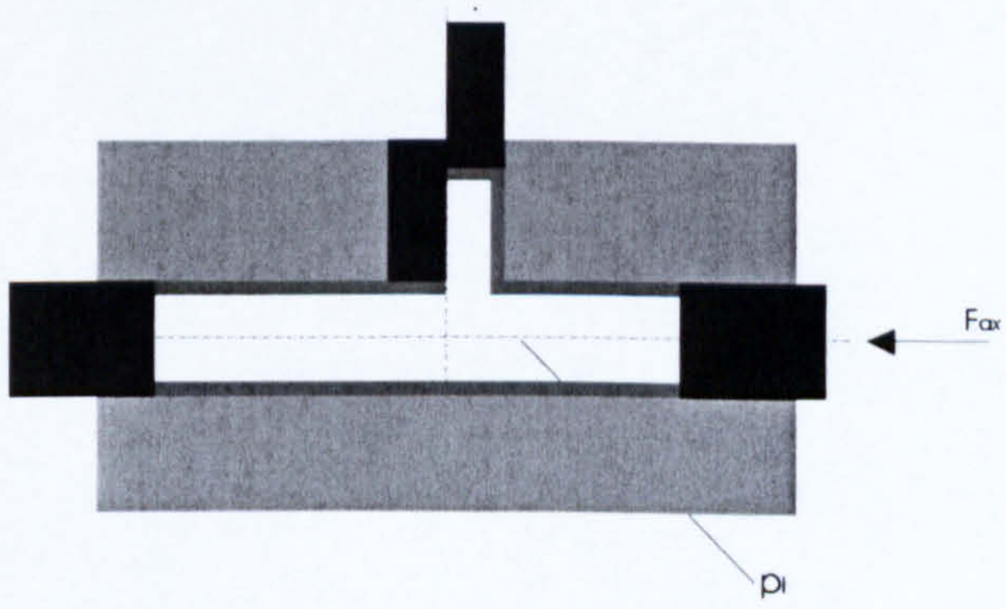

Figure 1-17 Expansion

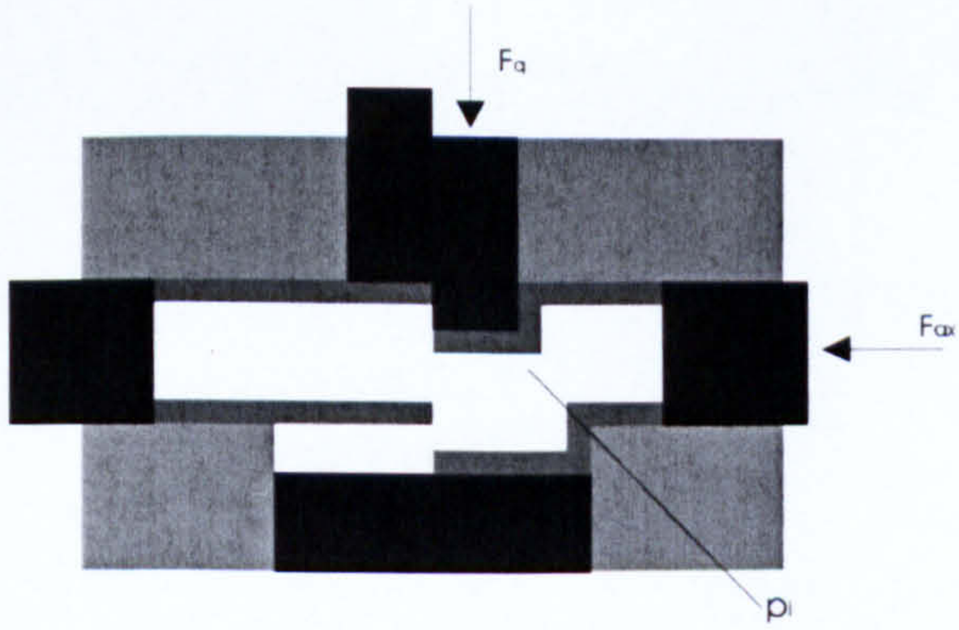

Figure 1-18 Transverse Forming (carry trough)

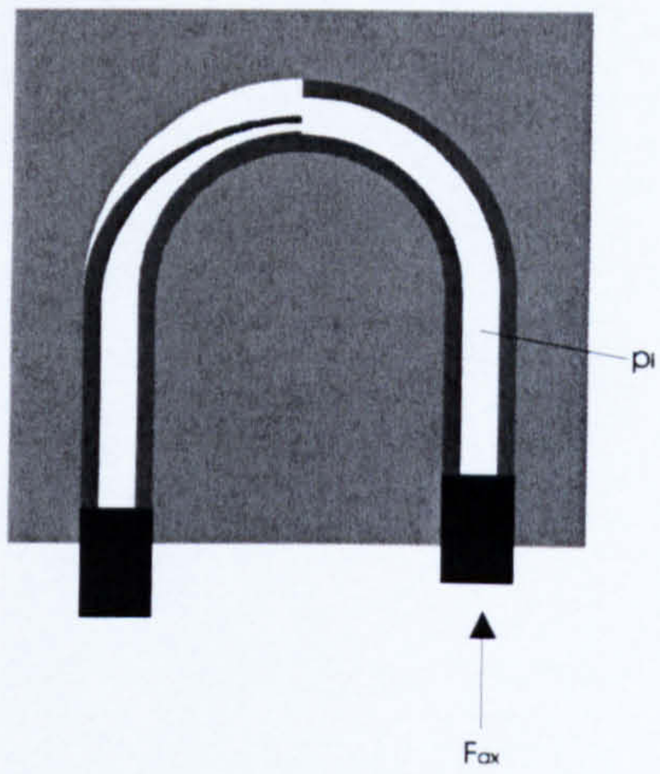

Figure 1-19 Calibration

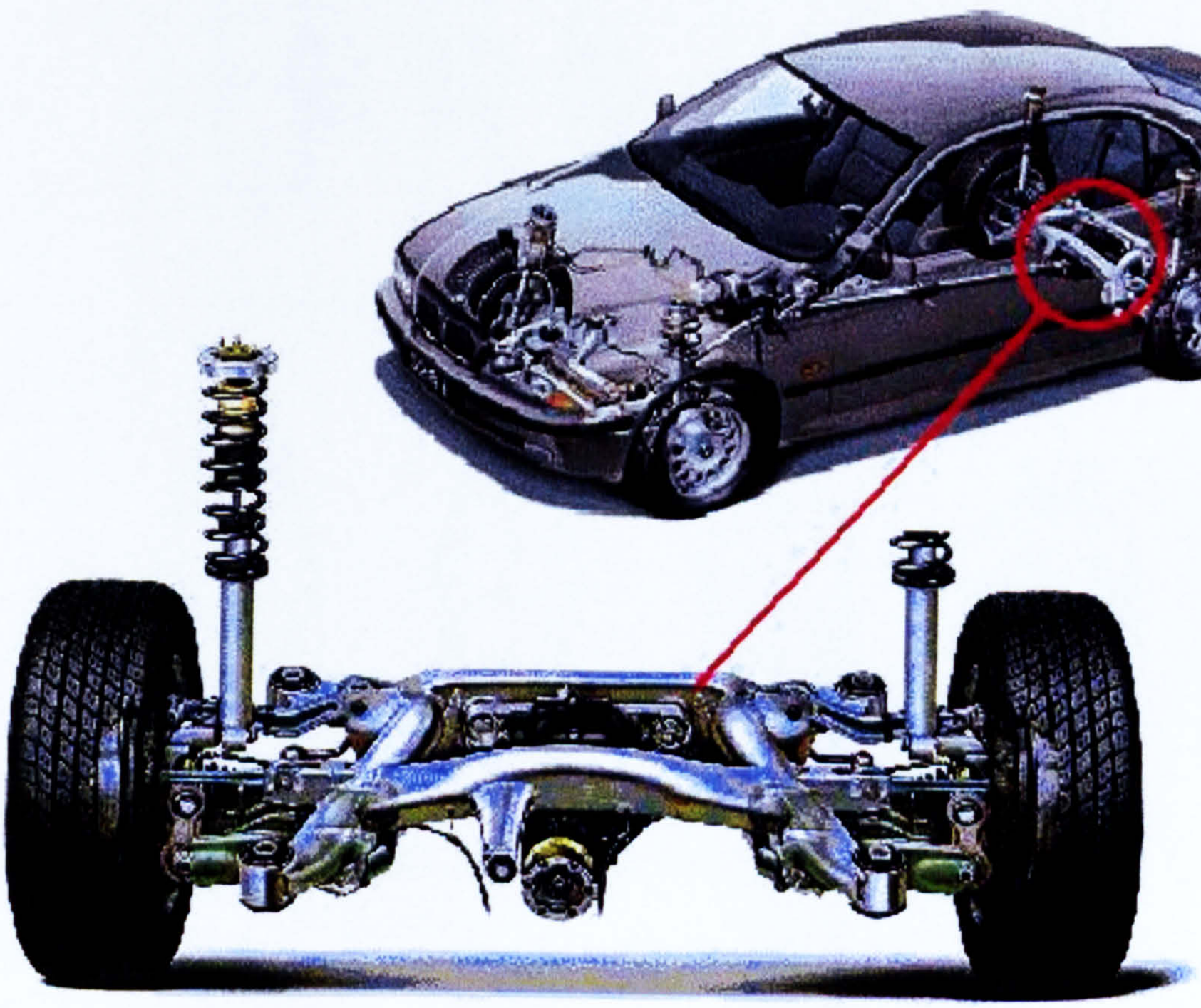

Figure 1-20 Rear Axle BMW 5er Series (BMW Company Prospectus)

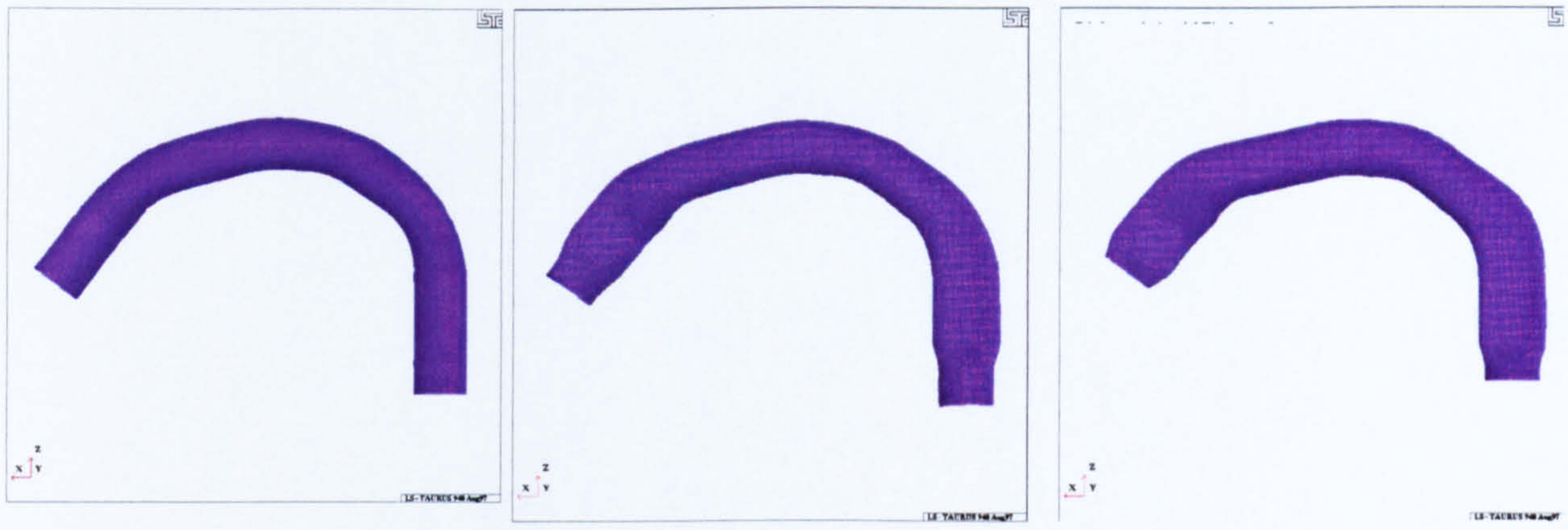

Figure 1-21 Forming Steps Rear Axle BMW: Side Member – Bending, Pre-forming, IHP

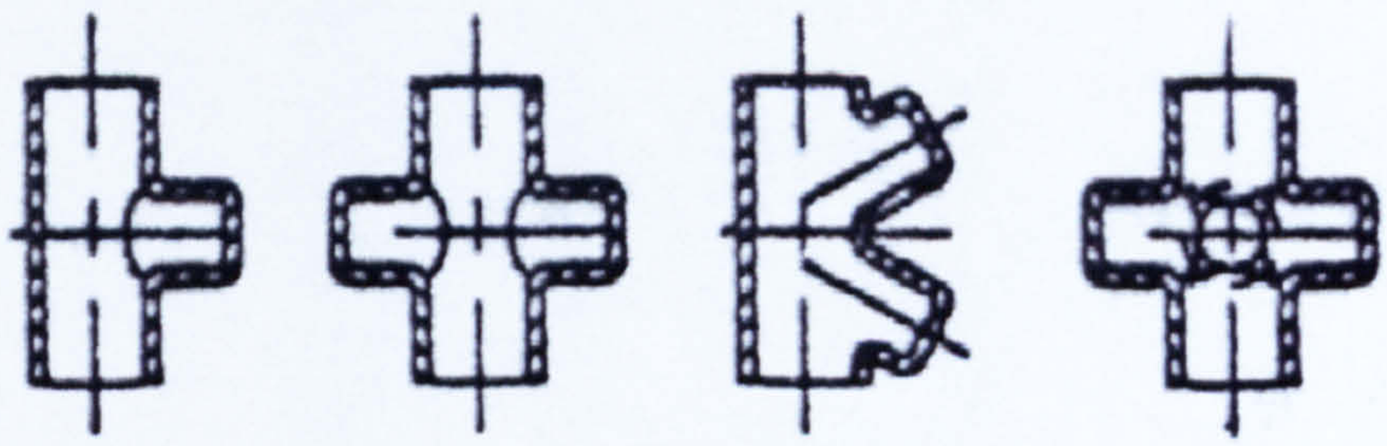

Figure 1-22 Typical Shapes: Partial (local) Expansion(s)

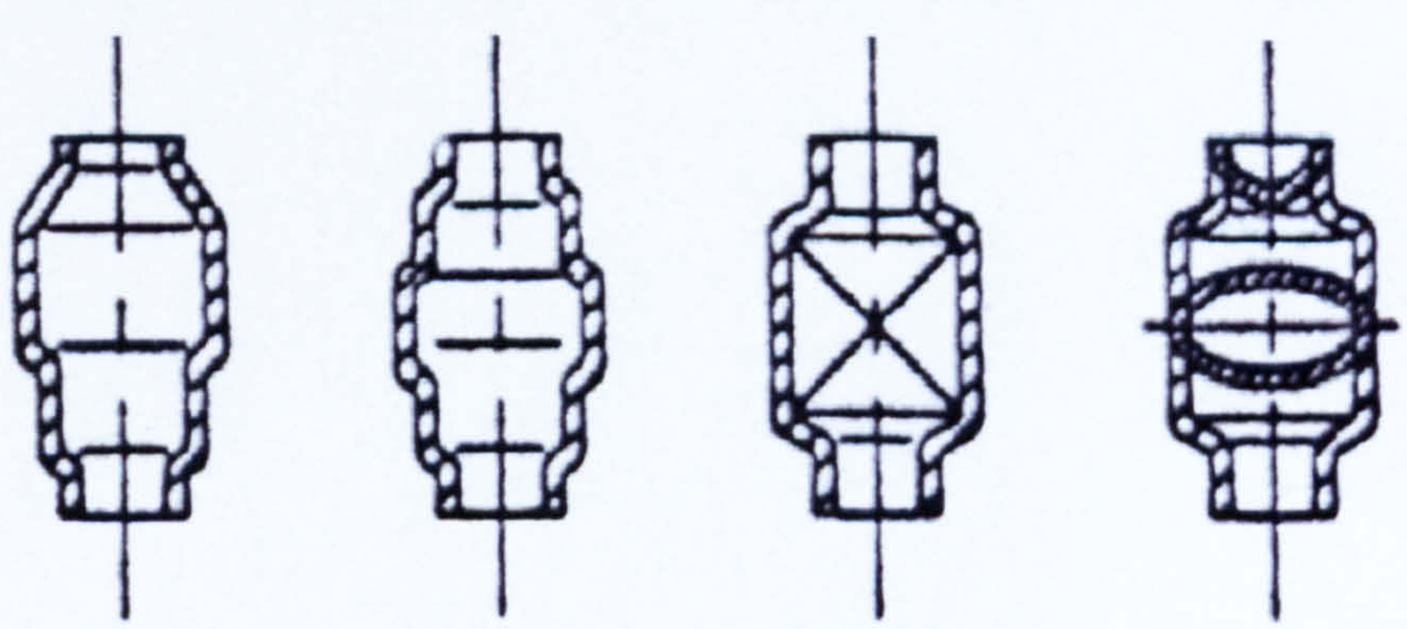

Figure 1-23 Typical Shapes: Rotational Expansion

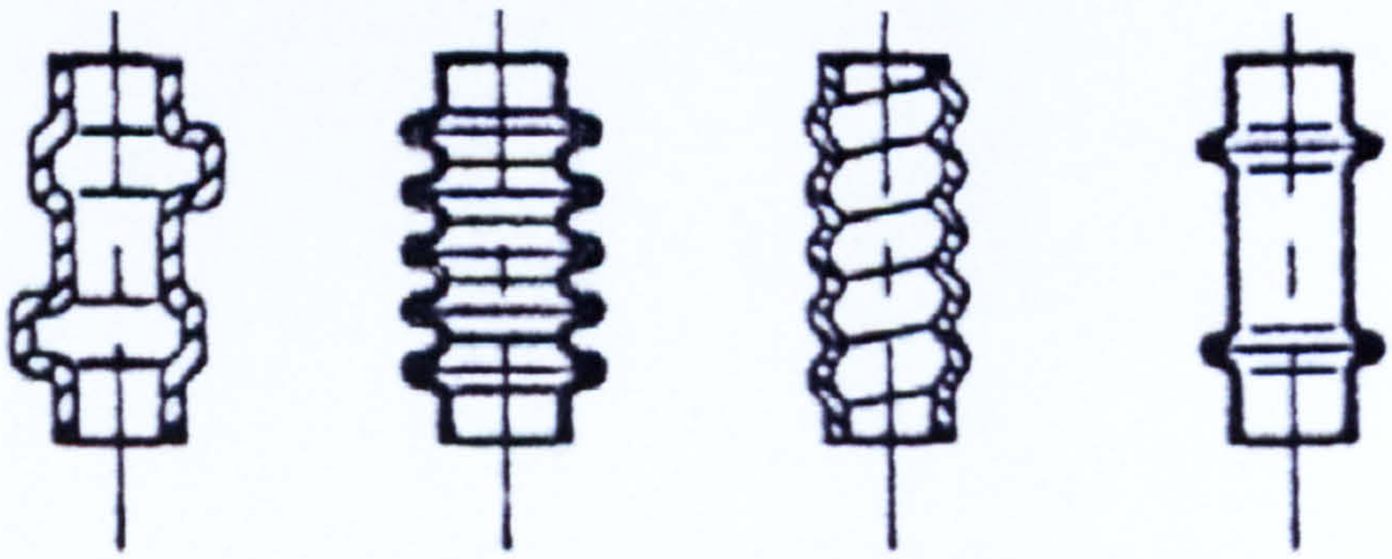

Figure 1-24 Typical Shapes: Undercut(s)

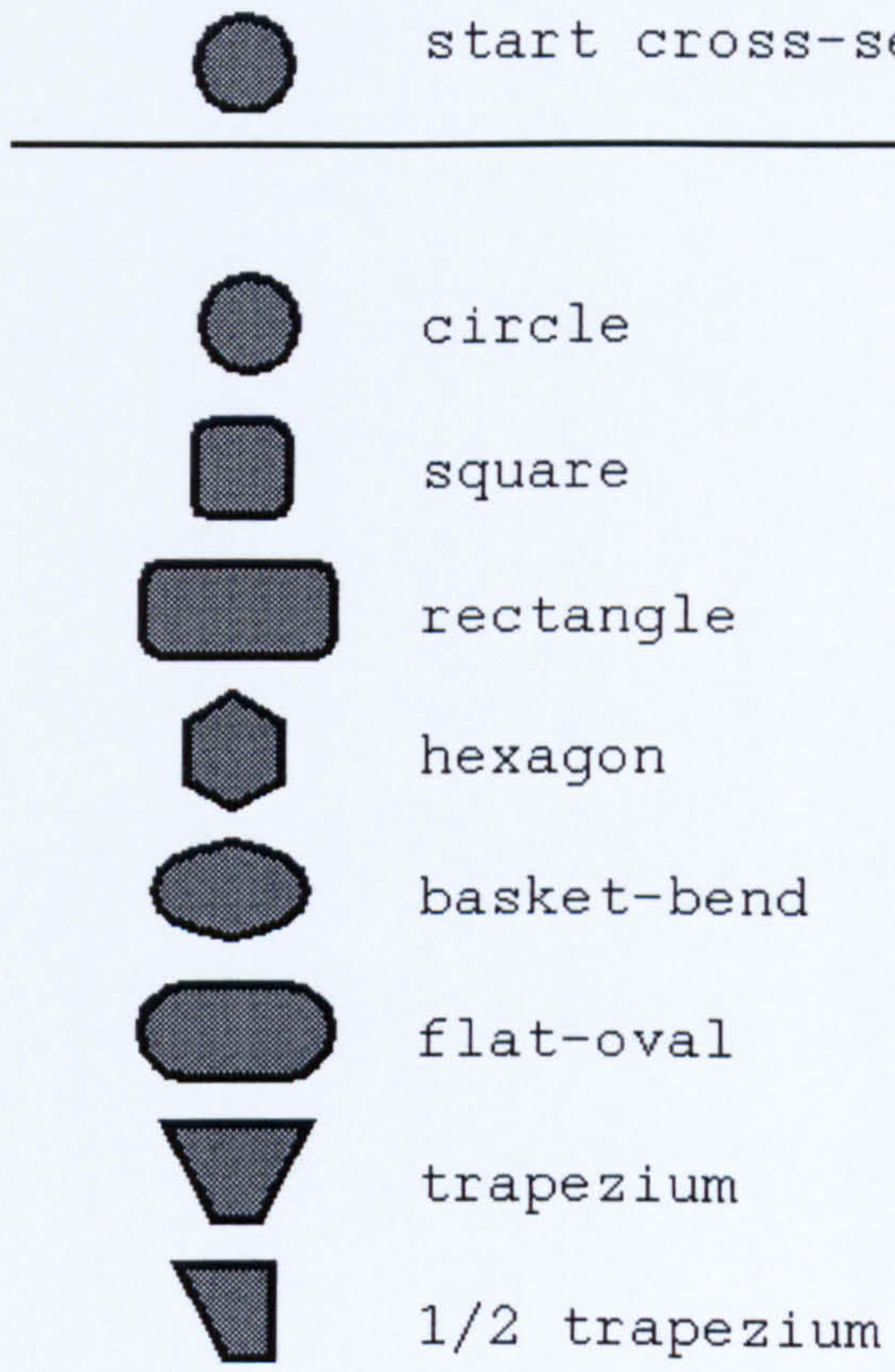

Figure 1-25 Cross-Sections Commonly used for IHP Products

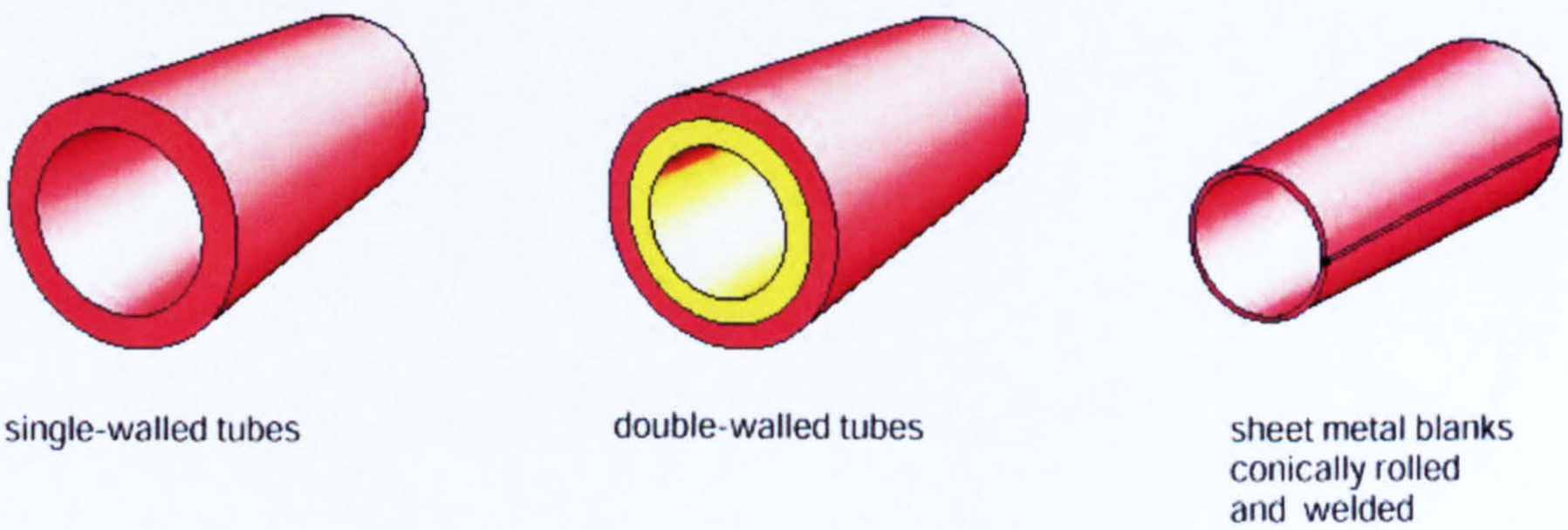

Figure 1-26 Blank Shapes (Schuler Metal Forming Handbook)

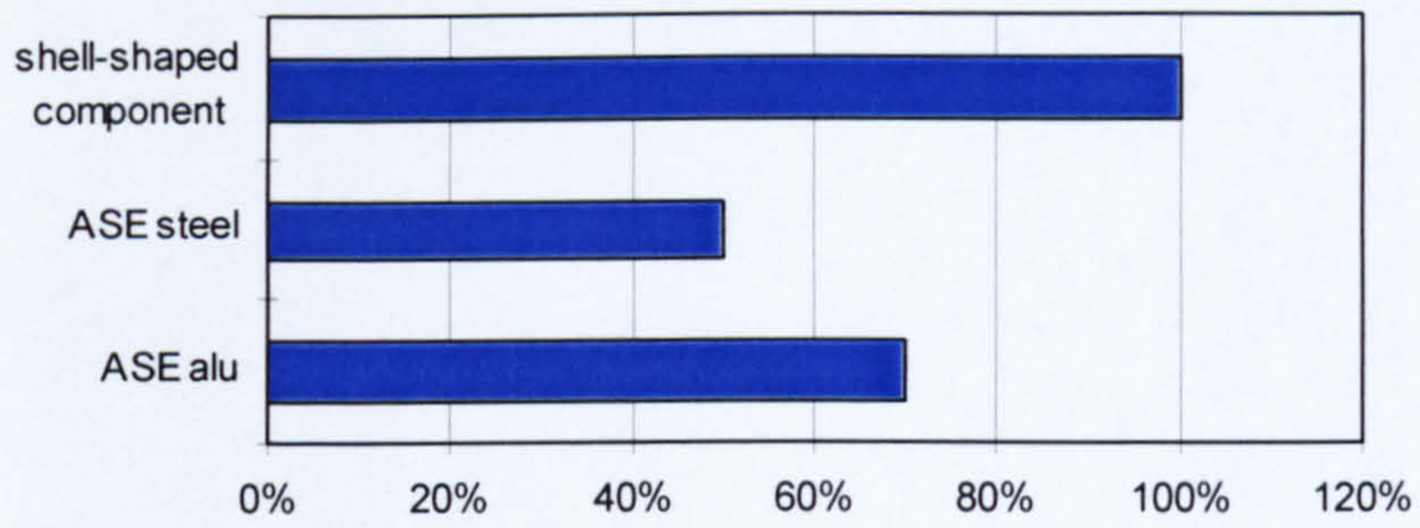

Figure 1-27 Comparison of the Costs for Prototypes

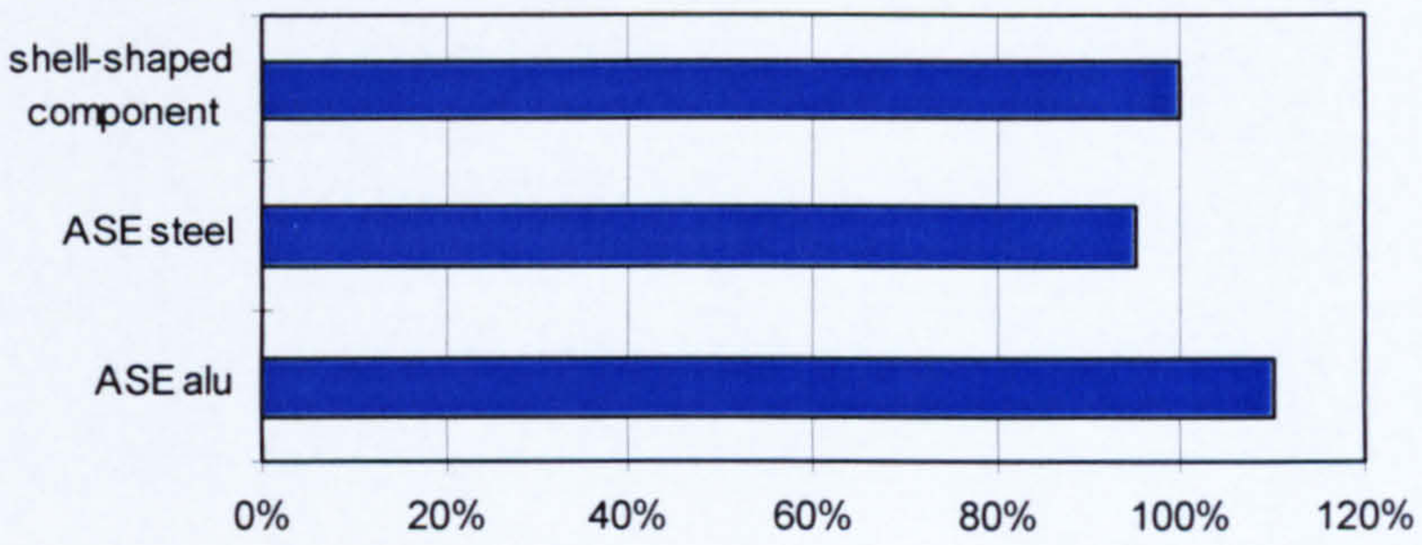

Figure 1-28 Comparison of the Costs for Serial Production

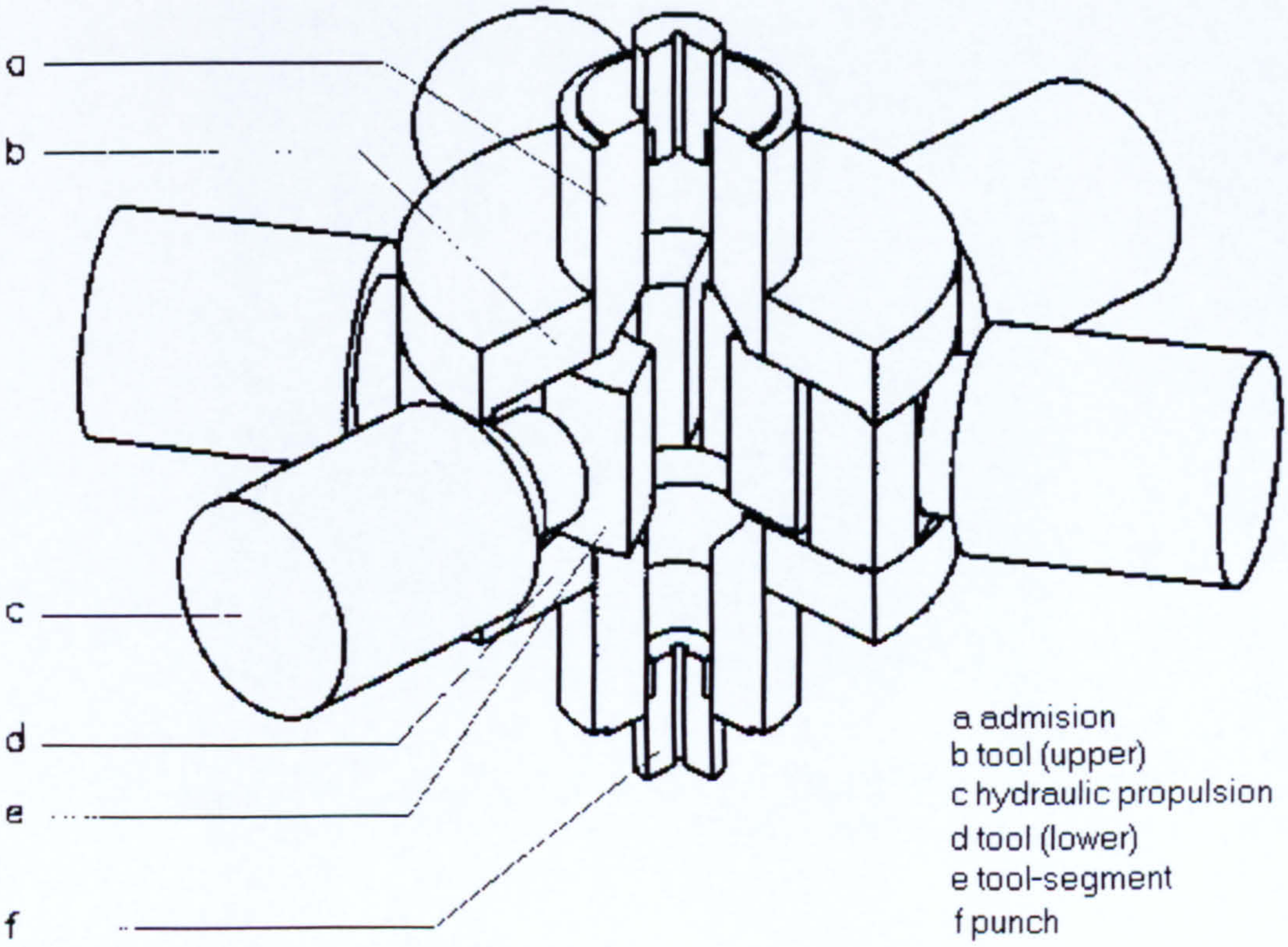

Figure 1-29 Structure of the Flexible Tool System

Figure 1-30 50000 KN Press for the Development and Production of Large Hydroforming Parts for the Automotive Industry (Picture: Siempelkamp)

Figure 1-31 35000 KN Press for the Automated and Integrated Production of Engine Cradles for the Opel Astra (Picture: Schuler SMG)

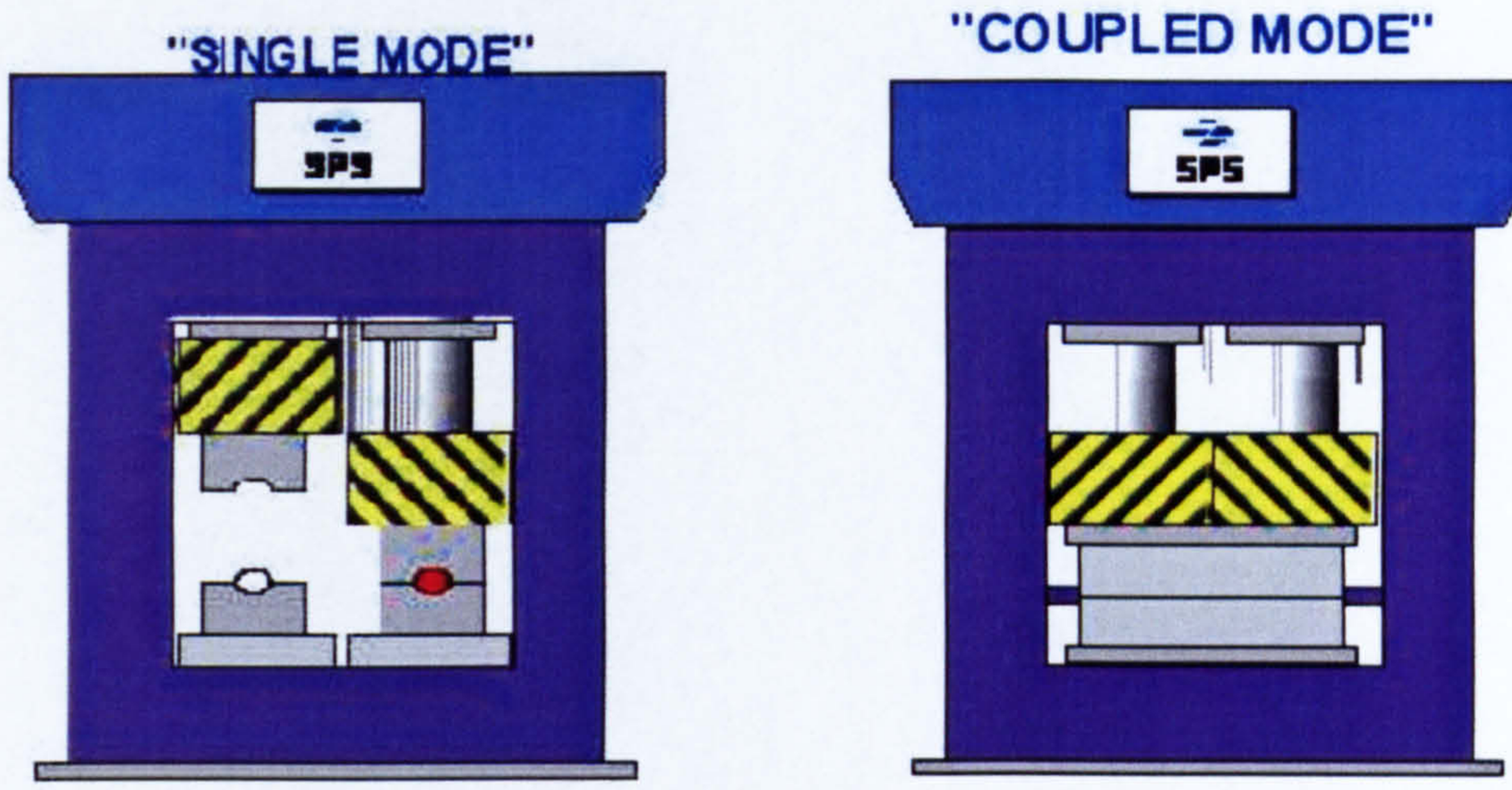

Figure 1-32 Double Ram Press System (Böhm, 1997)

CHAPTER 2
Literature Survey

This chapter gives a critical literature review of previous work carried out in the field of sheet metal forming process simulation using FE techniques, with a special focus at the IHP process simulation. It discusses the benefits gained from previous work as well as pointing out the shortcomings of such research.

2 Introduction

The optimisation of sheet metal forming processes with the help of the simulation techniques is much cheaper and faster than by trial and error. The numerical investigation delivers information about the material flow, stress and strain distribution, forming limits and the tool loads. Simulation is a very efficient tool by which new products, designs and their manufacturing process can be verified without having to manufacture a physical prototype, or perform a costly and time consuming trial. Today it is much more important to shorten the development time of new products, and this is not possible without using simulation techniques. The development of the computers during the last decade has made it possible to solve large simulation problems on a standard PC workstation, where a few years ago a supercomputer was needed for such tasks.

2.1 Simulation of Sheet Metal Forming Processes

First attempts to present the plastic change of the shape with the FEM were presented around the year 1965 as an extension to linear-elastic study from **Argyris (1965), Zienkiewicz (1969), Yamada, Yoshimura** and **Sakurai (1968)**. An important use of the process-simulation within the forming technique was the study of elastic-plastic material laws. First investigations of **Hill (1971)** and **Lee (1973)** were converted by **McMeeking** and **Rice (1975)** into an FE formulation. Further developments were initiated from the development of accurate and stable numerical procedures for the integration of non-linear material laws, and for obtaining solutions for the non-linear equation systems.

The first attempts to solve sheet metal problems using explicit methods where made in the middle of the 1980's. These efforts were mainly inspired by the very positive experience gained in the use of explicit methods in car crash simulations. The analysis of the deformation of a passenger car during a collision is in many aspects similar to the analysis of a sheet metal forming. Both these types of problems involved large plastic deformations and complex contacts including friction. The early sheet metal forming problems that where solved with explicit methods mainly involved conventional sheet stamping or deep drawing types of loading.

2.2 Simulation of IHP

Sauer (1978) described the free bulge forming of tubes under internal pressure and axial compression. He developed a computer program for the simulation of the process, which estimated the shape of the tube under load until failure. The main task of his work was to predict the two different modes of failure – buckling due to excessive axial forging or bursting due to excessive internal pressure. He obtained an excellent correlation between theoretical and experimental results. The work of **Sauer (1978)** focused at the free expansion of a tube without tools, e.g. without contact between tool and tube.

Wilhelm and **Keck's (1989)** thesis was on the use of the FEM for the simulation of solid metal forming, e.g. they investigated the Rastegaev press test, by looking at the IHP process simulation of an axial symmetrical forming process. They investigated the use of the FE-program EPDAN, which was developed from **Tekkaya (1986)** work, for the simulation of forming processes. The experimental results determined by **Klaas (1987, Figures 2-1, 2-2, 2-3)** were the basics for the FE simulations. **Lange, Herrmann, Keck** and **Wilhelm (1991)** simulated the forming process of the free interior high pressure forming of a tube with different load curves. The interior pressure was applied depending on the axial direction of the stamps. Contrary to the trials of **Klaas (1987)**, he used a force-steered forming for his experiments, **Lange et al. (1991)** simulated with a direction-steered forming. The pressure curve is drawn from diagrams which contain some inaccuracy, the same is valid for the flow-curve, so the authors did not expect that the simulation can review the experiment very accurately. The folds build at the expansion of a hollow-ball were accurately reproduced, except that the folds are more intensive in the simulation. Like **Sauer (1978)** the simulation confines itself to the free expansion without tool, e.g. the further nonlinar contact conditions. Remarkable is the good representation of the details e.g. the differences in the formed shape at the conical crossing area.

Sauer, Wilhelm et al. (1978) achieved a good agreement of their simulations with the experimental results, but the free expansion of tubes is only very rarely used for real industrial applications.

Bauer (1989, Figure 2-4) also described the process simulation of built-in cam shafts with a very good correlation with experimental results. Built-in cam-shaft means that cams are each and every one pushed on the tube, the cams are positioned in a tool and the tube is expanded. Now the tube deforms plasticly but the cams only elasticly. Afterwards when the interior pressure is taken away the cams contract back and for this reason they are fixed on the tube. The hole in the cam is not exactly circular, though it also forms a conclusive connection.

Bauer and **Lang (1992)** described the simulation of the forming process of a t-piece (**Figure 2-5**). The simulation model was very primitive because it was without counter-holder. **Bauer et al. (1992)** used a displacement-steering for the axial forces, the simulation worked, but the strains in the tube after the forming process are extremely high. The simulation was done with an elastic-plastic material law with an infinite plastic range, and this is the reason why the simulation worked. The results show a good comparison with the true forming process, with the folds build at the opposite side of the dome formed such as in the real process.

The publication of **Weiss (1996)** described the forming process for t-pieces, however with a simulation model which had a better correlation to the real process, e.g. with a counter-holder. He obtained results similar to **Bauer et al. (1992)** but with a better strain distribution and therefore similar to the real process.

Brännberg (1994) investigated the numerical simulation of sheet metal forming with special attention to the simulation of fluid cell forming processes (**Figure 2-6, 2-7, 2-8**). Fluid cell forming is similar to IHP forming, it is a deep drawing with a fluid as a stamp. The simulations from **Brännberg (1994)** were carried out with explicit finite element methods, using both deformable (sheet) and rigid (tools) material models. He used the code LS-DYNA for the simulations. First he investigated three test cases (**Table 2-1**) with a different complexity of the simulation model, the component simulated was a part of a fuselage frame from a Saab 2000 aircraft.

Case	Comment
1	Blank + Pressure
2	Blank + First Rubber + Pressure
3	Blank + First Rubber + Second Rubber + Pressure

Table 2-1 Load Cases simulated from Brännberg

The goal was to study the influence of the various parameters (**Table 2-2**) of the result.

Parameter	Influence	Comment
System damping	Yes	Important
Extension of first rubber	< 95 mm	-
Extension of second rubber	No	-
Ramps on the die	Yes	Improves performance
Fluid pressure	< 10 Mpa	-

Table 2-2 Process Parameters

This simulation was done for three cases with a different relationship of width and length. The main goal was to compare the solution for a full dynamic system and a mass scaled solution. The results were exactly the same, but the calculation time for the mass scaled run was only 40% of the full dynamic system. **Brännberg (1994)** showed that the mass scaling can efficiently reduce the time needed to obtain an accurate solution. The comparison of the simulation with the experiments shows that the displacement of the centre point had a good correlation with the experiment, and that the thickness distribution had little correlation with the experiment. The numerical results showed less straining in the thickness direction compared to the experimental results.

Further examples were a fluid cell forming of flanges, deep drawing of cups including the investigation of different anisotropic yield criteria and stretching of a circular thin sheet by a hemispherical punch. For all these examples he achieved a good correlation with the experimental results. **Brännberg (1994)** concluded that the explicit finite element method was a suitable tool for the simulation of sheet metal forming problems. **Brännberg's (1994)** work did not consider the hydroforming of tubes, which is the main aim of this research work.

Roll (1994) investigated the forming process for a t-piece, a cross member and two pieces from an exhaust system at the division for the development of manufacturing technology of the Mercedes-Benz company in Sindelfingen/Germany. **Roll (1994)** used the software-package AUTOFORM for quick analyses, LS-DYNA to optimise the process and to recognise folds, INDEED and EPDAN for the calculation of spring-back and residual strains. For the simulation of the IHP part (a t-piece) he obtained a good correlation with practical production and found that it was possible to predict the course of the shell-thickness over time. The T-piece shown in **Figure 2-9** has however a shape which cannot be created out of steel or aluminium. **Roll's (1994)** work did not describe which material he had used for this simulation and there is no evidence of the existence of a physical part.

Furthermore he found that it was possible to prognosticate the start of folding or bursting. Overall **Roll (1994)** maintains that the software packages today are suitable for the simulation of forming processes, but there are problems when applied in industries. These software packages are difficult to integrate into the CAD/CAM process chain, and the interpretation of the results, under certain circumstance, is difficult because of the size of data involved. Therefore the use of the simulation within the process chain is too late, he concluded that the simulation is used normally only if there are problems during the manufacturing stage and not during the development phase of the product, and there are only simple models and data for friction and materials available. One main task of this research work is to improve the integration of the simulation technique into the concurrent engineering process chain.

Heath (1993) investigated the simulation of the interior high pressure forming process of simple workpieces shown in **Figure 2-10** and **2-11** as did **Wilhelm et al. (1989)** using PAM-STAMP software.

Further simulations of axial symmetrical interior high pressure forming processes with the program ABAQUS were published by **Böhm (1993).** He described the simulation of the interior high pressure forming process hollow with a lengthways axis's and rotary symmetrical geometry. Therefore **Böhm (1993)** created the simulation with 2D FE-elements shown in **Figure 2-12,** he used the implicit FE program ABAQUS for the simulation. However at this time the program needed considerable time for the solution of the problem (20-60 hours on a SUN 4/ 233).

Duzidak (1995) developed a process model founded on theoretical assumptions. He used the results of **Klaas (1987)** and **Böhm (1993)** to create a program to estimate the process parameters online in the production machine, he tried to create a real-time process simulation tool directly on the production machine, and for this reason the FE method was ruled. This proce-

dure is possible for simple work-pieces but is relatively inaccurate, because the equations used cannot represent the variety of shapes found in IHP products. IHP parts are more and more complex and therefor the way taken by **Duzidak (1995)** was not suitable for industrial application.

One year later **Duzidak (1996)** reported the development of a typical IHP part from the Daimler company including the use of the FE simulation. He found that the FE simulation was a suitable tool for the simulation of the IHP process.

Zhang and **Wang (1993)** describe the FE simulation of a spherical vessel. Spherical vessels have been used widely in industry for the storage of oil, LPG, LNG, liquid ammonia, liquid oxygen, liquid nitrogen and liquid hydrogen, etc. and also in other fields such as architecture, etc. However, traditional technologies for manufacturing spherical vessels all use heavy presses and expensive dies, employing stamping technology. **Wang (1985)** put forward dieless hydrobulging technology for the forming of spherical vessels, in which there is no need for presses and dies, and therefore most of the difficulties of conventional technologies were overcome. Up to now, many spherical vessels made using this technology have been used in industry, 32-petal spherical vessels being typical. In this work, the hydrobulging process of a 32-petal spherical tank is simulated and analysed using the non-linear finite-element method. The deformation and features of some typical positions of the shell are summarised and discussed, the stress and strain distribution and their variation are analysed, and the measures taken to improve the new technology are highlighted.

A methodology for including anisotropy in metal forming analysis was presented by **Beaudoin, Dawson, Mathur, Kocks** and **Korzekwa (1994)**. A finite element formulation was developed for the analysis of the inhomogeneous macroscopic deformations. Anisotropic material properties were derived from a microscopic description based on polycrystal plasticity theory. Efficient computation of the microscopic variables is achieved through massive data parallel computations. A procedure was set for the initialization of the microscopic state variables from experimental measurement of the metal texture. The feasibility of initializing (from experimental data) and evolving (through massive computations) a detailed microscopic description for a complex deformation process was demonstrated through a predictive simulation. The predicted location and height of ears in the hydroforming of aluminium sheets was in agreement with the experimental findings.

The principle technical procedure and features of the dieless hydroforming technology of double layer spherical vessels were introduced by **Zhang** and **Wang (1994)**. The structures and materials of the shells before bulging were discussed, as well as the technical problems associated with bulging of the shells, taking account of experiments on a few double layer spherical shells. The deformation process, the thickness distribution and the diameter variation are also analysed, together with the deformation process of the shell at the initial deformation stage, which was analysed by using elastoplastic finite-element method. Finally the industrial applicability was discussed.

A computational method based on the membrane theory for the analysis of axisymmetric sheet

metal forming processes such as punch stretching, deep drawing and hydroforming was presented by **Hsu** and **Chu (1995)**. The elastic-plastic finite element approach was based on the flow rule associated with Hill's quadratic yield criterion for anisotropic material. The total Lagrangian formulation and virtual work theory were used to derive the stiffness equations and the relationship between displacement and strain. Some examples on the stretching, drawing and hydroforming of metal sheets were considered, and the computed results were compared with experimental data and with the results from existing numerical solutions.

A limit theorem of plasticity has been developed by **Hsu** and **Hsieh (1996)** to investigate the hemisphere punch hydroforming process. The limit theorem of plasticity was used to predict the upper and lower bounds of the permissible fluid pressure. Loci representing the critical fluid pressures which resulted in the rupture and wrinkling were presented. The property of the sheet metal was governed by Hill's quadratic yield criterion with a power-law hardening for anisotropic material. The premature failure was avoidable if the fluid pressure path was restricted to travel only within the suggested bounds. The theoretical results which include the failure prediction and wrinkling distribution were verified by conducting a series of hydroforming experiments. The experimental data agreed well with the computed results and demonstrated the technological usefulness of the results.

The investigation of tubular hydroforming limits based on analytical and experimental examinations were the subject of a publication by **Liu, Meulemann** and **Thompson (1998)**. This paper summarized experimental and analytical results of a hydroforming process which expanded a circular tube into a rectangular cross-section. A better understanding was obtained by investigating the relationship between internal pressure, axial displacements, mechanism of buckling, splitting and corner fill-ins. Splitting, buckling and the tubular hydroforming zones were identified by the traditional Forming Limit Diagram (FLD). The authors examine the behaviour of a single steel tube for different load paths. The simulations, done with LS-DYNA, did not investigate the influence of the different material types or the flow criteria's. The result of the investigations agreed with the known fact that a high axial compression provides wrinkles and hence a high pressure bursting can be expected.

2.3 Discussion and Conclusions

The common problem in all FE simulations is the considerable cost induced by the time taken to complete the whole process. The FE-simulation of IHP processes achieved, in nearly all cases, a good or very good correlation to the real processes. The FE-simulation is an efficient tool to achieve an overview of the process and to judge the feasibility of such a process. For large structures, like a complete back axle or motor suspension, the time currently needed for a simulation of the whole part on a modern workstation like a HP C200 or a SGI OCTANE is too high. The simulation time for the motor suspension shown in **Figure 2-13** which has about 48.000 shell-elements excluding the tools, which are formulated only as VDA surfaces, is approximately 4 weeks. In this case it is useful to extract the critical sections of the part and only simulate the forming process of these sections. **Figure 2-14** shows one critical part of the motor suspension with the tools for pre-forming. In the near future with faster processors and software codes running parallel on multiple processors it is predicted that such simulation will be possible. The tendency today is to use very small elements for the FE simulation in order to get accurate results, e.g. elements with an edge length of 1 mm, this means for an engine cradle with a length of 2500 mm and a diameter of 50 mm will produce approximately 350.000 elements.

The advantages of the FE simulation of IHP processes are the reduction of the high trial expenditure saving time and money, and the creation of basic knowledge about the process. FE simulation will also assist in estimating the costs of new manufactured products using the IHP technique, as well as to assist in the feasibility study of whether such a part can be produced economically using such technique. For a quick assessment of the possibilities of the IHP technology for new products or the replacement of products manufactured with standard technology it is necessary to investigate the following areas :

- basis of the IHP technology under consideration of the rapid development of the scientific and technological conditions
- estimating the feasibility, design and realisation of the interior high pressure forming with a basic scientific knowledge
- development of rules for the design of IHP products
- development of innovative and inexpensive alternatives to the conventional manufacturing technique such as deep-drawing, punching and welding
- investigating the influence of friction on the IHP process
- development of efficient and accurate adaptive mesh refinement and de-refinement

The goal for medium-termed developments is to create a virtual press including all necessary components. This virtual press should make it possible to go through the press, look at the process and how it works and look also at the behaviour of the press, e.g. the response, the displacements of the tools and the surrounding press-frame.

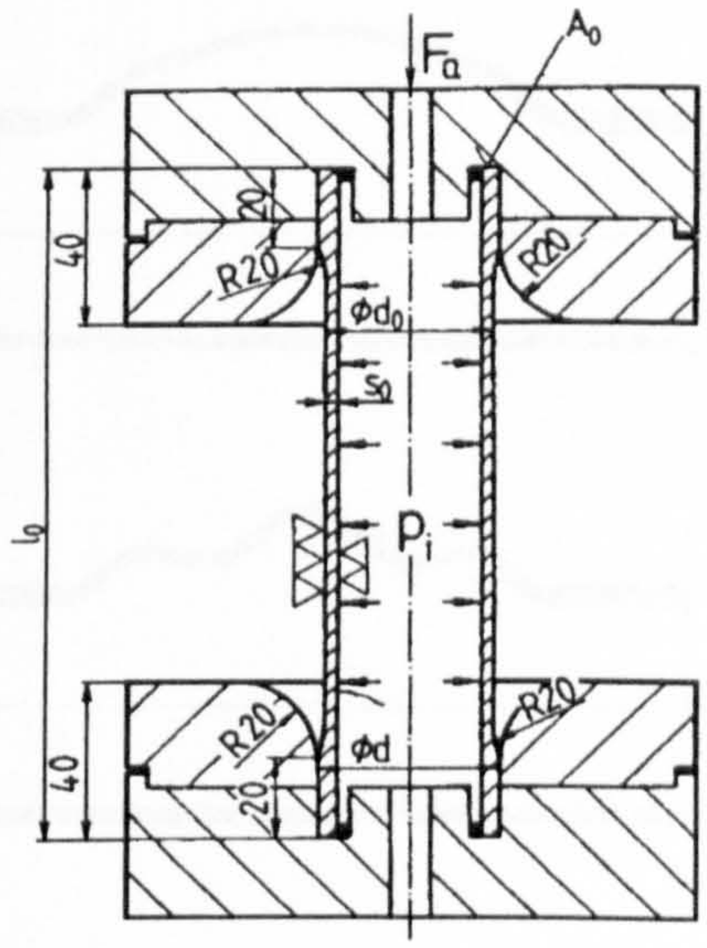

Figure 2-1 Free Expansion according to Klaas (1987)

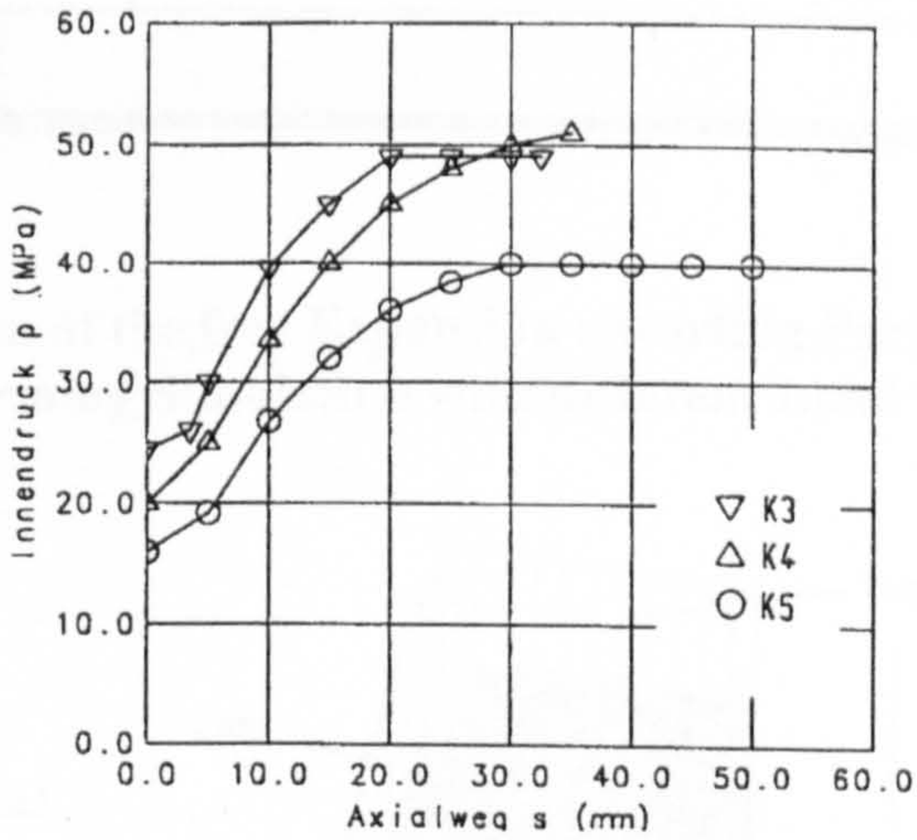

Figure 2-2 Interior Pressure vs. axial Way of the Tools for the three Load Cases K3, K4, K5

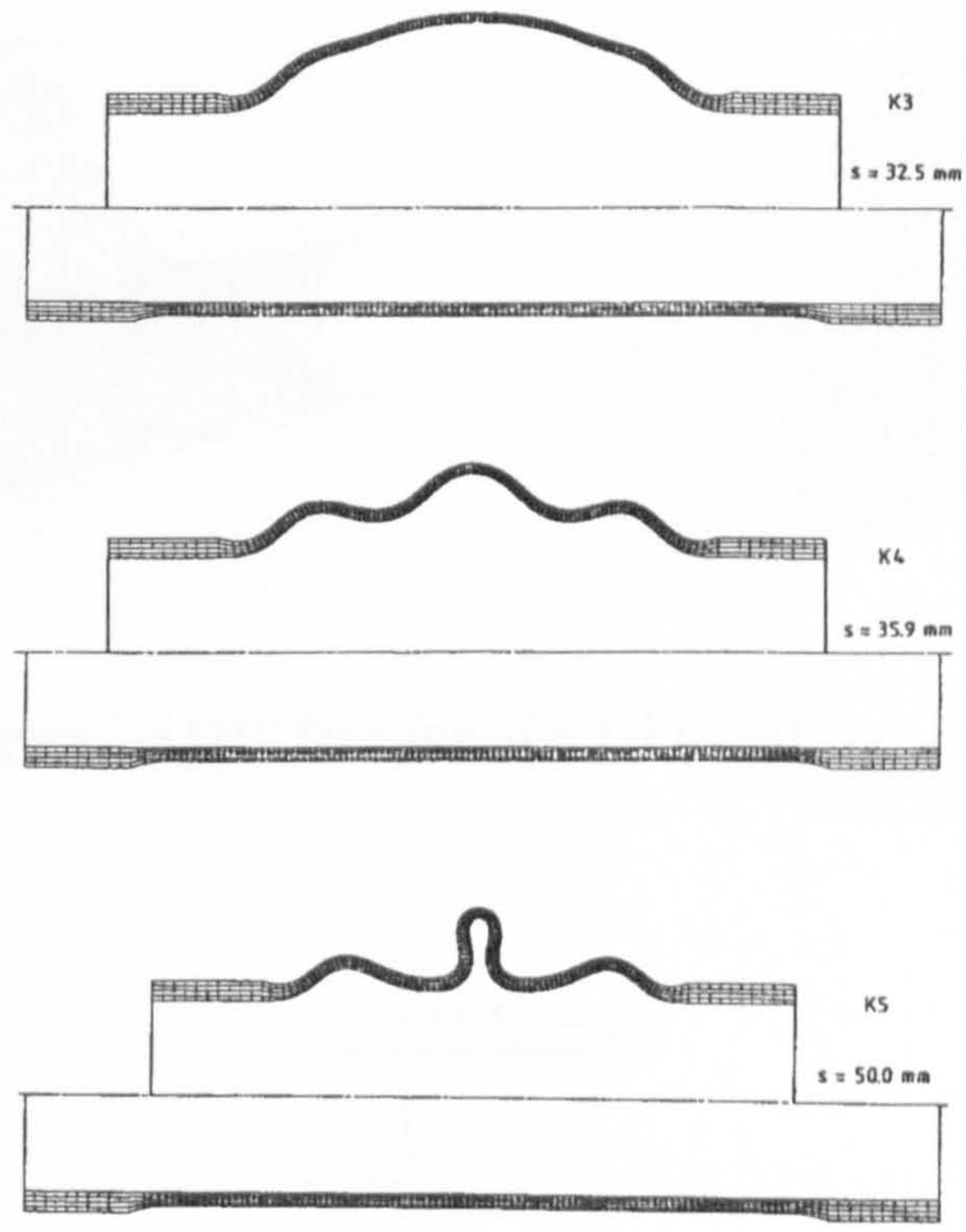

Figure 2-3 Simulation of the free Expansion : Starting Part and deformed FE Mesh at the End of the forming Simulation with different Load Cases according to Klaas

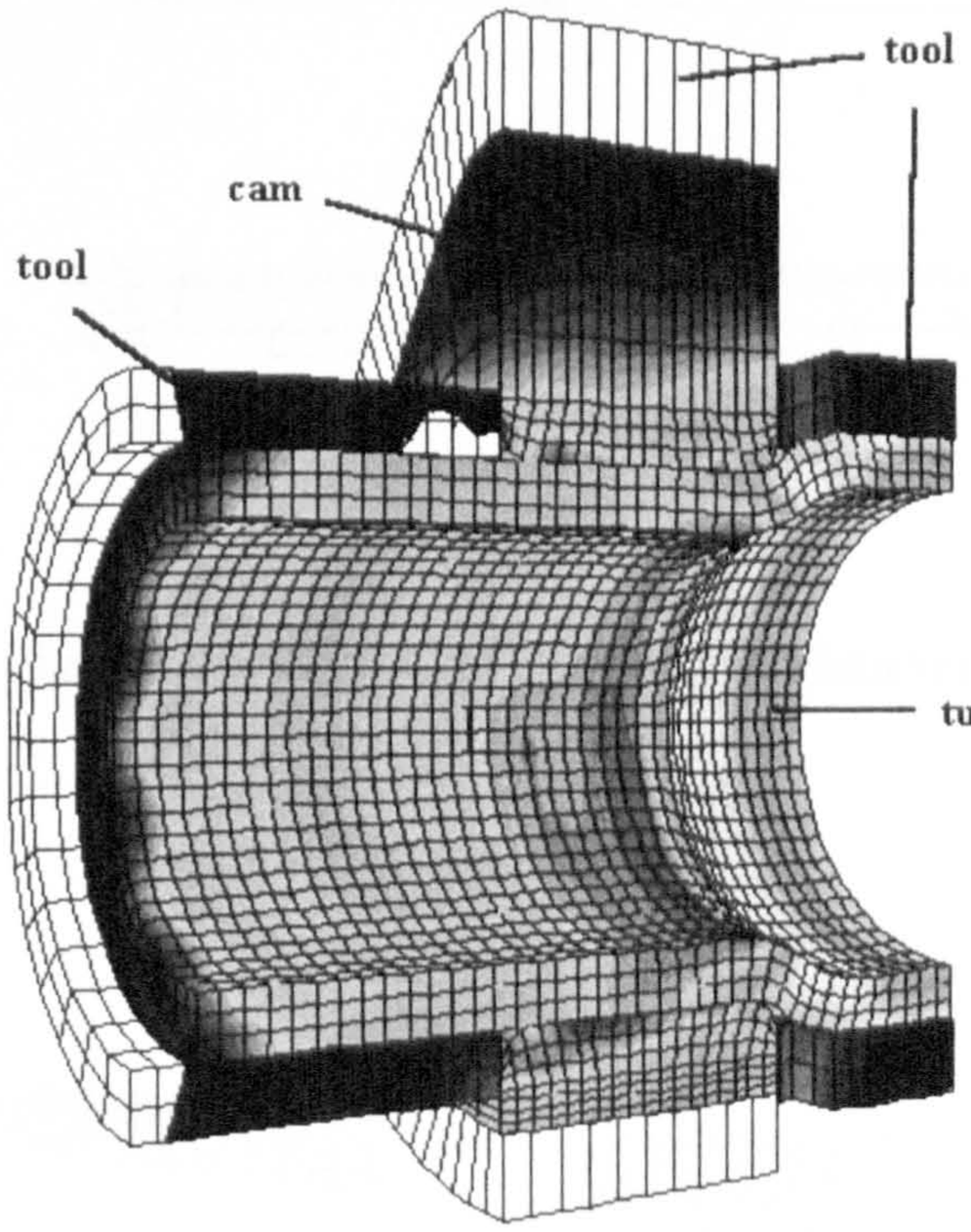

Figure 2-4 Built Cam-shaft (Bauer, 1989)

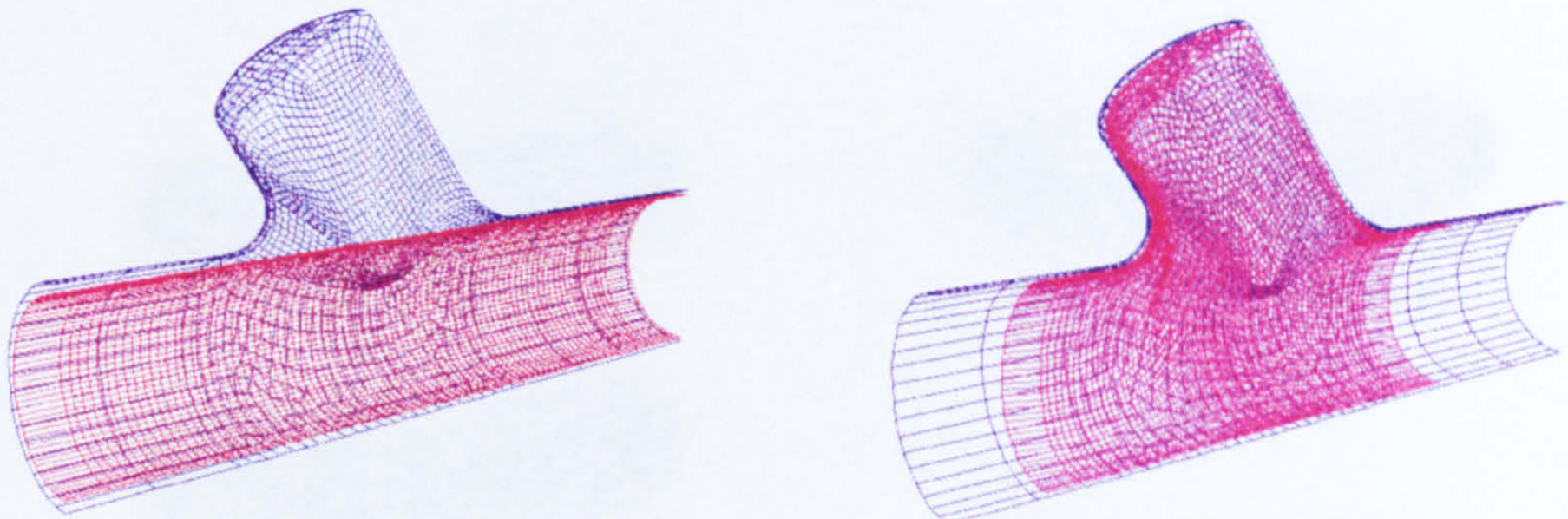

Figure 2-5 IHP forming of a T-Piece (Bauer et al., 1992)

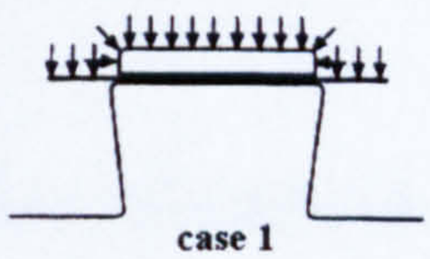

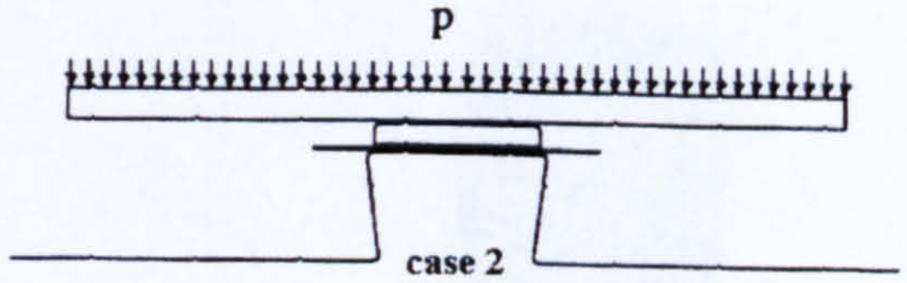

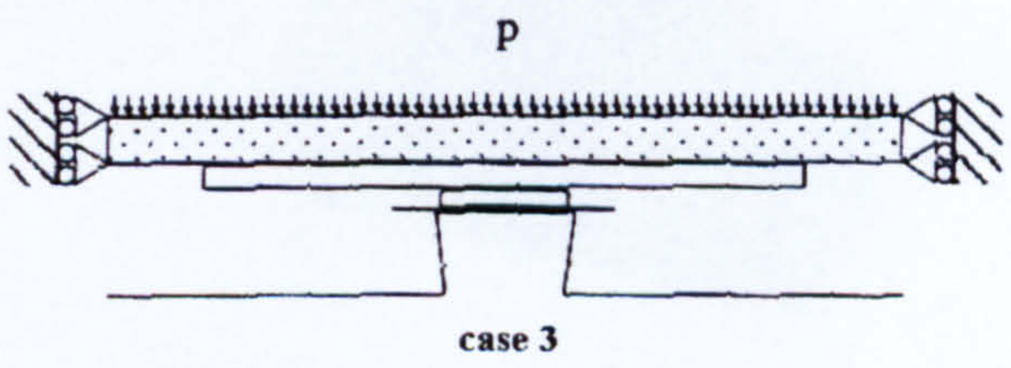

Figure 2-6 Fluid Cell Forming (Brännberg, 1994)

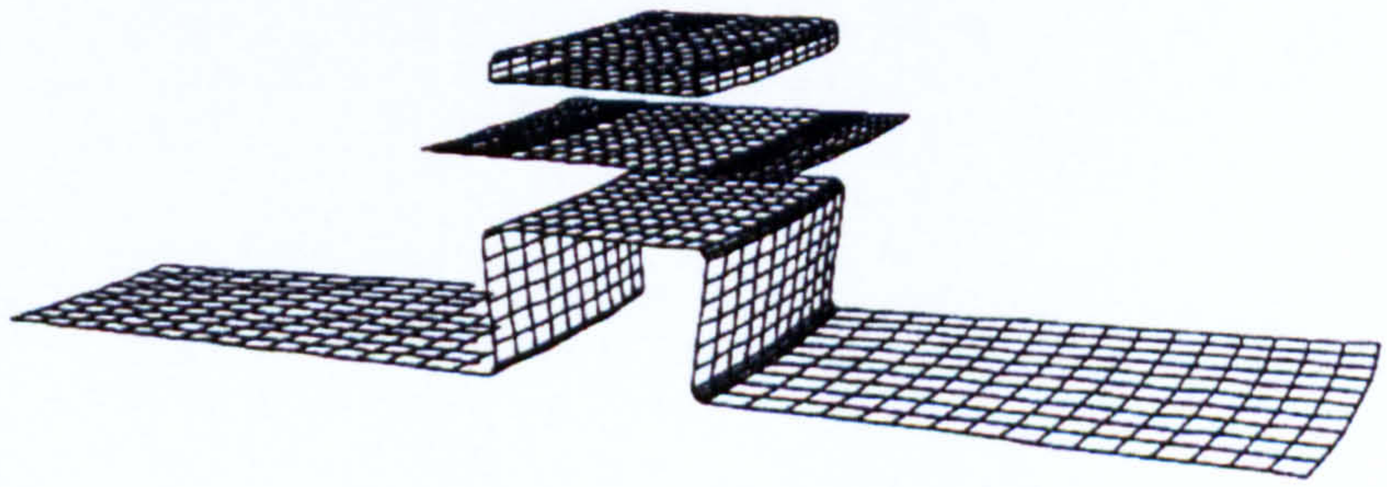

Figure 2-7 Fluid Cell Forming - FE model (Brännberg, 1994)

(a) Pressure 2 MPa

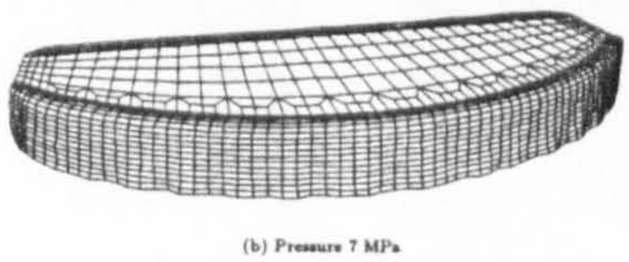

(b) Pressure 7 MPa

(c) Maximum pressure 20 MPa

Deformation of blank during pressing

Figure 4.24: Final shape of the flange after unloading

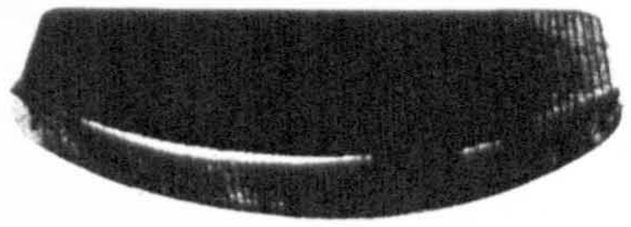

Final shape of the shrink flange from experiments

Figure 2-8 Hydrostatic Bulging of Rectangular Diaphragms (Brännberg, 1994)

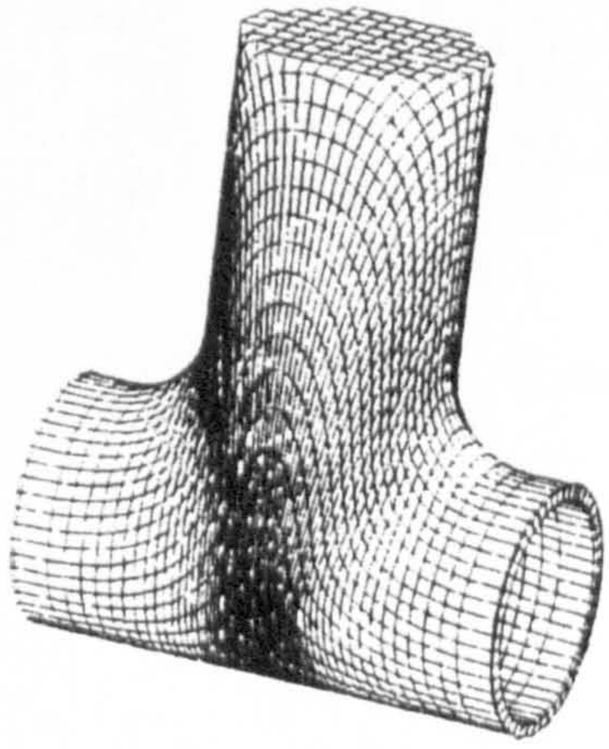

Figure 2-9 T-Piece (Roll, 1994)

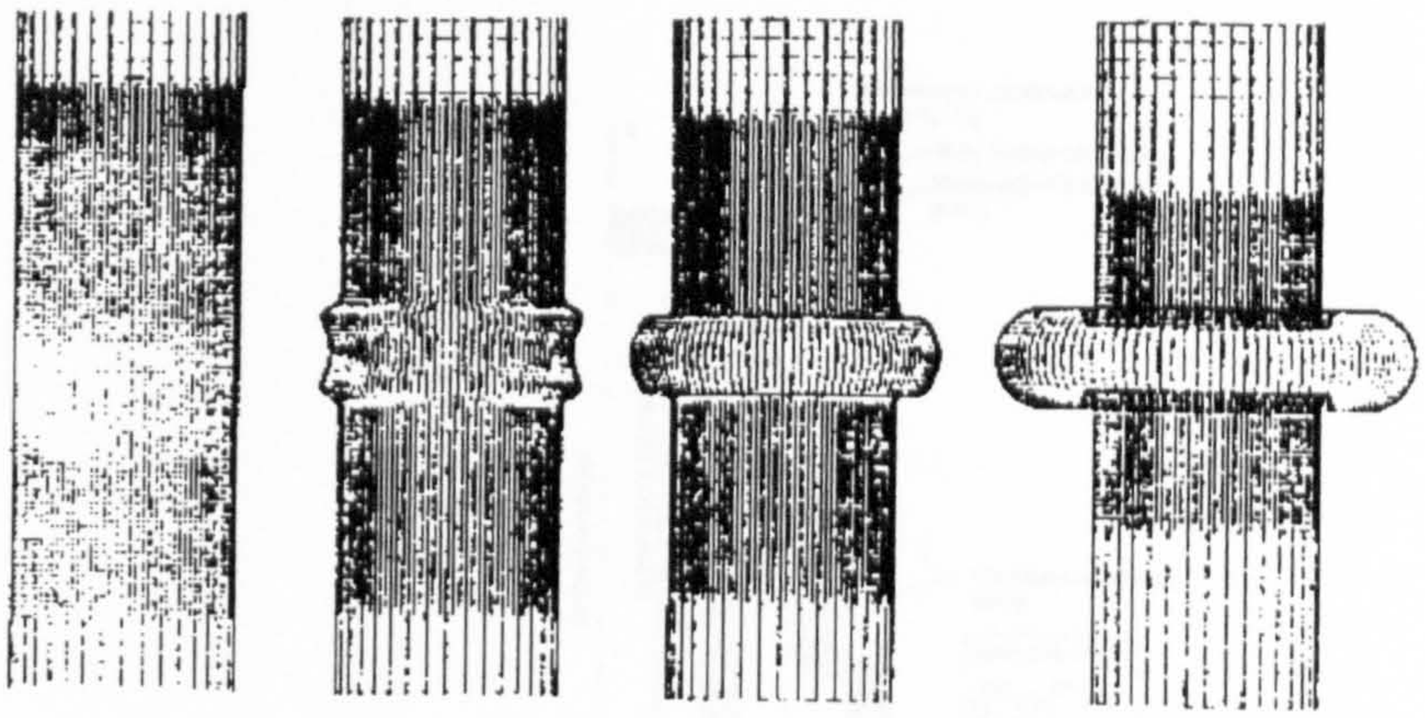

Figure 2-10 Simulation of a IHP Process - Case 1 (Heath, 1993)

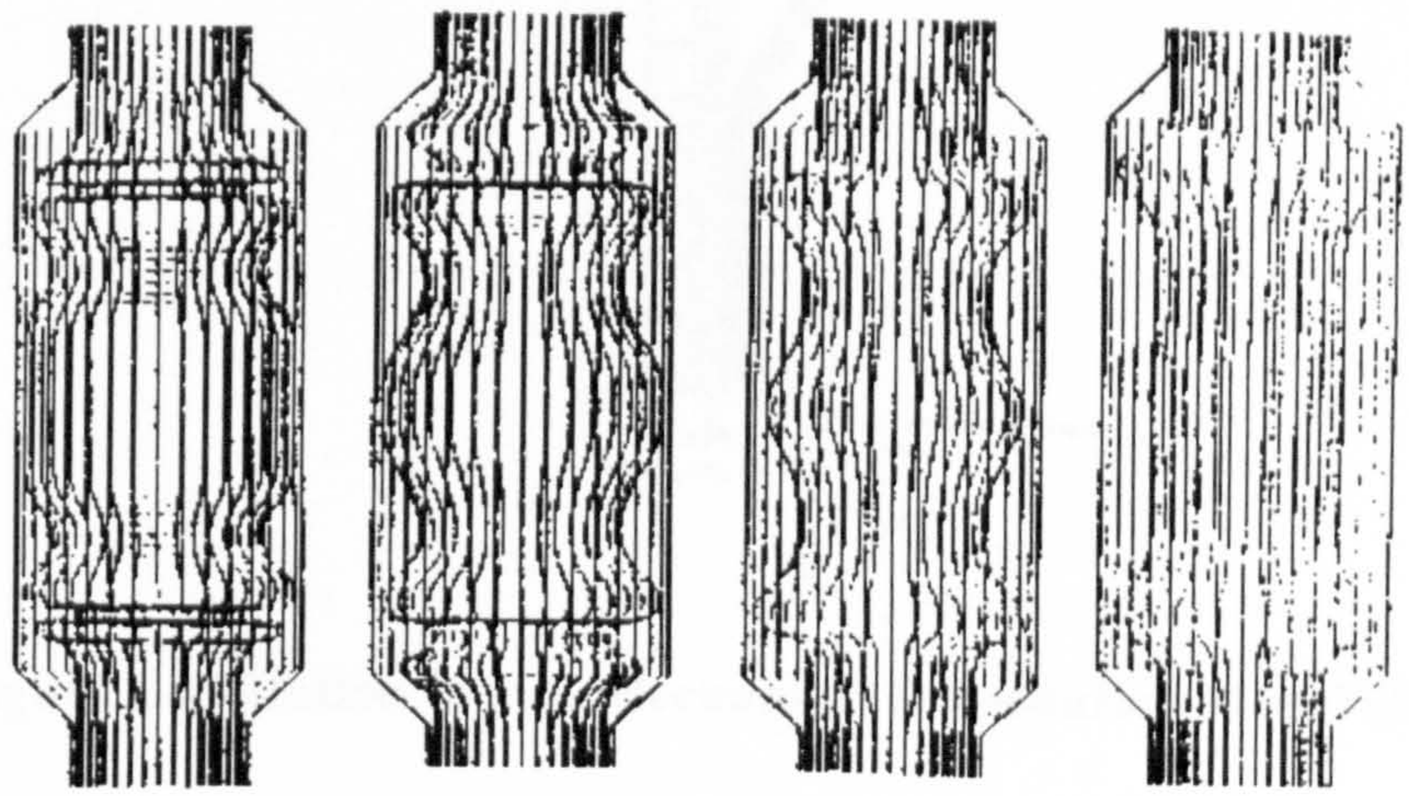

Figure 2-11 Simulation of a IHP Process - Case 2 (Heath, 1993)

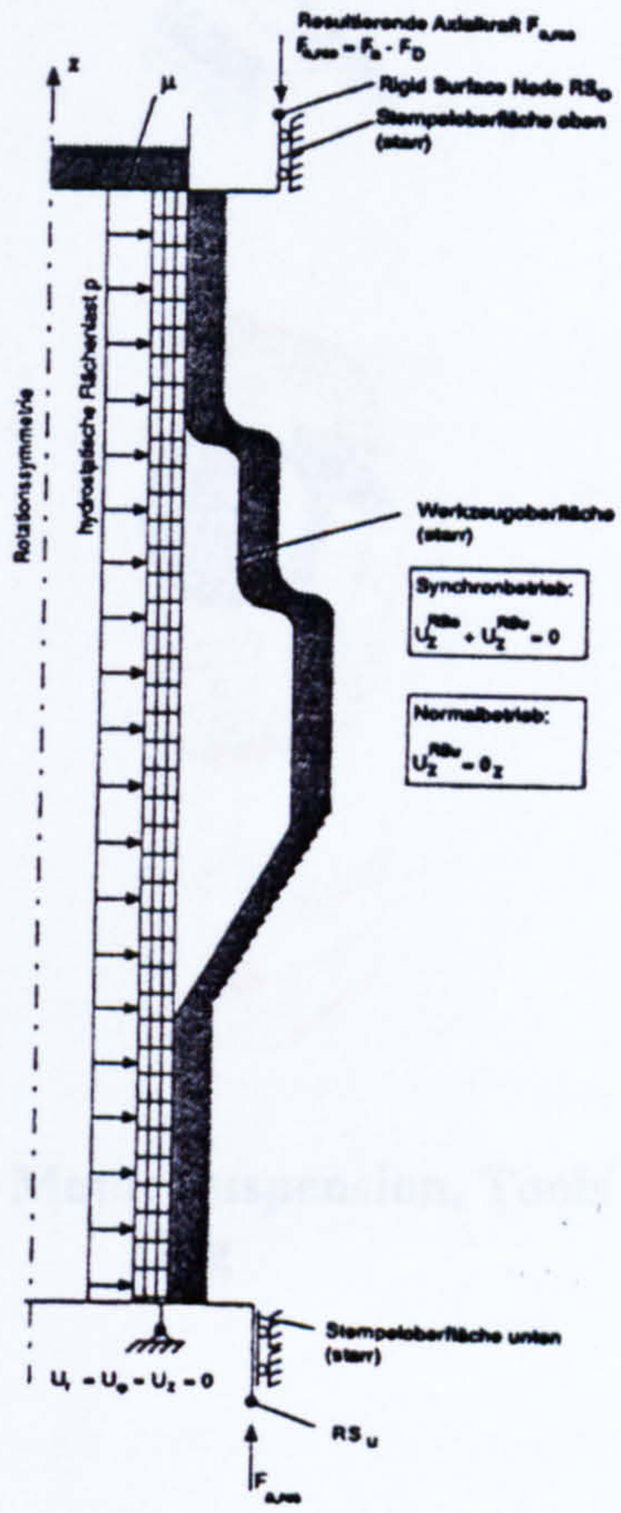

Figure 2-12 Hollow Wave, Mechanical Substitution Model (Böhm)

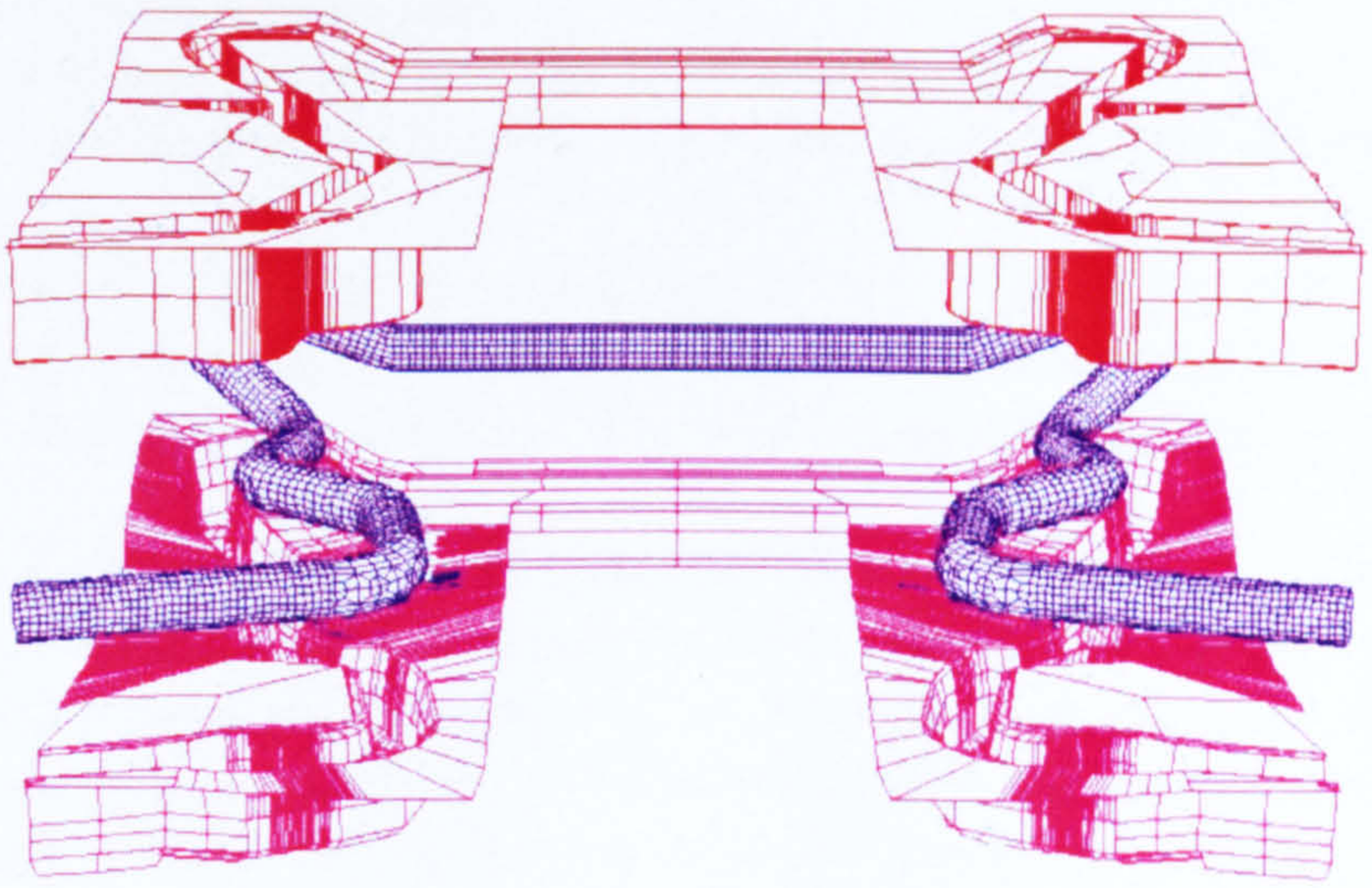

Figure 2-13 Motor Suspension, Tools and Tube

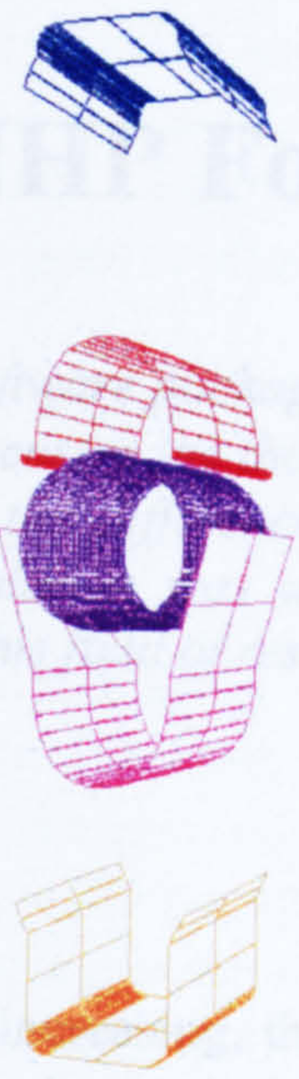

Figure 2-14 Critical Section of the Motor Suspension, Tools for Pre- and Mail Forming

CHAPTER 3

Simulation of the IHP Forming Process

This chapter gives an overview of the FE software packages that can be used for the simulation of the IHP forming processes. It also discusses the theoretical background of such simulation packages This chapter also discusses the difference between the explicit and implicit procedures. Finally it will show why simulation was used as the main approach in this research work, and discuss future trends in this field of research

3 Introduction

As world-wide competition is continuously increasing, there is a need to reduce the product cycle time in the IHP forming process, and further optimise this product development process. As the cost of modifications of the product becomes higher in the later stages of production, it would be beneficial to simulate the production process prior to the actual production of products.

The term "Process Simulation" refers to all methods that are able to estimate the process in advance (**Roll, 1996**). The estimation of these processes enables the economical production of components given a certain specification. The aims of the forming process simulation are :

- **Examine the feasibility of products**
- **Estimate the product properties**
- **Optimisation of the product and the production process**
- **Review whether the process is applicable within the present boundary conditions.**

Different procedures are existing for the simulation of various processes, such as the finite difference, the boundary element method (BEM) and the finite element method (FEM). The FEM is used for the simulation of sheet metal forming, which is in principal, similar to IHP forming.

Originally the FEM procedures were only used in the high technology sectors of industry (military, aircraft and space industries) as they use new materials and new manufacturing technology to satisfy the extreme requirements of their products. Simulation technique were used relatively early with a close connection to basic research in the material science field and experimental process analysis for the development of forming processes of engine components. The structures and methods of the aircraft and space industry cannot be compared with the structures in a medium sized company, but the requirements of the products in terms of quality and high process safety in combination with low material use are similar. Due to the rapid development of computer technology, the FEM procedures are now used in many areas, particularly in the field of the simulation of the behaviour of materials under static load. It has also been demonstrated, several times during the past 30 years, that the calculation of forming

processes is possible with numerical methods.

In future a further reduction of costs can be expected as a result of an improved production performance, hence further use of the simulation technology is expected. The software developed by the author within this project will not only optimise the production process, but will be user friendly and applicable to small, medium and large companies.

Prototyping tools for the IHP forming techniques are relatively expensive in comparison to conventional sheet-metal forming, and hence trial and error method leads to an unsatisfactory large cost and is time consuming. Due to the large experimental expenditure the product development costs for IHP work-pieces are very high, and precise cost estimation therefore is very difficult. The simulation of processes within production engineering ("Digital Prototyping") can help to reduce considerable costs and time. It is extremely important that the simulation is applied in the developmental stage of the product, and particularly advisable if a customisation of the configuration of the production process is still possible. The simulation of IHP processes can be applied to replace the classical prototyping, in order to reduce the product development time by up to 30% (**Figure 3-1**). Further development of the simulation techniques, one of the main tasks of this work, will significantly reduce the production time.

3.1 Why Simulation ?

FEM simulation can only be justified if it proves to be more economical than the trial and error method. This is very important in the case of IHP process due to the high expenditure cost involved, and therefore it is necessary that simulation can reduce the risk of inducing such high cost. The other major benefit in using simulation of IHP processes is the reduction in production the lead time. The use of simulation offers other advantages such as the reduction of practical experiments which often must be executed under production conditions. Problems with the forming process are noticed in an early stage of the development and therefor time and cost-consuming failure trials need to be avoided. The FE simulations make it possible to predict the properties of a new product which will be manufactured with the IHP techniques, and information about features such as the wall-thickness, hardening and outer shape can be estimated. Moreover the interior pressure necessary for the forming process and thus the closing forces are calculated. The FEM simulations ensure that the part can be produced reliably with the IHP technique and with the optimisation of the process parameters a higher product quality and process safety can be reached.

Fundamentally it can be said, that the simulation can be efficiently used for a fast change in the variation of all geometric parameters, but, if a **tool** is in **existence** the investigation of different materials is quicker and possibly cheaper on an IHP machine. The real process time on an IHP press is about 10 to 40 seconds, the time needed to calculate a simulation is between 2 hours and a few days.

3.2 Software Systems used for the Simulation of Forming Processes

During the last twenty years a number of experiments in the field of sheet metal forming have been carried out using different approaches. There are approximately 60 software packages presently on the market which are suitable for the simulation of forming processes, about 20 of these packages are commercially available. A summary of the most currently used packages relating to simulation of forming processes at the moment is presented in **Table 3-1.** Two of the listed packages (DEFORM, FORGE2/3) are especially developed for the simulation of solid forming processes, the other programs can be used for the simulation of sheet metal forming processes. At the moment within this section of the simulation of the forming processes there are implicit and explicit procedures which are competing intensively with each other.

Name	Producer, Country	Case	Application
ABAQUS	HKS,USA	Implicit	General
ANSYS	ANSYS, USA	Implicit	General
MARC	MARC,USA	Implicit	General
NIKE3D	LSTC,USA	Implicit	General
LARSTRAN	LASSO, Germany	Implicit	General
EPDAN	IFU STGT, Germany	Implicit	solid, sheet metal forming
INDEED	INPRO, Germany	Implicit	sheet metal forming
MARC	MSC, USA	Explicit	crash, solid, sheet metal
ROBUST	Prof. Nakamachi,J	Explicit, static	sheet metal forming
ANSYS/LS-DYNA	ANSYS, LSTC, USA	Explicit, dynamic	crash, solid, sheet metal
LS-DYNA	LSTC,USA	Explicit, dynamic	crash, solid, sheet metal
PAM-STAMP	ESI, France	Explicit, dynamic	crash, solid, sheet metal
OPTRIS	Dynamic Software, France	Explicit, dynamic	sheet metal forming
ABAQUS-explicit	HKS,USA	Explicit, dynamic	crash, solid, sheet metal
PSU	project-group, D/CH	Explicit, implicit	solid, sheet metal
UFO-3D	IABG, Germany	Explicit, dynamic	sheet metal forming
DETRAN	VW-Gedas, Germany	Spec. Formulation	sheet metal forming
AUTOFORM	AUTOFORM,CH	Spec. Formulation	sheet metal forming
IFU-ZH	IFU ZH, CH	Spec. Formulation	sheet metal forming
DEFORM	Batelle, USA, Germany	Stiff-viscoplastic	solid, forging
FORGE2/3	CEMEF, France	Stiff-viscoplastic	forging
ICEM-STAMP	CDC, Germany	Inverse procedures	sheet metal forming
SIMEX	SIMTECH, France	Inverse procedures	sheet metal forming
QWIKSIMM	H.G. Engineering, Canada	Inverse procedures	sheet metal forming
PreForm	ETHZ, CH	Inverse procedures	Hydroforming
FastForm3D	FTI, USA	Inverse procedures	sheet metal forming
ISO-PUNCHII	SOLLAC, France	Inverse procedures	sheet metal forming

Table 3-1 Programs for the Simulation of Forming Processes

The simulation programs can be divided into 4 groups .

- **Implicit procedures**

  Implicit time integration means a linear acceleration approach between two time steps. This procedure solves the equation at the time $t + \Delta t$. Normally as an iteration- procedure the Newton (Raphson)-method is used. The implicit methods lead to a non-linear structural equation system which have to be solved for each iteration. The matrix can become very large, so that the calculation-time for the structuring and analysing of the matrix dominate the simulation. The procedure converges if a determined criterion is reached. The implicit integration scheme can be made unconditionally stable. Thus, the time step can be chosen based on the desired time resolution only.

- **Explicit procedures**

  Explicit time integration means a linear displacement course between two time steps. Explicit time integration is, for some specific problems, the most efficient possibility to integrate the time variable in conjunction with spatial finite element discretizations of time dependent problems in structural mechanics. In particular highly non-linear problems arising in thin sheet metal forming such as large strain, contact, friction and multi-stage forming can be easily handled.

- **Inverse procedures**

  In contrast to the „Forward Simulation“ of explicit and implicit FE-systems, the inverse procedure uses a method called „Backward Simulation“. The „Backward Simulation“ uses the approach which starts from the final part shape and iterates back to the flat blank which has no stress and strain. The set-up and compute time required to run an inverse simulation test is very short compared to the „Forward Simulation“ method. The disadvantage of the inverse procedure is the lower accuracy of the results. Inverse procedures are good to get a fast overview about the process.

- **Special programs**

  There are a few programs available in the market which are made only for special applications like deep-drawing or forging. Programs with special formulation can be suitable to get a short overview of the process. The main disadvantage is that they support only very small specialised areas.

Explicit programs are applied to fast events and to calculate processes which are extremely non-linear (contact, large displacements, etc...). Explicit programs are also advantageous for virtually static events like metal forming.

In some instances both methods, implicit and explicit, are possible. Interior high pressure forming can be simulated using either implicit or explicit procedures. For the inverse procedures, the first applications with the programs ICEM-STAMP (**Doege et al. 1986**), AutoForm and PreForm (**Hora, 1998**) and FastForm3D (**Stelzmann, Stamm** and **Stühmeyer, 1999**) are known.

The application of the programs for the simulation of interior high pressure forming processes is even simpler in comparison with other forming processes, because only the tool is specified, the work-piece with the exception of the calibration procedure, is always a tube. This causes the expenditure cost of work required for the modelling to be reduced considerably. In many cases it can be seen that the model setting-up is the most time-consuming part of the simulation in the order of events for a simulation (model setting-up, calculation, evaluation).

The pressure characteristic for the forming process is usually defined as pressure against time function. During stability problems this description of the inside pressure can lead to problems, because in the case of failure the structure itself fails suddenly. In reality the interior pressure decreases, this effect is not included with a pressure vs. time control for the interior pressure, hence calculations become numerically unstable, and therefore the simulation predicts a failure which doesn't appear in reality. For a realistic simulation of the interior high pressure forming it is necessary to have a program option to define the pressure as a volume stream vs. time function of the pump instead of a pressure vs. time function, and therefore it would be possible to calculate the process correctly in the case of failure. The option of the pressure control is not included in all programs listed in the **Table 3-1**. After **Roll (1996)** the programs INDEED, LS-DYNA and PAM-STAMP provided such an option. Due to the reduction of computing time and to reduce the expenditure for the simulation this option is often not used.

The packages mentioned above offer the possibility to import CAD surfaces (IGES, VDA) and use it as rigid body for the tools. The advantage of using the CAD surfaces is that no FE mesh is necessary and the geometry of the tools is not falsified through the mesh. **Figure 3-2** shows the typical process chain for a IHP simulation.

3.3 Special Features of a FE Simulation

With FEM simulations it is possible to judge the influence of different parameters on the whole IHP process. The simulation works with transparent tools **(Figure 3-3)**, as it is possible to blank the tools out and have a look at the tube or sheet during the process. It is also possible to simulate with parameter-values which are not possible in reality, for example with a friction coefficient of 0.

3.4 Theoretical Background

The partial differential equations describing the mechanics of an IHP forming process are solved numerically by the finite element method (FEM). The choice of the time integration of semidiscretized finite element system has been discussed previously since the simulation of forming problem started. The first attempts were done with implicit time integration techniques (**Wilhelm et al., 1989**). However, solving more complex problems, convergence difficulties were encountered and the simulation failed. The use of the explicit method has proven to be both, efficient and robust, so today the explicit time integration is totally dominating the industrial application of sheet metal forming simulations.

Due to the relative slight complexity of the IHP process the theoretical process design can be based on the membrane or shell theory, and accurate results are obtained with the use of such theory because the bending effects are not neglected.

This chapter discusses the numerical aspects of the solution of sheet metal forming problems i.e. interior high pressure forming using the finite element method, and, as already said, implicit and explicit procedures compete intensely together (**Bathe 1990, Schweizerhof, Weimar, Hallquist** and **Stillman, 1991**). Implicit and explicit time integration will be distinguished in specialised literature with the matrix representation as follows:

If the equation of motion is solved for the unknown state $(t + \Delta t)$ the procedure is called implicit.

If the equation of motion is solved for known state t the procedure is called explicit.

FE program systems must fulfil the following requirements (**Bauer, 1999**):

- Consideration of geometric non-linearity (large strains)
- Multiple material laws for accurate representation of the material behaviour
- Accurate and fast contact algorithms
- Efficient elements
- Formulation of different friction laws
- Introduction of deformation dependent loads
- Fast algorithms for the solution of non-linear equations

The equation of motion, in general can be written as :

$$M \cdot \ddot{u} + C \cdot \dot{u} + R(u) = F(t) \qquad (3.1)$$

where *M* is the mass matrix; *C* the damping matrix; $\ddot{u}$, $\dot{u}$, u the acceleration, velocity and displacement vectors at the nodes of the FE mesh, respectively *R* is the vector of the internal forces, including the contact forces; *F* is the vector of the exterior time-dependent forces.

The solution can be done with an explicit or implicit time –integration scheme.

3.4.1 Explicit Time Integration

In recent times a procedure called **EXPLICIT** has become significant in the area of sheet metal forming. Explicit procedures solve the equation at the time t and needs no iterations. This procedure treats the forming process as a dynamic event and not like implicit procedures as a static problem. For the integration of the movement equation a central difference scheme is used. Explicit methods need no iteration and no tangential stiffness matrix, but they need, in contrast to implicit methods, for reasons of stability, a restriction of the time step. The time step size depends on the natural frequency of the system. For the simulation of a real forming process the velocities are of a range of 1 m/s. Therefore 10^5 to 10^6 time steps are necessary. The calculation time needed for such a simulation are unacceptably high and they are well over the calculation time needed for an implicit simulation. The problem is solved when the process is running faster than in reality. However it is necessary to suppress unwanted mass effects with appropriate measures, e.g. damping. Different publications show that it is allowable to increase the speed up to a factor of 10 without influencing the results. For forming problems the material properties often dependent on the velocity. In this case the velocity may not be changed. An alternative is to change the density whilst keeping the velocity constant, a reduction of the density reduces the sound velocity and allows greater time steps and reduces for this reason the calculation time. A increase of the density of 100 reduces the sound velocity around the factor 10 and allows a 10 times faster calculation. With this adjustment it is possible to simulate forming processes with acceptable calculation times.

For the explicit time integration a linear displacement course is assumed between the time steps.

Figure 3-4 shows the differences between the real and the linear displacement course. The displacements at the time $t + \Delta t$ are requested.

The solution for the time $t + \Delta t$ is based on the balance condition at the time t.

The mechanical equation of motion is the starting point :

$$v(t) = \frac{s}{t} \text{ and } a(t) = \frac{2 \cdot s}{t^2} \qquad (3.2)$$

According to the mechanical equations of motion s shall be u now.
The time t extends over the time period $2\Delta t$.

$$\dot{u} = \frac{1}{2\Delta t}(-u_{t-\Delta t} + u_{t+\Delta t}) \tag{3.3}$$

$$\ddot{u} = \frac{2 \cdot u}{t^2} = \frac{2 \cdot u}{2\Delta t^2} \tag{3.4}$$

$$\ddot{u} = \frac{1}{\Delta t^2} \cdot ((u_{t-\Delta t} - u_t) + (u_{t+\Delta t} - u_t)) \tag{3.5}$$

$$\ddot{u} = \frac{1}{\Delta t^2} \cdot (u_{t-\Delta t} - 2u_t + u_{t+\Delta t}) \tag{3.6}$$

From this attempt of the dynamic calculation comes the following equation:

equation of motion :

$$M \cdot \ddot{u} + C \cdot \dot{u} + K \cdot u = P(t) \tag{3.7}$$

M = mass matrix
C = damping matrix
K = stiffness matrix
u = displacement vector
P = load vector

Substituting the two equations 3.3 and 3.6 in 3.7 we obtain the following system of equations:

$$\frac{M}{\Delta t^2} \cdot (u_{t-\Delta t} - 2u_t + u_{t+\Delta t}) + \frac{C}{2\Delta t} \cdot (u_{t+\Delta t} - u_{t-\Delta t}) + K \cdot u_t = P(t) \tag{3.8}$$

with the solution

$$\frac{M}{\Delta t^2} \cdot u_{t-\Delta t} - \frac{2M}{\Delta t^2} \cdot u_t + \frac{2M}{\Delta t^2} \cdot u_{t+\Delta t} + \frac{C}{2\Delta t} \cdot u_{t+\Delta t} - \frac{C}{2\Delta t} \cdot u_{t-\Delta t} + K \cdot u_t = P(t) \tag{3.9}$$

Switched over after the requested displacement at the time $t + \Delta t$:

$$\left(\frac{M}{\Delta t^2} + \frac{C}{2\Delta t}\right) \cdot u_{t+\Delta t} = p(t) + \left(\frac{2M}{\Delta t^2 - K}\right) \cdot u_t + \left(\frac{C}{2\Delta t} - \frac{M}{\Delta t^2}\right) \cdot u_{t-\Delta t} \tag{3.10}$$

Regarding the calculation time, the demand for computer storage capacity and the robustness of the procedure it can be noticed that the explicit procedure is applicable for quasi-static analysis. The calculation time and the memory required, for fine meshes with a lot of elements, are reasonable.

Attention must be given to the model errors referring to the contact description and to coarse meshes. Beside this it must be checked that the time-scaling of the load-velocities and that the kinetic energies of the masses are not extremely large.

3.4.2 Implicit Time Integration

The solution of implicit problems is only accurate and effective if the idealization at the set up and solution of the gradient matrix (M, C, K) are fulfilled sufficiently. The gradient matrix (*M,C,K*) of implicit programs describes the communication between all discretisation points of the structure. Then it is possible to determine the response of the system with a single solving of the differential equation. Therefor implicit proceedings are suitable for linear static and dynamic problems. The system matrices are then known for the time step $t + \Delta t$ and the solution can be reached with the solution of the linear equation system. Implicit proceedings solve the balance at the time $t + \Delta t$. For the implicit time integration a linear acceleration course is accepted between the time steps.

$$M \cdot \ddot{u} + C \cdot \dot{u} + K \cdot u = P(t) \tag{3.11}$$

Attempt function for the implicit time integration: linear acceleration course

$$\ddot{u}_{t+\Delta t} = \frac{4}{\Delta t^2}(u_{t+\Delta t} - u_t) - \frac{4}{\Delta t}\dot{u}_t - \ddot{u}_t \tag{3.12}$$

$$\dot{u}_{t+\Delta t} = \dot{u}_t + \frac{\Delta t}{2}\ddot{u}_t + \frac{\Delta t}{2}\ddot{u}_{t+\Delta t} \tag{3.13}$$

Balance at the time t

$$\left(\frac{4}{\Delta t^2}M + \frac{2}{\Delta t}C + K\right)u_{t+\Delta t} = P_{t+\Delta t} + M\left(\frac{4}{\Delta t^2}\dot{u}_t + \ddot{u}_t\right) + C\left(\frac{2}{\Delta t}u_t + \dot{u}_t\right) \tag{3.14}$$

3.4.3 Time Step Size and Calculation Time

Another difference between the implicit and explicit time integration is the time step size Δt. For implicit procedures the time step can be taken as any quantity and is controlled by the user.

For the explicit time integration schemes the time step must be lower then a determined value. The reason is an instability of the system toward natural frequency.

From the basics of physics the following equation is known :

$$c = \frac{\lambda}{t} \tag{3.15}$$

c = speed of the wave
λ = wave length
t = duration of the period

With this formula it is possible to estimate the critical time step size Δt.The critical wave length is the shortest distance between two particles, or two nodes in this case.

$$\Delta t_c = \frac{l}{c} \tag{3.16}$$

c = speed of the wave
l = shortest distance between two nodes
Δt_c = shortest time step

So the time step is limited by the conditions above.

Speed of the wave for Steel :

$$c = \sqrt{\frac{E \cdot (1-\nu)}{(1+\nu) \cdot (1-2\nu) \cdot \delta}} \tag{3.17}$$

c = speed of the wave
E = young's modulus
γ = Poisson's ratio
δ = density

Shortest distance between two nodes (square shell element is shown in **Figure 3-5**).

The calculation time results from the shortest distance between two nodes of one element. A shorter element length reduces the calculation time.

From the equations 3-15 and 3-16 we can obtain the following connection :

$$c = \sqrt{\frac{1}{\delta} \cdot F} \qquad \textbf{(3.18)}$$

F= factor from young's modulus and Poisson's ratio

Equation 3-17 in 3-15 (F=const.)

$$dt = \frac{l}{c} = \frac{l}{\sqrt{\frac{1}{\delta}}} = \frac{l\sqrt{\delta}}{\sqrt{1}} \qquad \Delta(t \approx \sqrt{\delta}) \qquad \textbf{(3.19)}$$

The time step Δt corresponds directly to the density δ.

The increase of the density increases the time step and thus also the calculation time. **Figure 3-6** shows the relation between density and calculation time.

For the simulation of forming processes with the explicit method it is usual to scale the density with the factor 100 to 1000. Different publications demonstrate that mass scaling is allowed, and the results are almost identical (**Schweitzerhof (1999), Lang (1992), Brännberg (1994)**).

3.4.4 Comparison between Explicit and Implicit Methods

Based on the higher efficiency of implicit methods for problems with longer duration and rather low velocity loading, it is recommended that such methods should be used to obtain solutions for static or quasi-static problems.

Explicit finite element methods have been extensively used for problems involving high velocity and short duration loading, for example crash simulation. In these problems the high frequency response demands a high resolution time, and the solution does not suffer from the stability restriction $\Delta t \leq \Delta t_{krit}$. In contrast to high velocity transient problems, the solution of quasi-dynamic problems, like interior high pressure forming, suffers from the short stable time step and can take a considerable amount of time if solved without special measures.

Implicit finite element methods are effective for the calculation of springback and residual stress. It is possible to calculate these quantities, but the movement of the tools must be considered. This means that it is necessary to allow the calculation to run as long as the workpiece is at rest, i.e. dynamic effects have decreased to nothing. The calculation time needed is therefore very high, normally the same time needed for the simulation of the expansion is needed for the springback calculation. Implicit methods don't have this problem, because they have no dynamic dependence.

Some important differences between explicit and implicit time integration schemes as used in interior high pressure forming applications are listed below.

Features of the explicit time integration :

- Stability at the time t_n
- Only limited stablility, time step must remain below a required value
- Required time step orientates itself to high natural frequency
- Calculate a lot of time steps (< 100.000 at real applications)
- Single time steps very fast
- No large equation system build (storage) and solve (calculation time)
- No convergence problems
- Calculation time grows squarely

Features of the implicit time integration :

- Balance at the time t_{n+1}
- Absolutely stable, time step size arbitrary
- Time step so, that interesting natural frequency is contained
- Fewer, larger time steps
- Computation time per time step high
- Solution of a large equation system required
- Solve non-linearity in the time step using iteration, convergence not always guaranteed
- calculation time grows linearly

However, in real practical simulations the situation is rather different, both computational efficiency and the amount of data storage needed for the computation are dependent on the problem size. For a typical application of interior high pressure forming, where the finite elements are mostly shell elements, the solution time increases as the third power of the resolution of shell elements for the explicit method and as the fifth power of the shell element resolution for the implicit method. The data storage needed for the explicit solution increases as the second power for the explicit method and as the fifth power for the implicit method. Thus, for real industrial processes, the explicit method is more efficient and handles the very large models better. For the size of the models today, with a very high mesh resolution, it seems to be unacceptable to use implicit algorithms due to the limited computer resources and the limitations of current equation solvers; possibly this will change in the future with faster computers and further developed solvers. The explicit and implicit methods are compared in **Table 3-2**, where n represents the element resolution in each topological direction.

	Storage requirements	CPU requirements
Element type	2D	3D
Implicit	n^5	n^7
Explicit	n^2	n^3

Table 3-2 Cost Comparison between Explicit and Implicit Methods (Brännberg)

3.5 Conclusion and Outlook

The simulation of IHP forming processes can be successfully done with the help of the FE method. The critical areas can be discovered, failure can be predicted and the properties of the final product can be determined. The problem of the FE simulation is the considerable amount of solution time required. Today the development of IHP products runs in two parallel ways – one way is the simulation of the forming process and parallel to that the construction and manufacturing of the tools. This means that the problems for the production of the part are carried out with the simulation, but at a moment when the tool is already finished. What we need for the future will be tools for a very fast global simulation of the process, to get a coarse overview about the process to work out the critical areas. What we further need will be faster computer processors, a development of the parallel processor techniques and optimisation of the algorithms in the FE systems. The way for the future seems to be to use a fast one-step solver to get a coarse overview of the process and afterwards to use a combined implicit/explicit code to optimise the critical areas determined from the previous one-step analysis (see **Figure 3-7**). Developments in this direction will be done at the Swiss Federal Institute of Technology (ETHZ) from **Reissner** and **Hora**. At the ETHZ a few tools for IHP simulation are under development. IHU-Plan for the layout of the process, e.g. the set-up of the bending line. A one-step solver named PreForm gives a fast and coarse overview about the pre-form and hydro-forming operation. For the simulation of the critical areas the tool ExForm can be used.

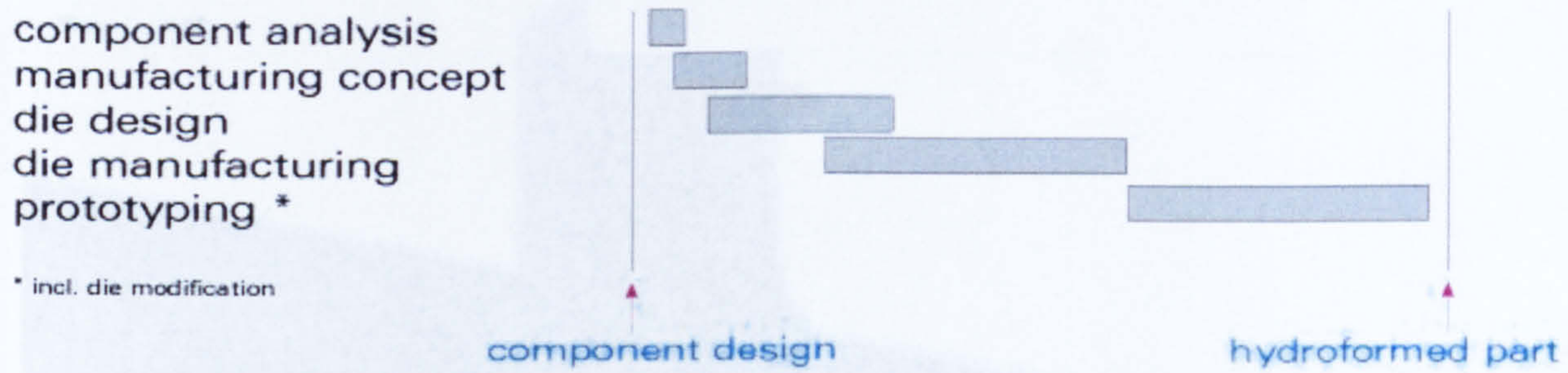

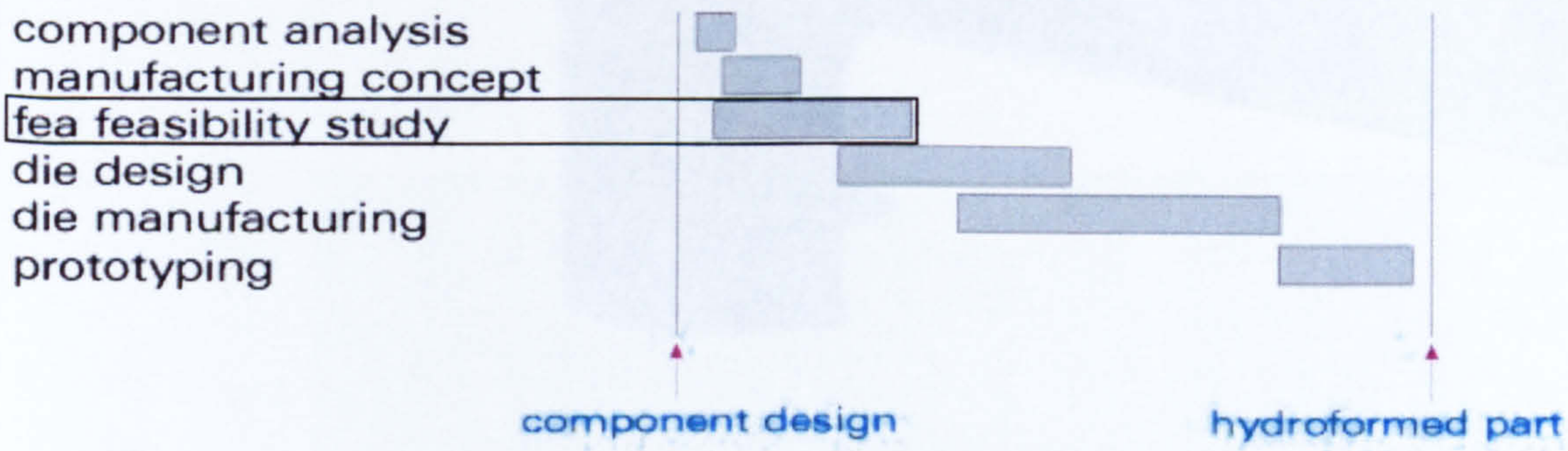

Figure 3-1 Product Development Time, without/with FEA

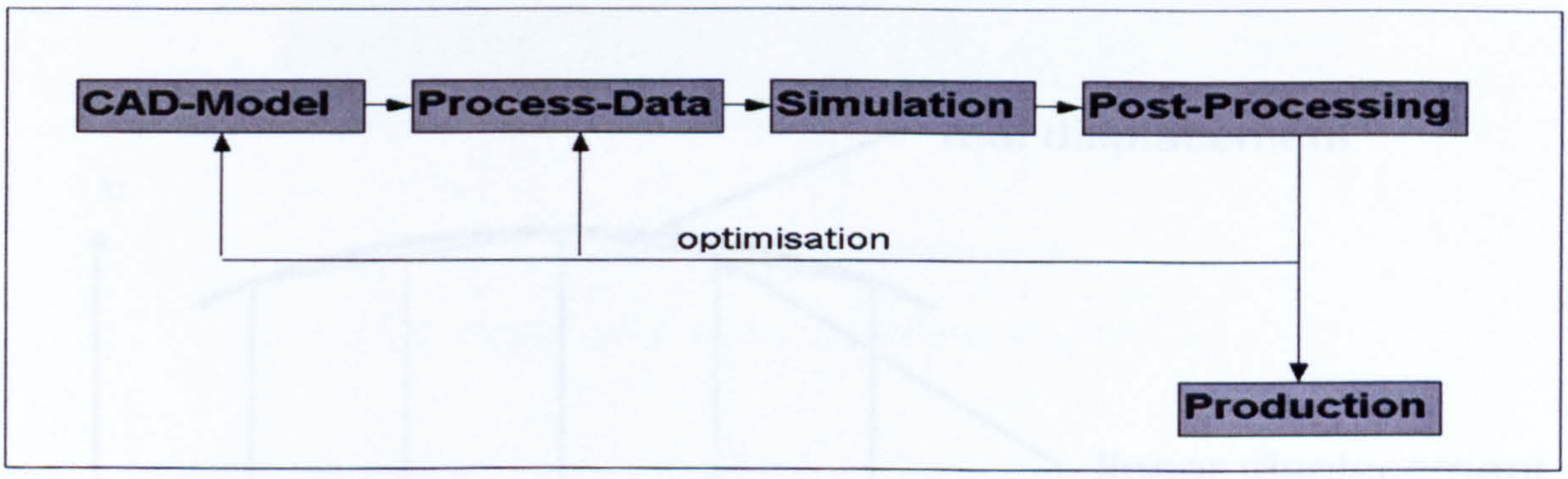

Figure 3-2 Process Chain for the IHP Forming Simulation

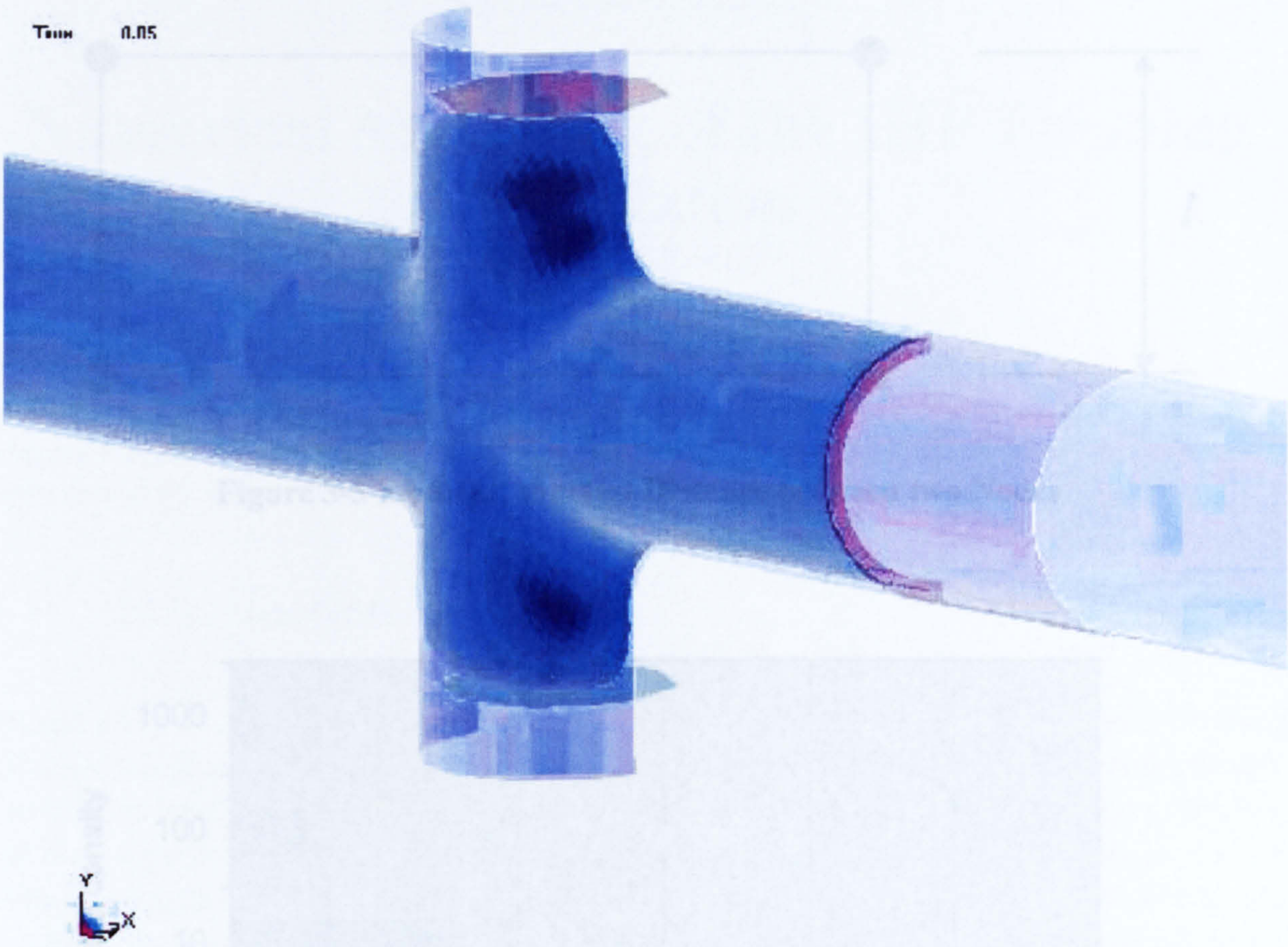

Figure 3-3 Transparent Tools

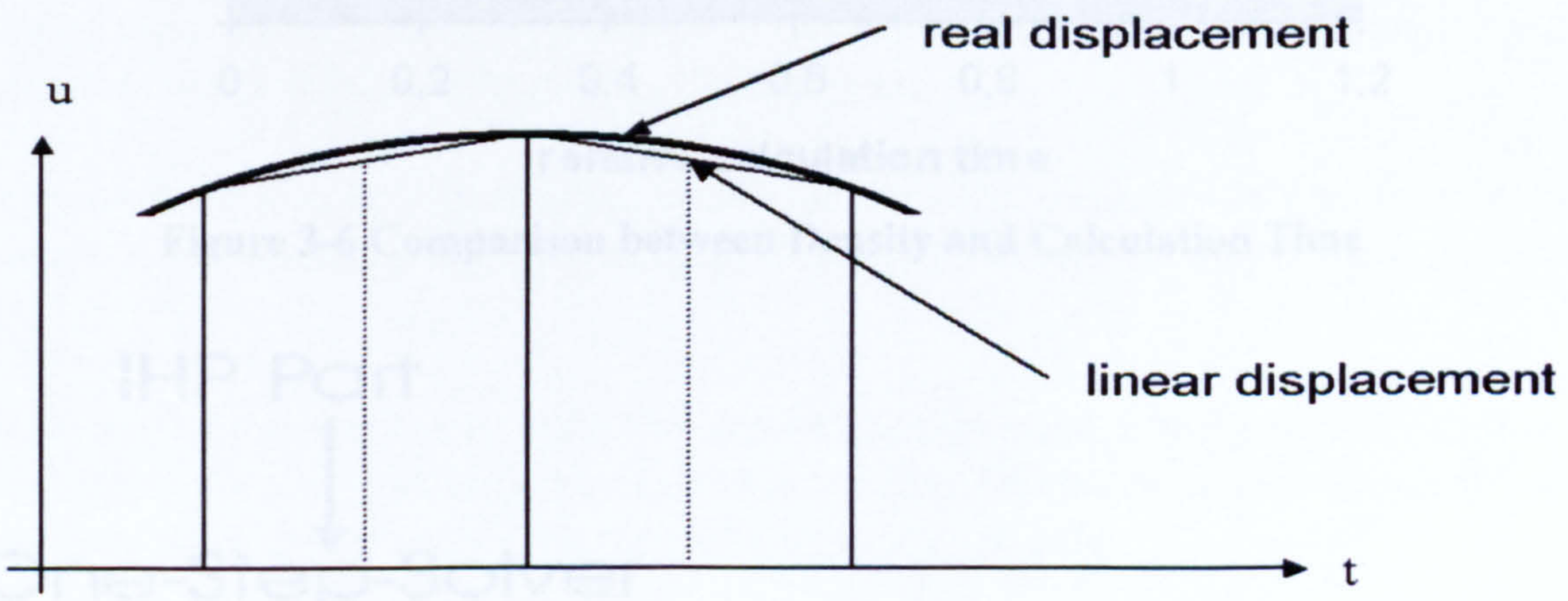

Figure 3-4 Representation of the Linear Displacement Course

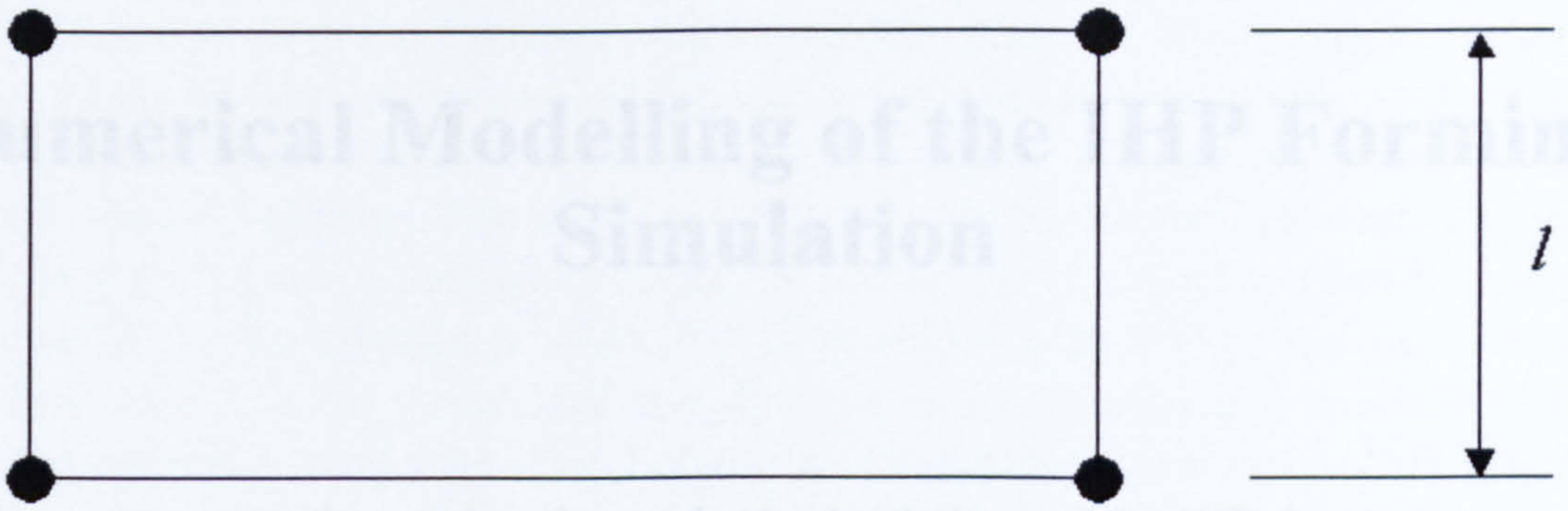

Figure 3-5 Element, shortest Distance between two Nodes

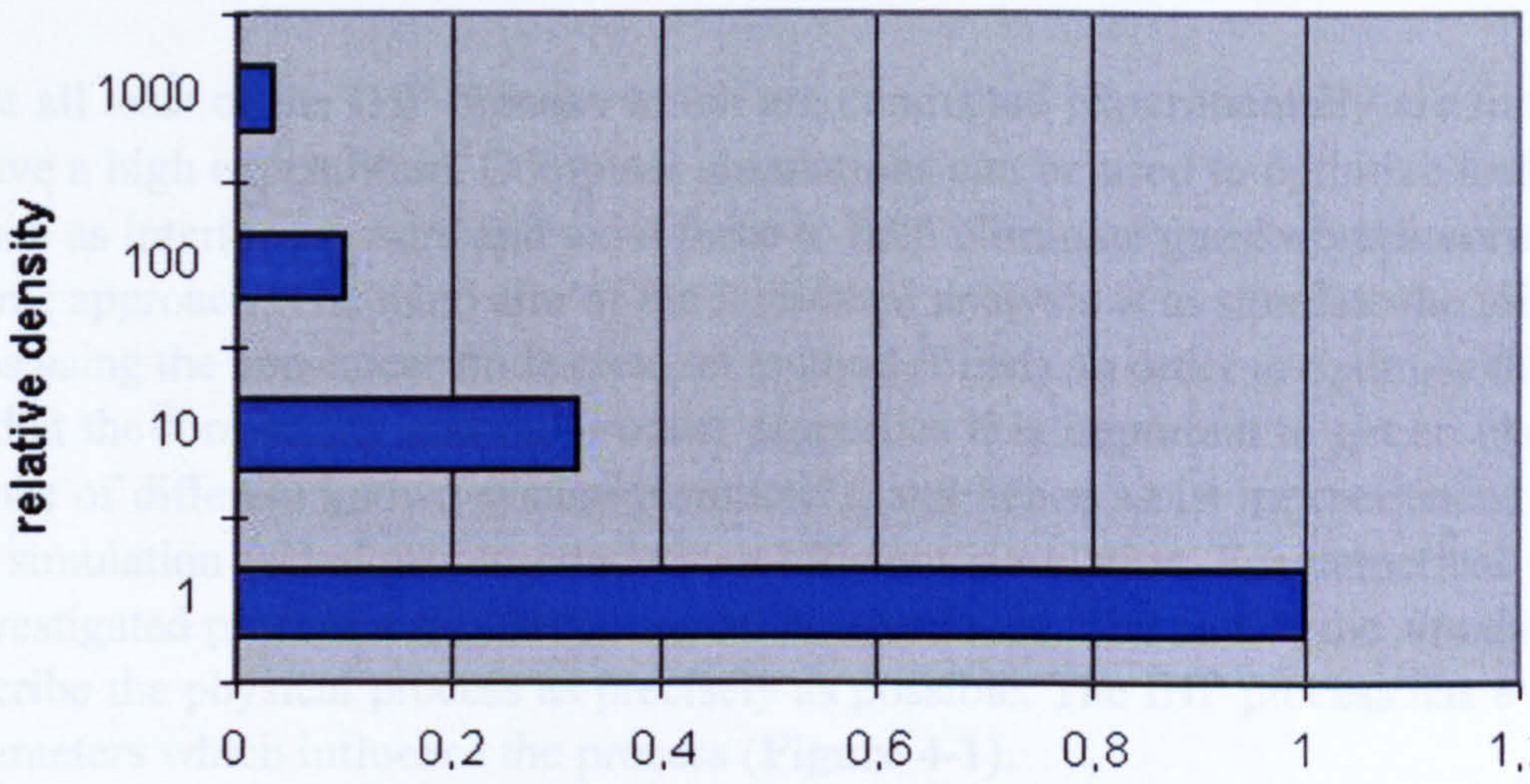

Figure 3-6 Comparison between Density and Calculation Time

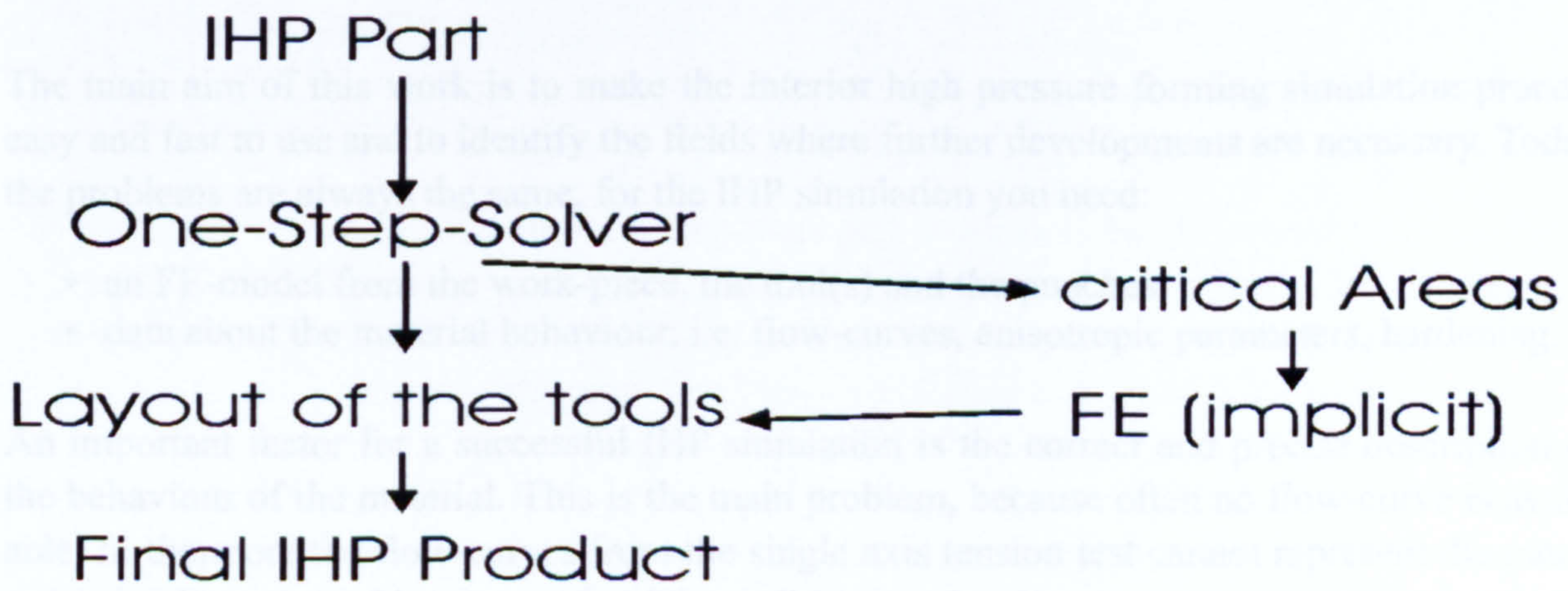

Figure 3-7 Simulation of IHP Parts – Process Chain

CHAPTER 4

Numerical Modelling of the IHP Forming Simulation

This chapter presents the results of some basic simulations of the IHP forming process. The general material behaviour theory is discussed. The influence of the friction on the forming process and the effects developed by using thick tubes are also investigated.

4 Introduction

Almost all tests of the IHP-process which are conducted experimentally are time consuming and have a high expenditure. Computer simulations can be used to optimize forming parameters such as interior pressure and axial force to help eliminate guesswork involved in the trial and error approach. The main aim of the numerical analysis is to simulate the total production process using the non-linear finite element method (FEM). In order to optimise the process and to predict the formability and the product properties it is important to get an overview of the influence of different known system parameters, and hence assist inexperienced or new users of the simulation techniques to conduct an efficient simulation. For numerical simulation of the investigated process a simulation model is introduced. The aim of the simulation model is to describe the physical process as precisely as possible. The IHP process has a large number of parameters which influence the process (**Figure 4-1**).

Human factors are also important to the simulation, which depends on the qualifications and experience of the simulation engineer, who must create the simulation model and interpret the results.

The main aim of this work is to make the interior high pressure forming simulation process easy and fast to use and to identify the fields where further developments are necessary. Today the problems are always the same, for the IHP simulation you need:

- an FE-model from the work-piece, the tool(s) and the punches
- data about the material behaviour, i.e. flow-curves, anisotropic parameters, hardening.

An important factor for a successful IHP simulation is the correct and precise description of the behaviour of the material. This is the main problem, because often no flow-curve is available, furthermore the flow-curves from the single axis tension test cannot represent the material behaviour under bi-axis or tri-axial conditions and only represents a restricted material behaviour.

The input for the IHP simulation (i.e. the LS-DYNA input deck) consists of the FE-Model (workpiece, tool(s), punch(s), counterholder(s)), non-linear material properties, load-curves, contact definitions, control information and if necessary dampers. If it is possible to use shell elements for the simulation process the FE-model can be created with a surface/solid modeller. Program such as Pro/ENGINEER or CATIA, which include efficient pre-processors for the commonly used FE systems. For rigid tools, it is possible to use shell elements in nearly all cases. Generally the use of shell elements for the work-piece causes no problems, because it is a thin tube. If the work-pieces consists of a thick walled tube than it may be necessary to design them with 3D solid (brick) elements. In this case FE-systems such as ANSYS or PAT-RAN must be used to create the mesh because unfortunately there is not a CAD system that has the functionality to mesh a solid geometry with brick elements. Non-linear analysis requires brick elements because the tetrahedron elements available today cannot satisfy the demands of accuracy and efficiency. Future developments can possibly remedy this disadvantage, on the other hand new efficient automatic brick element mesh generation tools integrated into CAD systems might be developed.

The loads for interior pressure and axial force are defined with load-curves (**Figure 4-2**). A load-curve describes the course of the load (force, displacement, pressure) over time. Successful IHP forming is dependent upon remaining within a narrow process window defined by the correct combination of interior pressure and axial force at the ends of the tube. Excessive pressure without sufficient axial force will cause bursting of the tube, excessive axial force without appropriate pressure will lead to buckling of the tube. With the information about the model geometry (wall thickness, diameter...) and the material properties it is possible to create the load-curves for interior pressure and axial forging.

4.1 Material

The material behaviour can be described with different models :

- Rigid/plastic
- Rigid/visco-plastic
- Elastic-plastic
- Visco-elastic-plastic

The rigid/plastic material law neglects the elastic part of the deformation which is insignificant in comparison to the plastic part of deformation of the forming processes. For this material model only the rigid plastic behaviour exists. Rigid/plastic material models are used for the simulation of solid forming processes like forging and cold extruding. This material model is not suitable for the simulation of IHP processes. For the simulation of the IHP process it is necessary to know the elastic-plastic material behaviour. The plastic behaviour of the material is also important for the material flow during the forming process; the elastic behaviour is crucial for the springback after the forming operation. Furthermore it is necessary to know the material behaviour for the prediction of failure. The basic information about material behaviour is obtained by tension and compression tests, **Figure 4-3** shows a typical tensile test bar.

Using flow-curves, i.e. the relation between stress and strain (**Figure 4-4**), the material behaviour under load are thus obtained. The principal structure of such elastic-plastic material model formulation can be subdivided into:

- A flow-criteria which describes a flow area; this identifies the pure elastic from elastic-plastic conditions
- A flow-rule, which describes the behaviour in the case of plastic flow
- An elastic component rule, which represents the elastic material behaviour

The visco-rigid-plastic and visco-elastic-plastic material law take the viscose part of the material behaviour into consideration. This means that the flow stress is not only dependent on the equivalent degree of deformation but also on the equivalent strain deformation rate. This model is not, or only partly, implemented into the software packages available today. The users of IHP techniques are also considering the introduction of heat into the hydroforming process; the simulation of such process the visco-elastic-plastic material laws are absolutely necessary.

4.1.1 Mathematical Background of the Material behaviour

Metallic materials may be shaped by applying external forces to them without reducing their structural cohesion. This property is known as the formability of metal. Deformation or flow occurs when the rows of atoms within the individual crystalline grains are able, when stressed beyond a certain limit, to slide against one another and cohesion between the rows of atoms takes place at the following atomic lattice. This sliding occurs along planes and directions determined by the crystalline structure and is only made possible by, for example, dislocations (faults in the arrangement of the atomic lattice). Other flow mechanisms such as twin crystal formation, in which a permanent deformation is caused by a rotation of the lattice from one position to another, only play a minor role in metal forming technology.

During the forming process the volume of the body stays theoretically constant.

The volume (V) of a rectangular body with the starting dimensions h_0, b_0 and l_0 will be compressed to the final dimensions h_1, b_1 and l_1 (**Figure 4-5**) is :

$$V = h_0 \cdot b_0 \cdot l_0 = h_1 \cdot b_1 \cdot l_1 = \text{constant} \qquad \textbf{(4.1)}$$

The plastic material behaviour, i.e. the growth of the non-reversible deformation, can be characterised by different values including :

- **Nominal Strain** (relative deformation, usually in %)

$$\varepsilon_h = \left|\frac{h_1 - h_0}{h_0}\right|; \quad \varepsilon_b = \left|\frac{b_1 - b_0}{b_0}\right|; \quad \varepsilon_l = \left|\frac{l_1 - l_0}{l_0}\right| \tag{4.2}$$

- **True Strain** (Actual deformation, also called logarithmic or true strain)

$$\varphi_h = \int_{h_0}^{h_1} \frac{dh}{h} = \ln \frac{h_1}{h_0} = \varphi_1; \quad \varphi_b = \int_{b_0}^{b_1} \frac{db}{b} = \ln \frac{b_1}{b_0} = \varphi_2; \quad \varphi_l = \int_{l_0}^{l_1} \frac{dl}{l} = \ln \frac{l_1}{l_0} = \varphi_3 \tag{4.3}$$

The relationship between true strain and nominal strain is:

$$\varphi_l = \ln \frac{l_1}{l_0} = \ln \frac{l_0 + \Delta l}{l_0} = \ln(1 + \varepsilon_l) \tag{4.4}$$

With the law of the constant volume (equation 4-1) it can be concluded that the sum of all deformation values is always equal to zero:

$$\varphi_h + \varphi_b + \varphi_l = 0 \tag{4.5}$$

4.1.2 Yield Stress and Yield Curve

Metallic materials show a proportional behaviour up to the yield point due to their crystalline structure. The elastic deformation arise through reversible lattice stretching and compression. At the yield point large areas of the lattice structure slide into the non-reversible region. For small strains, the difference between original strain at cross section area S_0 and the actual strain for cross section area **S** is negligible. On the contrary, when the strains are large, the difference is considerable. Therefore there is a difference between the nominal stress $\sigma' = \frac{F}{S}$ and the true stress k_f. There is also a single-axial state of stress within the range of the proportional elongation, for this condition the nominal stress $\sigma' = \frac{F}{S}$

F actual force
S actual cross section area

is equal to the true stress k_f. The characteristics of metallic materials are described with a stress-strain diagram (**Figure 4-4**), determined with a standardized tensile test.

The yield stress is the stress which introduce the flow of a material within the single axial homogenous stress condition.

The yield stress will normally be applied over the degree of deformation (**Figure 4-6**).

Publications of results on stress-strain curves simulations are now available. They are differentiated by the shape of the trails at the loading; the chosen stress-srain curves represent the basis properties of the actual forming process. The yield stress depends on the degree of deformation φ, the forming velocity $\dot{\varphi}$, the temperature υ, the hydrostatic pressure σ_m and the material.

For anisotropic materials k_f is also dependent on the load direction.

In the elementary theory of the forming techniques the criterion of the maximum shear stress according to Tresca and the criterion of the maximum octahedral shear stress according to **v.** Mises are used **(Figure 4-7).**

Multi-axial stress conditions are reduced to single-axis stress condition with the aid of flow criteria, e.g. the criterion of the maximum octahedral shear stress (v. Mises, Henchy, Maxwell, Huber) or the criterion of the maximum share stress (Tresca, Mohr). These criteria indicate under which conditions the material starts to flow under multi-axial stress by making a connection between the characteristic stress and the multi-axial stress **(Figure 4-8).**

With $\sigma_1 > \sigma_2 > \sigma_3$ as principal stresses (**Figure 4-8**) and σ_v as equivalent stress the following yield criteria are formulated:

v. Mises:
$$\sigma_v = \sqrt{\frac{1}{2}\left[(\sigma_1-\sigma_2)^2+(\sigma_2-\sigma_3)^2+(\sigma_3-\sigma_1)^2\right]} \qquad \textbf{(4.6)}$$

Tresca:
$$\sigma_v = |\sigma_1-\sigma_3| = 2\cdot\tau_{max} = k_f \qquad \textbf{(4.7)}$$

The criterion of the maximum shear stress only considers the shear stress, however the criterion of the maximum octahedral shear stress cover the whole stress condition. The deviation between the hypotheses depends on the stress condition. The greatest difference appears in a pure shear stress. The v. Mises hypothesis results in up to 15 % higher stresses as the Tresca criterion of the maximum share stress **(Figure 4-9).**

The influence of one or multi axial stress conditions on the course of the shear yield locus τ_F and shear yield strength τ_B is shown in **Figure 4-10,** where the Mohr stress circles are shown for the start of yielding. The diagram shows that for multi-axial compression conditions; more plastic deformation is possible under tension conditions.

4.1.3 Characteristic Values of Sheet Metals

The evaluation of the forming suitability of sheet metals (applies also for thin walled rolled tubes) is based on the characteristic values from the single axis traction test. The traction test stretches the sample slowly with a constant velocity until it reaches breaking point.

In the testing of materials it is usual to indicate the stress as working strength F on the output cross section A_0. The stress σ over the elongation ε is determined in such a way which results in a stress - strain diagram (**Figure 4-11**).

Characteristic values from the single axis traction test are:

- Tensile stress R_m [N/mm^2]
- Proof stress $R_{p\,0,2}$ [N/mm^2]
- Ultimate elongation A [%]
- fracture necking Z [%]

The ultimate elongation is the lasting length variation referred to the output length after the break of the sample. The fracture necking is the relation between the starting cross section of the tensile test bar and the cross section are at fracture.

For the traction test within the plastic area the cross section A is smaller as the starting cross section A_0, the stresses $\sigma = \frac{F}{A_0}$ is also much smaller in relation to the real direct-axis components of stresses. In order to obtain the true stress in longitudinal direction, the strength F must refer to the momentary cross section A.

Within the area of the strain ε_{gl}, to the beginning of the necking, a single axial state of stress is present with the traction test. Within this area the stress in the plastic area corresponds to the yield stress k_f.

At the beginning of the necking the true stress and the yield stress starts to deviate from each other as shown in **Figure 4-12.**

Further characteristic values for the forming suitability of sheet metals are

- the hardening exponent n
- the anisotropic value r

4.1.4 Hardening Exponent

The flow curves of most non-alloyed and low-alloy steel can be approximated (for deformations $\varphi < 1{,}0$) using the power function:

$$k_f = (C_\phi)^n \qquad (4.8)$$

The hardening exponent n, which represents a measure for the material hardening occurring when forming, and the quantity C are specific material constants.

If the flow curve is plotted in doubly logarithmic representation, then it presents itself as straight lines, whose upward gradient corresponds to the hardening exponent (**Figure 4-13**).

After **Reihle** the following relations applies:

$$n = \varphi_{gl} \tag{4.9}$$

$$C = R_m\left(\frac{e}{n}\right)^n \tag{4.10}$$

The uniform degree of deformation can be determined from the uniform strain A_g measured in the traction test according to the following equation:

$$\varphi_{gl} = \ln(1 + A_g) \tag{4.11}$$

Here the accuracy, with which the uniform strain A_g is determined, directly affects the accuracy of the flow curve. The effect of a high hardening exponent, for example on the behavior of the sheet metal material when stretch-forming, shows up in the fact that with rising values of n the danger of high local strains and thus the inclination to the necking decreases.

In deep-drawing a high hardening exponent has both positive and negative effects. Large values for n increase the base fracturing strength, but, at the same time the drawing force necessary rises. The drawing limit ratio with increasing n value increases in particular if the relation of stamp diameter to sheet thickness is high.

4.1.5 Anisotropy

With so many procedures for sheet-metal forming, it is considered that a material does not have the same characteristics in all directions, i.e. the material has an anisotropic behaviour. The anisotropy of a much-crystalline material is thereby indicated, and the grains are not irregularly oriented, but it is preferentially aligned certain planes and directions. Such referenced orientation, which is also called texture, can develop during both, the production (e.g. a casting) and the subsequent treatment (forming, thermal treatment). Conditionally and among other things the tensile strength and plastic characteristics are direction-controlled.

There are different characteristic values, which indicate the plastic behaviour due to the anisotropy of the sheet metal.

- vertical Anisotropy r

This characteristic value describes the relation of the log. change of the sheet width change φ_b to the log. sheet thickness change φ_s.

r = 1 means isotropic, plastic behaviour of the material in the sheet metal-normal direction

r ≠ 1 means anisotropic, plastic behaviour in the sheet metal-normal direction

r > 1 means larger resistance of the tensile test specimen against reduction of the plate thickness s

A high perpendicular anisotropic value r is desired.

- middle vertical anisotropy $\bar{r}$

Usually the anisotropic values in the different directions of the sheet metal plane do not correspond to each other. Therefore the tensile test specimens (**Figure 4-14**) are taken under different angles to the direction of rolling out of the sheet metal (**Figure 4-15**).

$$\bar{r} = \frac{1}{4}(r_0 + 2r_{45} + r_{90}) \qquad \textbf{(4.12)}$$

A value of $\bar{r} > 1$ is desired.

Deep-drawings sheets should be easily formable on the surface, however it should have resistance against deformation in the plate thickness direction. For sheet metal to be suitable for deep-drawing it should have both, a high value of vertical anisotropy r and middle vertical anisotropy $\bar{r}$.

- plane anisotropy $\Delta \bar{r}$

A substantial measure for the variance of the vertical anisotropy over the sheet metal plane is the plane anisotropy Δ r (**Figure 4-16**).

The so-called plane anisotropy leads to irregular edges of punched hollow forms. This appearance is called "distorted edges". This is caused by different r-values in the sheet metal plane. If the range of "mountains" of the distorted edges of the r-value is larger then there is a large resistance against the sheet thickness change. However the range of "valleys " of the distorted edges of the r-value is smaller and the sheet thickness is larger.

The plane anisotropy Δ r is calculated as folows:

$$\Delta r = \frac{r_0 + r_{90}}{2} - r_{45} \qquad \textbf{(4.13)}$$

The dependency of the distorted edges of cups on the plane anisotropy is shown in **Figure 4-**

17 and 4-18. The Δ r-value should be as small as possible.

- Influencing the anisotropy

Using deep drawing of steel St 14, it can be demonstrated that high r-values can come by a combination of different production measures. An outline of the different possibilities is shown in **Figure 4-19.**

The most important prerequisite for the height of the r-value falls when hot-rolling. The hasp temperature must be keep less than 600°C, so that a connection between the aluminium and nitrogen in the hot-rolled strip is prevented. Both items should be only together after cold-rolling and during the recrystallizing heat treatment to fine aluminium nitrides. The interaction between the separating aluminium nitride particles and the recrystallisation leads to the desired orientation selection.

4.2 Influence of the Friction

Friction is a relatively unknown field in the IHP technique. Normally the friction law from Coulomb are used. The goal is to keep the friction low in order to allow the process to work, and to minimize the wear of the expensive dies. The tubes will be coated with graphite and/or other lubricants before forming. The question is now if the friction really is an important parameter for IHP processes, then it must be clarified if there is a considerable movement between the tool and the tube. For processes which only calibrate a part it can be supposed that there only a small movement between tool and tube. Therefore some FE simulations are nedeed.

The friction-force depends on the area, the force which acts vertical (normal) to the area and the friction coefficient (**Figure 4-20**).

F_R	=	friction force
F_n	=	normal force
μ	=	friction coefficient

Different types of friction must be distinguished - static friction and dynamic friction. Static friction acts between resting parts which are placed against each other during movement. The liability of the adhesion must be broken at contact areas (often cold welding for metals). Afterwards, e.g. if a movement already exists, generally a lower movement friction accurs.

According to the material combination the friction coefficient for dry friction have the following range :

static friction coefficient	$\mu = (0{,}15 .. 0{,}8)$
dynamic friction coefficient	$\mu = (0{,}1 .. 0{,}06) < \mu_0$

Friction coefficients are tribologic parameters which must be estimated with experiments, e.g. with a slide trial on a inclined plane with a changeable angle a.

The range of the friction-value normally used varies between 0.01 to 0.15. Now the question is, how important is the influence of the friction for the IHP process. We can distinguish two cases. The first is friction in the radial direction, and the second is in the axial direction.

4.2.1 Friction in Radial Direction

For this analysis the FE model (**Figure 4-21**) for the investigation of the definition thin/thick tube from section 4.4.4 is used. The simulation is done only with interior pressure and no axial force. The influence of the friction in radial direction questioned here. If the friction has a significant influence it can be assumed that with a low friction a greater degree of deformation is possible. Therefore the strains would also be of interest.

Parameter of the simulation model:

outer diameter of the tube	$D_a = 60$ mm
wall thickness	$s_0 = 4$ mm
wall thickness relationship	$wv = s_0 / D_a = 0.066 \Rightarrow 6.6\ \%$
tool dimension	rectangle 65 * 65 mm
calibration pressure	p=3000 bar
material	St 36-2 mod

For this investigation the influence of the friction is in the radial direction, and the following cases are simulated (**Table 4-1**):

case	static friction	dynamic friction
1	1.0	1.0
2	0.5	0.5
3	0.5	0.0
4	0.0	0.5
5	0.15	0.06
6	0.0	0.0

Table 4-1 Simulation Trails

In this investigation the influence of the friction and the displacements of three nodes are considered, concentrating on the nodes after being applied to the tool. The moment when the node come into contact with the tool can be determined by looking on the displacements in Y direction, from that time the node has no further displacements in the Y direction. The displacements of three nodes is considered. **Figure 4-22** diplays the displacement path vs. time of node 294, **Figure 4-23** shows the location of the nodes.

displacement in X direction	node	1	2	3	4	5	6
1.80	A	0.05	0.06	0.06	0.20	0.14	0.2
6.64	B	0.12	0.13	0.13	0.83	0.61	0.83
9.88	C	0.38	0.37	0.37	1.32	1.01	1.29
strain		57.76	57.76	57.76	50.38	52.14	50.38

Table 4-2 X and Y Displacements of the considered Nodes

Between cases 4, 5 and 6 a relatively small difference is detected. Even for cases 1, 2 and 3 about half of the node displacement can be noticed, but these two cases are unrealistic. For example a friction coefficient of 0.5 means steel to rubber. **Table 4-2** and **Figure 4-24** show that the dynamic friction has no great influence on the results. The only important parameter is the growth of the static friction.

The analysis has shown that the influence of the **friction** on the expansion without axial force, thus for all **calibration processes, is insignificant.**

4.2.2 Friction in Axial Direction

The IHP process is based on the principle of pushing material in the axial direction. It is of course necessary to minimise the friction, because a good forming result can only be achieved when material can be carried into the expansion area.

4.3 Wall-thickness and Degree of Deformation of a Thin/Thick Tube

An important failure case of an IHP process is cracking at the inner/outer side of the tube. Cracking on the outer side can be recognised relatively easily with a visual control, but cracking on the inner side of the tube is a greater problem. The cracks cannot be localised with the eyes. It is only by the destruction of the part what makes it possible to find defects. This of course is not possible for a line production. The important question is that what is the limiting factor of the relationship between tube-thickness and tube-diameter, that can be regarded as an economical and technological value for using the IHP process. There are different strains between the inner and outer sides of the tube. From experience it is known that thick tubes develop cracks on the inner side of the tube, therefore it can be assumed that the strains at the inner side are greater than these at the outer side.

Today, in industry, tubes with a wall thickness relationship of up to 18% of the outer diameter are used. The normal area for IHP products will be a wall thickness between 3% and 12% of the outer diameter. This section investigates the strain values across the wall for thin/thick tubes and defines what is a thin/thick tube.

Is it possible to use shell elements to investigate the strains over the wall-thickness? The first question is, whether shell elements are able to show the strains over the wall-thickness correctly. To answer this question a number of simple simulations must be made. The following analysis will be based on a tube which is widening up constantly. The material-volume during the forming process is constant, i.e. the volume of the tube before, during and after the forming process are the same. The length of the tube during the expansion is uncharged.

4.3.1 Wall-thickness - Analytical Solution

A tube with a diameter of 48 mm and a wall-thickness of 6 mm will be blown up to a diameter of 57.6 mm.

Parameter :

$D_{A0/1}$	outside diameter	(0 before IHP, 1 after IHP)
$D_{I0/1}$	inside diameter	
$s_{0/1}$	wall thickness	
l	length of the tube	
$A_{0/1}$	cross-section area	
$V_{0/1}$	Volume of the tube	
ε_I	strain on the inner side of the tube	
ε_M	strain in the middle of the tube	
ε_O	strain on the outer side of the tube	

The wall thickness after the forming process s_1 can be calculated over the volume of the tube, in this case the length is constant so it is possible to look at the cross-section area. The cross

section area must be the same before and after the forming process.

$$s_{0/1} = \frac{D_{A0/1} - D_{I0/1}}{2} \tag{4.14}$$

$$A_0 = \left[\left(\frac{D_{A0}}{2}\right)^2 - \left(\frac{D_{I0}}{2}\right)^2\right] \cdot \pi \tag{4.15}$$

$$A_1 = \left[\left(\frac{D_{A1}}{2}\right)^2 - \left(\frac{D_{I1}}{2}\right)^2\right] \cdot \pi \tag{4.16}$$

$$V_0 = V_1 = A_{0/1} \cdot l = const. \tag{4.17}$$

as defined before the area must be constant $A_o = A_1$

$$\left[\left(\frac{D_{A0}}{2}\right)^2 - \left(\frac{D_{I0}}{2}\right)^2\right] \cdot \pi = \left[\left(\frac{D_{A1}}{2}\right)^2 - \left(\frac{D_{I1}}{2}\right)^2\right] \cdot \pi \tag{4.18}$$

resolved to D_{I1}

$$D_{I1} = 2 \cdot \sqrt{\left(\frac{D_{A1}}{2}\right)^2 + \left(\frac{D_{I0}}{2}\right)^2 - \left(\frac{D_{A0}}{2}\right)^2} \tag{4.19}$$

with the following relation

$$D_{I0} = D_{A0} - 2 \cdot s_0 \tag{4.20}$$

$$D_{I1} = D_{A1} - 2 \cdot s_1 \tag{4.21}$$

substitution of (4.21) into equation (4.19)

$$D_{A1} - 2 \cdot s_1 = 2 \cdot \sqrt{\left(\frac{D_{A1}}{2}\right)^2 + \left(\frac{D_{A0} - 2 \cdot s_0}{2}\right)^2 - \left(\frac{D_{A0}}{2}\right)^2} \tag{4.22}$$

solved to s_1

$$s_1 = s_{min} = \frac{D_{A1}}{2} - \sqrt{\left(\frac{D_{A1}}{2}\right)^2 + \left(\frac{D_{A0} - 2 \cdot s_0}{2}\right)^2 - \left(\frac{D_{A0}}{2}\right)^2} \tag{4.23}$$

It is now necessary to find out if wall-thickness s_{min} follows for different starting diameters of the tube the same ratio of expansion. As an example a tube with a wall-thickness of 4 mm will be expanded about 20%.

D_{A0} (mm)	D_{A1} (mm)	s_{min} (mm)
40	4.8	3.21
60	72	3.25
80	96	3.27
100	120	3.29
120	144	3.30

Table 4-3 s_{min} for Different Ratio of Expansion

Table 4-3 shows that the outer diameter has little influence on the minimal wall-thickness s_{min}, and for the curves in Figure 4-25 the results for different starting diameters are averaged. In Figure 4-25 the relationship between expansion and wall-thickness s_{min} can be seen.

4.4 Degree of Deformation of a Thin/Thick Tube

4.4.1 Analytical Solution – Regular Expansion

For the evaluation example, the inner diameter after the forming process can be calculated as:

$$D_{I1} = 2 \cdot \sqrt{\left(\frac{57.6}{2}\right)^2 + \left(\frac{36}{2}\right)^2 - \left(\frac{48}{2}\right)^2} = 48.06 \text{ mm}$$

$$s_1 = \frac{D_{A1} - D_{I1}}{2} = \frac{57.6 - 48.06}{2} = 4.76 \text{ mm}$$

Now the strains on the different locations can be calculated as follow:

Strain at the outer side :

$$\varepsilon_O = \frac{D_{A1}}{D_{A0}} \qquad \varepsilon_O = \frac{57.6}{48} = 1.2 \text{ -> 20 \% strain}$$

Strain at the middle

$$\varepsilon_M = \frac{D_{M1}}{D_{M0}} \qquad \varepsilon_O = \frac{52.84}{42} = 1.2581 \text{ -> 25.58 \% strain}$$

Strain at the inner side :

$$\varepsilon_I = \frac{D_{I1}}{D_{I0}} \qquad \varepsilon_O = \frac{48.06}{36} = 1.335 \text{ -> 33.5 \% strain}$$

The strain at the inner side is also 13.5 % greater that the strain on the outer side. This shows that there is a significant difference between the inside/outside strains of the tube.

4.4.2 Solution with FE – Regular Expansion

For the comparison of the FE results with the analytical solution four different types of shell elements are investigated. **Figure 4-26** shows the FE model used for the investigation.

- **Belytschko-Lin-Tsai** shell with 3 integration points (BLT 3IP) This is the standard shell element with the smallest calculation time. This element cannot be used for great twisting and thrust deformation
- **Belytschko-Lin-Tsai** shell with 5 integration points (BLT 5IP)
- **Hughes-Lui** shell with 3 integration points (HL 3IP) This shell element is very accurate for great deformations, twisting and thrust distortion. The calculation time is 2.5 times of the Belytschko-Lin-Tsai shell
- **Hughes-Lui** shell with 5 integration points (HL 5IP)
- **Belytschko-Wong-Chiang** shell with 3 integration points (BWC 3IP)
- **Belytschko-Wong-Chiang** shell with 5 integration points (BWC 5IP) This shell element is a further development of the Belytschko-Lin-Tsai and the Hughes-Lui shell which has a calculation like the BLT and an accuracy like the HL.
- **3D solid elements** (5 over the thickness)

		1	2	3	4	5	6	7
Strain	ana-lytic	BLT 3IP	BLT 5IP	HL 3IP	HL 5IP	BWC 3IP	BWC 5IP	Solid 5 El
outer	20.0	26	27	26	26	26	26	22
Middle	25.58	25	25	25	25	25	25	26
Inner	33.5	28	28	28	28	28	28	32
shell-thick-ness	4.76	4.88	4.88	4.89	4.89	4.88	4.88	4.8

Table 4-4 Comparison of the Strains for Different Types of Shell Elements (%)

The results presented in **Table 4-4** shows that the shell elements are not suitable to describe the strain course over the wall thickness. The results for the outer and inner side of the tube are shown to be too large for the inner and respectively too small for the outer side. Investigation of the exact strain values over the tube-wall shows that it is necessary to use a FE model with solid elements. The shell elements implemented today in the FE system only consider the

strains due to bending and not the strains effected through a thickness change during the forming process. To avoid this disadvantage of the shell elements new thick shell elements should be developed.

4.4.3 Diagram for the Estimation of the Strain Rate Difference

The ratio between wall-thickness and tube diameter for IHP processes is between 3 % and 12%.

The starting tube diameter must first be investigated by the same degree of expansion and ratio of wall-thickness which influences the degree of deformation. **Table 4-5** shows the difference in the degree of deformation for different diameters, expansions and wall-thickness.

D_0	expansion	D_1	s_0	s_1	d_0	d_1	φ_{Innen} Degree of deformation (inside)	φ_{aussen} Degree of deformation (outside)	φ_{dif} Difference
80	10	8.8	10	8.9	60	70.2	1.1	1.17	0.07
64	10	70.4	8	7.12	48	56.16	1.1	1.17	0.07
80	20	96	10	8.1	60	79.8	1.2	1.33	0.13
64	20	76.8	8	6.45	48	63.9	1.2	1.33	0.13
80	10	88	5	4.45	70	79.1	1.1	1.13	0.03
64	10	70.4	4	3.56	56	63.28	1.1	1.13	0.03
80	20	96	5	4.05	70	87.9	1.2	1.26	0.06
64	20	76.8	4	3.25	56	70.3	1.2	1.26	0.06
80	10	88	2.5	2.23	75	83.55	1.1	1.11	0.01
64	10	70.4	2	1.78	60	66.84	1.1	1.11	0.01
80	20	96	2.5	2.03	75	91.95	1.2	1.23	0.03
64	20	76.8	2	1.61	60	73.57	1.2	1.23	0.03

Table 4-5 Influence of the Wall-Thickness Ratio at the Degree of Deformation

Table 4-5 shows that the starting diameter D_0 of the tube has no influence on the difference of the degree of deformation φ_{dif}.

$$\varphi_{dif} = \varphi_{Innen} - \varphi_{Aussen}$$

With this information a general diagram to determine the strain rate difference can be created. The strain rate depends on the diameter and wall-thickness before and after the expansion. The strain rate further depends on the wall-thickness relationship. This wall-thickness relationship is introduced as *wr.*

wall-thickness relationship = wr = s_0/D_0

The expansion *er* is the ratio between the outer diameter before and after IHP.

$$er = D_1/D_0$$

Figure 4-27 shows the difference in the degree of deformation for different values for the expansion *er.*

From **Figure 4-27** it can be concluded that:

- The thicker the wall of the tube, the greater are the differences in the degree of deformation between the inner and outer side.
- The difference in the degree of deformation grows with the expansion *er*
- The maximum degree of deformation is always on the inner side of the tube
- With a greater difference in the degree of deformation, there is a risk of a crack inside growth.

Up to now only a constant circular expansion of a tube is considered. The next section looks at the strain conditions for the expansion of a tube into a rectangular section with rounded edges.

4.4.4 Expansion of a Circle Tube into a Rectangle – Strain Values

In order to investigate the strains inside the wall of a tube during the forming process a tube was expanded into a rectangle **(Figure 4-28).**

The model is symmetrical, so ¼ of the model can be used for the FE simulation **(Figure 4-29).** For all trials the geometric relationships are the same, e.g. the expansion is always 32.6. A tube with a diameter of 30 mm is expanded up to 32.5 mm, a tube with 60 mm to 65 mm and a tube with 120 mm up to 130 mm.

4.4.5 Results

Figure 4-30 shows that the greatest strains are not within the radius, but at the crossing between the straight section to the radius section. It is interessting to note that the greatest strain occur for all relationships between wall-thickness and tube-diameter. Practical experiments shows that the assumption that thin tubes fail on the outer side is not always true. If thin tubes begin cracking they are most likely to burst. This is the reason from which the opinion

came that thin tubes fail at the outer side.

Figure 4-31 shows that the strains increase significantly at the point at which the straight side turns into the radii. This confirms the conclusions gained from the practical work (**Bögel, 1997**).

This trial is made for the following cases (wr = wall-thickness relationship)

$$wr = \frac{s_0}{D_0}$$

Diameter (mm)	Wall-thickness (mm)	Wr
30	2.	0.067
60	3	0.05
60	4	0.067
60	5	0.083
60	6	0.1
120	6	0.05

Table 4-6 Test Trials

Figure 4-32 shows the results for the different test trials. Because the geometric relationships for all cases are the same is be possible to interpolate a single curve out of the diagram as shown in **Figure 4-33**.

With such a radius curve it is possible to determine the necessary interior pressure. This diagram makes it is now possible to find the corresponding strain. And now it is possible to decide if it is possible to produce the configuration in question with the proposed material. This procedure, of course, works also backwards, i.e. it is possible to determine which radius can be formed for a certain strain value. This curve must be verified using practical experiments.

4.5 Expansion of a Pre-Formed Workpiece

A lot of IHP workpieces, especially parts for exhaust systems, are bent before the expansion process. The simulation of the bending process is difficult i.e. very time consuming. Normally, the simulation will be done without the bending process, but it is known that the bending process has a significant influence on the simulation results through the thickening/thinning of the tube wall, and the introduction of cold hardening. In order to consider the strains and the wall-thickness from bending, the properties of the pre-formed workpiece must be defined in the FE-

system.

This section describes the considerations done for the definition of the pre-formed part. The presented method leads only to a coarse approximation of the real relations and can be used to save time. More and more parts are pre-bended before the hydrofoming operation and the properties introduced through the bending have a crucial influence onto the forming result. Therefore it is often inevitable to use approximation for the simulation of the bending and the real process circumstances must be used (**Haas et al., 1999**)

4.5.1 Background for the definition of the pre-formed part

A compensation model must be created for the real pre-formed part. The tube will be divided into 4 parts (**Figure 4-34**). A strain and a wall-thickness must be assigned to all of these parts.

At first the strains for the different sections of the tube must be calculated. On the outer side there are tensile strains, on the inner side compressive strains.

On the outer side of the tube the bending-incident must be considered for the calculation of the strain. The dimension parameters are shown in **Figure 4-35**.

$$\text{outer strain}: \varepsilon_a = \left[\frac{R_a}{R_m} - 1\right] \cdot \text{bending} - \text{incident}$$

$$\text{inner strain}: \varepsilon_i = \left[\frac{R_i}{R_m} - 1\right]$$

Furthermore the wall-thickness after bending must be calculated.

$$\text{outer wall-thickness}: s_a = s_0 \cdot [1 - \varepsilon_a]$$

$$\text{inner wall-thickness}: s_i = s_0 \cdot [1 - \varepsilon_i]$$

4.5.2 Example

The strains and wall-thicknesses from the pre-forming for a tube with the following parameters should be calculated.

So	=	2 mm
d0	=	50 mm
R_a	=	225 mm
R_m	=	200 mm
R_i	=	175 mm

bending-fall-in = 15 % = 0.85

Strains

$$\varepsilon_a = \left[\frac{R_a}{R_m} - 1\right] \cdot bending - fall - in = \left[\frac{225}{200} - 1\right] \cdot 085 = 0.10625$$

$$\varepsilon_i = \left[\frac{R_i}{R_m} - 1\right] = \left[\frac{175}{200} - 1\right] = |-0.125| = 0.125$$

Wall-thicknesses :

$$s_a = s_0 \cdot [1 - \varepsilon_a] = 2 \cdot [1 - 0.10625] = 1.8$$

outer wall-thickness = 1.8 mm

$$s_i = s_0 \cdot [1 - \varepsilon_i] = 2 \cdot [1 - (-0.125)] = 2.25$$

inner wall-thickness = 2.25 mm

4.6 Conclusion

This chapter has shown some basic analysis concerning about the material behaviour and fundamental investigations about the influence of the friction and the course of the strain over the tube wall.

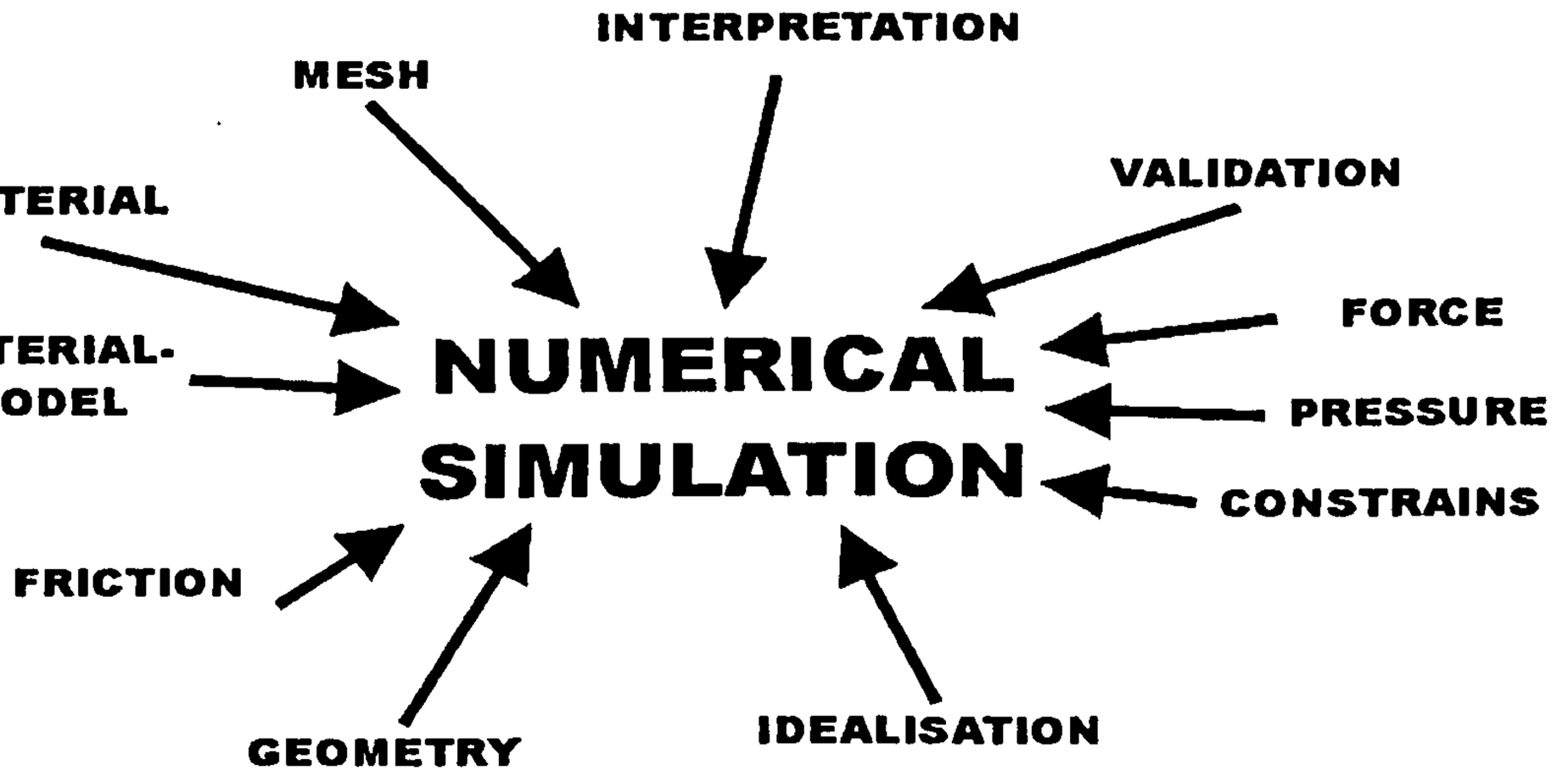

Figure 4-1 Numerical Simulation - Influence Parameters

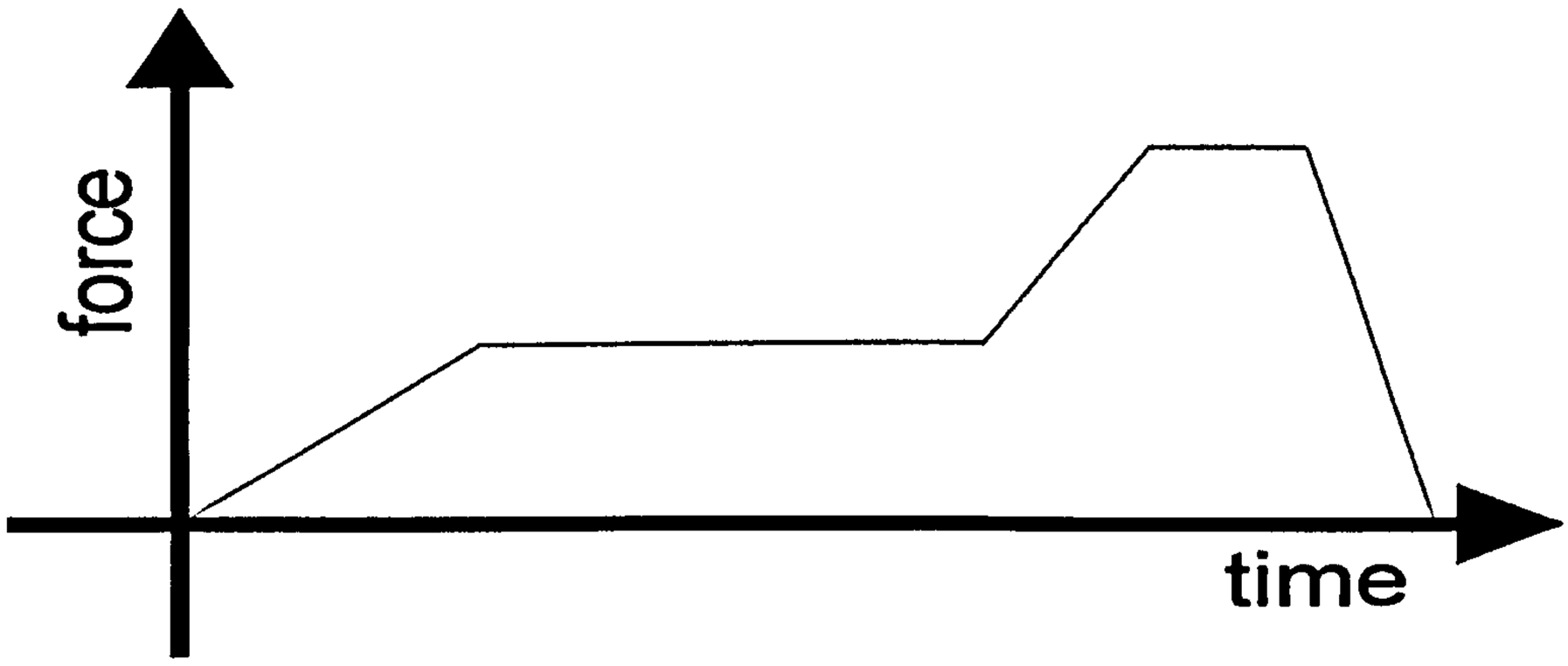

Figure 4-2 A typical IHP Load-Curve (axial compression - in principal)

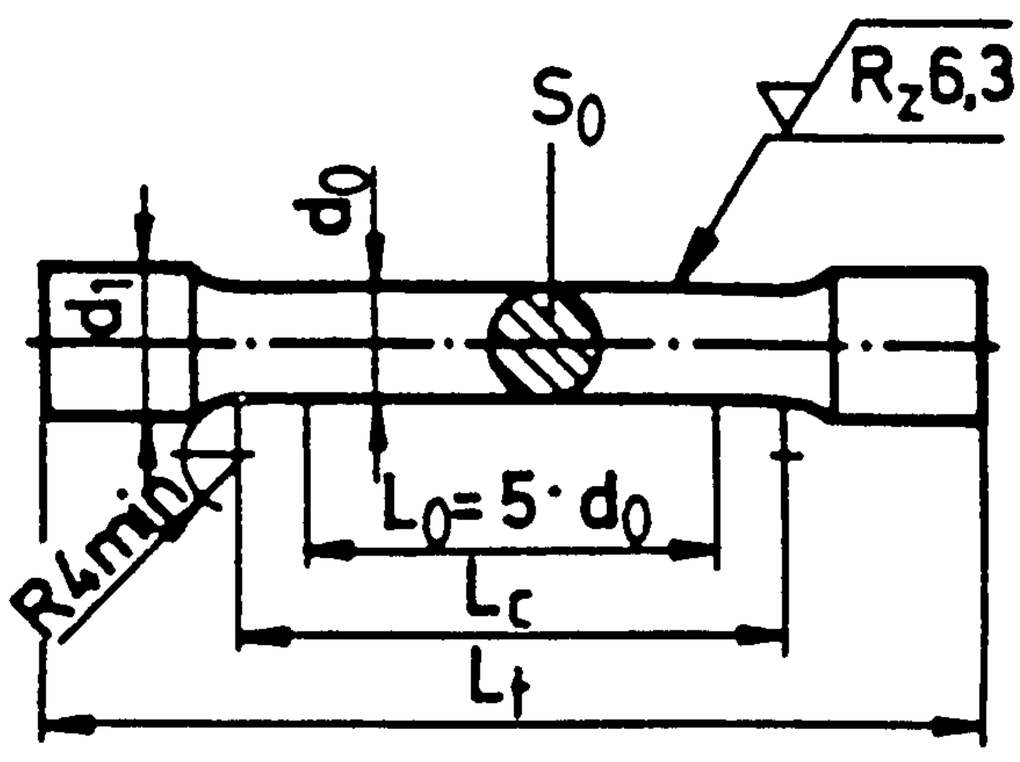

Figure 4-3 Tensile Test Bar (DIN 50125)

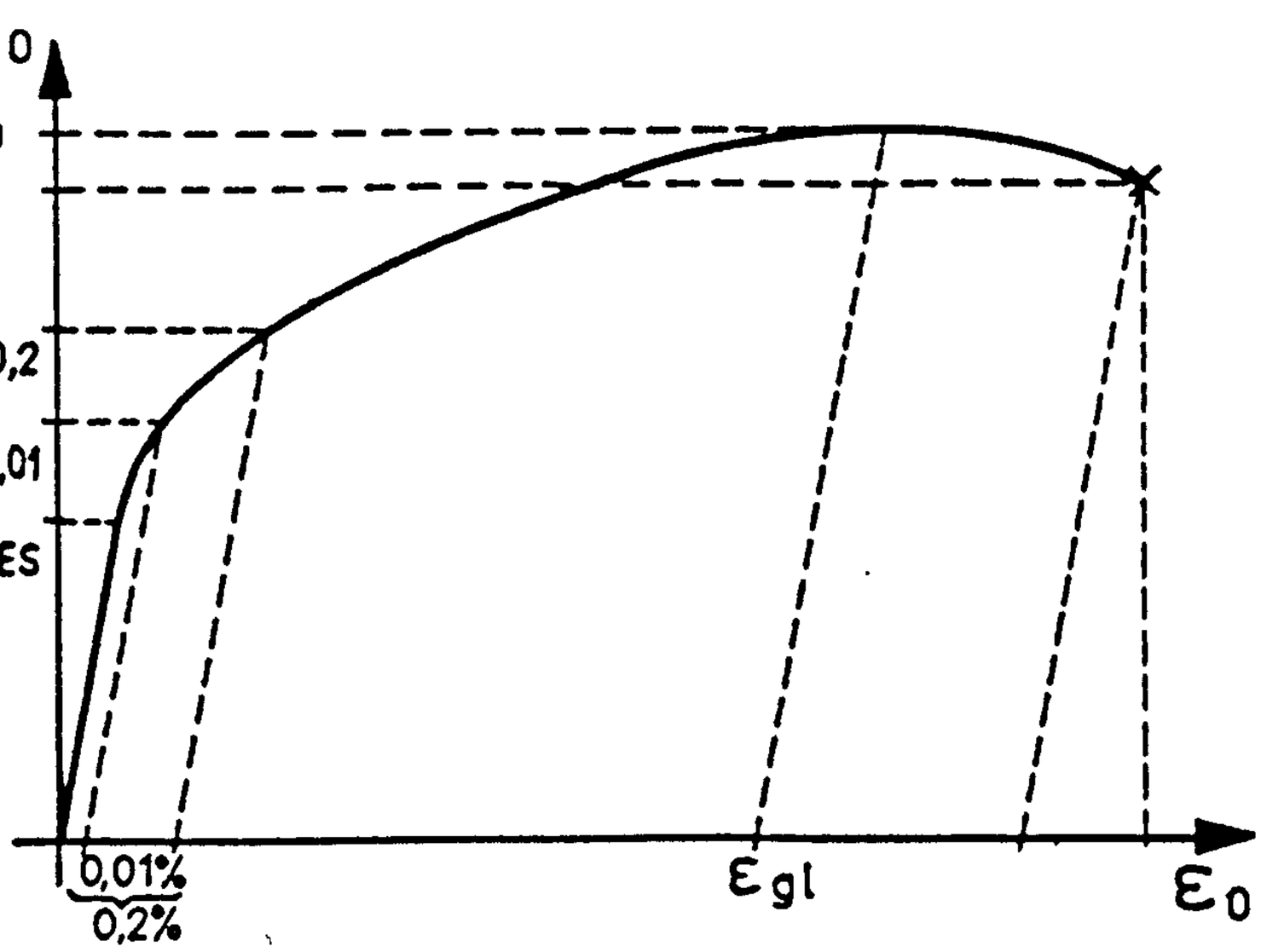

Figure 4-4 Stress – Strain (nominal) Diagram (mild steel, ST 37)

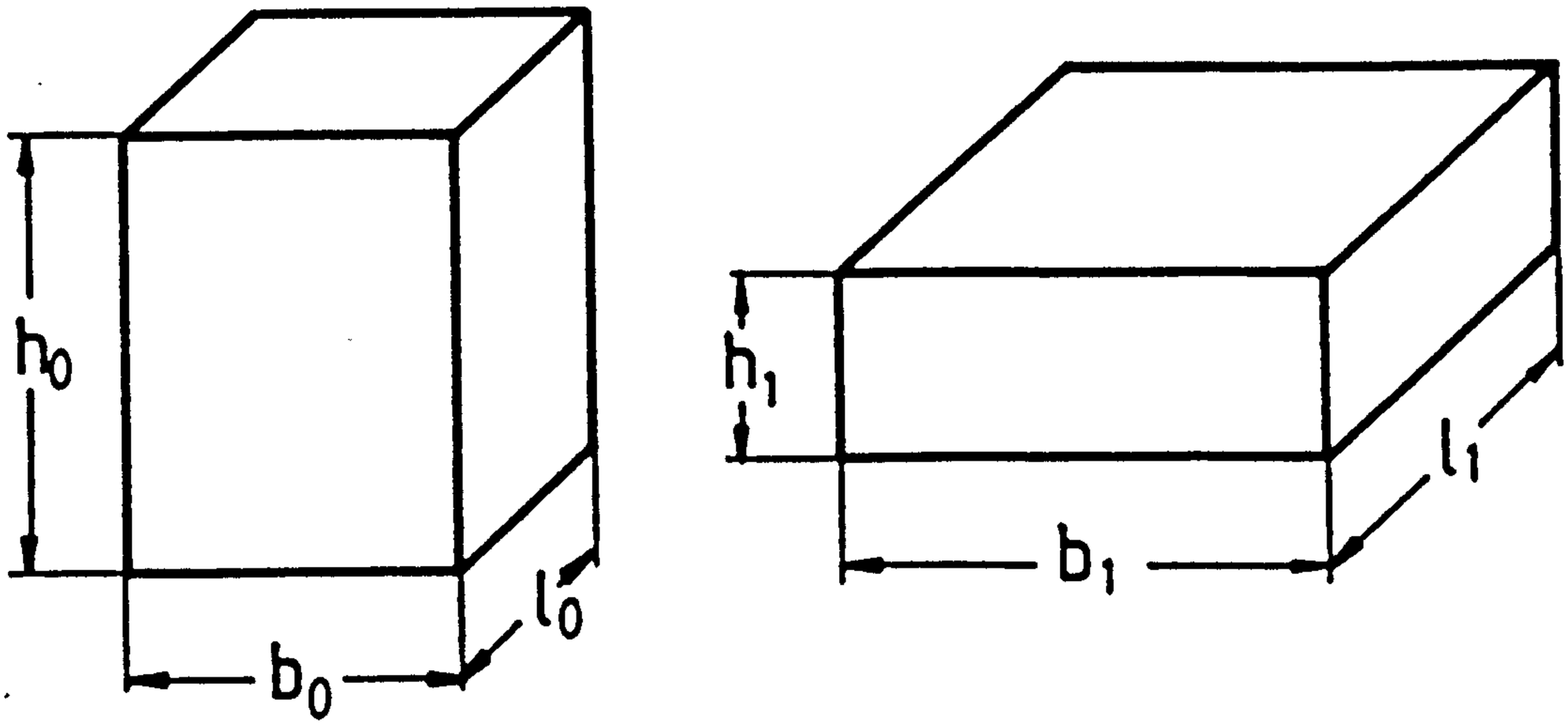

Figure 4-5 Converted Body

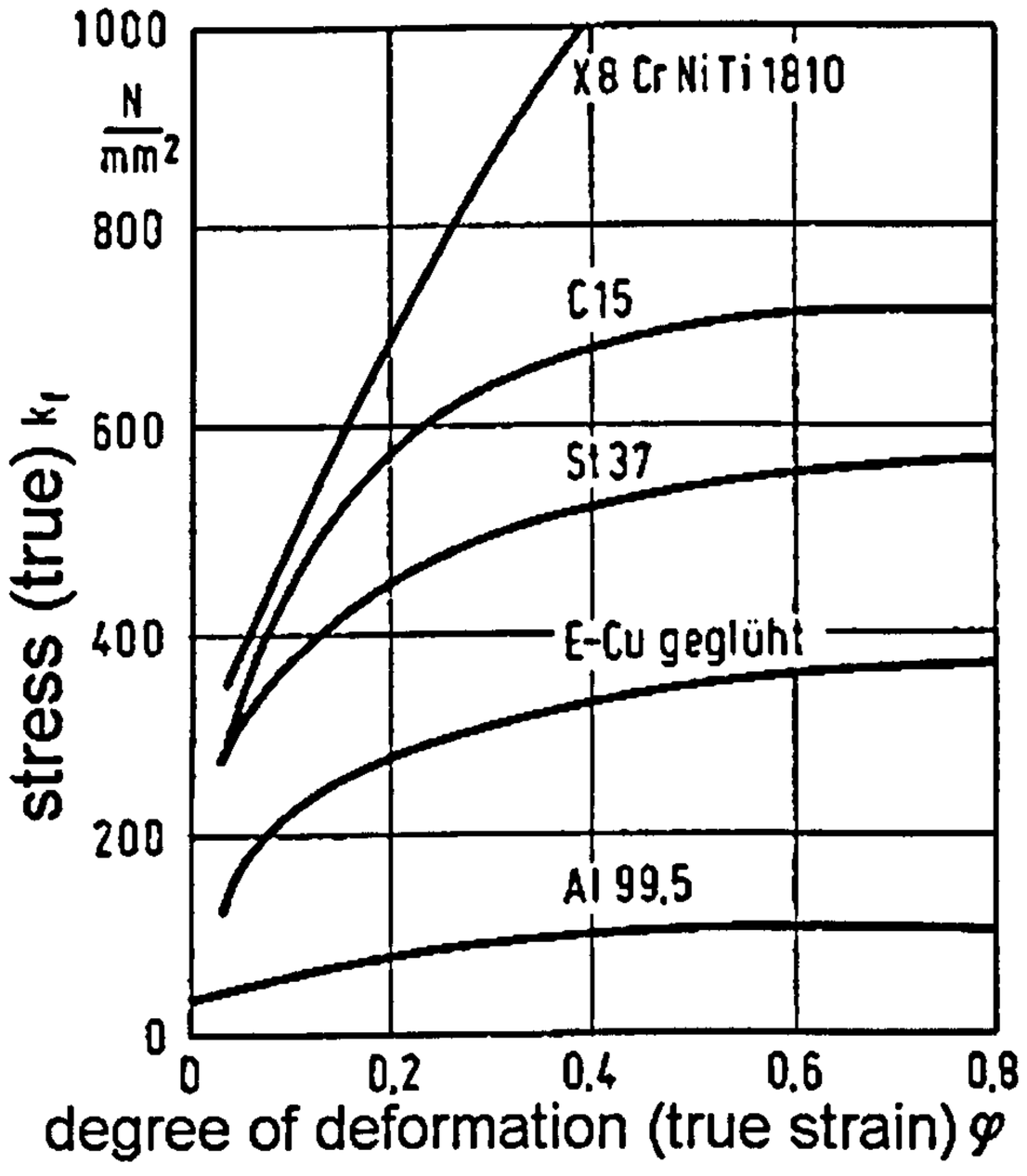

Figure 4-6 Flow-Curve

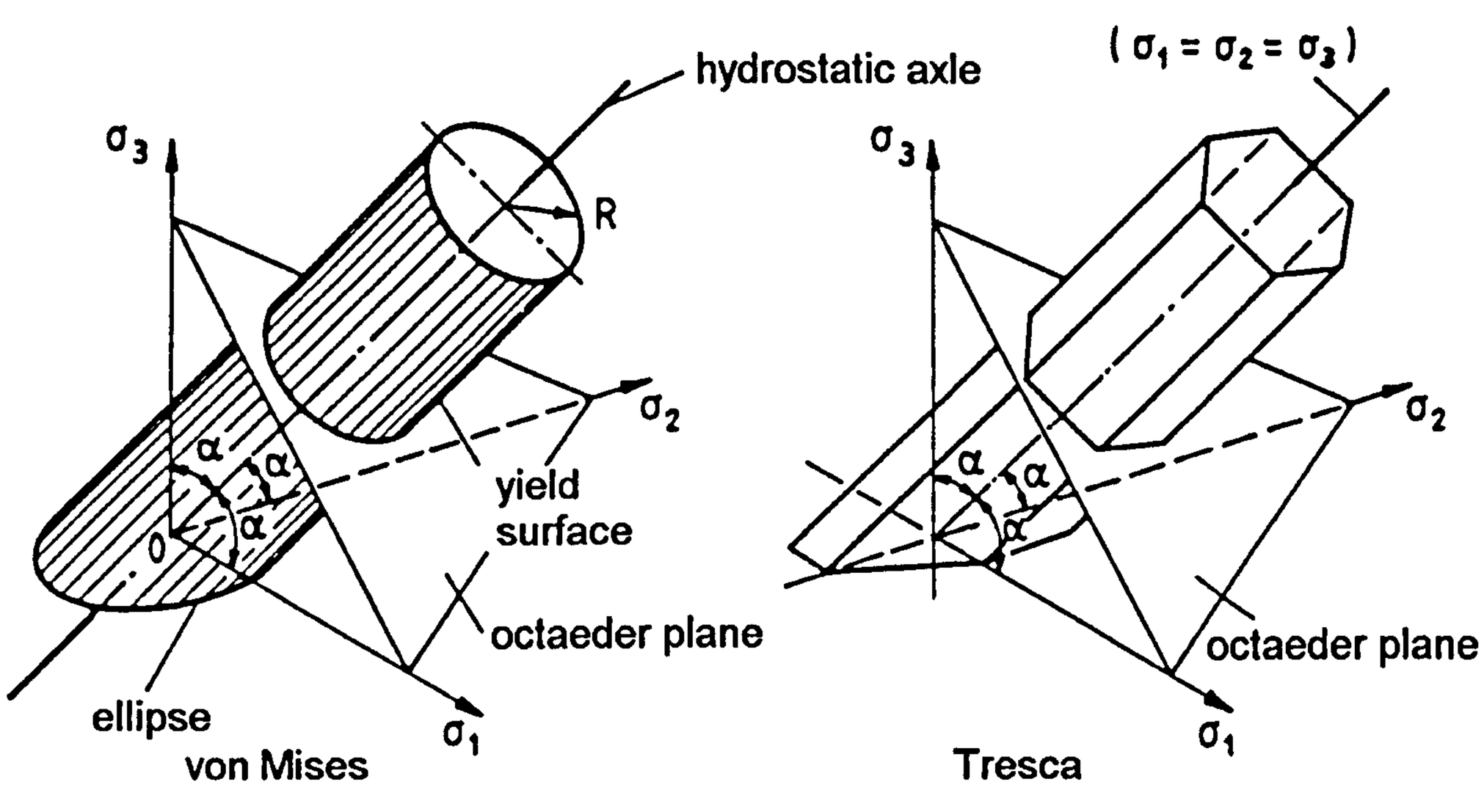

Figure 4-7 Yield Surface (v. Mises, Tresca)

Multi-axial load
(e.g. rope-casting)

Single-axial load

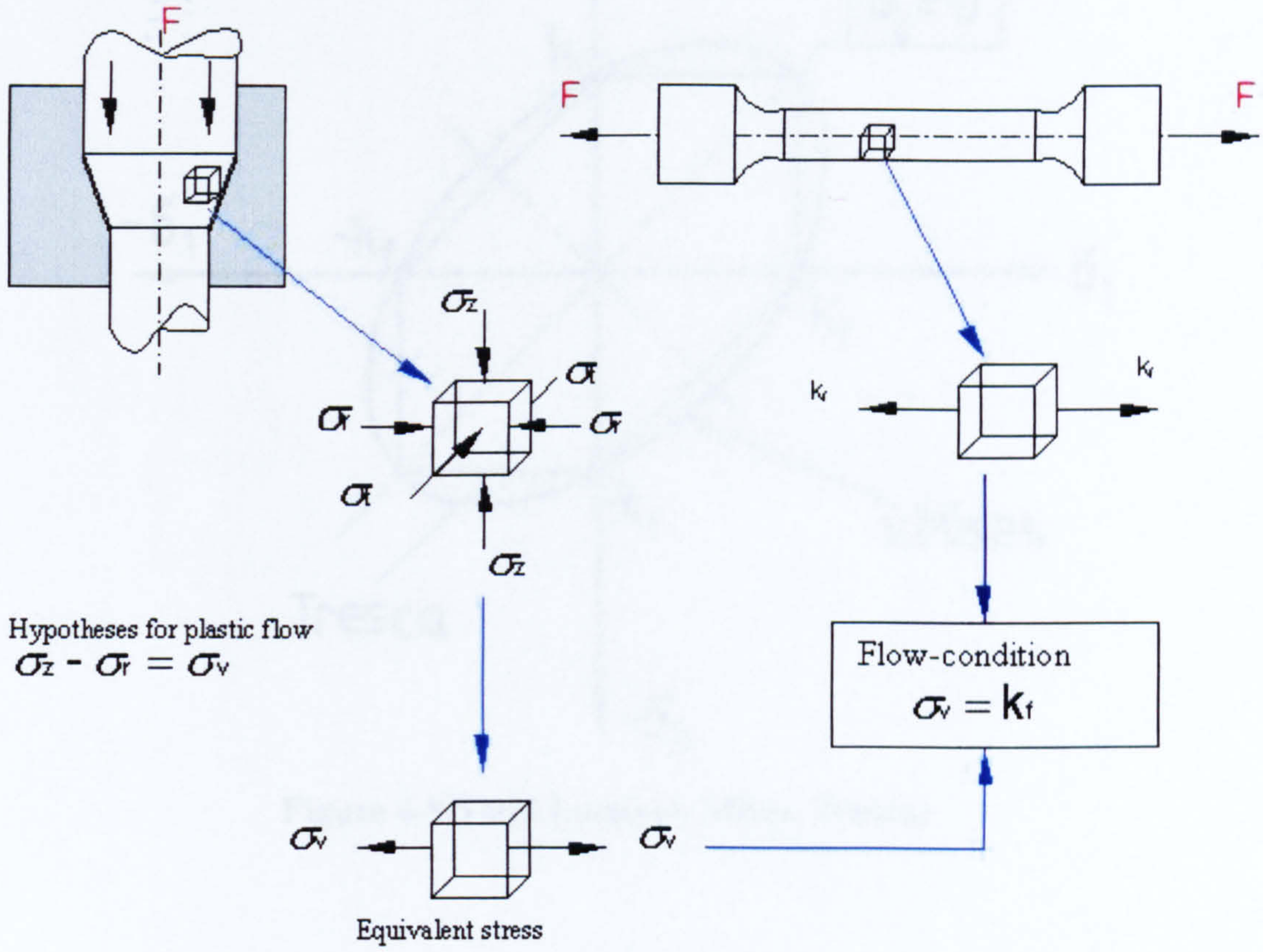

Figure 4-8 Universal Stress Condition

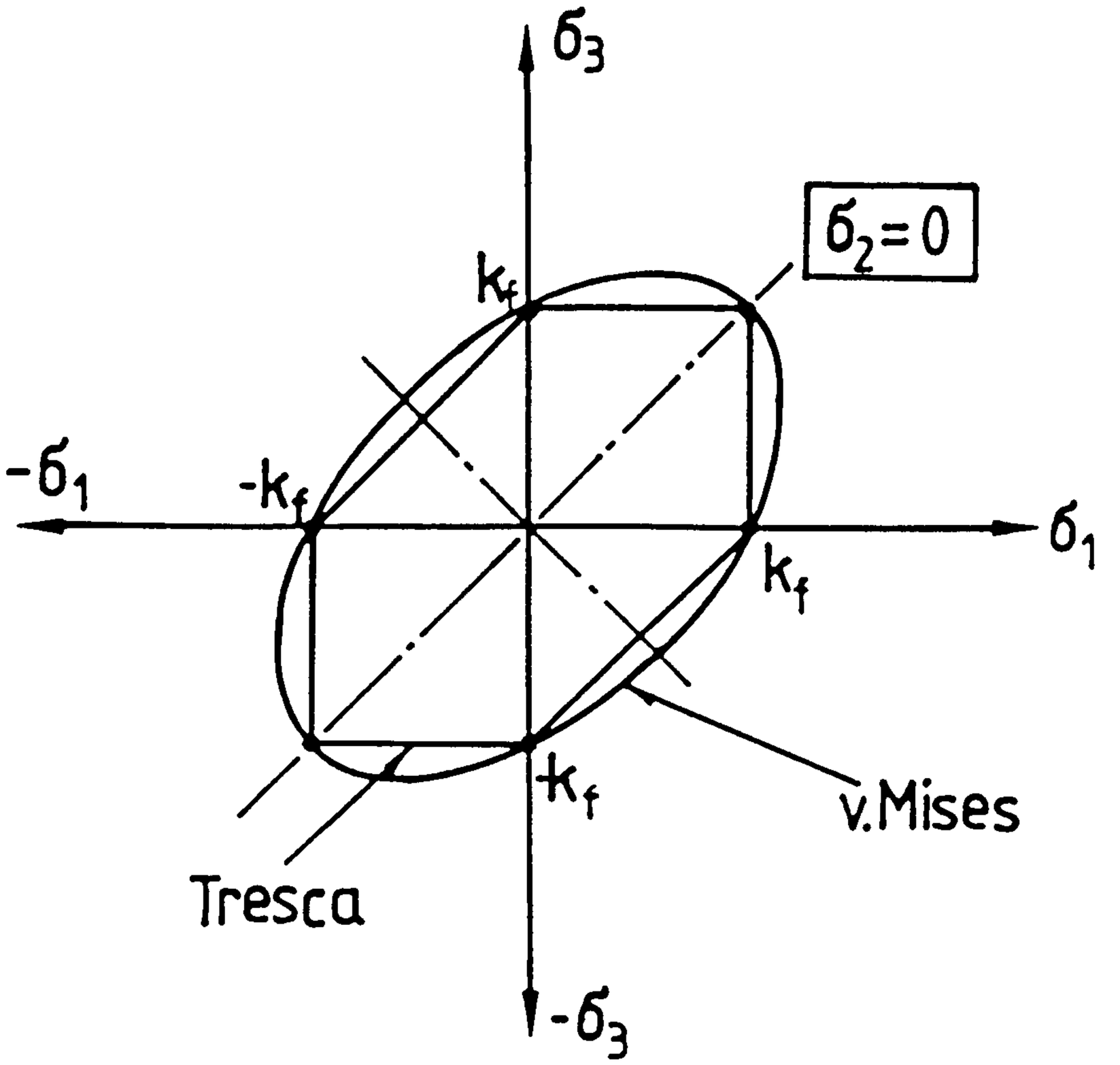

Figure 4-9 Yield Locus (v. Mises, Tresca)

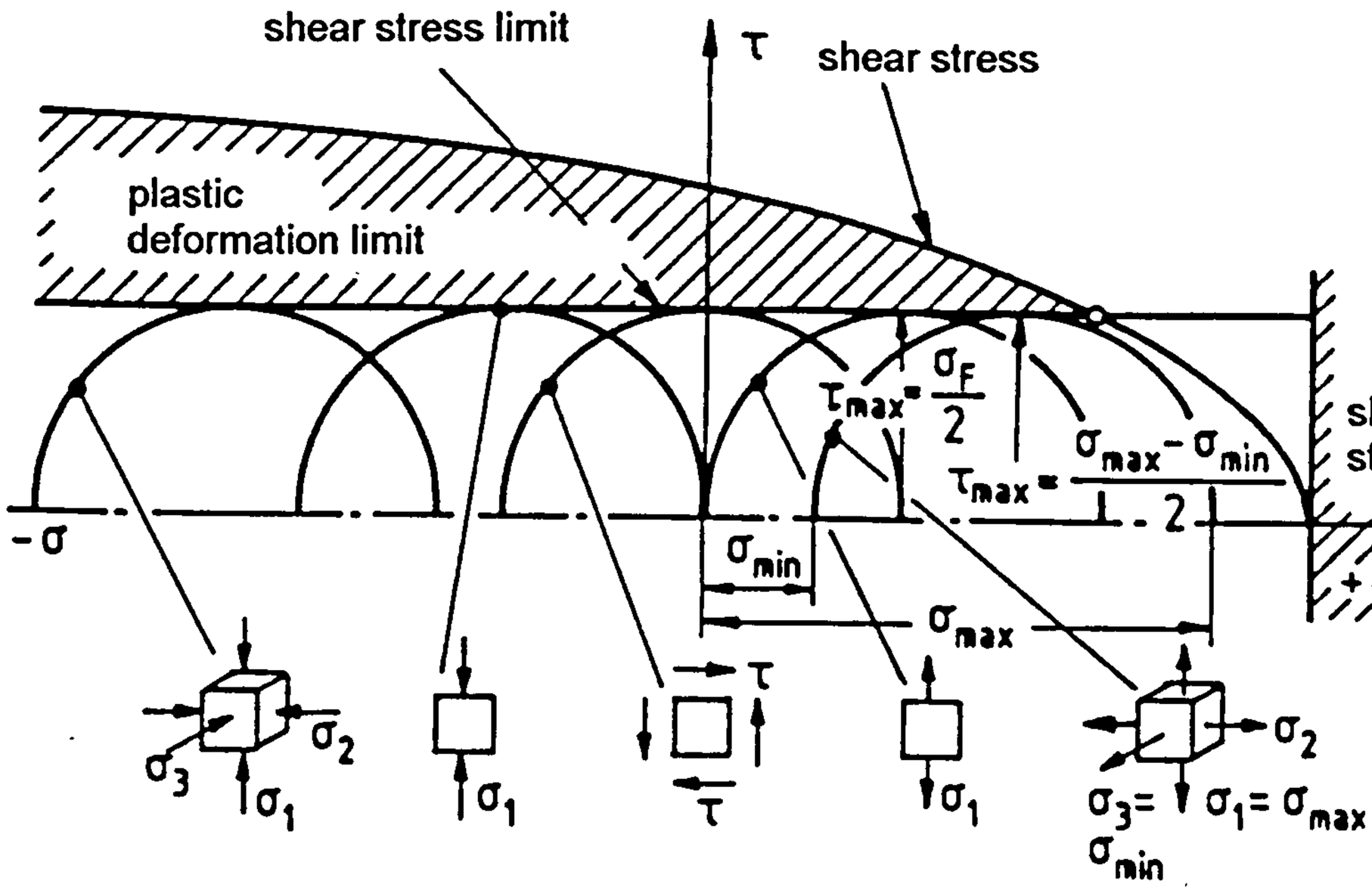

Figure 4-10 Influence of the Stress Condition at the Shear Strength

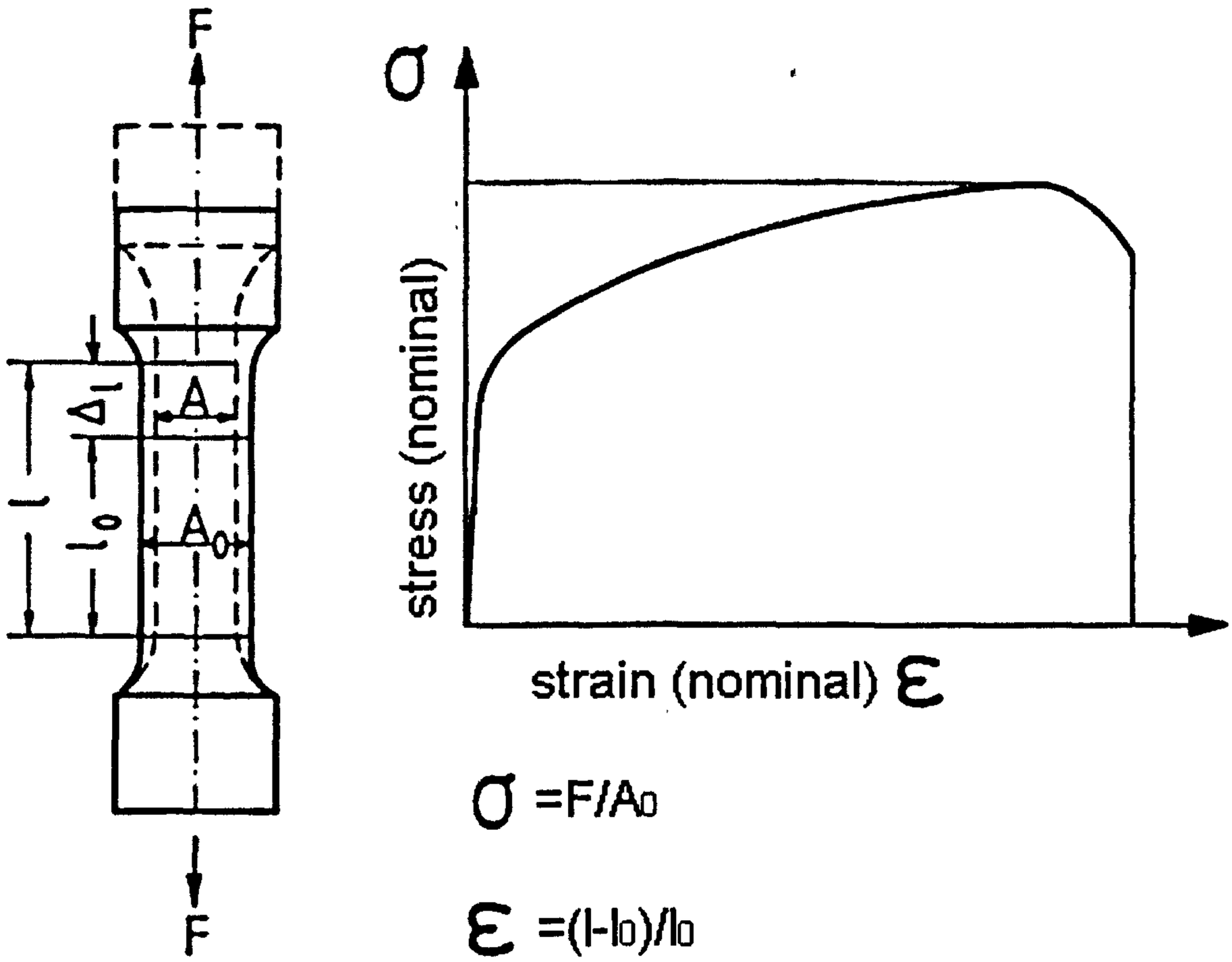

Figure 4-11 Stress - Strain Diagram

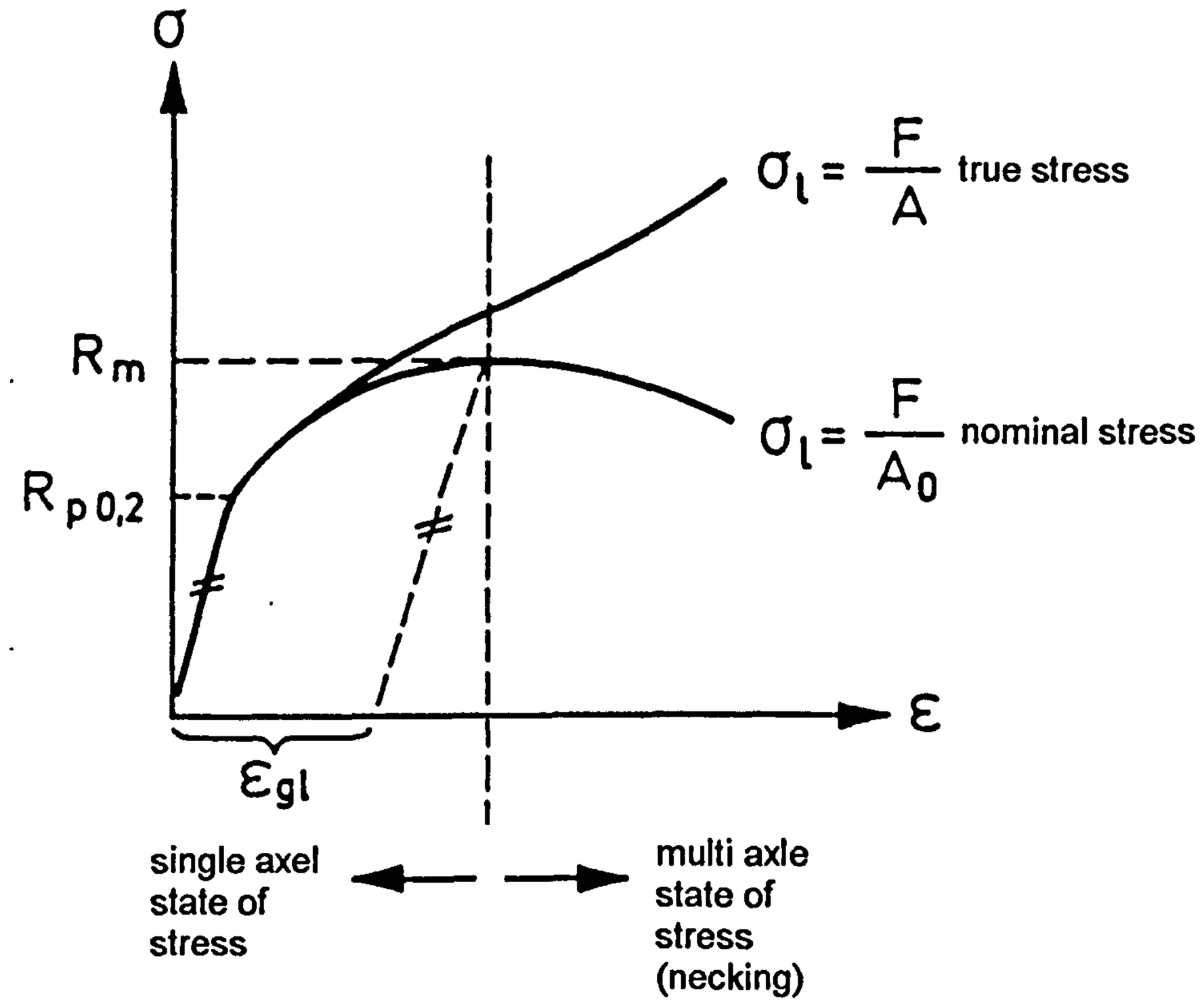

Figure 4-12 True Stress and Yield Stress

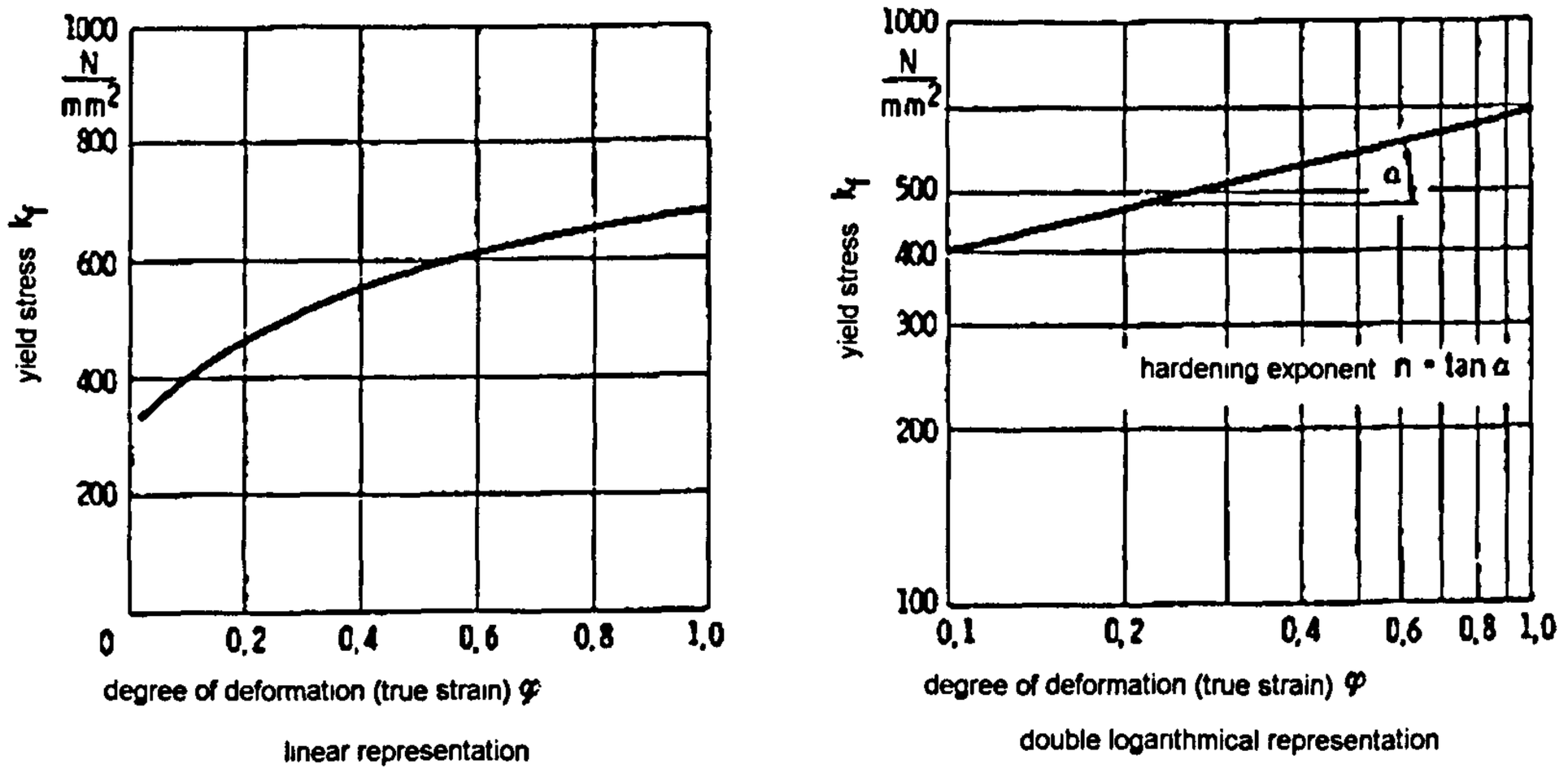

Figure 4-13 Flow-Curve and Hardening Exponent n

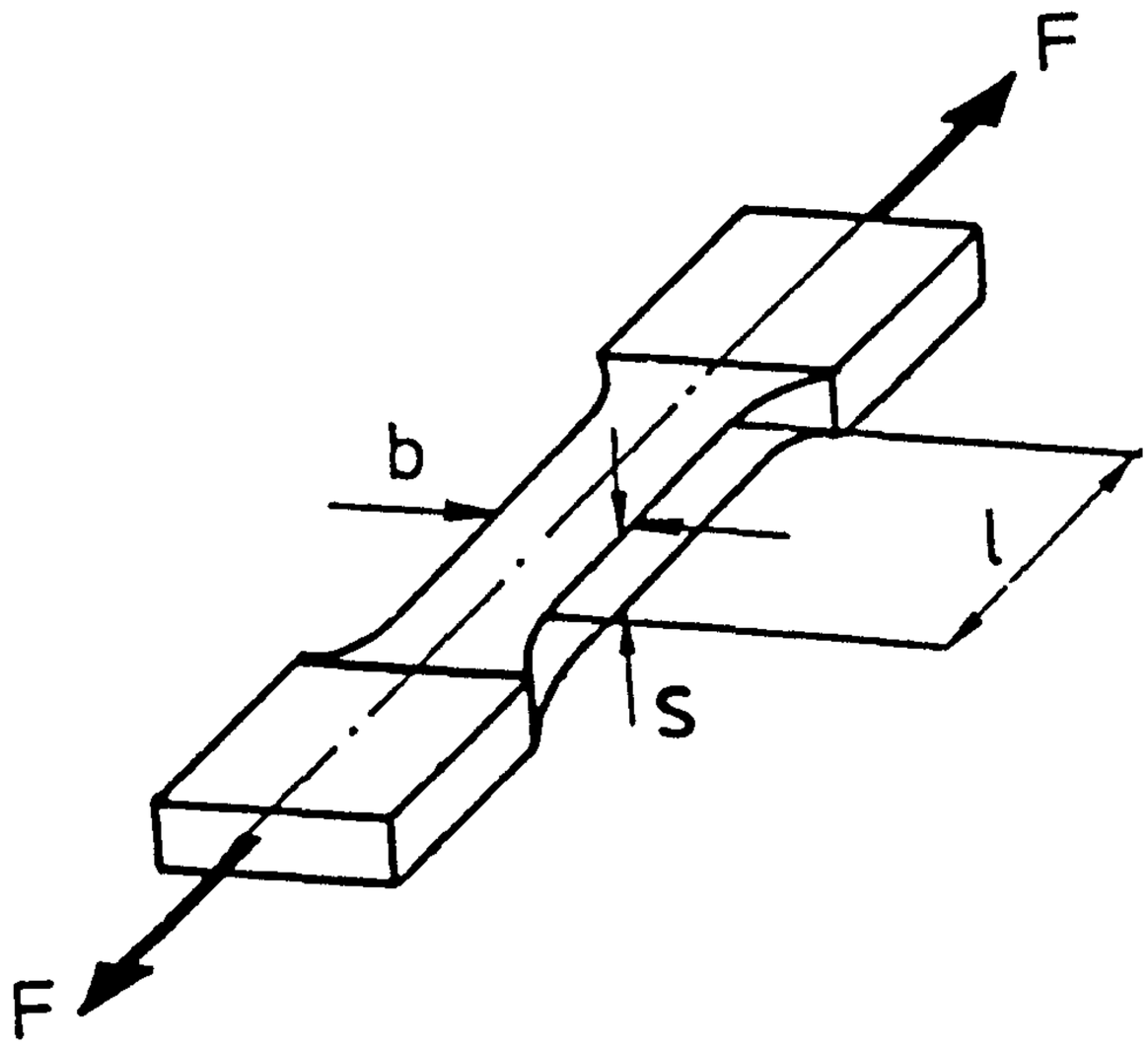

Figure 4-14 Determination of the Perpendicularly anisotropy r with the Traction Test

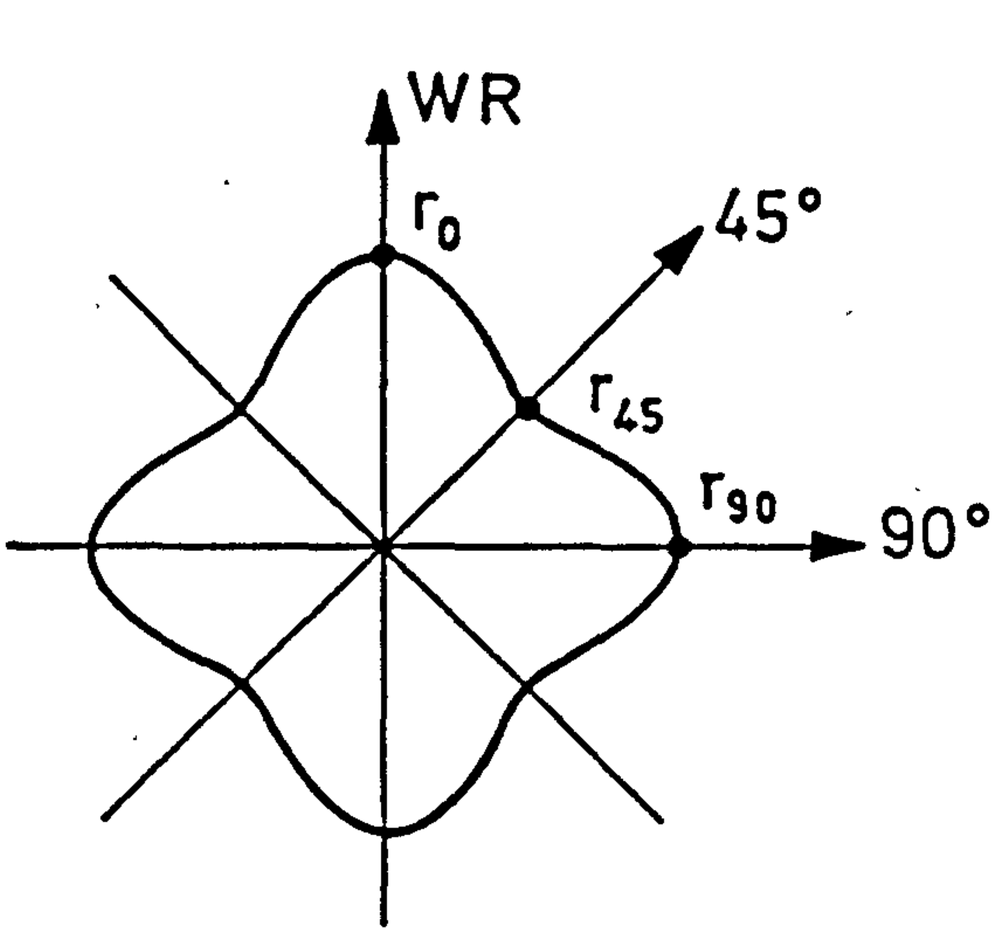

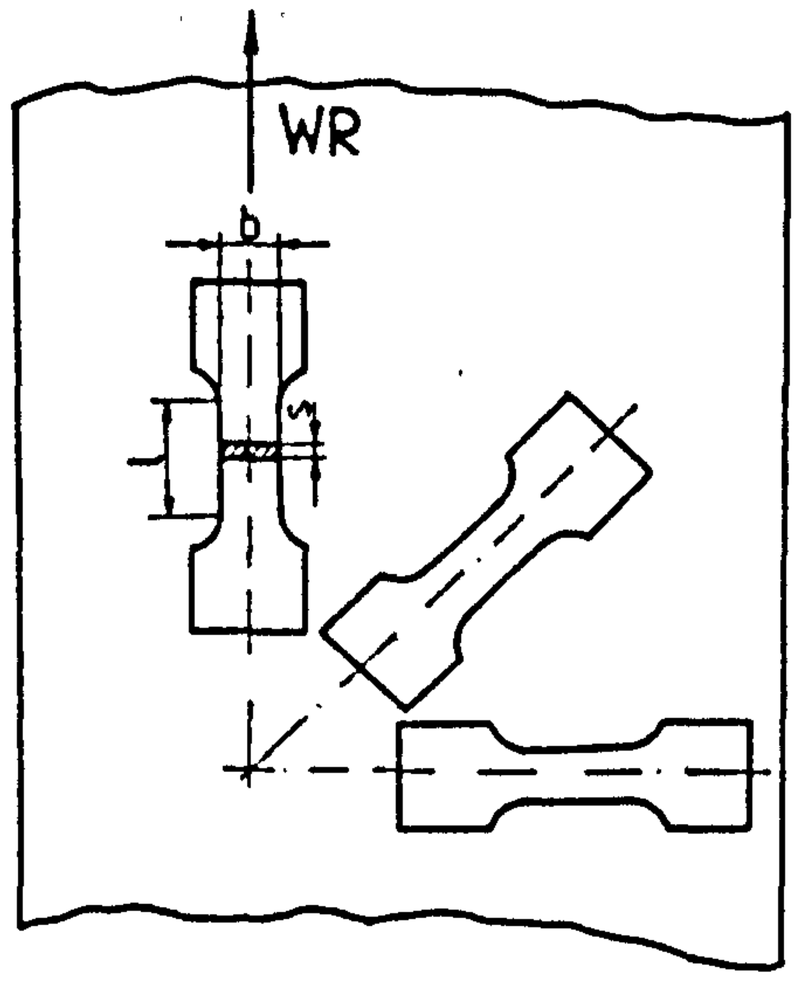

Figure 4-15 Arrangement of the Traction Test Rehearse, which are taken out of the Sheet

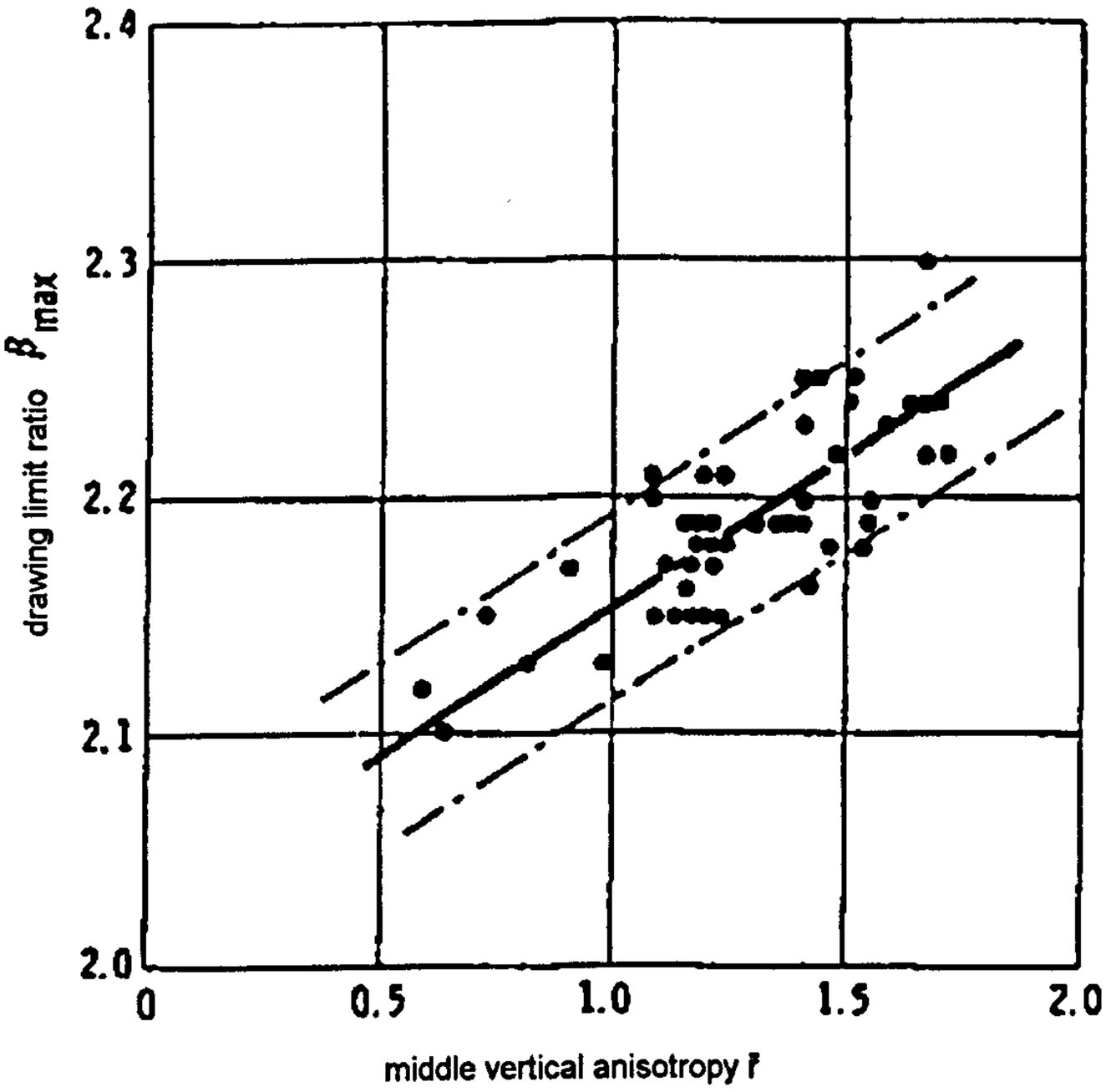

Figure 4-16 Effect of the Perpendicularly Anisotropy onto the Forming Limit

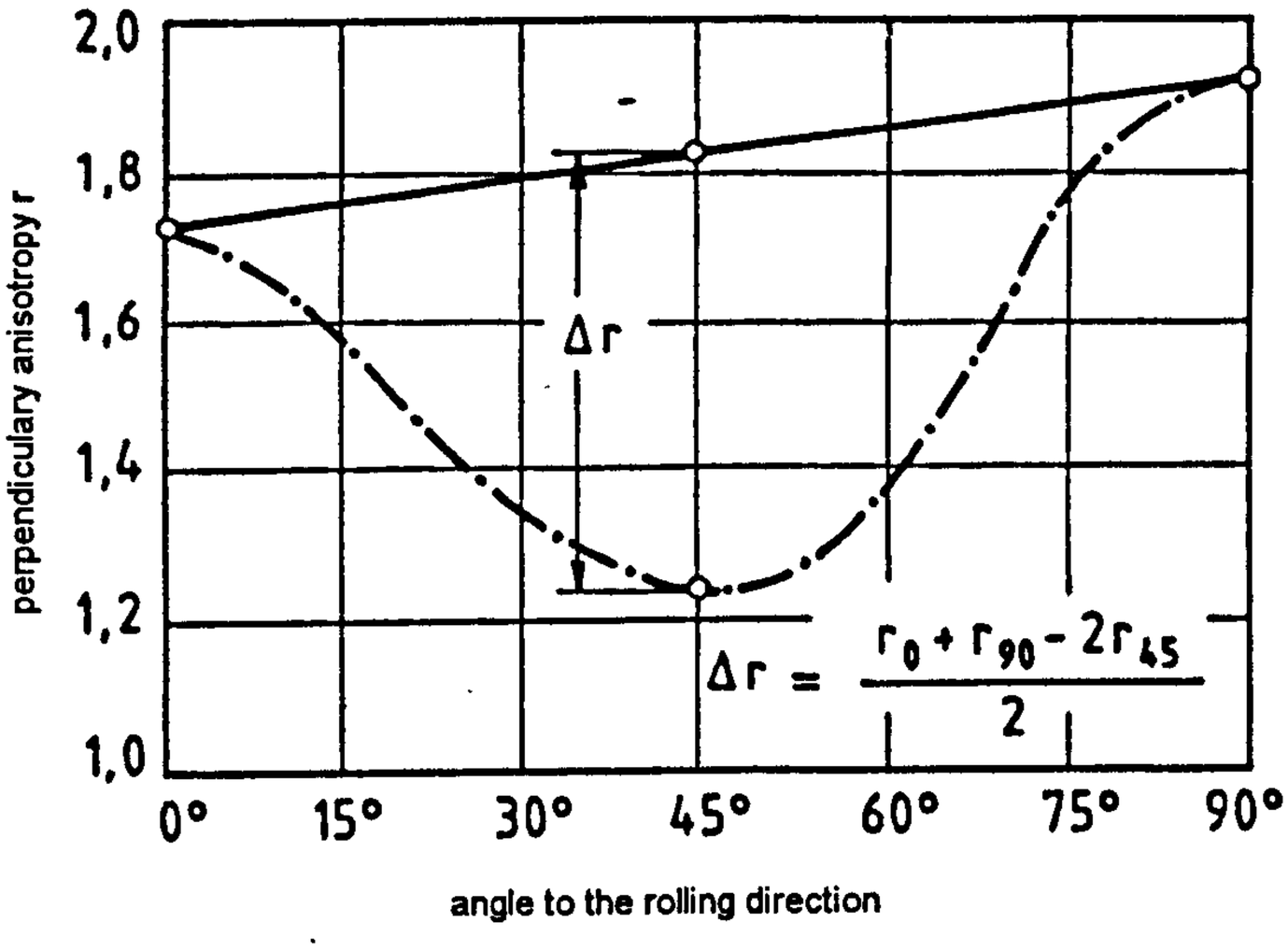

Figure 4-17 Perpendicularly Anisotropy dependency of the Rolling Direction

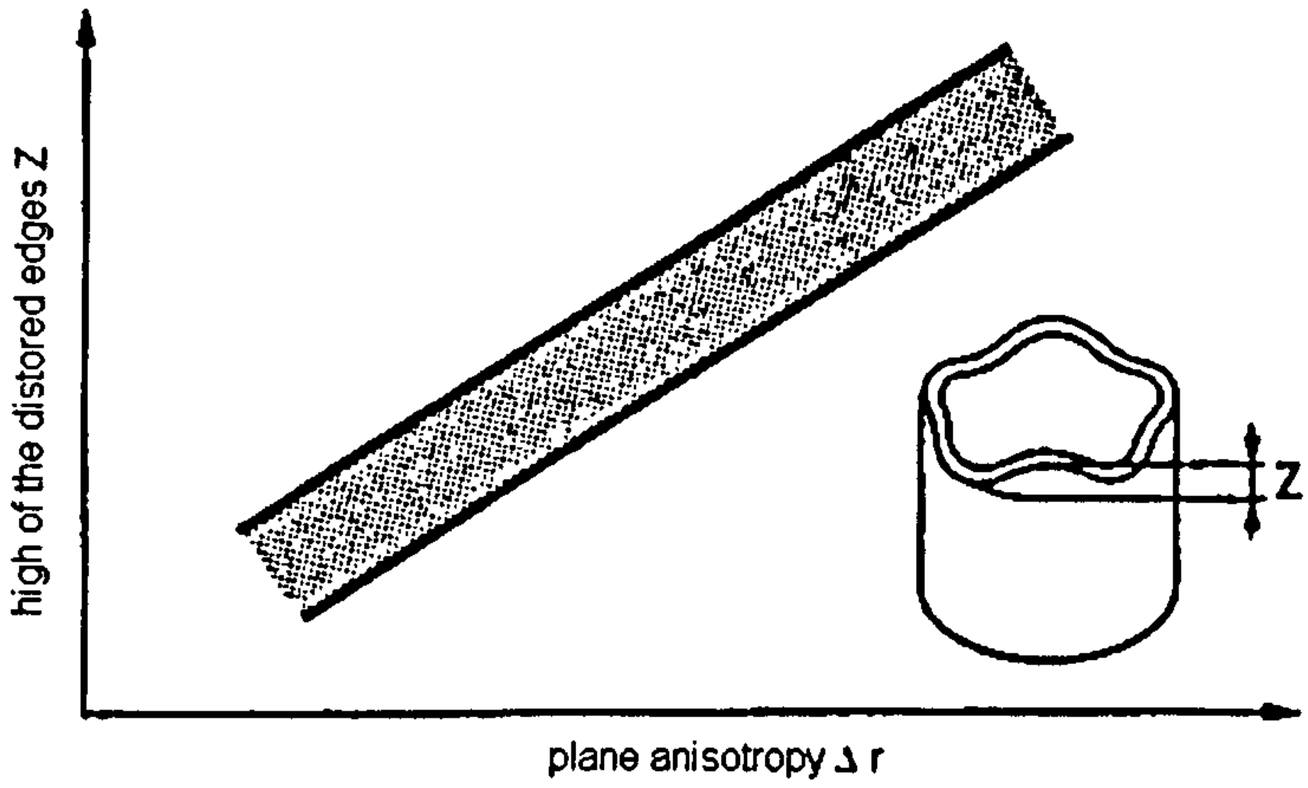

Figure 4-18 Plane Anisotropy

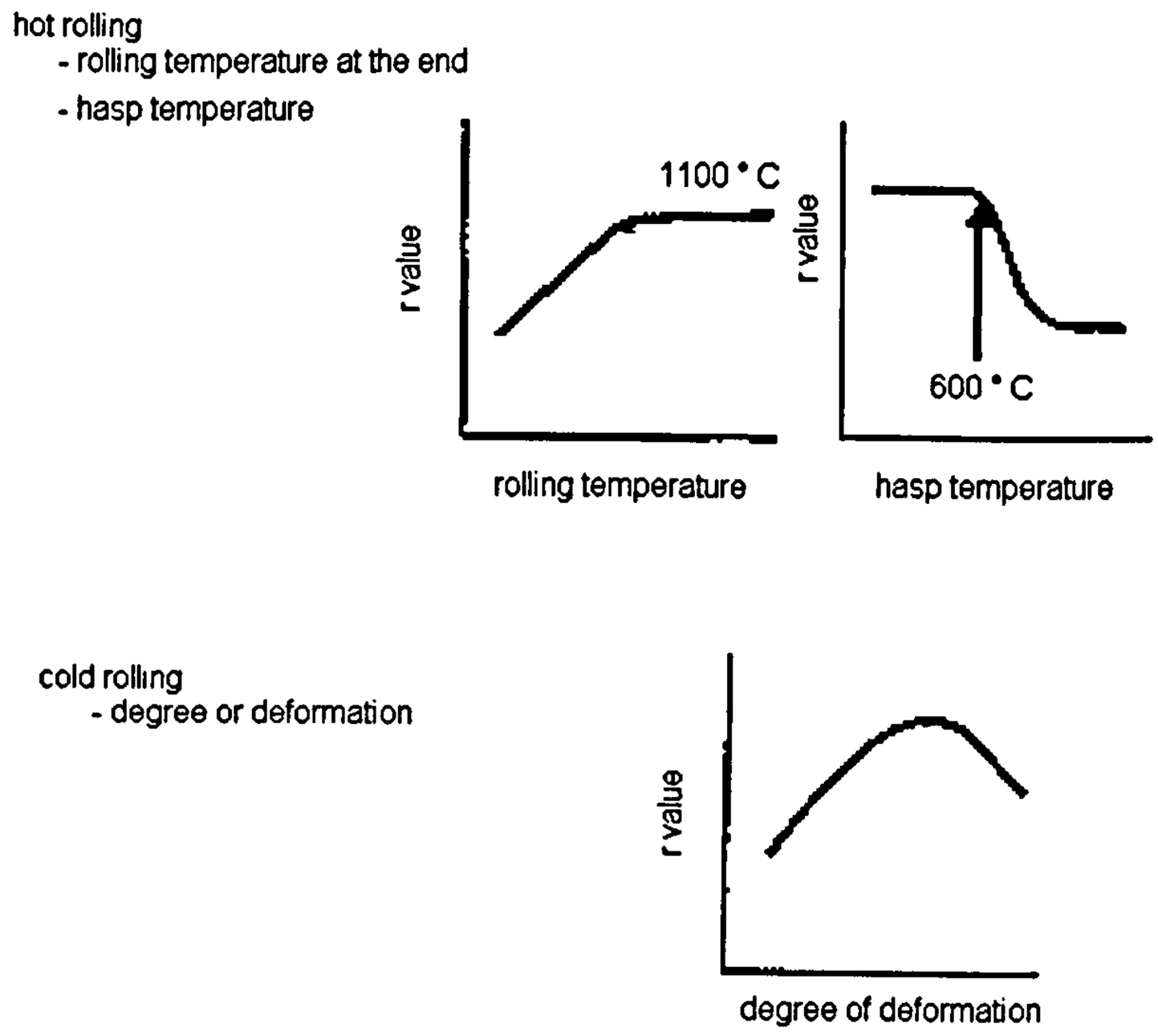

Figure 4-19 Possibilities of influencing the r Value

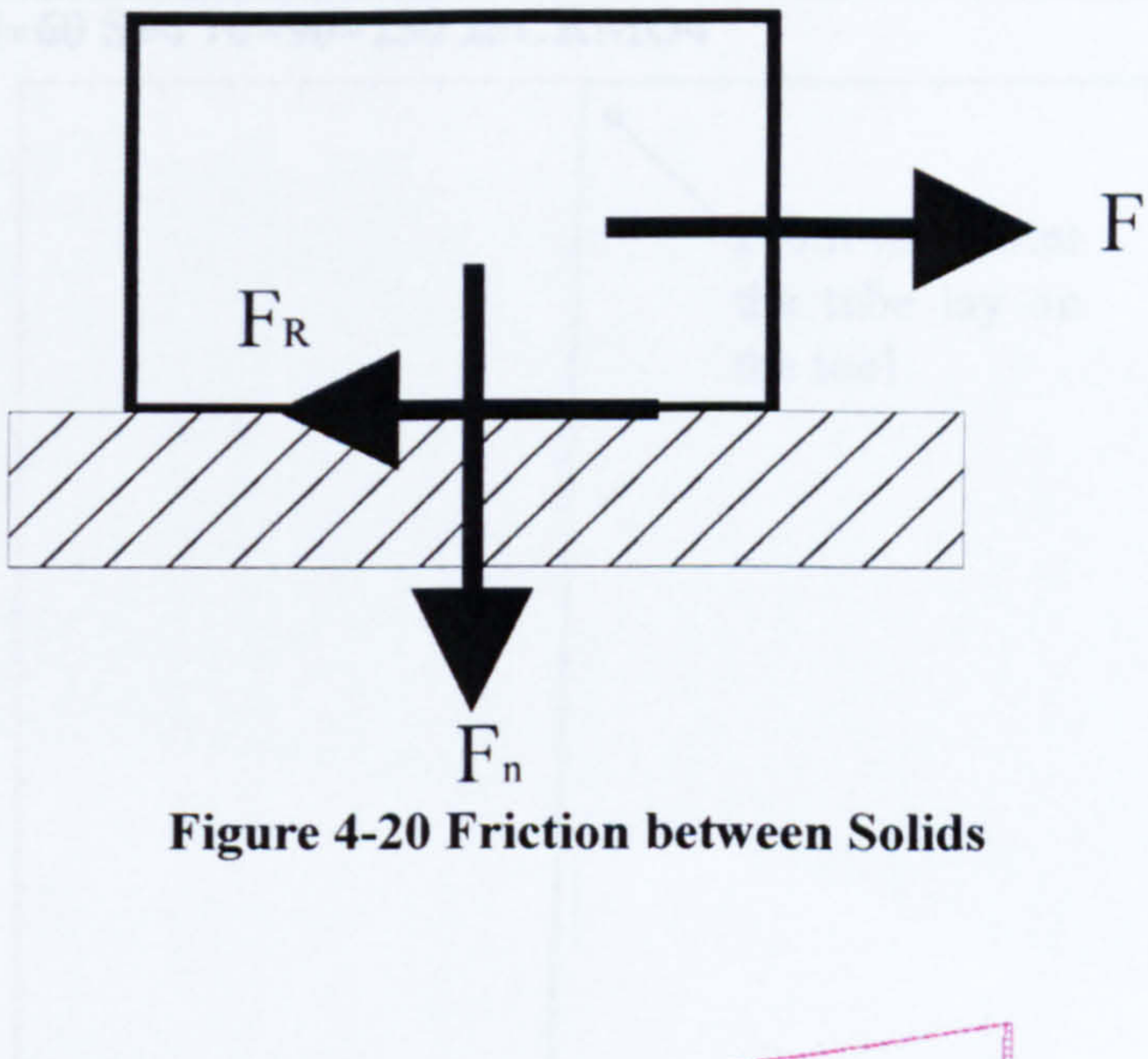

Figure 4-20 Friction between Solids

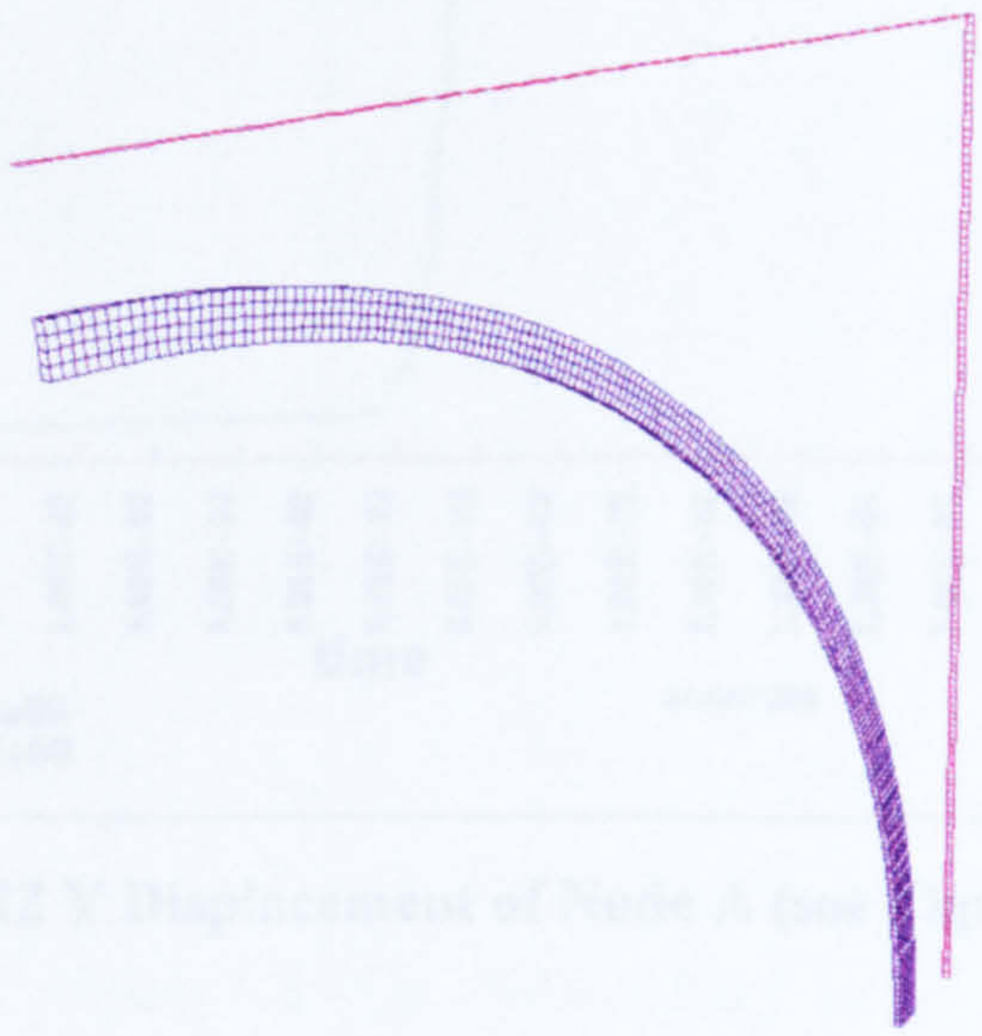

Figure 4-21 FE Model

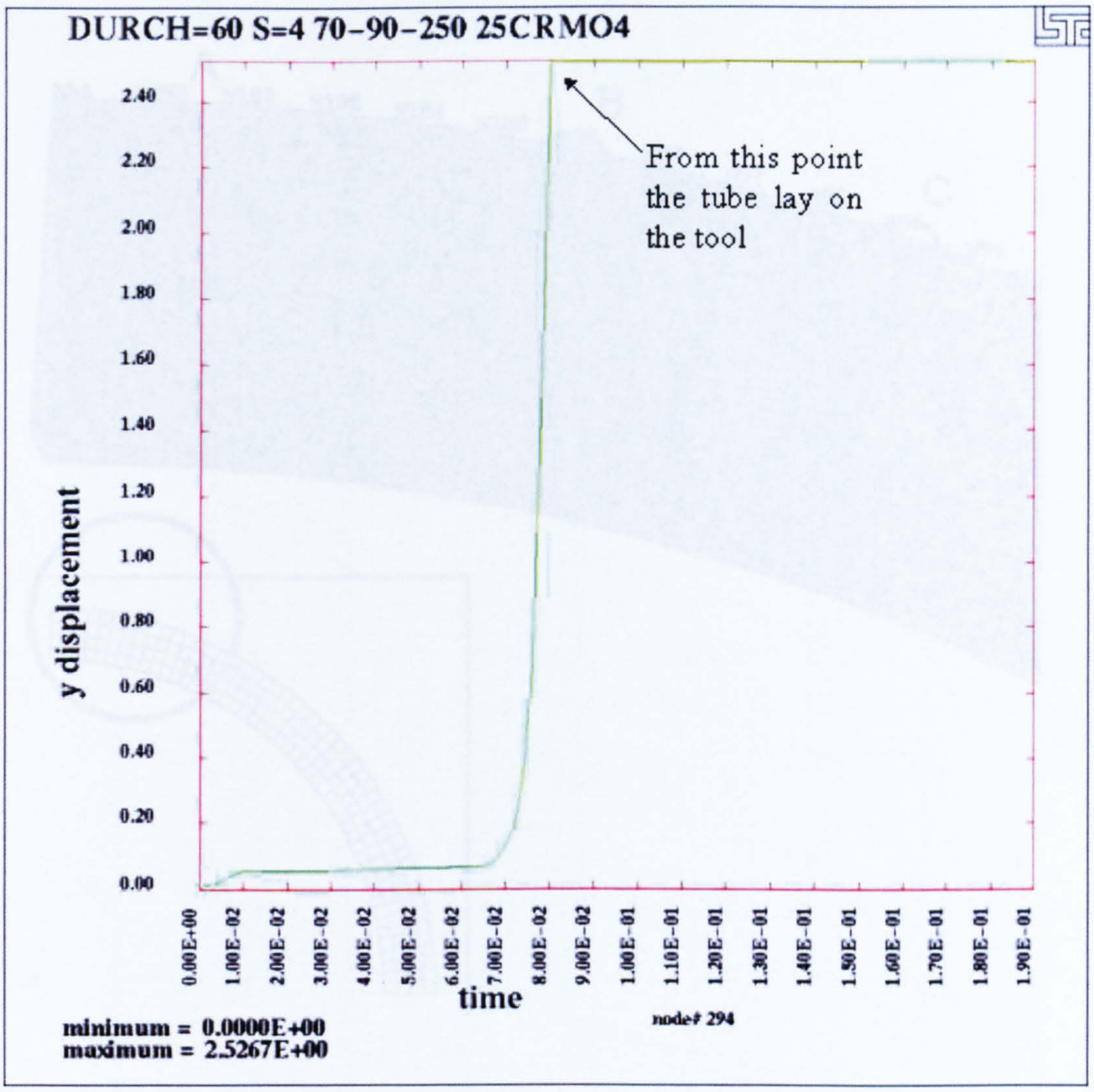

Figure 4-22 Y Displacement of Node A (see Figure 4.23)

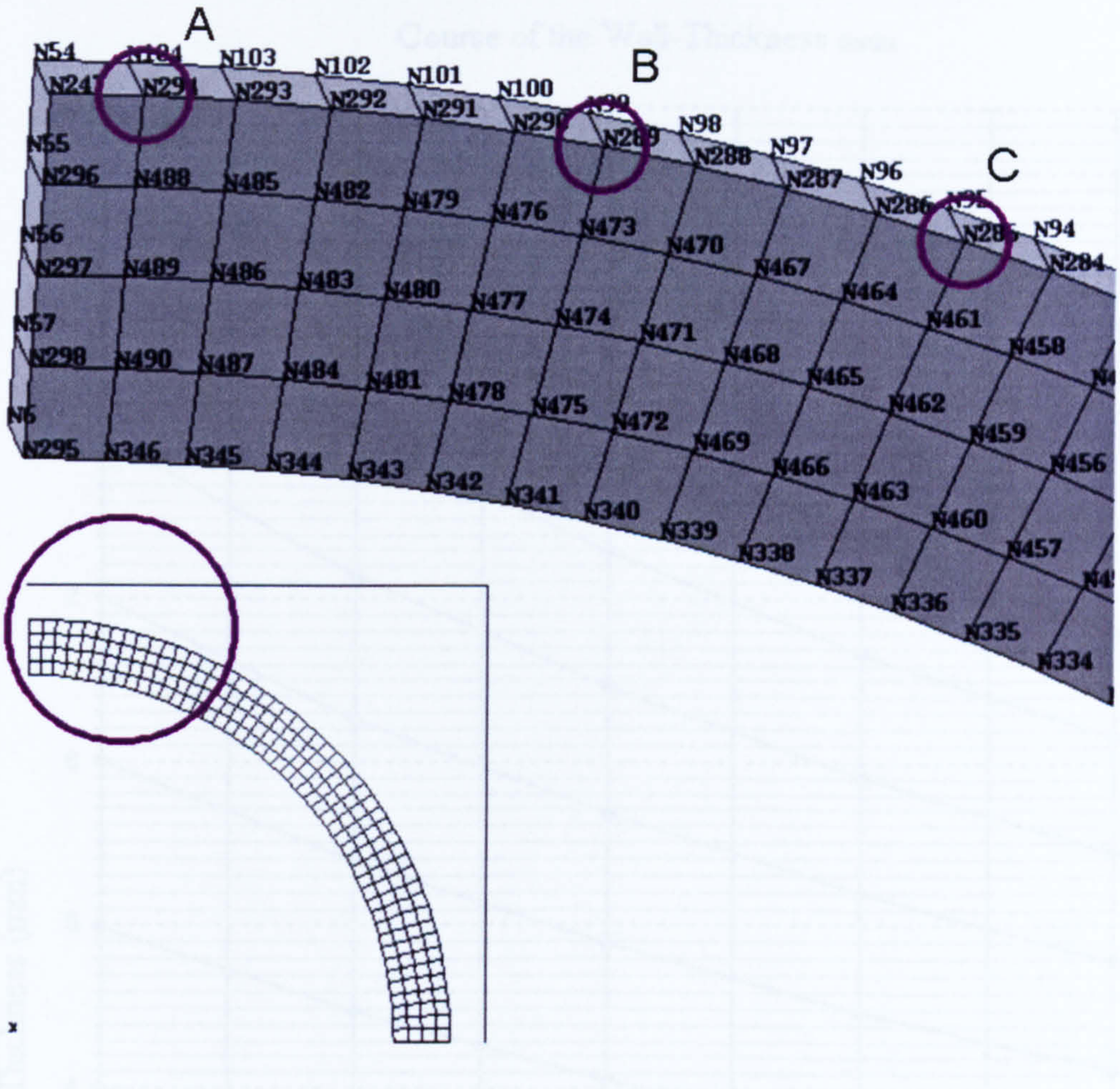

Figure 4-23 Location of the Nodes

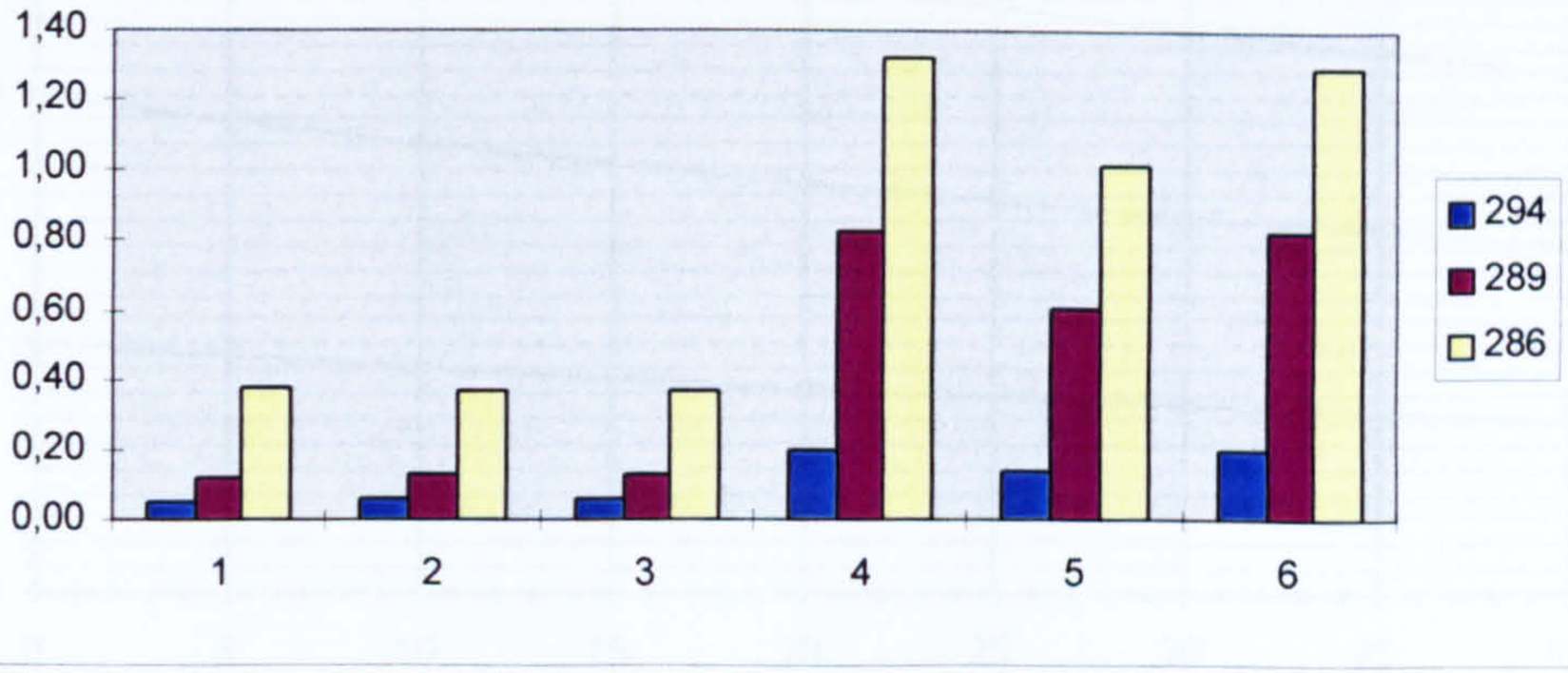

Figure 4-24 Diagram - Displacement of the Nodes for the 6 Cases

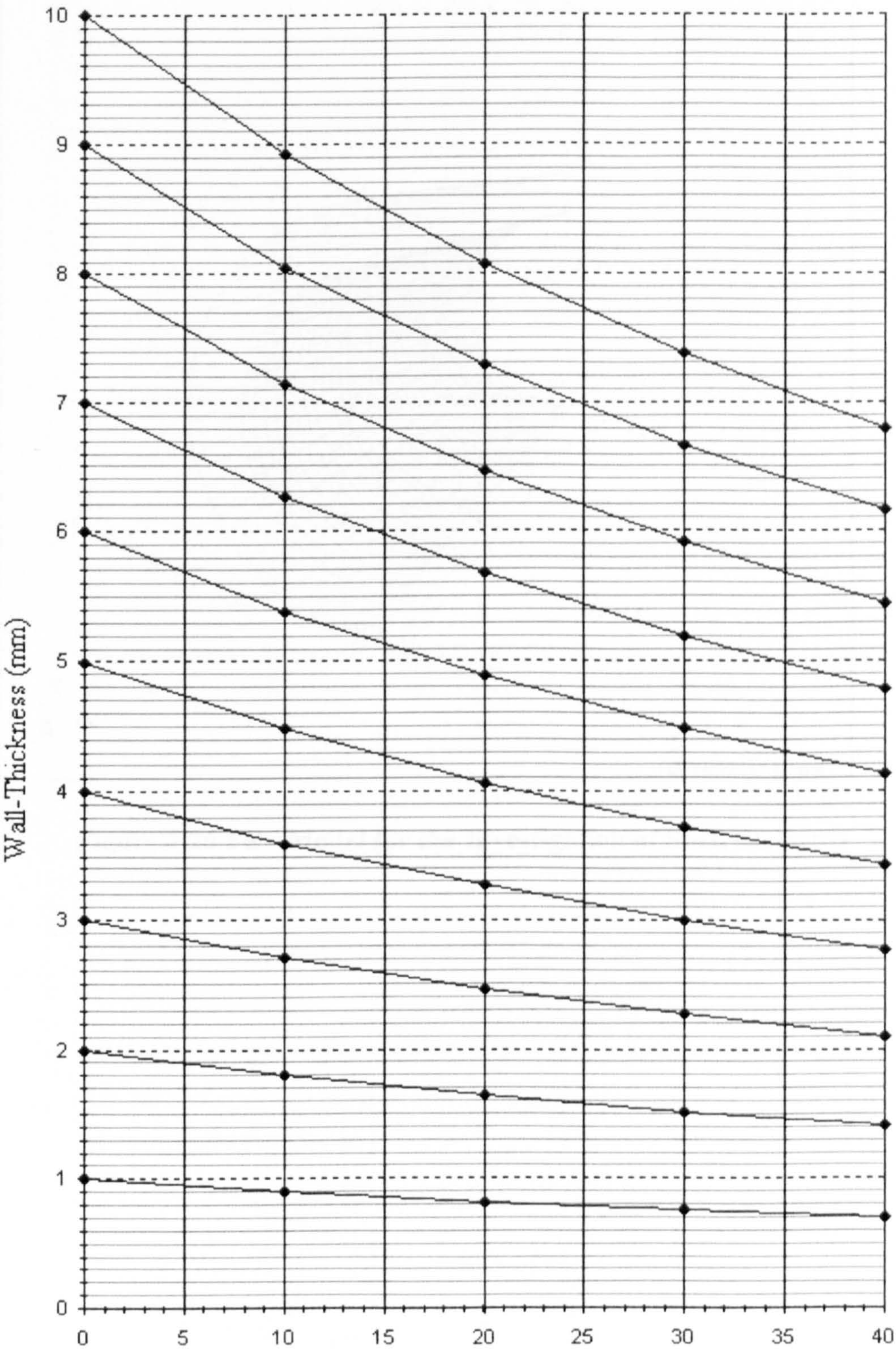

Figure 4-25 Course of the wall-thickness s_{min}

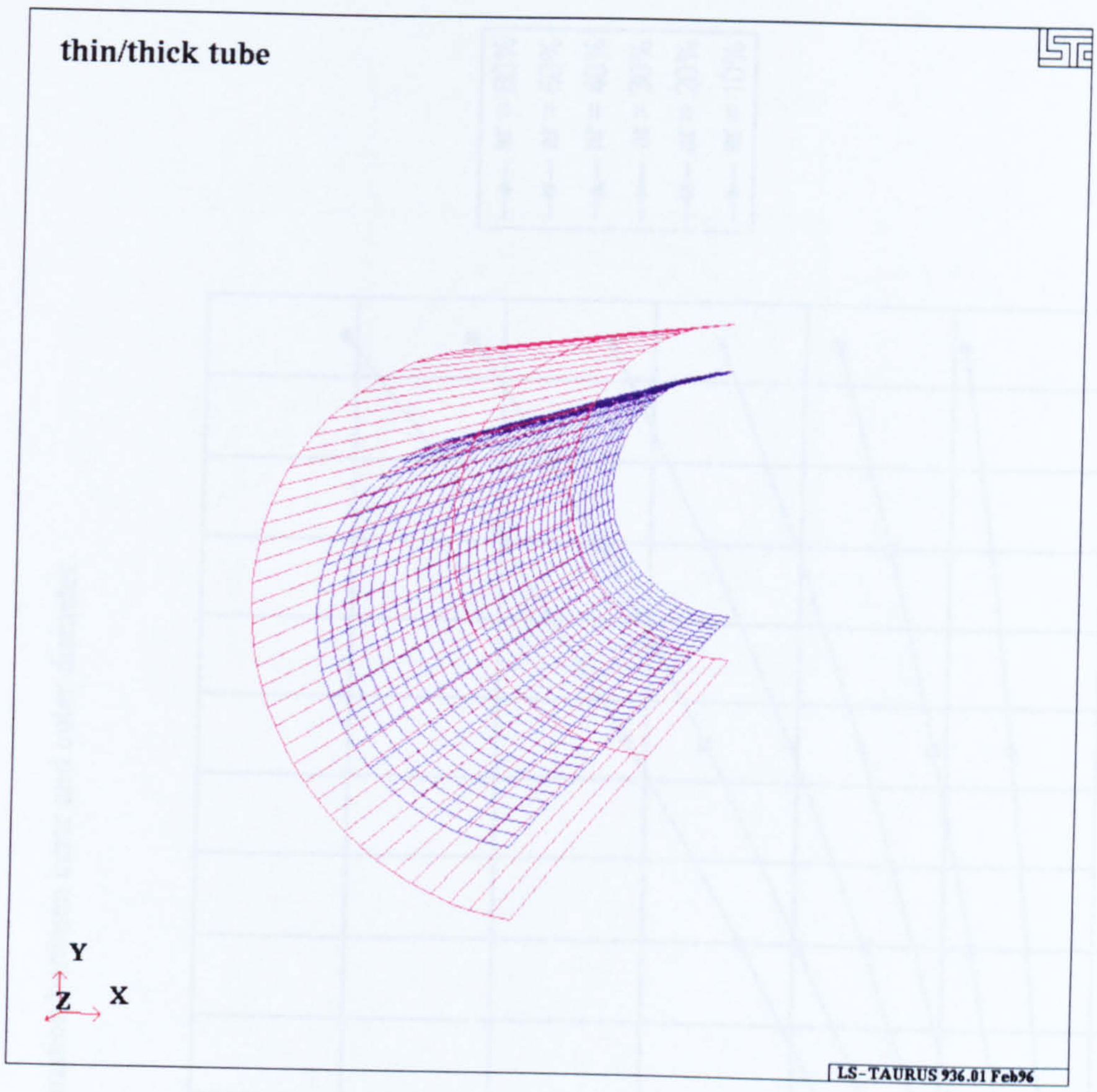

Figure 4-26 FE - Model for the Investigation of Shell Elements

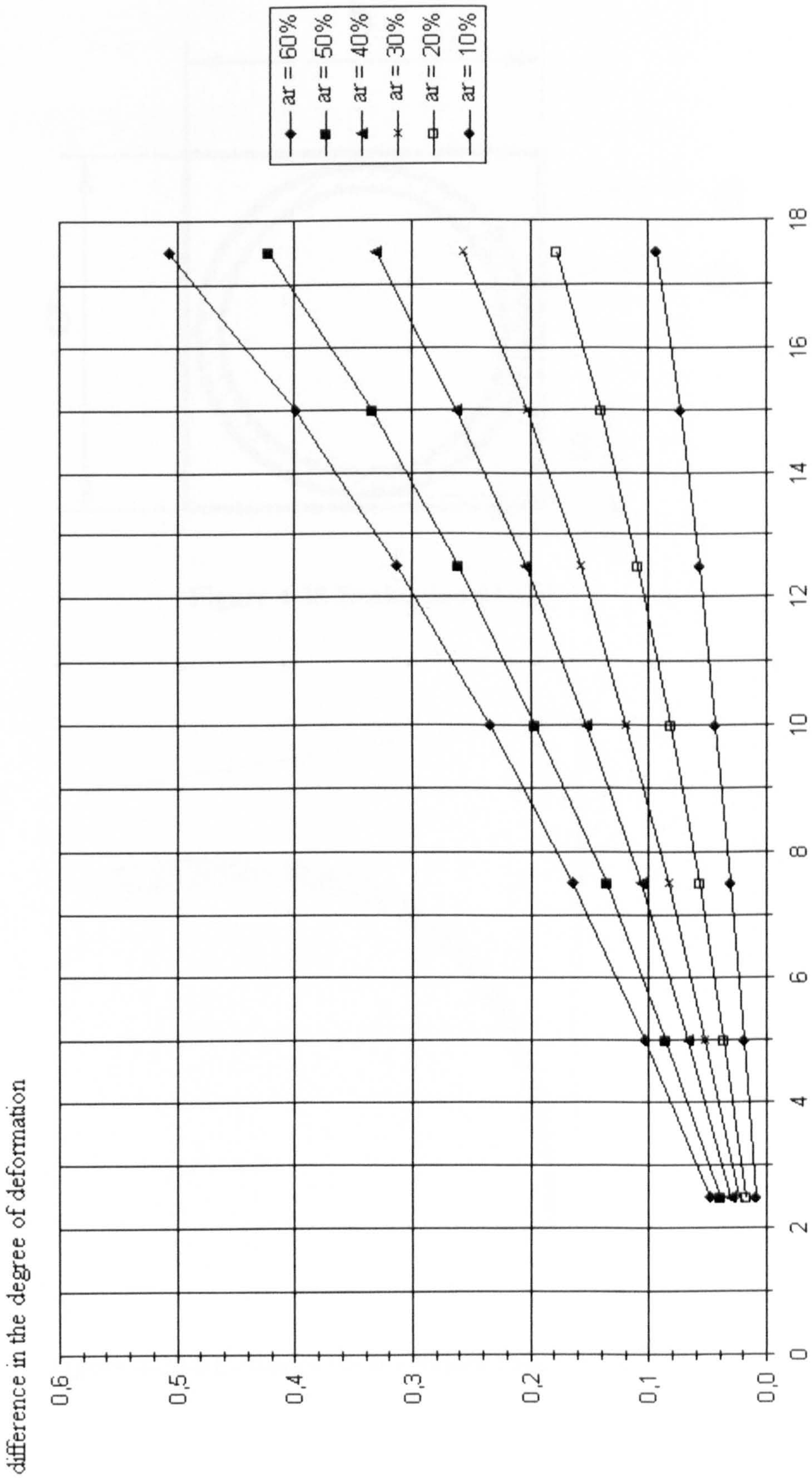

Figure 4-27 Difference in the Degree of Deformation

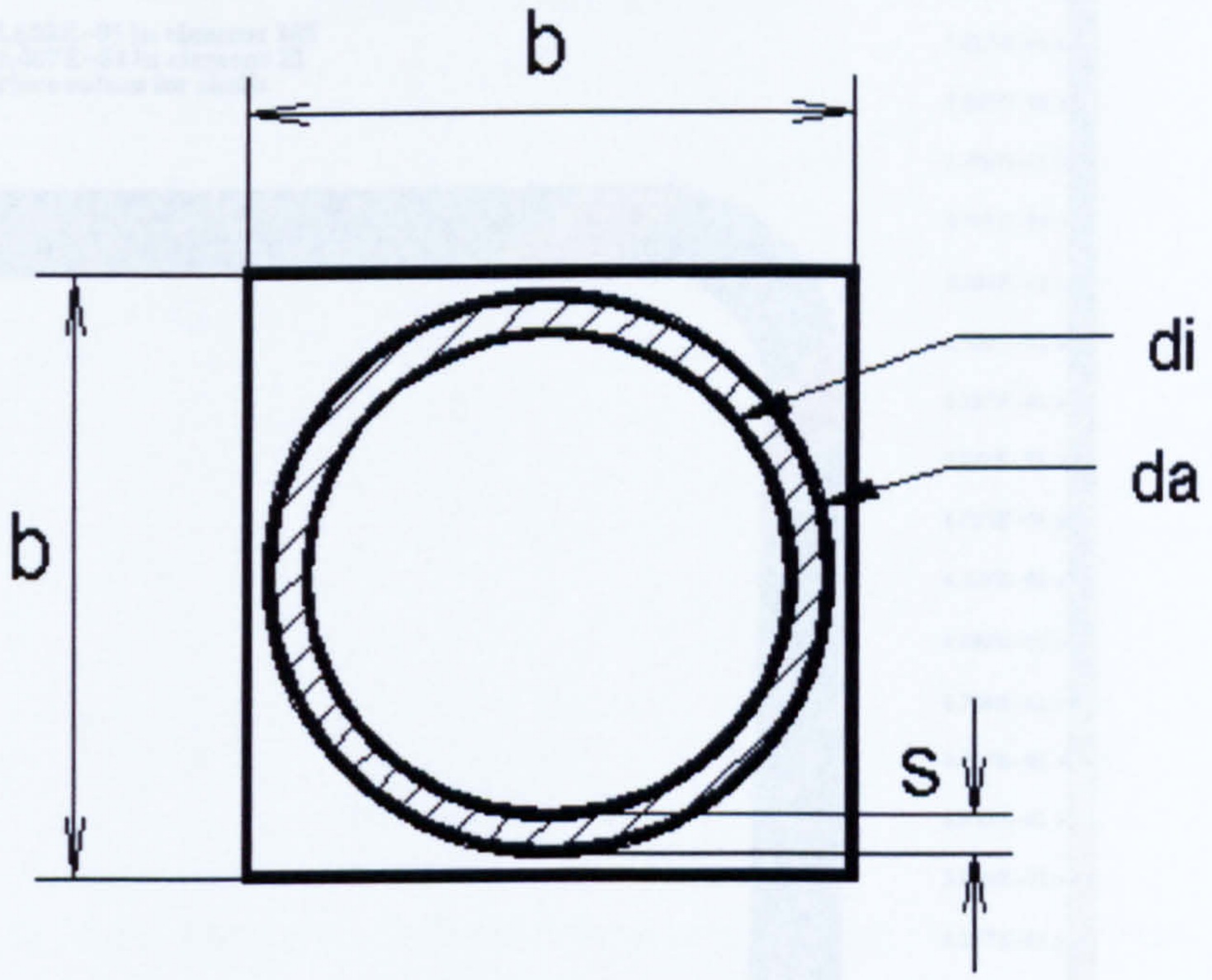

Figure 4-28 Evaluation Model

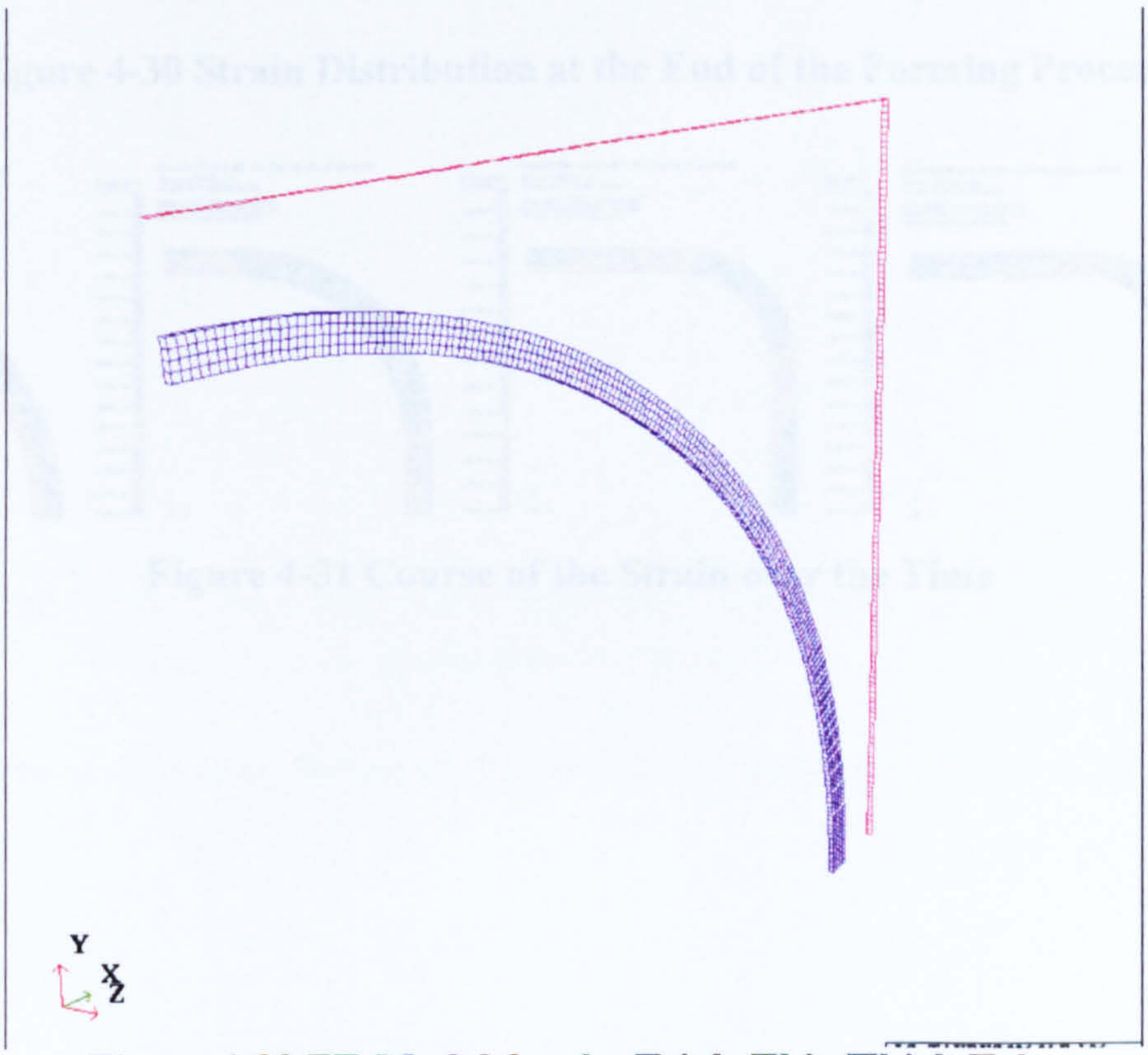

Figure 4-29 FE-Model for the Trials Thin/Thick Tube

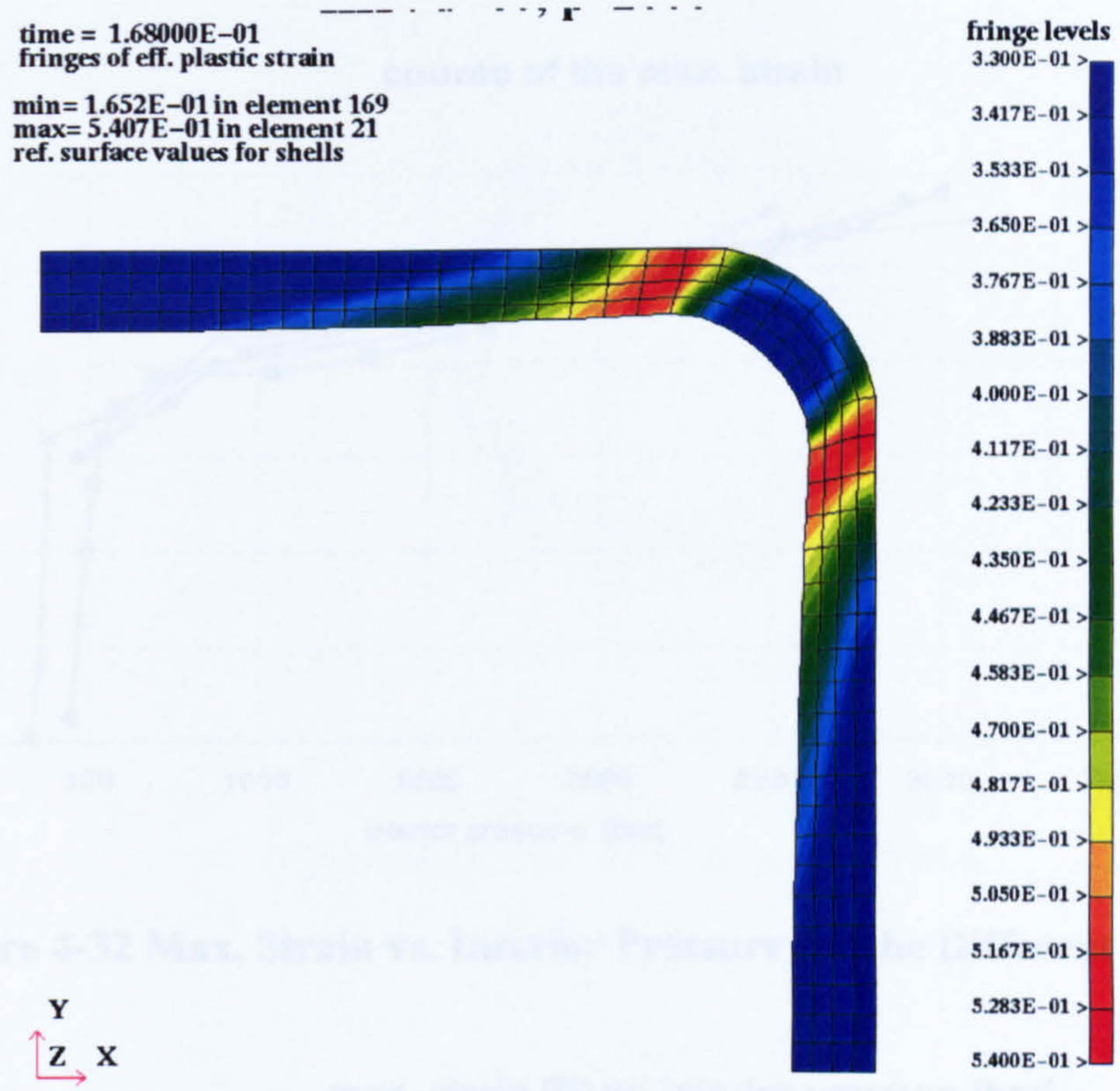

Figure 4-30 Strain Distribution at the End of the Forming Process

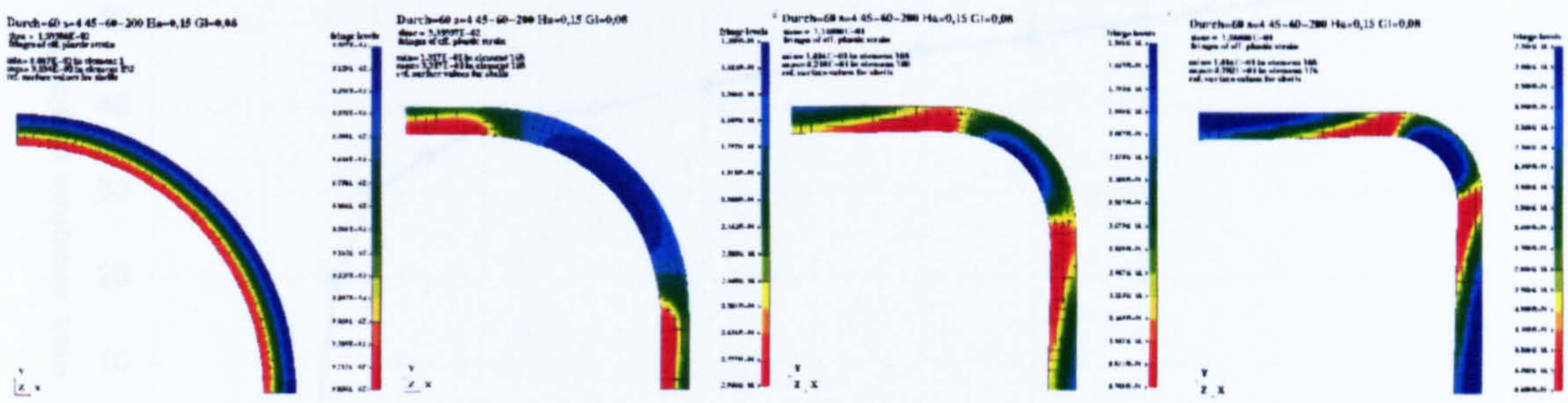

Figure 4-31 Course of the Strain over the Time

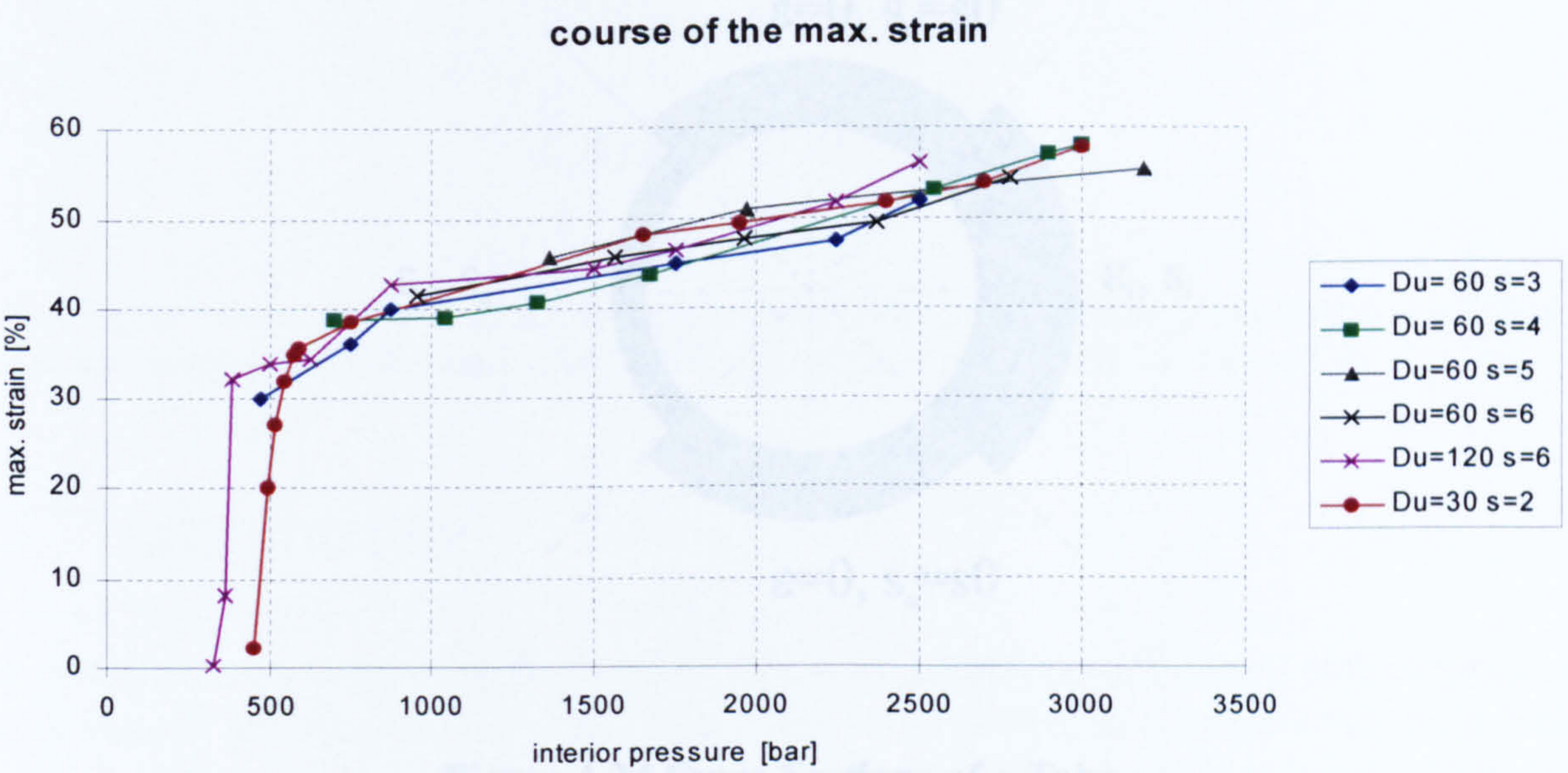

Figure 4-32 Max. Strain vs. Interior Pressure for the Different Test Trials

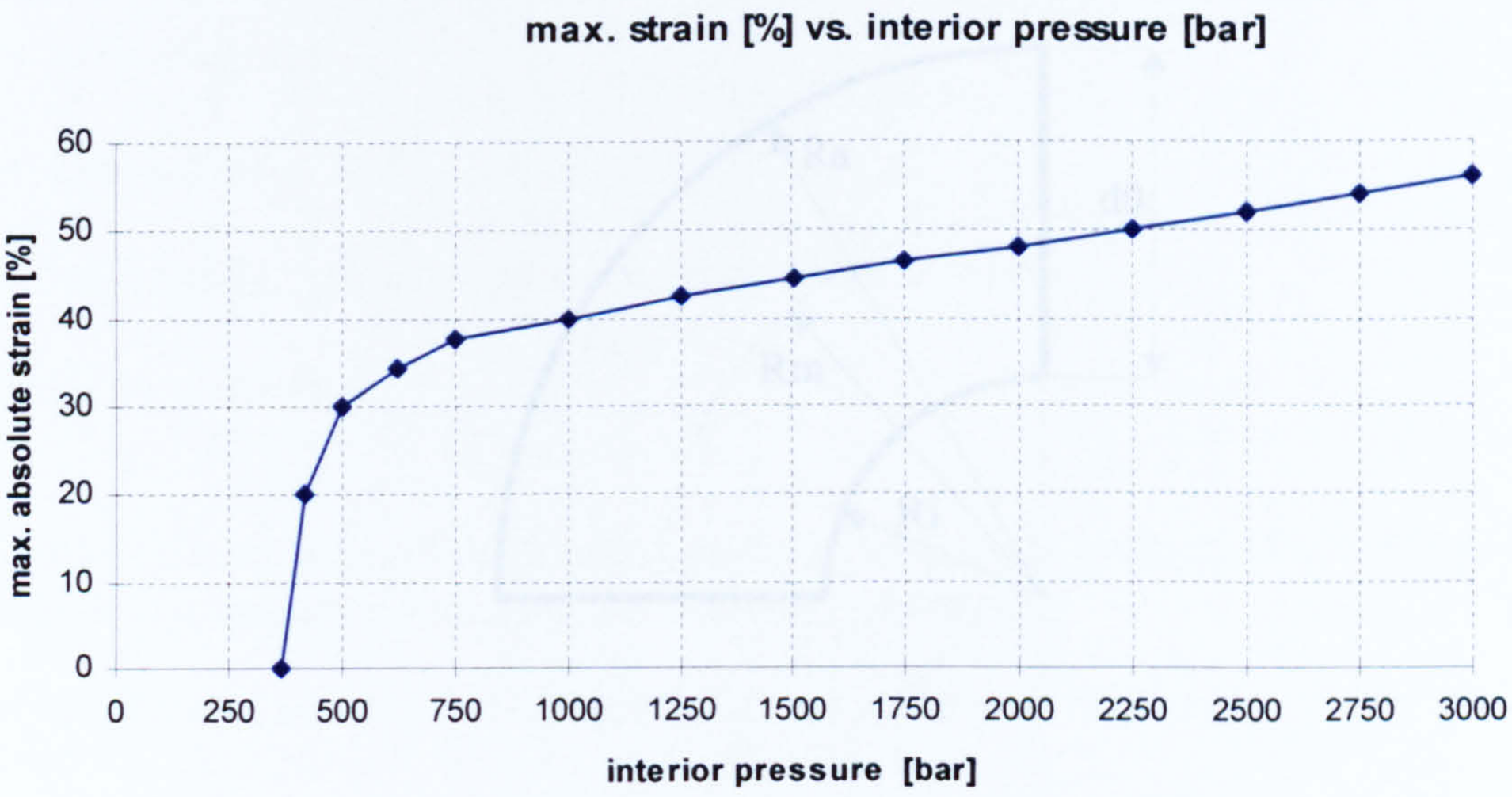

Figure 4-33 Max. Strain vs. Interior pressure (Interpolated Curve)

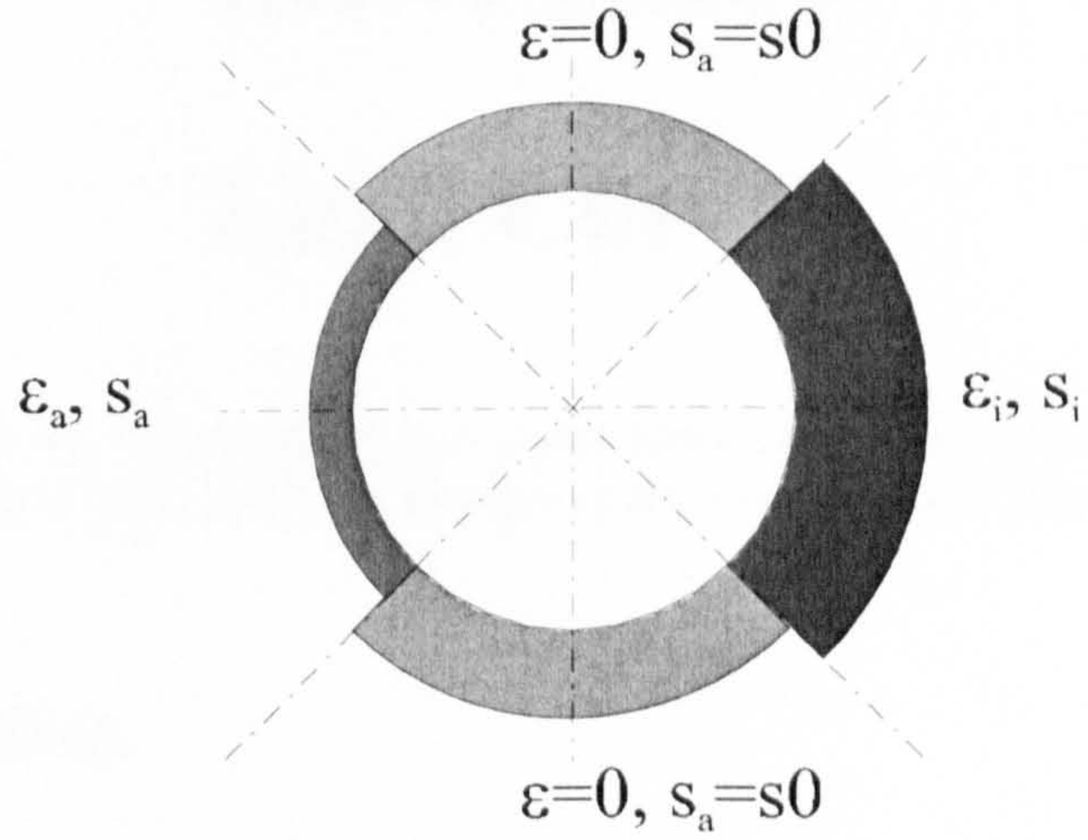

Figure 4-34 Cross-Sections of a Tube

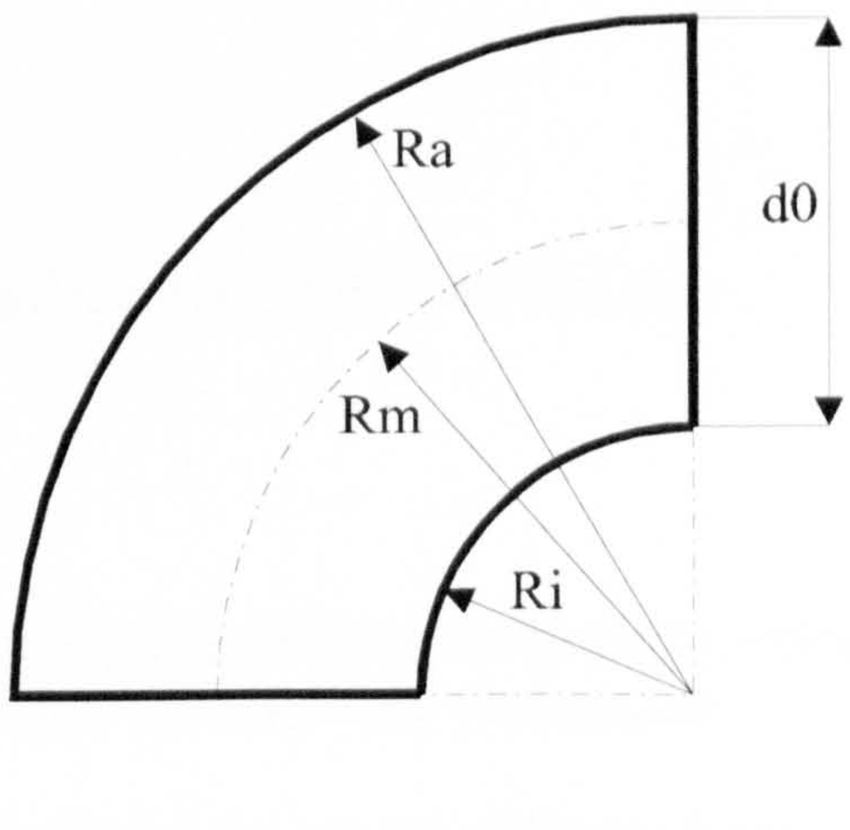

Figure 4-35 Dimensions Tube Bending

CHAPTER 5

Load Curves

This Chapter shows how the load-curves for axial force and interior pressure can be created and hence diagrams for the easy and fast design of these curves are developed.

5 Introduction

IHP processes are steered using load-curves. The forming process is initiated with the application of interior pressure and the axial force. These two parameters are controlled using load-curves, the load-curve defines the loads history. For the design of the load curves the following parameters are significant:

- material
- shell thickness
- tube diameter
- relationship between shell thickness and tube diameter
- forming radius

To conduct a simulation of the forming process successfully, using the Finite Element Method (FEM), it is necessary to calculate the following parameters:

- axial force, necessary to control the course of the wall thickness
- forming pressure, necessary to press the tube into the tool (**Figure 5-1a, 5-1b**)
- calibration pressure, necessary to form the (smaller) radii (**Figure 5-1c**)

A correct relationship between the interior pressure and the axial force is absolutely necessary in order to prevent the failure modes like buckling, folding or bursting (**Figure 5-2**). Too much interior pressure and too less axial force leads to bursting, for too less interior pressure and too much axial force folding or buckling occurs.

Figure 5-3 shows a typical load-curve for interior pressure with the various phases during the IHP process.

point 0 - 1 : fill the tube, point 1 - 2 : expansion, point 2 - 3 : calibrate

5.1 Axial Force

The axial force consists of two parts, the first is Fa0 shown in **Figure 5-4,** which is necessary to make the tube tight. The second is Fa1 which is necessary to pull material into the forming region. The axial force acts against the two ends of the tube and control the change in the wall thickness.

During the calibration phase (**Figure 5-1b**), no material can be pushed into the forming area due to the friction between the tube and the tool caused by the high interior pressure. The level of the interior pressure and the time history of the axial force are critical parameters for an accurate forming process.

Figure 5-4 shows a typical load-curve for an axial force showing the following points :

Point 1 : force F_{a0} when the process starts - necessary to make the tube tight

Point 2 : force F_{a1} at the end of the forming phase

Point 3 : force F_{a2}, equal to F_{a1}

5.1.1 Calculation of F_{a0}

The axial pre-force or pre-load, F_{a0} given in equation (5-1) is necessary for the forming process holding the tube tight, as the pressure acts against the punches. During the simulation this is not necessary when applying pressure on the elements, but it is necessary when using a fluid-cell option for the hydro-forming application.

$$F_{a0} = p_{a0} \cdot A_{R0} = p_{a0} \cdot (D_0^2 - d_0^2) \cdot \frac{\pi}{4} \qquad \textbf{(5-1)}$$

According to practical experiments (**Böhm, 1994**) the value of p_{a0} can be calculated using the following relation:

$$p_{a0} = 0.15 * k_{f0} \qquad \textbf{(5-2)}$$

where:

F_{a0}	force at point 1
p_{a0}	axial compress pressure before forming
k_{f0}	flow stress
A_{r0}	cross section area
D_0	outer diameter of the tube
d_0	inner diameter of the tube

This ensures that the tube is held tight and therefore failure of the work-piece can not occur.

5.1.2 Calculation of F_{a1}

It is possible to estimate the axial force at the end of the forming phase, F_{a1}, with the aid of the ideal forming work done *Wid* (virtual forming energy) according to Siebel, and is given by the equation :

$$W_{id} = V \cdot k_{fm} \cdot \varphi_1 \qquad \textbf{(5-3)}$$

where:

V	constant volume of the material
k_{fm}	average flow stress during the forming phase
φ_1	degree of deformation after the forming phase

The constant volume V can be calculated as follows:

Cross section area before and after forming:

$$A_{R0} = \left(D_0^2 - d_0^2\right) \cdot \frac{\pi}{4} \qquad \textbf{(5-4)}$$

$$A_{R1} = \left(D_1^2 - d_1^2\right) \cdot \frac{\pi}{4} \qquad \textbf{(5-5)}$$

and the volume:

$$V = V_0 = V_1 = A_{R1} \cdot l_1 \qquad \textbf{(5-6)}$$

The initial length l_0 is calculated as:

$$l_0 = l_1 \cdot \frac{A_{R1}}{A_{R0}} \qquad \textbf{(5-7)}$$

where:

D_0	outer diameter before forming
D_1	outer diameter after forming
s_0	shell thickness before forming
s_1	estimated thickness after forming
l_0	length of the forming area before forming

l_1 length of the forming area after forming

A_{R0} Cross sectional area before forming

A_{R1} Cross sectional area after forming

The degree of deformation at the end of the forming phase, φ_1, is given by :

$$\varphi_1 = \ln \frac{A_{R1}}{A_{R0}} \tag{5-8}$$

Middle flow-stress, k_{fm}, is the average of the flow-stress at the beginning, k_{f0}, and the flow-stress at the end of the forming phase, k_{f1}, and is given by:

$$k_{fm} = \frac{k_{f0} + k_{f1}}{2} \tag{5-9}$$

The necessary ideal forming work done for the forming process is:

$$W_{id} = V \cdot k_{fm} \cdot \varphi_1 \tag{5-10}$$

The work W_{id} necessary for the forming process consists of two parts:

W_{pi} work from interior pressure

W_{pa} work from axial force

$$W_{id} = W_{pi} + W_{pa} \tag{5-11}$$

The work due to interior pressure can be calculated as follows:

$$A_{proj} = d_m \cdot l_m \tag{5-12}$$

where (see **Figure 5-5**) :

A_{proj} = projected inner area

d_m = middle inner diameter

l_m = middle forming length

p_{i0} = interior pressure before forming = 0

p_{im} = middle interior pressure

p_{i1} = interior pressure after forming

and:

$$d_m = \frac{d_0 + d_1}{2} \tag{5-13}$$

$$l_m = \frac{l_0 + l_1}{2} \tag{5-14}$$

$$p_{im} = \frac{p_{i0} + p_{i1}}{2} = \frac{p_{i1}}{2} \tag{5-15}$$

Then the work due to interior pressure, W_{pi}, is given by :

$$W_{pi} = p_{im} \cdot A_{proj}\left(\frac{d_1 - d_0}{2}\right) \tag{5-16}$$

and the work from axial force, W_{pa}, is given by :

$$W_{pa} = \left(\frac{p_{a0} + p_{a1}}{2}\right) \cdot A_{Rm}\left(l_0 - l_1\right) \tag{5-17}$$

where:

W_{pa} = work from axial force

A_{Rm} = middle cross-section area

p_{a1} = axial compress pressure after forming

With both these values known it is now possible to calculate the ratio between them,(va):

$$va = \frac{W_{pi}}{W_{pa}} \tag{5-18}$$

The value of *va* varies between 2 to 3, depending on the final geometric shape of the formed components, as shown in **Figure 5-6**. The value of *va* is normally estimated from practical experiments (**Duzidak, 1995**).

The pressure p_{a1} can be calculated from:

$$p_{a1} = \frac{2 \cdot W_{pa}}{A_{Rm} \cdot \left(l_0 - l_1\right)} - p_{a0} \tag{5-19}$$

and the axial force at the end of the forming phase, F_{a1} is given by :

$$F_{a1} = p_{a1} \cdot A_{R0} \tag{5-20}$$

and F_{a2} is equal to

$$F_{a2} = F_{a1} \tag{5-21}$$

5.1.3 Maximum Axial Force

The size of the axial force varies between the calculated value F_{a2} and a maximum force F_{amax} calculated using the formula

$$F_{a\max} = A_{Rm} \cdot p \tag{5-22}$$

where:

p approximately the tensile strength

5.1.4 Work due to Friction, W_r

It is assumed that the friction originating from the interior pressure is due to the contact between the tool and the tube. It is also assumed that Coulomb's friction law is valid. This assumption represents the upper limit for the friction force, because the stresses introduced from interior pressure will be reduced over the tube-wall.

W_r can be calculated as :

$$W_r = \mu \cdot s \cdot F_N \tag{5-23}$$

where:

s = displacement of the punch
μ = coefficient of friction

and F_N is given by :

$$F_N = p_{im} \cdot A \tag{5-24}$$

where:

p_{im} = interior pressure (average)
A = friction area, e.g. coat-area of the tube

and the average interior pressure, p_{im}, is calculated by:

$$p_{im} = \frac{p_{il}}{2} \tag{5-25}$$

where p_{il} is given by equation (5-27).

Appendix C shows that the work from friction is small in comparison to the work from axial force and interior pressure.

As a summary it can be said that it is possible to estimate the load-curves with the presented methods. The procedures for the estimation of the interior pressure is simple. The following section describes a way of estimating the calibration pressure.

The estimation of the axial force is time consuming and under some circumstances can be difficult for some geometric shapes. It is useful to divide the work-piece into several sections and calculate the forming work required by applying step by step.

5.2 Interior Pressure

The pressure load-curve has two phases, one at the forming phase where pressure is needed to expand the workpiece, and the second, at the calibration phase where it is needed to calibrate radii (as shown in **Figure 5-3**).

5.2.1 Forming Pressure

The pressure time history of the forming pressure depends on the shell thickness, the outer diameter of the work-piece and the tensile strength of the material. **Figure 5-3** shows a typical load-curve of the interior pressure against time.

The forming pressure can be calculated using the following formula:

$$p_f = \frac{2 \cdot s_0 \cdot R_m}{d_0 - s_0} \qquad \textbf{(5-26)}$$

p_f = forming pressure(N/mm^2)

s_0 = shell thickness

d_0 = outer diameter of the work-piece

R_m = tensile strength (N/mm^2)

The interior pressure at point 1 (**Figure 5-3**) should be 10% smaller than p_f and the interior pressure at point 2 should be 20 to 40% higher than p_f. These values are based on practical experiments (**Böhm, 1993**).

$$p_{i1} = 0.9 \cdot p_f \qquad \textbf{(5-27)}$$

$$p_{i2} = 1.3 \cdot p_f \qquad \textbf{(5-28)}$$

5.2.2 Calibration pressure

For the interior high pressure forming process in a closed tool, a distinction is made between the expansion phase and the calibration phase (**Figure 5-1 a,b,c**). At the beginning of the calibration phase most of the work-piece will be in contact with the tool, during the calibration phase the complex sections, e.g. small radii of the work-piece, will be brought in full contact with the tool cavities. To save energy and to avoid needless tool loads, the interior pressure only needs to be as high as necessary. The calibration phase will be described as follows :

- at the beginning of the calibration phase most of the work-piece is expanded
- at the end of the calibration phase the work-piece is in full contact with the tool
- during the calibration phase the highest interior pressure that will be reached is the calibration pressure
- during the calibration phase the axial force is constant

The calibration pressure has a significant influence on the design and construction of the IHP processes and work-pieces. Therefore the interior pressure has to be determined first. The aim of this section is to develop a method of estimating the original calibration pressure.

The methods proposed here have the following advantages:

- easy and fast to use (user friendly)
- possibility of using many different parts
- easy input of the parameters

5.3 The Estimation Procedure

For the estimation procedure, it is important that the parameters for the growth of the calibration pressure are determined. The growth of the calibration pressure depends on the following parameters :

- the radius to be calibrated
- the wall-thickness of the part
- the material

For the estimation model (**Figure 5-7**), the following boundary conditions are assumed :

- the start position for the estimation will be a tube expansion at the end of the expansion phase. Furthermore the tube has no residual stresses.

- for the trials the details, shown in **Figure 5-8,** will be used to create the FE-trial model. **Böhm (1993)** has shown that it is possible to use the results of the FE simulation.

- the tool is a rectangular square without a radius.

- the interior pressure will be constantly increased. The adjusted radius is estimated.

- the experiments should depend on the wall-thickness and the material.

For the estimation, the following considerations are necessary :

The starting point for the trials is that the tube has already formed at the end of the expansion phase, at this moment the examined area within the tube has a smaller wall-thickness, which is not constant. The wall-thickness at the beginning of the process will be called *s'*. An assumed radius will be adjusted at the end of the expansion phase. The size of the radius will be defined depending on the wall-thickness. From real forming processes it is known that the radius at the end of the expansion phase, *r*, is approximately equal to the wall-thickness' multiplied by four **(Böhm, 1994)**:

$$r = 4 \cdot s' \tag{5-29}$$

where:

s' = expected wall thickness after forming

Furthermore the hardening of the material needs to be considered and the estimation of an increased flow-curve must be used. It is assumed that the degree of deformation at the end of the forming phase amounts to 20%.

Figure 5-7 shows the work-piece to be calibrated, and the detail for the FE-simulation. In order to save processing time and computer memory the reduced model shown in **Figure 5-8** is simulated, in this way a fine FE-mesh is generated.

For accurate results it is necessary to define the boundary conditions for the cut boundaries. The following constraints are defined :

- Cut A : due to the symmetries no displacements in tangential direction direction are possible

- Cut B : no radial constrains, i.e. the material can flow from the end of the tube

The calibration trails will be carried out without axial forging in order to reduce the complexity

of the problem. For the presented configuration the axial force is insignificant.

For other configurations with flat angles the axial force can be utilised to press the material into the corner.

5.3.1 Calibration Trial with the Equal Material

Now components of the same material but with different wall thicknesses are examined with the help of the FE techniques. For these trials the material 25 CrMo 4 with an increased flow-curve is used (**Figure 5-9**).

trial 1 : wall-thickness 4 mm, starting radius 16 mm
trial 2 : wall-thickness 6 mm, starting radius 24 mm

Figure 5-10 shows that the radii developed from the interior pressure depend on the wall-thicknesses. The interior pressure increases up to 10000 bar. It can be seen, that the bigger the wall-thickness, the harder it is to calibrate the work-piece.

The intention of the next step is to examine the sensitivity of the wall-thicknesses. The aim is to receive a single radius-curve for all wall-thicknesses. Instead of the radius on the y-axis, a y-factor shall be taken down on the y-axis. The y-factor is defined as :

$$y = \frac{r}{s'} \qquad \textbf{(5-30)}$$

y = y-factor
r = outer radius
s' = wall-thickness after forming (see **Figure 5-7**)

Figure 5-11 presents the radii curves calculated with the help of the equation (5-30). It can be seen that the curves are almost identical for the two values of the wall thicknesses, and can now be used for all wall-thicknesses.

5.3.2 Example using the Y-Factor Radius-Curve

A work-piece made of 25 CrMo 4 has a starting wall-thickness of 5 mm. The calibration pressure needed to calibrate a radius of 12 mm is required. It is estimated that the wall-thickness after the expansion will be reduced to 4.5 mm (**Figure 5-1b**).

s' = 4.5 mm
r = $r = 12\,\text{mm}$
y = r/s'=12 mm/4.5 mm = 2.66

Using equation (5-30) the y-factor is 2.66. From **Figure 5-11** the calibration pressure can be estimated at 2700 bar.

5.3.3 Calibration trial with the different materials

The next trial is to find out if it is possible to create a curve which is independent of the material. For this trial the model with a wall-thickness of 4 mm and a starting radius of 16 mm are used:

trial 1 : material 25 CrMo 4
trial 2 : material St 37

To consider the solidification from precede expansion process flow-curves with an increased strain are used for the simulation (**Figure 5-12**).

Figure 5-13 shows that different radii are resulting from the two different materials. The steel St 37 is softer, hence smaller radii are created due to a smaller interior pressure.

In order to remove the material dependence for material group 1, the ratio x is introduced as :

$$x = \frac{p}{k_{f,20}} \qquad \textbf{(5-31)}$$

where:

x = x-factor
p = interior pressure
$k_{f,20}$ = flow-stress for 20% strain

where for:

St 37 $\quad k_{f,20} = 420\ N/mm^2$

and for:

25 CrMo 4 $\quad k_{f,20} = 565\ N/mm^2$

Figure 5-14 presents the radii curve calculated with the help of equation (5-31)

5.3.4 Example using the X-Factor Radius-Curve

A workpiece with a wall thickness of 4 mm, a flow-stress of 500 N/mm^2 and 20% strain is considered. In order to calibrate an outer radius of 10 mm the following interior pressure is necessary:

$$P = 0.5 * 500\ \text{N/mm}^2 = 250\ \text{N/mm}^2 \approx 2500\ \text{bar}$$

5.3.5 Investigation of the Flow-Curves

The next investigation was to establish if it is possible to remove the material dependence out of the radius-curve. The flow-curves can be calculated using the procedure described in the VDI-guideline 3146 which is suitable for practical applications.

It is covered by the following equation (**Doege et at., 1986**) :

$$k_f(\varphi) = R_m\left(\frac{e}{n}\right)^n \cdot \varphi^n \qquad \textbf{(5-32)}$$

and:

$$n = \tan\alpha \qquad \textbf{(5-33)}$$

where:

k_f	flow-stress
R_m	tensile strength
α	hardening (slope of the flow-curve, see **Figure 5-15**)
φ	degree of deformation
n	hardening exponent
e	basis of the natural logarithm

The hardening of various materials are (**Doege et al., 1986**):

25 CRMo 4	$\alpha = 12°$
Ck 10	$\alpha = 16°$
Ck 45	$\alpha = 12°$
17 CrNi 18 9	$\alpha = 10°$
X5 CrNi 18 9	$\alpha = 25°$
X6 CrNiTi 18 19	$\alpha = 23°$

From equation (5-8) it can be seen that the flow-stress is a function of the degree of deformation φ, the tensile strength R_m and the hardening exponent.

Figure 5-15 shows the calculated flow-curves with different tensile strength. The flow-curves are parallel and differ only by the level of the flow-stress.

Figure 5-16 shows the stress strain curves for materials with a different tensile strength.

Figure 5-17 shows two flow-curves with a different hardening. The hardening has an influence on the gradient of the curves.

To remove the dependence on the material from the radius-curve, the flow-curves of different materials must have identical gradients and therefore the hardening exponent must be the same. Therefore the radius-curves must be divided into two groups of materials. Group one contains only normal steel with a hardening exponent between 10 - 16 degree. The second group consists of the stainless steel with a hardening between 22 -25 degrees.

5.3.6 Calibration Trials with Different Expansion Diameters

Now it is time to investigate the relationship between the expansion diameter and the radius-curve. Therefore two different configurations are investigated.

The two workpieces have a starting wall-thickness of s'= 4 mm. The material is 25 CrMo 4. The starting radii are calculated using equation (5-29).

$$r = 4 * s' = 4 * 4 \text{ mm} = 16 \text{ mm}$$

The first trial is to expand a workpiece from a diameter of 60 mm to 100 mm. The second trial is to expand a work-piece from 50 mm to 80 mm.

Figure 5-19 shows that the results of both trials are identical.

5.3.7 Results of the Calibration Trails

Now the results of the different FE calibration trials can be summarised. The aim is to create a curve, which is independent of the material and wall-thickness.

Here are some notes on the use of the radius-curve:

- The flow-curves have a different gradient due to the hardening exponent. To get a radius-curve independent of the material, the gradients of the material must be similar, i.e. the

flow-curves must be parallel. Therefore the materials are divided into two groups. Within a material-group the flow-curves have a similar hardening exponent.

- The wall-thickness (s') is the wall-thickness at the end of the expansion phase.

- The radius-curves are created only with interior pressure. Axial forces are not considered. If the process works with axial forces, it is possible to get smaller radii. Thus radii read out from the radius-curves can be securely created.

The growth of the calibration pressure depends on the shell thickness, the material and the radius which has to be calibrated. To estimate the calibration pressure **Figure 5-20** and **5-21** are used. The materials to be calibrated are classified into two categories.

- material group 1 : most steel except stainless steel

- material group 2 : stainless steel

For using the radius curves, the knowledge of the following parameters is necessary : shell-thickness, material and smallest corner radius.

5.3.8 Radius Curve 1

The radius-curve 1 (**Figure 5-20**) is based on the flow-stress at 20% strain.
The radius-curve is valid for a hardening of:

$$\alpha = 10° \div 16°$$

The following materials belong to this group :

25 CrMo 4, Ck 10, Ck 45, 17 CrNi 6, St37

$$x = \frac{p}{k_{f,20}}$$

x = x-factor
p = interior pressure
$k_{f,20}$ = flow-stress for 20% strain

$$y = \frac{r}{s'}$$

y = y-factor
r = outer radius
s' = wall-thickness

5.3.9 Radius Curve 2

The radius-curve 2 (**Figure 5-21**) is based on the flow-stress at 20% strain.

This radius-curve is valid for a hardening of:

$$\alpha = 21° \div 25°$$

The following materials belong to this group :

X5 CrNi 18 9, X6 CrNiTi 18 10

$$x = \frac{p}{k_{f,20}}$$

x = x-factor
p = interior pressure
$k_{f,20}$ = flow-stress for 20% strain

$$y = \frac{r}{s'}$$

y = y-factor
r = outer radius
s' = wall-thickness

Appendix D shows how the calibration pressure can be calculated using the radius curve. Appendix E investigates the developed radius curves by a verification using a FE simulation.

5.4 Use of the Fluid Cell Option for the IHP Process

Some publications (**Heath et al., 1993, Roll, 1994**) claims that the FE simulation does not work correctly with a load applied as pressure on FE elements, especially in the case of failure, because the pressure acts further onto the elements. In reality the pressure falls down very quickly. Therefore different FE-systems offer the capability to use a fluid cell for the expansion of the work-piece, for instance the programs INDEED, LS-DYNA and PAM-STAMP provide this option. The roots of this option are the simulation of the expansion of airbags. With the fluid-cell option it is possible to define a volume-stream vs. time function.

But, on the other hand, the manufacturer of the stamping machine claims that the steering of the IHP machines is very fast (**Böhm,1998**). This means that it is better to simulate using pressure on the elements or to define the volume-stream with a pressure vs. time function.

For simulation of IHP forming processe which works only with the fluid filled into the tube and without a volume-stream during the expansion, the fluid cell option is the only way.

5.5 Conclusion

This chapter has presented methodologies to derive load-curves for the internal pressure and axial force easily. The load curves provide initial values of pressure and an axial load which can be optimised for a specific steel component using either an FE-simulation or experimentally using an IHP machine.

The methodologies are only valid for steel. Future work should investigate if it is also possible for other materials like aluminum and copper. Furthermore implementation of the developed knowledge into a software system could be done.

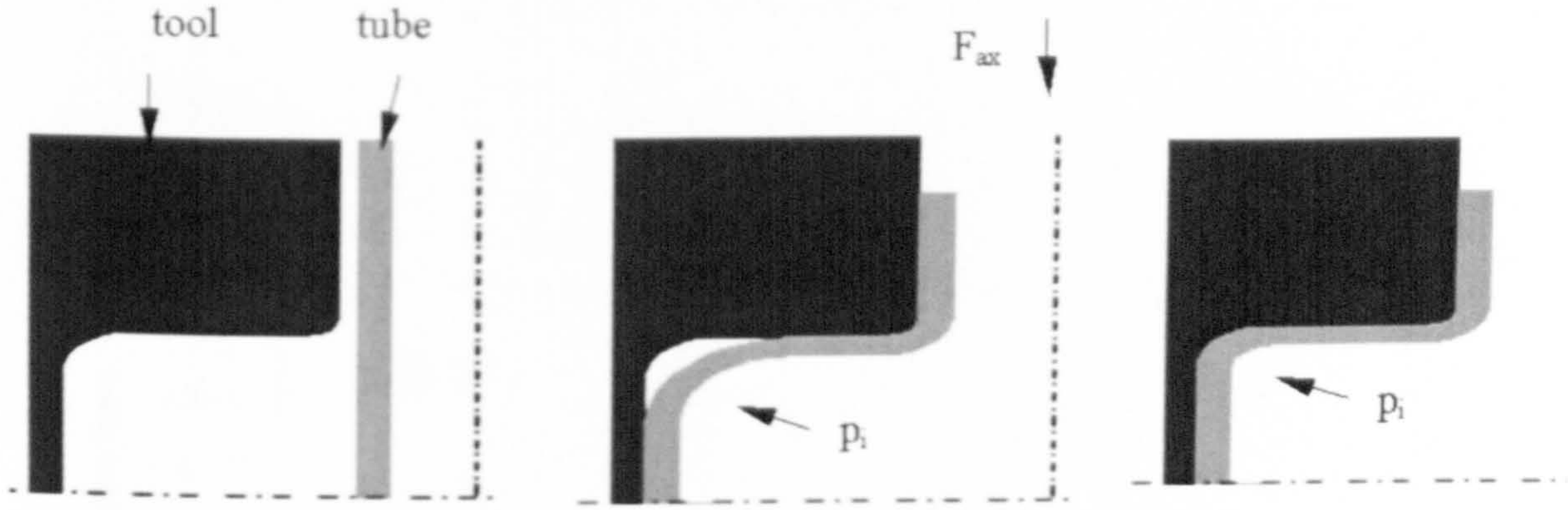

Figure 5-1 Phases of the Interior High Pressure Forming Process

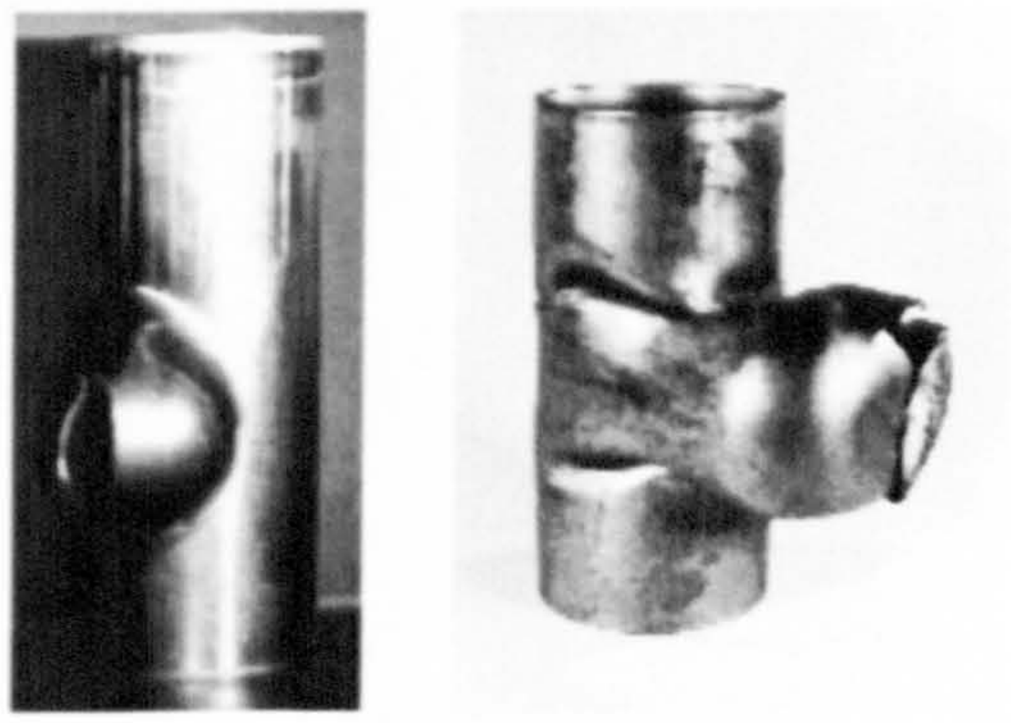

Figure 5-2 Failure Modes (bursting, folding)

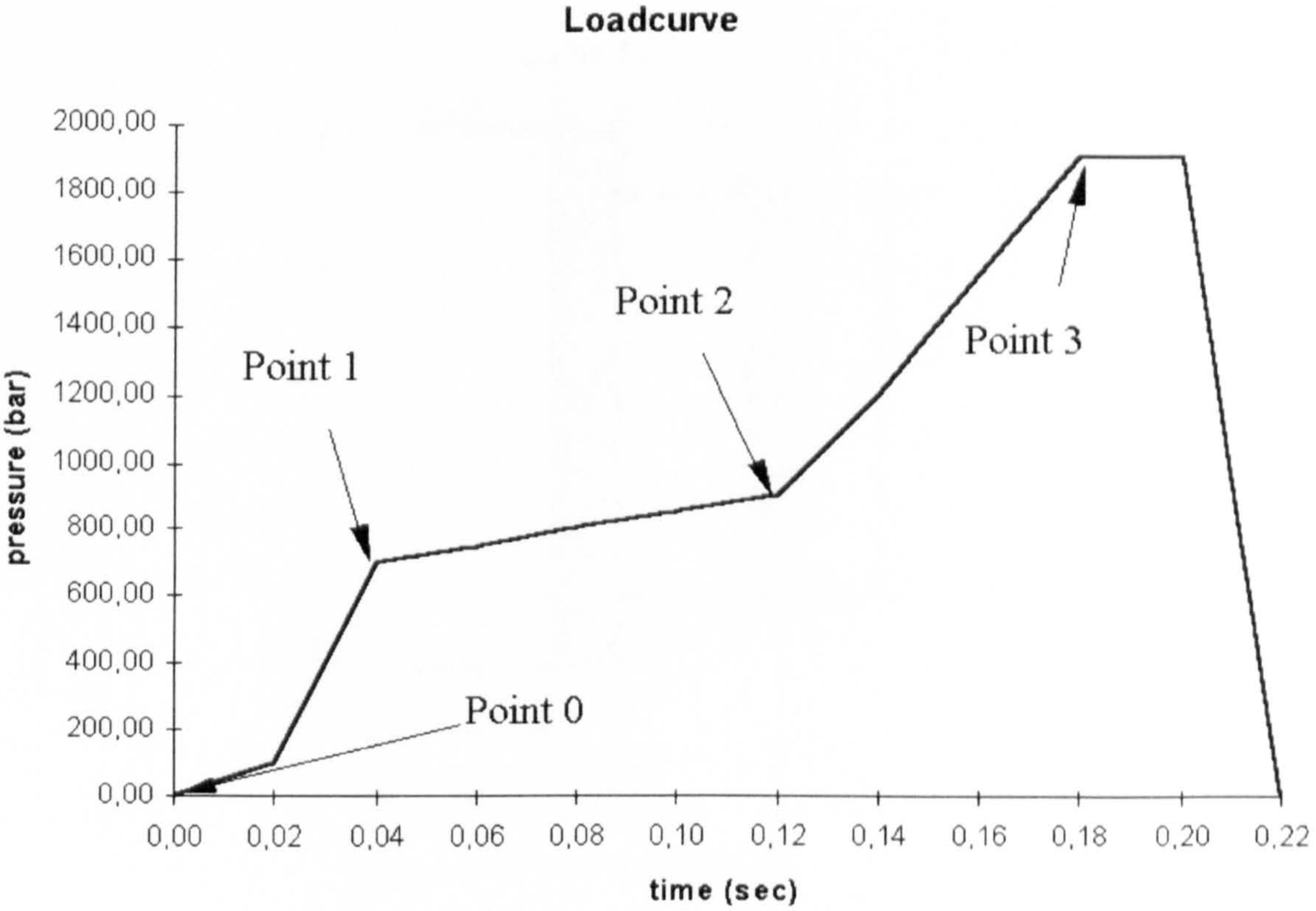

Figure 5-3 Load-Curve for Interior Pressure vs. Time

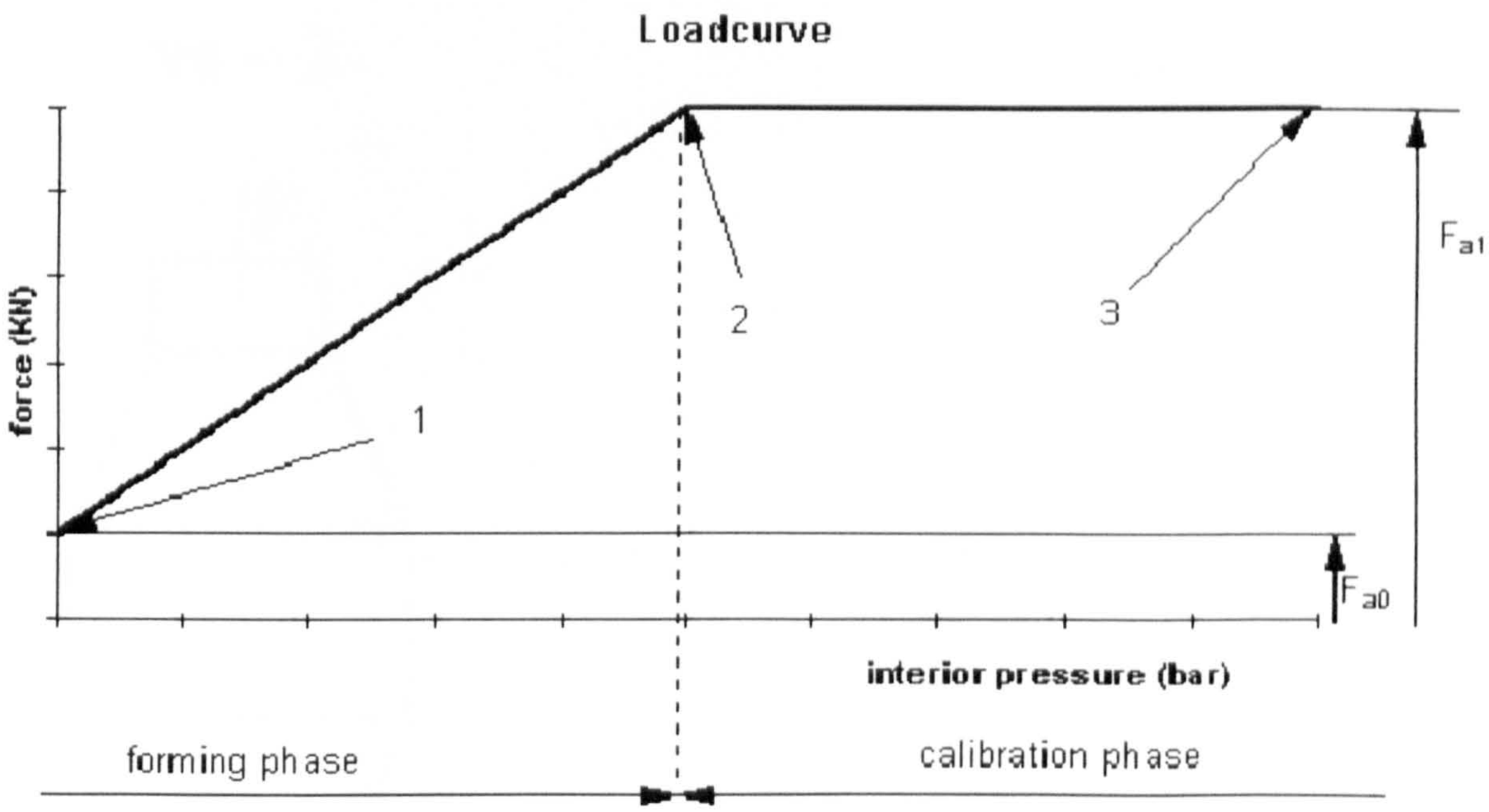

Figure 5-4 Load-Curve for the Axial Force vs. Pressure, Important Points

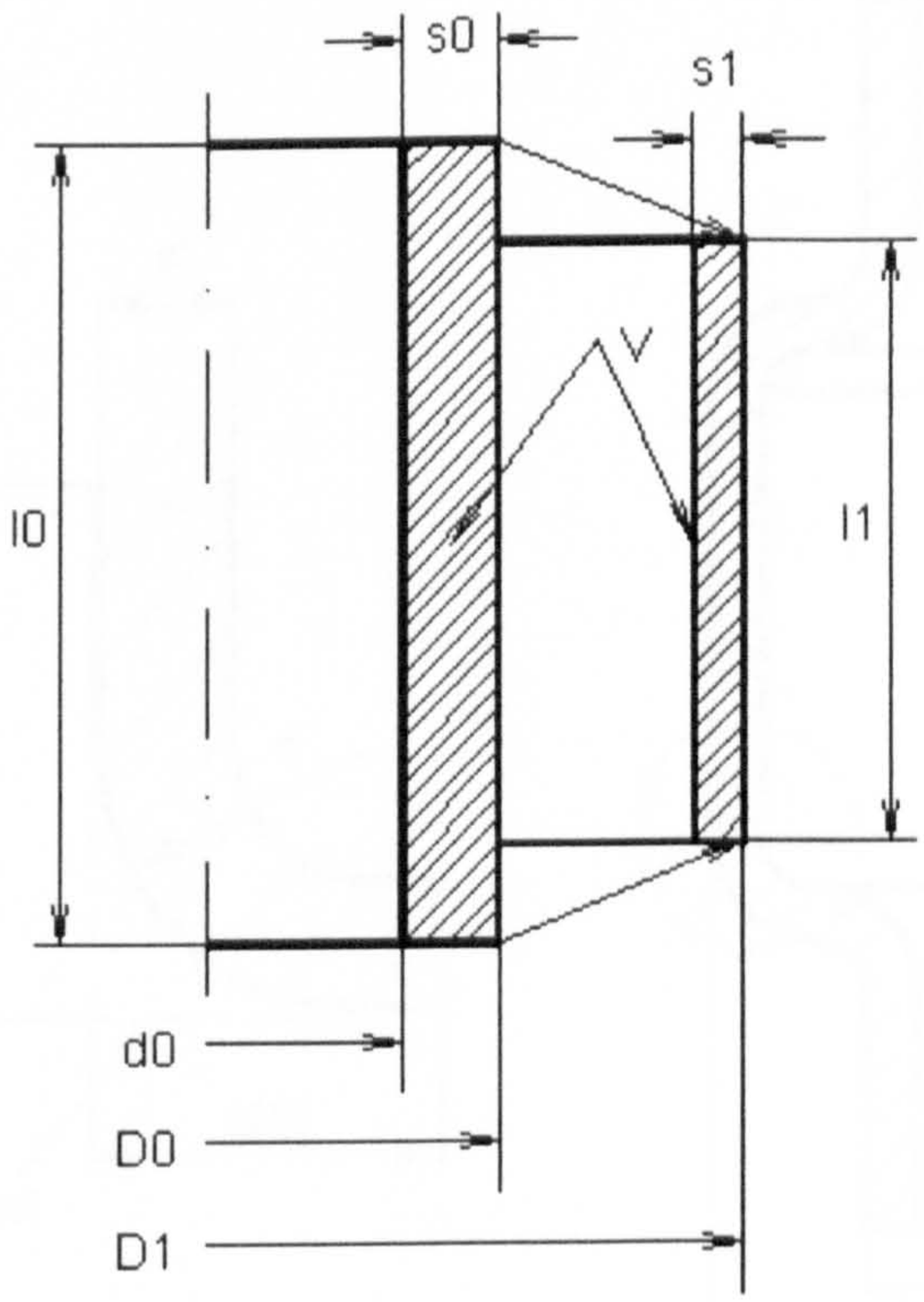

Figure 5-5 Dimensions for the Calculation of the Volume V

va ~ 2

va ~ 3

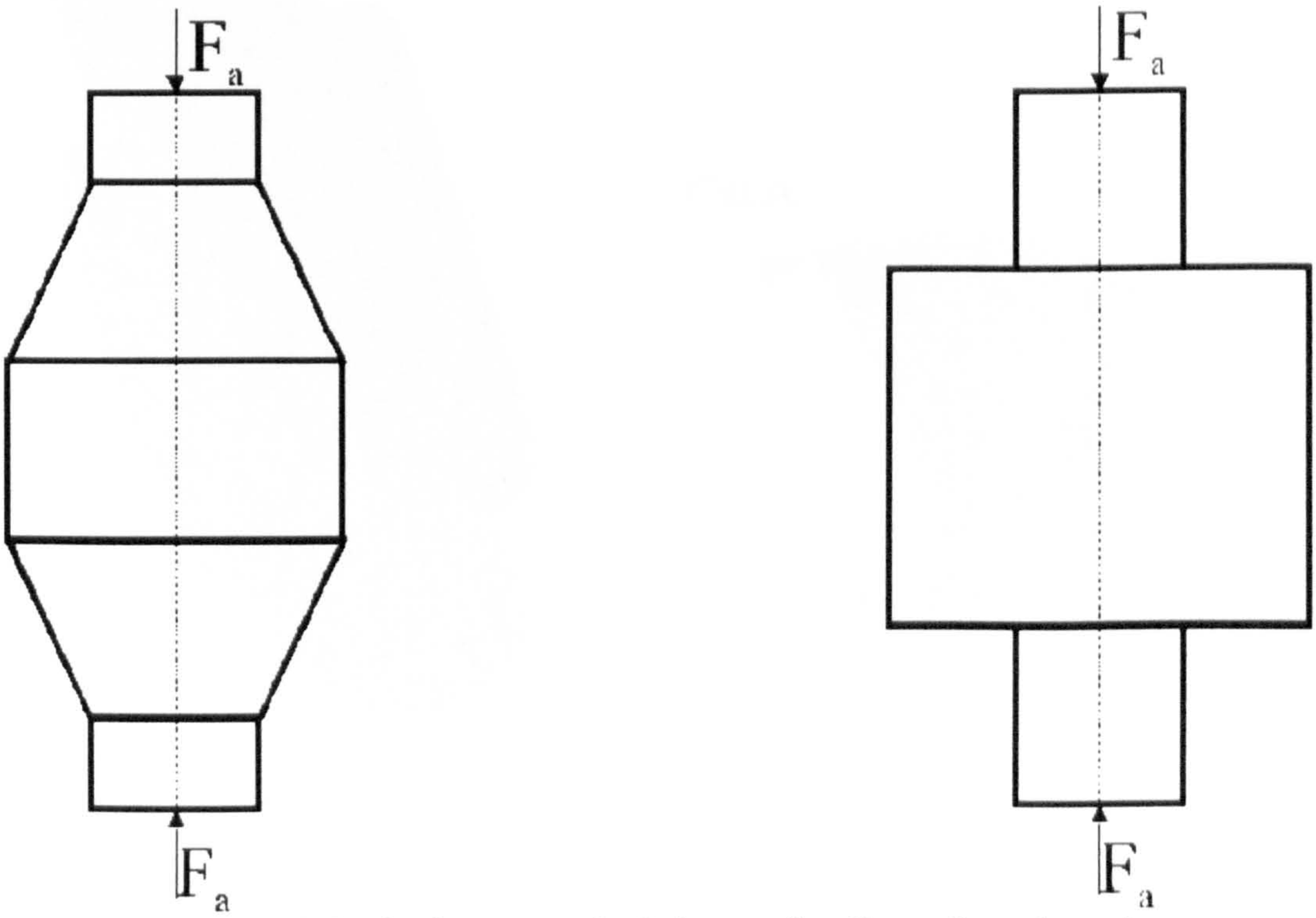

Figure 5-6 Typical geometrical shapes for the estimation of va

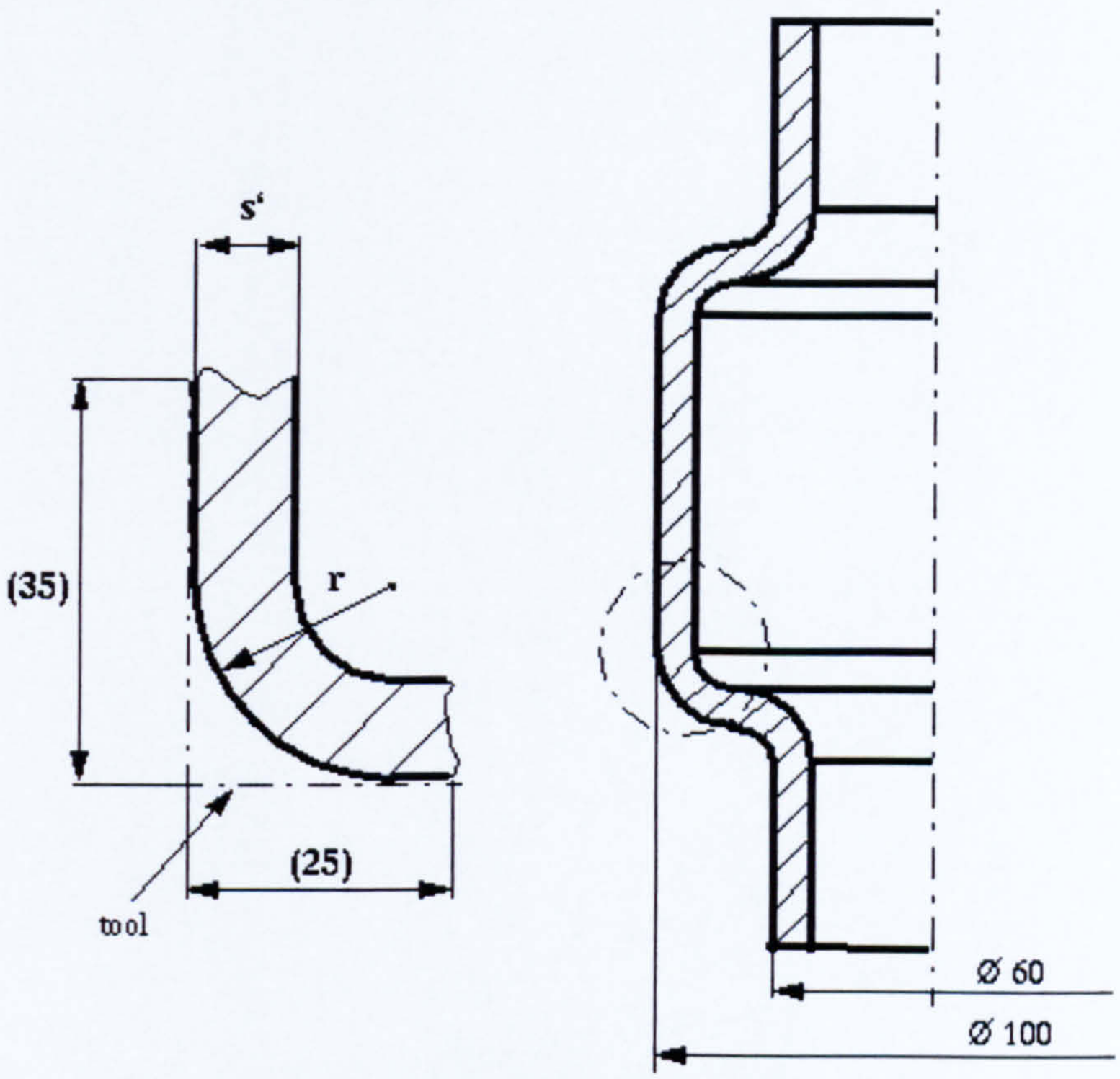

Figure 5-7 Estimation Model

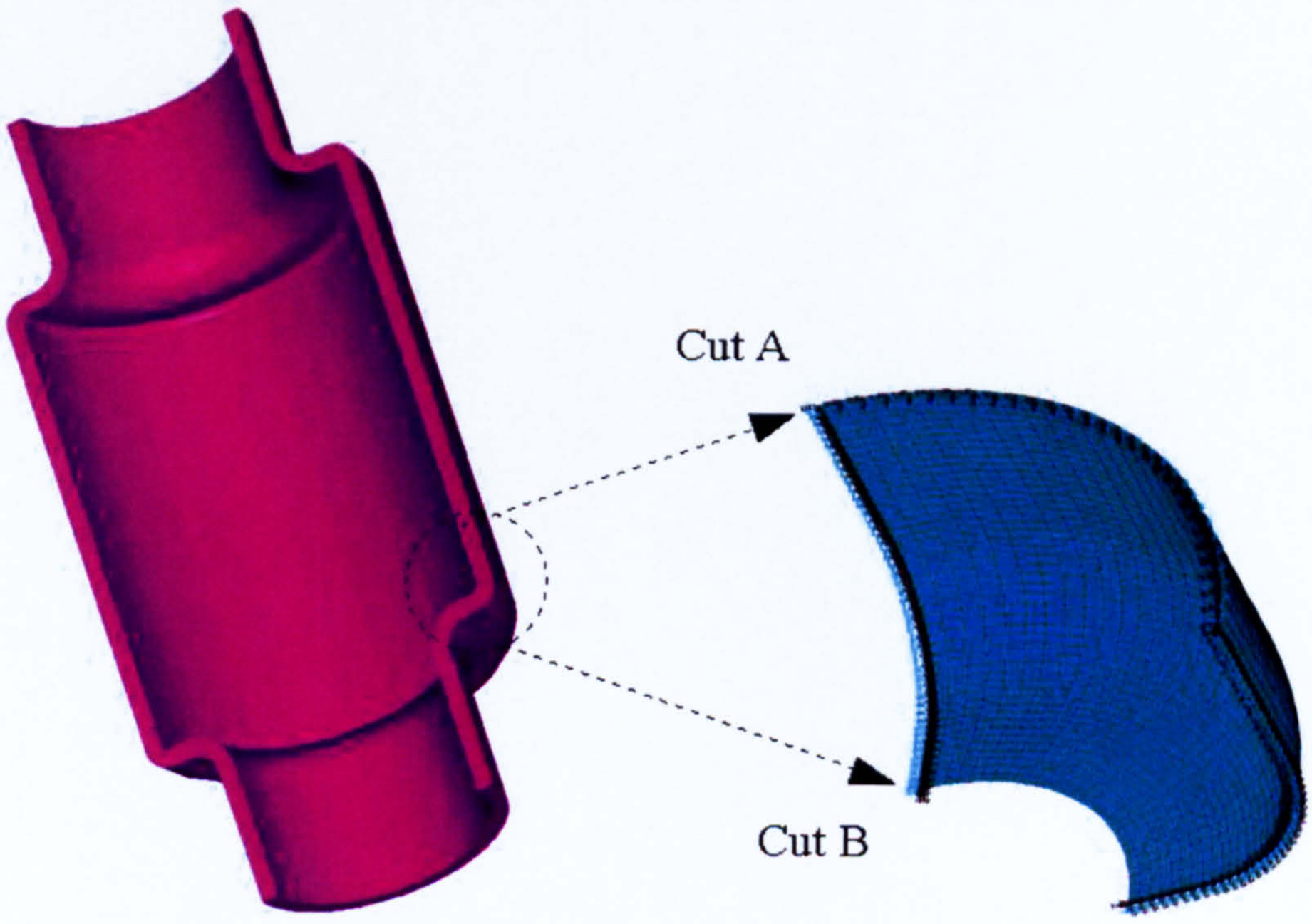

Figure 5-8 Work-Piece, Detail for the Simulation as FE Model

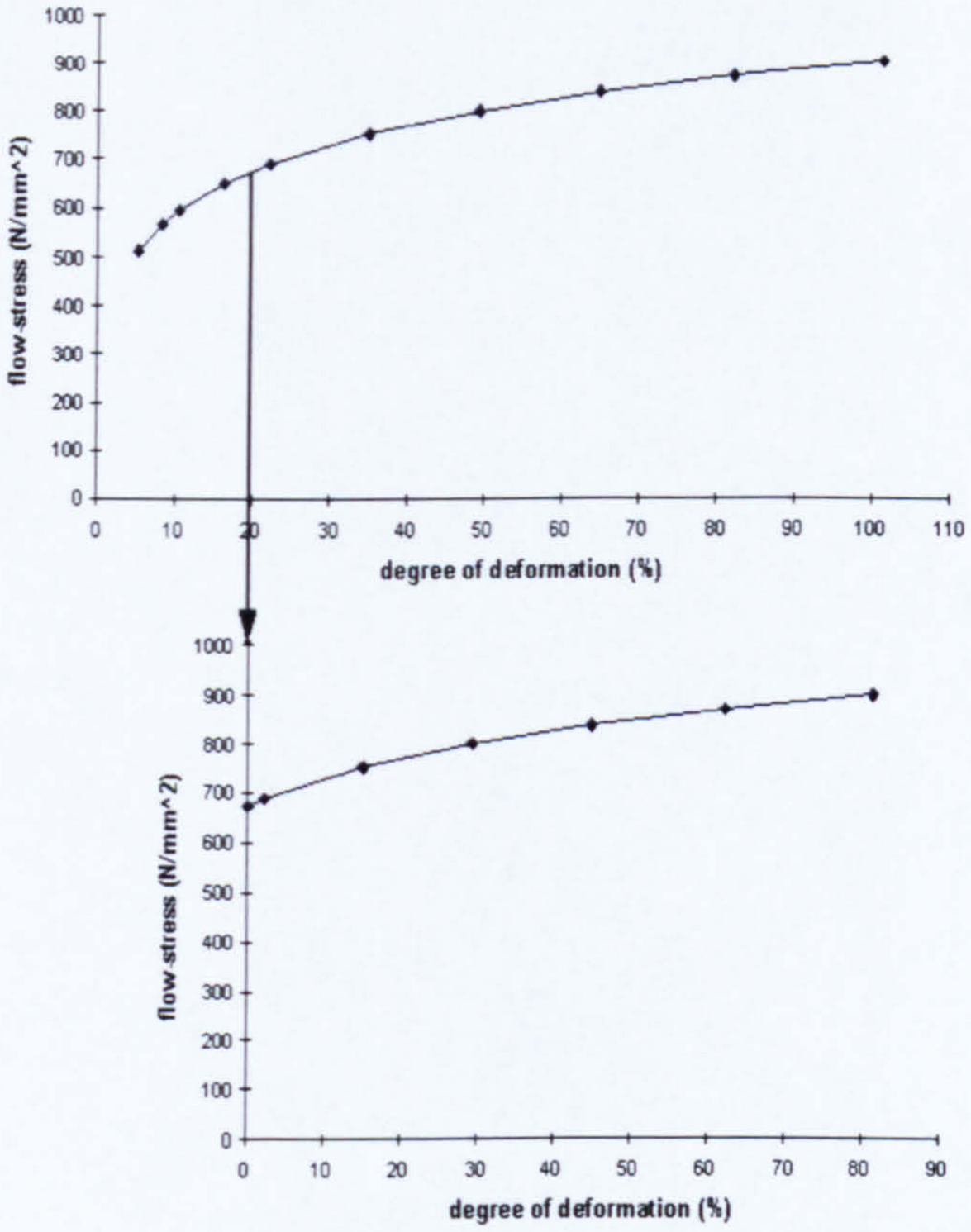

Figure 5-9 Flow-curve for 25 CrMo 4, Increased Flow-Curve for 25 CrMo 4 , used for the Calibration Procedures (true stress - strain)

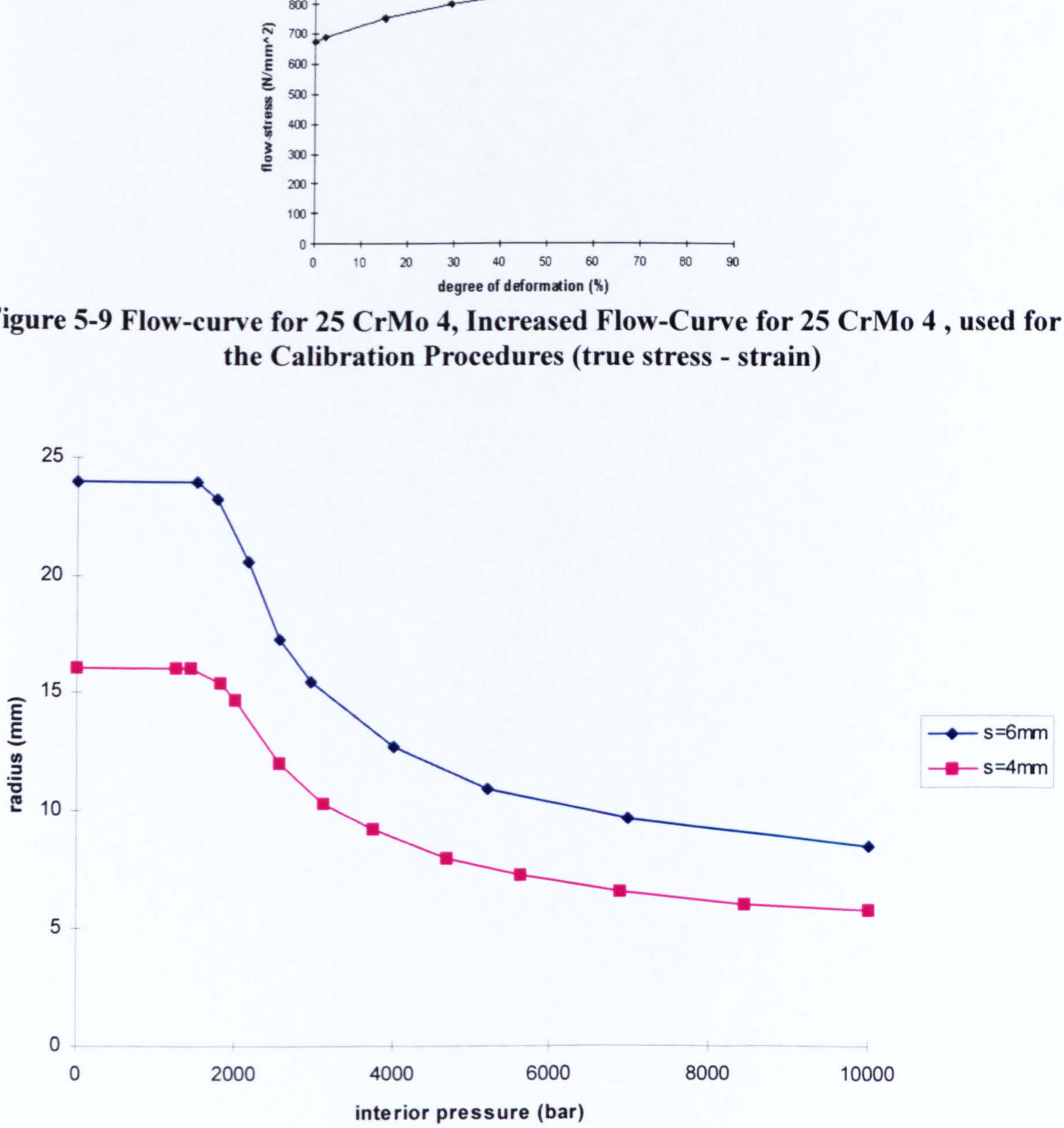

Figure 5-10 Radius-curve depending on the wall-thickness

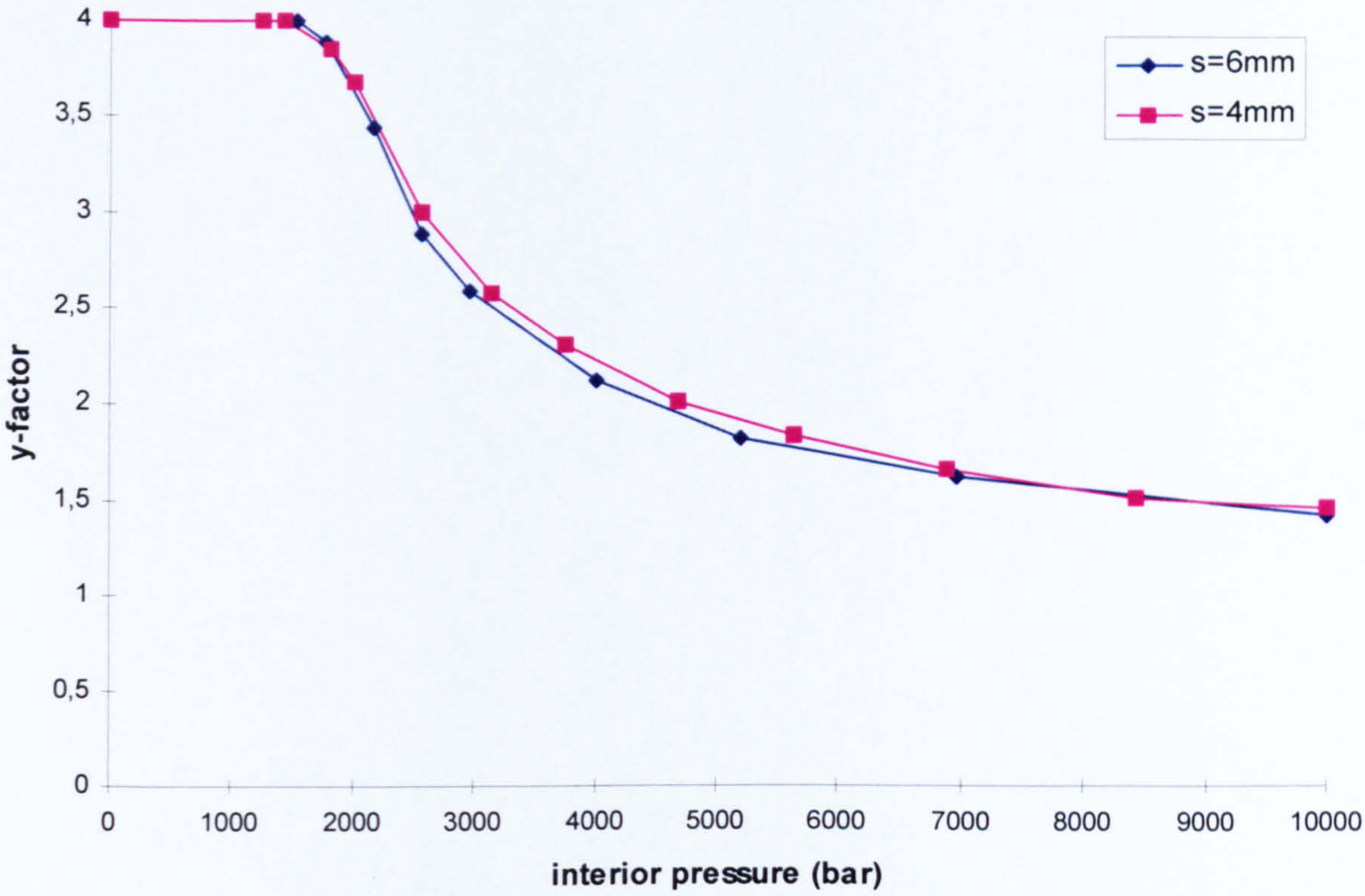

Figure 5-11 Radius-curve depending on the y-factor

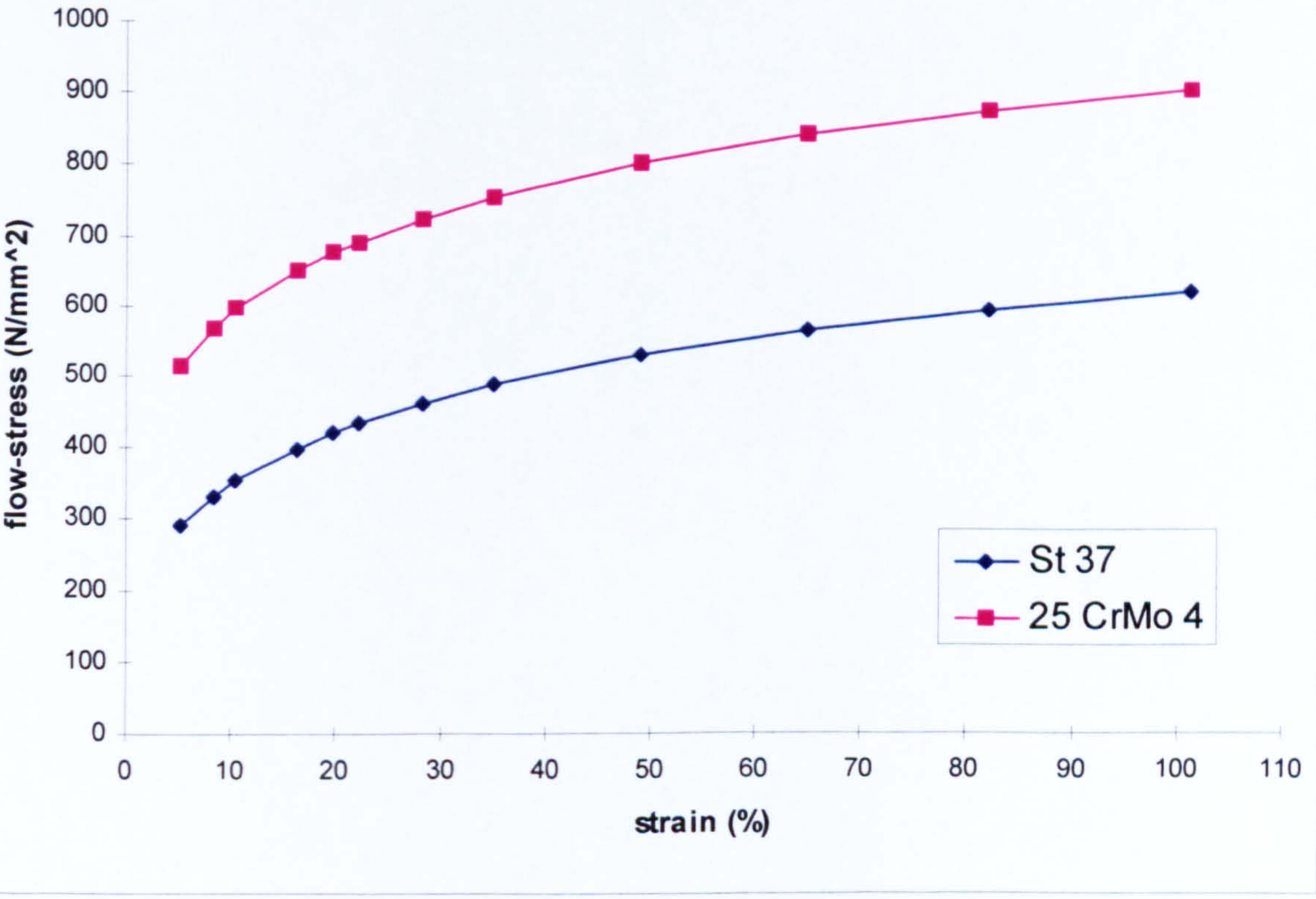

Figure 5-12 Flow-curve for the trial-materials (true stress-strain curve)

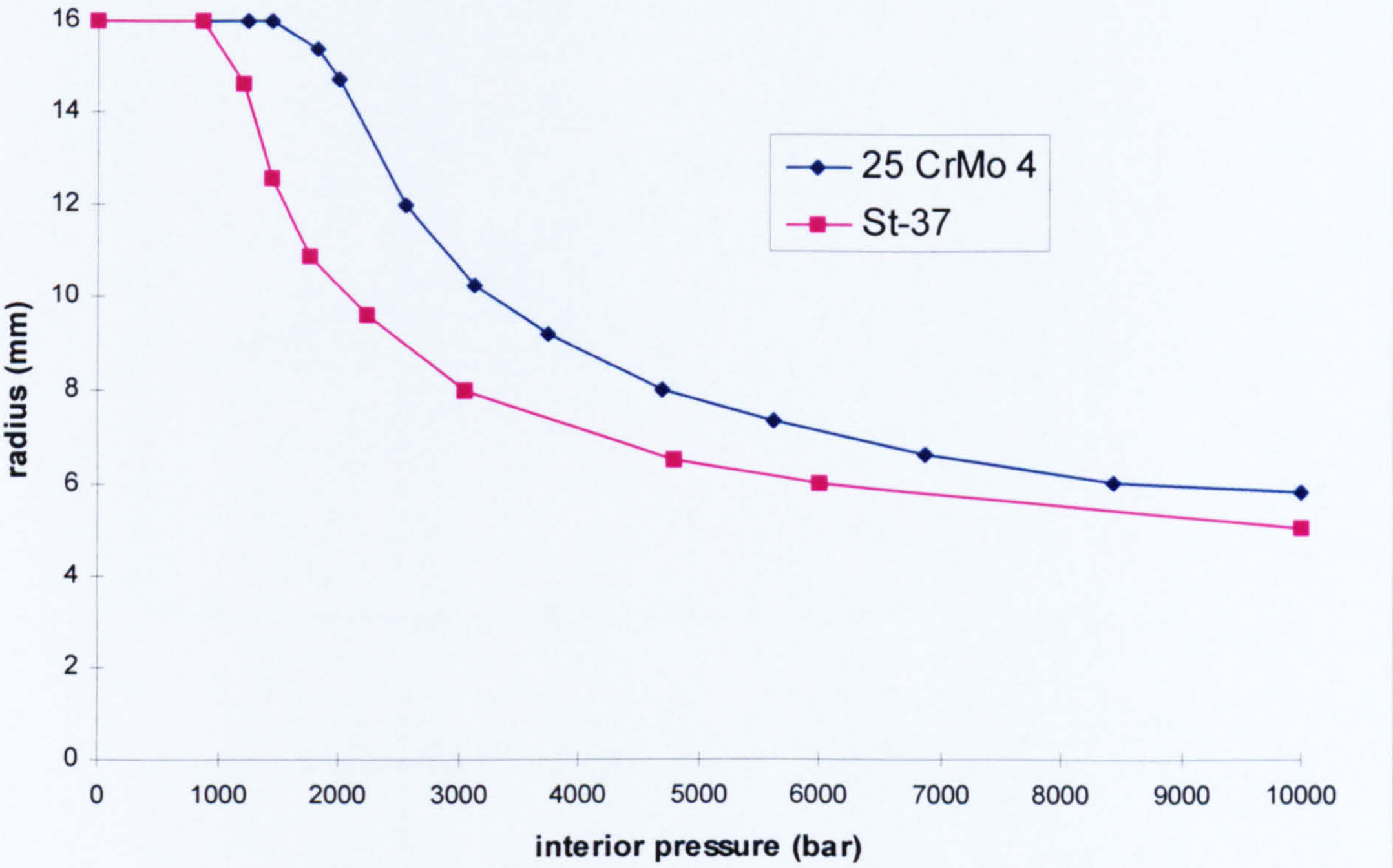

Figure 5-13 Radius-curves for both examination materials

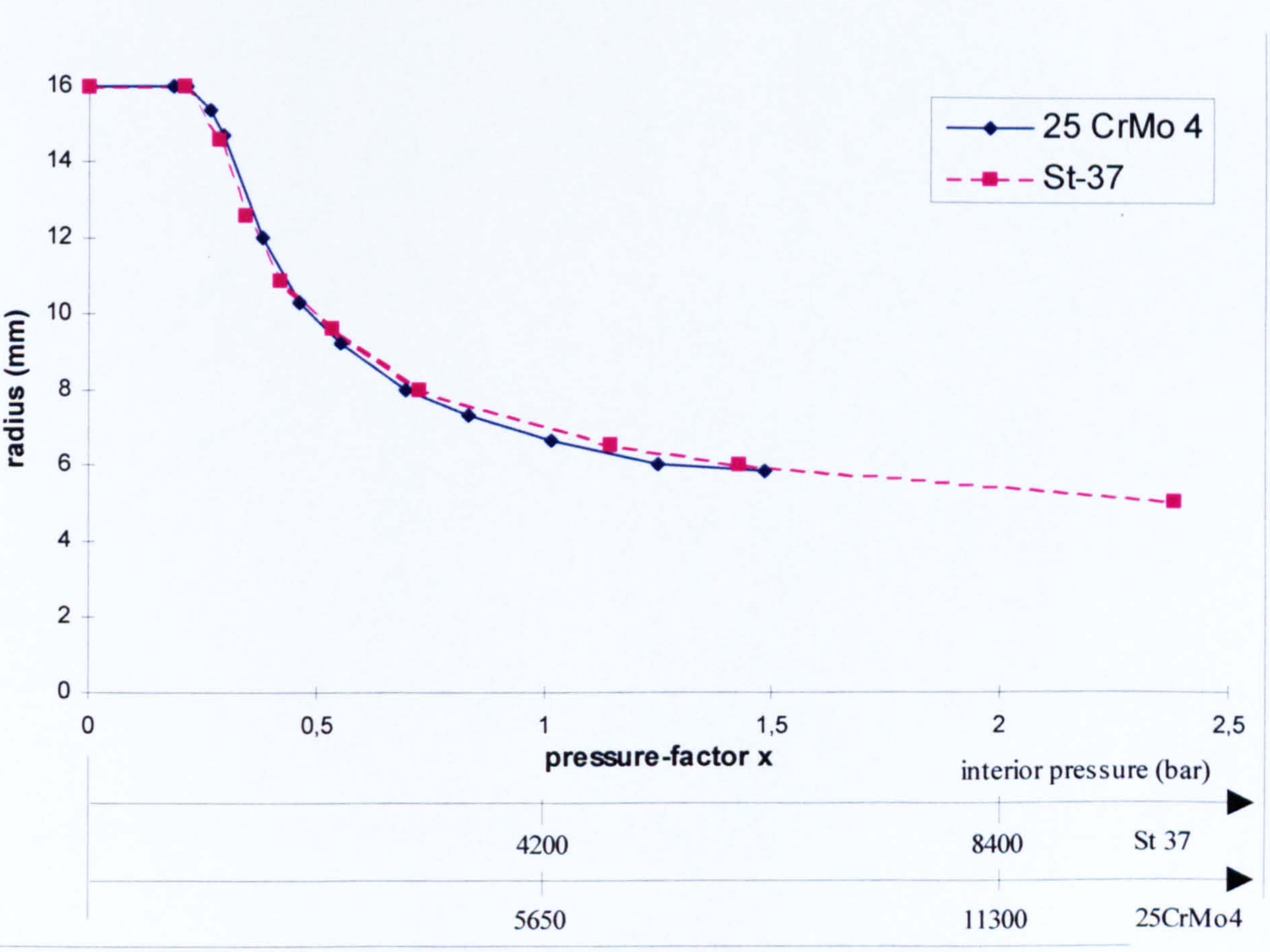

Figure 5-14 Radius-curves dependent on the x-factor

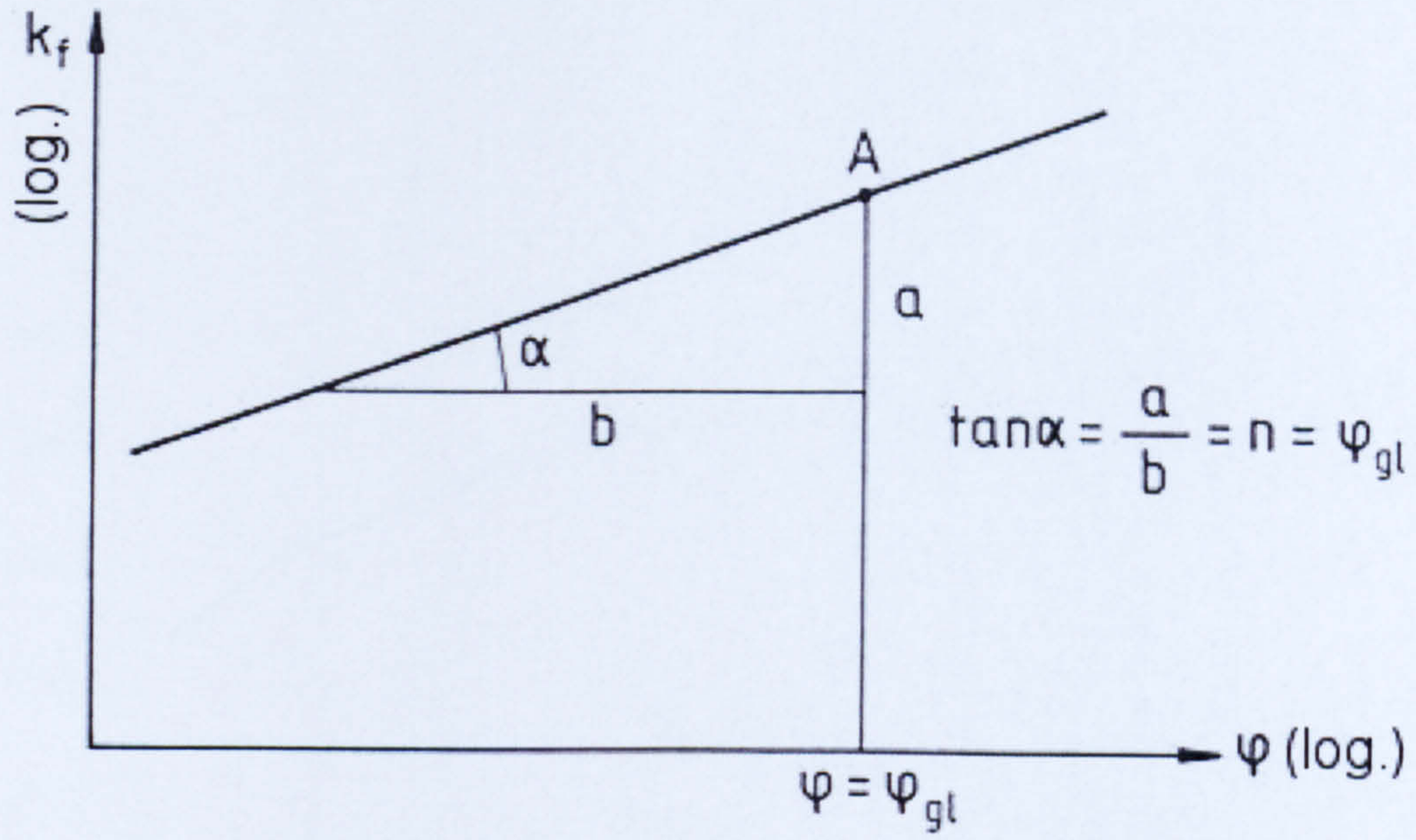

Figure 5-15 Calculation of α (Doege et al., 1986)

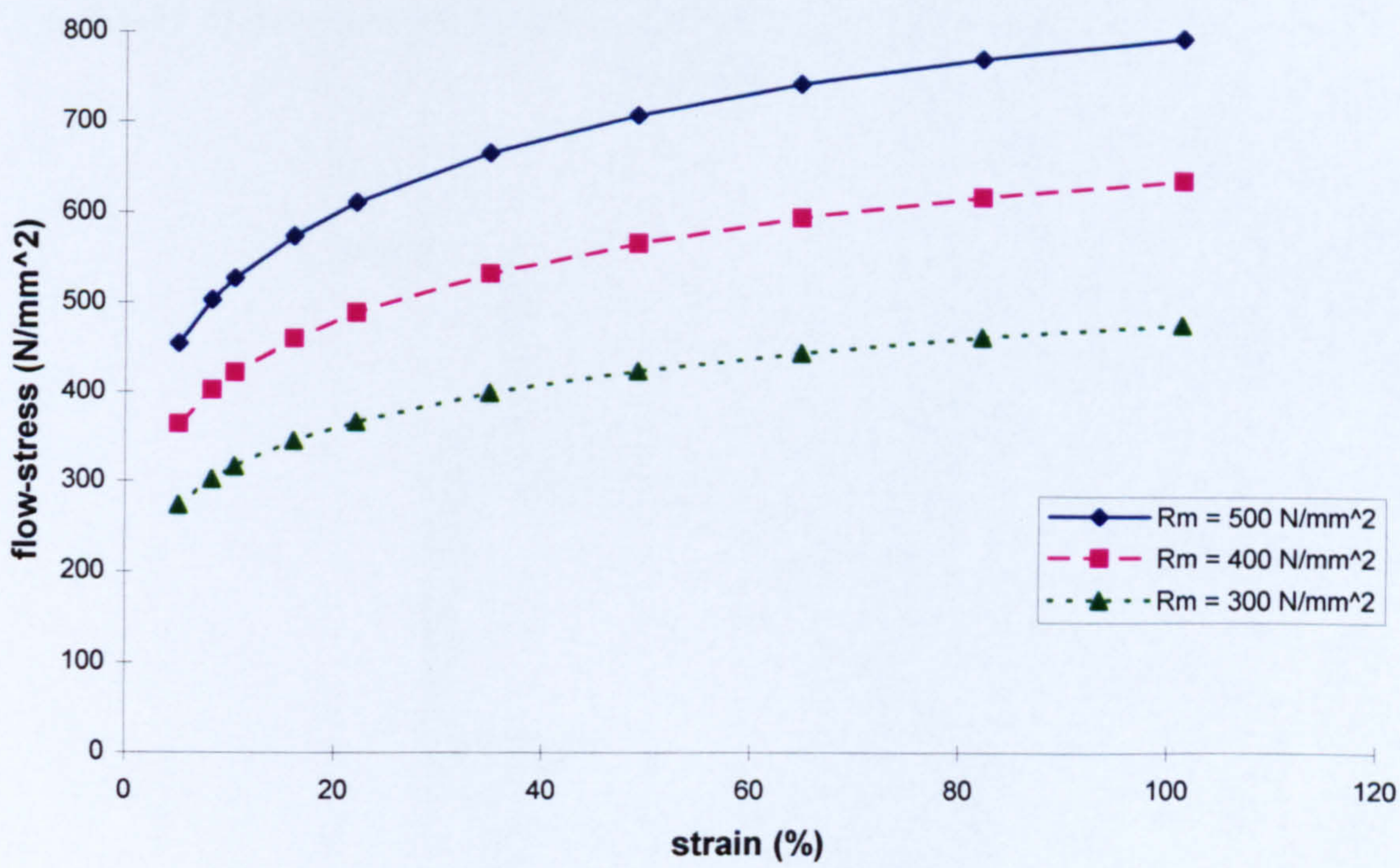

Figure 5-16 Flow-Curves with Different Tensile Strength (true stress - strain curve)

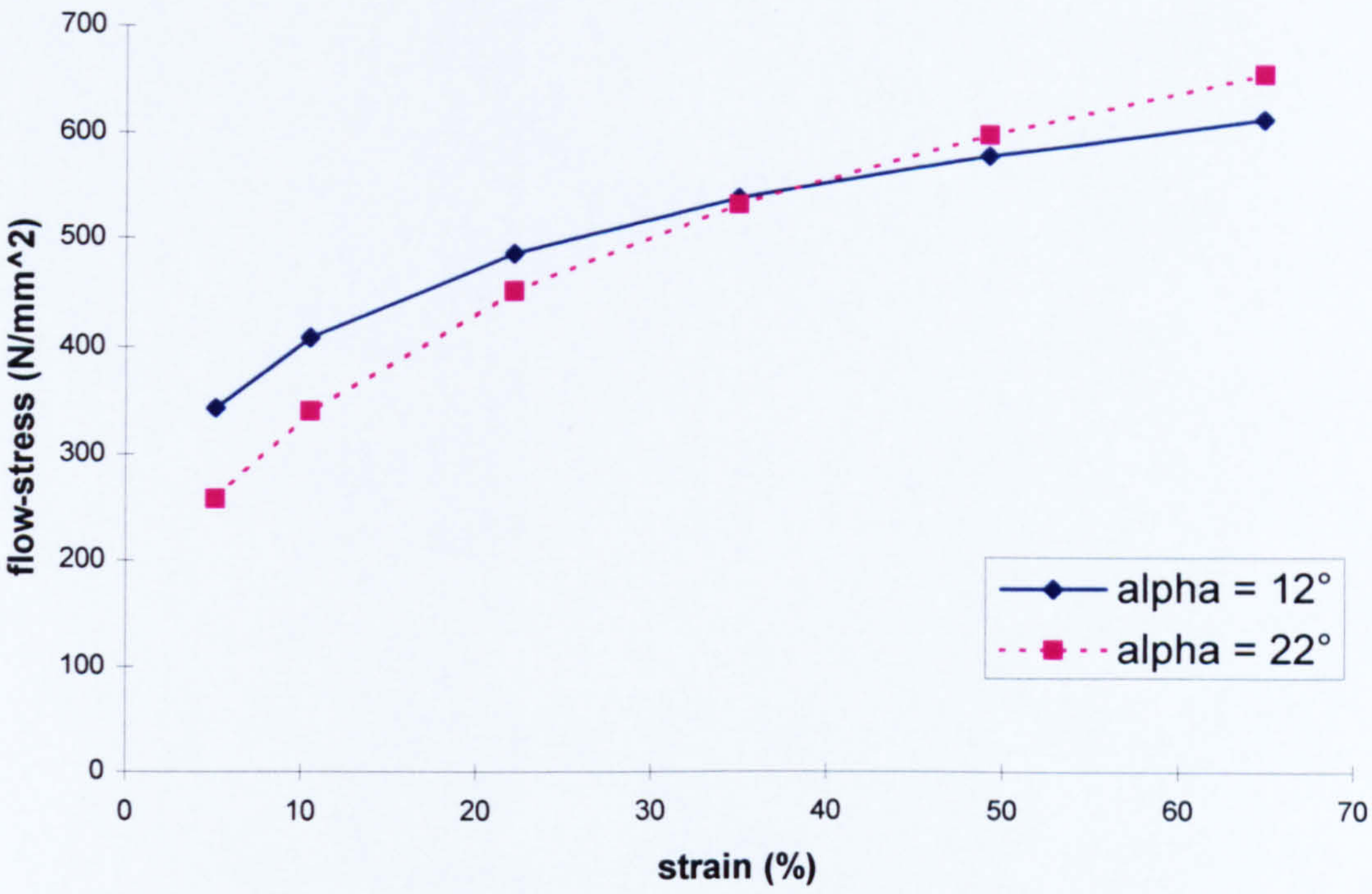

Figure 5-17 Flow-stress for material with different hardening exponent (true stress - strain curve)

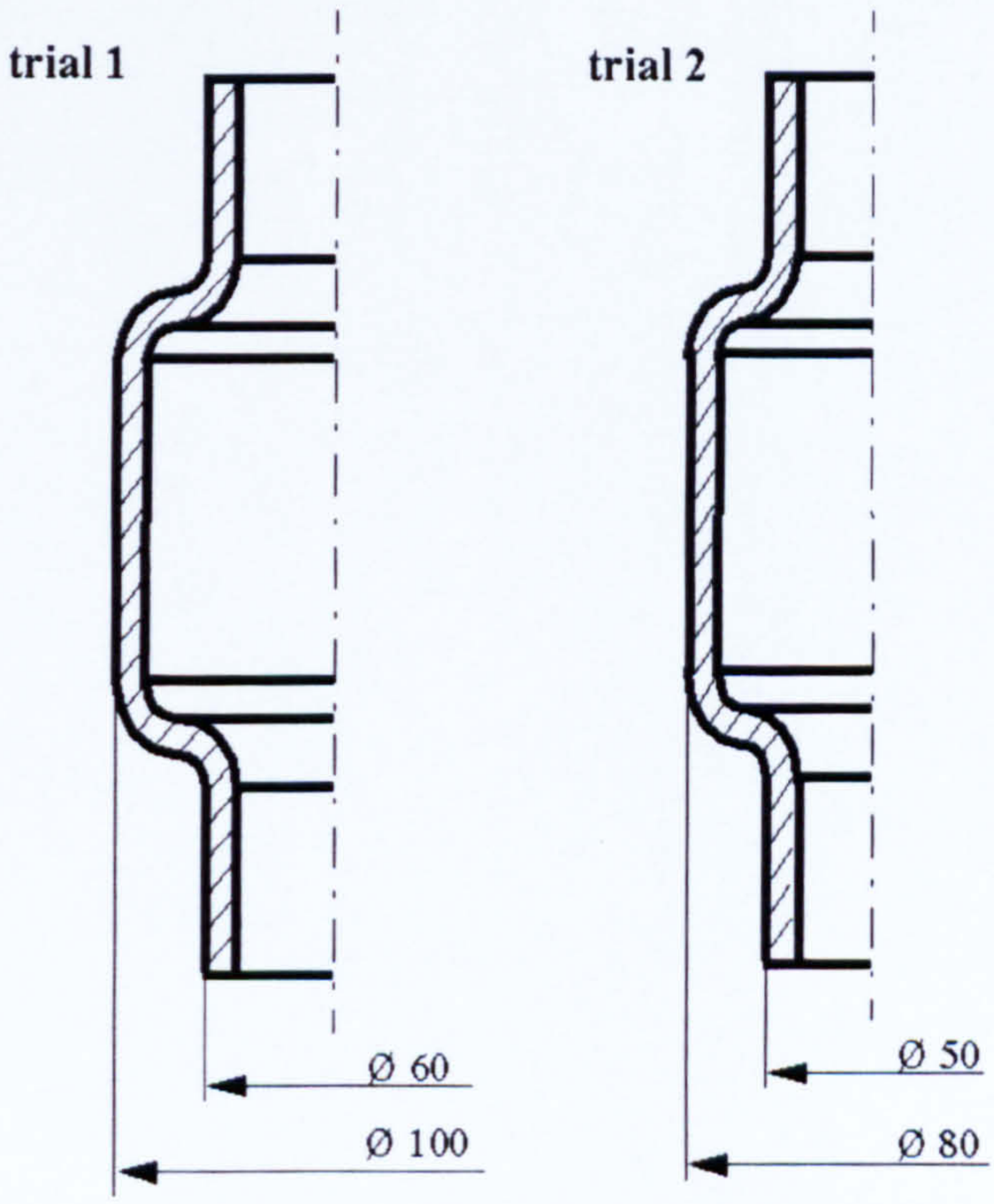

Figure 5-18 Work-Pieces with Different Expansion Diameters

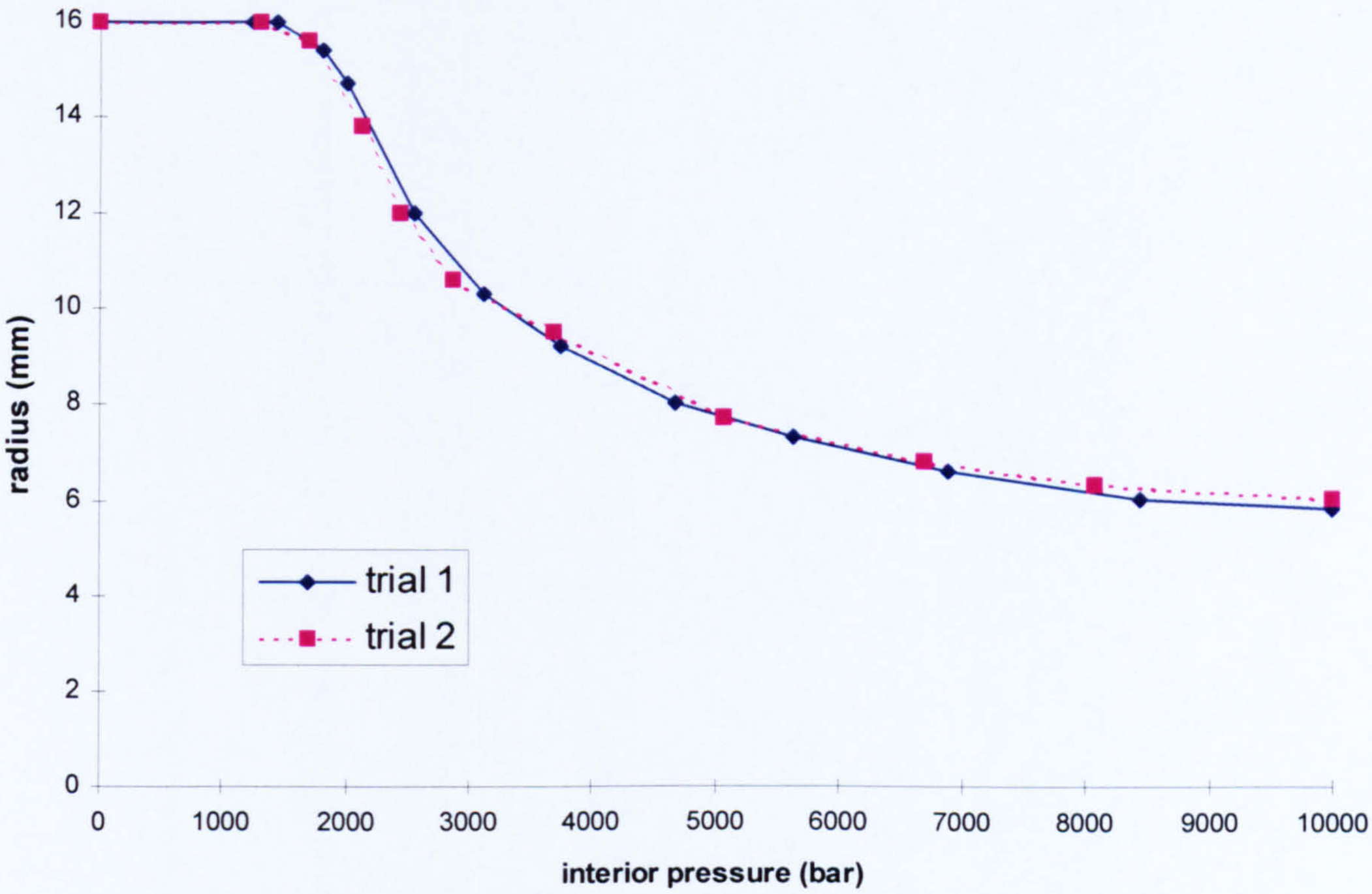

Figure 5-19 Radius-Curves for Different Expansion Diameter

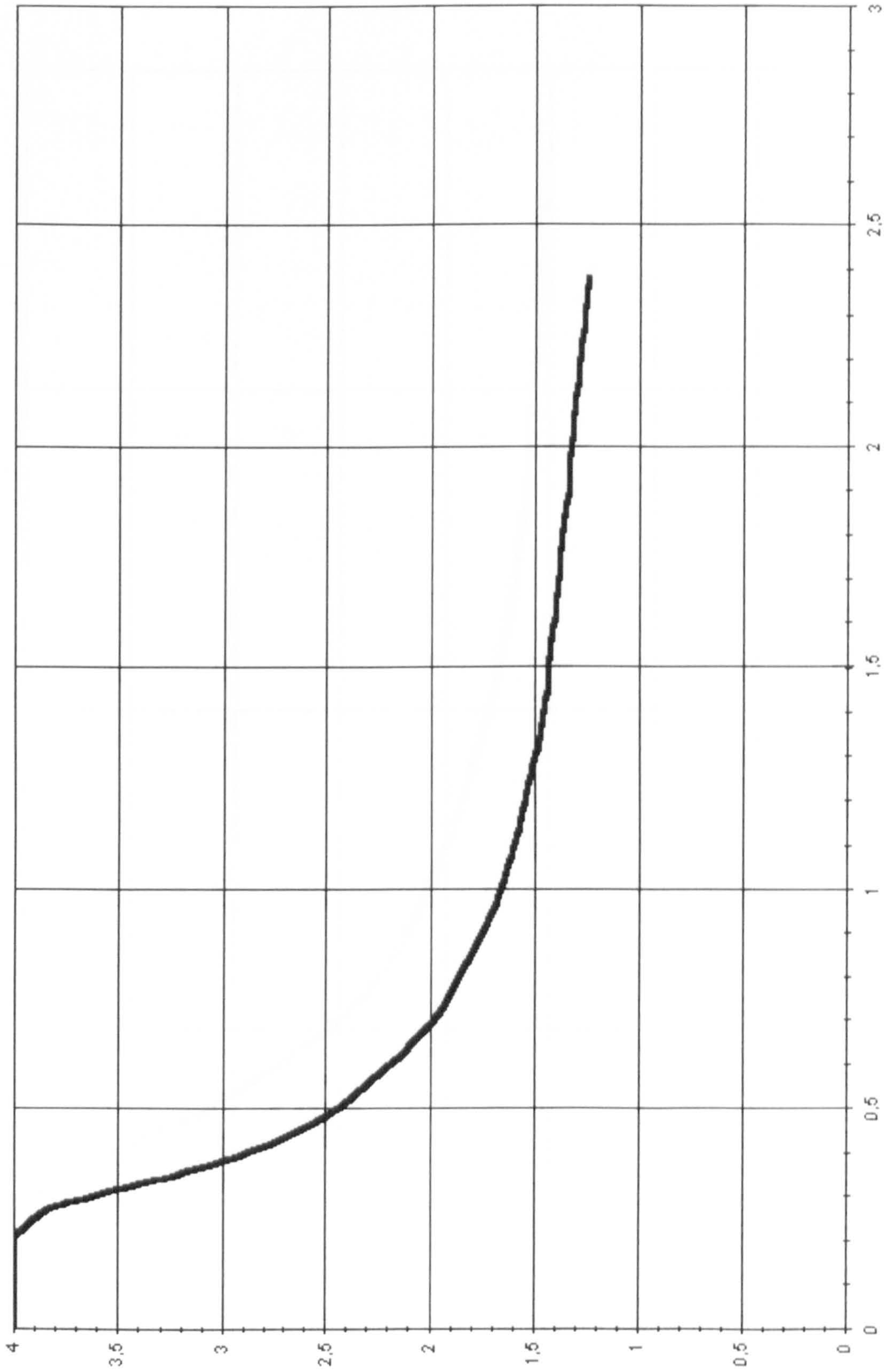

Figure 5-20 Radius-Curve for Material Group 1

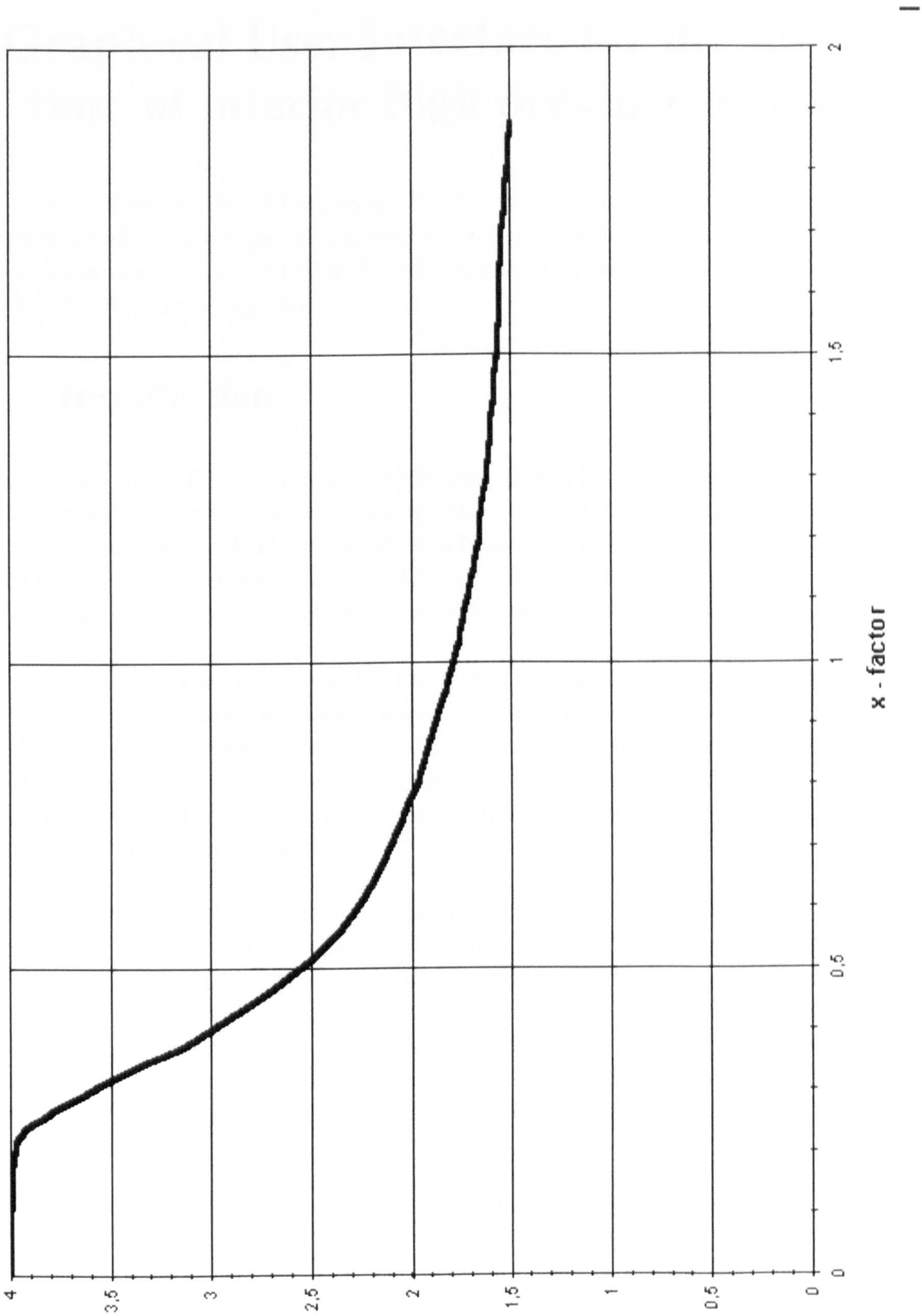

Figure 5-21 Radius-Curve for Material Group 2

CHAPTER 6
Graphical User Interface for the simulation of interior high pressure forming

This chapter describes the development of a fast user-friendly FE-interface program which simulates a hydroforming operation using the interior high pressure (IHP) process. The interface program has been integrated with the FE software package ANSYS and uses the explicit code LS-DYNA for the simulation.

6 Introduction

The efficiency of the FE-simulation of an IHP process and its importance for the whole design process strongly depends on the rate of integration between finite element system, 3D-CAD-system and database (i.e. load curves, material behaviour, friction laws etc). With the integration of the FE-simulation and modern 3D-CAD-techniques it is possible to create a design system which allows an interactive modification of the design variables using the FE-results.

Nowadays the use of the non-linear FE simulation is complex and time consuming because there is no user-interface for the inexperienced user to allow an easy simulation of the IHP process. For other sheet metal procedures like deep-drawing special interfaces are in existence. Therefore industrial users, especially in small or medium sized companies, often don't use the advantageous tool of simulation; this is true for LS-DYNA as well as other simulation packages available in the market today.

A recently available package which integrates LS-DYNA into ANSYS makes it relatively easy to develop a graphical user interface for IHP applications. The aim is, to integrate software tools for the IHP technique into an existing FE System. This would make it possible for the tool constructor or the process developer to use the simulation arbitrarily within an appropriate time and with a minimal expenditure. The interface facilitates the definition of the contact elements in an IHP process, friction between tool and work-piece, and other features are the main modules in this program. Meaningful default values can be adjusted.

6.1 Modelling of the forming processes with LS-DYNA

The program LS-DYNA is a numerical solver, with no pre/post processing capabilities. The input of the simulation data is processed through a so-called LS-DYNA input deck. The creation of the input deck for LS-DYNA can be achieved through a number of pre-processors.
There are a number of third party products for pre/post processing of LS-DYNA available (**Table 6-1**). However they are specialised in either, crash applications (EASi-Crash, Animator3) or simulation of deep drawing processes (Eta/DYNAForm), and they have major

limitation when analysing IHP processes such as the lack of ability to display the shell thickness distribution.

Product	Company	Remark
ANDY	CADFEM, Germany	Pre – Processing
ANIMATOR3	GNS, Germany	Crash, only Post – Processing
ANSYS/LS-DYNA	ANSYS, USA	
EASi-CRASH	EASI, USA	Crash
eta/DYNAFORM	ETA, USA	Deep drawing
FEMB	ETA, USA	
HYPERMESH	Altair, USA	Universal application
LS-PREP, LS-POST	LSTC, USA	
PATDYN	MacNeal-Schwendler, USA	Limited functionality

Table 6-1 Pre/Post Processors for LS-DYNA

6.2 Process Chain for the Simulation

A possible process chain for the simulation of IHP forming processes is shown in **Figure 6-1.** The first step is to design the geometry of the finished IHP product with a CAD system, for example Pro/ENGINEER or CATIA. Using the surface of the finished IHP product, the shape of the tool and additional tools like punch and counted-holder are then derived. This tool geometry is exported in a VDA or IGES format, LS-DYNA can then apply such geometry directly into the simulation (it is not necessary to mesh the tools). The blank, normally a simple tube will be meshed with the CAD system and exported as an ANSYS format or of course it can be created directly within ANSYS. Additional information like boundary conditions and loads will be defined in ANSYS. Using ANDY, a subroutine for ANSYS developed by CADFEM, the German distributor of ANSYS, the LS-DYNA input deck are now created. ANDY interfaces ANSYS with LS-DYNA, however, it supports only a small portion of the capabilities of LS-DYNA. Normally it is always necessary to modify the input deck created with this interface using an editor.

The steps described in **Figure 6-1**, which are relatively error susceptible, require an experienced user.

With ANSYS/LS-DYNA we now have a pre/post-processor for LS-DYNA which is integrated into a commonly used software system, but the ANSYS/LS-DYNA module is not easy to use, and a significant training time is then required.

The author has developed a user interface which is integrated into the general-purpose soft-

ware, ANSYS. The interface incorporates a Graphical User Interface (GUI) which supports an interactive definition of the problem. Returning events such as the definition of the contact between tool and work-piece run in the background. The interface also facilitates input data checking.

The programming of the GUI has been developed using ANSYS UIDL and APDL, making the design of menus relatively easy. However it was not possible to implement all functionalites, the risk being that they may not be compatible with future versions of ANSYS/LS-DYNA. For example it is desirable to have a button at the input of load curves for the graphical visualisation of the curve and the possibility to modify the values using the mouse, this function is offered by the control system of the IHP machine.

Unfortunately ANSYS/LS-DYNA does not support the full functionality of LS-DYNA, especially the possibility of using the CAD surfaces (IGES/VDA) for the tools (stamps), which would be very useful for the simulation of forming processes.

The interface program is realised with ANSYS APDL (**A**nsys **P**arametric **D**esign **L**anguage) and UIDL (**U**ser **I**nterface **D**efinition **L**anguage). APDL is the programming language of ANSYS, which allows teh user to define variables and program structure (IF, THEN, ...). UIDL is a X-Windows/Motif like programming language for the design of adaptive ANSYS Menus. UIDL programs will be only interpreted, and it is not possible to compile the final programs. The disadvantage of UIDL is that it is relatively slow and the code cannot be protected from unauthorised access and modifications. A further disadvantage is that the possibilities for the design of menu's are not so flexible as desirable. It is for example not possible to create a interactive window for the definition/design of load-curves including an graphical representation of the curve and the opportunity to move the load-curve point with drag and drop. The post-processing of the simulation results from LS-DYNA can be done in ANSYS, but it is not advisable because the post-processing in ANSYS is very slow and restricted. LS-POST the new post-processor for LS-DYNA from the LSTC company is much faster and the functionality has better capabilities than ANSYS, and the use of LS-POST is relatively easy and self explanatory.

6.3 The ANSYS/LS-DYNA/IHP-Interface

The IHP interface is designed for the preparation of the LS-DYNA input, e.g. the pre-processing. The IHP main menu (**Figure 6-2**) includes the selection of components like the work piece, the tool and the stamp (**Figure 6-3**) as well as the contact definition, the load curve definition and other control parameters.

First of all the geometry, e.g. nodes and elements, must be defined. This can be done directly in ANSYS or within a CAD system like Pro/ENGINEER or CATIA which has an interface to ANSYS. Most important is that every component has a separate material definition, the material groups are used to define the components, and the components are then used for the automatic contact definition.

Using the *Work piece* menu (**Figure 6-4**), it is possible to import the geometry (*Read File*) into ANSYS. The menu option *Work piece* is used to pick an element and define a component for all elements with the same material 6-number. The non-linear material behaviour will then be defined using the *Material properties* option **(Figure 6-5)**.

From the material library a material for the forming process can then be chosen. The stress-strain curve for the selected material will be displayed.

The next step is the definition of the interior pressure **(Figure 6-6)**.

Using the *Define* option (**Figure 6-6**), the load-curve for the interior pressure is defined. The load-curve is entered as a couple of X-Y value-pairs.

The creation of other components, tools and stamps, is done in the same way as the work piece was defined. The material properties (density, joung's-modulus, etc ...) for the rigid components are taken from the work piece. Tools and stamps are automatically defined as rigid bodies. For each tool or stamp the degrees of freedom (X,Y,Z,XY,XZ,YZ,XYZ) and the concerning load-curves are then defined **(Figure 6-7, 6-8)**

The contact definition is made almost automatically, only the contact type and the static/ dynamic coefficients of friction must be entered. The contacts between work piece, tool(s) and stamp(s) are then automatically defined **(Figure 6-9)**.

The *Control Card* (**Figure 6-10**) menu option is used to define different basic adjustments of the simulation process such as the process time and output options. The simulation can now be started within ANSYS, or alternatively LS-DYNA input deck can also be programmed to start the simulation separately.

6.4 Conclusion

The first version of the GUI for the simulation of IHP processes has been developed and IHP processes with a low to medium complexity can be easily simulated. Two variants of the interface are available, one for ANSYS/explicit and one for ANSYS/ANDY. ANSYS/ANDY is a free FORTRAN subroutine for ANSYS which allows the user to write a LS-DNYA input deck out of the ANSYS database. ANSYS/ANDY has no graphical interface.

It is desirable for future developments that a graphical check of the tool and punch motions to be available including visual control to show whether the directions and/or the relations between the different moving tools are correct. Furthermore an auto-positioning for the punches and counter-holders are useful.

Further integration of different functions and the integration of the IHP GUI itself into a CAD system would be desirable, for example CATIA or Pro/ENGINEER is under development.

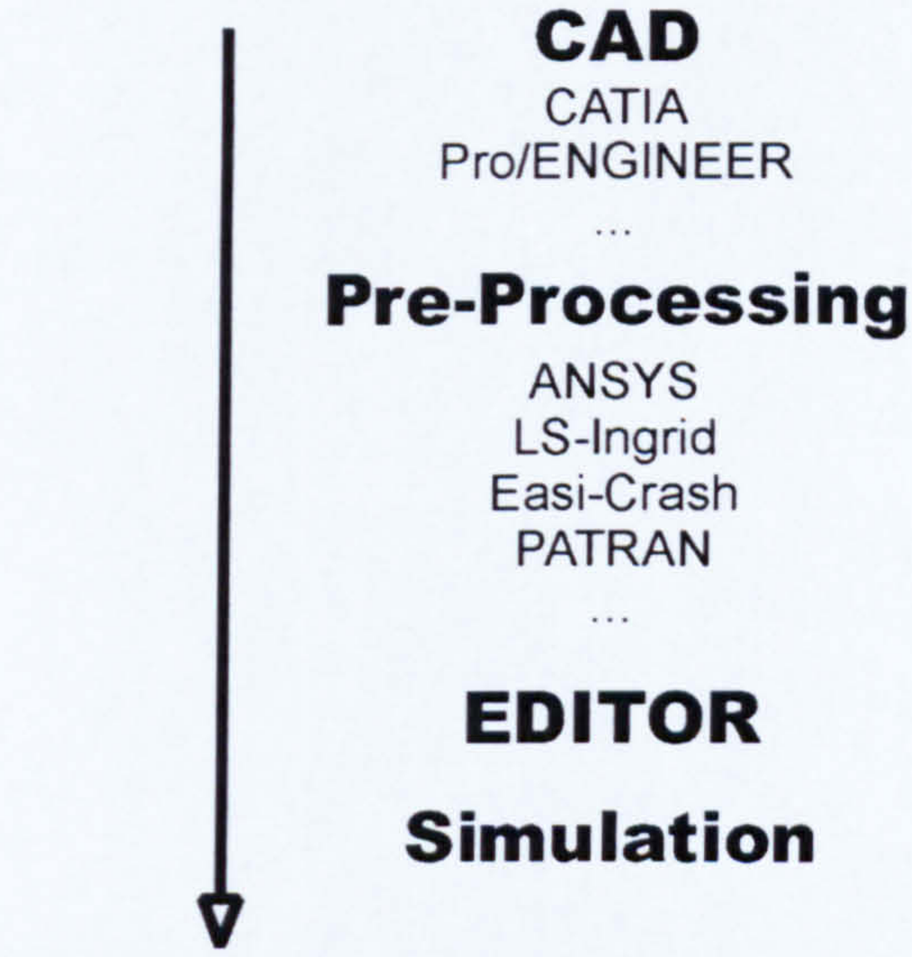

Figure 6-1 Block Diagram IHP Simulation

Figure 6-2 IHP Main Menu

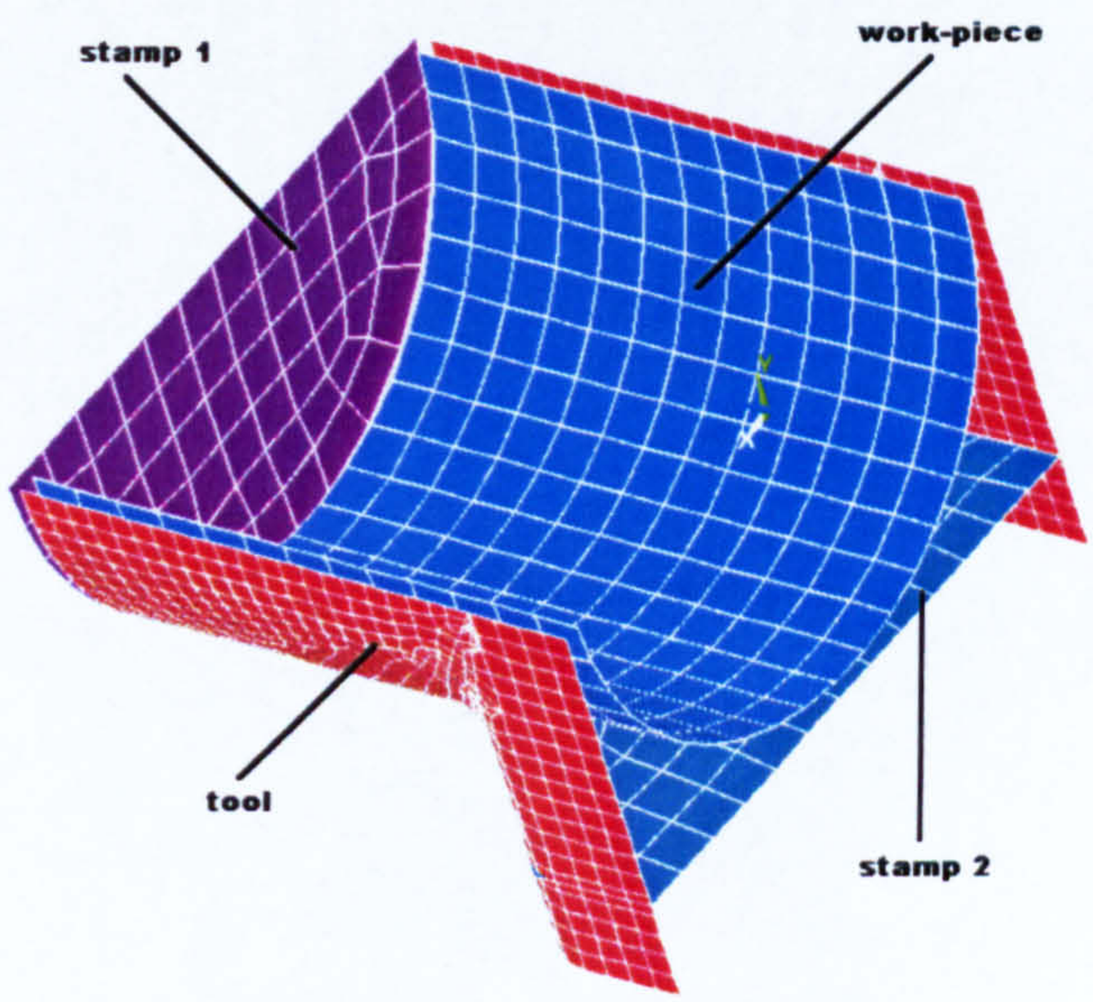

Figure 6-3 Typical IHP Situation

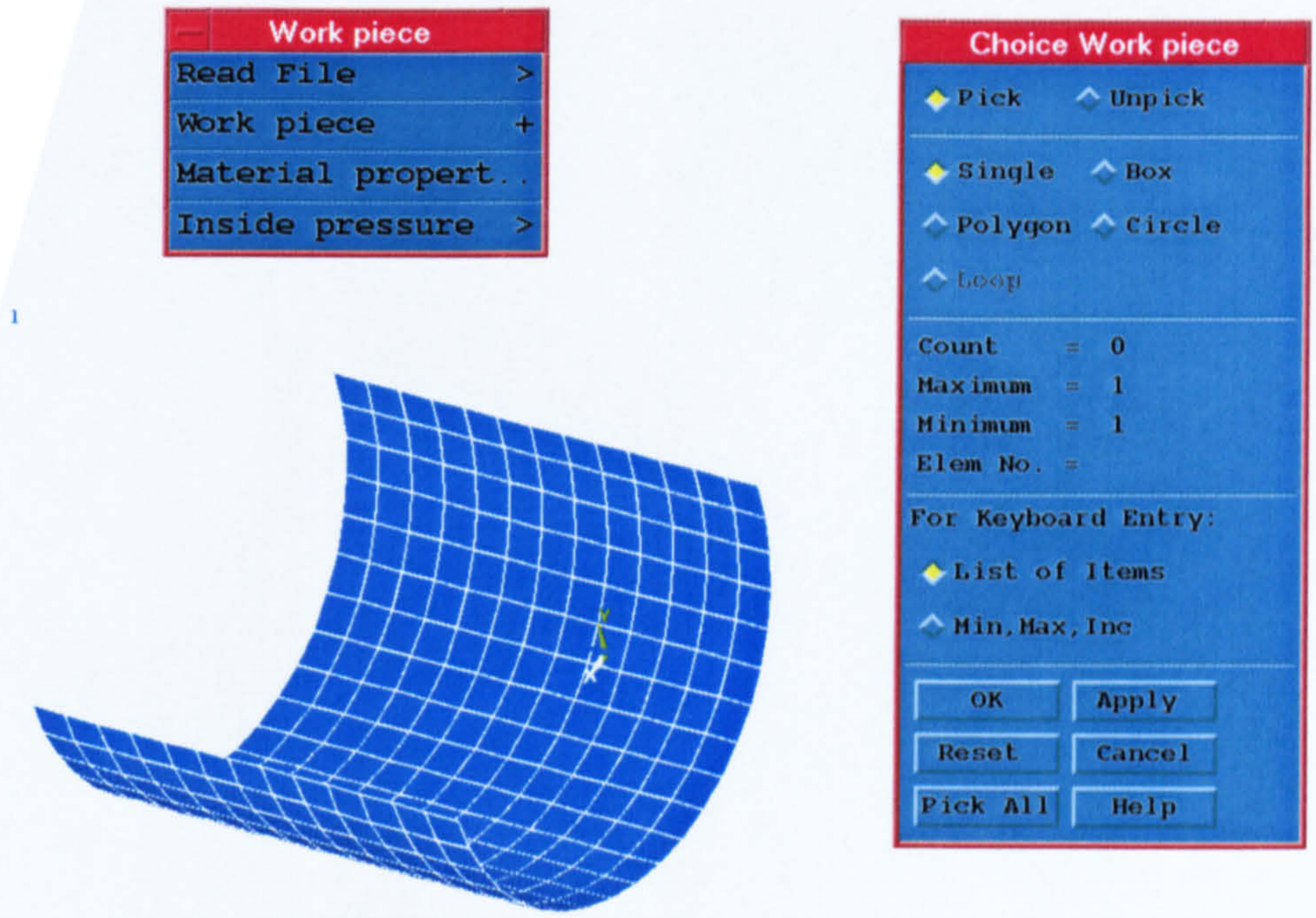

Figure 6-4 Work Piece Definition

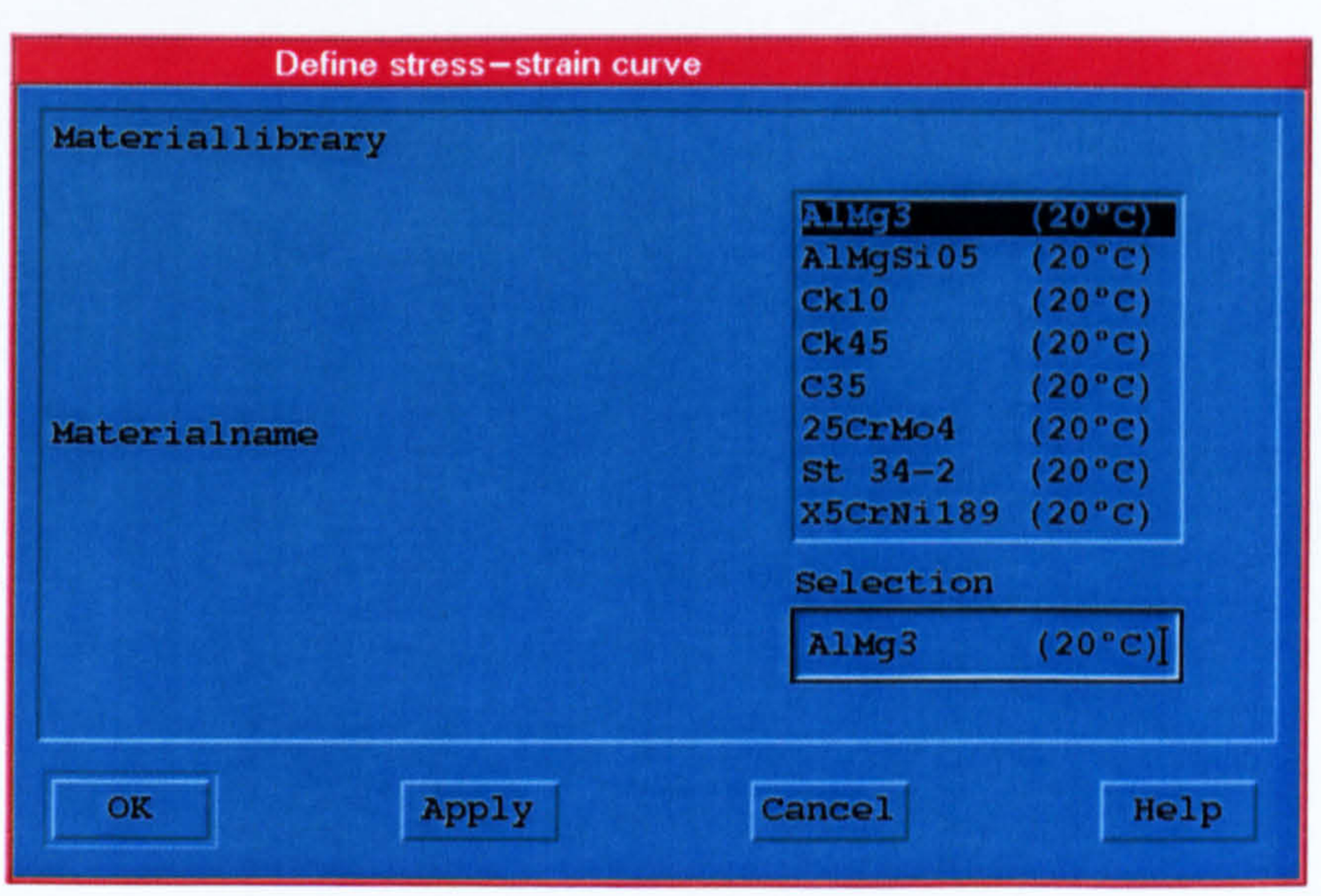

Figure 6-5 Menu for the Material Selection from the Material Library

Figure 6-6 Definition of the Interior Pressure

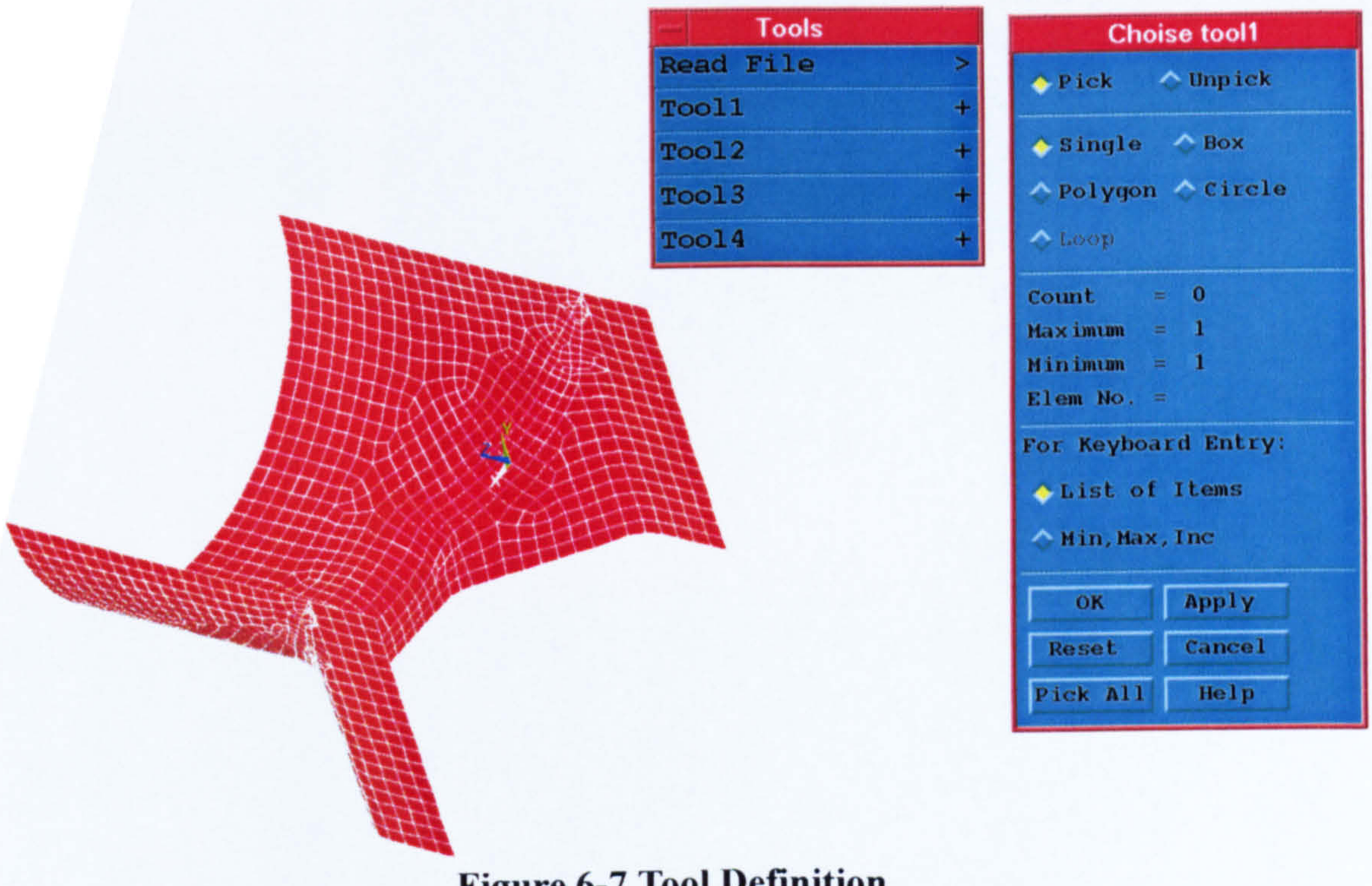

Figure 6-7 Tool Definition

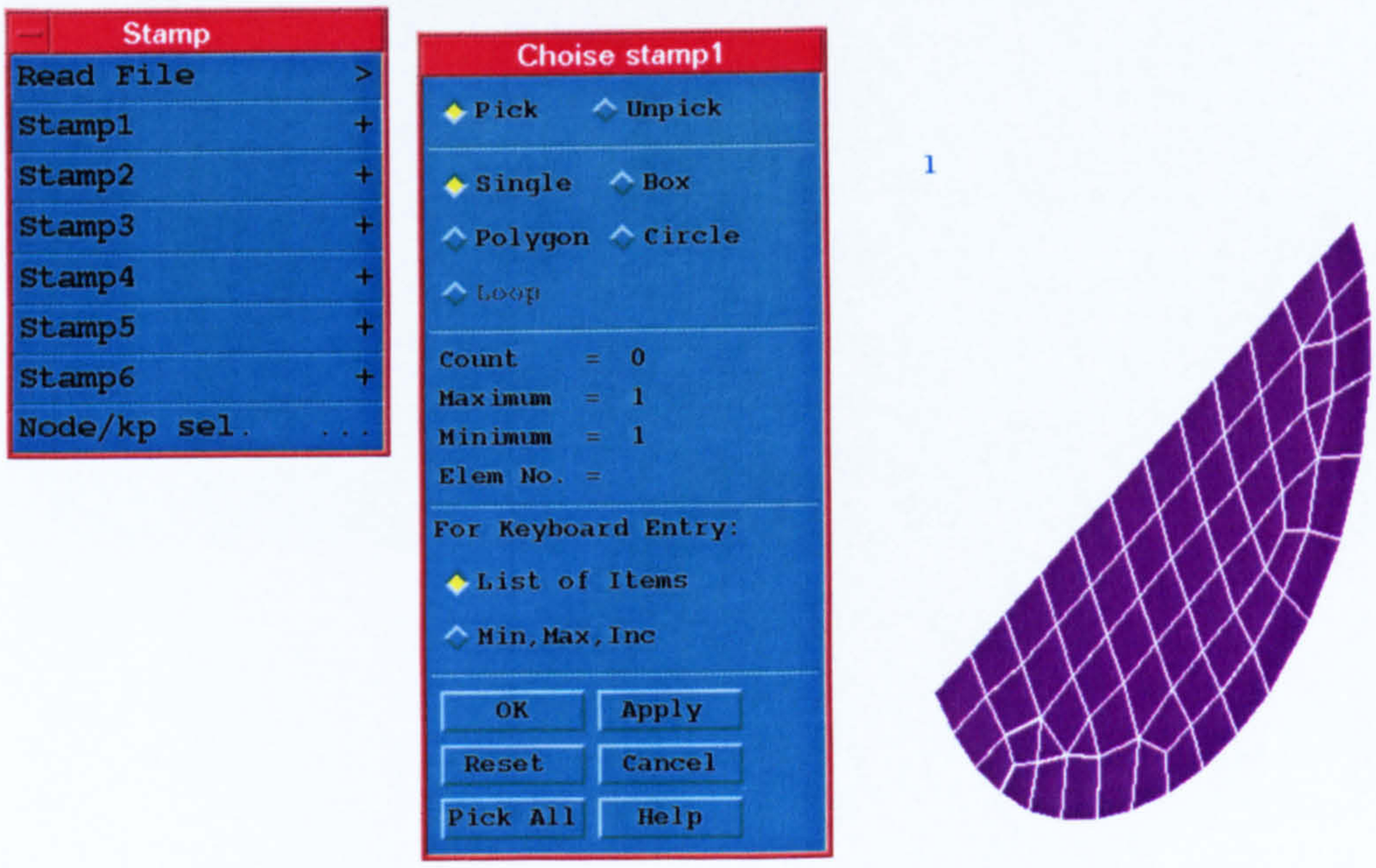

Figure 6-8 Stamp Definition

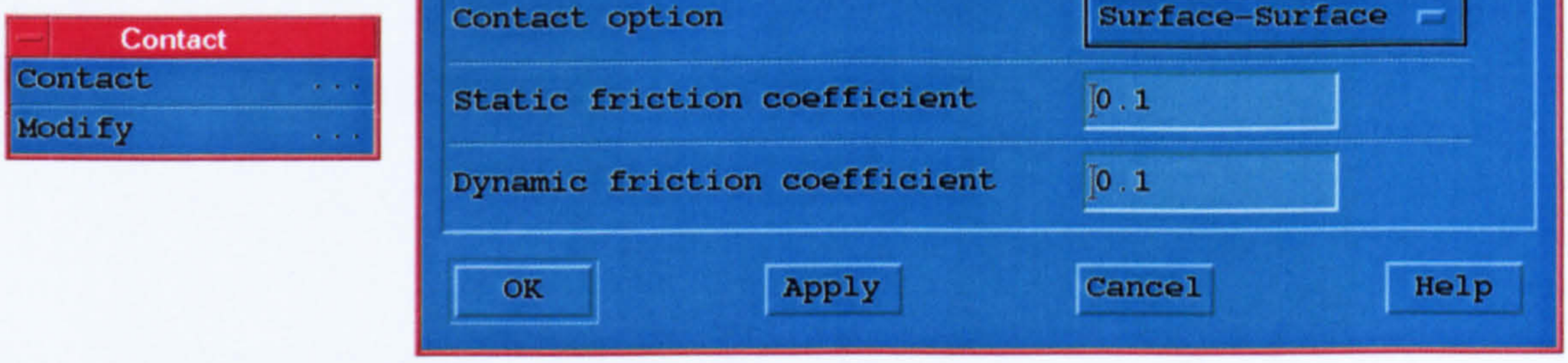

Figure 6-9 Contact Definition

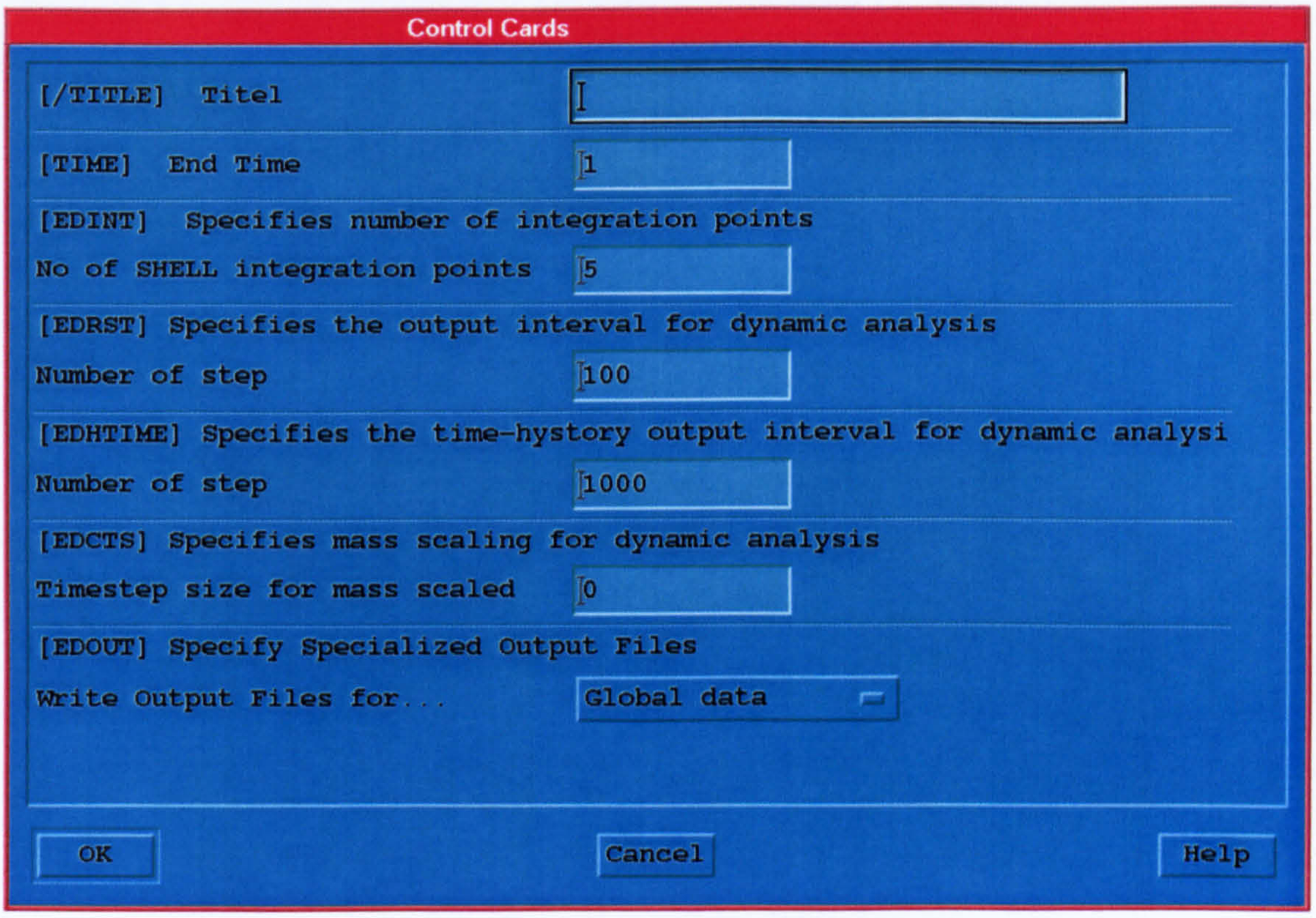

Figure 6-10 Control Options

CHAPTER 7

IHP Optimisation using Surface Reconstruction

Today the simulation of forming processes is only applied to find out how the process works, and the investigation of the part properties is done after the forming operation, e.g. the distribution of the wall thickness and plastic strains, or the possibility of calculating the springback behaviour. The demand of the automotive industries is more and more for investigating the behaviour of the produced components while in action. This means the calculation of the daily loads requirements and also the use of the components including the real shape, the real residual stresses and wall thickness distribution in case of a crash. This Chapter introduces a method for feeding back the simulation results into the CAD system for further processing. For multi-stage forming processes this procedure can also be used to feed back the geometry of the intermediate states into the CAD system, e.g. for the construction of special shaped punches.

7 Introduction

The staring point for each IHP simulation is the design of the component to be produced and the corresponding dies with the help of a CAD system or under certain circumstances by a FE pre-processor. The IHP part and the involved tools are meshed using the CAD system or a separate meshing tool. After completing the mesh with the process information, e.g. material data load-curves for interior pressure and axial feeding, the IHP forming simulation is done. At the end of the forming simulation, normally done with shell elements for the work piece, the shape of the final part is investigated, e.g. the co-ordinates of the nodes and the wall thickness and strain distribution for each element. This information is then used to develop a new CAD model of the part that was received from the forming process. The information out of the forming simulation must be prepared for the CAD system, the aim is to represent the received work-piece as a 3-dimensional volume model. This reconstructed geometry can then be compared with the target geometry and also can be used for further structural analysis and calculations, e.g. the simulation of the component behaviour in installation position under load. **Figure 7-1** shows the complete process chain for the developed procedure. In this case Pro/ENGINEER was used as the CAD system.

The problem of this surface reconstruction is similar to the processing of measuring points from a co-ordinate measuring system. There are some programs available on the market today for this approach (Surfacer – Imageware, IntiSurf - IntiTec, Scan-Tools - PTC), but they are not directly able to use the output from the FE system. Furthermore they are not capable of processing any information about elements, e.g. the structural context of the part available

through the elements and their corresponding nodes, and they also can not process the thickness distribution. In this case the points must be connected by hand. A further disadvantage of this program system of surface reconstruction, is the high cost.

The objective of this work is to design a program which fills this gap. The program should be able to calculate the outer and inner cloud of points representing the co-ordinates of the nodes and the thickness information. There is the possibility of using an existing program for surface reconstruction, a CAD system, to create the inner and outer surface using this information. Also the points from the outer and inner surface can be processed further and a spline curve may be created and converted into a fitting format, e.g. VDA or IGES for additional processing within a CAD system. These two proposals should be investigated and evaluated. A further possibility is to use the available information in Pro/ENGINEER directly to create spines and surfaces.

7.1 LS-DYNA Output

The geometry of the component to be reconstructed was saved to a file named DYNAIN (**Figure 7-2**). This file consists of the co-ordinates of the nodes after the forming operation, and the geometric element information, e.g. which node belongs to which element, the element thickness' and the residual stresses for each element. **Figure 7-3** shows a corresponding thickness distribution of a typical IHP part. The residual stresses are not of interest in the case of the reconstruction of geometry within the CAD system as the CAD system is not able to process this information. The residual stress conditions within the component of the forming process is only of interest for additional FE calculations. This case will be not considered in this work and can be a topic for further work.

7.2 Approaches for the surface reconstruction

There are different approaches for the reconstruction of the surfaces, as shown in (**Figure 7-4**) or excluding the element information as shown in (**Figure 7-5**).

For all solutions it is necessary to create a facility for calculating the inner and outer surface points because the simulation program provides only the co-ordinates of the middle node and the corresponding thickness.

Different approaches are available for the reconstruction of the surface:

- Create the Surfaces Directly with a Utility
- Create cloud of arranged points
- Solution using Pro/TOOLKIT
- Solution with Pro/SCANTOOLS
- Solution with an existing Surface Reconstruction Tool

The following sections discuss the advantages/disadvantages of the different solutions. **Figure 7-4** and **Figure 7-5** show the flow-diagram for the surface reconstruction.

7.2.1 Approach to Create the Surfaces Directly with a Utility

The first attempt is to write a utility which creates the inner and outer surfaces directly out of splines. The splines must be placed through the neighbouring nodes in a radial or longitudinal direction. Surfaces and/or splines must be converted and saved as a IGES or VDA format so that they can be imported into Pro/ENGINEER. If only splines are generated then they must be connected afterwards to the surfaces within Pro/E using the standard Pro/E functionality in order to create a surface.

Advantages of this solution

- Fast reconstruction possible
- Reconstruction tools independent from surface
- Cheap

Disadvantages

- High overhead for the programming
- Splines and surfaces must be described mathematically

This solution will not be used, because of the high programming overhead as well as being time consuming .

7.2.2 Approach to create cloud of arranged points

A further attempt is to write a utility which sorts the point of the outer and inner surface in a radial or longitudinal direction. The points are sorted using the node and element information available from the LS-DYNA output. The points of one spline are summarised and saved into an IBL file in Pro/ENGINEER and the splines are then created selecting the point from the screen.

Advantages of this solution

- Fast reconstruction possible
- Reconstruction tools independent from surface
- Cheap
- Not necessary to describe the splines mathematically
- Simple to write an IBL file

Disadvantage

- Manual labour necessary

This solution has been chosen, because of the low programming overhead required.

7.2.3 Solution using Pro/TOOLKIT

Pro/ENGINEER offers the possibility to integrate user written programs into the software using the programming interface Pro/TOOLKIT. This module includes a number of C libraries for the creation and manipulation of Pro/ENGINEER geometry. These possibilities can be used to create the inner and outer surface automatically.

This approach needs a considerable efford of personal involvement. The work described in the previous section must also be carried out in this case, and for that reason the integration can be done later.

7.2.4 Solution with Pro/SCANTOOLS

The points on the outer and inner surfaces will be imported into Pro/SCANTOOLS. Afterwards a manual adjustment of the scanned curves and the creation of the surfaces are necessary.

Advantages of this solution

- No additional programming necessary
- Curves can be modified
- Data reduction possible

Disadvantage

- Time consuming manual labour necessary
- No influence on how the points are imported

7.2.5 Solution with an existing Surface Reconstruction Tool

A further approach is to use an existing surface reconstruction tool, for example Surfacer. Inti-Surf, Pointmaster, etc ... . The points must be arranged into a format which can be imported into the surface reconstruction software and following manual adjustment of the points to arrange them in a fitting order the surfaces are created. The created surfaces can be exported out of the surface reconstruction software in a standard exchange format and imported into Pro/ENGINEER.

Advantages of this solution

- No additional programming necessary
- Many functions for manipulation of the points
- Data reduction possible

Disadvantage

- Time consuming manual labour necessary
- High costs
- Personal involvement necessary

7.3 Surfaces in Pro/ENGINEER

The modelling of free-form surfaces in Pro/ENGINEER is always performed by (spline) curves created before. The boundary curves of an already existing geometry can be used, or new curves must be created. Pro/ENGINEER only offers the possibility to create interpolating splines curves through points. However interpolated spline-curves have the disadvantage of being more wavy than approximated splines. The creation of curves and surfaces in Pro/ENGINEER is easy but not necessary for an optimum solution.

7.3.1 IBL-file

Curves out of points which are to be imported from a file into Pro/ENGINEER must be written in a special format (IBL-file). **Figure 7-6** shows the format of this IBL file. The imported points (**Figure 7-7**) are referenced to a co-ordinating system within Pro/ENGINEER. Imported curve or curves (**Figure 7-8**) will be handled as a single feature. However the creation of the surfaces of the curves can be individually selected.

Different keywords can influence the appearance, e.g. **[open]** to start a new curve and **[closed]** to create a closed curve, in this case the co-ordinates of the first and the last point must be identical.

7.4 Requirements of the User

Today industry and above all the automotive industry uses more and more parts manufactured using the IHP technique. These mostly tubular IHP parts have a varying wall thickness in comparison to conventional produced parts. For crash simulations and structural analysis the variation of the wall thickness is of great importance, therefore, it is necessary to bring back the simulation results into the CAD system.

7.5 User Interface Requirements

The use of the program for the reconstruction of the part must be quick and easy. Ideally the execution of the surface reconstruction should be possible without a handbook or training. Furthermore it is desirable that the surface reconstruction runs quickly and without errors, and that little manual post-processing is needed.

An advantage would be the integration of the surface reconstruction into Pro/ENGINEER, but additional costs for programs or licenses would arise.

7.6 Utility to Create the Outer and Inner Surface Points

The first step for the surface reconstruction is to calculate the outer and inner points (**Figure 7-9**) out of the node co-ordinates from the LS-DYNA output DYNAIN. Each node from the FE mesh amounts to 2 points on the solid structure.

Any element has four attached nodes. These four nodes are situated in the same plane and represent a parallelogram. One node and the neighbouring node allows the calculation of the vectors V_1 and V_2 (**Figure 7-10**). The cross-product of these two vectors amounts to the normal vector. The order of the nodes is chosen in such a manner that the normal vector points to the outside.

$$V_1 = K_2 - K_1$$

$$N1 = V1 \times V2$$

$$V_2 = K_4 - K_1$$

A node is always attached to a certain number of elements, for quadratic elements two at the boundaries and 4 inside the structure, see **Figure 7-11**. The normal vector of a node will be determined using the normal vectors of the attached elements. To calculate the element normal vector, the elements are valenced corresponding to their area. An element with an area twice as big as the neighbouring element will have twice the weight. The area of an element will be calculated using the normal vectors of the opposite corners and the amounts are then added together.

The normal vector (N_5) would be calculated using the standard vectors of elements 1 to 4, and are then weighted corresponding to their area. This calculated normal vector must now be transformed into the standard vector.

Each element has an attached thickness, i.e. each node has four (two) thicknesses. The average of these thicknesses is the thickness of the part at that position. This value will now be halved and multiplied with the standard vector for the node to obtain the co-ordinates of the point at the outer and inner surfaces.

These newly calculated points will now be written into two separate files. These files can be created depending on other procedures, i.e. with or without using the element information.

7.7 Surface Reconstruction using Pro/SCAN-TOOLS

An optional module of Pro/ENGINEER has the capability of importing digitised points (Pro/SCAN-TOOLS). This module is able to import IBL, IGES or VDA files. Pro/SCAN-TOOLS generates automatically, what is called scan curves out of the imported points.

The surface reconstruction with Pro/SCAN-TOOLS runs with the following steps

- Import of the IBL-file
- Process the scan curve(s) **(Figure 7-12)**
- Modify the scan curve(s) **(Figure 7-13)**
- Convert the scan curves into style curves **(Figure 7-14)**
- Process the style curves
- Create a style surface
- Merge the style surface to a surface
- Repeat same procedure for inner and outer points
- Create the front surfaces
- Merge the surfaces
- Create the solid

The scan curves must be modified because they are not in the desired shape.

The style curves must be lengthened up to the boundary curves **(Figure 7-15)**.

The next step is to create the surfacte through selecting the style curves **(Figure 7-16)**. As Pro/ENGINEER does not allow the creation of a single tubular surface it is necessary to generate two partly tubular surfaces.

Figure 7-17 shows the result of the first operation, the upper surface, and **Figure 7-18 shows** the result of the second step, the lower surface.

Both surfaces must now be merged. The outer curves would be processed in the same manner to get the outer surface. **Figure 7-19** shows the inner and outer surface.

To create the solid model it is necessary to close both open ends of the tubular body. **Figure 7-20** shows the forehead surface.

As a result of merging both surfaces all surfaces of the solid component can be generated **(Figure 7-21)**.

7.8 Problems of the Surface Reconstruction using Pro/SCAN-TOOLS

The user has no influence on how the scanned curves are placed through the points, except through editing the IBL file. Under some circumstances, a costly post-processing of the scanned curves is necessary.

Surface reconstruction with Pro/SCAN-TOOLS is relatively time consuming. Most of the time is needed at the post-process stage of scanned curves, the convertion of the scanned curves into stile curves, and the lengthening of the stile curves to boundary curves. The selection of the stile curves to create the surfaces in the correct order is costly, as errors can be easily made. The complete surface reconstruction of a typical IHP component takes up to approximately 2 hours interactive user time.

Because it is not possible to create a single surface in one step and the surfaces of the two halves must be merged at the boundary line, a slight fold can arise as the tangential stability of the surface is broken.

If the IBL file contains triangular elements (**Figure 7-22**) the order in which the points are numbered changes. The scanned curves which are placed through are then useless. A surface reconstruction of such a file is only possible with a very costly post-processing.

7.9 C-Utility to sort the nodes

7.9.1 Description of the Utility

The LS-DYNA output file contains information about the node co-ordinates and additional information about which nodes are attached to which elements. No existing surface reconstruction tool is able to make use of this additional information to create the surface. For that reason the idea is to create a utility which is able to work with this information and sort the nodes in radial direction (**Figure 7-23**), and then save them again into a new IBL file.

The utility checks how many nodes are connected to each element. If a node is only attached to two elements then it is identified as a boundary node (**Figure 7-24**), and sorting starts at such a boundary node (**Figure 7-25**).

Starting from the node which has the position Pos2 at element EL1 (see **Figure 7-25**), the element on which the node is on Pos1 will be searched. In this way all boundary nodes are processed until node 1 is reached (**Figure 7-26, 7-30, 7-31**).

The same procedure is used for all other nodes starting from node 1 on EL 1 (**Figure 7-27**).

Each circular set of nodes results in a single scan curve in the IBL file.

7.10 Surface Reconstruction with radial sorted Nodes

After processing the data from the LS-DYNA output through the sorting utility and importing of the new IBL file into Pro/ENGINEER, the following scan curves are generated (**Figure 7-28**). A single surface can now be created out of these curves (**Figure 7-29**). The same procedure must be carried out for the outer surface.

The benefit of this procedure in comparison to curves in longitudinal direction is that a single surface can be created for the inner and outer area and that no problems with tangential conditions are present.

7.11 Problems with the current Solution

With the surface reconstruction utilities currently available the thickness distribution from the IHP simulation can be used to generate the corresponding 3-dimensional part. The fastest method for the surface reconstruction is the use of the radially sorted splines.

However the current version of this tool has some restrictions. It is not possible to reconstruct parts which are simulated as half- or quarter- symmetries. Furthermore it is not possible to reconstruct simulation results which contains triangular elements (**Figure 7-32**) or those which contains transitions resulting from an adaptive mesh refinement (**Figure 7-33, 7-34**).

7.12 Conclusion and Outlook

Various approaches to solve the problems arising during surface reconstruction are investigated. The aim of the work is to introduce a solution which is cost effective and achieves good results. Two approaches were investigated in detail, the use of Pro/SCAN-TOOLS and the task with radial reordered points. The surface reconstruction with the points sorted in radial direction has been proved to be the best solution, due to the shorter processing time.

The commercially available tools for surface reconstruction have proved less helpful, because they were not able to process the element information. Using such tools a greater deal of manual operation was necessary. As said before the costs for the commercial tools are too high and the process is very time consuming.

An integration of the developed utilities into Pro/ENGINEER with the programming interface Pro/TOOLKIT should be useful to further reduce the time necessary for the surface reconstruction. This approach can also be used to insert the conversion of the scan curves into stile curves and the costly selection of the splines for the production of the surface into the utility. In this way the surface reconstruction can be automated so that the necessary manual labour is reduced considerably.

The automotive industries are demanding more and more predictions of the behavior of the produced components in operation. This means calculating the loads under daily requirements

and also the simulation of the components, including the real shape, the real residual stresses and wall thickness distribution in case of a crash. An additional step towards the use of manufactured parts for further processing is to include the stress and strain conditions in the reconstructed model, and to use this information for crash analysis or the simulation of the car under load.

Appendix F shows some examples for reconstructed parts.

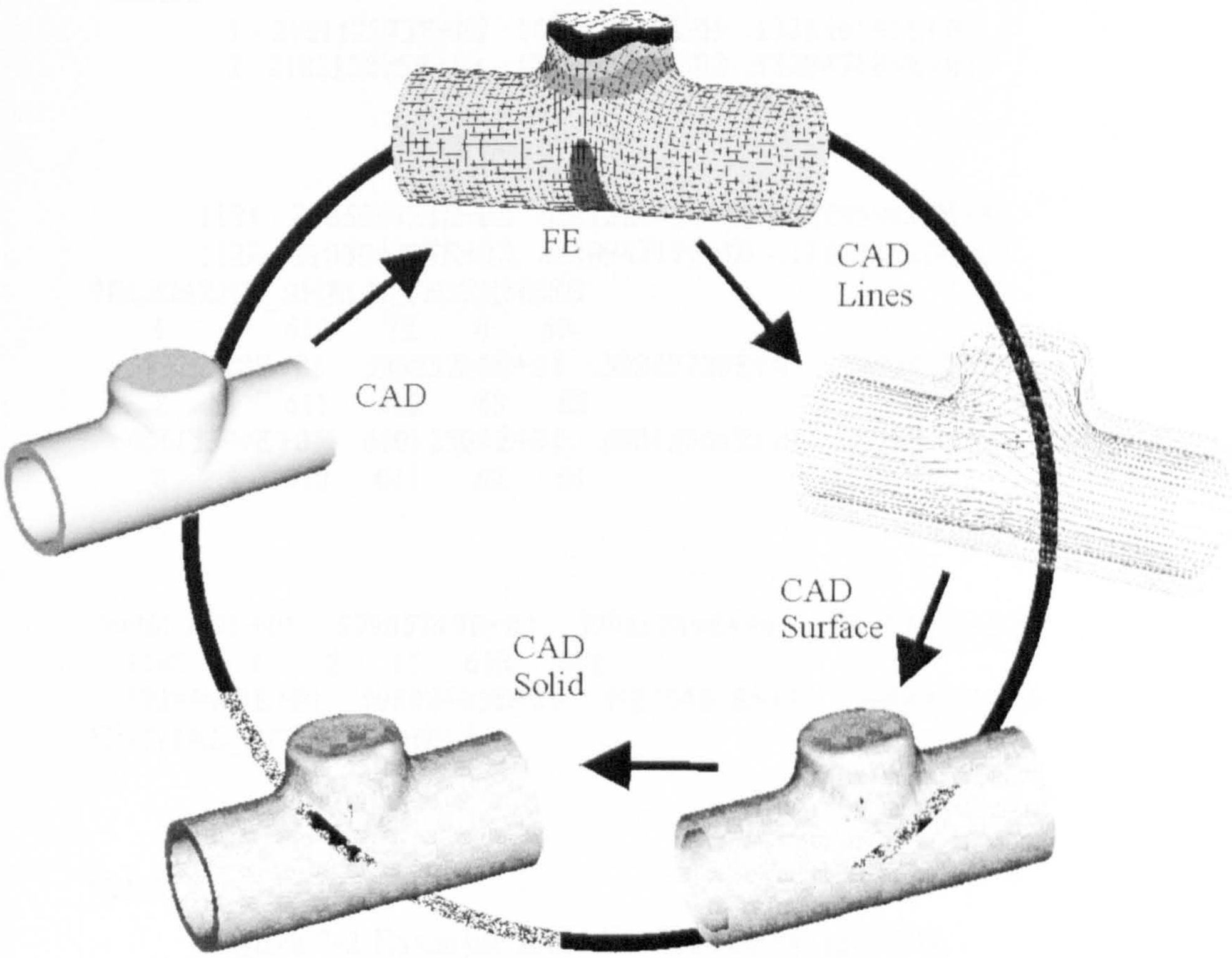

Figure 7-1 Process Chain – Surface Reconstruction

```
*NODE
        1 -.218112373E+02  .167041421E-01  .132846191E+03
        2  .218213825E+02 -.187020935E-02  .132847885E+03
                .
                .
                .
     1121 -.210596733E+02  .614122248E+01 -.120899628E+03
     1122 -.210804787E+02  .613094711E+01 -.126884705E+03
*ELEMENT_SHELL_THICKNESS
    1     1   612    73     4    63
  .59925728E+01  .59925728E+01  .59925728E+01  .59925728E+01
    2     1   611   612    63    62
  .60013304E+01  .60013304E+01  .60013304E+01  .60013304E+01
    3     1   610   611    62    61
                .
                .
                .
 .59965749E+01  .59965749E+01  .59965749E+01  .59965749E+01
   1100     1     2    15   633   613
  .59898405E+01  .59898405E+01  .59898405E+01  .59898405E+01
*INITIAL_STRESS_SHELL
      .
      .
      .
*END
```

Figure 7-2 Example for a LS-DYNA Output File

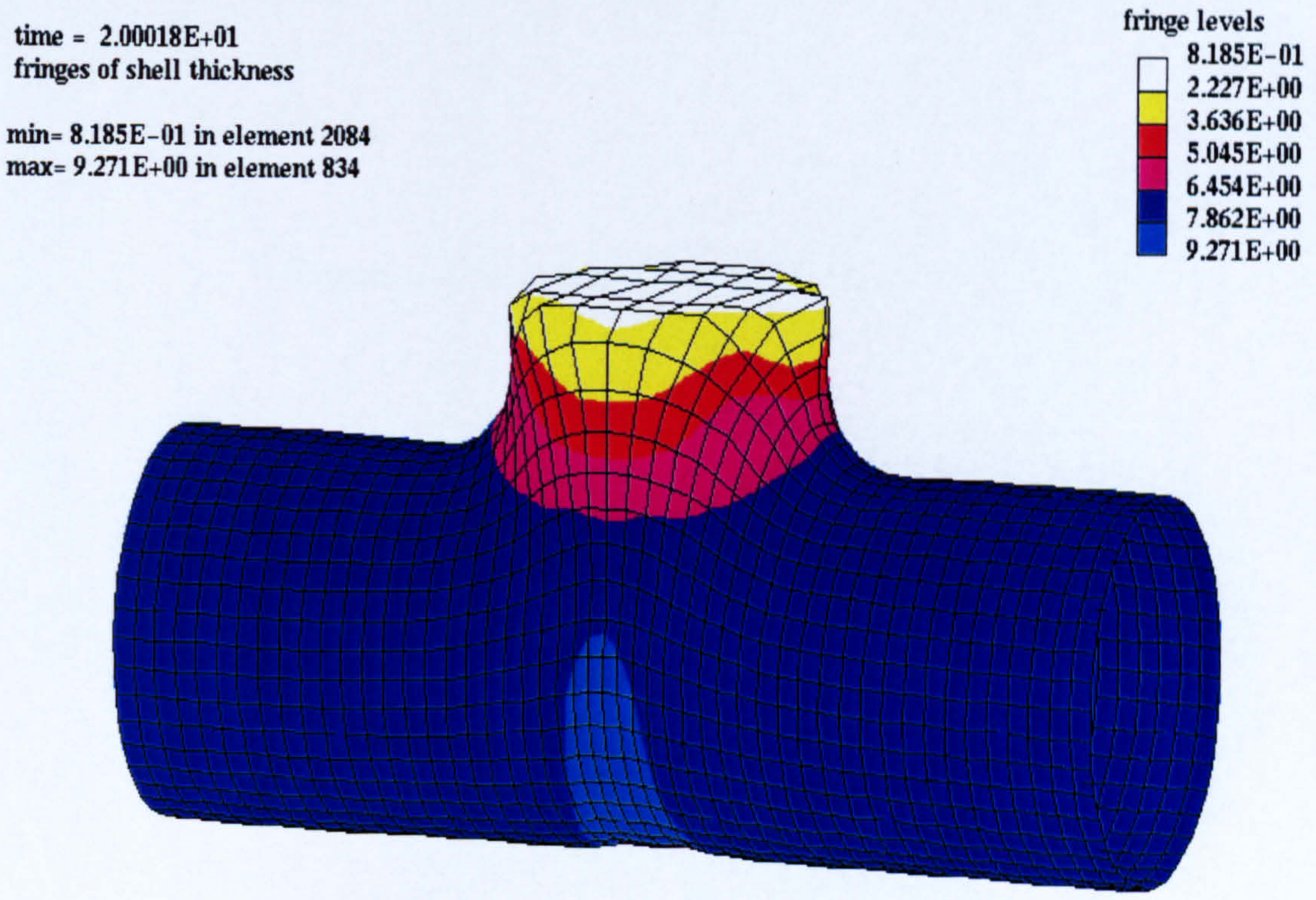

Figure 7-3 Wall-thickness Distribution (LS-Taurus)

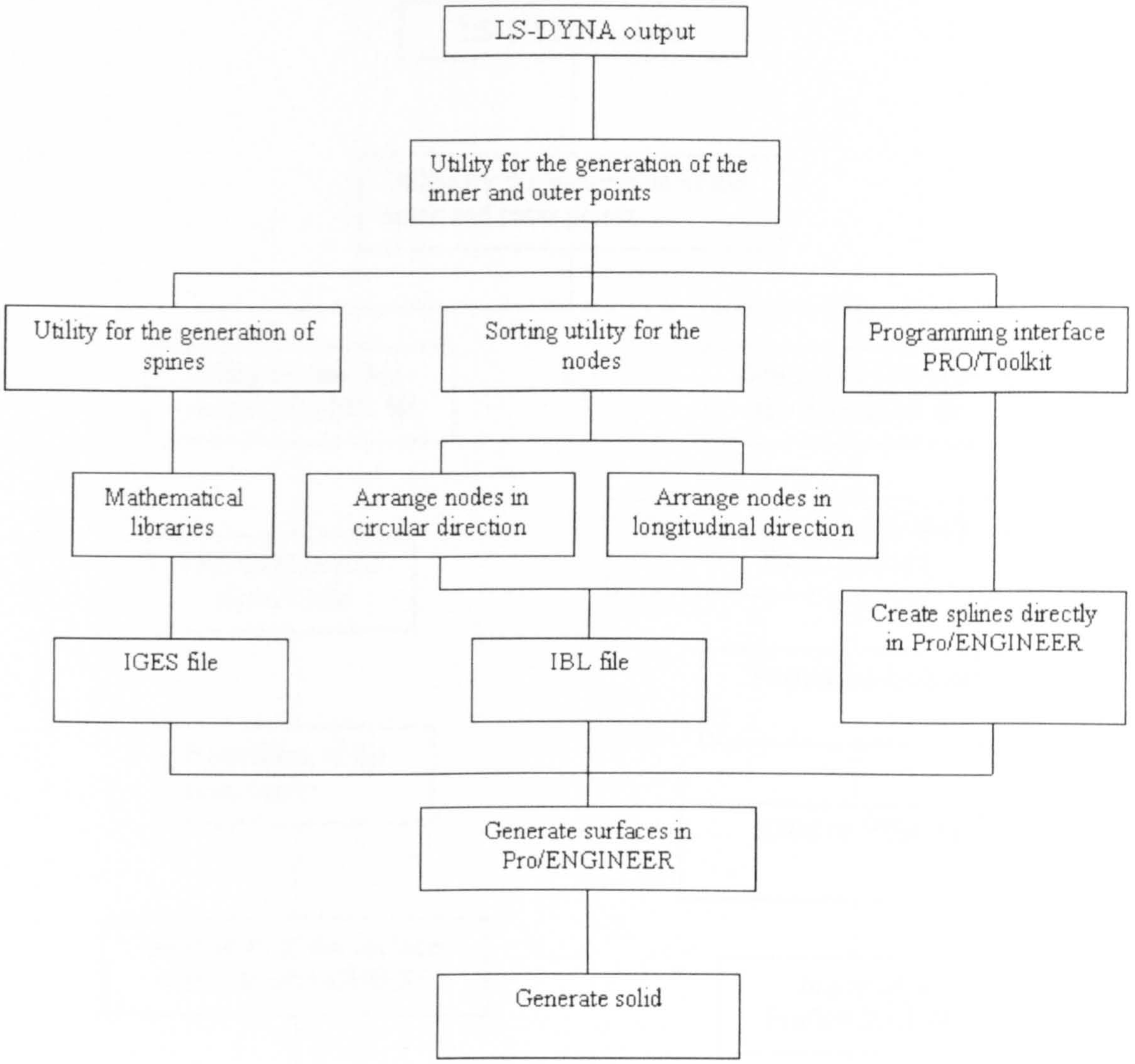

Figure 7-4 Solutions for the Surface Reconstruction

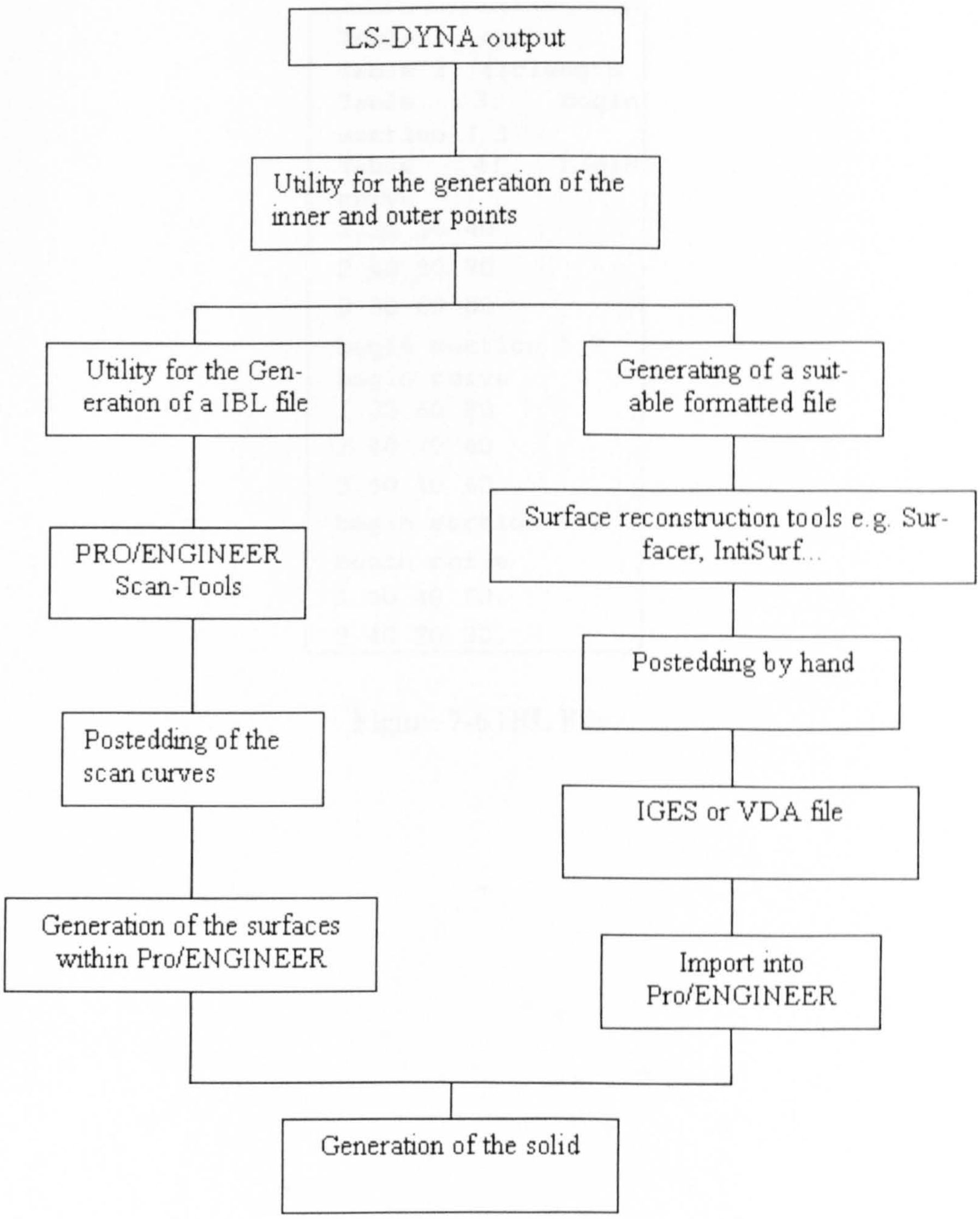

Figure 7-5 Solutions for the Surface Reconstruction

```
Table 1: open
Table 2: arclength
Table    3:    begin
section ! 1
Table    4:    begin
curve
1 20 30 40
2 40 50 70
3 30 60 80
begin section ! 2
begin curve
1 30 60 80
2 40 70 40
3 50 40 60
begin section ! 3
begin curve
1 50 40 60
2 40 20 30
```

Figure 7-6 IBL File

Figure 7-7 Spline-Curves Created out of Imported Points

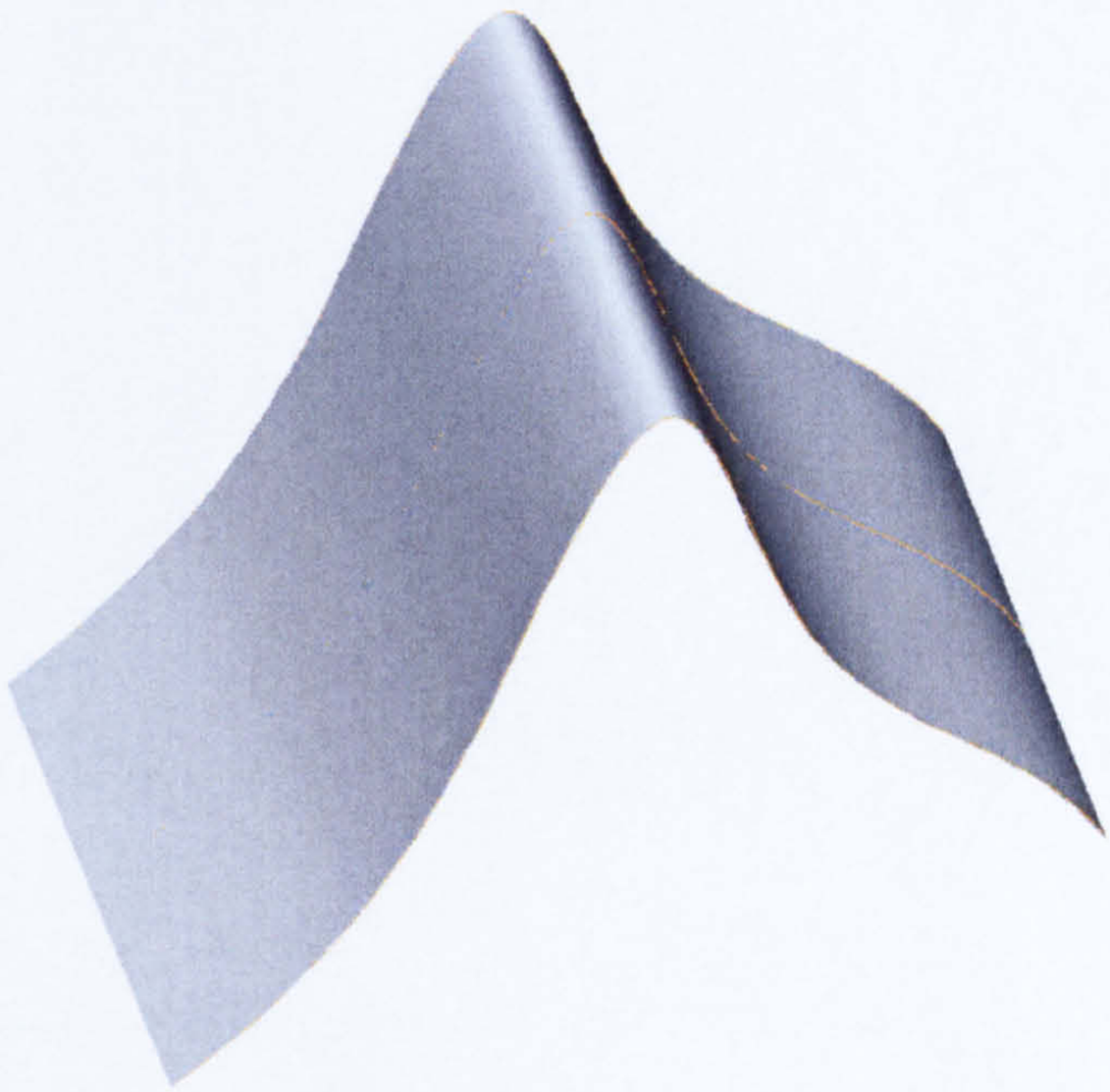

Figure 7-8 Surface Created from Imported Curves

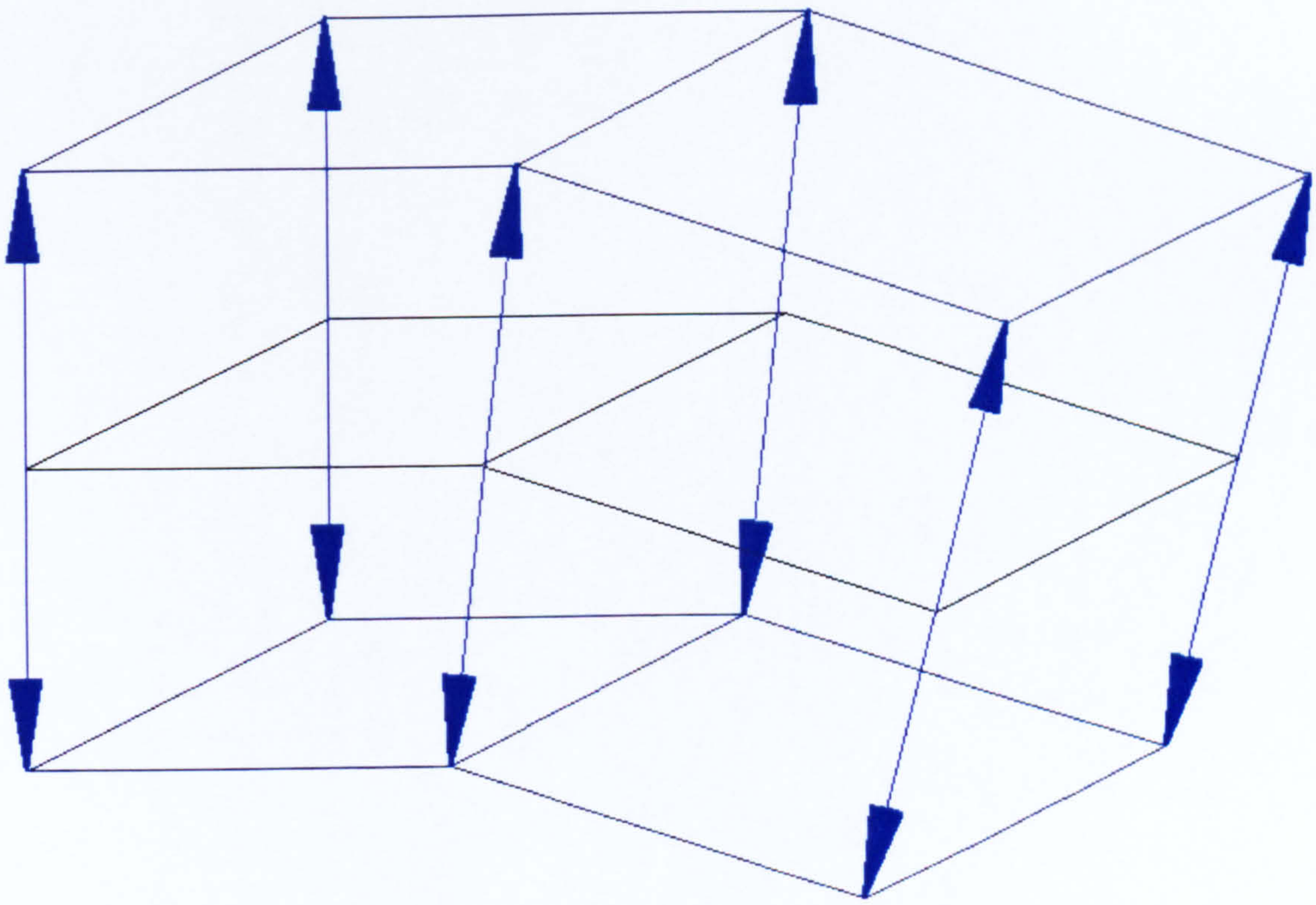

Figure 7-9 Points at the Outer and Inner Surfaces

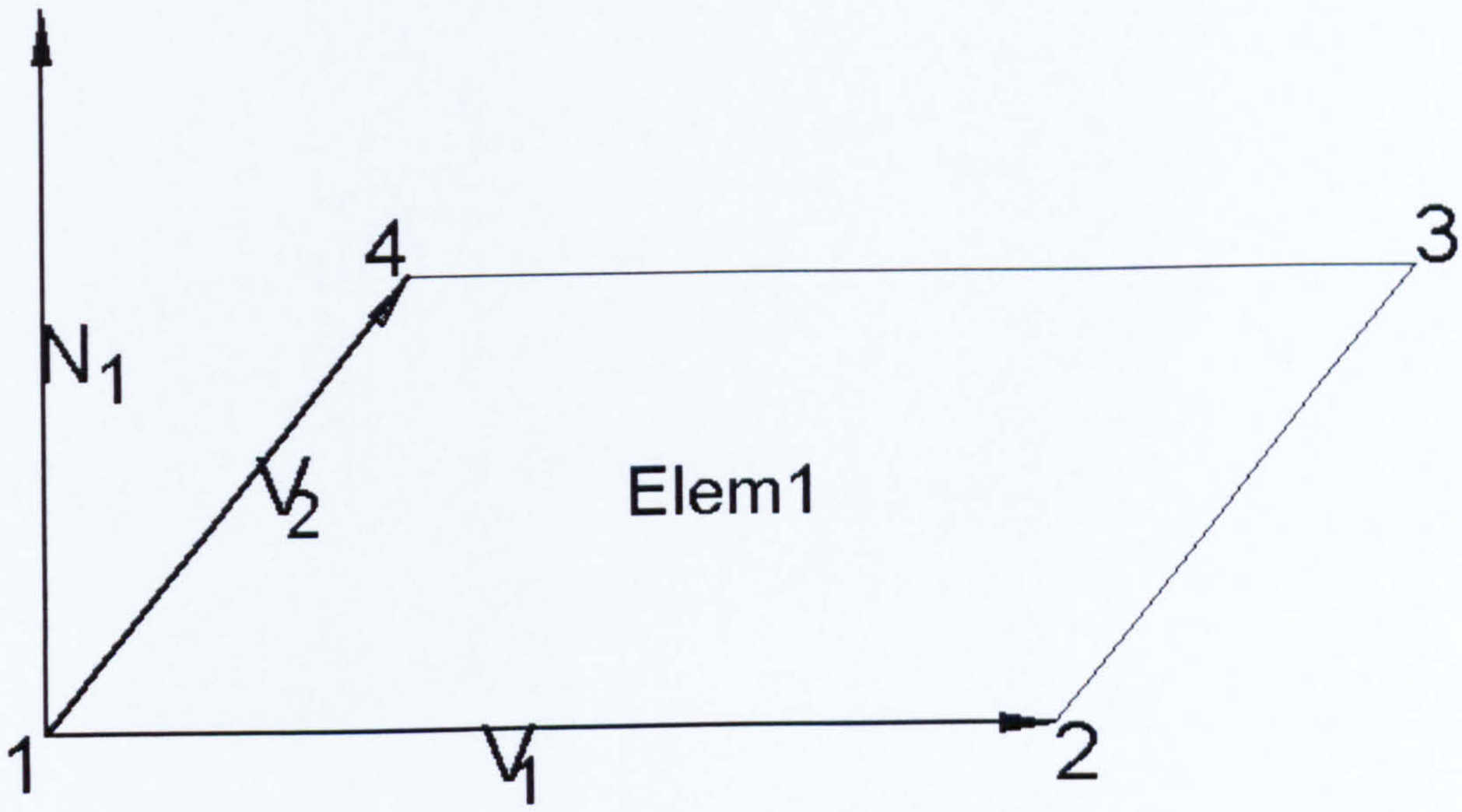

Figure 7-10 Vectors V_1, V_2, Normal Vector N_1

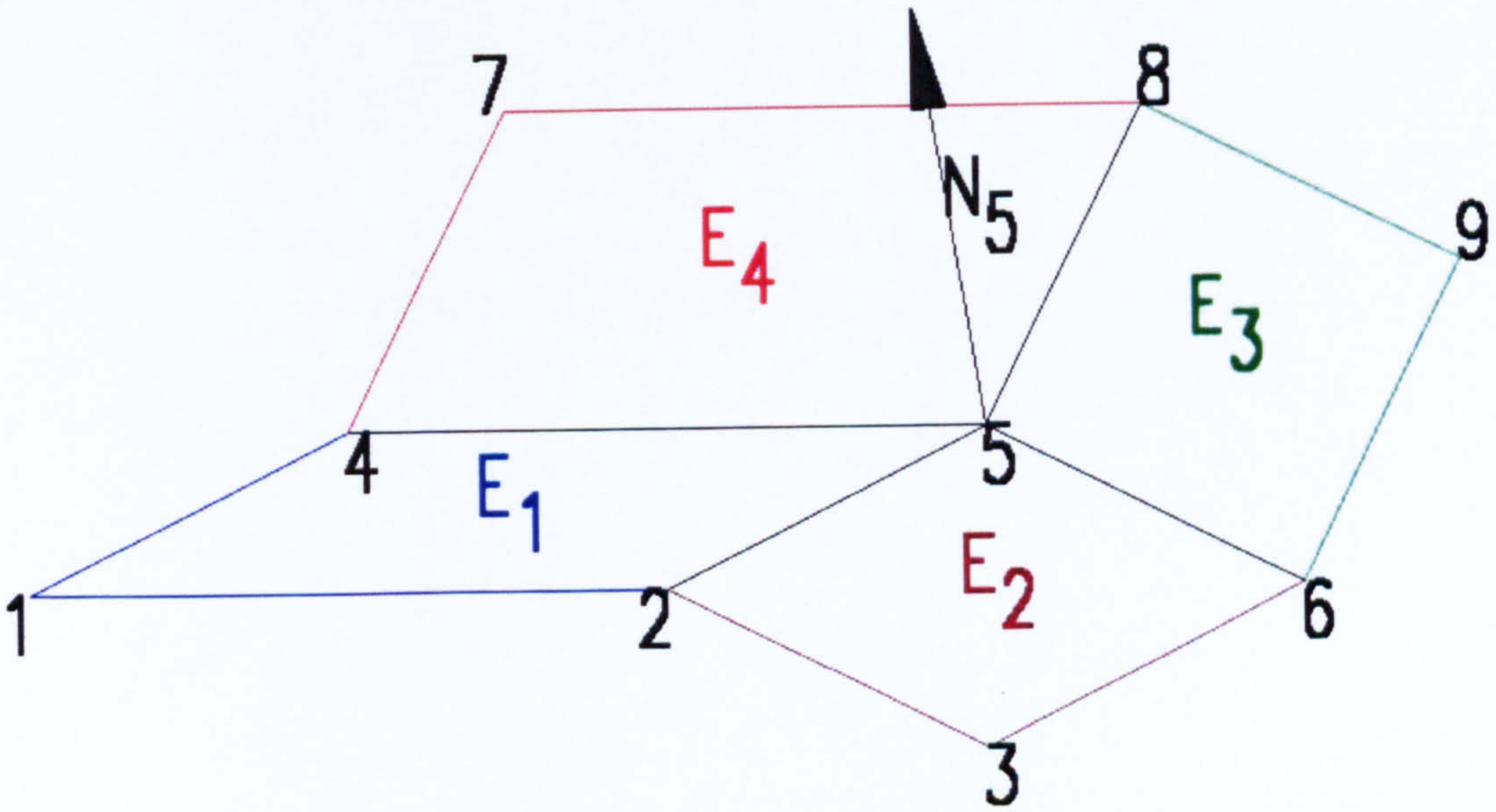

Figure 7-11 Node Normal Vector N_5

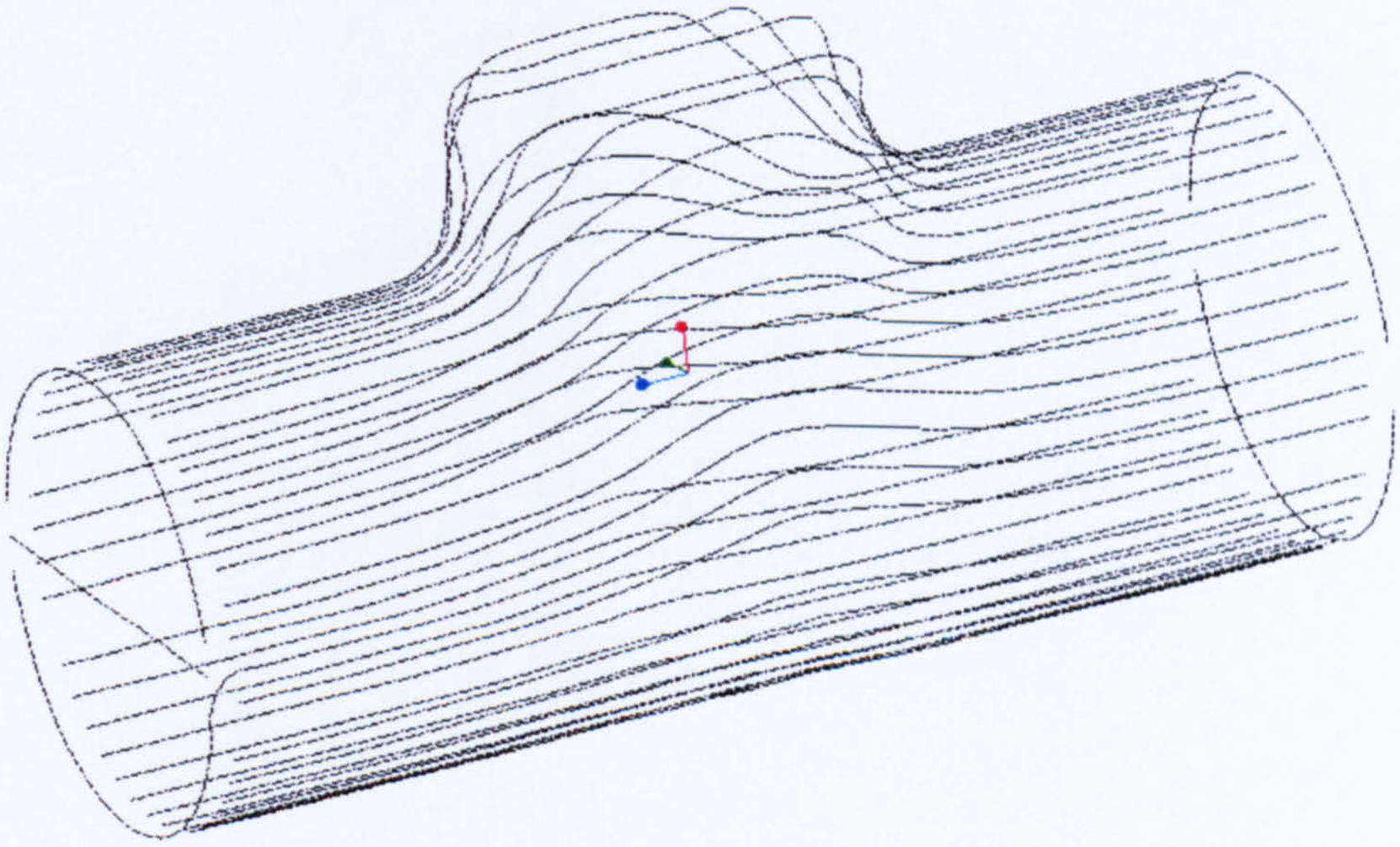

Figure 7-12 Scan Curves

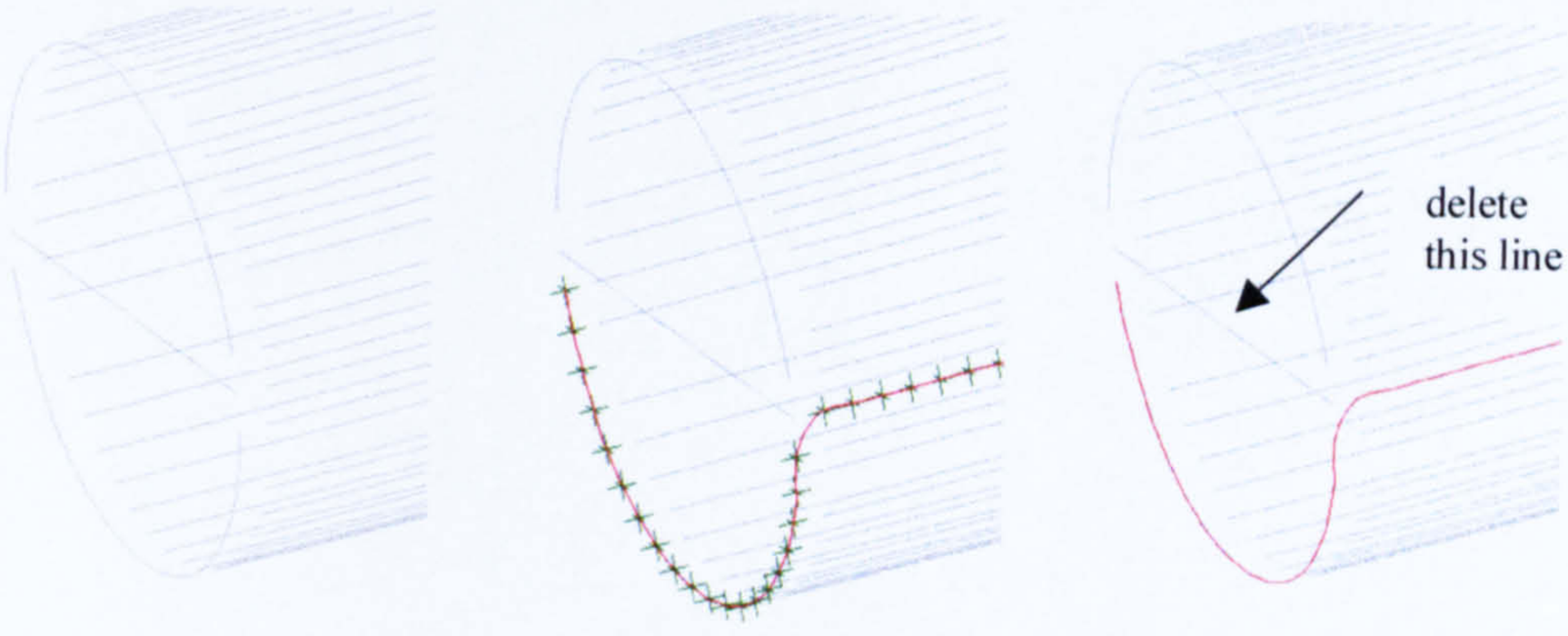

Figure 7-13 Modification of the Scan Curves

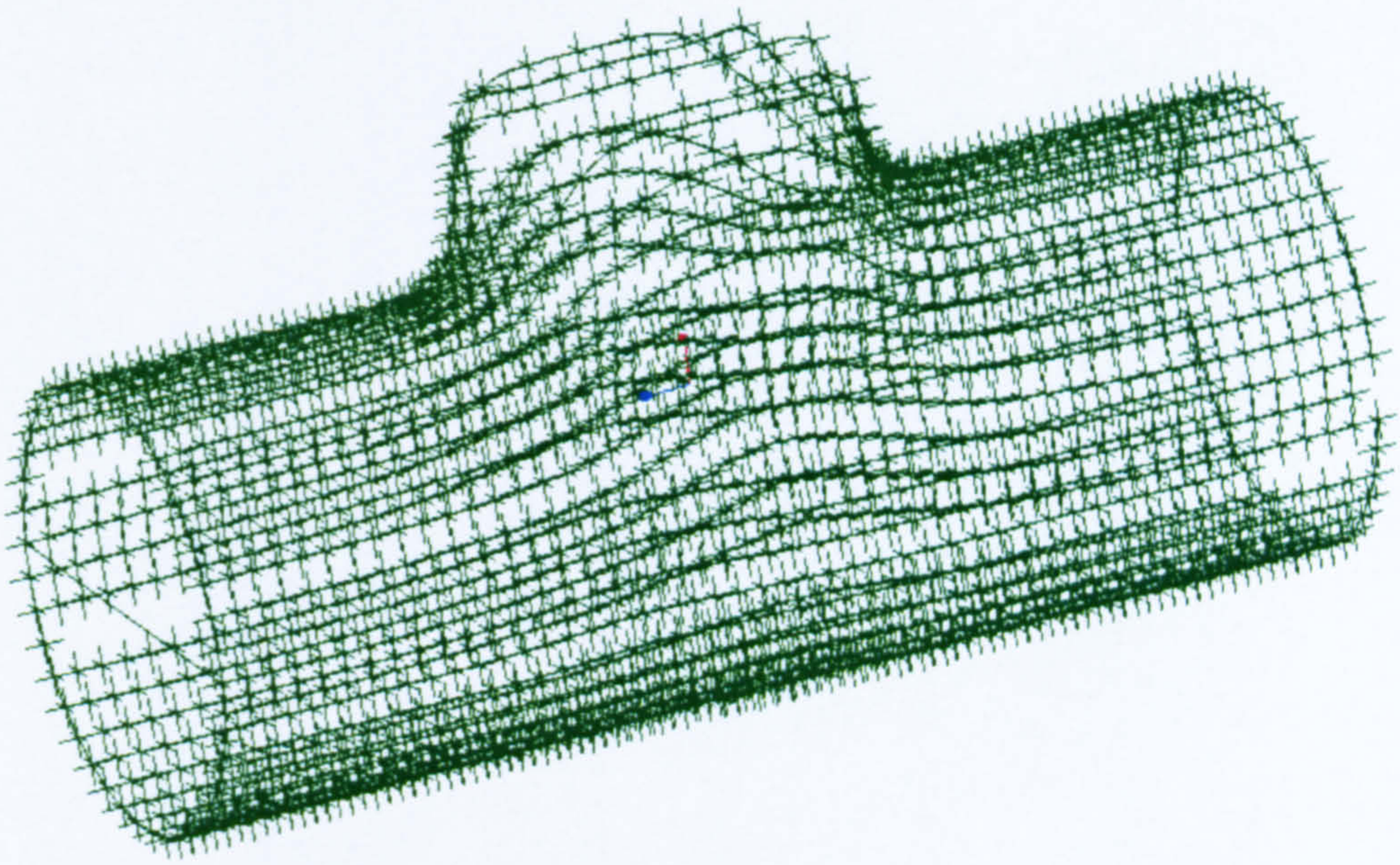

Figure 7-14 Style Curves

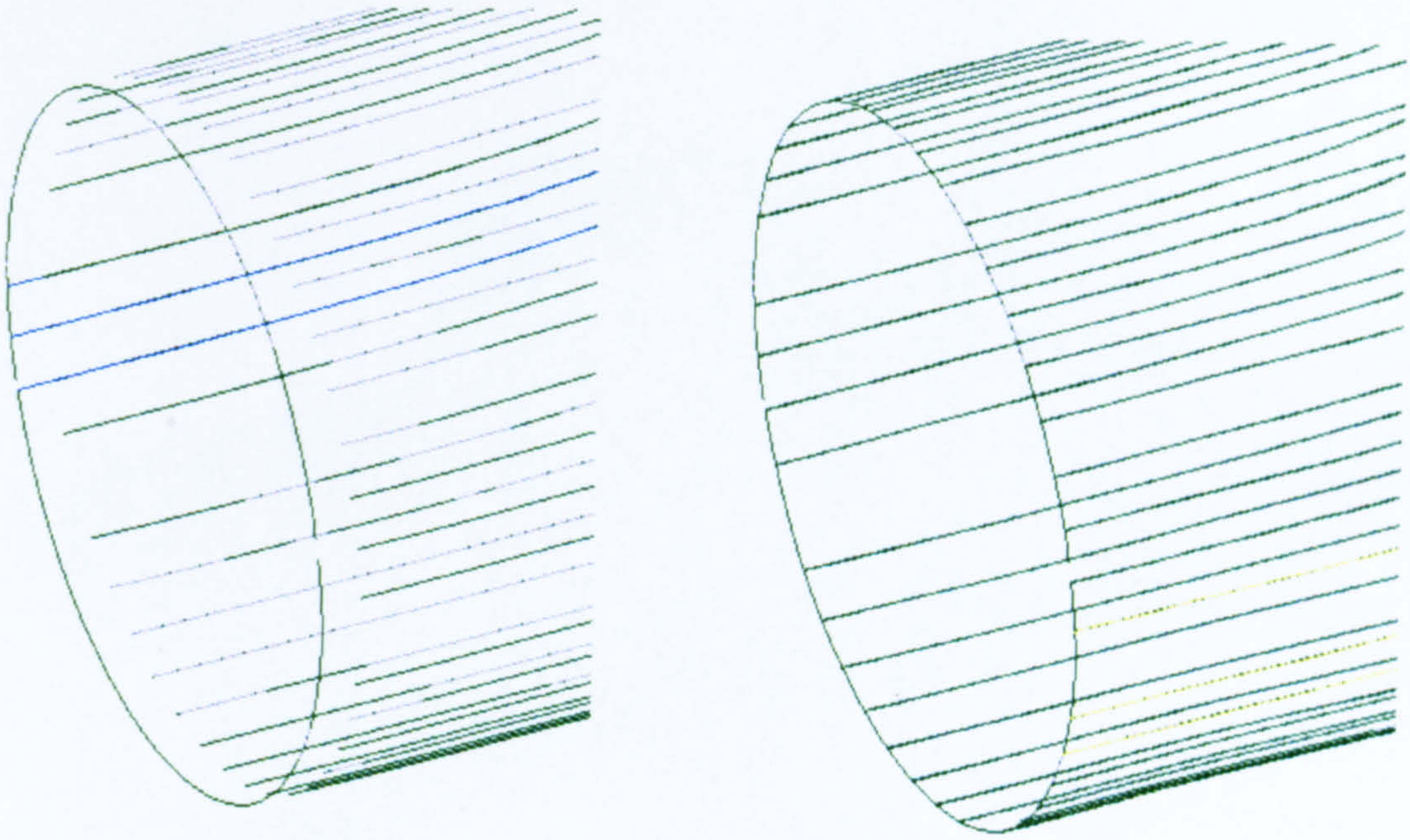

Figure 7-15 Lengthening of the Style Curves

Figure 7-16 Selection of the Style Curves to create the Surfaces

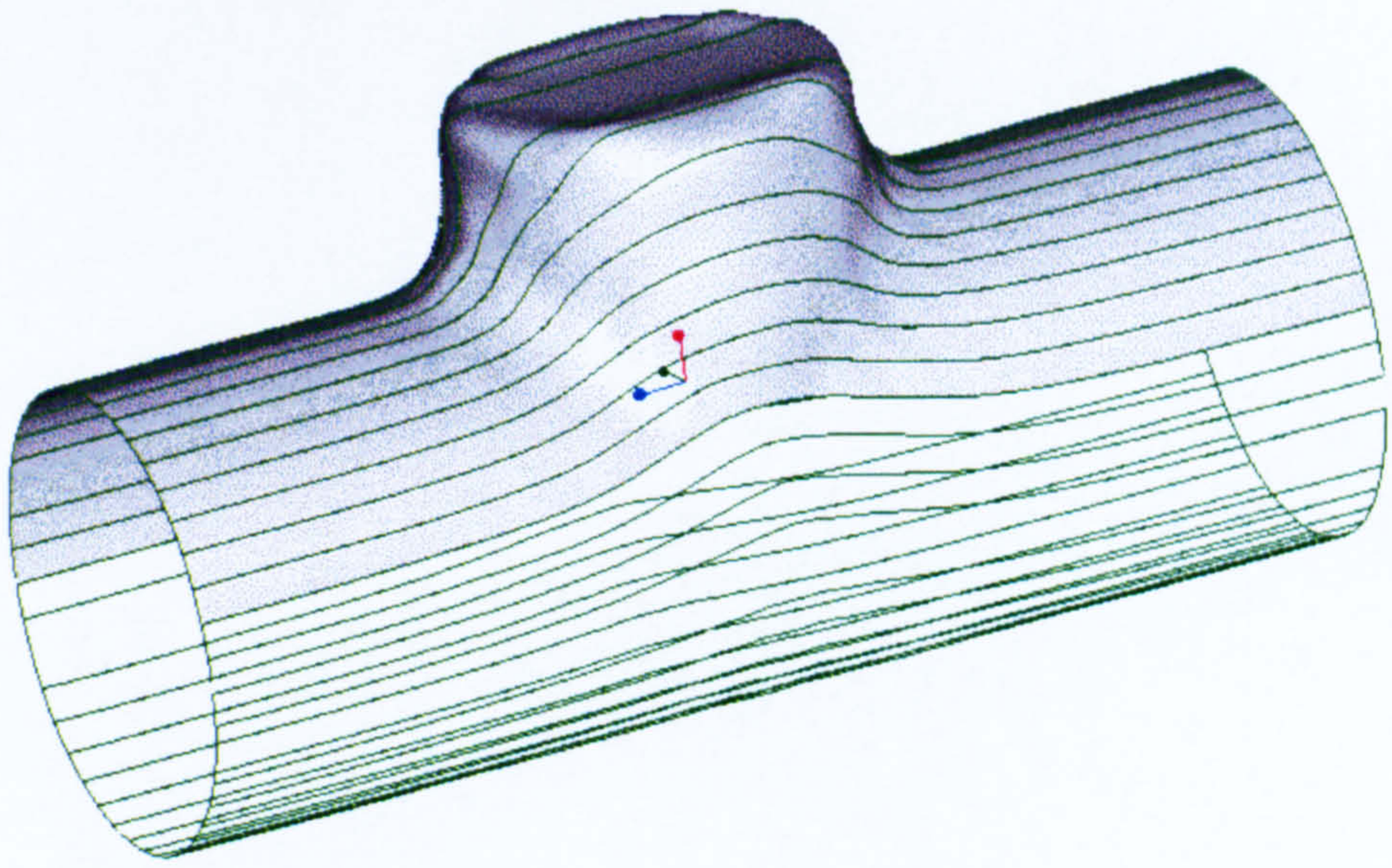

Figure 7-17 Upper Surface

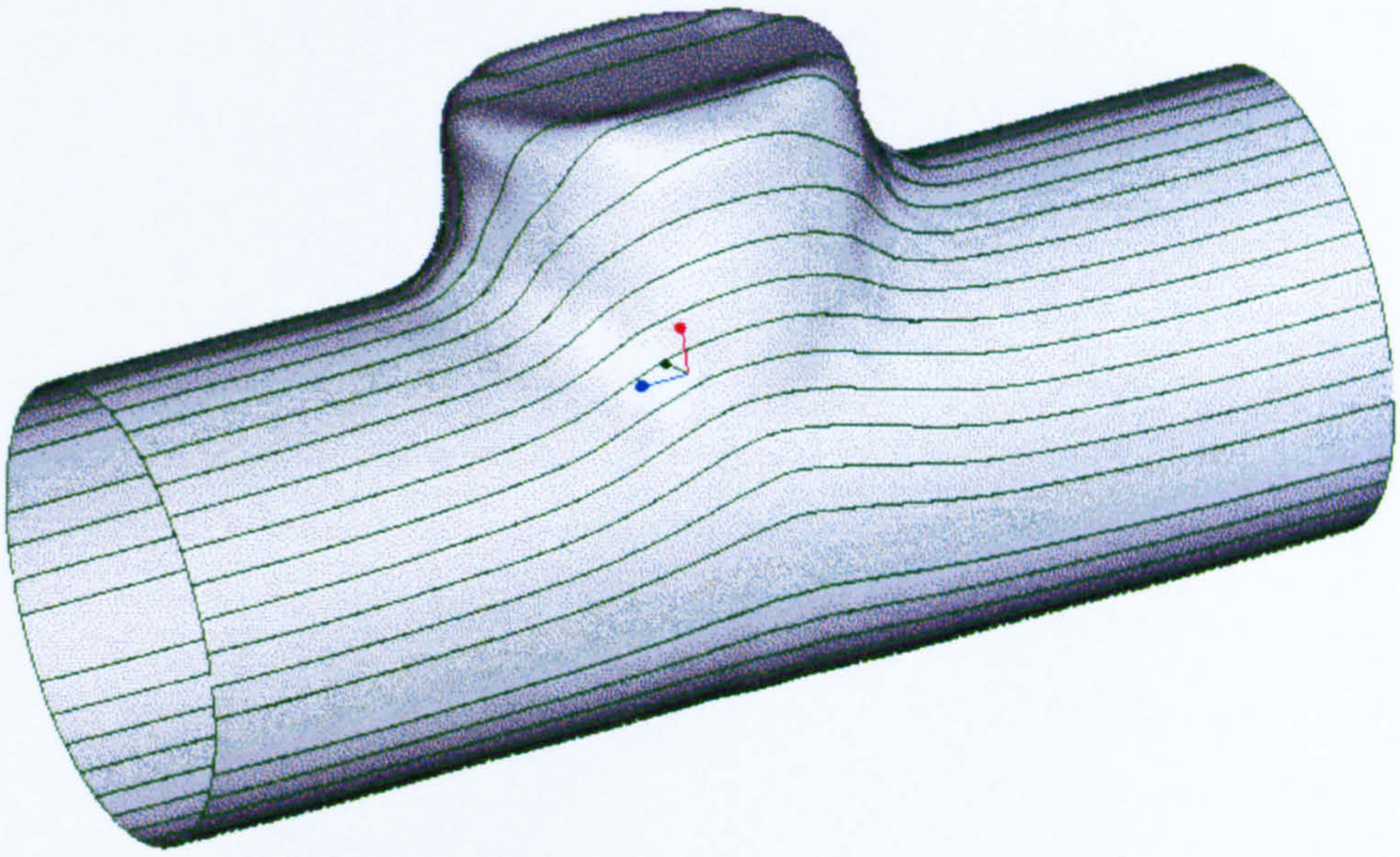

Figure 7-18 Lower Surface

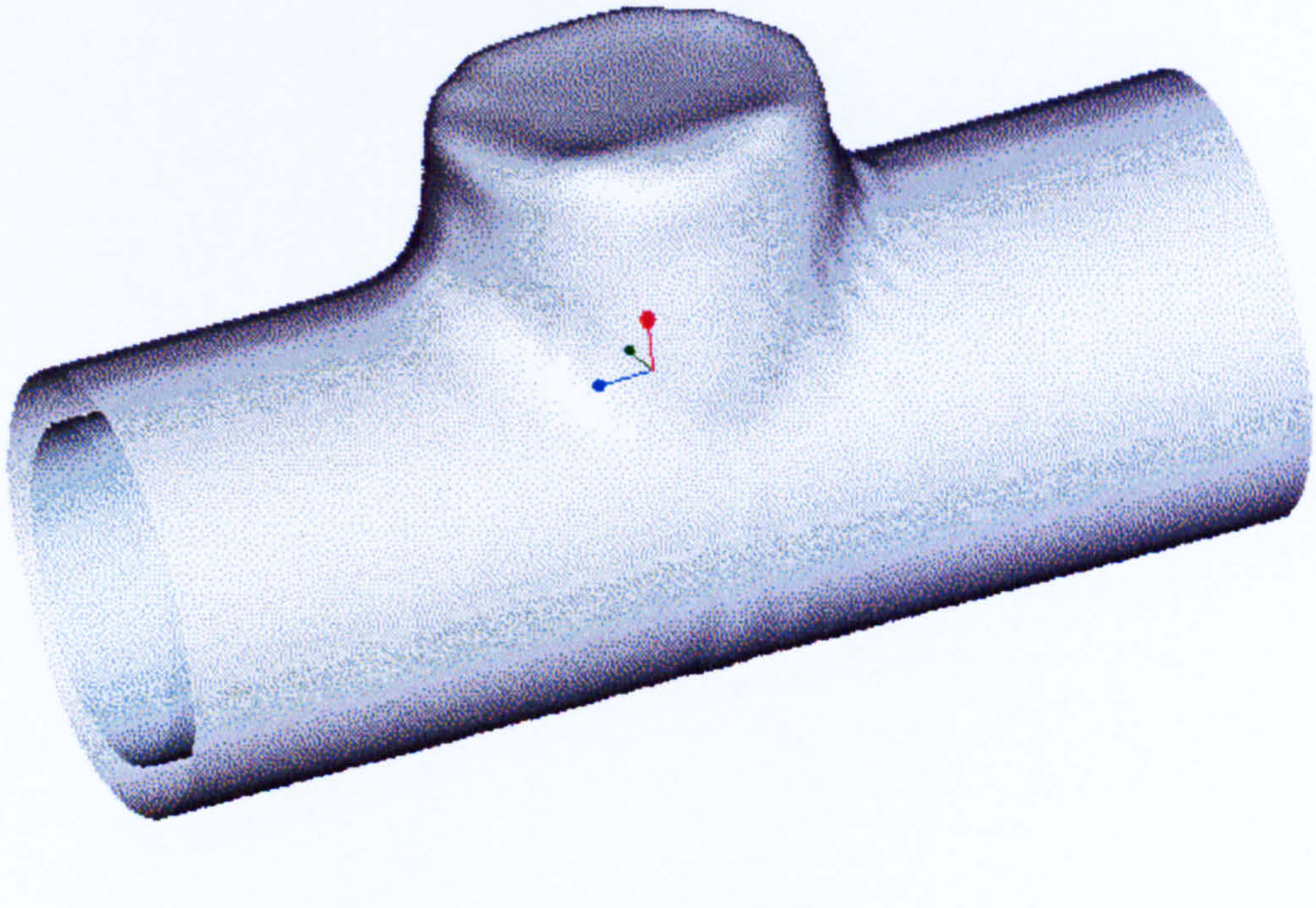

Figure 7-19 Inner and Outer Surface

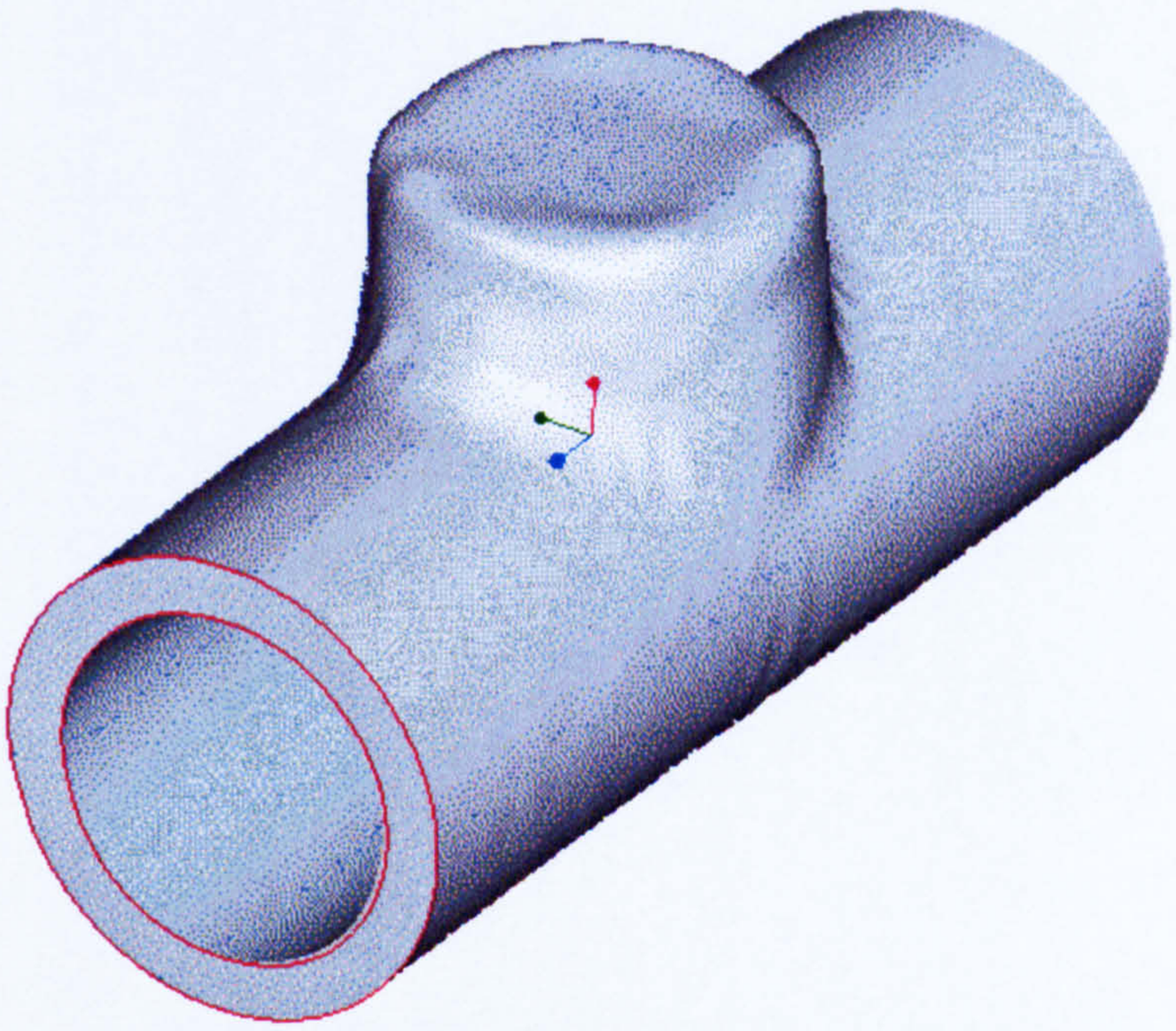

Figure 7-20 Front Surface

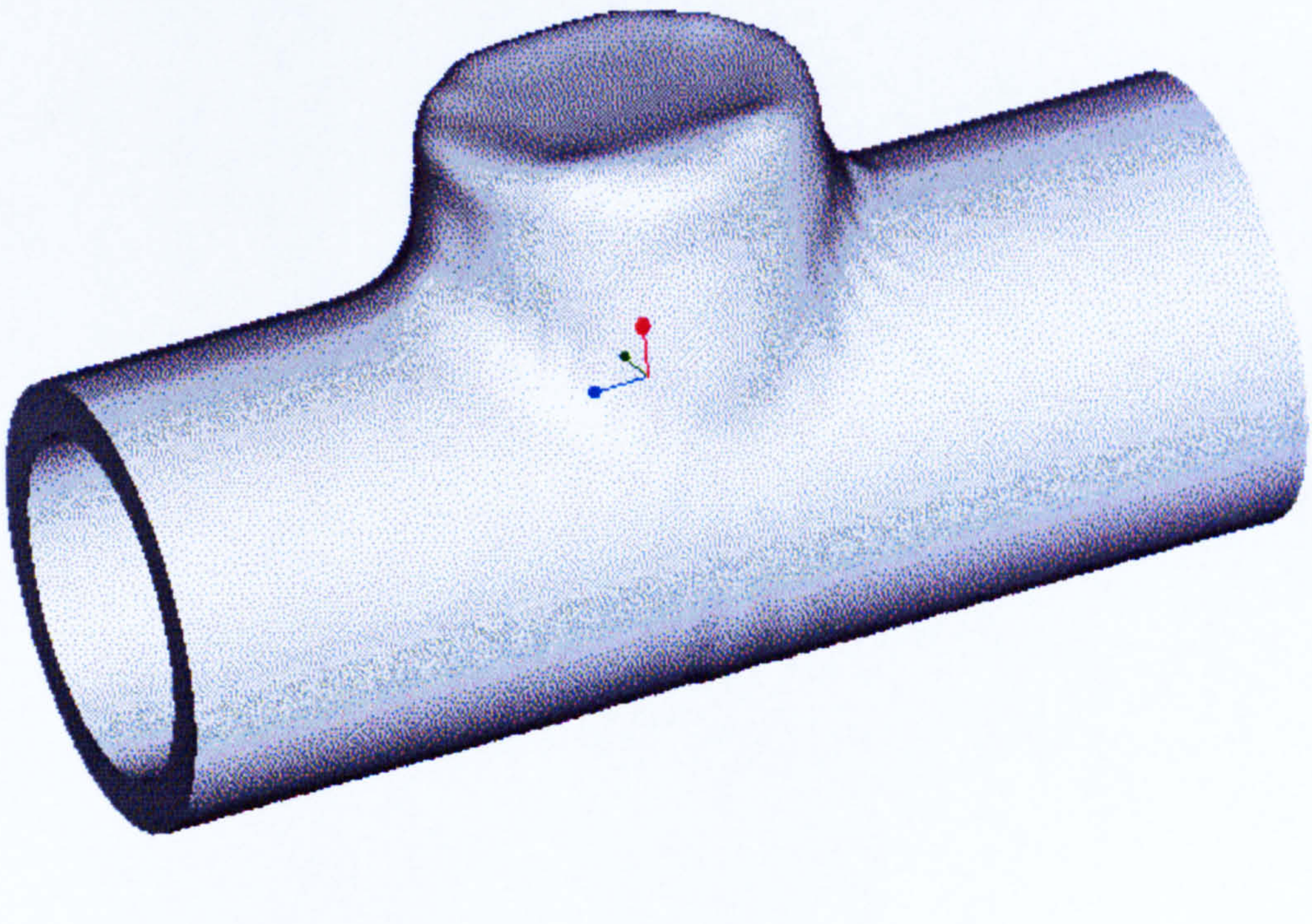

Figure 7-21 Finished Part

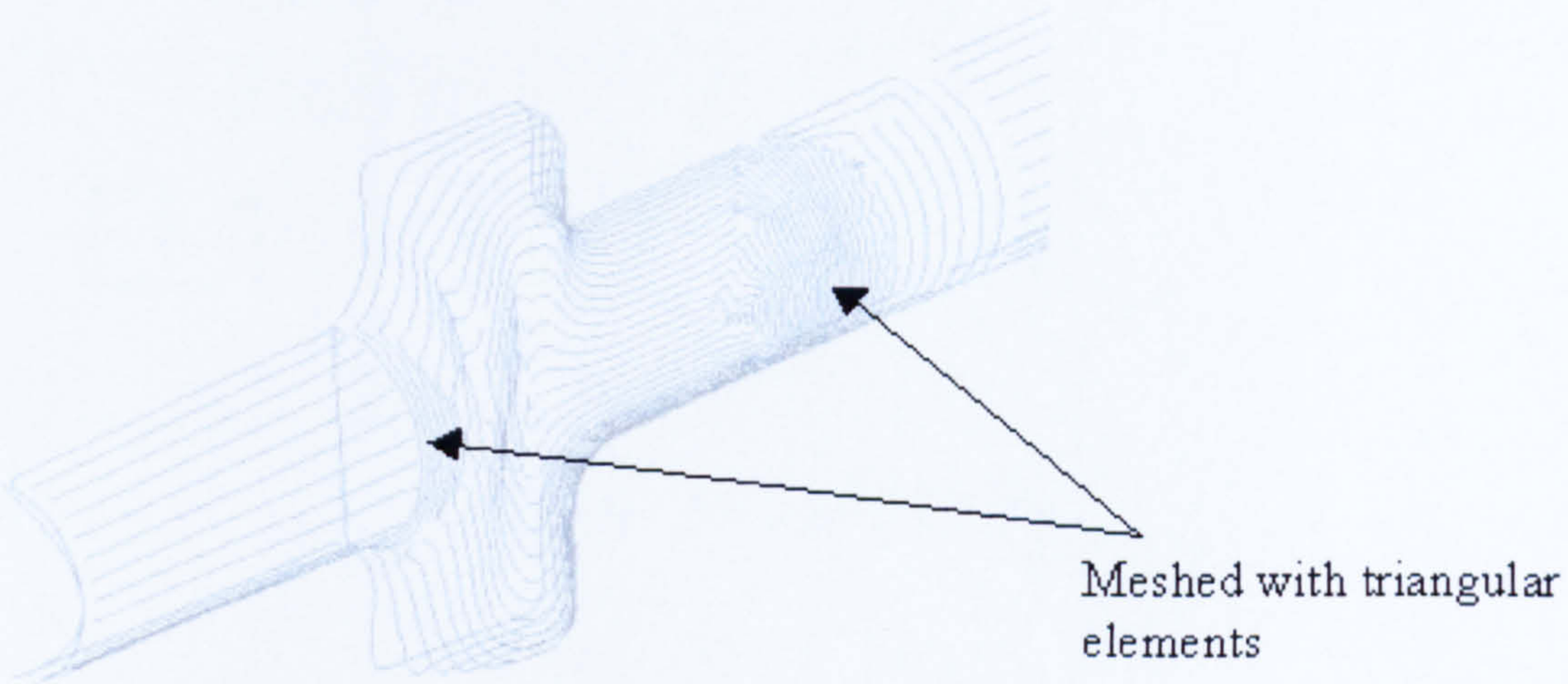

Figure 7-22 IBL-File with Triangular Elements

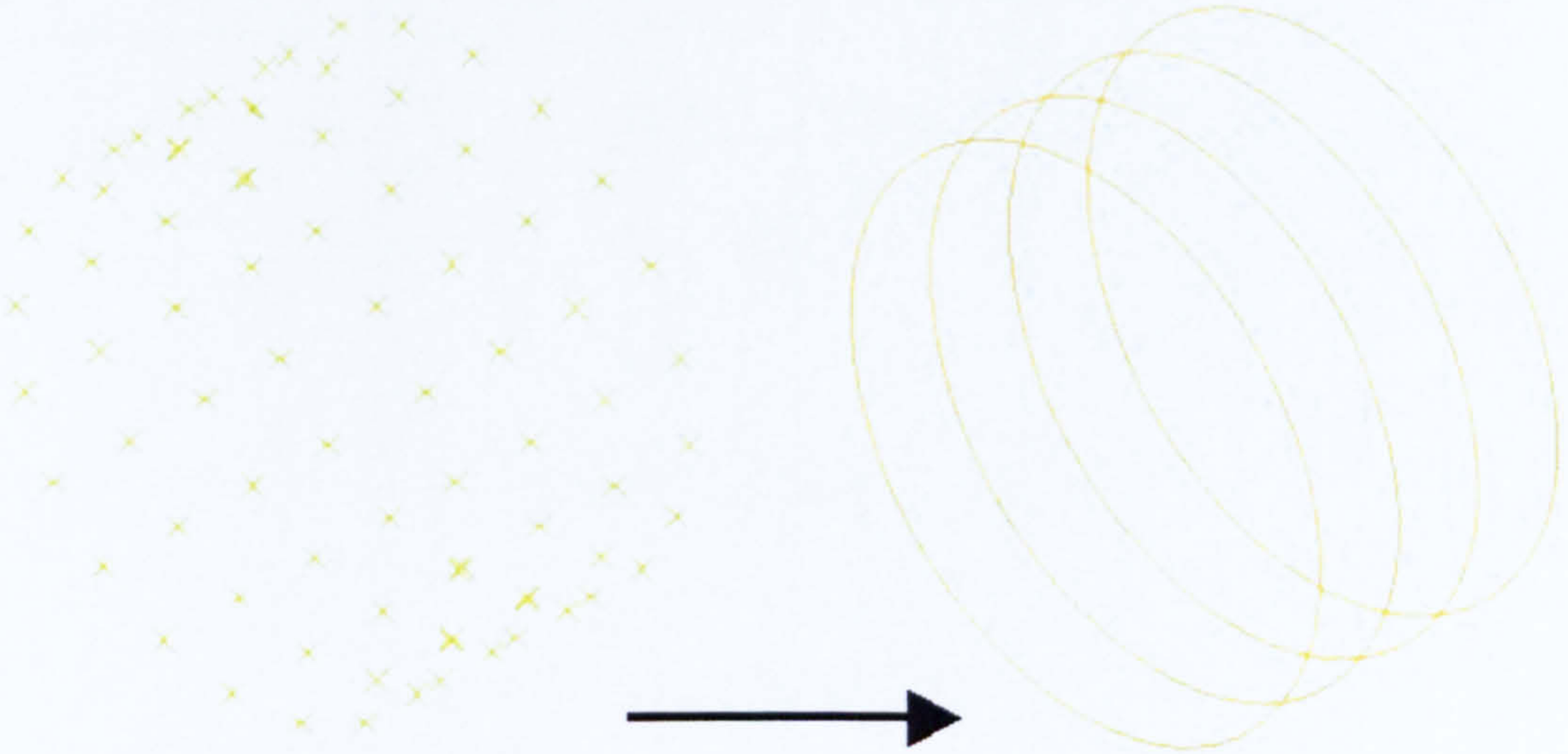

Figure 7-23 Radial sorted Points, Scan Curves

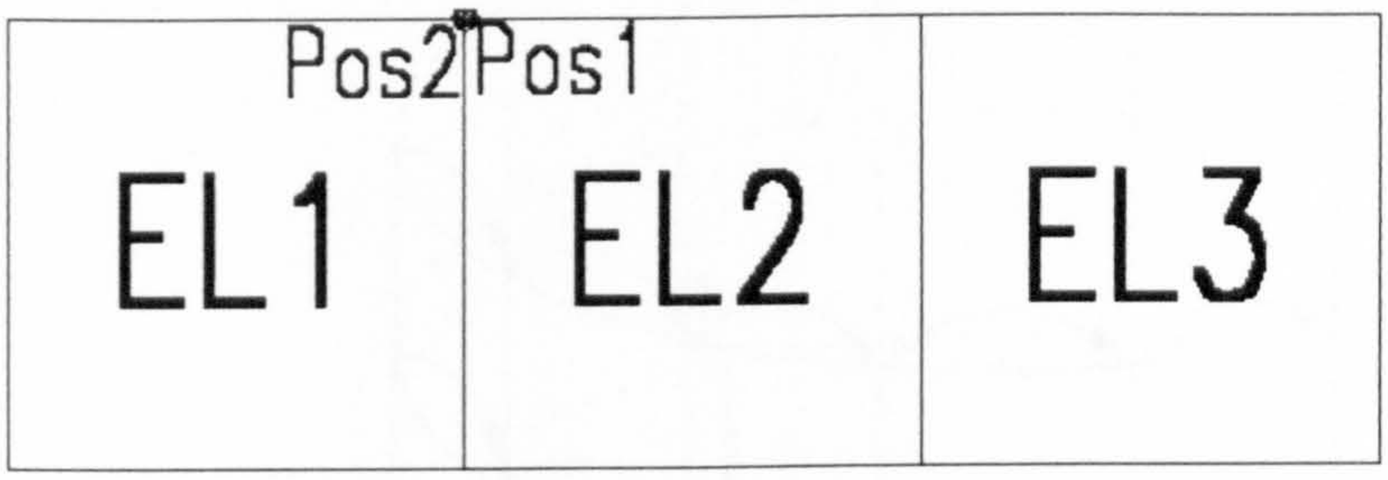

Figure 7-24 Boundary Nodes

element	node			
	Pos1	Pos2	Pos3	Pos4
1	14	1	16	15
2	1	2	17	16
3	2	3	18	17
4	3	4	19	18
5	4	5	20	19
6	5	6	21	20

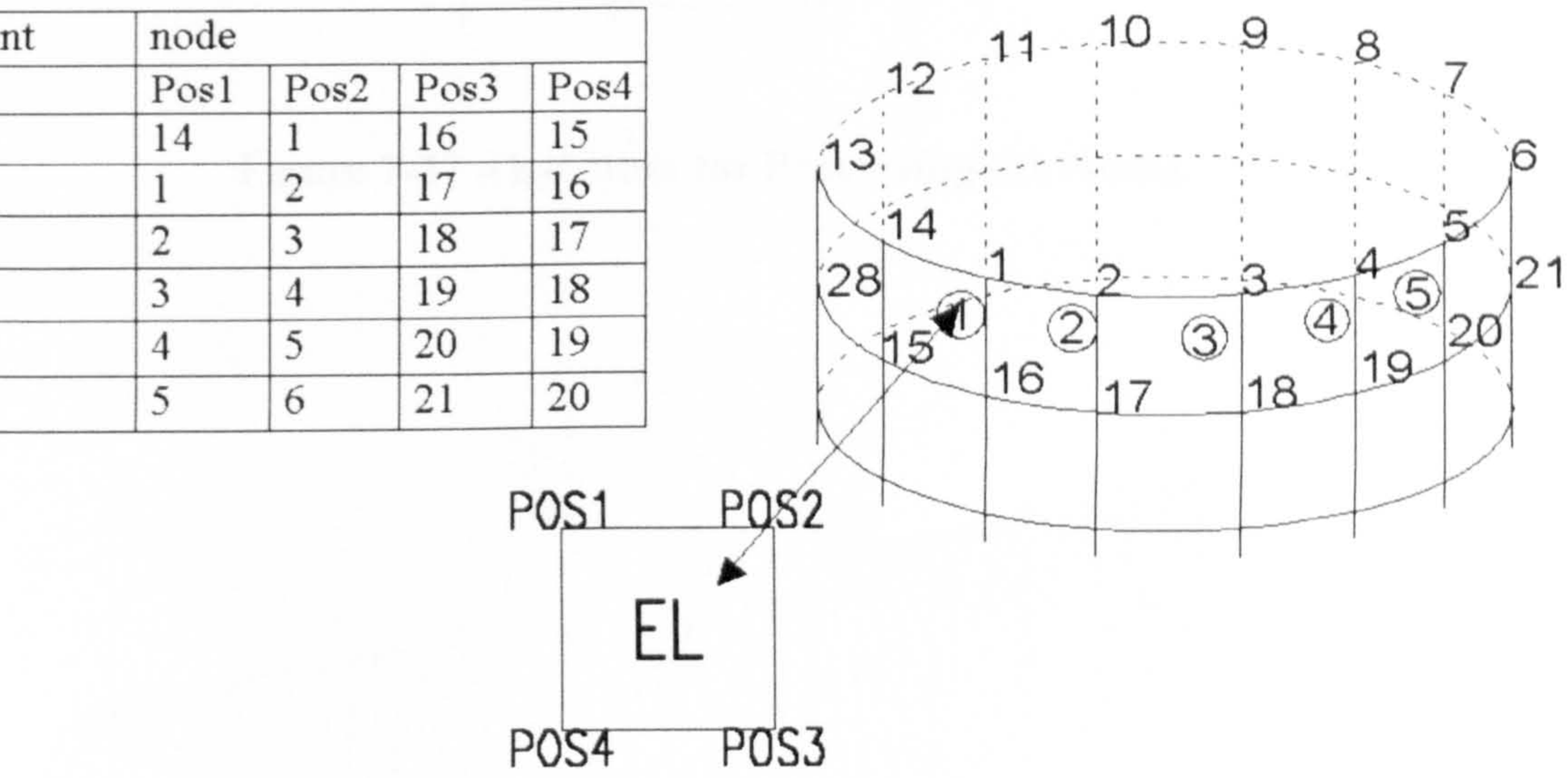

Figure 7-25 Order of Nodes

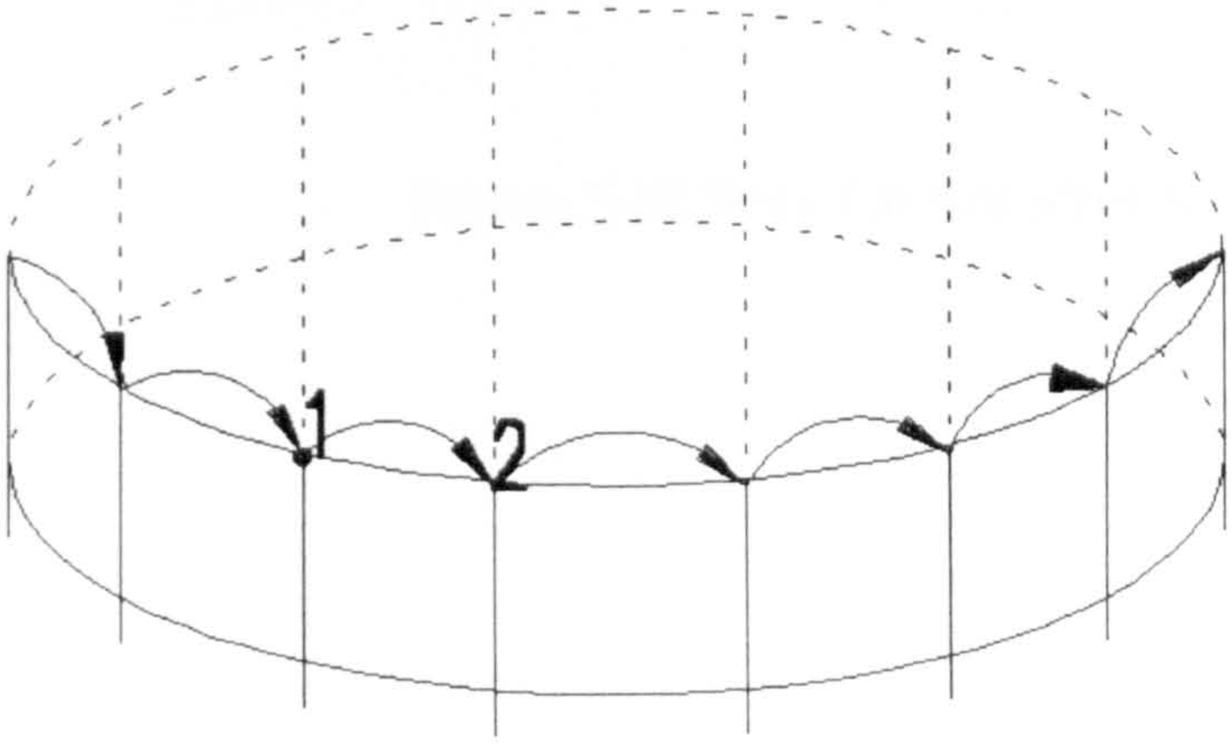

Figure 7-26 Sorting of the Boundary Nodes

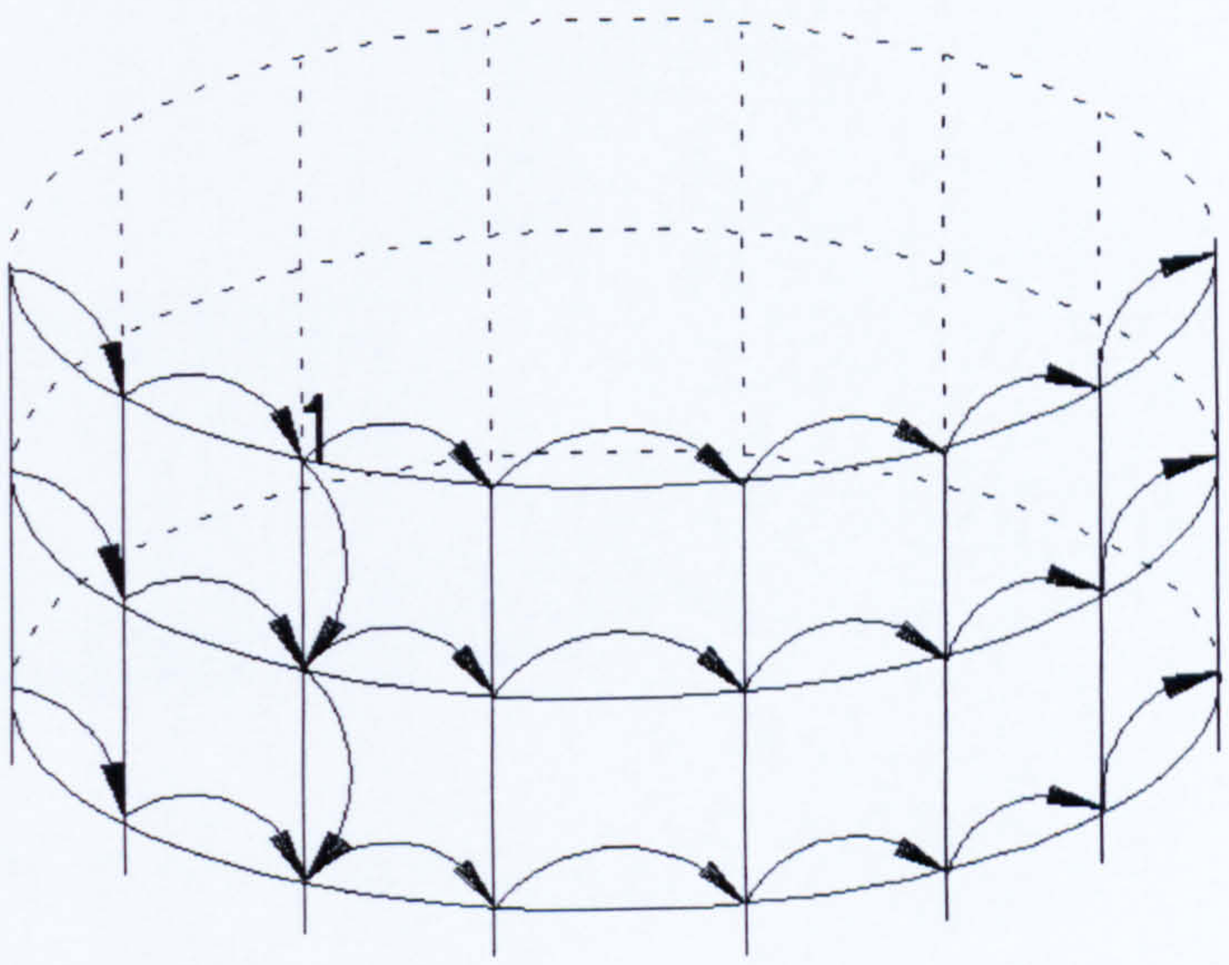

Figure 7-27 Algorithm for Processing the Nodes

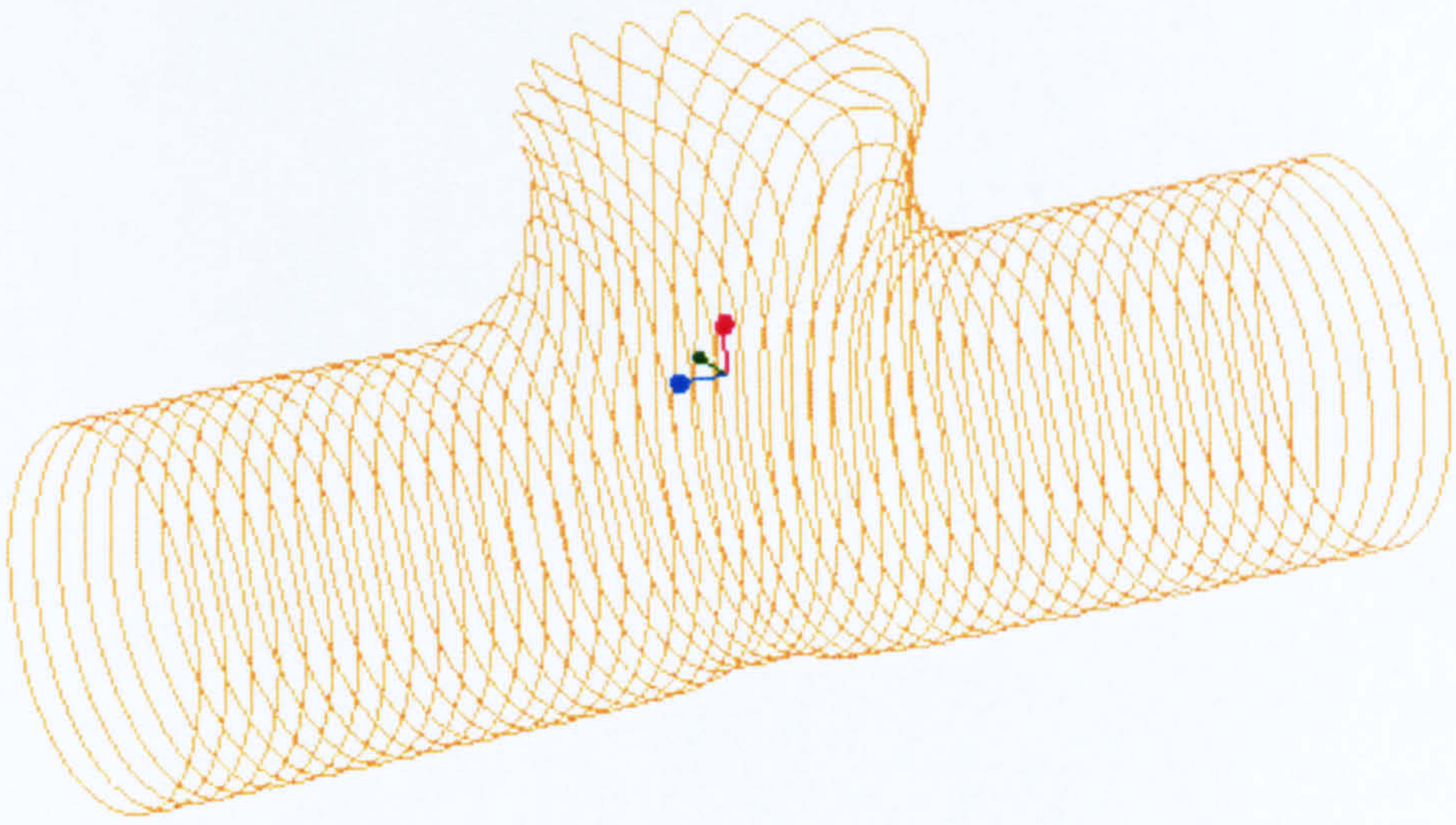

Figure 7-28 Scan Curves after Sorting

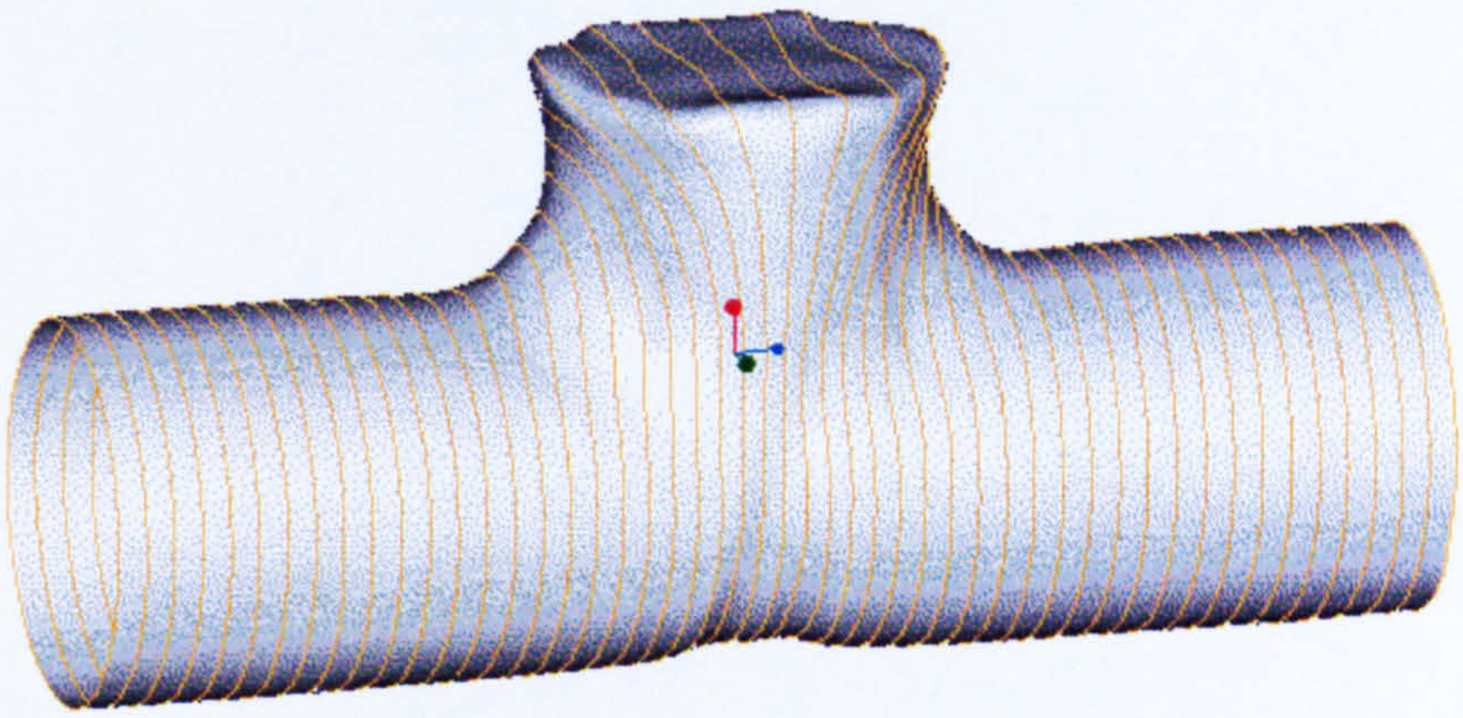

Figure 7-29 Inner Surface out of Radial sorted Points

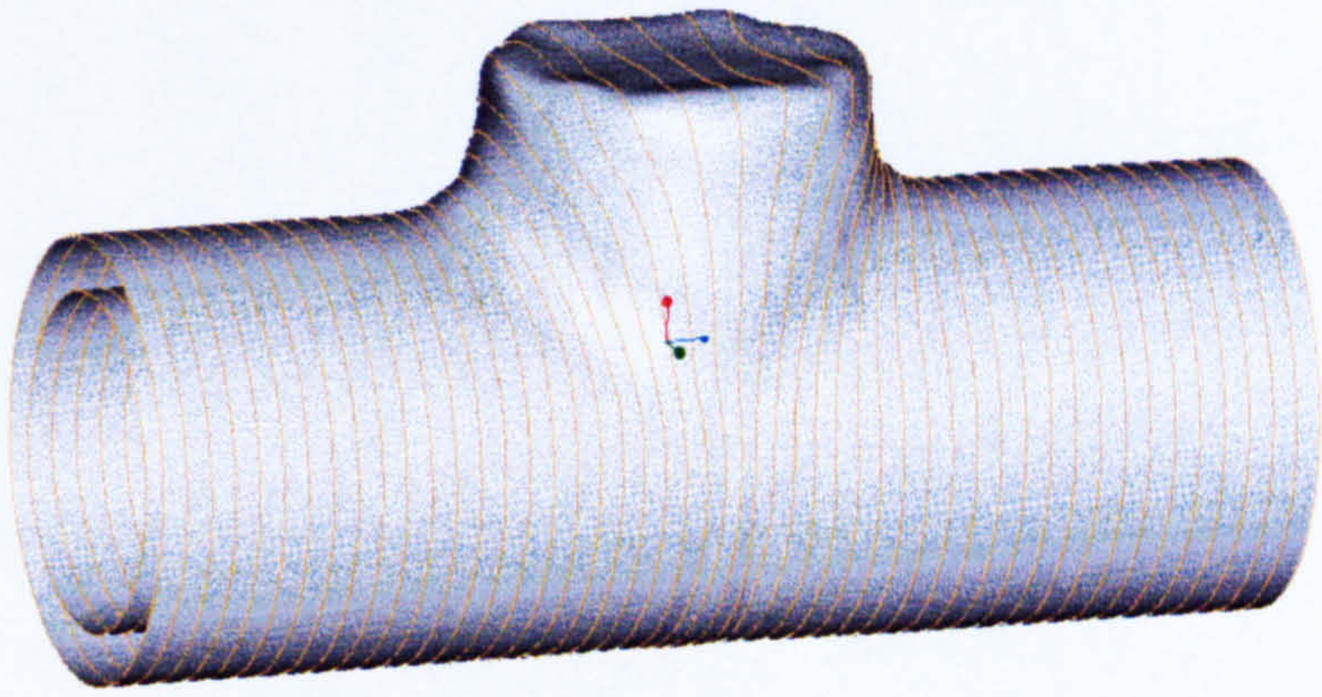

Figure 7-30 Outer Surface

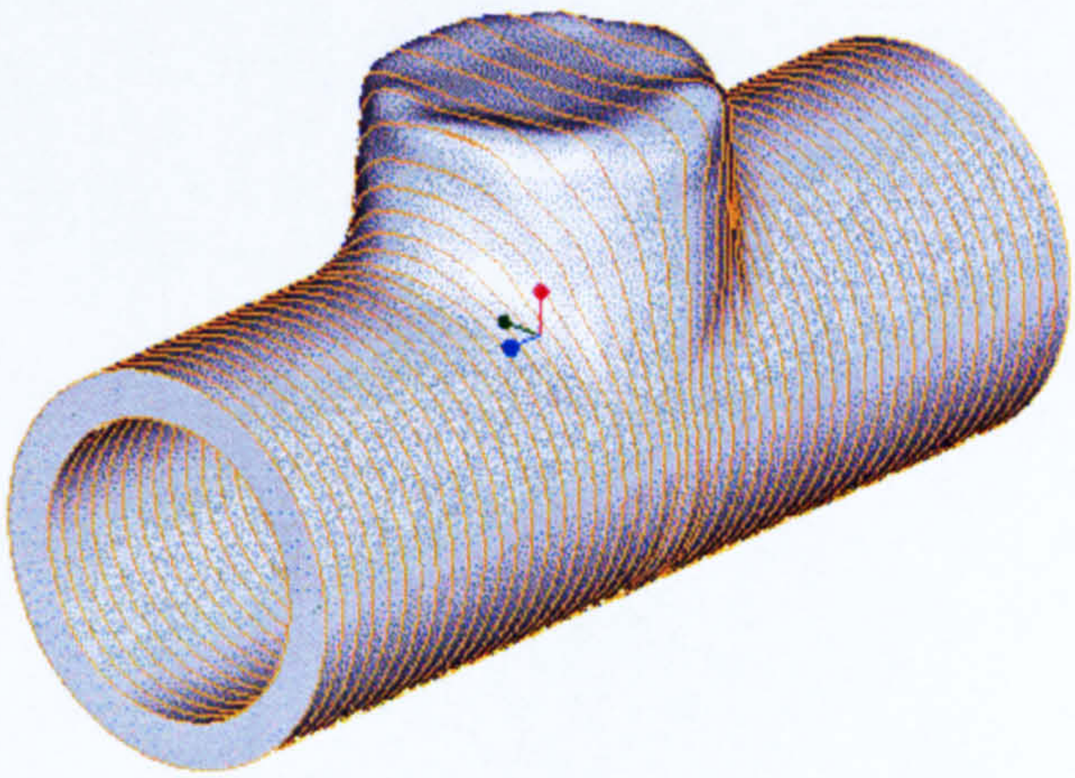

Figure 7-31 Reconstructed Component with Boundary Surfaces

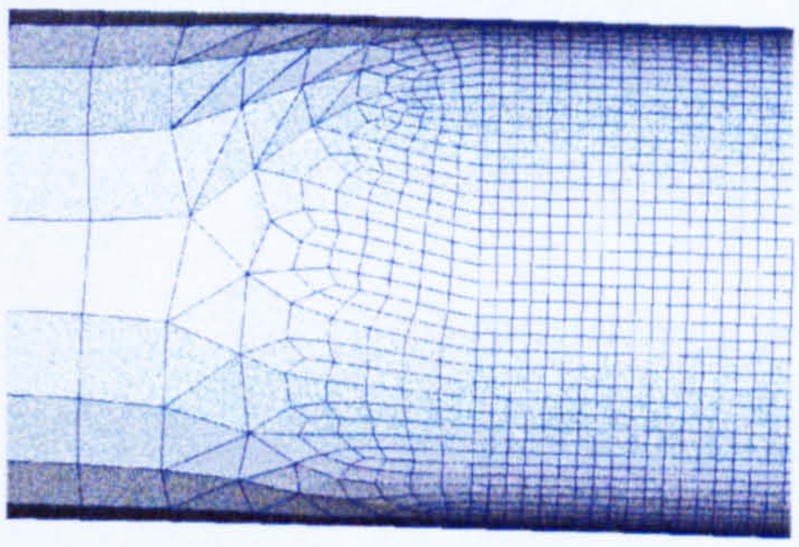

Figure 7-32 Triangular Elements

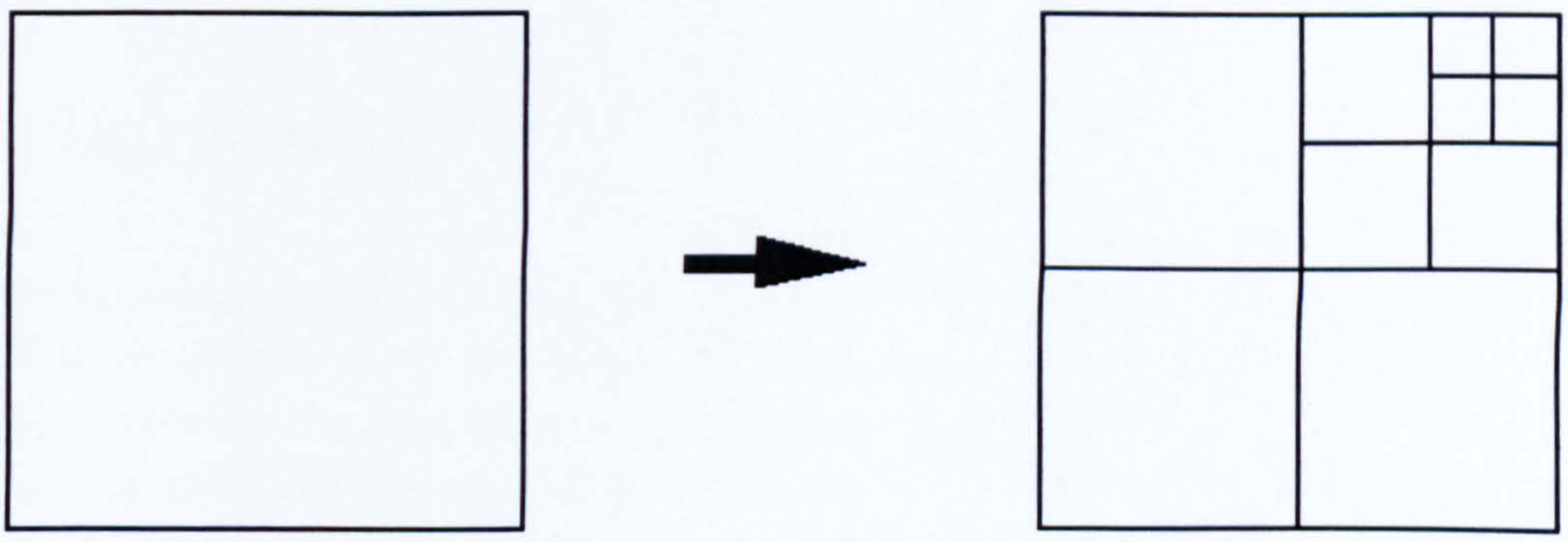

Figure 7-33 Adaptive Mesh Principle

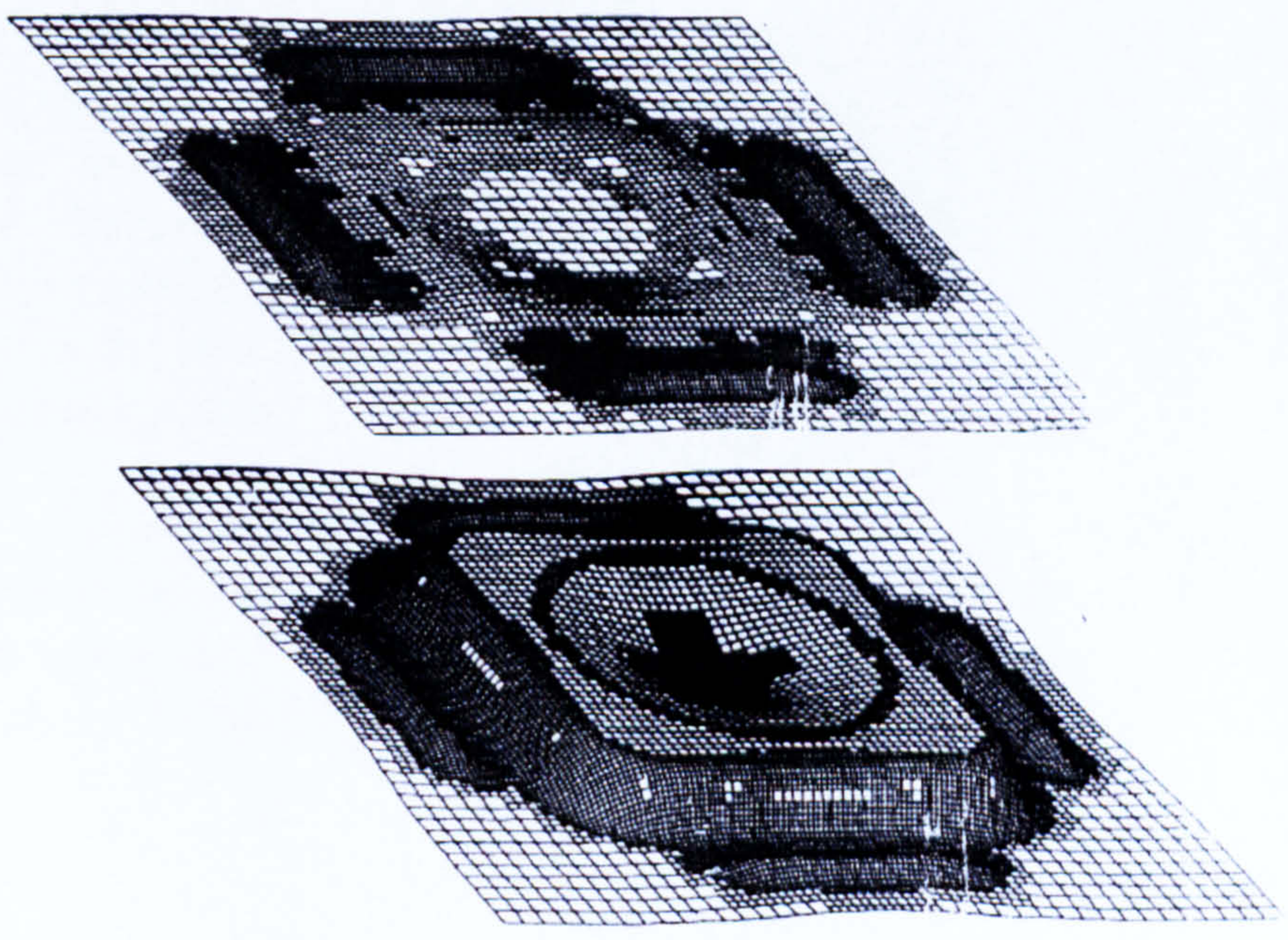

Figure 7-34 Adaptive Mesh - Deep Drawing Example

CHAPTER 8
Experimental Investigation of the IHP Process

This chapter verifies the use of the FE simulation technique by investigating two real applications. The results of the real forming process will be compared with the virtual forming results. Within this chapter the different material models offered from the simulation program LS-DYNA are compared and the influence of the anisotropic material (tube) properties is exploited. It should be shown whether the FE simulation is a suitable method to predict the complex characteristics of the process parameters (interior pressure, axial force and material behaviour) acting during the IHP forming process. In particular the possibilities of displaying the feasibility of the application and to determine the failure modes should be investigated.

8 Introduction

The virtual production (IHP forming simulation) was investigated through a number of experiments. The conclusion of these experiments was based on the variation of the wall thickness distribution between the real and the simulated part used in the experiment. Furthermore, the plastic strains were also investigated and compared. The main aim of this investigation was to determine how exactly the simulation results correspond with the real part and what are the best material model in LS-DYNA for the IHP forming simulation. This chapter should be show if the FE simulation is a suitable tool for the prediction of the feasibilty of an IHP component.

The parts for the investigations are done using the hydroforming press at the Siempelkamp Press Systems (SPS) research and development center in Aalen, Germany. This was possible because a close connection between the Aalen University and the Siempelkamp company exists. **Figure 8-1** shows the press at the Siempelkamp plant with a clamping force of 2500 ton and a internal pressure of up to 10000 bar. The hydroforming press was kindly provided by the SPS company for the tests. The tools for the parts were available from previous projects running with industrial partners.

For the part „Windshield Wiper Mounting“ the measured load-curves for interior pressure and axial displacement could be saved directly from the press steering on a floppy disk. The load-curves for the „End-Tube“ were only available as paper hardcopies. Both simulations were carried out with the real load-curves from the actual production process.

8.1 Material Models in LS-DYNA

LS-DYNA offers more than 100 material types for all the different types of simulations that can be done using this software package. For metal forming simulation there are four material types available. The material types in LS-DYNA are identified by a number which depends on historical issues, and hence the keyword format is available with a corresponding keyword value.

8.1.1 Material 24 (MAT_PIECEWISE_LINEAR_PLASTICITY)

Material Type 24 is an elasto-plastic material (**Figure 8-2**) An stress/strain curve and its strain rate dependency can be defined. Also, failure based on a plastic strain or a minimum time step size can be defined. The stress strain behavior may be treated by a bilinear stress/strain curve by defining the tangent modulus. Alternately, a curve similar to that shown in **Figure 8-3** is expected to be defined by an effective stress/plastic strain curve. The computation time is approximately the same for both approaches.

There are three possible options to account for strain rate effects. Strain rate may be accounted for using the Cowper and Symonds model which scales the yield stress. If the viscoplastic option is active, then the dynamic yield stress is computed from the sum of the static stress, which is typically given by a load curve and the initial yield stress, multiplied by the Cowper-Symonds rate term **(Hallquist, 1999)**.

8.1.2 Material 36 (MAT_3-PARAMETER_BARLAT)

This Material was developed by **Barlat** and **Lian** for modelling sheets with anisotropic materials under plane stress conditions. Material 36 allows the use of the Lankford parameters Parameter r_0, r_{45} and r_{90} for the definition of the anisotropy and take the hardening into consideration **(Hallquist, 1999)**.

8.1.3 Material 37 (MAT_TRANSVERSELY_ANISOTROPIC_ELASTIC_PLASTIC)

This material model is for simulating sheet forming processes with anisotropic material. It was developed by **Hill** in 1948. Only transverse anisotropy can be considered. Optionally an arbitrary dependency of stress and effective strain can be defined via a load curve. This material model is only available for (thin) shell elements.

8.1.4 Material 103 (MAT_ANISOTROPIC_VISCOPLASTIC)

Material Model 103 was developed by **Berstad et at. (1994)**, **Hopperstad** and **Remseth (1995)**, and **Berstad (1994).** It is useful for the description of anisotropic – viscoplastic material. Beside the three Lenkford - parameters an isotropic hardening can be considered. Kinematic, isotropic or a combination of kinematic and isotropic hardening can be used (**Figure 8-2**). The material constants can be fitted directly, or if desired, stress versus strain data may be input and a least squares fit will be performed by LS-DYNA to determine the constants. This material is the newest available in LS-DYNA.

8.2 Windshield Wiper Mounting

Currently the windshield wiper mounting consists of a number of components (tube, bearing elements for the wiper axle and the propulsion axle and connecting components). The idea was to produce the whole part out of one tube using the IHP technique. If possible the parts which take up the bearing for the wipers should be in such a shape that they prevent twisting (the dome can have a hexagon or a octagonal shape).

8.2.1 Material

The following investigation describes the results of producing a tube using stainless steel (1.4301). **Table 8-1** shows the designation of the used steel in different countries. X5 CrNi 18-10 is the most common of the stainless steel types. It is a general purpose alloy suited for a variety of corrosion resistant applications. In **Figure 8-4** the stress - elongation curve for this material can be seen, **Table 8-2** shows the further material parameters.

EN 10088-1 Name	EN N°	Italy UNI	USA AISI	Germany DIN	France AFNOR	Sweden SIS	ILTA INOX
X5 CrNi 18-10	1.4301	X5 CrNi 1810	304	1.4301	Z 7 CN 18-09	2333	304

Table 8-1 Designation for the used Steel in different Countries

In this case the dome has a circular shape. Dimensions of the tube before forming are: a 22 mm diameter, a wall thickness of 1 mm, and a length of 375 mm. **Figure 8-5** shows the CAD model of the whole configuration of the tube, tool, stamp and counter-holder. The material properties for X5 CrNi 18-10 are :

Parameter	Value
Young's Modulus	210000 N/mm^2
Poisson's ratio	0.3
Density	7.85000E-9 t/mm^3
Yield stress	314 N/mm^2
R00	0.830
R45	1.150
R90	0.870
Rolling direction	+Y (perpendicularly to the longitudinal axis, see **Figure 8-6**)

Table 8-2 Material Properties X5 CrNi 18-10

These material parameters values are determined from tests carried out by the Institute of Production Engineering and Forming Technology (PTU) in Darmstadt, Germany.

8.2.2 Process Parameters

As said before the load-curves for the part „Windshield Wiper Mounting“could be saved directly from the press steering on a floppy disk. **Figure 8-7** shows the course of the interior pressure vs. time for the simulation and also for the real process. The movement of the stamps is induced by the pressure applied, and the amount of displacement is known. **Figure 8-8** shows the displacement vs. time relationship used for the simulation. The same is valid for the counter-holder displacement (**Figure 8-9**).

8.2.3 Results

Figure 8-10 shows the tube before forming [1], the final part [2] (see also **Figure 8-11**), furthermore a lengthwise [3,4] and crosswise [5,6] divided tube. For the analysis of the wall thickness distribution the tubes were cut lengthwise and crosswise.

Prior to the forming process the tubes are provided with a circular grid pattern (**Figure 8-12**) with the intention to determine the plastic strains caused by the deformations of the circles. Unfortunately the grid pattern will be destroyed in the zone where the dome is generated through the motion between tool and tube, for that reason it is not possible to determine the plastic strains appearing in the tube. The analysis of the plastic strains generated through the forming process is not considered to be a solved problem yet. Using the grid pattern is possible if the deformations are not too large, i.e. components which are mainly calibrated with the IHP technique like axle components.

The wall thickness distribution of the real forming process are compared with the simulation results (**Figure 8-13**) for some different cuttings sections as shown in **Figure 8-15** for the real component, and **Figure 8-16, 8-18 and 8-21** for the simulation model.

Figure 8-17, 8-19,8-20 and **8-22** show the course of the wall thickness for the real part and the different material models for the different path.

The results for path 1 shows slight differences between the four material models of the simulation and an average deviation of approximately 5% from the real part. **Table 8-2** to **8-5** contain the min./max. and the average value for the different material models all applied for the wall thickness of the tube.

	mt37	mt36	mt24	mt103
average	95.24	94.61	95.31	93.76
max.	100.91	101.11	100.85	98.88
min.	84.73	83.14	84.16	83.86

Table 8-3 Path 1, Thickness, deviations from the Real Part

	mt37	mt36	mt24	mt103
average	99.60	99.50	99.77	99.50
max.	117.13	117.64	116.71	116.92
min.	73.38	69.89	74.65	70.071

Table 8-4 Path 2, Thickness, deviations from the Real Part

	mt37	mt36	mt24	mt103
average	98.99	98.95	99.16	99.09
max.	127.99	128.53	127.80	128.02
min.	74.02	70.43	76.08	75.47

Table 8-5 Path 3, Thickness, deviations from the Real Part

	mt37	mt36	mt24	mt103
average	101.66	101.89	101.86	99.34
max.	120.39	121.66	121.02	121.78
min.	82.28	82.64	82.53	57.76

Table 8-6 Path 4, Thickness, deviations from the Real Part

It can be stated that the simulation with shell elements are not able to represent the conditions in the region where the stamps are acting. The simulation forecasts a much larger wall thickness. A reason for this is that the shell elements are not able to bear loads in the shell thickness direction. The contact algorithm detects the penetration, but on both sides and applies 2 identical forces onto the node, the resulting force thus is 0 (**Figure 8-14**). So thickness results which are larger than the gap between tool and stamp normally cause no problem, because the results in the area where the stamp acts are not of interest. Otherwise the simulation must be done with 3D solid elements

Therefore it can be said that the results for using material types 24, 36 and 37 are quite similar.

The deviations for path 2,3 and 4 from the real part are approximately 20%. It seems that the shell elements are not very accurate for pressure loads, i.e. the shell elements are not able to represent the conditions through the IHP process (pressure and axial feeding) accurately. The results for the thickness distribution of path 1, where are mostly in tension, are much more accurate. Material 103 shows partly a larger deviation than the other materials.

Figure 8-23 shows the part reconstructed using the tools described in chapter 6 out of the LS-DYNA simulation results. The following **Figures 8-24, 8-25** and **8-26** shows the cross - sections out of the reconstructed part (yellow) and the same cross - sections for the real component.

The comparison of the cross - sections of path 2 and 4 (2 is identical with 3) shows that the shape of the part in the lenghtwise direction fits together with a good correlation. For path 1 the radii predicted from the simulation are larger than the real part. This agitates probably because the material is somewhat softer than the flow curve, which was used in the simulation.

The next diagrams (**Figure 8-27, 8-28, 8-29** and **8-30)** display the course of the plastic strains for the four sections (path 1-4) determined through the simulation. As discussed earlier the plastic strains in the real component could not be measured, and hence could not be compared to the simulation results.

Material Type	CPU (s)	CPU (h)
MT 24	8748	2,43
MT 36	14728	4.1
MT 37	8560	2.38
MT 103	12249	3.4

Table 8-7 CPU Time needed for the Different Material Types

Table 8-7 and **Figure 8-31** shows how much CPU time the different element types was needed for the process simulation of the windshield wiper mounting.

Therefore it can be concluded that the selection of the material model has no considerable influence on the wall thickness distribution. Because of this the cheapest (from the view of the calculation time) material model 24 should be used as it is the most cost effective option. Furthermore the simulation show, as in reality, that the IHP forming process works successful with the selected boundary conditions.

8.3 End-Tube

The second part investigated was the end-tube of the exhaust system from the BMW Z3 sports car. **Figures 8-32** and **8-33** shows a picture of the car and the end-tube. In order to obtain two end-tubes out of an IHP work-piece, the tube was cut at there symmetric plane. The shape of this part is relative simple, but the expansion is quite large; the relation between starting and final outline in the middle of the part is approximately 1.5. This means for a evenly expansion in the middle section of the part a plastic strain of approximately 50% can be expected.

8.3.1 Material

The material for the end-tube is equal to the material used for the windshield wiper mounting described in section 8.2.1 (X5 CrNiTi 18 8, Ø 46 x 2 mm).

8.3.2 Process Parameters

The load-curves for the „End-Tube“ were only available as paper hardcopies. **Figure 8-34** shows the course of the interior pressure vs. time for the simulation, **Figure 8-35** shows the load curve for the velocity/displacement of the stamp for axial feeding.

8.3.3 Results

As for the real component the simulation for the end-tube shows a general feasibility of the IHP process.

The wall thickness distribution of the real forming process are compared with the simulation results for some different cuttings sections. The **Figures 8-36** to **8-44** show the location of the cuttings sections (path 1 to 3) and the corresponding results for plastic strain and wall-thickness distribution.

Figures 8-45 to **8-52** show the strain and thickness distribution of the end-tube at the end of the forming process for the different material types. As described for the first part investigated, the windshield wiper mounting, it was not possible to measure the plastic strains of the real part.

For path 2 the plastic strain is as expected around 50 %, with exception of the area containing elements which are extremely deformed. Comparing the simulation results for the different material types with the real part the material type 103 predicts the best results. Material type 24 shows a pronounced necking behaviour in the middle area of the tube which can not be observed in reality (**Figure 8-40**). Material type 36 and 37 show the same tendency in these regions. Also similar to the „Windshield wiper mounting“, the wall thickness at the end of the

tube, where the stamp acts, is too large in comparison to the real part. The reason for this is the same as described in the previous part. The shell elements are not able to bear loads in the shell thickness direction. As in reality the simulation shows that the process only works correctly on a narrow path and that an exact coordination between interior pressure and axial force is absolutely necessary. A wrong coordination of the load-curves leads to folding at A or bursting at B **(Figure 8-53)**.

The use of material type 103 justifies that more computing time is needed (**Figure 8-54**) to simulate this part.

8.4 Conclusion

The results of the simulations shows a small wall thickness distribution and a large plastic strains, compared to the measured value. These results hence using large element deformations, above all, in the area where the largest plastic strains occur (**Figure 8-55**).

A solution with accurate results could be achieved using a remap of the part properties two or three times over the simulation time. Remap means to project the actual values for shell thickness and plastic strains onto a new mesh. LS-DYNA provides this possibility, but only for brick elements and not for shells. Remapping has two problems, one is the production of a new mesh onto the deformed structure, the other is the projection of the part properties onto the new mesh. Together with the Institute of Technology of the State of Nordrhein-Westfalen in the new Federal Republic of Germany (RWTH Aachen) first attempts are made to solve this problem. The RWTH offers a tool for the remeshing of solid structure normally used for the forging simulation. A modified version of this tool makes it is possible to also remesh shell structures using LS-DYNA (**Figure 8-56**).

Currently there is no solution available for the problem of projecting the part properties onto the new mesh. This could be the subject of further developments and research.

Haas et al. (1998) have shown that the simulation provides accurate results for medium sized degrees of deformation (< 40%). In this case the deviation of the wall-thickness distribution between the simulation and the real component is less than 5%.

The investigations in this work show that for large degrees of deformations the results for shell thickness and plastic strains are not very accurate, but the simulation can help with referencing the material flow, the occurring of folds and bursting. The results of the simulation are always within the safety region, and if the simulation predict a well working process, it is most likely to work correctly and efficiently. Using the simulation techniques can help substantially to understand the IHP process better.

Figure 8-1 Siempelkamp Hydroforming Press

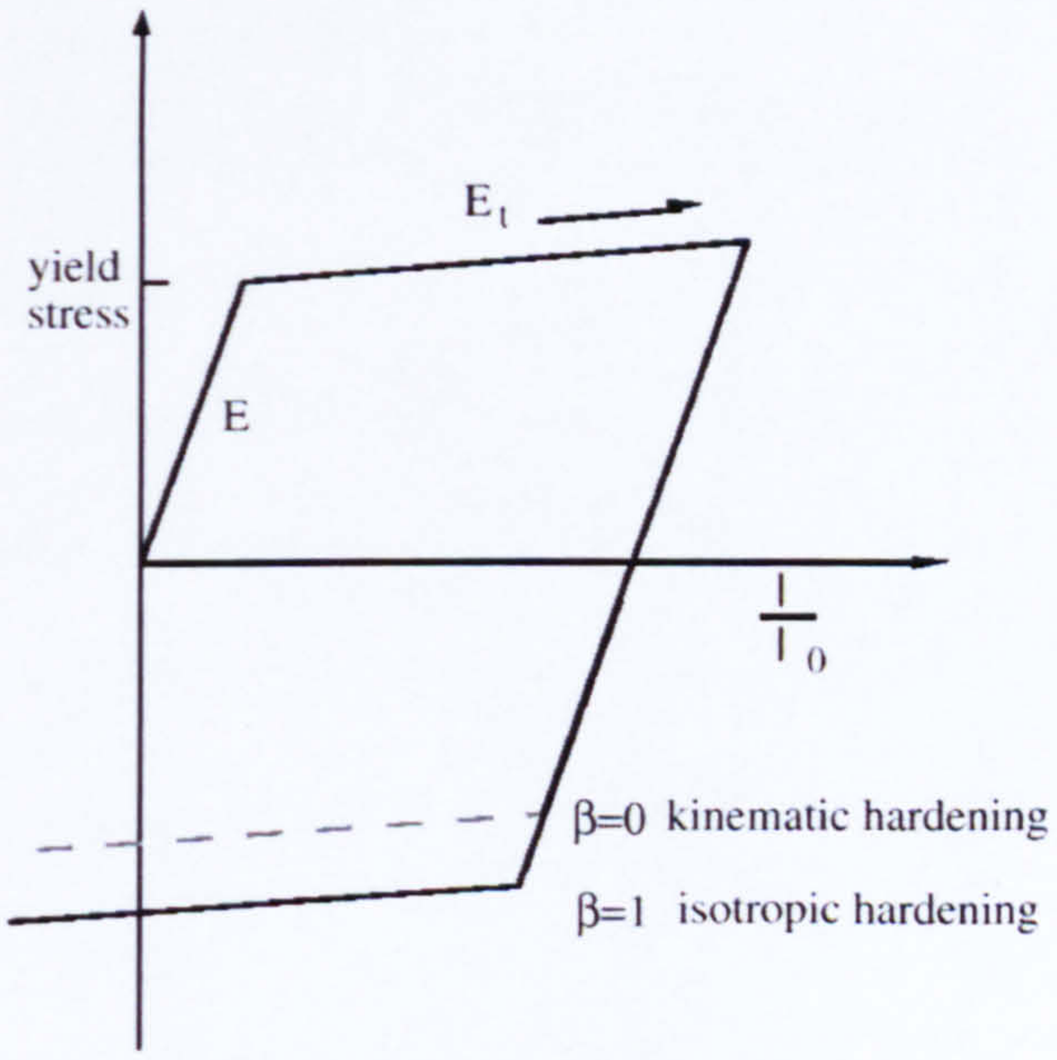

Figure 8-2 Elastic – Plastic Material behaviour

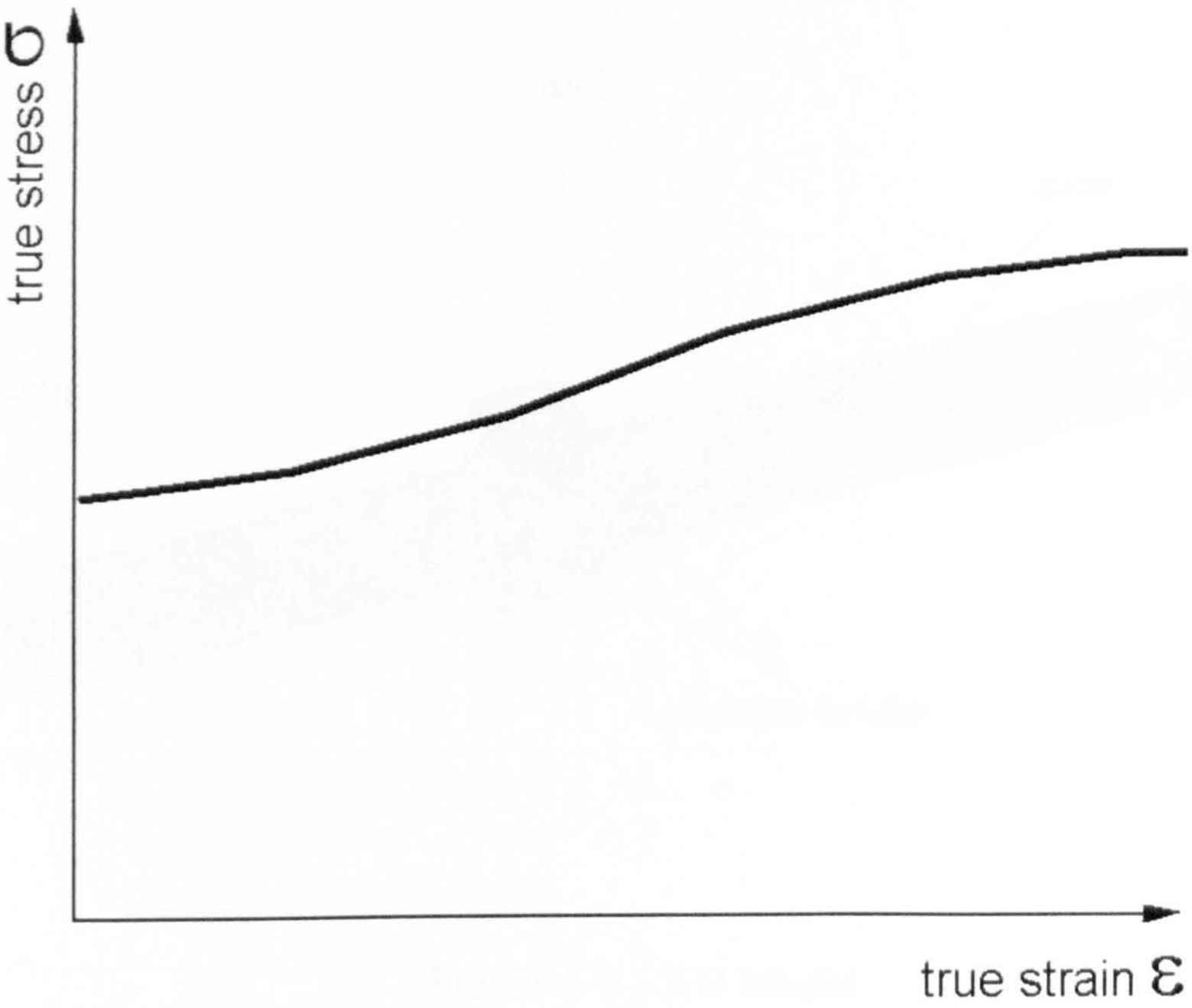

Figure 8-3 Effective Stress (true) versus effective plastic Strain (true) Curve

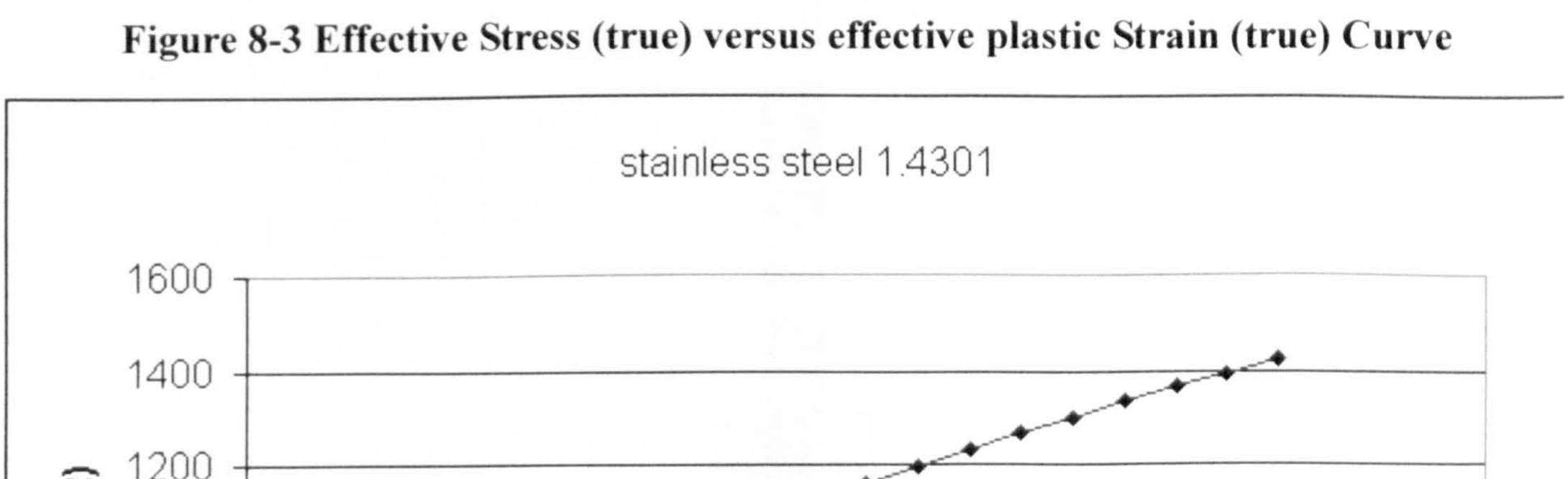

Figure 8-4 Stress - Strain Diagram for 1.4301

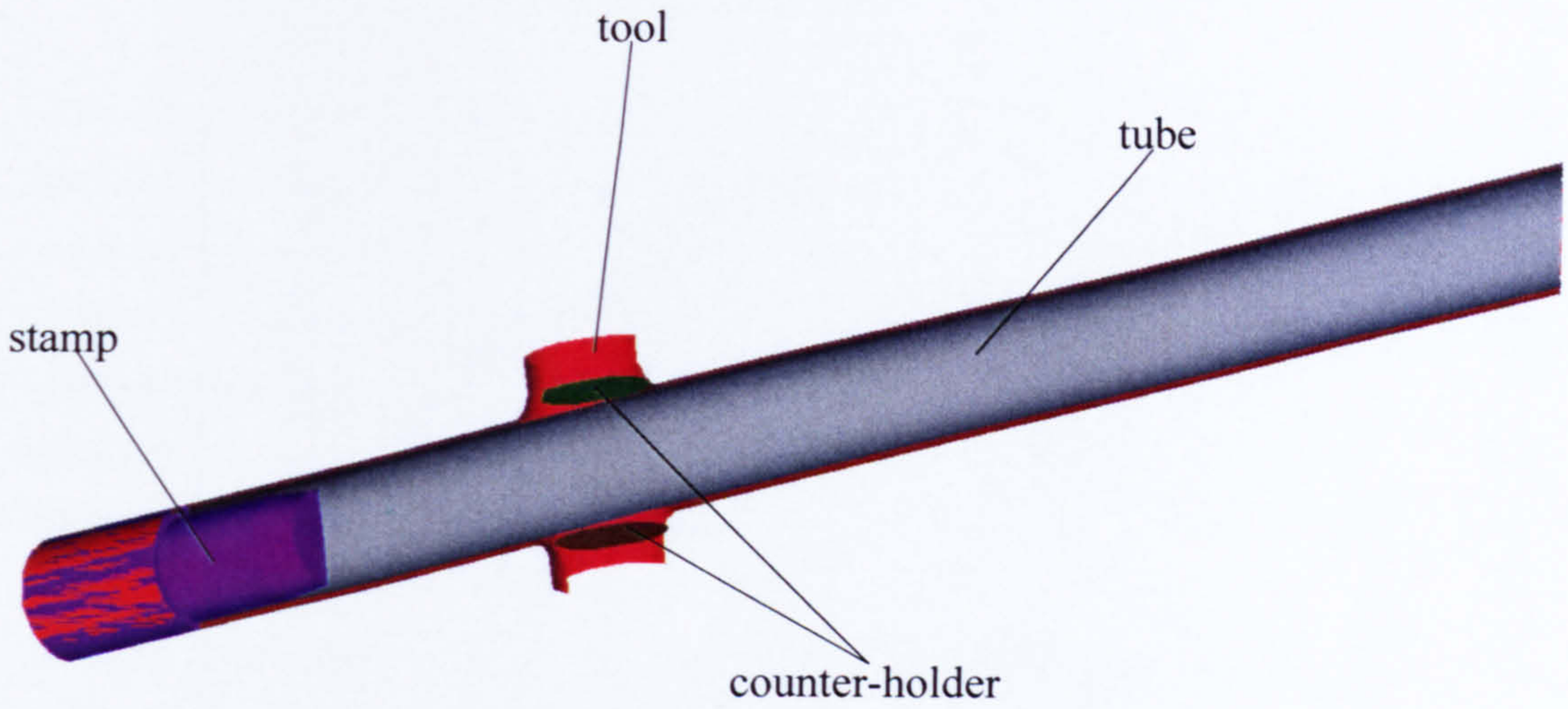

Figure 8-5 CAD Model

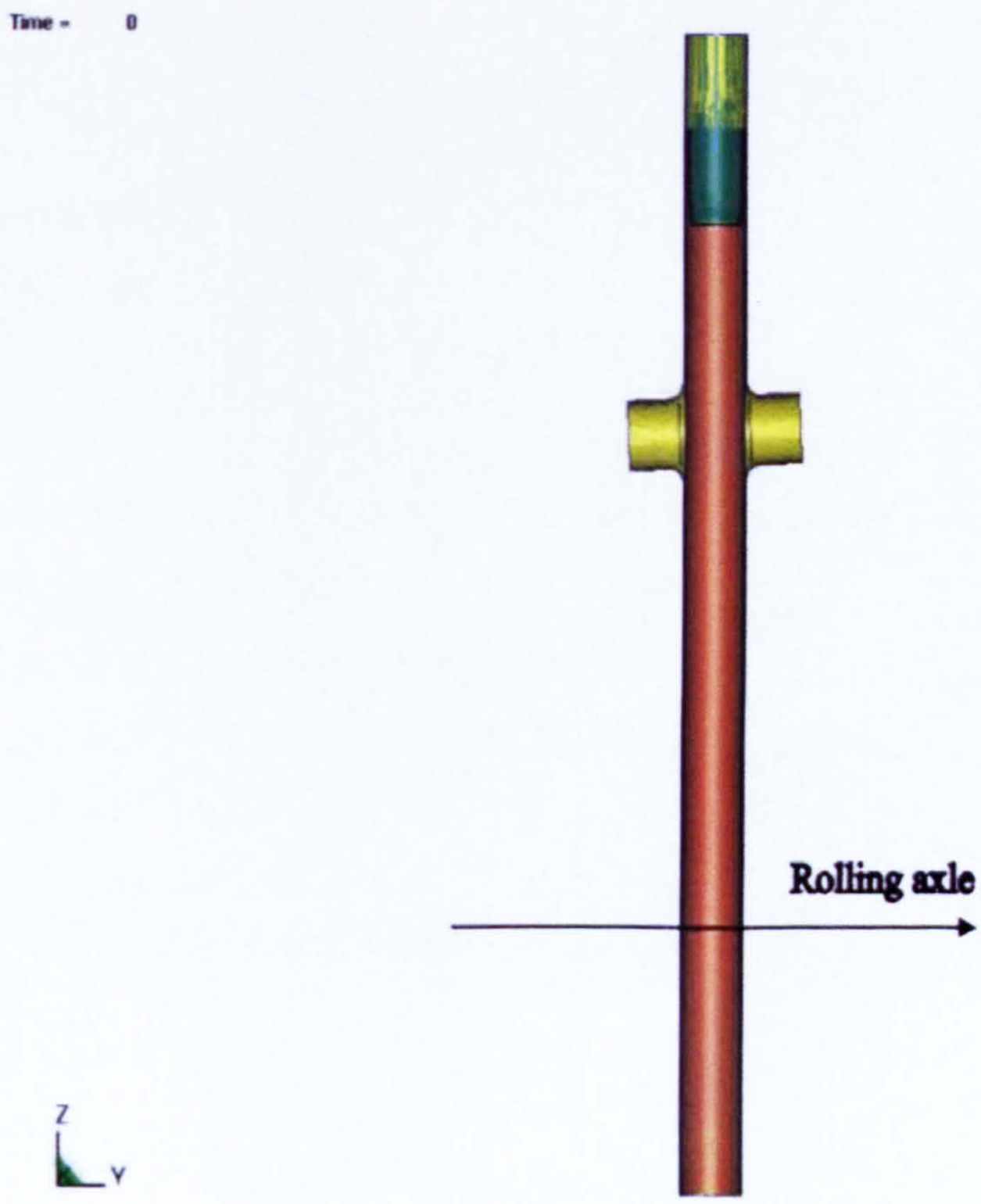

Figure 8-6 Rolling Direction

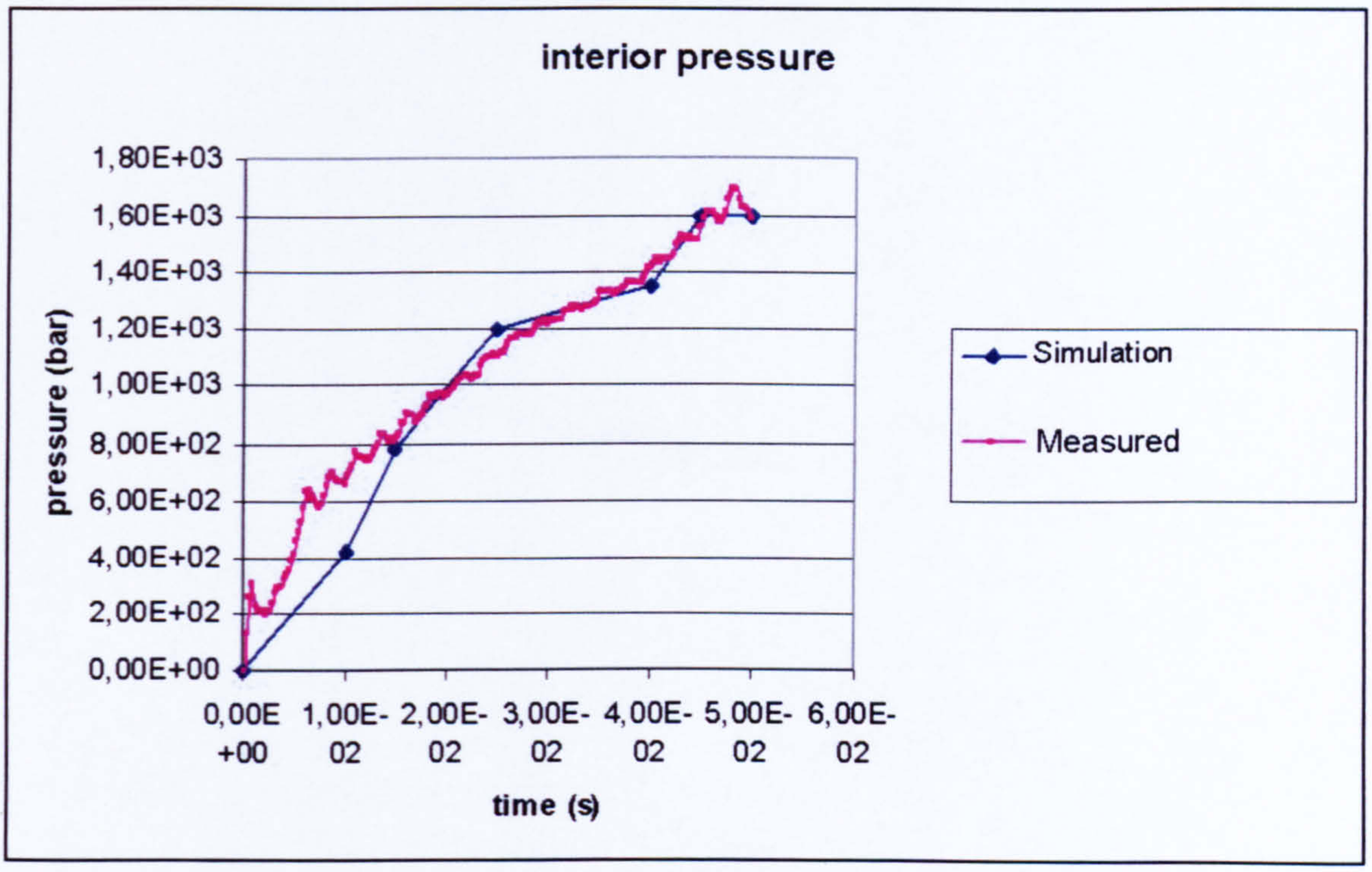

Figure 8-7 Load - Curve for Interior Pressure

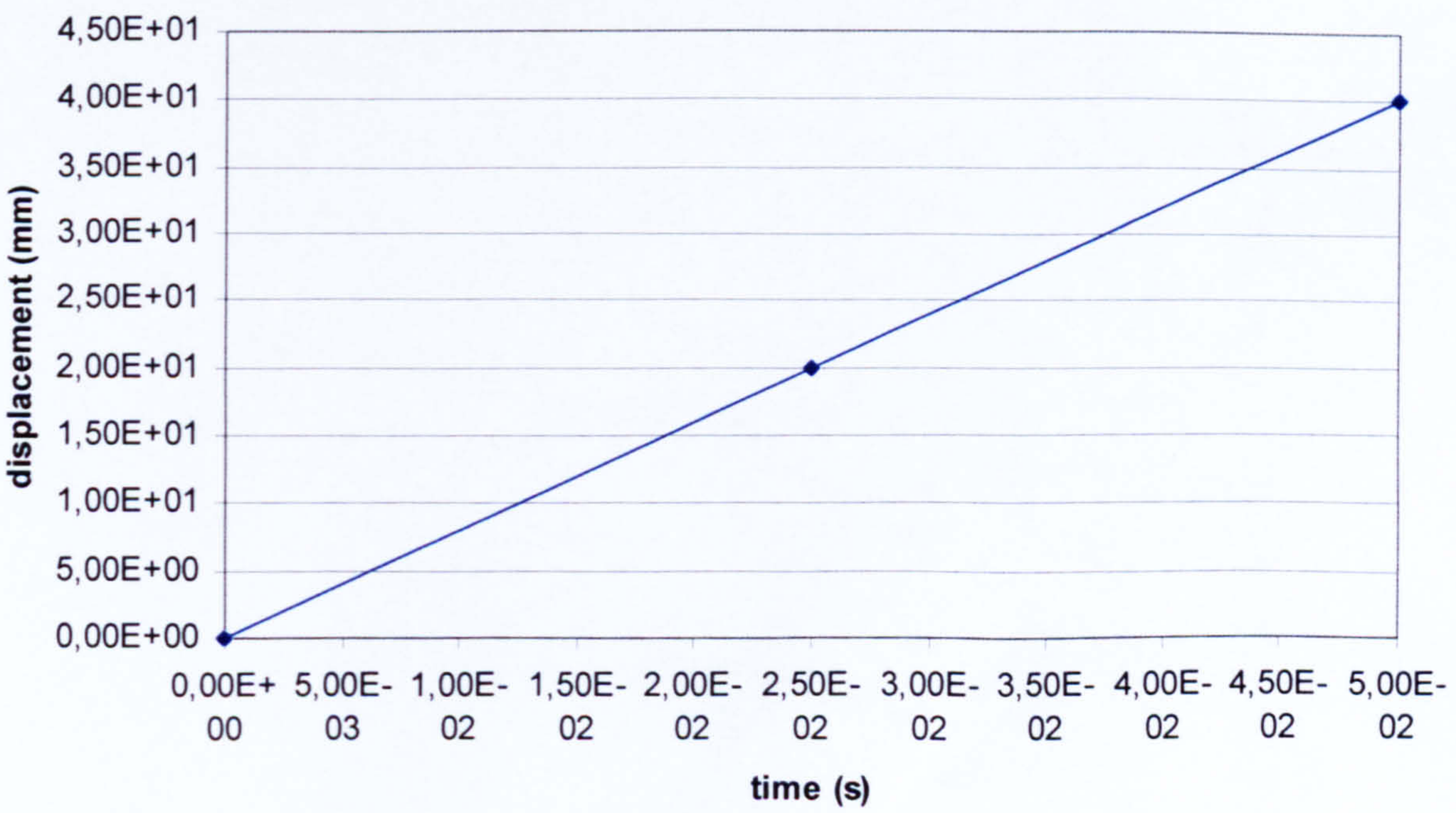

Figure 8-8 Load - Curve for axial Feeding (Simulation)

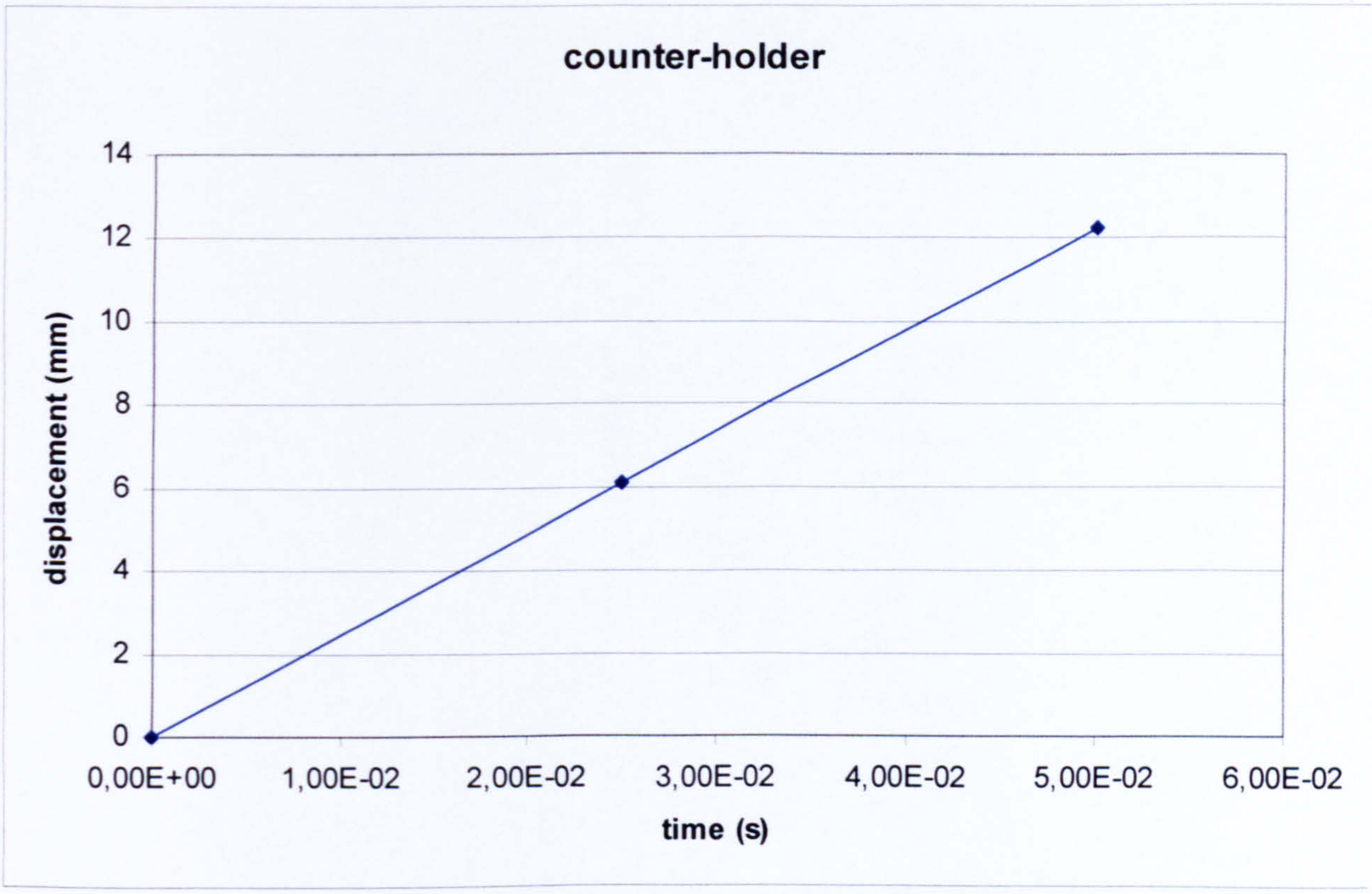

Figure 8-9 Load - Curve Counter-Holder (Simulation)

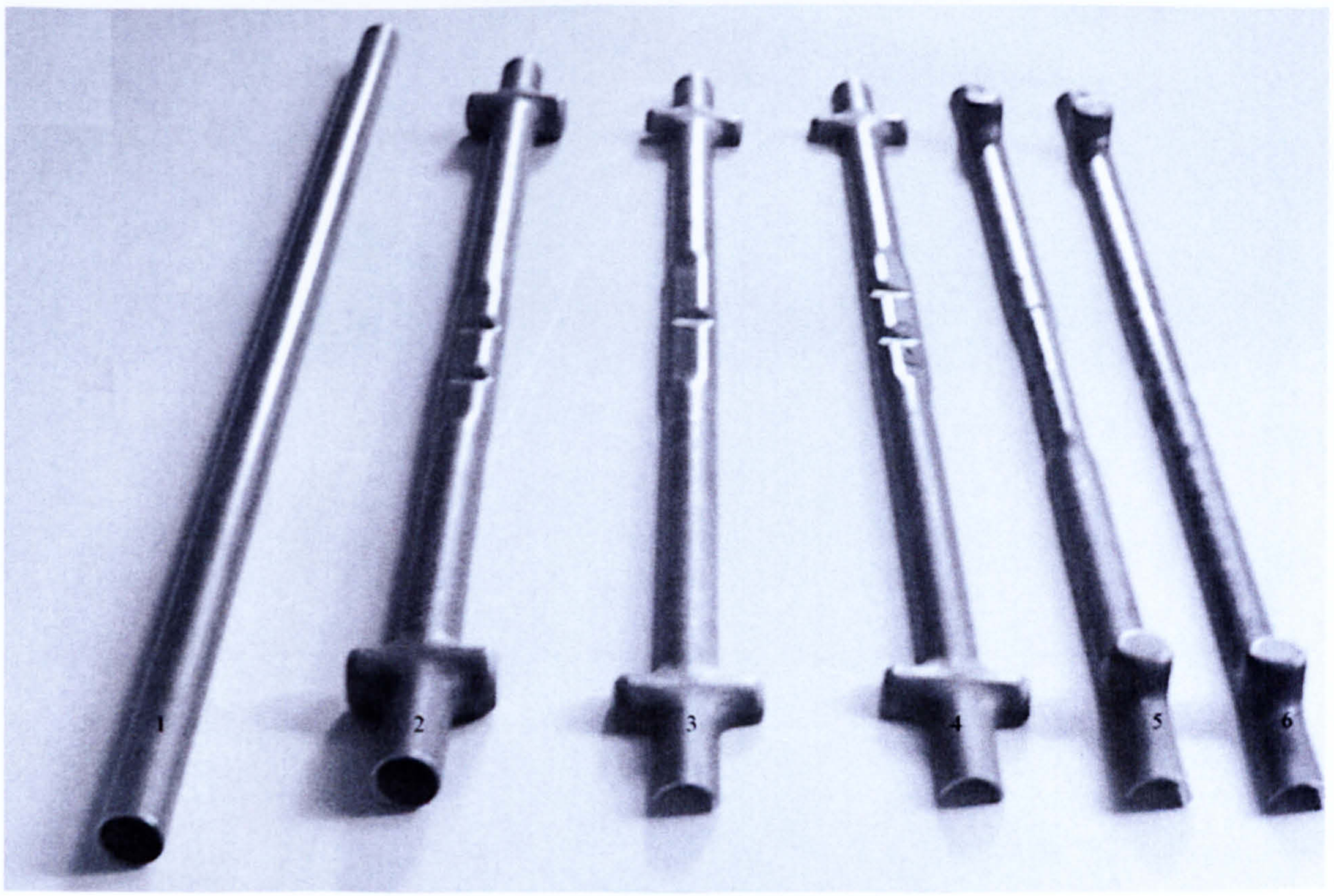

Figure 8-10 Windshield Wiper

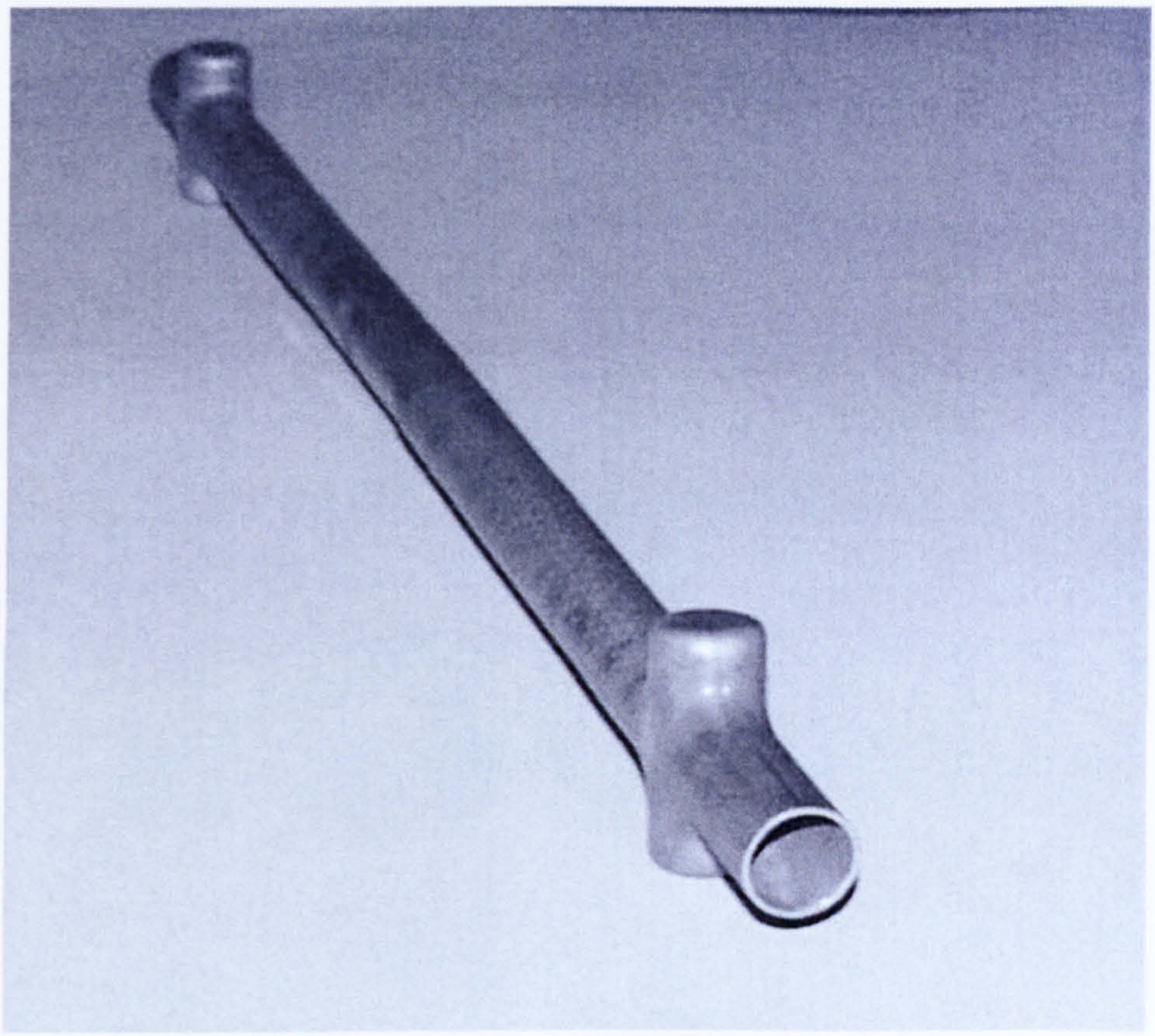

Figure 8-11 Windshield Wiper

Figure 8-12 Tube with grid

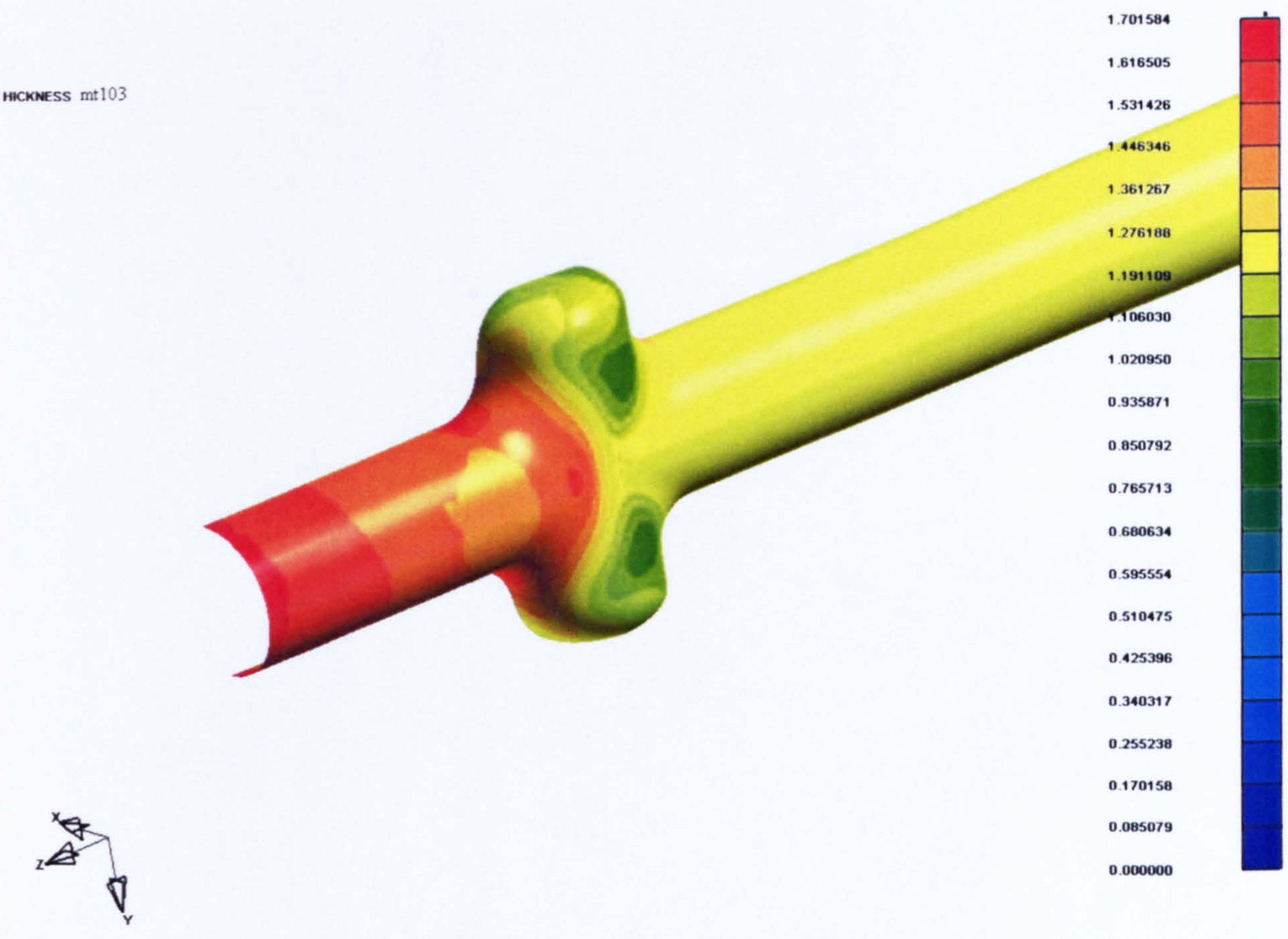

Figure 8-13 Wall - Thickness Distribution (mt103)

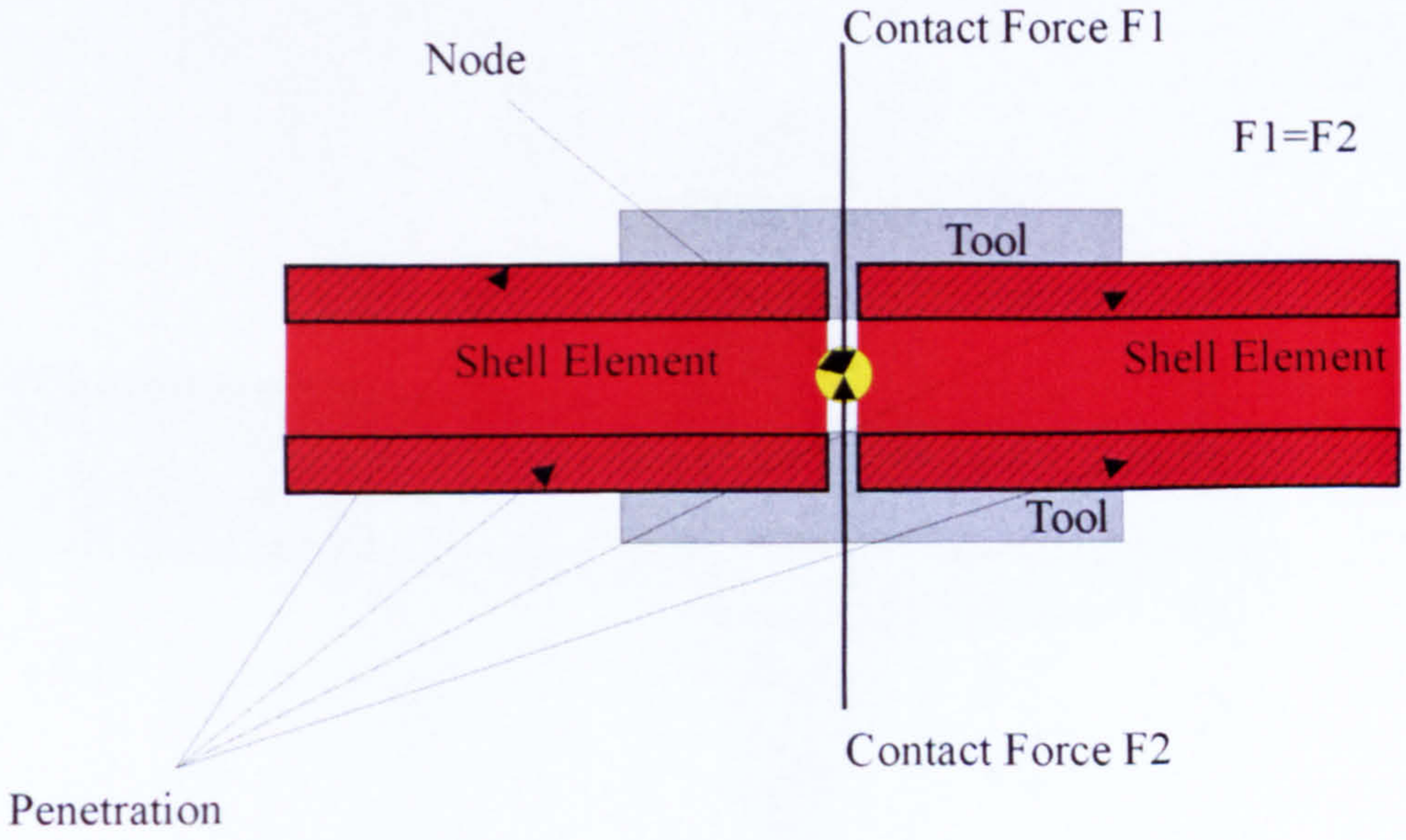

Figure 8-14 Contact and Shell Thickness

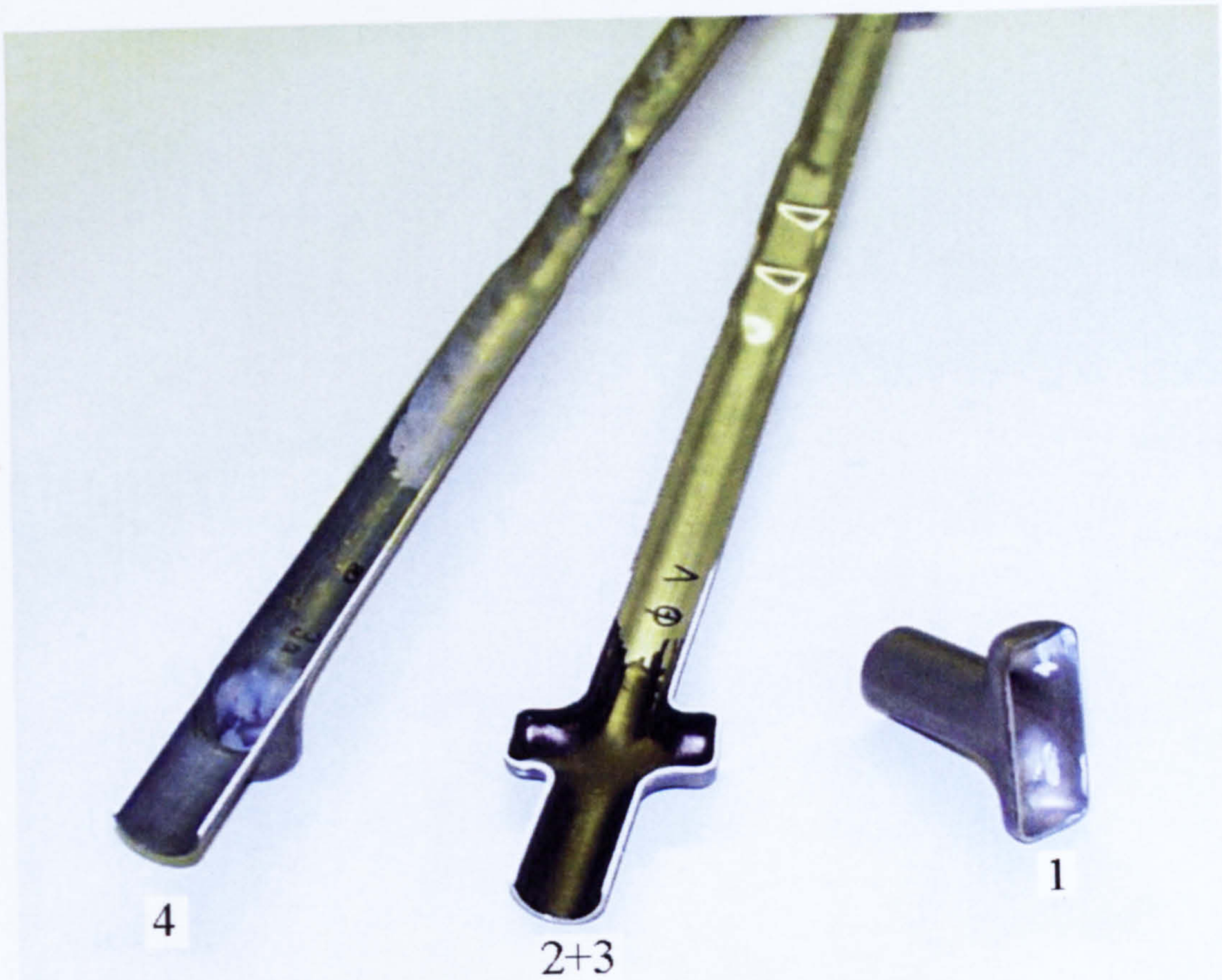

Figure 8-15 Tubes – Path 1-4

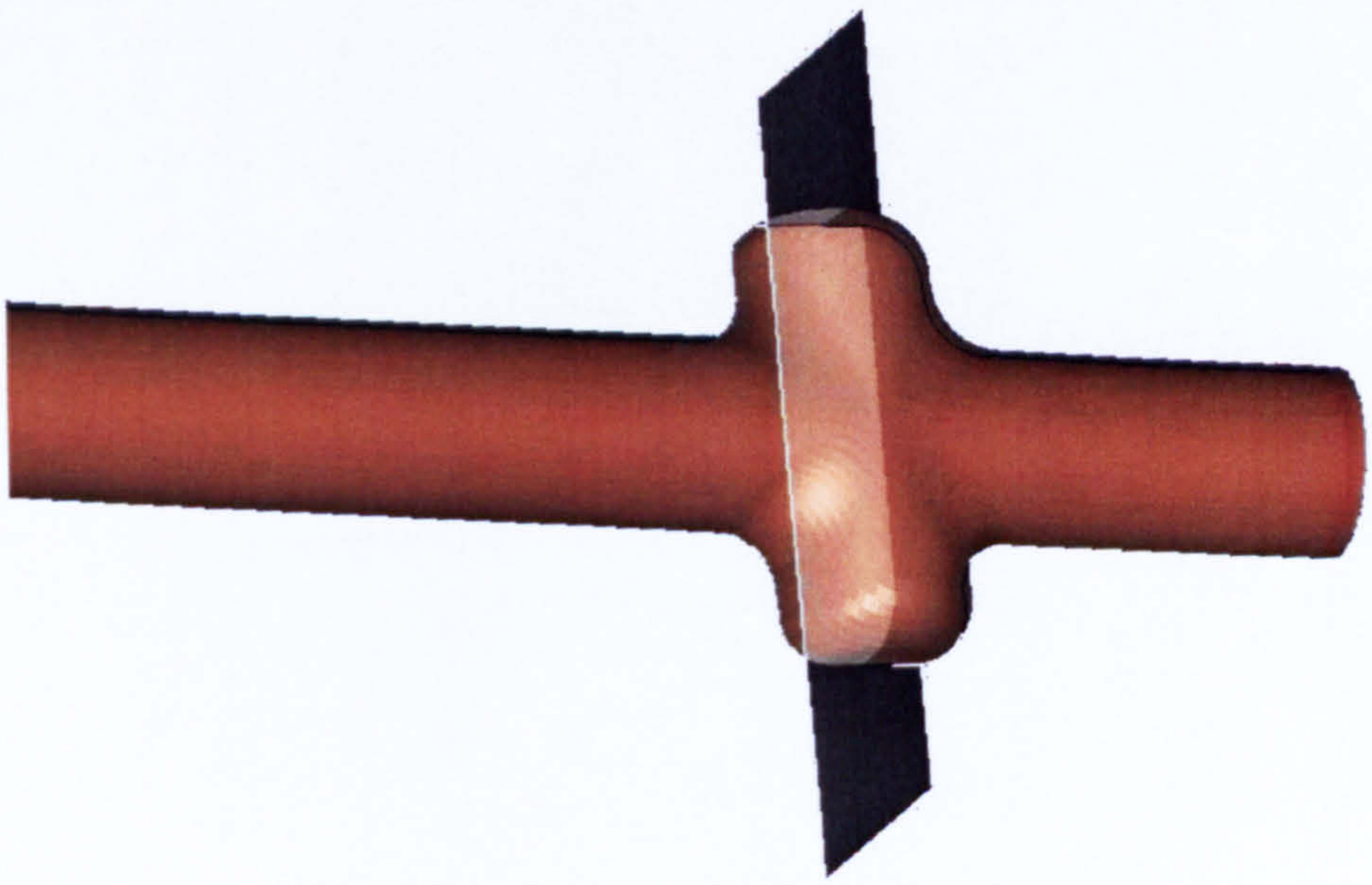

Figure 8-16 Path 1

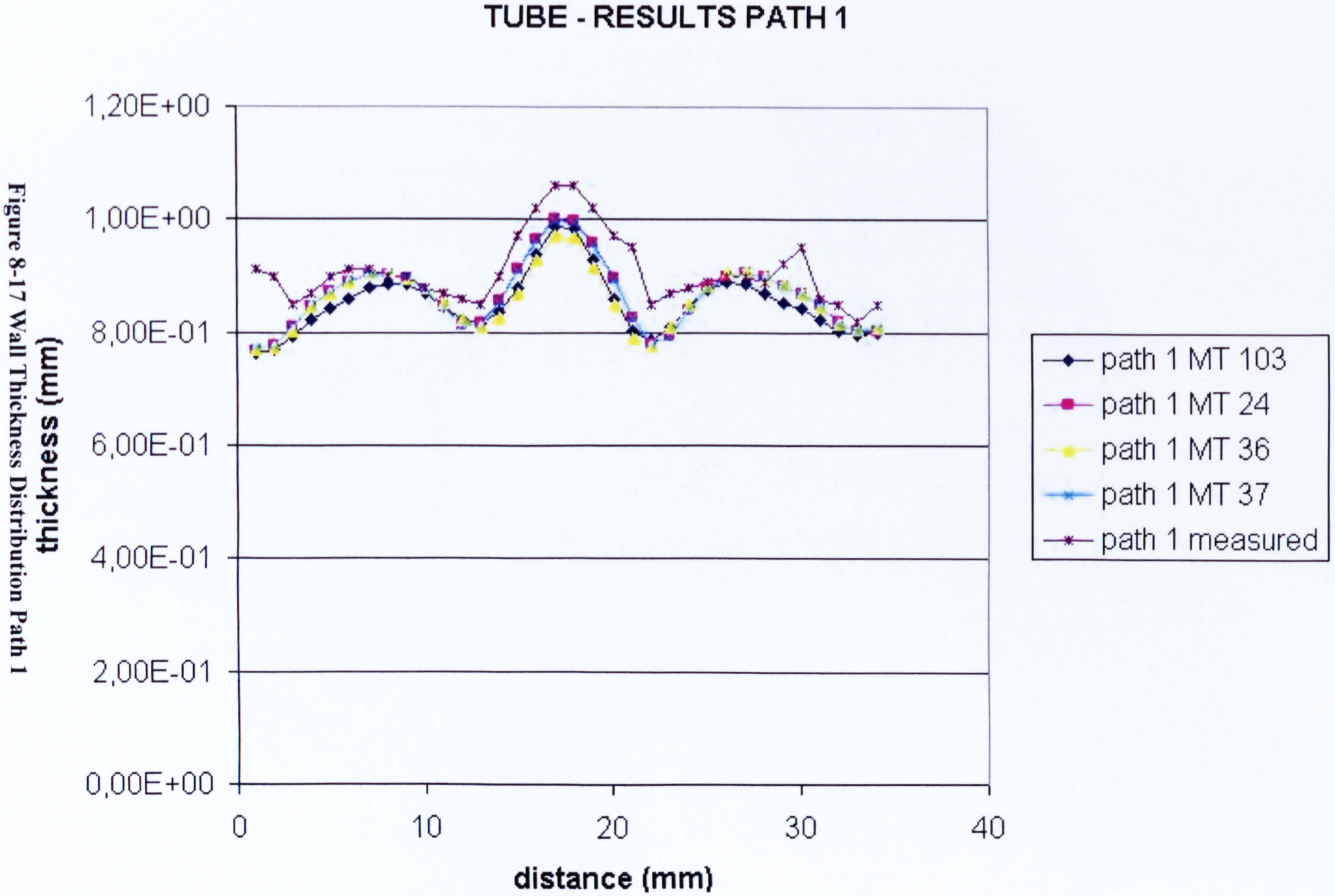

Figure 8-17 Wall Thickness Distribution Path 1

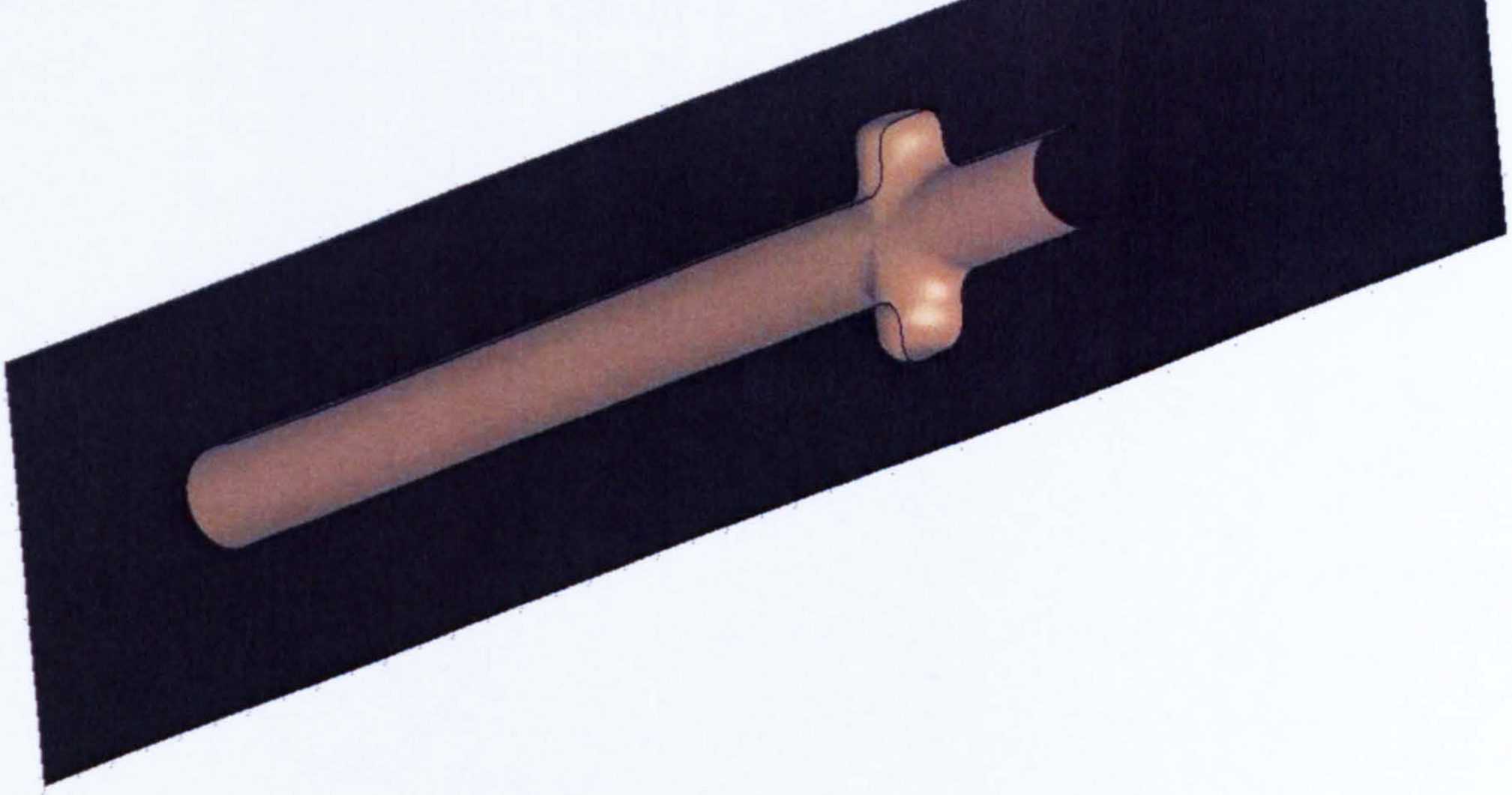

Figure 8-18 Path 2 + 3

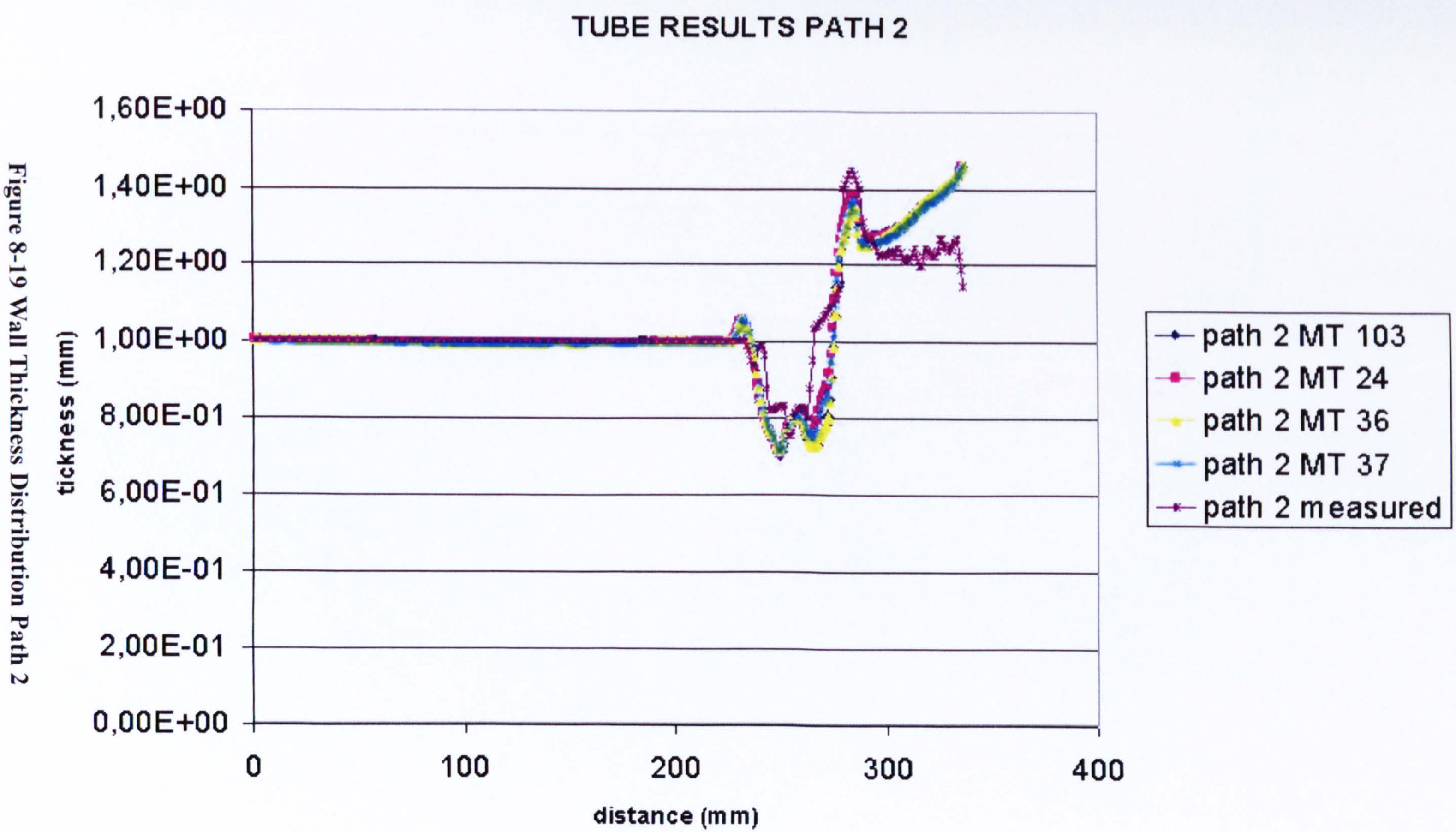

Figure 8-19 Wall Thickness Distribution Path 2

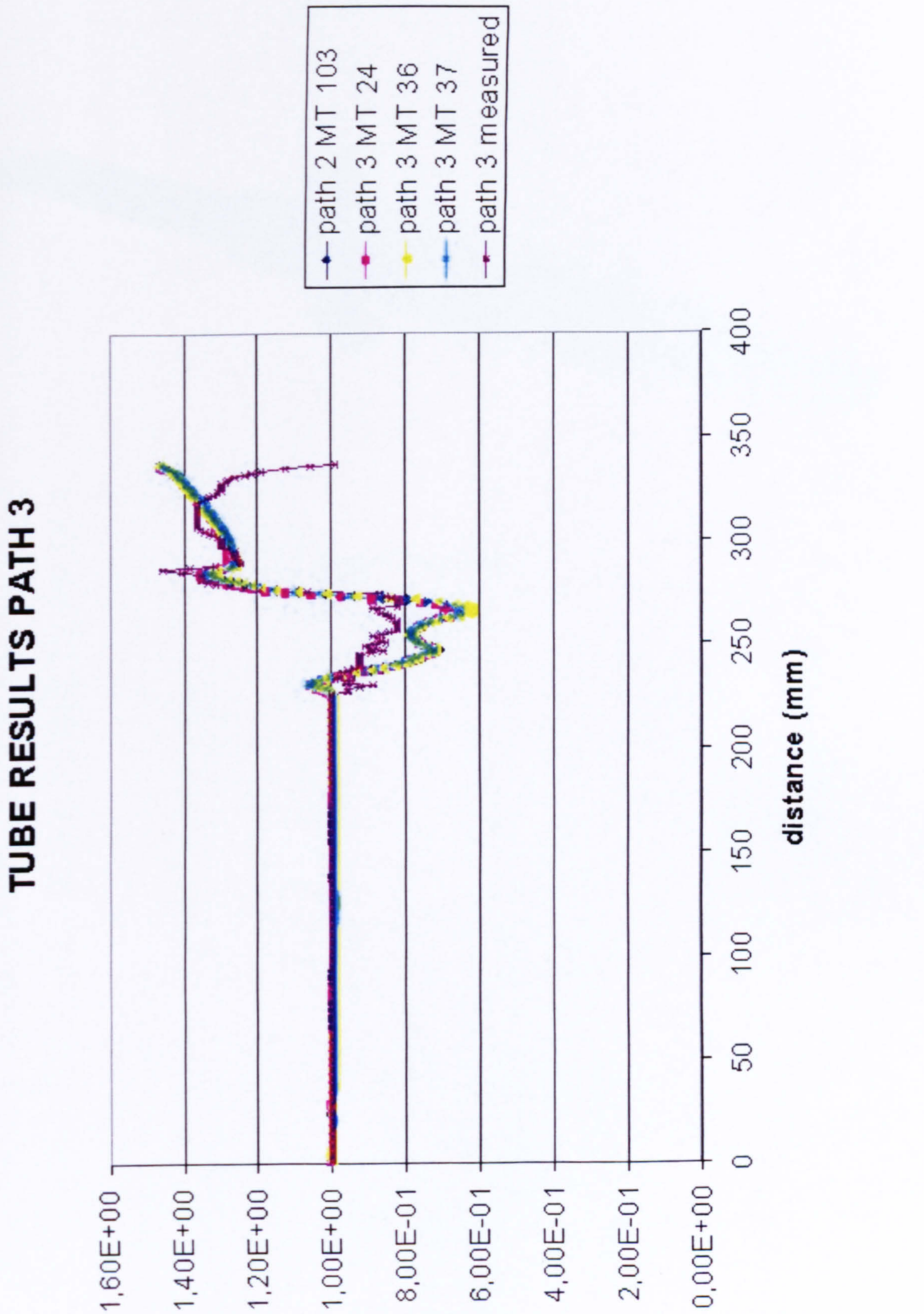

Figure 8-20 Wall Thickness Distribution Path 3

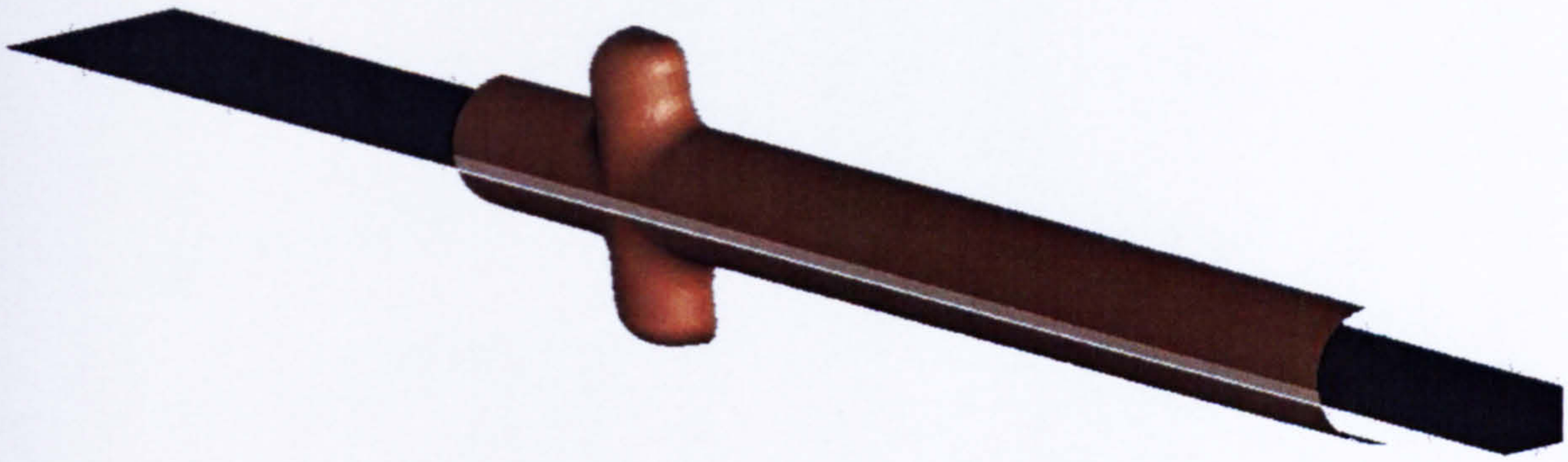

Figure 8-21 Path 4

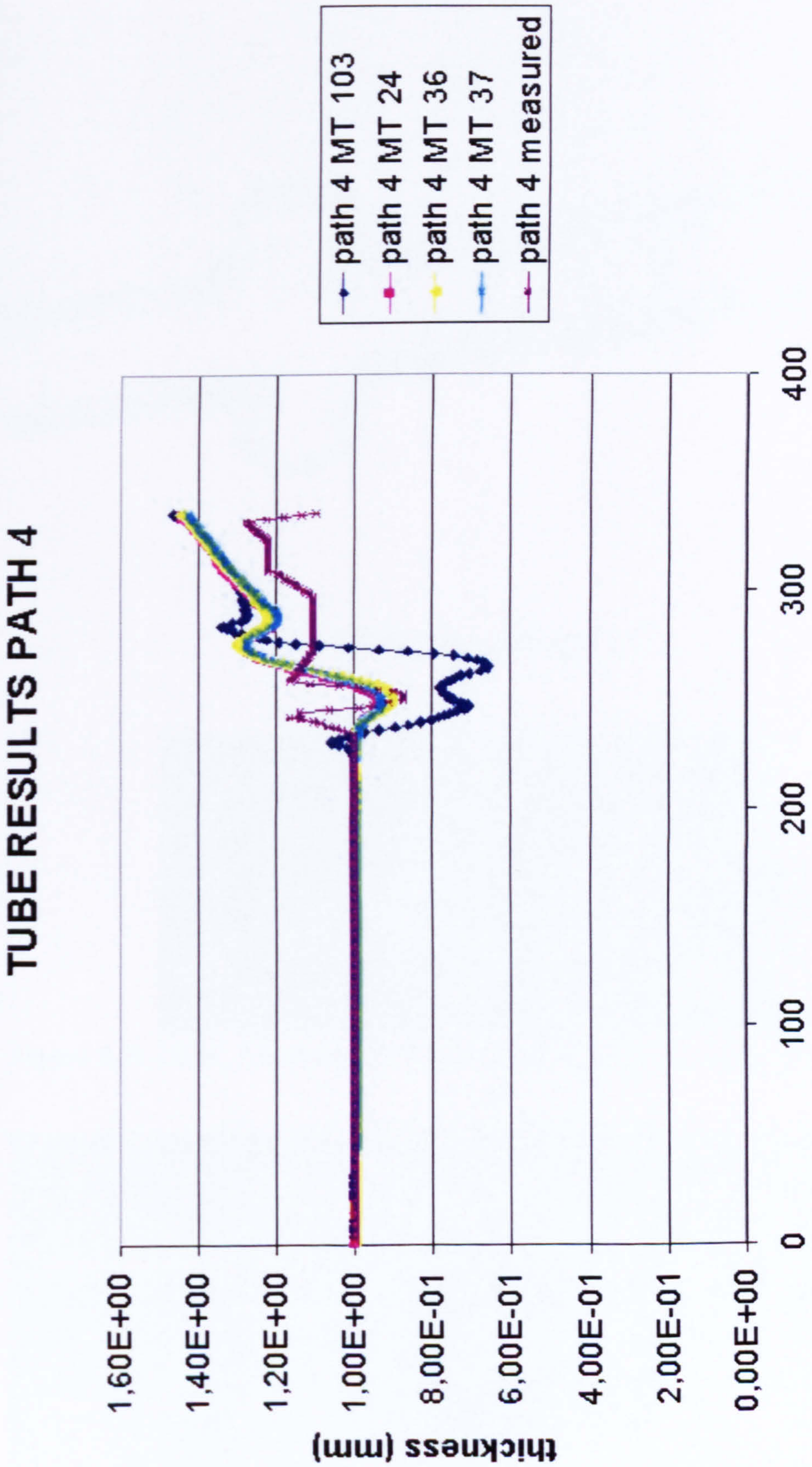

Figure 8-22 Wall Thickness Distribution Path 4

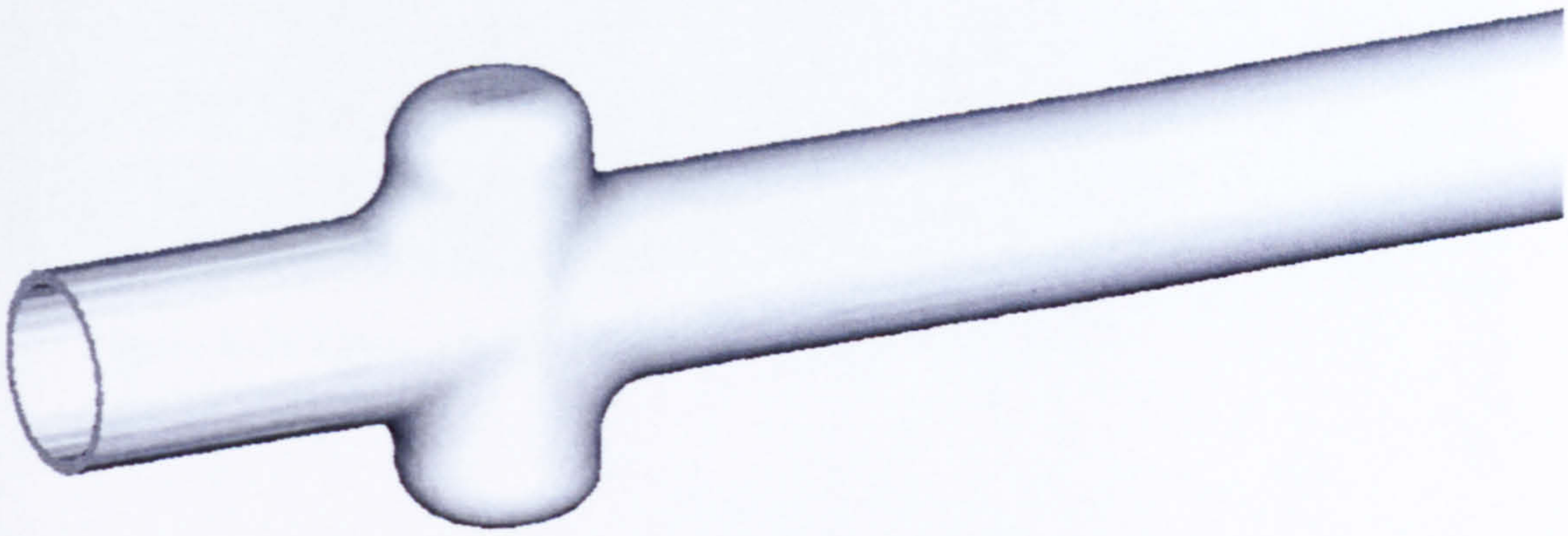

Figure 8-23 Reconstructed Part

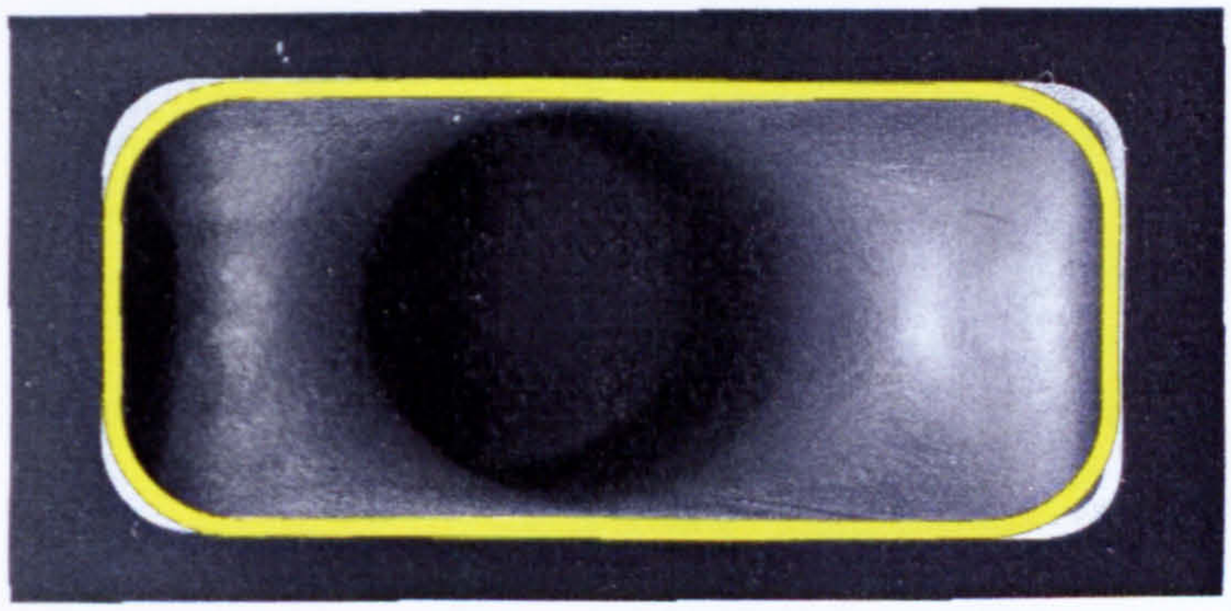

Figure 8-24 Cross - Section Path 1 - Simulation (yellow) and Real Part

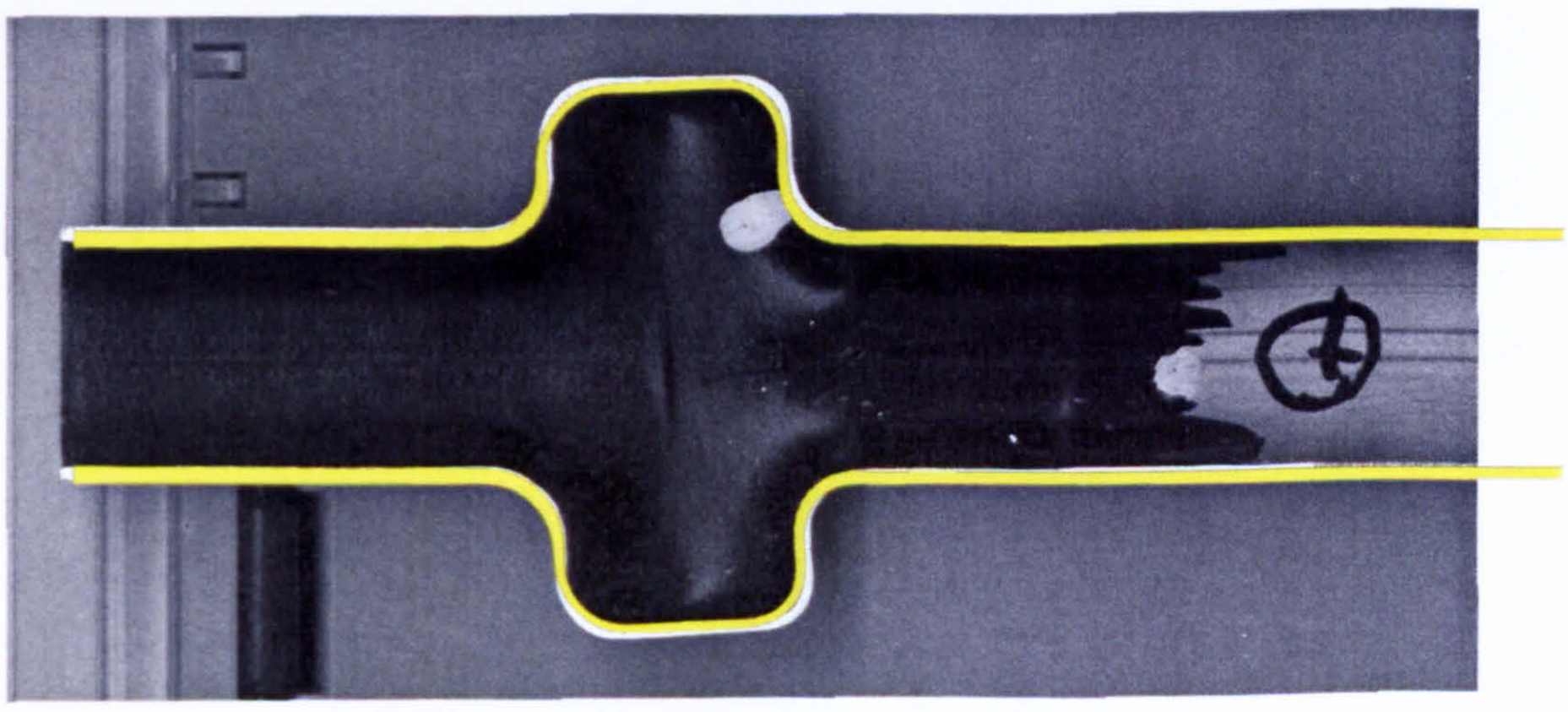

Figure 8-25 Cross - Section Path 2 - Simulation (yellow) and Real Part

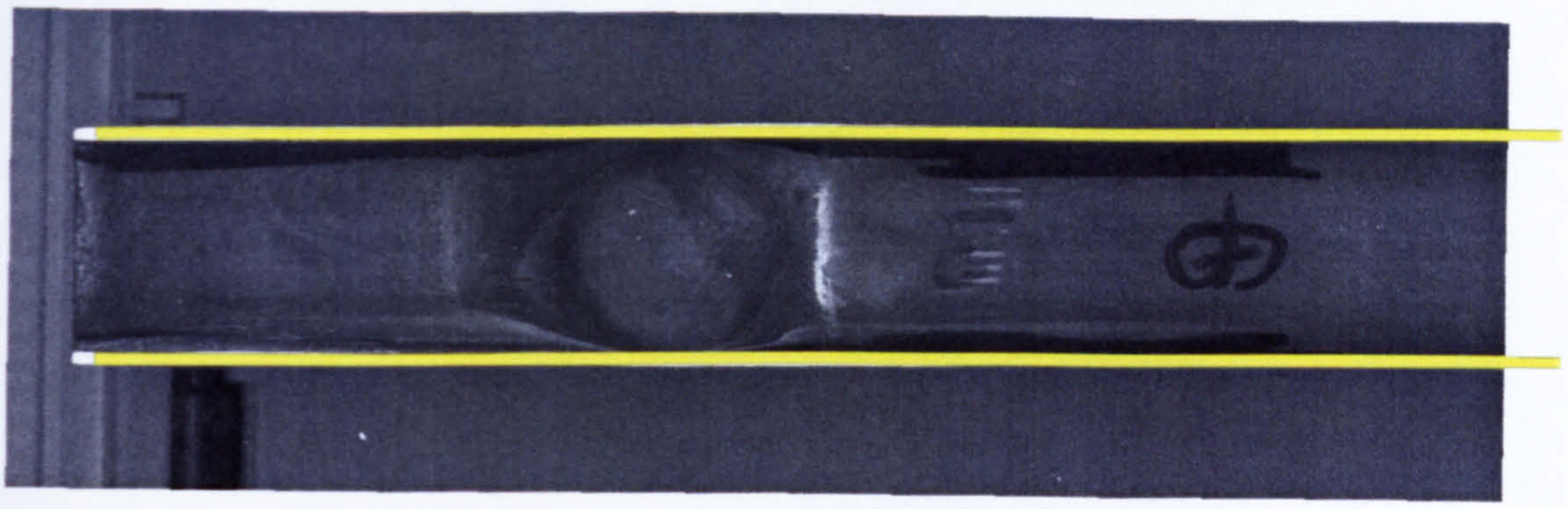

Figure 8-26 Cross - Section Path 4 - Simulation (yellow) and Real Part

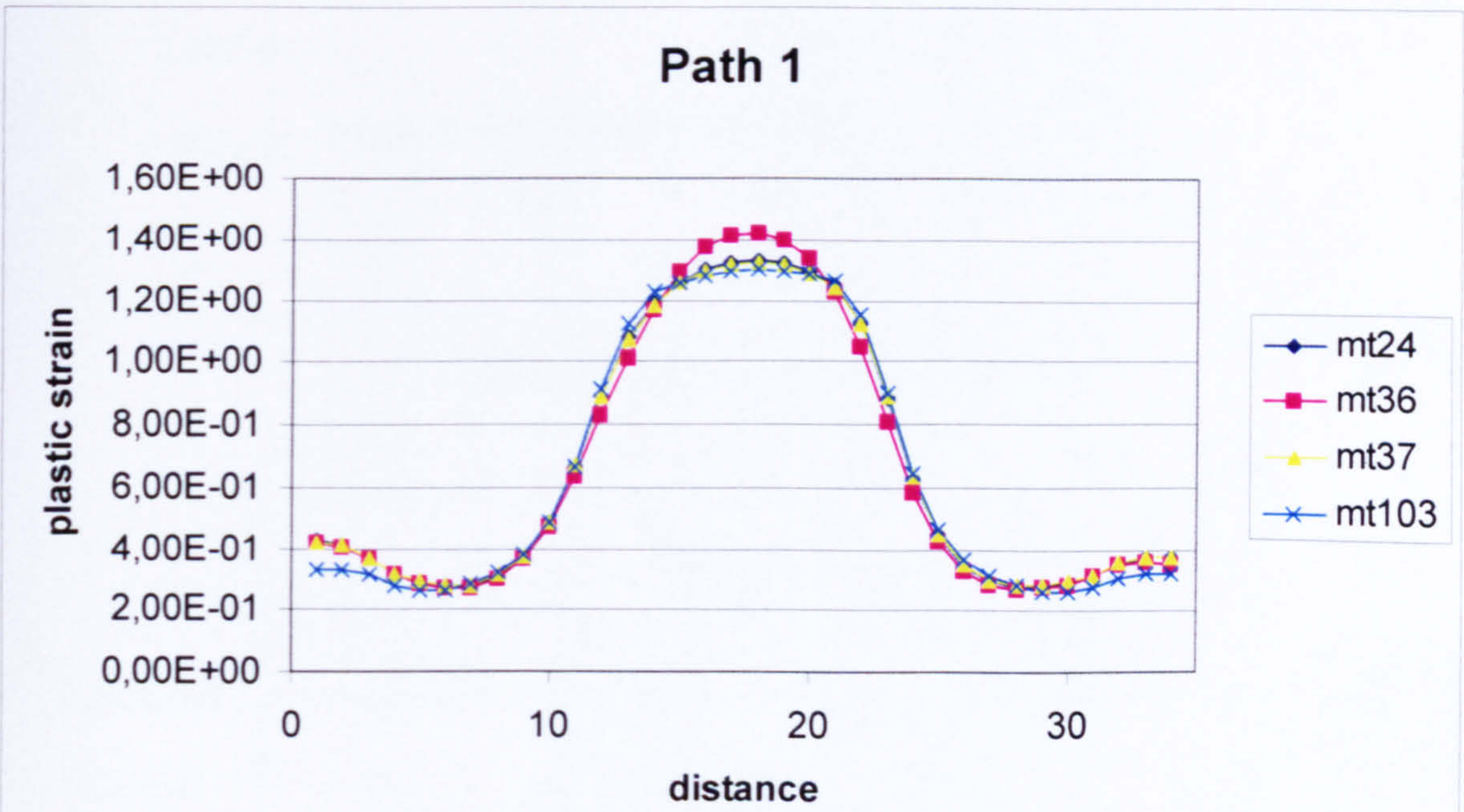

Figure 8-27 Plastic Strain Path 1

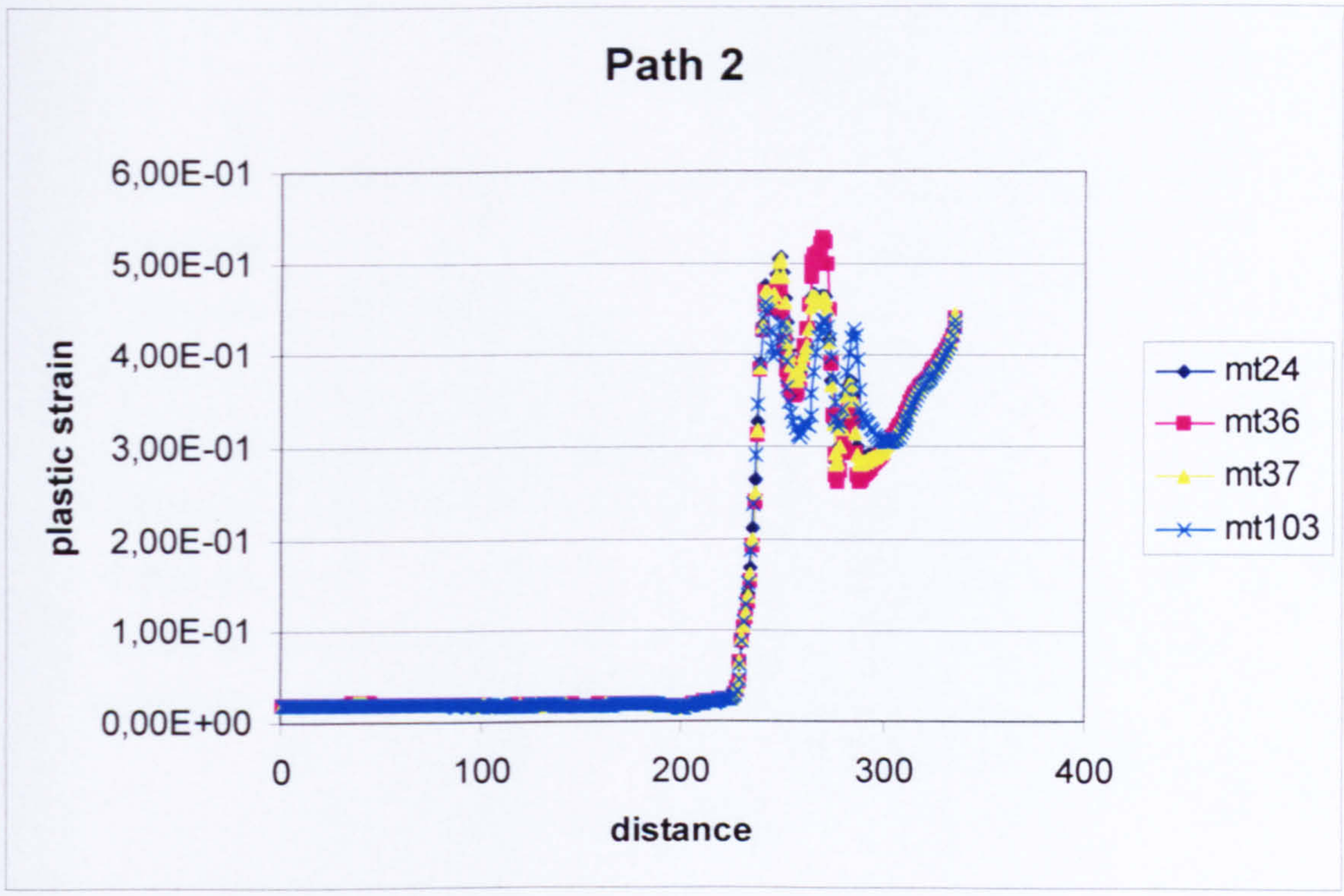

Figure 8-28 Plastic Strain Path 2

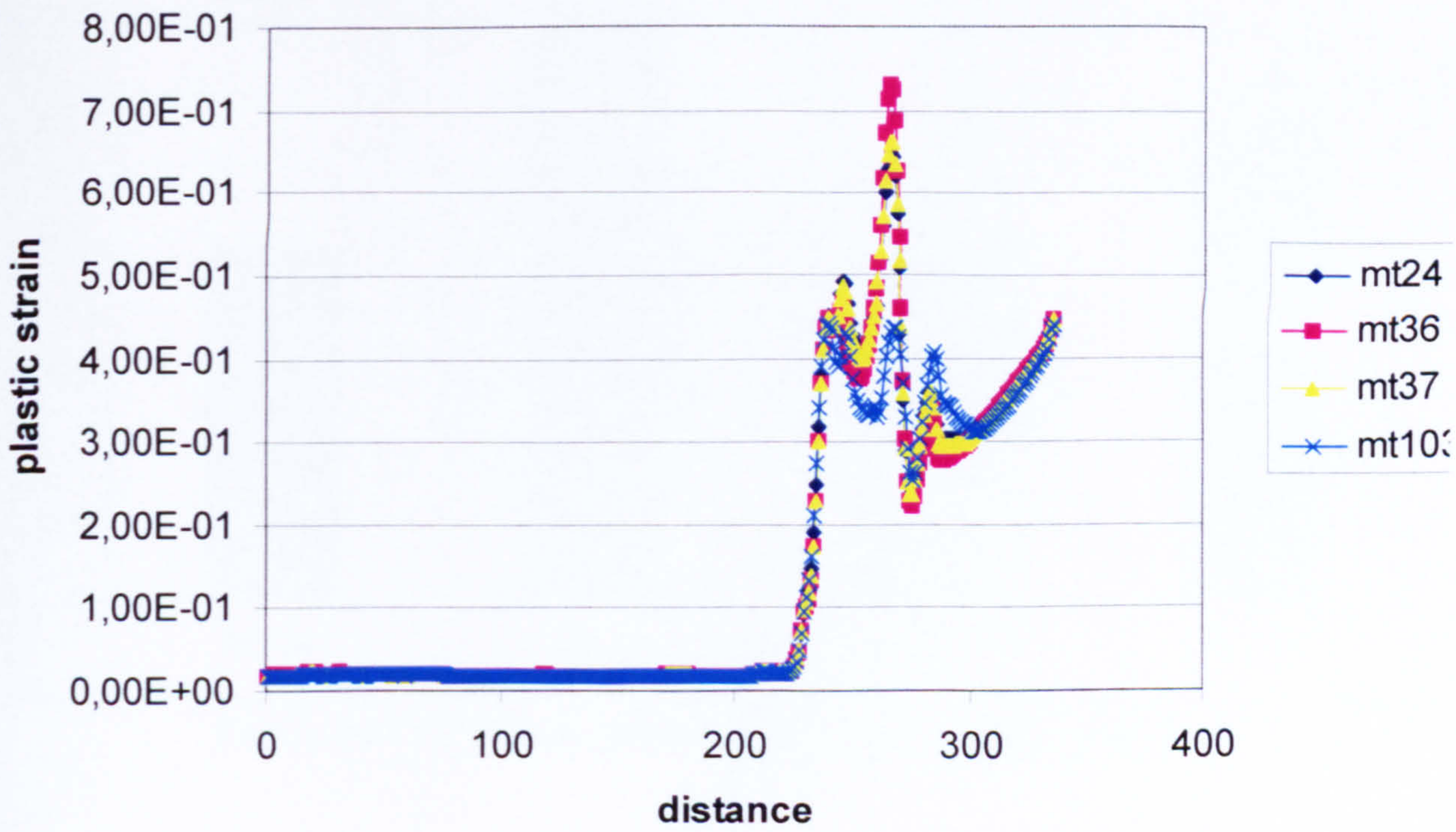

Figure 8-29 Plastic Strain Path 3

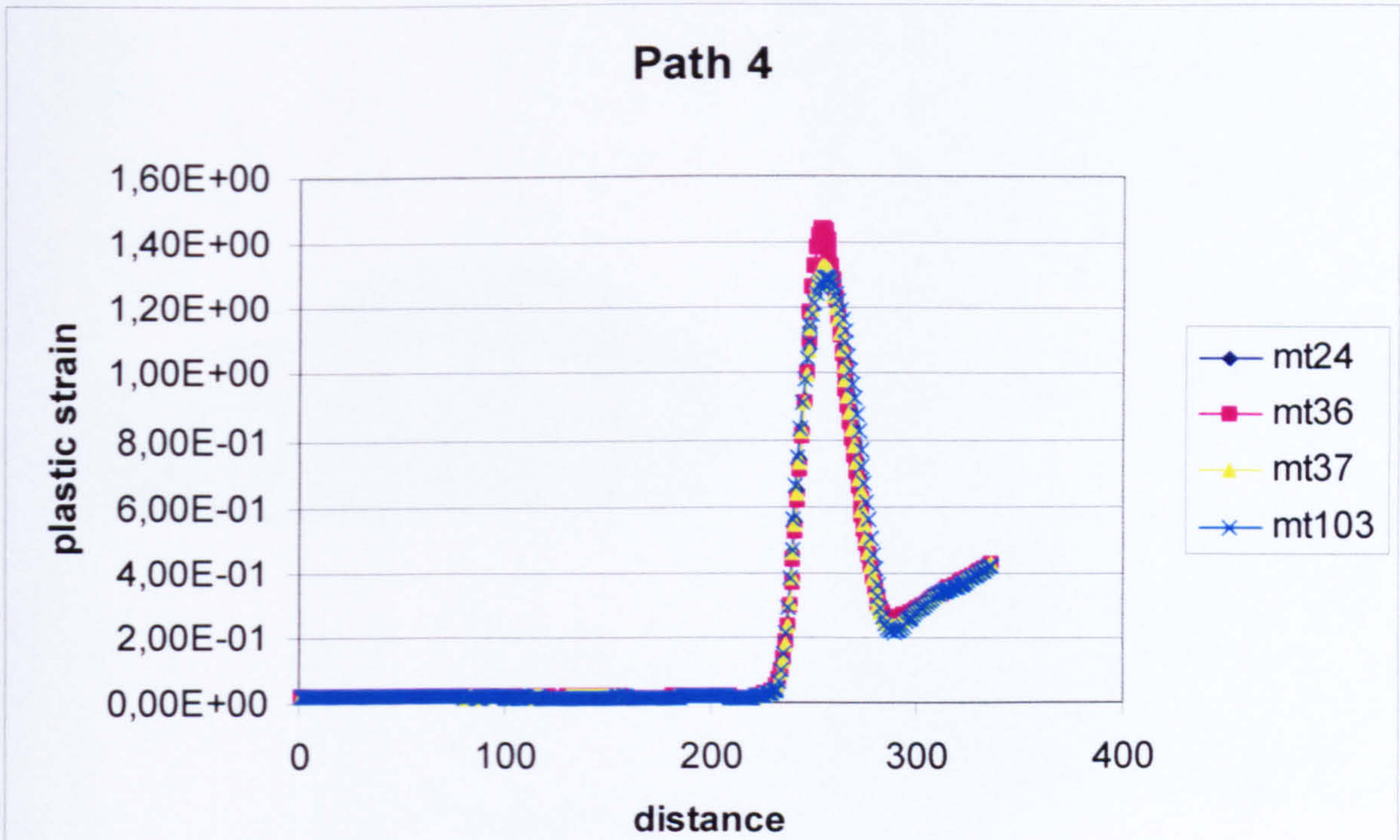

Figure 8-30 Plastic Strain Path 4

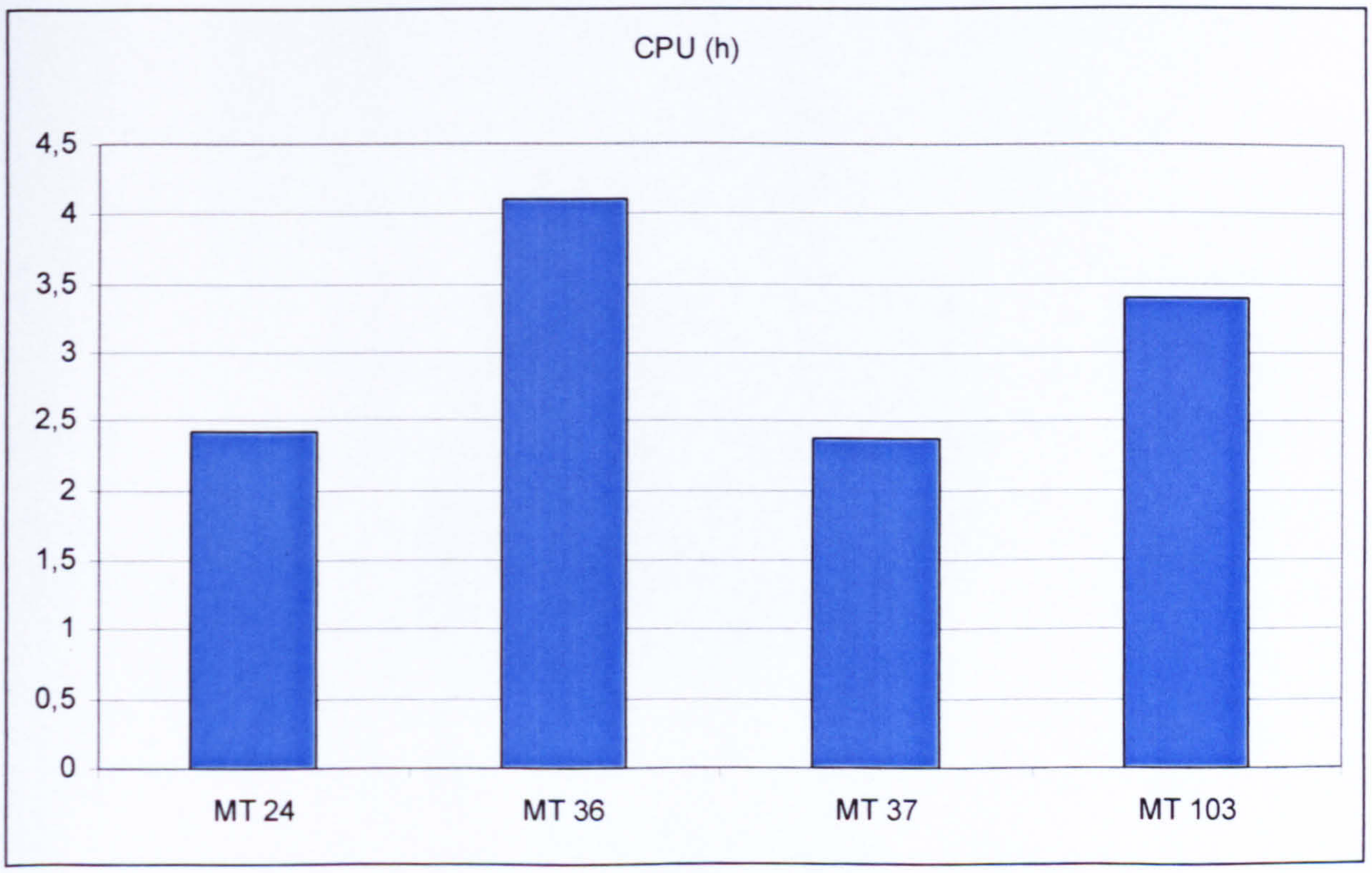

Figure 8-31 CPU Time needed for the Different Material Types

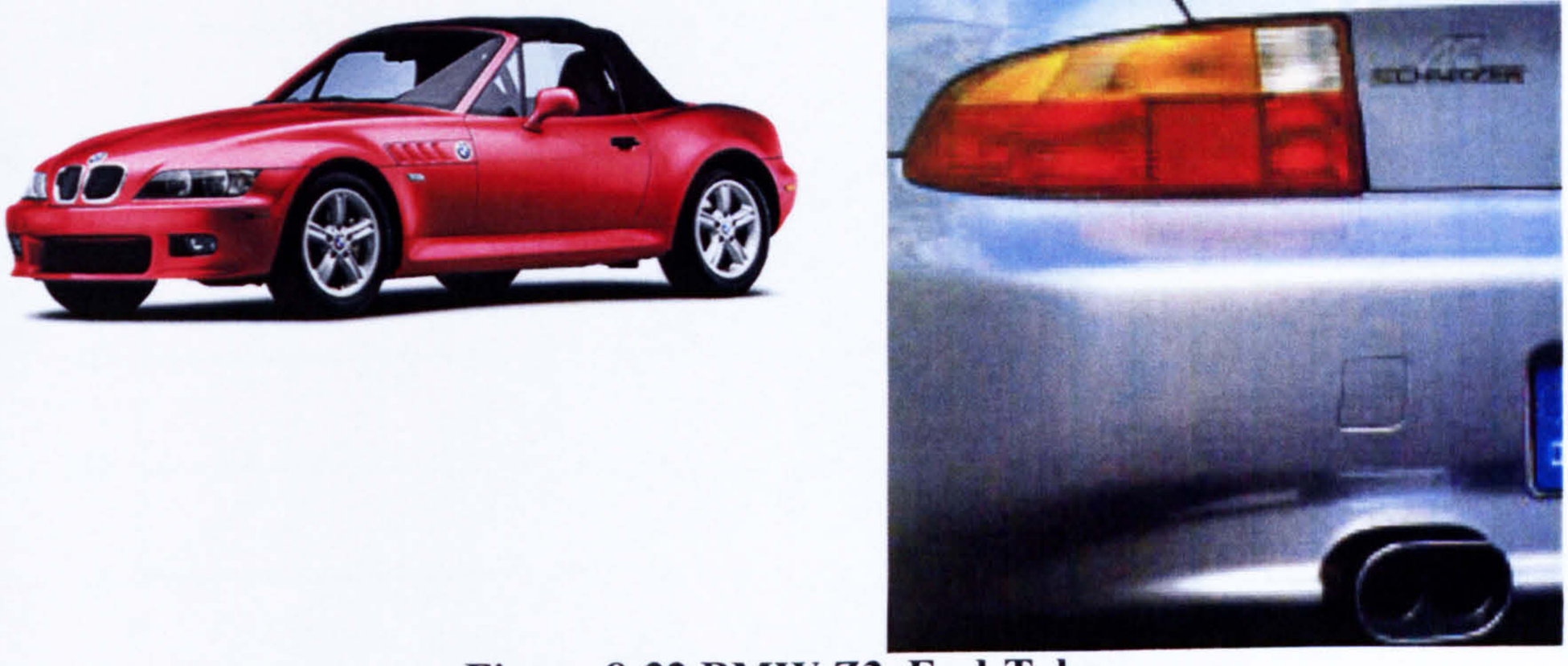

Figure 8-32 BMW Z3, End-Tube

Figure 8-33 End-Tube

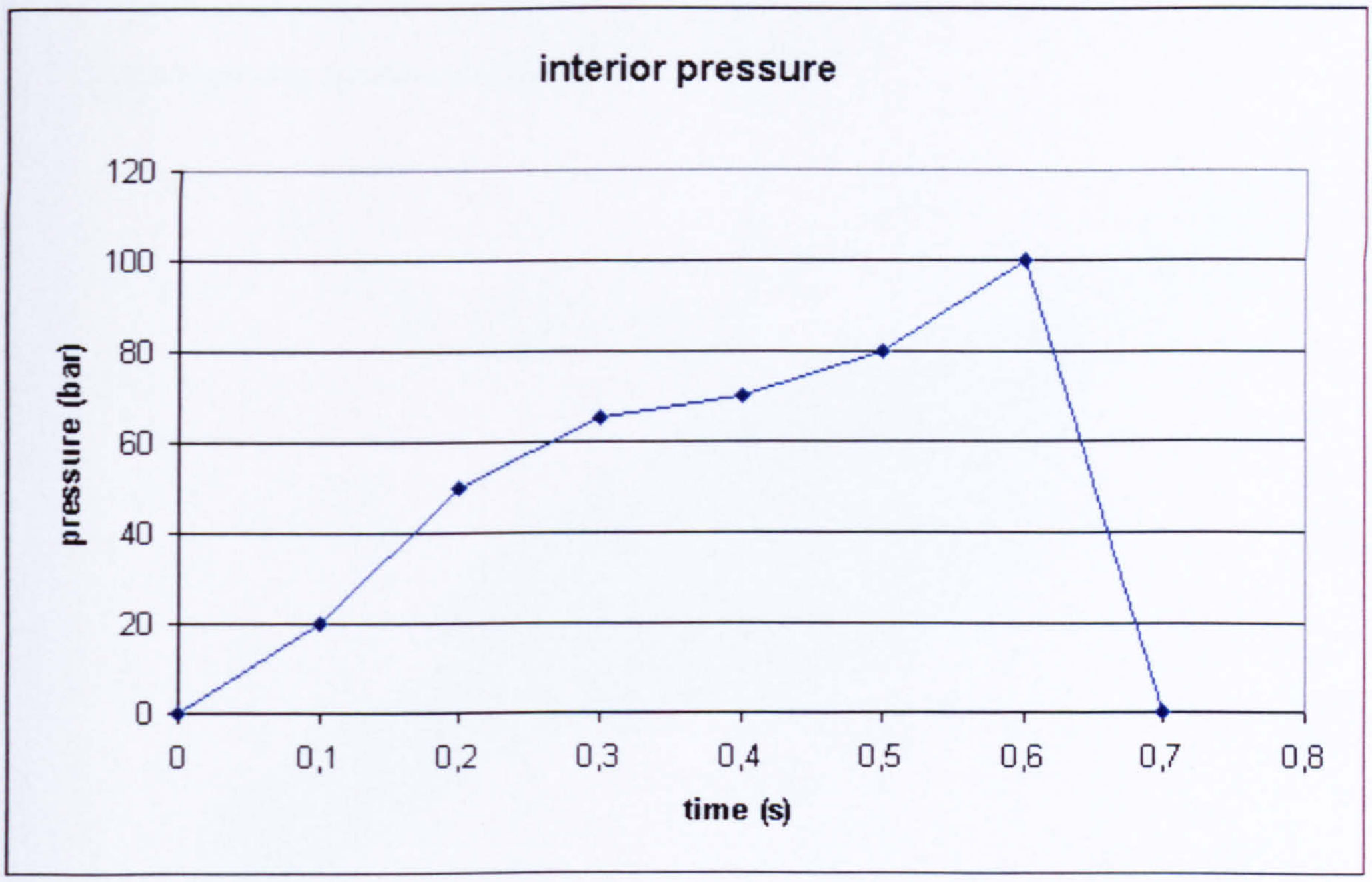

Figure 8-34 Load - Curve for Interior Pressure

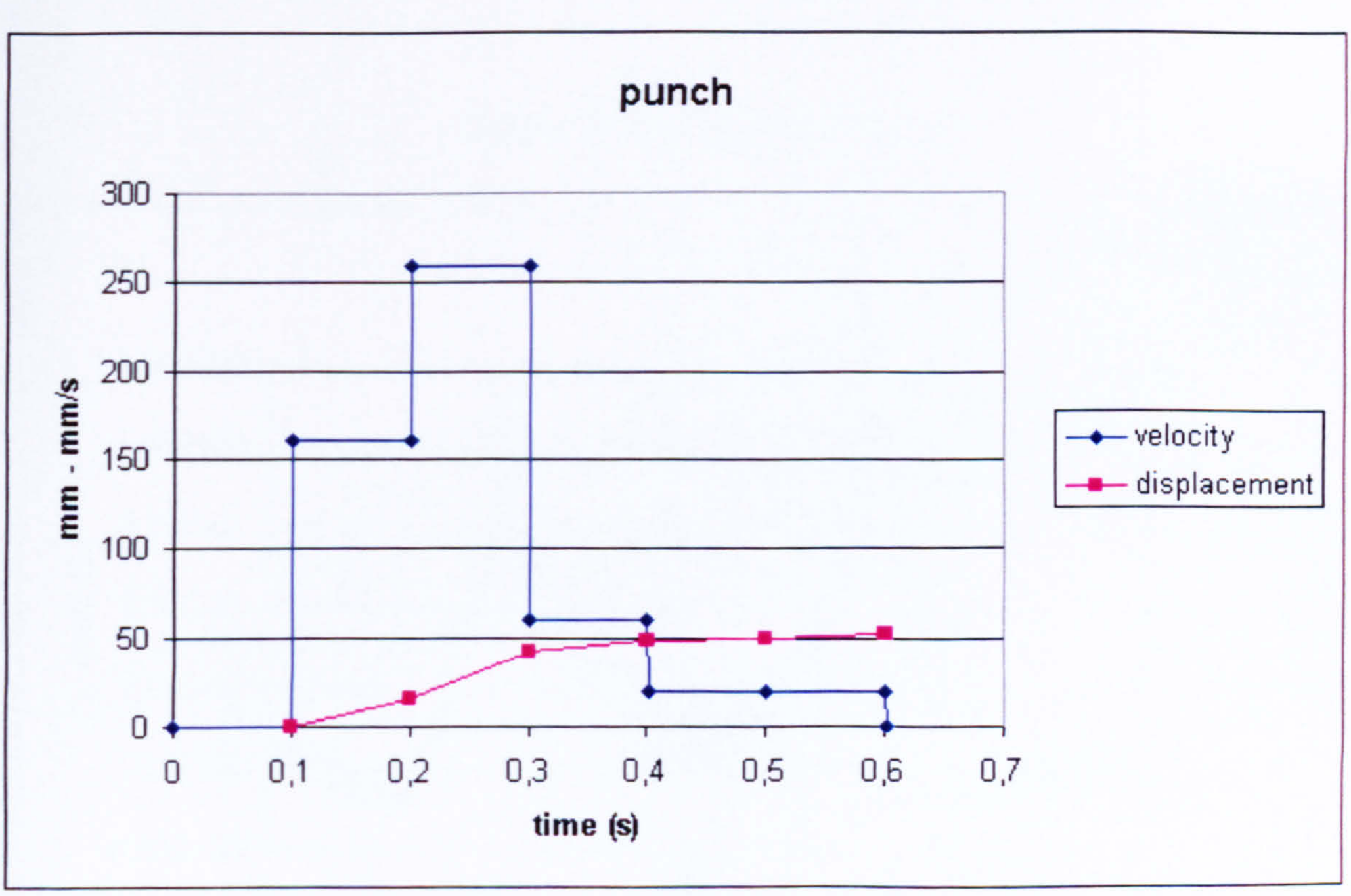

Figure 8-35 Load - Curve for axial feeding

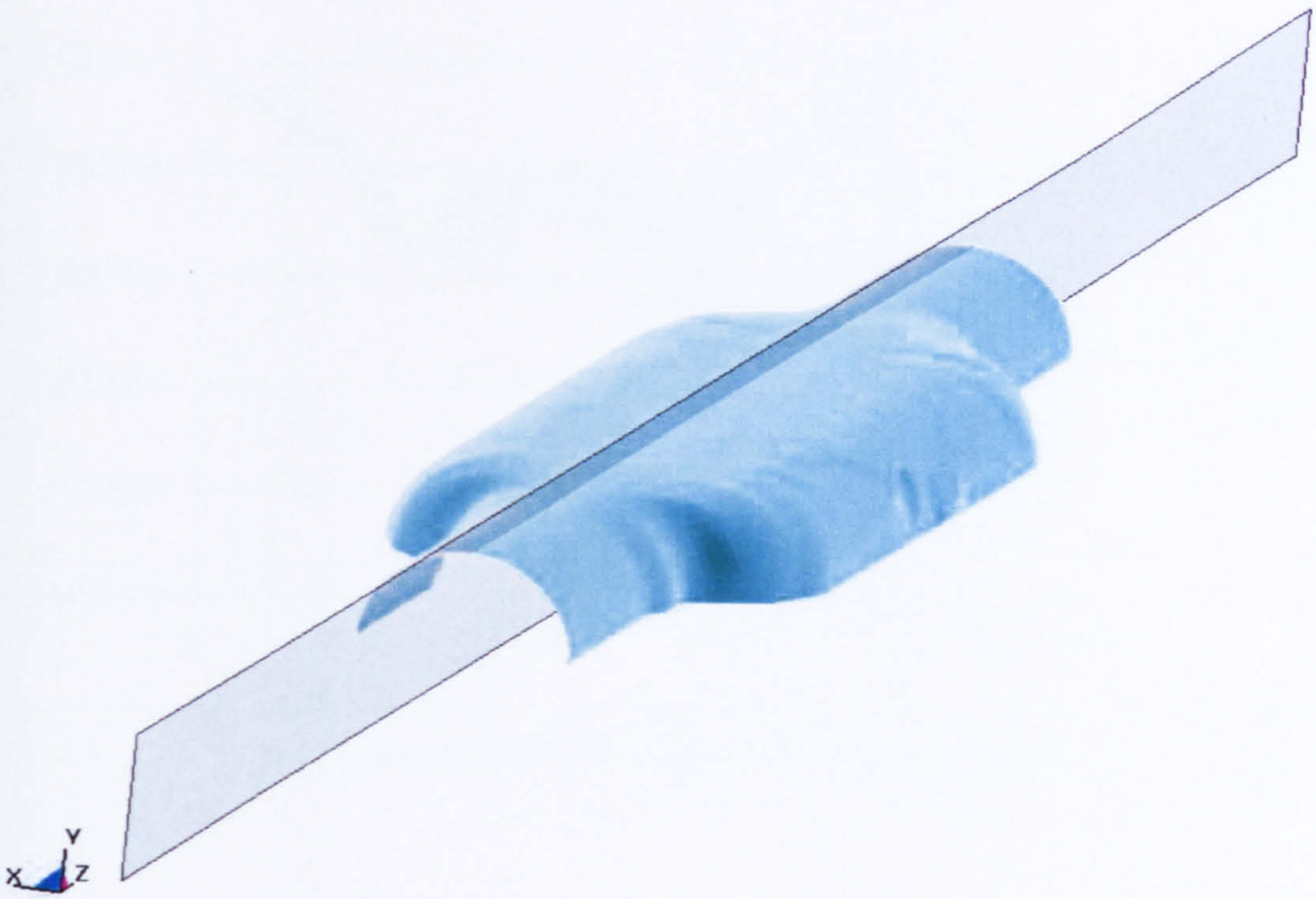

Figure 8-36 End-Tube Path 1

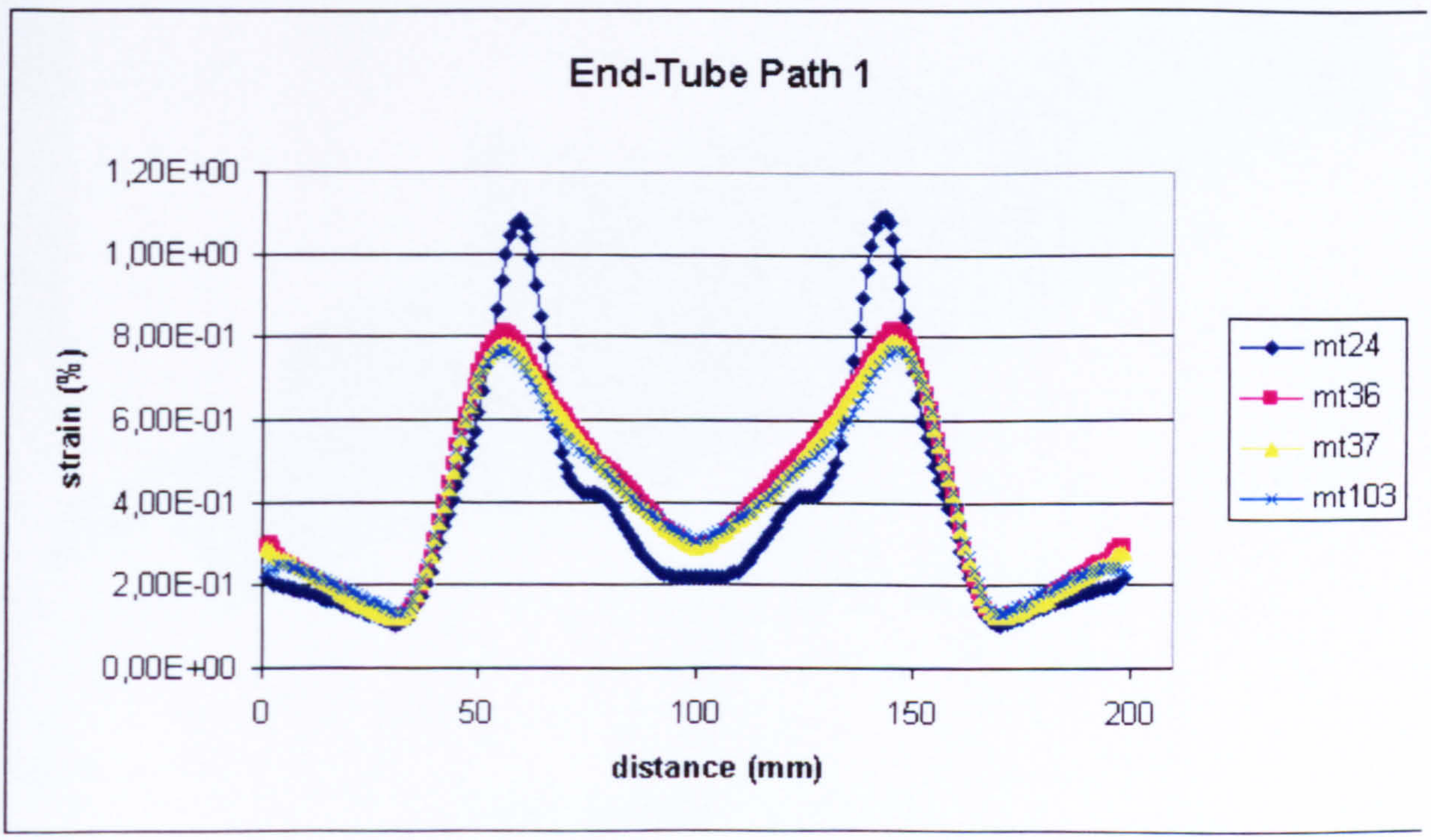

Figure 8-37 Plastic Strain Path 1

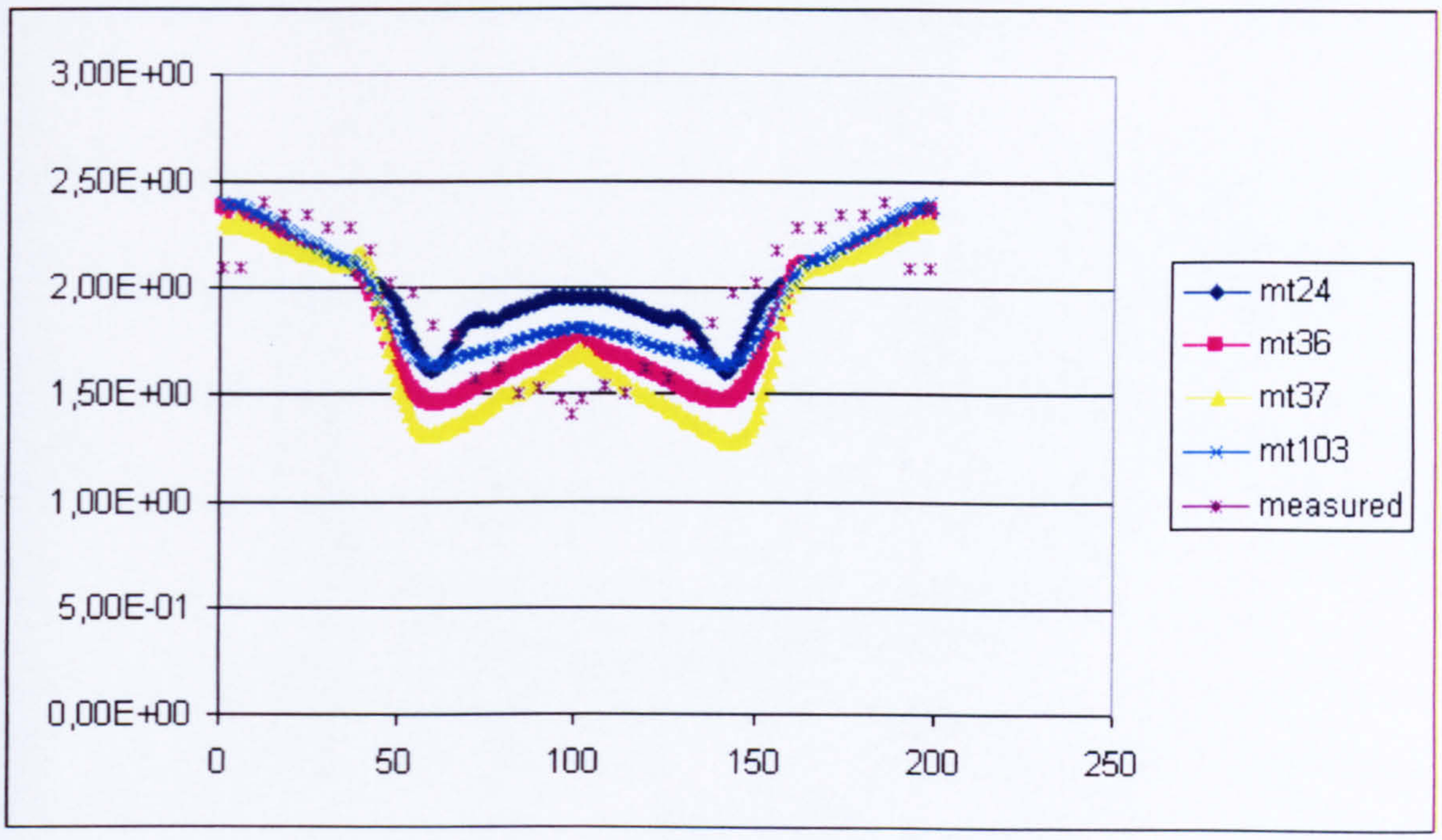

Figure 8-38 Wall-thickness Distribution Path 1

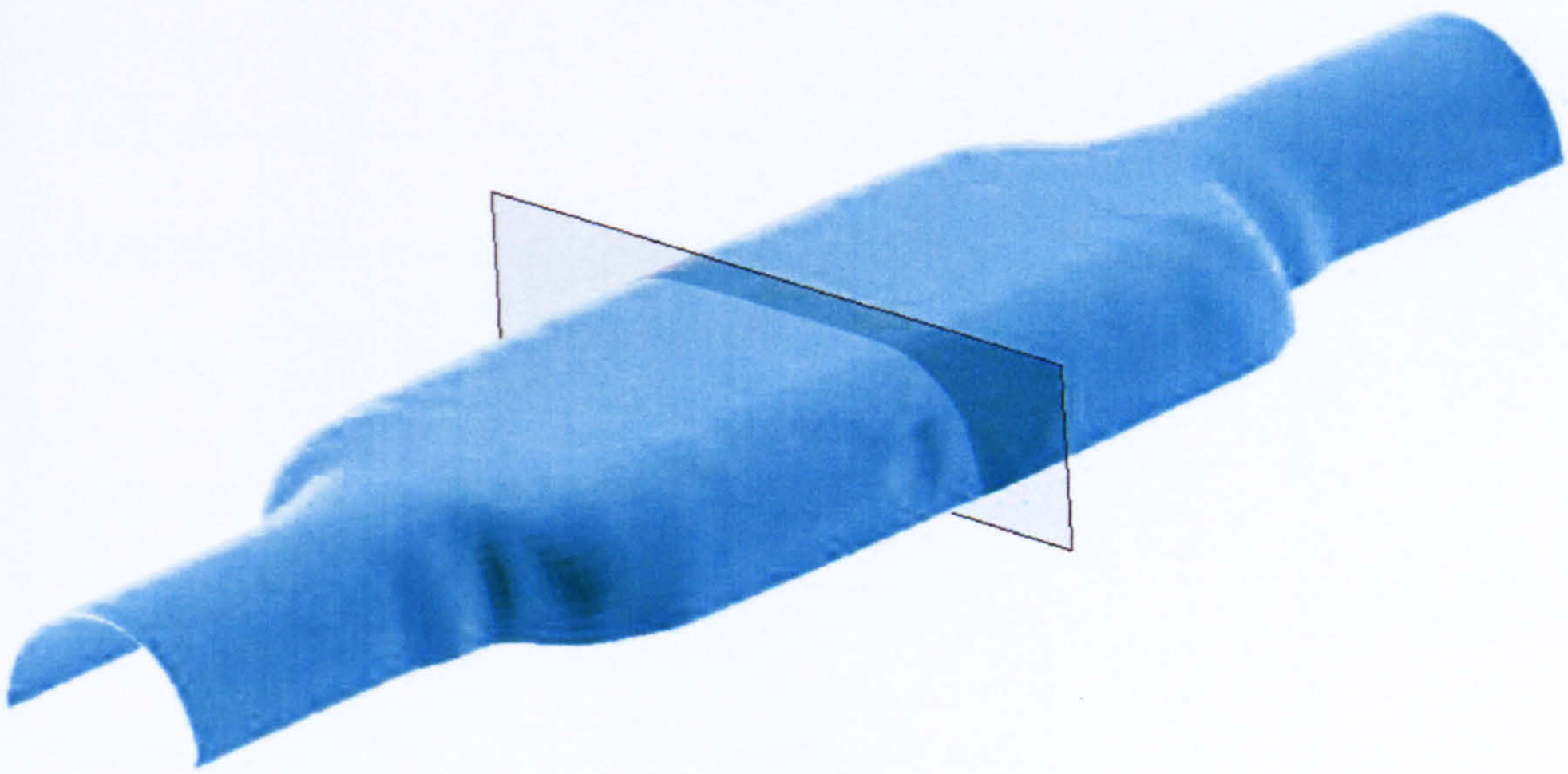

Figure 8-39 End-Tube Path 2

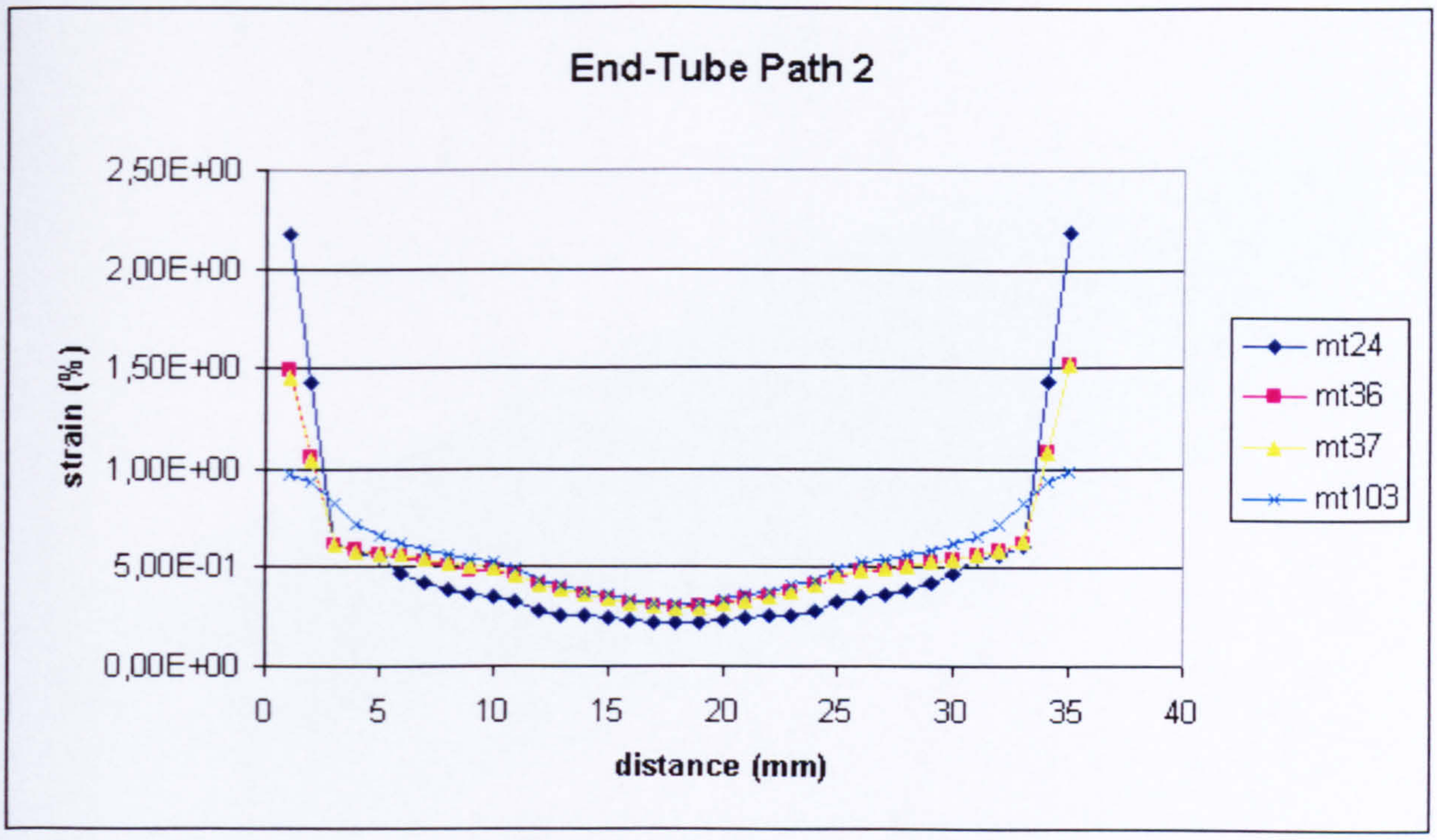

Figure 8-40 Plastic Strain Path 2

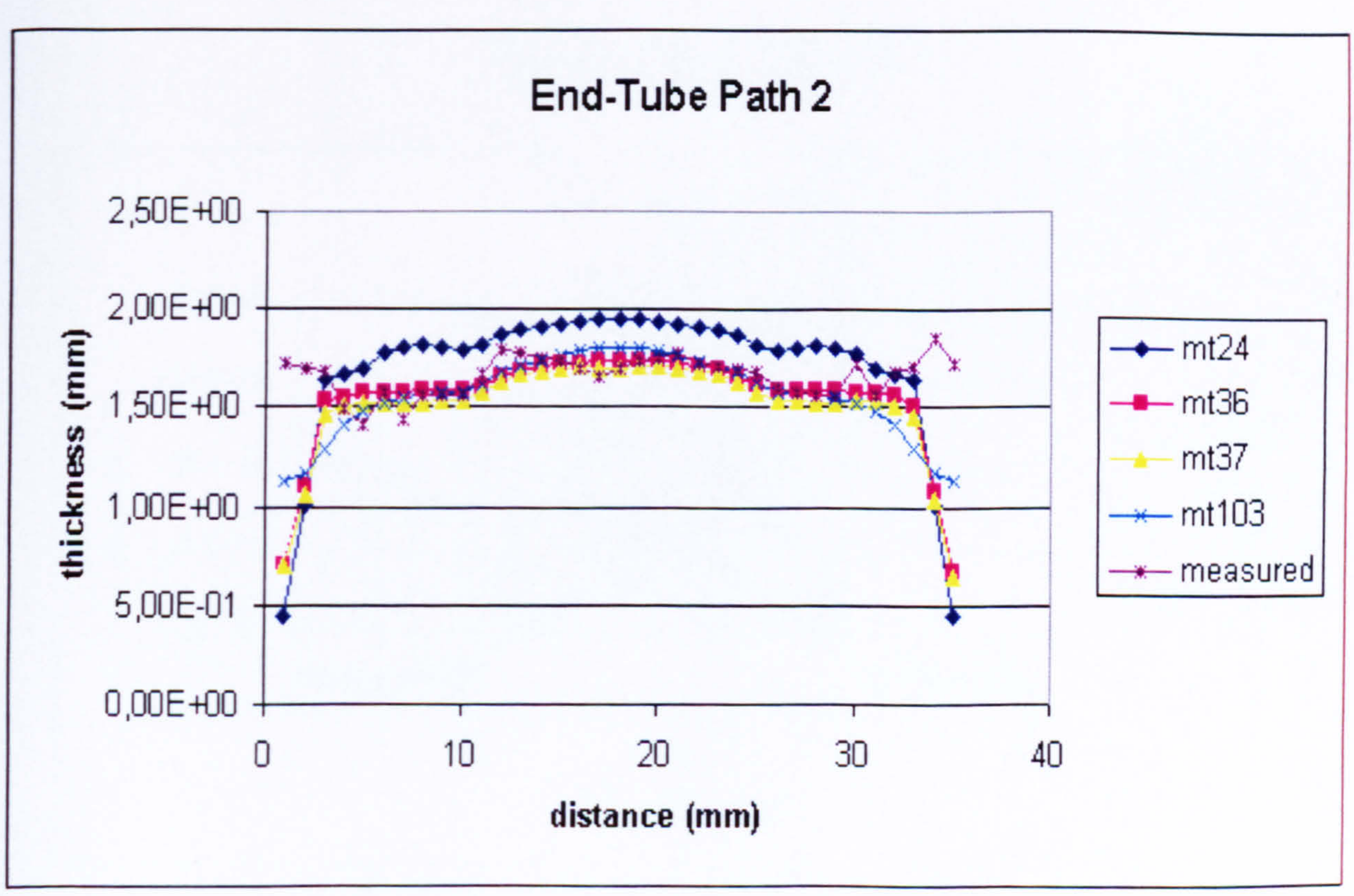

Figure 8-41 Wall-thickness Distribution Path 2

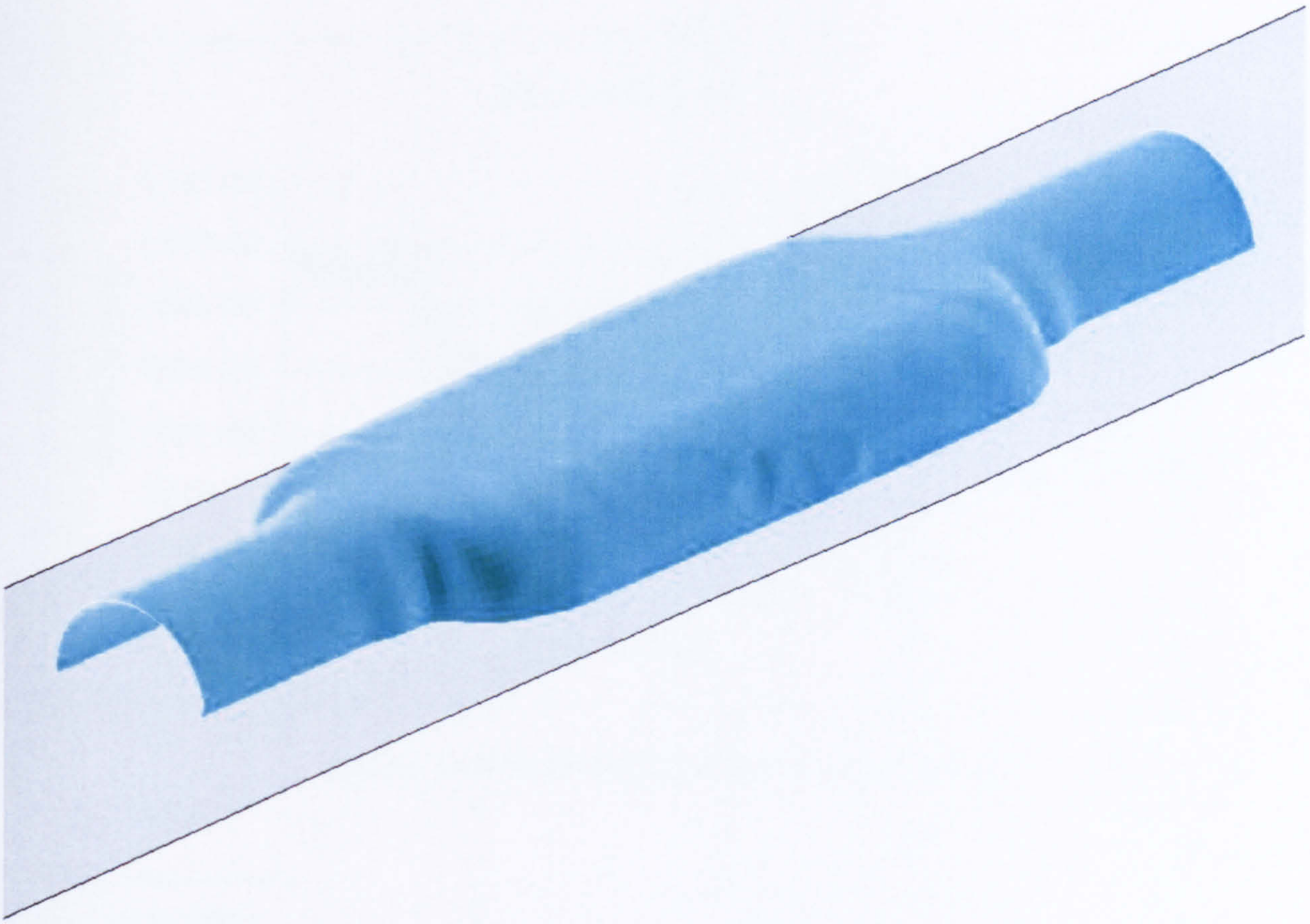

Figure 8-42 End-Tube Path 3

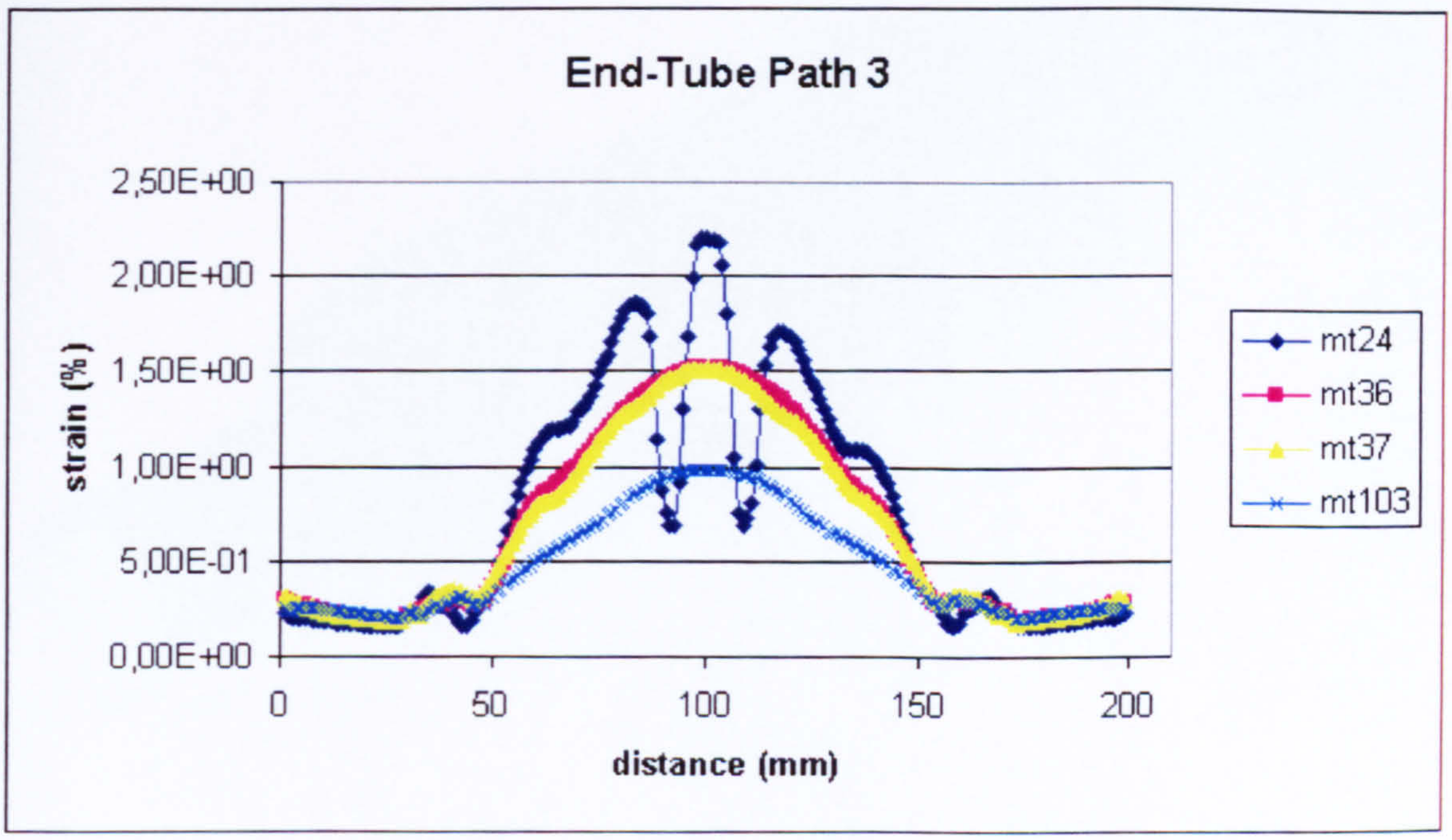

Figure 8-43 Plastic Strain Path 3

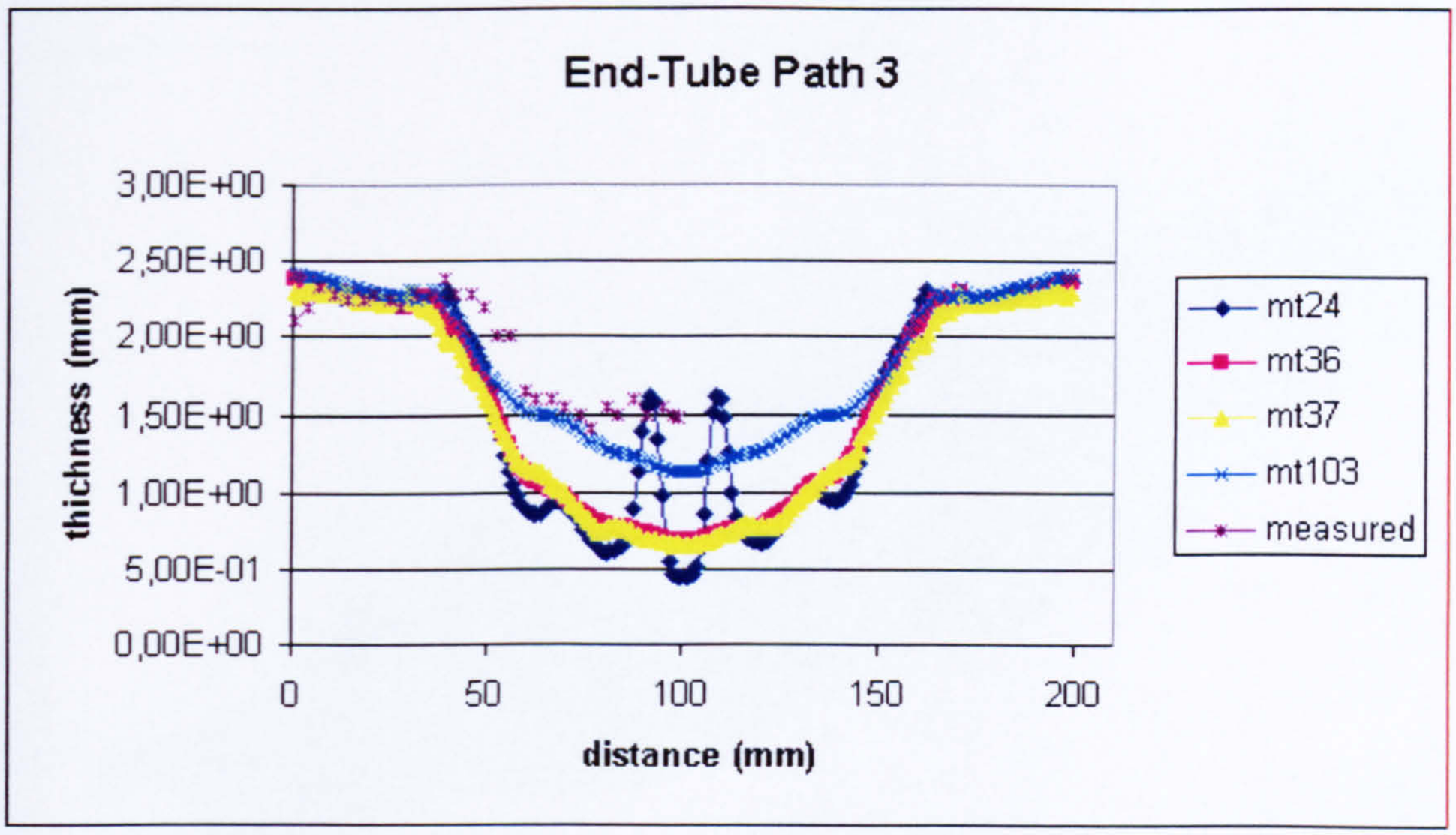

Figure 8-44 Wall-thickness Distribution Path 3

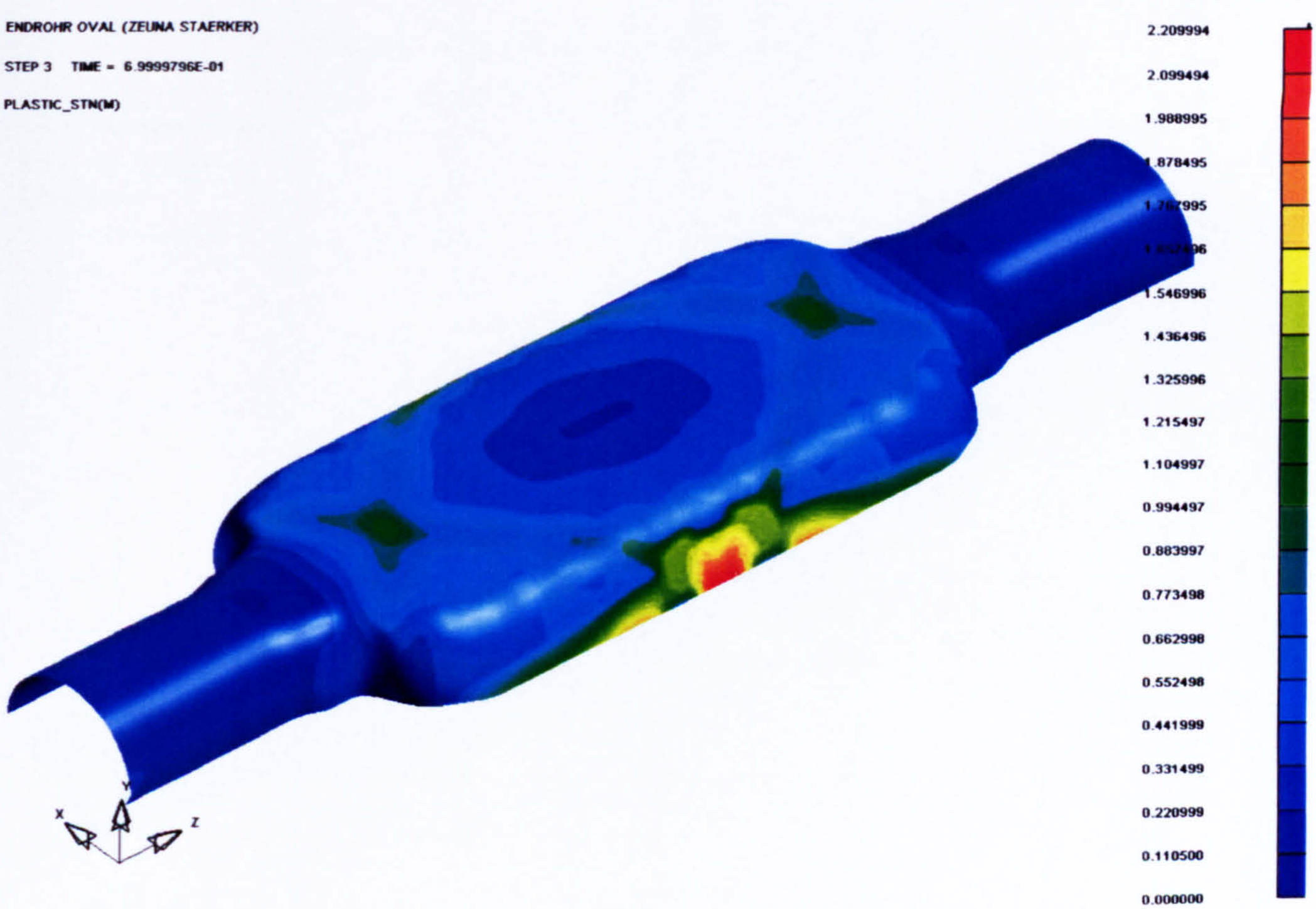

Figure 8-45 Plastic strain distribution (MT24)

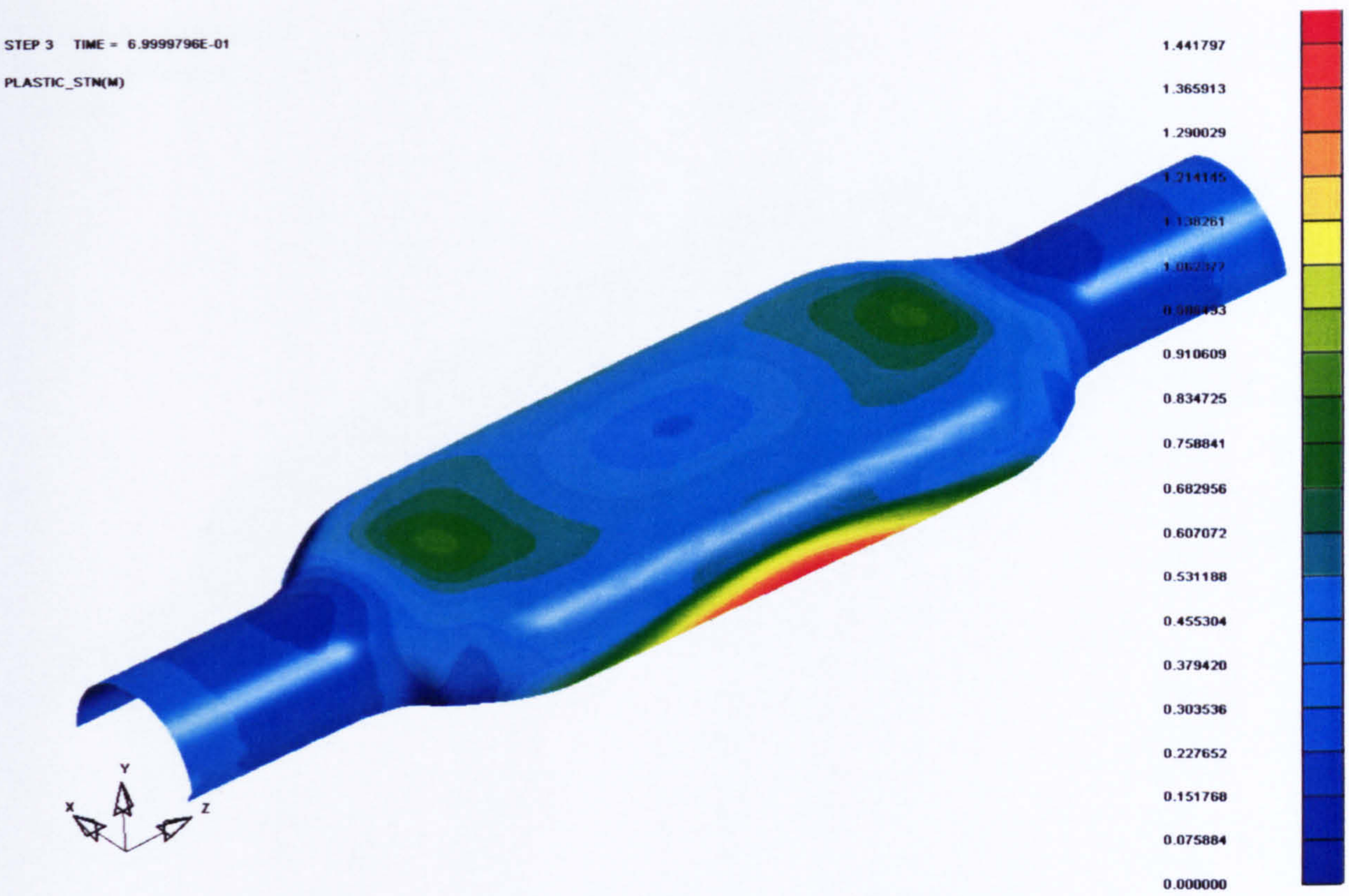

Figure 8-46 Plastic strain distribution (MT36)

Figure 8-47 Plastic strain distribution (MT37)

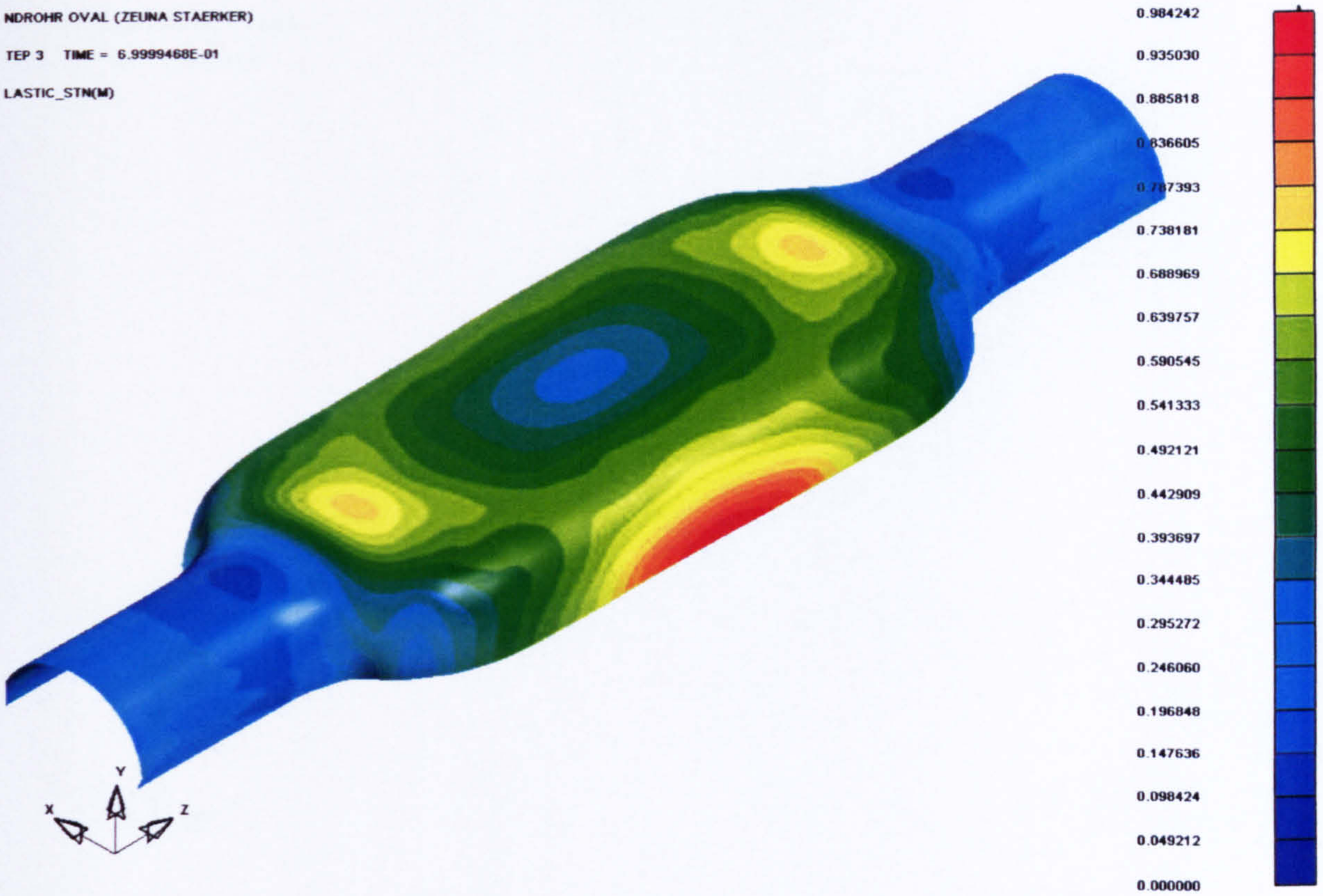

Figure 8-48 Plastic strain distribution (MT103)

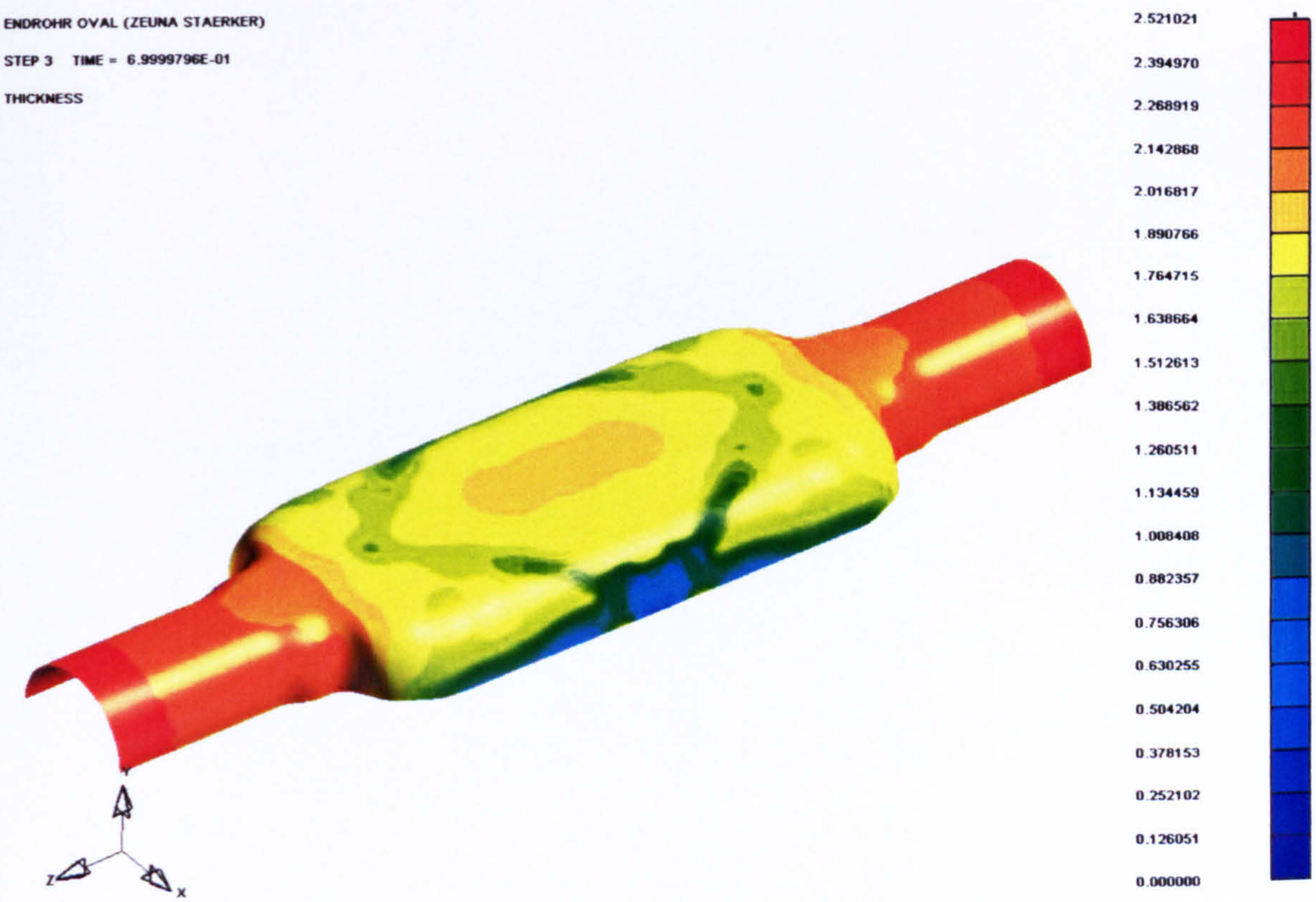

Figure 8-49 Thickness distribution (MT24)

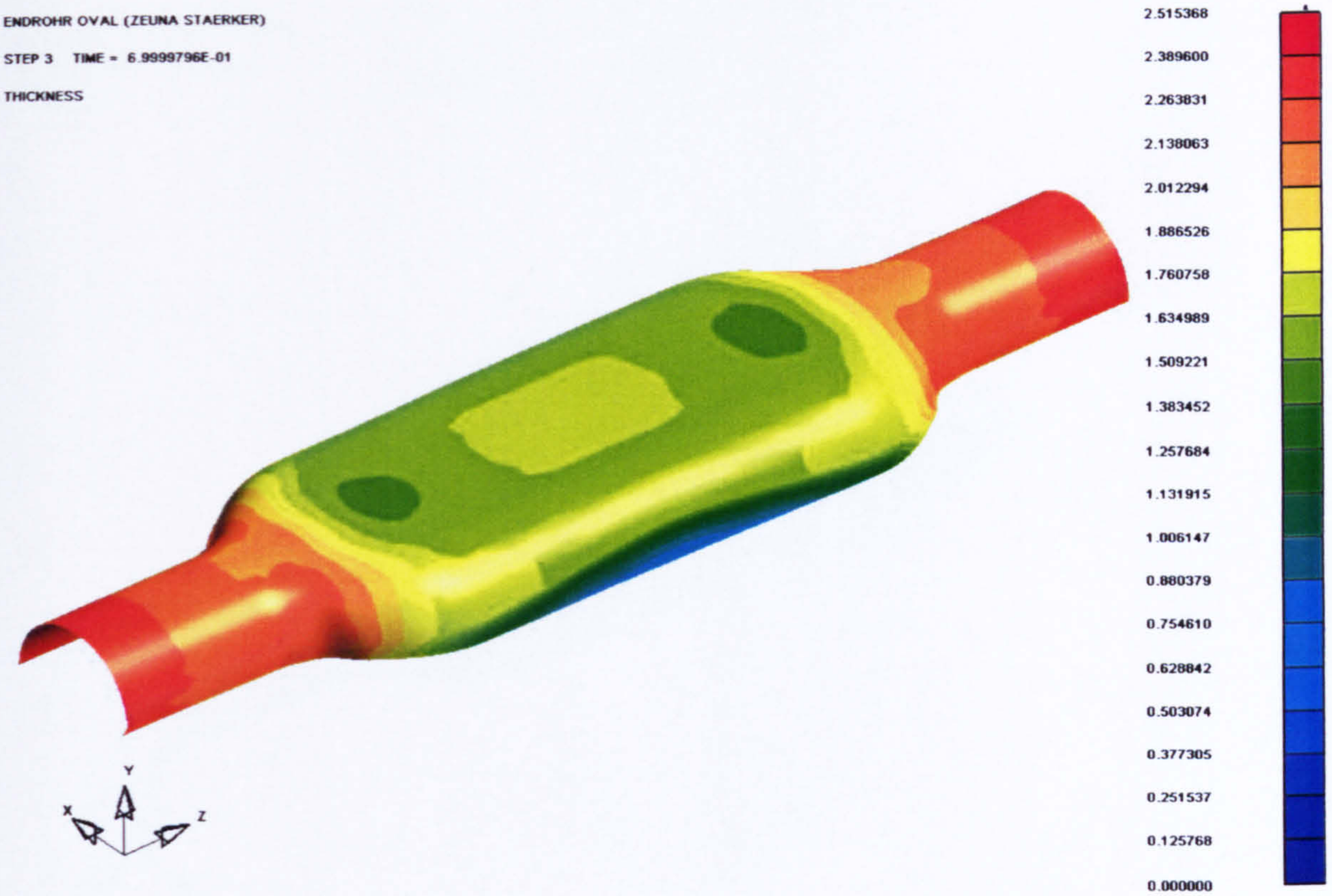

Figure 8-50 Thickness distribution (MT36)

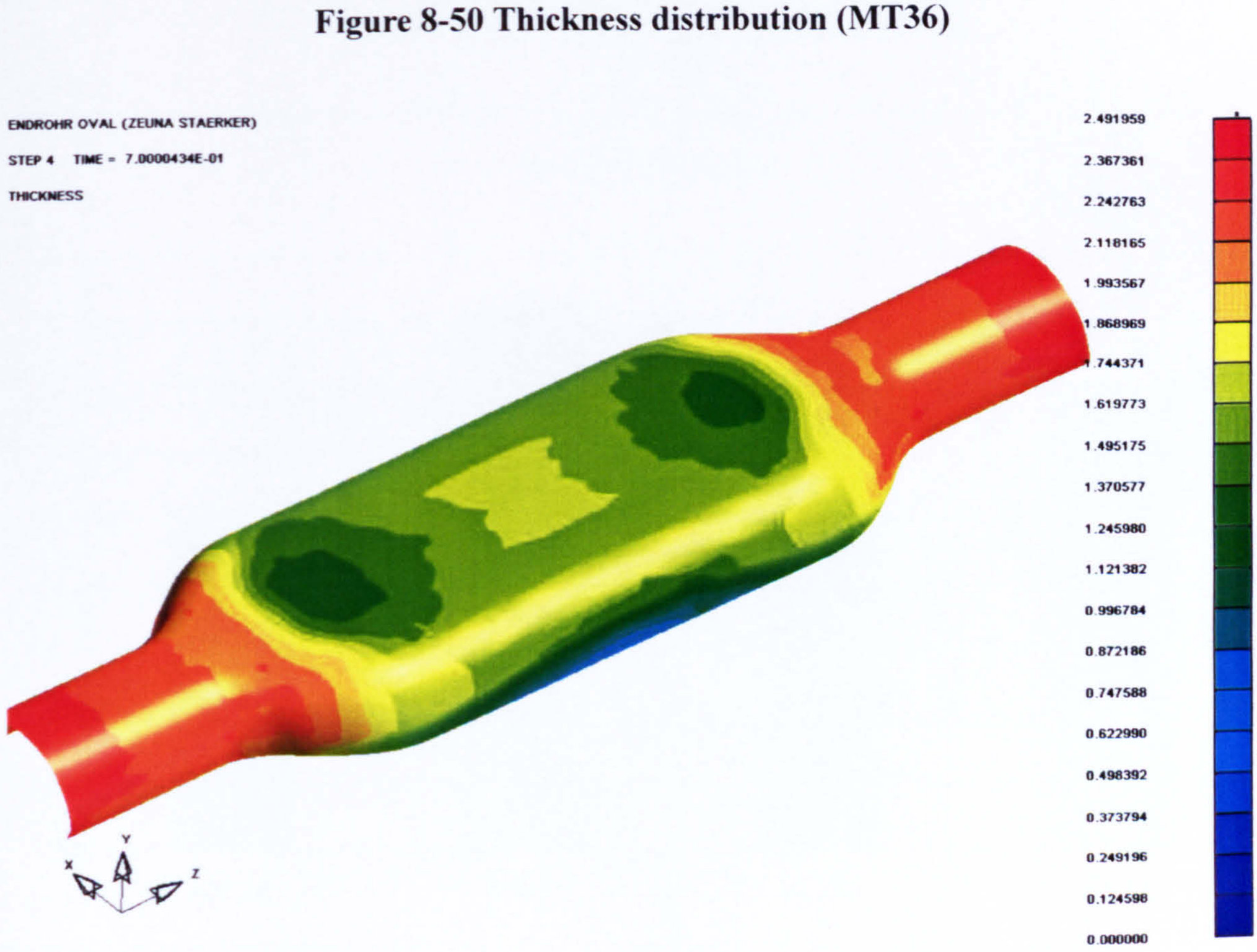

Figure 8-51 Thickness distribution (MT37)

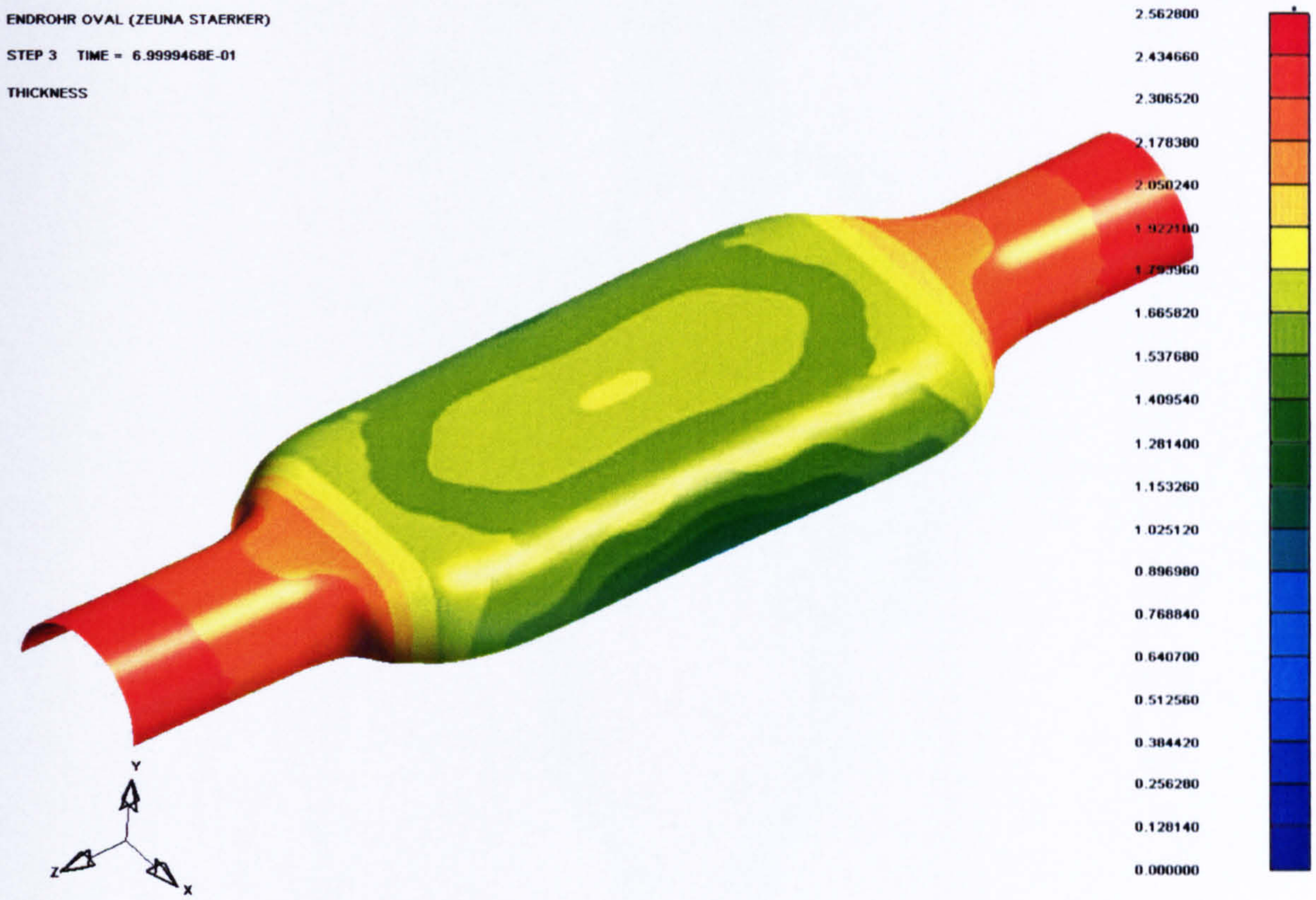

Figure 8-52 Thickness distribution (MT103)

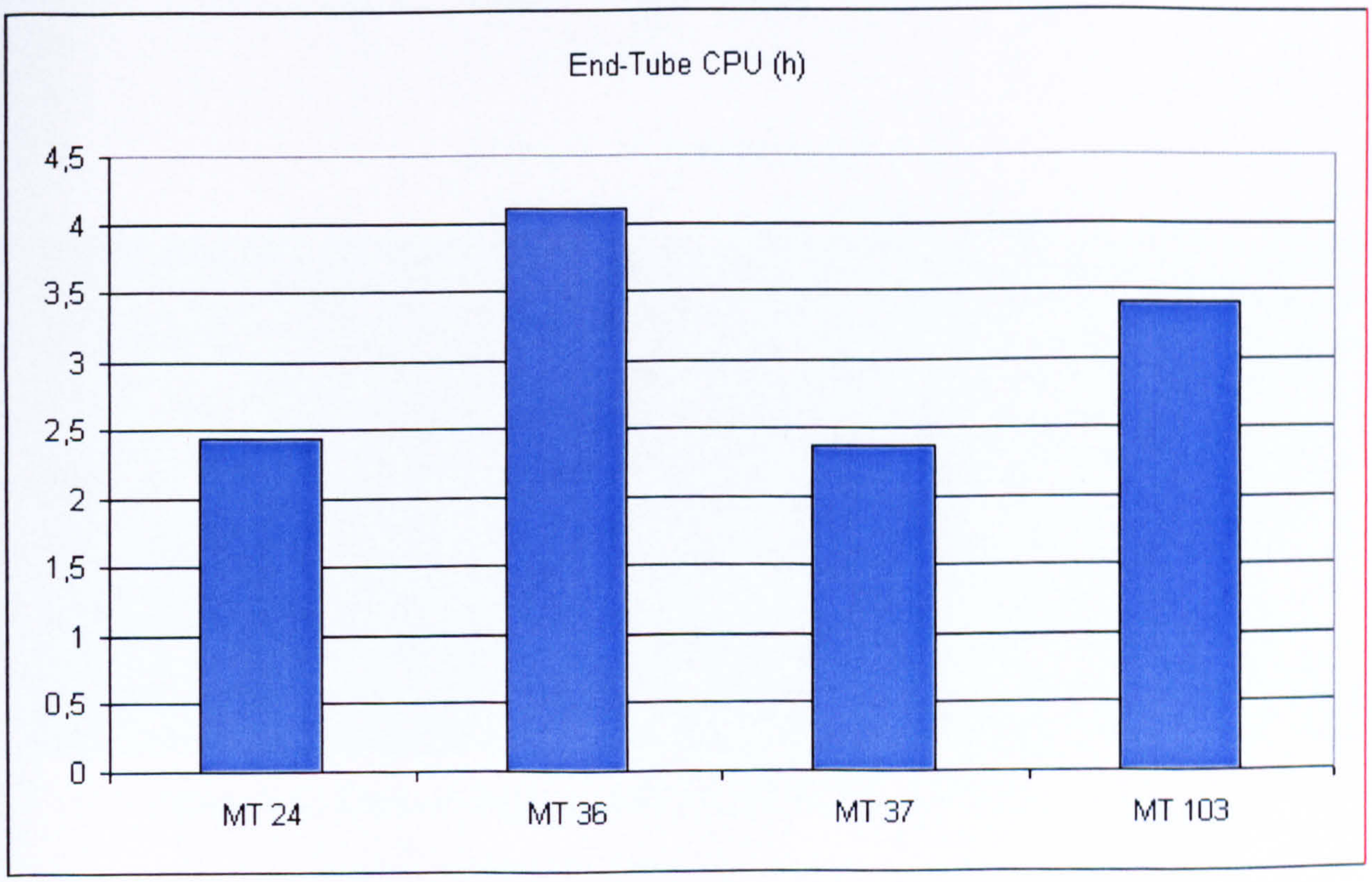

Figure 8-53 CPU Time needed for the different material types (End-Tube)

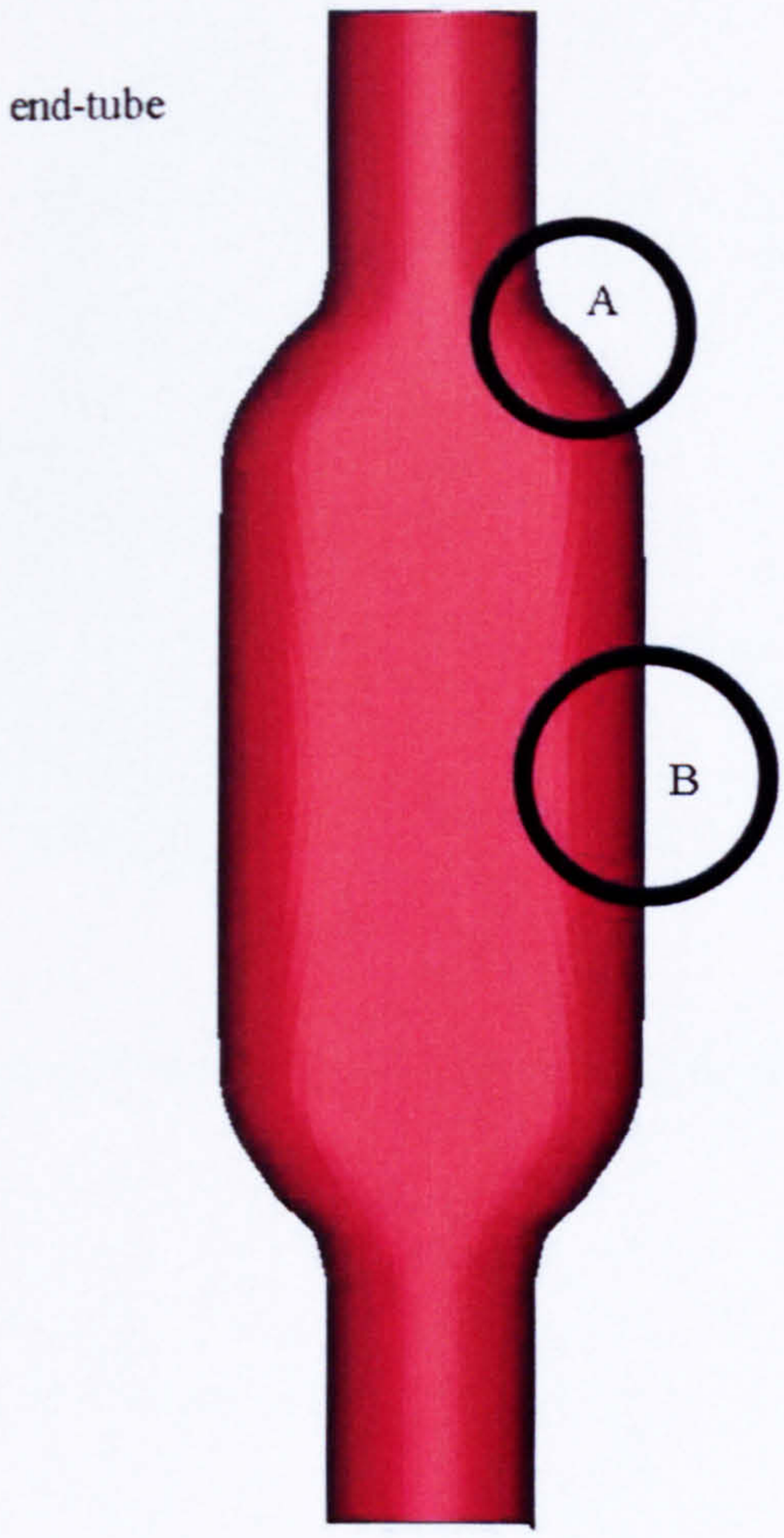

Figure 8-54 Problematic Areas

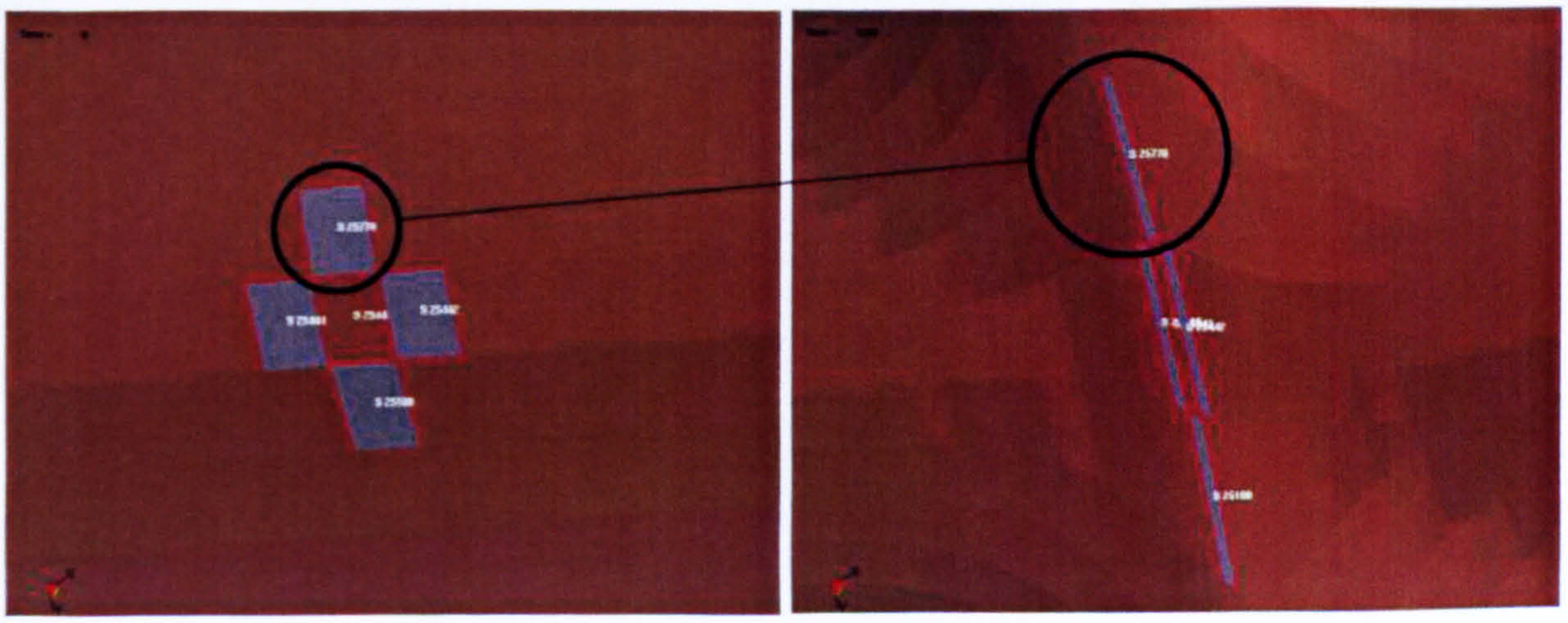

Figure 8-55 Element Deformations (starting shape, shape after forming)

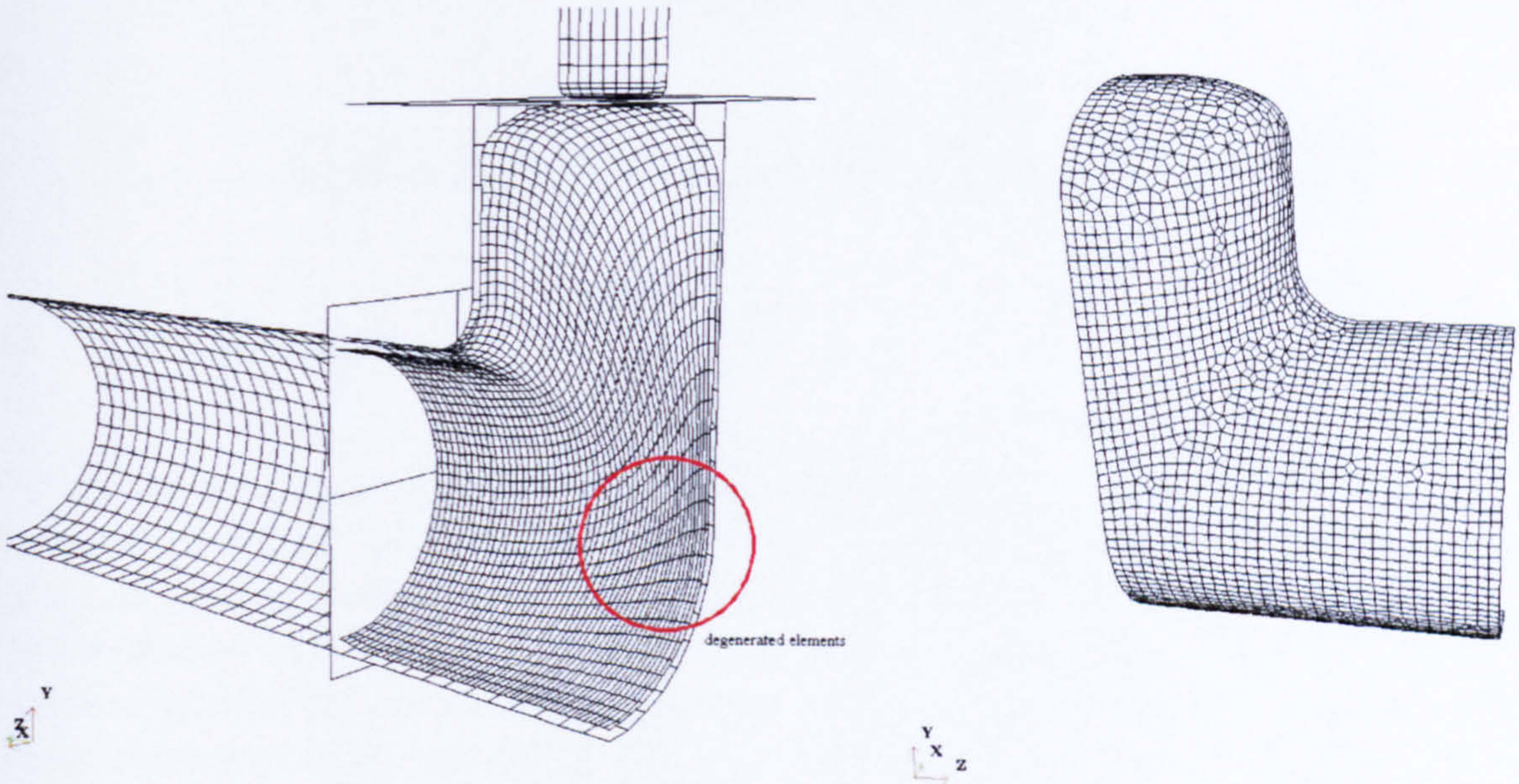

Figure 8-56 Remesh of degenerated Elements

CHAPTER 9

Conclusion and Future Work

9 Conclusion

One of the main aims of the sheet-metal processing industry is the optimization of its products in terms of weight, strength and rigidity characteristics, and naturally the minimization of costs. In the search for alternative production processes, IHP forming – the manufacture of hollow bodies with complex geometry by means of fluid pressure – has been shown to offer an interesting technical and economic potential to sheet metal manufacturers. The achievement of beneficial component characteristics using this process is only possible where component and process configuration are selected by considering the overall system design.

There has been a rapid growth in the interest shown in IHP technique during the last ten years. A fact which was underlined during 1999 when international conferences attracted up to 500 participants mainly from the automotive industry. Above all industry in the United States has started to use the technology very intensively, they are well on the way to making progress and even exceeding the expectations in this field of work in comparison to Europe.

There is undeniable euphoria about the broad spectrum of applications which can be expected in the future. Particularly within the automotive industry which looks forward to producing many car parts, for example chassis, exhaust and intake systems, add-on parts, drive system, seats, frames/bodywork and steering components, cross members, side members, manifolds, roof rails, spoilers, gear shafts, seat frame components, A/B/C pillars, roof frame profiles, steering column with compensation. In spite of this the economical aspect of the IHP technique should not be forgotten, as not all components can be produced with an acceptable price/ performance relationship.

Computer aided design (CAD) and computer aided manufacturing (CAM) are used today by large business and also by medium sized companies. The use of computer applications within the forming techniques has received new impetus with the appearance of fast workstation techniques since the start of the 90's. Due to this fact and with the growth of the IHP technique the FE simulations of such processes have more and more importance for a fast, accurate and economic development of new products. The merger of companies leads to developments in a more and more distributed environment. Today it is more important than ever to integrate the simulation process into the Digital Mock-up (DMU) and Product Data Management (PDM) chain. The objective of FE is to replace costly and elaborate experimental testing by fast, low-cost computer simulation.

The simulation technique is an advantageous tool to study the feasibility of new products. When developing hydroformed components, the precise analysis of all boundary conditions is

essential. Optimum design of components, taking into consideration special process-specific factors enhances safety and also the cost-effectiveness of series production. The feasibility study, the component configuration and definition of a production sequence are closely interlinked. Once these processes have produced a positive result, it is possible to start with prototype development of the components.

The following information can be predicted using a suitable simulation program:

- equivalent plastic strain
- effective stress
- thickness distribution
- distribution of plastic strain rate
- principal strains
- distance between outer wall of workpiece and the die wall

The aim of this research project was to investigate the existing methodologies and procedures for the simulation of IHP hydroforming processes, development of new methodologies which would improve the existing mode of operation in terms of ease of use, robustness and practicality, and to verify the evaluation of the simulation results by the comparison with real components. The main objectives of this research were to:

- investigate the existing tools and identify the limitations of these procedures
- improve the integration of the hydroforming simulation into the simultaneous engineering process chain.

A comprehensive and critical literature review of the previous work done was carried out in the field of sheet metal process simulation, especially the interior high pressure forming process. The literature review has shown that there is no work, which considers the entire process chain of modeling with a CAD system, preparing the FE model, simulation, analysis of the results and the transfer back into the CAD system. Furthermore no systematic basic work about the design of load-curves exists.

For a quick assessment of the possibilities of the IHP technology for new products or the replacement of products manufactured with standard technology it is necessary to investigate the following areas :

- estimating the feasibility, design and realisation of the interior high pressure forming with a basic scientific knowledge
- development of rules for the design of IHP products
- investigating the influence of friction on the IHP process

The presented work shows how the simulation technique can be used efficiently, provide detailed advice for doing an accurate and fast simulation. Diagramms and formulas for the calculation and estimation of the load-curve paramaters (interior pressure and axial forging) needed were developed. These diagramms and formulas make it possible to determine the necessary load-curves very fast.

A graphical user interface for the definition and processing of the IHP simulation data was developed to facilitate a simultaneous engineering (SE) process within a closed process chain. The choice of this interface ensures that all cogent inputs, for instance the contact definition, are done automatically and hence adjusting all other parameters default values. The necessary steps (work-piece, tool and stamp(s) definition) are worked out step-by-step gradually. This tool makes the definition of the geometry and the parameters for the IHP simulation very easy and enables the tool designer to use the simulation techniques for the layout and optimization of the process.

This work has shown that the simulation of IHP forming processes can be successfully done with the help of the FE method. The critical areas can be discovered, failure can be predicted and the properties of the final product can be determined. This fact is impressively shown by the comparison of the simulation results with real components out of the automotive industries done as a part of this work.

Furthermore a utility for the reconstruction of the simulation results was created. This utility for the reconstruction allows the creation of a 3D solid geometry out of the results of the simulation program, in this case LS-DYNA. An example of a possible application for the reconstructed component would be the comparison of the part produced using the IHP technique with the expected part or the construction of the shape of punches for further processing of pre-formed parts. Without this tool a time consuming trial and error method is necessary to create the tools for pre-formed parts with a complex geometrical shape. A further advantage is the simulation of the component behaviour under load, with a true wall-thickness distribution, assembled into the whole construction e.g. a car.

With the tools developed as a part of this thesis the process chains from the preparation of the simulation model with the IHP interface, the actual simulation of the IHP process using FE techniques and finally the reconstruction of the part carried out from the simulation results are closed. Presented work point out the needs for a simultaneous engineering process chain and developes tools to close the existing gaps in this chain.

9.1 Outlook & Future Work

The developed tools and the investigated knowledge about the simulation technique presented in this work satisfies the current requirements in this area, and provides a methodology for the simulation and optimization of IHP manufacturing processes.

However there is some room for further development of the graphical user interface, i.e. a better, graphically oriented definition of the load-curves and then implementation of the knowledge about load-curves to create them automatically.

Within the simulation tool, LS-DYNA, the options for the optimization of load-curves should be tested. Since the latest version there is an option to influence the loads depending on measured values during the simulation process. A trail of this option must be done and an extension should be requested if necessary by or in co-operation with the developers of the software code.

Within the field of results utilization (the post-processing), new packages *like LS-POST or eta/* PostGL come into use. These software tools fulfil some important user requirements, but the possibilities to judge failure must be further developed.

The virtual reality (VR) technique develops from a presentation-tool to an addition to classical CAD and FE tools. Through the process of a rapid product development (RPD) the fast evaluation of complex data e.g. complex simulation results by specialists within a suitable virtual environment has a main role to play today and above all in the future. Crash simulation with cars built out of components which are afflicted with their real properties – wall-thickness distribution, residual strains and cold hardening – or just the simulation of the behaviour of the car under everyday use, is also an important task of the future. There are already first attempts in existence (**Remensperger et al., 1997; Dutton et al., 1999**), where **Dutton et al., 1999** show that the real component properties have a significant influence on the crash behaviour of a side-rail. For virtual product development and the virtual prototyping (VP) within a VR environment it is of course necessary to build the specific components as realistically as possible. Therefore the approach shown in chapter 7 (IHP Optimization using Surface Reconstruction) is of enormous importance. The reconstruction of simulation results must also be further improved to create components with all properties which are important in real life. VR application for computer supported co-operative work (CSCW) will be available in the future to lead this vision to reality. On the basis of the high speed network technology and the new high-end graphic workstation, collaborative virtual prototyping (CVP) can be used for the next generation of product development.

The properties induced in the component after forming are of importance, not only for the springback of the part through the releasing of the loads, pressure and force, but also for additional operations like pulling out of the tool cavity and additional working steps like cutting and punching. There has been up to now very little investigation into this field of springback calculation, although for parts manufactured today in the automotive industry - i.e. large carrier structures with multiple bendings – this is of great necessity. Up to now investigations in

this field are mainly done as a minor matter of forming simulations.

Today and in the near future the way to do a feasibility study for an IHP product is to determine the expected circumferential expansions, set up the bending line and decide if pre-form operations are necessary. The shape of the planed product must also be checked as to its suitability for an IHP process and if necessary modified, where possible without modifying its functional characteristics. For all these operations a planing or design tool like the IHP-Plan developed from **Longchang et al., 1999** should be used (**Figure 9-1**). The first simulation will then be done with a single step solver to study the fundamental feasibility of the planed product and to find out problematic areas. Because of the small computing time for a single step analysis, a number of simulations can be done to study the effect of the modification of the geometry or process parameters. With this first improved process layout an explicit/implicit simulation can be done to create the final process design for the prototyping.

The IHP process often works correctly on only a very small path, this means the course of the load-curves and combination of the different load-curves only leads to a successful result after a time consuming optimization process. A further main task of new developments is therefore to use computer techniques for automatic optimization or improvement of the IHP process layout. From today's point of view there are three approaches for this optimization :

- **Fuzzy Logic**
- **Stochastic Procedures**
- **Use of a Expert System**
- **Parameter Optimization**

The use of the fuzzy logic is based on an investigation by **Schmoeckel** and **Engel, 1996.** The characteristic of the fuzzy logic is that it avoids the problems of a mathematical model representation. The fuzzy logic observes and describes the course of the process parameter variation linguistic. This means that this regulation works similar to a machine worker, the parameters would not be described as absolute, but in quantity. The fuzzy regulation works based on production rules. **Schmoeckel et al., 1996** report the successful experimental use of the fuzzy logic. An industrial use of the fuzzy logic for the simulation of IHP processes is not known until today.

Recent simulations, based on stochastic methods, have been used successfully for the improvement of processes, mainly in the area of crash simulation (**Reuter** and **Watermann, 1999**). At this time, at the Aalen University, a project is investigating the use of these methods for the IHP simulation. It will be checked if it is possible to verify the sensitivity of the FE model and furthermore if an optimization or improvement of the IHP process simulation is possible. Simulation with stochastic methods requires high CPU power, i.e. supercomputers from SGI (Cray) or HP (Convex). First results have shown that the verification of the model sensitivity is possible and this gives hope that the improvement of the IHP process is also possible.

Work to investigate an expert system for the layout and optimization of an IHP process is presently unavailable, but initial ideas are in existence to develop an expert system for sheet metal forming based on the software STONErule and CATIA from **Müller, 1999**. An additional

advantage of an expert system is the preservation of expert knowledge and the possibility of reproducing and reusing development steps and results.

A further possibility is the use of the standard parameter design optimization. **Stander** and **Münz, 1999** described the use of LS-OPT, a parameter optimization tool for the improvement of a sheet metal forming process. **Stander et al., 1999** optimize the thinning of the sheet based on an FLD constraint governing a maximum thickness reduction. An accurate optimal design was found by **Stander et al., 1999** using the LS-OPT design tool, but the parameter optimization had some restrictions, i.e. the problem of how to find the correct boundaries for the parameters.

It is possible that a combination of the different methods can also lead to a meaningful solution.

Nowadays one of the main problems in applying simulation is the time needed. For complex structures it is often necessary to start with the tool manufacturing before the simulations are complete. This means that the problems determined in the simulation can be established by the prototyping at the same time. This is desirable, but not satisfactory. A task for the future would also be to speed up simulation, possibly up to the real process times. The development of the computer technology during the last 10 years shows that this aim can be reached in the near future. An improvement of the simulation codes, the use of the best method for the respective case of simulation – single step, implicit, explicit – and the ability to switch between the methods, the speeding up of the processors and the massive use of the multi-processor technology – local and in a local or global network – can also help to achieve this goal.

The vision for the next decade is to develop and optimize IHP products with a virtual press. The Institute of Forming Techniques at the University of Stuttgart plans to initiate a project on this area, together with industrial partners and educational institutions, in the year 2000.

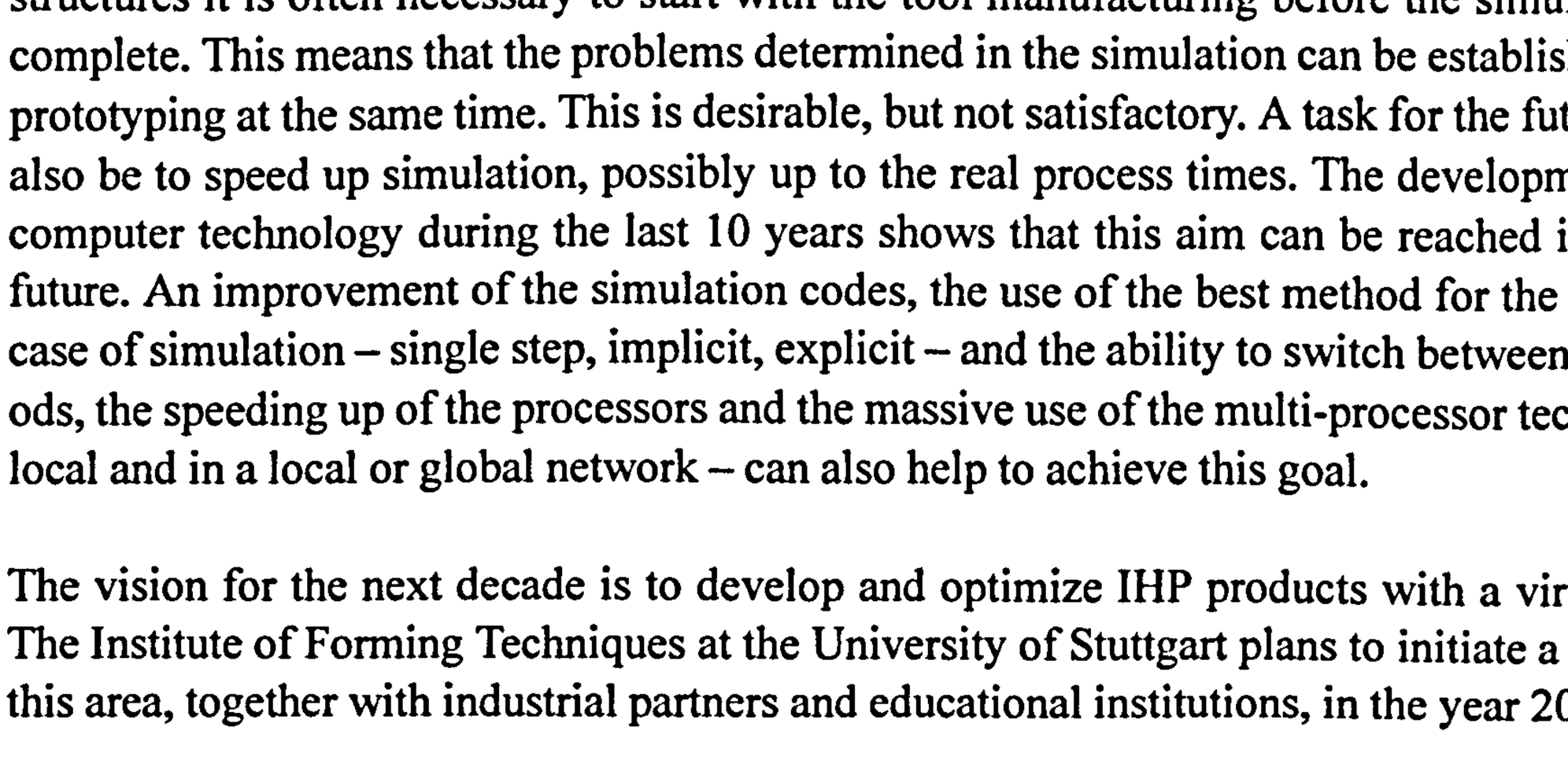

Figure 9-1 Process Chain - Use of the Design Tool

References

Argyris, J.; Elasto-plastic matrix displacement analysis of three-dimensional media, *Journal of Royal Aeronautic Society, 69, 1965, 633-635*

Argyris, J.; Die Methode der finiten Elemente in der Strukturmechanik, *Bd 3, Einführung in die Dynamik, Vieweg Verlag, 1988*

Ahmed, M. & Hashmi, M.S.J.; Estimation of mechine parameters for hydraulic bulge forming of tubular components, *Journal of Materials Processing Technology, 64, 1997, 9-23*

Ahmed, M. & Hashmi, M.S.J.; Three dimensional finite element simulation of bulge forming, *Proc. Intl. Conf. On Advances in Materials and Processing Technologies, AMPT '99 & 16th Ann. Conf. Of the Irish Manufacturing Committee, IMC 16, Dublin, Vol. 1, August 1999, 153-161*

Ahmed, M. & Hashmi, M.S.J.; Finite element simulation of manufacturing metal bellows from tubes, *Proc. Advances in Materials & Processing Technologies '98, Kuala Lumpur, Vol. II, August 1999, 982-989*

Ahmed, M. & Hashmi, M.S.J.; Finite-element analysis of bulge forming applying pressure and in-plane compressive load, *Journal of Materials Processing Technology, Vol. 77/1-3, May 1998, 95-102*

Bathe, J.; Finite Elemente Methoden, *Springer Verlag, 1990*

Bathe, J.; Crash simulation of cars with FEA, *Mechanical Engineering, 1998, 82-83*

Bauer, H.; H., Sicherheit durch Simulation, *Blech, Heft 3,1995, 46-50*

Bauer, H. & Rimkus, W.; Fast and Efficient FE Simulation of Hydroforming Problems, *Proceedings First European LS-DYNA User's Conference, Stratford, 1997*

Berg, H. & Hora, J.; Numerical Simulation of 3-D Sheet Metal Forming Process, *Proceedings 3rd int. Conference Numisheet, 1996*

Bieling; Untersuchung zum Aufweitstauchen von Rohren zu Hohlwellen, *Dissertation, TH Darmstadt, 1992*

Bogojavlenskij, K.N.; Hydraulisches Formen von T- und Kreuzstücken, *Kunz-stamp. Proizvodstvo 4, 1972, 22-24*

Bogojavlenskij, K.N.; Ausbauchen von Teilen für Fahrradrahmen, *Kunz-stamp. Proizvodstvo 21, 1979, 21-24*

Bogojavlenskij, K.N.; Entwicklung und Gestaltung des Hydromechanischen Ausbauchens für die industrielle Anwendung, *Fertigung und Betrieb 28, 1978, 563-565*

Bogojavlenskij, K.N.; Umformen von Hohlkörpern mit elastischen Medien und Flüssigkeiten, *Metallverarbeitung 28, 1974, 78-79*

Bögel, H.; Private communication, 1997

Böhm, A.; Numerische Simulation von Verfahren der Innenhochdruckumformung unter besonderer Berücksichtigung des Aufweitens im geschlossenen Werkzeug Dissertation, *Uni. Paderborn, 1994*

Böhm, A.; Part cost reduction in the hydroforming process, *Technical paper of: The 2nd International Conference on Innovations in Hydroforming, Columbus/Ohio, September 15-17, 1997*

Böhm, A.; Private communication, 1998

Brännberg, N.; Computational Aspects on Simulation of Sheet Metal Forming, *Dissertation, Institute of Technology, Dept of Mech Eng, S-581 83 Linköping, Sweden, 1994*

Breuer, J. & Maus, W. & u.a.; Verfahren zur Herstellung einer gebauten Nockenwelle sowie gebauten Nockenwellen aus einem Wellrohr und aufgeschobenen Elementen, *Patent DE 3633435A1, 1988*

Buerk, E.; Hydromechanical Drawing, *Sheet Metal Industries March, 1967*

Burkhardt, B; Communication Platform at Hydroforming, *http://www.hydroforming.net/, web resource, 1999-2000*

Chalupczak, J. & Sadok, L.; The Problem of Forces and Stresses in the Hydromechanical Process of the Bulge Forming of Tubes, *Metalurgia I Odlewnictwo Tom 9 Zeszyt 1, 1983, 59-66*

Cheng, J.-L.; Automatic Adaptive Remeshing for Finite Element Simulation of Forming Processes, *International Journal for numerical Methods in Engineering, Vol. 26, 1988, 1-18*

Chenot, J.-L.; Recent contributions to the finite element modelling of metal forming processes, *Journal of Materials Processing Technology 34,1992, 9-18*

Danzberg-J & Hora-P & Reissner-J.; Effizienzsteigerung bei der rechnergestuetzten Methodenplanung. Numerisch gestuetzte Prozesse, *Baender Bleche Rohre, Band 38 (1997) Heft 10, Seite 22-25*

Doege, E. & Nolkemper, H. & Saeed, I.; Fließkurvenatlas metallischer Werkstoffe, *Hanser Verlag München, 1986*

Dohmann, F. & Böhm, A. & Dudziak, K.-U.; The Shaping of Hollow Shaft-Shaped Work-pieces by Liquid Bulge Forming, *Advanced Technology of Plasticity, 1993*

Dohmann, F. & Hartl, Ch.; Liquid-Bulge-Forming as a Flexible Production Method, *Journal of Material Processing Technology 45, 1947, 377-382*

Dohmann, F. & Hartl, Ch.; Prozeßführung von Innenhochdruckumformverfahren, *Tagungs-band EFB Kolloquium "Innenhochdruck - eine Alternative in der Fertigungstechnik, Stuttgart, 5.-6. März, 1996*

Dohmann, F. & Hartl, Ch.; Tube hydroforming - research and practical application, *Journal of Material Processing Technology 71, 1997, 174-186*

Dohmann, F. & Hartl, Ch.; Hydroforming - a method to manufacture light-weight parts, *Jour-nal of Material Processing Technology 60, 1996, 669-676*

Dohmann, F. & Hartl,Ch.; Finite element analysis of forming hollow camshafts using internal high pressure, *Int. Conf. Modelling and Simulation in Metal Engineering and Material Sci-ence, June 11-13, 1996, 640-645*

Dohmann, F. & Klaas, F.; Verfahren zum Umformen von Rohren, *Bänder Bleche Rohre 4, 1986*

Dohmann, F. & Klaas, F.; Innenhochdruckumformen rohrförmiger Werkstücke, *Bänder Bleche Rohre 6, 1986*

Drapela & Pechacek & Tomas; Anforderungen an die Entwicklung einer IHU-Anlage - Tech-nologische und ökonomische Aspekte, *EFB-Kolloquium, 1996*

Dudziak, K.-U.; Mit Hilfe der FEM-Simulation zum prozeßsicheren IHU-Produkt, *Tagungs-band EFB Kolloquium "Innenhochdruck - eine alternative in der Fertigungstechnik, Stuttgart, 5.-6. März 1996*

Dudziak, K.-U.; Prozeßmodell zum Innenhochdruckumformen von hohlwellenförmigen Werkstücken, *Dissertation, Uni. Paderborn, 1995*

Ebbinghaus, A.; Hohlteile materialsparend hergestellt, *Industrie-Anzeiger Nr. 20, 1984*

Ebbinghaus, A.; Wirtschaftliches Konstruieren mit innenhochdruck-umgeformten Präzisions-Werkstücken, *Werkstatt und Betrieb 123, 1990*

Eberlein, L., Zscheckel, R.; Das Hydromechanische Ausbauchen von Rohrstücken - ein neues Verfahren zur Herstellung von Rohrverbindungselementen, *Wissenschaftliche Zeitschrift der Universität Dresden, Heft 3/4, 1978*

Ekholm; Method of producing fittings, *US-Patent 2 837 810, 1958*

Fuchs, H.-J.; Hydrostatic pressure, its role in metal forming, *Mechanical Engineering, April 1966, 34-40*

Geckeler, J.W.; Abhänigkeit des Formänderungsvermögens metallischer Werkstoffe vom Spannungszustand bei unterschiedlich hoher Temperatur und Formänderungsgeschwindigkeit, *Bänder Bleche Rohre, Nr. 8,1972, 387-395*

Geiger, M & Vollertsen, F. & Hein, P.; Neue Wege der Innenhochdruckumformung *Tagungsband EFB Kolloquium "Innenhochdruck - eine alternative in der Fertigungstechnik, Stuttgart, 5.-6. März, 1996*

Greve, A. & Haase, F. & Keßler, L. & Schilling, R.; Calculation of metal forming processes by means of FEM, *Steel Research 65 No.7, 1994, 284-290*

Gruszka, T. & Lenze, F.-J. & Rösen, H.; Werkstoffgerechte Simulation des Vorformens für hydromechanisches Umformen, *EFB09/23-24/99 Technical Paper, 1999, 188 ff.*

Haas, A. & Rimkus, W. & Bauer, H.; Höhere Prozeßsicherheit beim IHU, *17. CADFEM Users Meeting, Sonthofen, Germany, 1999*

Handbuch der Umformtechnik, *ISBN 354061099-5, Springer Verlag Berlin, 1996*

Hallquist, J.; LS-DYNA Keyword User's Manual, Version 950, *Livermore, 1999*

Hallquist, J.; LS-DYNA Theoretical Manual, *Livermore, 1998*

Hasek, V.; Über den Formänderungs- und Spannungszustand beim Ziehen von grossen unregelmässigen Blechteilen, *Dissertation, Uni. Stuttgart, 1973*

Heath, A.N. & Pasquale, E.; Case Studies in FEM-Simulation of Industrial Sheet Metal Forming, *XXII. International FEM-Congress, Baden-Baden, 15.-16. November, 1993*

Hein, P. & Vollertsen, F.; Hydroforming of sheet metal pairs, *Journal of Material Processing Technology 87, 1999, 154-164*

Heßler; Beitrag zur Entwicklung des hydraulischen Rohr-Innendruck Umformens, *Dissertation, TH Darmstadt, 1991*

Hielschler, C. & Sitzmann, B.; Erfahrungen mit dem Innenhochdruckumformen, *Werkstatt und Betrieb 129, 1996, 840-850*

Hill, R.; The Mathematical Theory of Plasticity, London Oxford University Press, 1971

Hora-P & Kubli-W.; Prozessbegleitende Umformoptimierung in der Fahrzeugentwicklung. Numerisch gestuetzte Prozesse, *Baender Bleche Rohre, Band 39 (1998) Heft 1/2, Seite* 32-36

Klaas, F.; Aufweitstauchen von Rohren durch Innenhochdruckumformung, *Blech Rohre Profile 35, 1988, 175-180*

Klaas, F.; Weniger Werkstoff - Spanloses Fertigen innovativer Hohlteile mit den Innenhochdruck-Umformverfahren, *Maschinenmarkt 3, 1994*

Klaas, F.; Aufweitstauchen von Rohren durch Innenhochdruckumformung, Dissertation, *GHS Uni Paderborn, 1987*

Klaas, F.; Formenvielfalt - Innenhochdruck-Umformen von Hohlteilen: Anwendungsmöglichkeiten und Verfahrensgrenzen, *Maschinenmarkt 16, 1994*

Kochan, A.; ISATA highlights trends in automotive assembly techniques, *Assembly automation Vol. 17 Nr. 4, 1997, 287-290*

Kolleck, R.-B.; Finite Element Simulation wirkmedienbasierter Blechumformung als Teil einer virtuellen Fertigung, *Dissertation, Uni. Dortmund, 1999*

Krahn, M. & Hellmann, M.; Kopplung von PEP und LS-DYNA zur Simulation umformtechnischer Prozesse, *16. CADFEM Users Meeting, Bad Neuenahr - Ahrweiler, Germany, 1998*

Kursetz, E.; Flüssigkeit formt Rohrteile, *Maschinenmarkt 14, 1970, 270-271*

Lange, K. & Roll, K.; Prozeßsimulation in der Umformtechnik, *Aachener Stahl Kolloquium, 1988, 5.2.1-5.2.14*

Lange, K. & Herrmann, P. & Keck, P. & Wilhelm, M.; Aplication of an elasto-plastic finite-element code to the simulation of metal forming processes, *Journal of Materials Processing Technology, 27, 1991, 239-261*

Lee, C.H.; New solutions to rigid-plastic deformation problems using a matrix method, Journal of Engineering Industry 95, S. 865-873, 1973

Lichtenberg, S.; Möglichkeiten und Grenzen des Umformens von Stahlwerkstoffen mit hydraulischen Wirkmedien, *Forschungsbericht P 305, Studiengesellschaft Stahlanwendungen e.V., Düsseldorf, 1996*

Longchang, T. & Hora, P. & Skrikerud, M. ; Moeglichkeiten und Grenzen der FEM-Simulation von Innenhochdruck-Umformprozessen, Hydroumformung von Rohren, Strangpressprofilen und Blechen, *Internat. Konf., Hydroumformung, Bd. 1, Stuttgart, D, 12.-13. Okt., 1999, Band 1 (1999) Seite 531-550*

Lücke, U.; Sorgfältig auf Nummer Sicher, *Blech Nr. 1, 1995, 26-30*

Lücke, U.; Innenhochdruckumformung - Reduzierte Teilekosten durch optimierte, Produktionsprocesse, *Stahl Nr. 46,1998*

Lundqvist, J.; Numerical Simulation of Tubular Hydroforming with an Adaptive Loading Procedure in DYNA 3D, *11th Nordic Seminar on Computational Mechanics, KTH, the Royal Institute of Technology, Stockholm, Sweden,16.-17. October, 1998*

Maisch, R.-P. & Reissner, J.; Appropriate Modelling of Contact and Friction in the Finite-Element (FE) Simulation of Forming Processes as a Contribution to Better Product and Tool Design, *ICCIM 91, 1991, 227-230*

Marczyk, J.; Principles of Simulation-Based Computer-Aided Engineering, *Dissertation, 1999*

Marezyk, J.; Statistical Mechanical Designs Uncertainly Management in CAE via Monte Carlo Simulation, *Benchmark, January 1999, 11-14*

McMeeking, R.M. & Rice, J.R.; Finite element formulations for problemsof lerge elastic plastic deformations, *Int. Journal Solids Structures, Vol. 11, 1975, pp. 601-616*

Mikkelsen, L. P. & Tvergaard, V.; A 2D non-local analysis of hydroforming for thin sheets, *Journal de Physique IV, 1998, 249-256*

Mücke, K.; IHU in der Serienfertigung, *Blech Rohr Profile Nr. 1, 1995, 17-20*

Müller, G; Private communication, 1999

Nakamachi, E.; A Finite Element Simulation of the Sheet Metal Forming Process, *International Journal for numerical Methods in Engineering, Vol. 25, 1988, 283-292*

Neubauer, A.; Formen von Blechhohlteilen mit Wirkmedien: Vergleich der Verfahrensvarianten, *Maschinenmarkt 104, 1998, 22-25*

NN; Plastic Flow in the Elliptical Bulging Test., *Int. J. Mech Sci. 37 4, 1995 373-389*

NN; Bedeutung der Prozesssimulation beim Innenhochdruckumformen, *BBB Band 33, 1992, 26-28, 33-34*

NN, Plastisches Knicken der Wandung von Hohlzylindern und einige andere Faltungserscheinungen an Schalen und Blechen, *Zeitschrift für angewandte Mathematik und Mechanik, Bd. 8, Heft 5, Oktober 1928, 341-351*

NN; Hydrostatic forming of hollow parts; state of the art and future, *Proceedings of the fourth conference on sheet metal vol. 2 University of Twente NL S, 1996, 111-122*

Nowack, H. & Jung, M. & Hachmann, B. & Schweitzer, K.-H.; Ein Innenhochdruck-Umformverfahren mit besonderen Vorteilen, *Bänder Bleche Rohre 3, 1996, 52-56*

Ogura, T. & Ueda, T.; Liquid bulge forming, *Americal Machinist, August 26, 1968*

Panknin, Prof. Dr.; Grundlagen des hydraulischen Tiefziehens Hydroform und hydraulische Tiefzieheinrichtungen, *Werkstatt-Technik und Maschinenbau, 1957*

Raghavan, K. S. & Arwashan, N.; Analysis of quasi-Static Denting Behavior of Automotiv Sheet Steels, *SAE Technical Paper Series 970984, 211-221*

Ratjen, R.; Hochenergie-Umformverfahren Hydropunch, *Werkstatt und Betrieb 104,* 1971, 41-44

Reissner, J, & Kubli, W. & Linder, R.; Schnelle Auslegung einer mehrstufigen IHU-Fertigung durch Einsatz eines mit einer Mehrschritt-Simulation gekoppelten Plaungssystems, *Tagungsband EFB Kolloquium "Innenhochdruck - eine Alternative in der Fertigungstechnik, Stuttgart, 5.-6. März 1996*

Reissner, J.; Integrierte Experten-Simulationssysteme in der Umformtechnik, *Wissenschaftliche Zeitschrift der techn. Univ. Magdeburg; Heft 4; 1991, 17-21*

Reuter, R. & Gärtner, T.; Stochastische Crashsimulation mit LS-DYNA am Beispiel des Kopfaufpralls nach FMVSS 201, *Tagungsband 17. CADFEM Users Meeting 1999, Sonthofen Germany, 1999*

Reuter, R. & Watermann, A.; Application of Uncertainly Management to MADYMO Occupant Simulations, *2th EUROPEAN MADYMO USERS' CONFERENCE, Stuttgart, 1999*

Rimkus, W.; Investigation into Interior High Pressure Forming (IHP) using Finite Elemente (FE) Techniques, *Transfer Report, 1997*

Rimkus, W.; Simulation of IHP Processes, *CAD-FEM Firmenzeitschrift, 1997*

Rimkus, W.; Simulation der Innenhochdruckumformung, *FH Aalen Hochschulmagazin, 1998*

Rimkus, W. & Bauer, H & Hertell, K,; Neue FE-Simulationen beim Innenhochdruckumformen, *14. CADFEM USERS' MEETING 1996, Bad Aibling, Tagungsband, 1996*

Rimkus, W. & Bauer, H.; Integration of the IHP simulation into the CAX chain, *Pro/Engineer Day, Aalen University, 1997*

Rimkus, W. & Bauer, H. & Haas, A.; Increased Production Integrity for Hydroforming Products by using FEA Techniques, *ISS Conference Detroit, 1999*

Rimkus, W. & Bauer, H. & Lerch, J.; Entwicklung einer Benutzeroberfläche zur Simulation des IHU, *Tagungsband 15. CADFEM USERS' MEETING, Fulda, Germany, 1997*

Rimkus, W. & Haas, A. & Bauer, H.; Numerische Verfahrenssimulation zum IHU, *EFB Fortbildungspraktikum, Magdeburg, 1998*

Rimkus, W. & Mihsein, M. J. A. & Bauer, H.; Design of Load-Curves for Tube Hydroforming,
National Conference on Manufacturing Research, Bath, UK, 6. - 8. September, 1999

Roll, K. & Gröber, M.; Anforderungen der Praxis an Programme zur Umformsimulation, Tagungsband, Simulation von Umformprozessen in der Industrie, Baden-Baden, 28.-30. September, 1994

Roll, K. & Tekkaya, A.E.; Prozeßsimulation in der Umformtechnik mit der Methode der Finiten Elemente, *Bleche Rohre Profile 32, 1985, S. 284-289 und S. 327-330*

Sauer, W. J.; Free Bulge Forming of Tubes under internal Pressure and axial Compression, 6th North Americal Metalworking Res. Conf. Proc. SME, Uni. of Florida, Gainsville, 16.-19. April, 1978, 228-235

Schilling, R. & Zicke, G.; Einsatz der Finite-Elemente-Methode in der umformenden Fertigung, *Festschrift zum 60. Geburtstag von Prof. Dr. Ing. E.v. Finkenstein, Univ. Dortmund, 1992, 107-126*

Schmoeckel, D. & Speck, F.-D.; Finite Element Simulation of the Axial-Radial Forming Process, *Production Engineering Vol. II/1, 1994, 193-196*

Schmoeckl, D. & Engel, B.; Weiterentwicklung des Innenhochdruckumformens durch überlagerte Biegung, *EFB-Kolloquium, Innenhochdruckumformen - eine Alternative in der Fertigungstechnik, 1996*

Schuler; Handbuch der Umformtechnik, *ISBN 354061099-5, Springer Verlag Berlin, 1996*

Schweizerhof, K. & Weimar, J.O. & Hallquist, & D.W. Stillman: Improving Standard Shell Elements, Friction Models and Contact Algorithms for the Efficient Solution of Sheet Metal Forming Problems with LS-DYNA3D, *Proc. VDI Conference on 'FE-Simulation of 3-D Sheet Metal Forming processes in Automotive Industry', VDI Berichte 894, VDI Verlag, Düsseldorf, 1991, 499-516*

Schweitzerhof, K. & Walz, M., Quasi-statische Berechnungen mit LS-DYNA - Möglichkeiten und Grenzen, *17. CADFEM Users Meeting 1999, Sonthofen, Germany, 1999*

Schweitzerhof, K. & Walz, M. & Rust, W., Franz, U.; Quasi-static Structural Analysis with LS-DYNA - Merits and Limits, *Second European LS-DYNA Users Conference Gothenburg, Sweden, 1999*

Seifert, M.; Einsatz des Innenhochdruck-Umformverfahrens im Automobilbau unter den Bedingungen des Leichtbaus am Beispiel von Space-Frame-Komponenten, *Kolloquium "Innovative Karosseriefertigung" Chemniz, 1996*

Seifert, M.; Body & Chassis Systems Hydroforming of Tubes, *University of Magdeburg/Germany, Technical Paper, 09/23 -24/99; 188 ff.*

Sommer, B.; Entwicklung der Fertigung von hohlen Achsen der Schienenfahrzeuge durch inneren Wasserdruck, *Hüttenblätter, Nr. 3, 1964, 173-181*

Srinivasan, T-M & Shaw, J-R & Thompson, K.; Tubular hydroforming: correlation of results., *Automotive Engineering International, Band 106 Heft 7, 1998, 85-88*

Stander, N. & Münz, T.; A Successive Response Surface Approximation Approach to Design Optimization using LS-OPT, *17. CADFEM Users Meeting 1999, Sonthofen, Germany, 1999*

Stelzmann, U. & Stamm & Stühmeyer; Tiefzeihsimulation eines BMW-Federbeindomes: Gegenüberstellung der Einschrittlösung mit FAST_FORM3D und inkrementeller Lösung mit LS-DYNA, *17. CADFEM Users Meeting 1999, Sonthofen, Germany, 1999*

Tang, J. & Wu, W.T. & Walters, J.; Recent development and application of finite element method in metal forming, *Journal of Materials Processing Technology 46, 1994, p 117-126*

Tekkaya, A.; Ermittlung von Eigenspannungen in der Kaltmassivumformung, *Berichte aus dem Institut für Umformtechnik, Uni Stuttgart, Nr. 83, Springer Verlag, 1986*

Tscheckel, R.; Ein Beitrag zur Entwicklung des hydromechanischen ausbauchens für die Fertigung T-förmiger Rohrverbindungsstücke, *Dissertation, TU Dresden, 1977*

Ueda, T. & Ogura, T. & Takagi, R.; Über die Anwendung eines hydraulischen Ausbauchverfahrens, *Industrie-Anzeiger Nr. V, Mai 1966*

Ueda, T. & Ogura, T.; Liquid bulge forming, *Metalworking Prod. Apr., 1968 73-81*

Verein Deutscher Ingenieure; Innenhochdruck-Umformen – Grundlagen, *Richtlinie VDI 3146, Blatt 1 (Entwurf), 1999*

Weiss, K-H., Innen-Hochdruck-Umformen - eine Fertigungtechnologie fuer das Umformen von Rohren und Platinen. *Konferenz-Einzelbericht: Innenhochdruckumformen - eine Alternative in der Fertigungstechnik, EFB-Kolloquium, Fellbach, Germany, 1996, Band T 16, 4.1-14*

Wilhem & Keck; FE-Methode als Werkzeug zur Stoffflußbetrachtung in der Massivumformung, *Tagungsband, Neuere Entwicklungen in der Massivumformung, 1989, 16/1-16/18*

Zang, S.H. & Danckert, J.; Development of hydro-mechanical deep drawing, *Journal of Material Processing Technology 83, 1998, 14-25*

Yamada, Y & Yoshimura, N, & Sakurai, T.; Plastic stress strain matrix and its application for the solution of elasticplastic problems by the finite element method, *Int. Journal mech. Sci., 10, 1968, 343-354*

Zienkiewicz, O. C.; Elasto-plastic solutions of engineering problems, 'Initial Stress' finite element approach, *Int. Journal Num. Meth. Engg., 1, 1969, 75-100*

Zienkiewicz, O. C.; Methode der finiten Elemente, *VEB Fachbuchverlag, 1983*

Author's Publications

Rimkus, W. & Bauer, H & Hertell, K,; Neue FE-Simulationen beim Innenhochdruckumformen, 14. CAD-FEM USERS' MEETING 1996, Bad Aibling, Tagungsband

Rimkus, W.; Investigation into Interior High Pressure Forming (IHP) using Finite Element (FE) Techniques, Transfer Report, 1997

Bauer, H. & Rimkus, W.; Fast and Efficient FE Simulation of Hydroforming Problems, First European LS-DYNA User's Conference, Conference Proceeding, 1997, Stratford upon Avon, UK

Rimkus, W.; Simulation of IHP Processes, CAD-FEM Firmenzeitschrift, 1997

Rimkus, W. & Bauer, H.; Integration of the IHP Simulation into the CAX Chain, Pro/Engineer Day, FH Aalen University for Applied Sciences, 1997

Rimkus, W. & Bauer, H. & Lerch, J.; Entwicklung einer Benutzeroberfläche zur Simulation des IHU, 15. CAD-FEM USERS' MEETING 1997, Fulda, Tagungsband

Rimkus, W.; Simulation der Innenhochdruckumformung, FH Aalen Hochschulmagazin, 1998

Rimkus, W. & Haas, A. & Bauer, H.; Numerische Verfahrenssimulation zum IHU, EFB Fortbildungspraktikum, Magdeburg, 1998

Rimkus, W. & Bauer, H. & Haas, A.; Increased Production Integrity for Hydroforming Products by using FEA Techniques, ISS Conference 1999, Detroit

Haas, A. & Rimkus, W. & Bauer, H.; Höhere Prozeßsicherheit beim IHU, 17. CADFEM Users Meeting, 1999, Sonthofen, Germany

Rimkus, W. & Mihsein, M. J. A. & Bauer, H.; Design of Load Curves for Tube Hydroforming, National Conference on Manufacturing Research, 6. - 8. September 1999, Bath, UK

Bauer, H. & Haas, A. & Rimkus, W. & Lerch H.; Examples of Hydroforming Fem Process Simulations, International Conference on Hydroforming, 12. - 13. October 1999, Stuttgart, Germany

Rimkus, W. & Mihsein, M. J. A. & Bauer, H.; Design of Load Curves for Hydroforming applications, Journal of Materials Processing Technology, volume 108 issue 1, 2001

Appendix A

A.1 Source Code for the Program to Reconstruct Surfaces

A.2 Program to convert the LS-DYNA output dynain

Available on attached disk.

Appendix B

B.1 Source Code for the IHP Modul (ANSYS UIDL)

Available on attached disk.

Appendix C

C.1 How to create Load-Curves - Example

The following example will serve to explain the use of the formulas.
Parameter :

D_0 = 50 mm
D_1 = 80 mm
s_0 = 6 mm
l_1 = 100 mm
material : St 30 AL NBK

Now we have the two unknown parameters s_1 and l_0. It is necessary to estimate one of these parameters. So we estimate that the wall-thickness decreases linearly.

s_1 = 4.9 mm

C.2 Estimation of the interior pressure

The material used for this example has a tensile strength of 300 N/mm**2

$$p_f = \frac{2 \cdot s_0 \cdot R_m}{d_0 - s_0} = \frac{2 \cdot 6mm \cdot 300 \frac{N}{mm}}{50mm - 6mm} = 81.82 \frac{N}{mm^2}$$

The flow-pressure of 81.82 N/mm^2 corresponds to a pressure of 818.2 bar. Now the pressures at point 1 and 2 (**Figure 4-22**) can be estimated.

$$p_{ipo\,int\,1} = 0.9 \cdot p_f = 0.9 \cdot 820bar = 738bar$$

$$p_{ipo\,int\,2} = 1.2 \cdot p_f = 1.2 \cdot 820bar = 984bar$$

C.3 Calculation of the Axial Pre-Force

For the present material the flow-stresses are 280 N/mm^2.

$$p_{a0} = 0.15 \cdot k_{f0} = 0.15 \cdot 280 \frac{N}{mm^2} = 42 \frac{N}{mm^2}$$

$$F_{a0} = p_{a0} \cdot A_{R0} = p_{a0} \cdot \left(D_0^2 - d_0^2\right) \cdot \frac{\pi}{4} = 42 \frac{N}{mm^2} \cdot \left(50^2 - 38^2\right) mm^2 \cdot \frac{\pi}{4} = 37.5kN$$

To be sure that the tube is tight the axial pre-force will amount to 50 kN.

C.4 Calculation of the Axial Force at the End of the Expansion Phase

The first step is the calculation of the cross-section area before and after the forming process.

$$A_{R0} = \left(D_0^2 - d_0^2\right) \cdot \frac{\pi}{4} = \left(50^2 - 38^2\right) mm^2 \cdot \frac{\pi}{4} = 829.4 mm^2$$

$$A_{R1} = \left(D_1^2 - d_1^2\right) \cdot \frac{\pi}{4} = \left(80^2 - 70.2^2\right) mm^2 \cdot \frac{\pi}{4} = 1156 mm^2$$

Now the volume is

$$V = V_0 = V_1 = A_{R1} \cdot l_1 = 1156 mm^2 \cdot 100 mm = 115600 mm^3$$

Moreover the origin length can be calculated

$$l_0 = l_1 \cdot \frac{A_{R1}}{A_{R0}} = 100 mm \cdot \frac{1156 mm^2}{829.4 mm^2} = 139.4 mm$$

Degree of deformation after expansion

$$\varphi_1 = \ln \frac{A_{R1}}{A_{R0}} = \ln \frac{1156 mm^2}{829.4 mm^2} = 0.33 \quad \text{and} \quad \varepsilon_1 = e^{\varphi 1} - 1 = 0.39$$

Furthermore we need the average flow-stress. It can be calculated from the flow-stress at the beginning and at the end of the expansion stage.

$$k_{fm} = \frac{k_{f0} + k_{f1}}{2} = \frac{280 \frac{N}{mm^2} + 400 \frac{N}{mm^2}}{2} = 520 \frac{N}{mm^2}$$

The ideal forming work done necessary for the forming process is now

$$W_{id} = V \cdot k_{fm} \cdot \varphi_1 = 1156 mm^3 \cdot 4 \frac{N}{mm^2} \cdot 0.33 = 15259200 Nmm = 15.26 kNm$$

We also need the average inner diameter and length

$$d_m = \frac{d_0 + d_1}{2} = \frac{38mm + 70.2mm}{2} = 108.2mm$$

$$l_m = \frac{l_0 + l_1}{2} = \frac{139.4mm + 10mm}{2} = 119.7mm$$

and the projected inner area of the tube

$$A_{proj} = d_m \cdot l_m = 108.2mm \cdot 119.7mm = 129.5mm^2$$

as well as the average interior pressure

$$p_{im} = \frac{p_{i0} + p_{i1}}{2} = \frac{p_{i1}}{2} = \frac{980bar}{2} = 490bar$$

$$W_{pi} = p_{im} \cdot A_{proj}\left(\frac{d_1 - d_0}{2}\right) = 49\frac{N}{mm^2} \cdot 12951mm^2 \cdot 16.1mm = 10.22kNm$$

$$W_{id} = W_{pi} + W_{pa} \Rightarrow W_{pa} = W_{id} - W_{pa} = 15.26kNm - 10.22kNm = 5.04kNm$$

In the next step the relationship between work from interior pressure and from the axial force can be estimated

$$va = \frac{W_{pi}}{W_{pa}} = \frac{10.22kN}{5.04kN} = 2.03$$

A relationship of work from 2.03 permits a high axial force.

Now we still need the axial pressure at the end of the expansion phase.

$$p_{a1} = \frac{2 \cdot W_{pa}}{A_{Rm} \cdot (l_0 - l_1)} - p_{a0} = \frac{2 \cdot 5040000Nmm}{992.7mm^2 \cdot 39mm} - 42\frac{N}{mm^2} = 215.8\frac{N}{mm^2}$$

thus the axial force can be calculated

$$F_{a1} = p_{a1} \cdot A_{R0} = 215.8\frac{N}{mm^2} \cdot 829.4mm^2 = 179kN$$

C.5 Work from Friction

$$\mu = 0.04$$
$$s = 65mm$$

$$p_{im} = \frac{p_{i1}}{2} = \frac{104.4\frac{N}{mm^2}}{2} = 52.2\frac{N}{mm^2}$$

$$A = U \cdot l = \pi \cdot d_{i0} \cdot l = \pi \cdot 38mm \cdot (300mm - 152) = 1766mm^2$$

$$F_N = p_{im} \cdot A = 52.2\frac{N}{mm^2} \cdot 1768mm^2 = 922300N$$

$$W_r = \mu \cdot s \cdot F_N = 0.04 \cdot 65mm \cdot 922.3kN = 24000Nmm = 0.024kNm$$

This shows that the calculated work from friction is very small in comparison to the work from interior pressure and from axial force.

C.6 Load-Curves

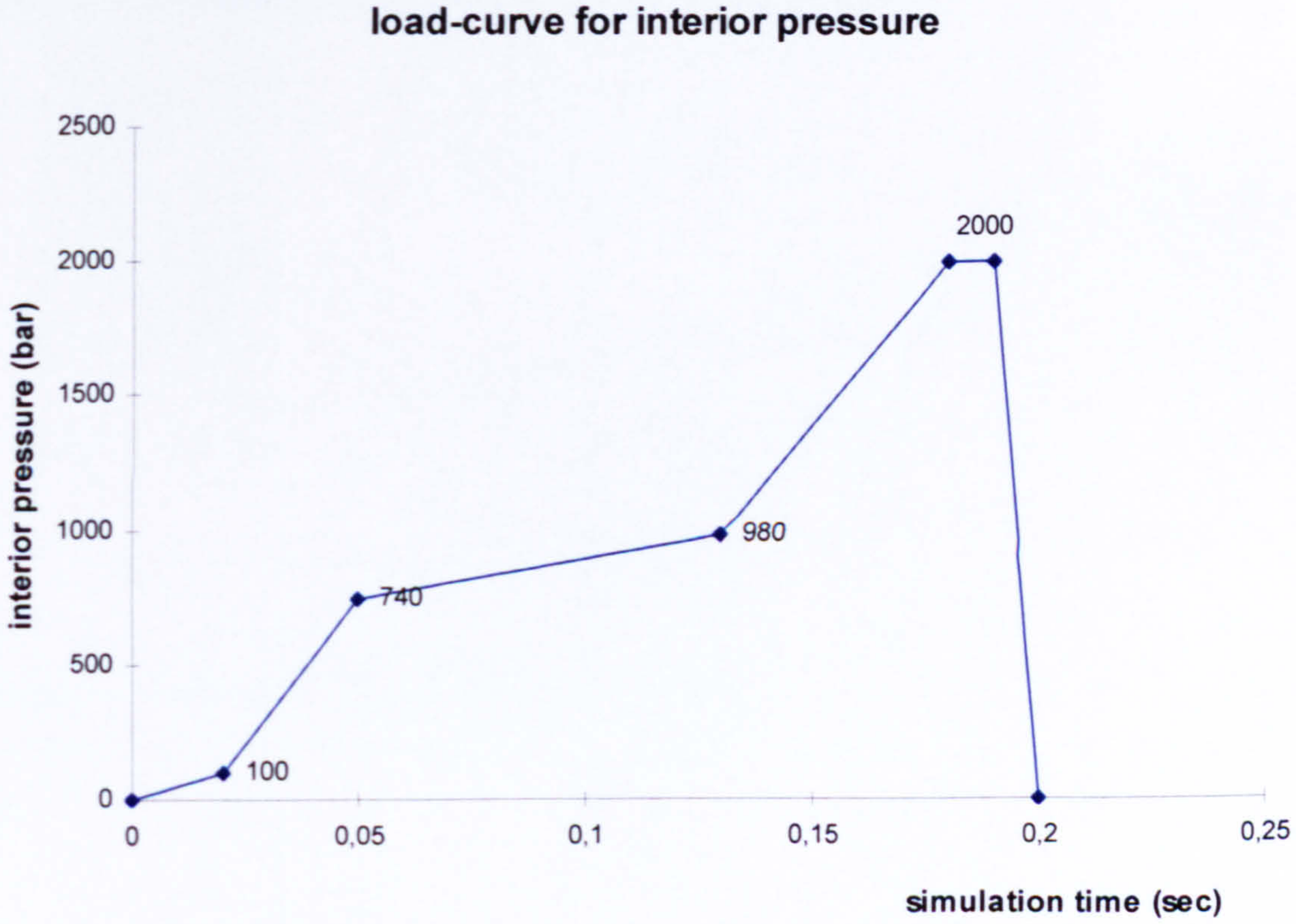

Figure C-1 Load-curve for interior pressure

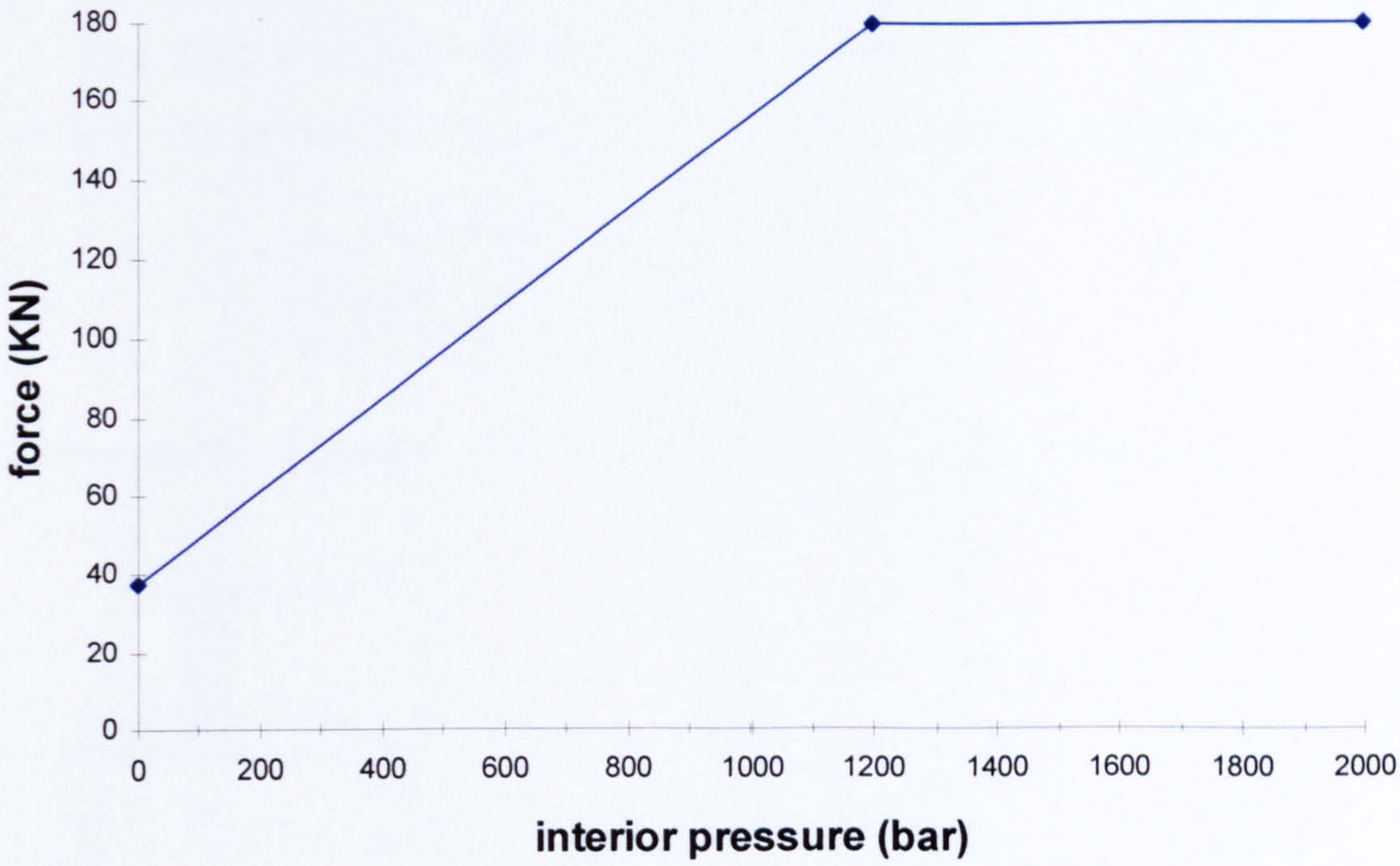

Figure C-2 Load-curve for axial force vs. interior pressure

Appendix D

D.1 Calculation of the Calibration Pressure - Example for the use of the Radius Curve

The workpiece to be formed using interior pressure has the following parameters:

shell thickness	s = 3 mm
material	16 MnCr 5
smallest outer radius	r = 7 mm.

The interior pressure necessary to calibrate a radius of 7 mm is required.

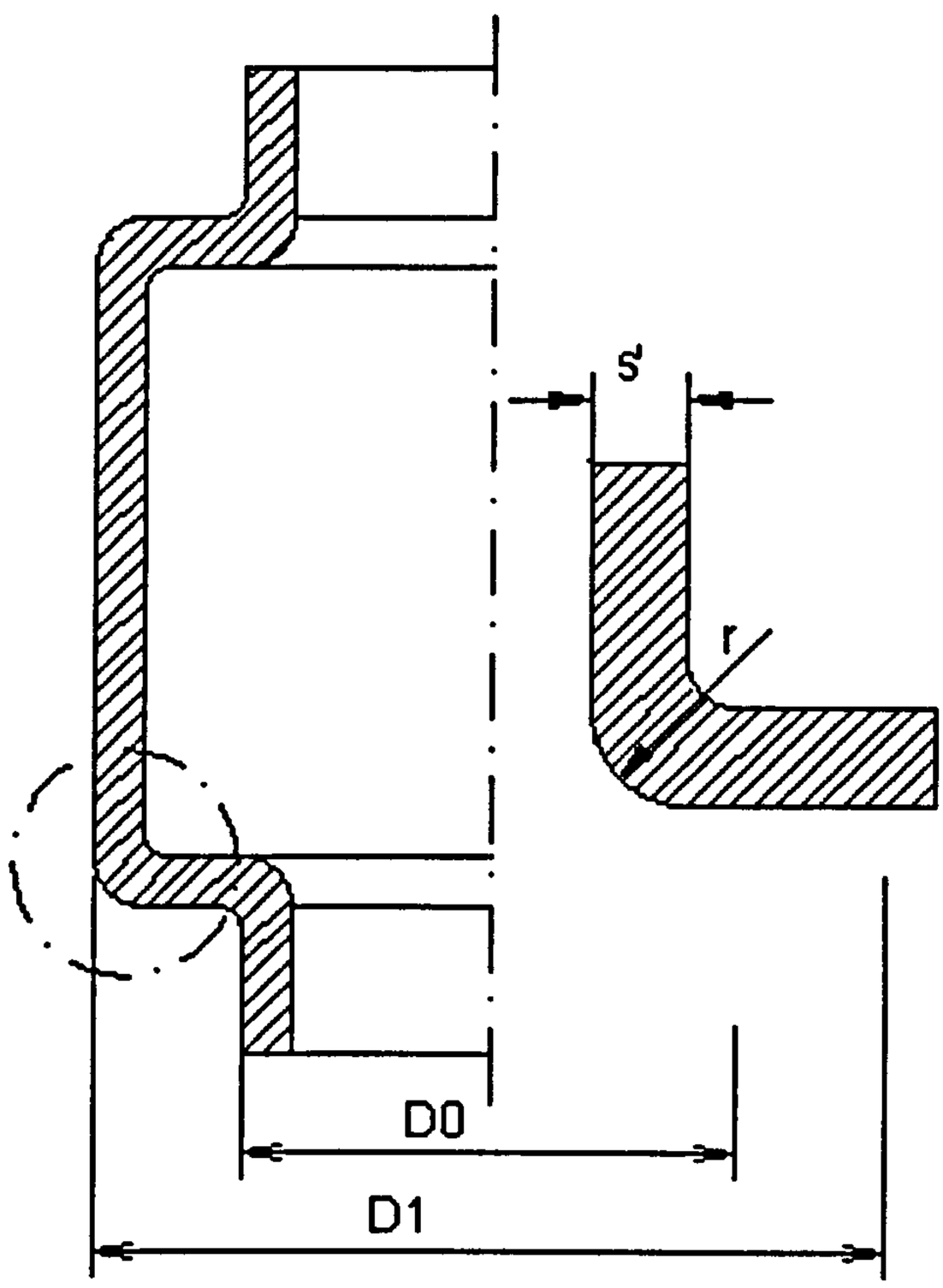

Figure D-1 Drawing - Radius and Shell Thickness

It is possible to estimate that the shell thickness after the forming phase is 2.5 mm (**Figure 4-25**).

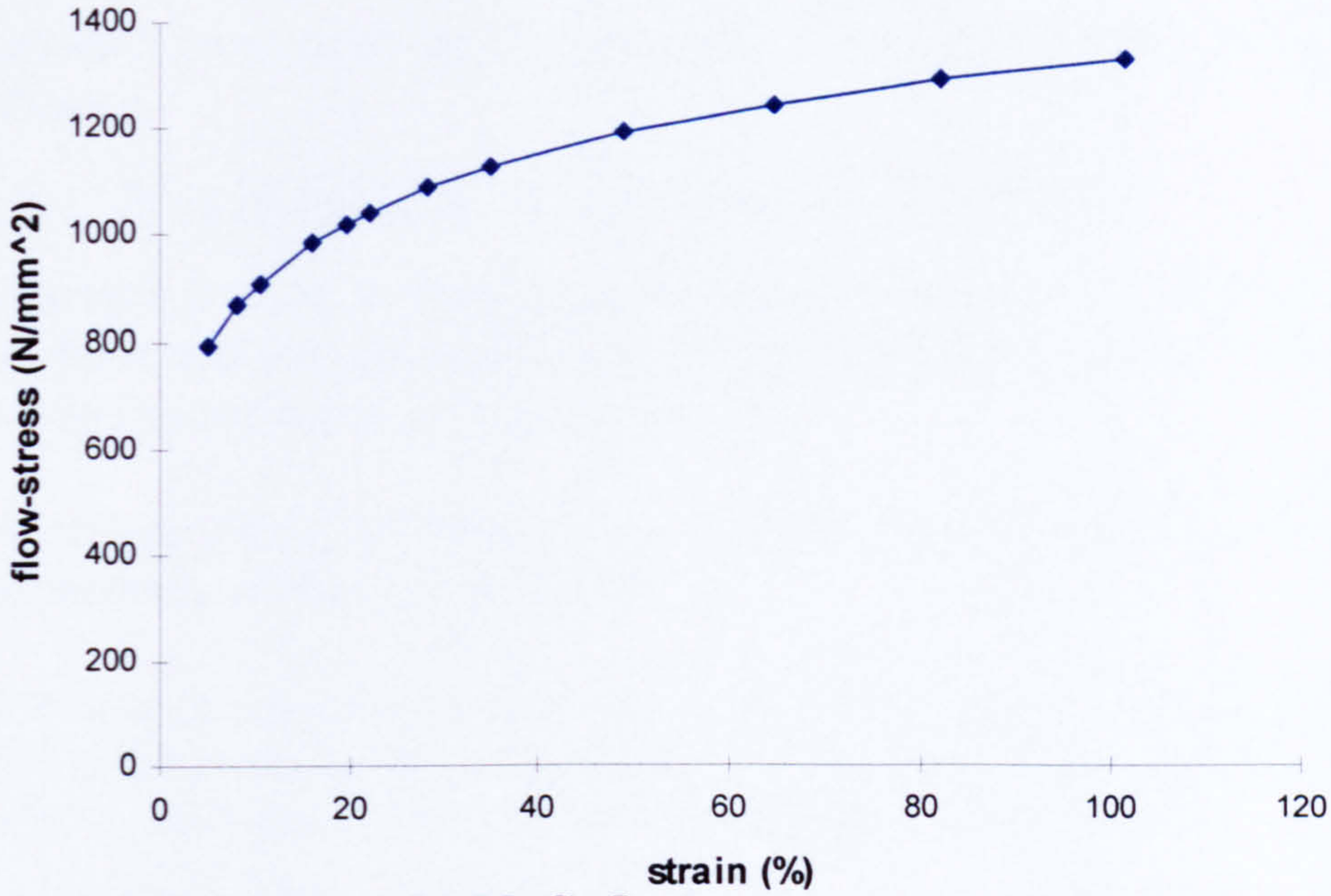

Figure D-2 Flow-Curve 16 MnCr 5

From the flow-curve for 16 MnCr 5 a flow-stress of $k_{f,\,20} = 1000\frac{N}{mm^2}$ for 20 % strain can be determined.

The y-factor can then be calculated from radius and shell thickness

$$y = \frac{r}{s'} = \frac{7\,mm}{2.5\,mm} = 2.8$$

Out of the radius-curve for the material group 1 a x-factor of x = 0.4 can be determined.

The calibration pressure can now be calculated as

$$p = x \cdot k_{f,20\%} = 0.4 \cdot 1000\frac{N}{mm^2} = 400\frac{N}{mm^2}$$

Pressure needed for calibration amounts to 400 N/mm^2 or 4000 bar.

Appendix E

Appendix E investigates the developed radius curves in chaper 5 by a verification using a FE simulation.

E.1 Verification of developed Methods

This section investigates the summarised methods for the design of IHP loads, as there are the axial force and the interior pressure for expanding and calibration. The correctness of the developed radius-curves is investigated.

A workpiece with a wall thickness of 4 mm and a starting diameter of 60 mm is expanded up to an diameter of 90 mm as an example.

Particularly of interest is the outer radius, marked with X in the **Figure E-6**. The tool has no radius at this place, i.e. the radius results only from the interior pressure. The interior pressure, needed for the forming process is determined from the radius-curve.

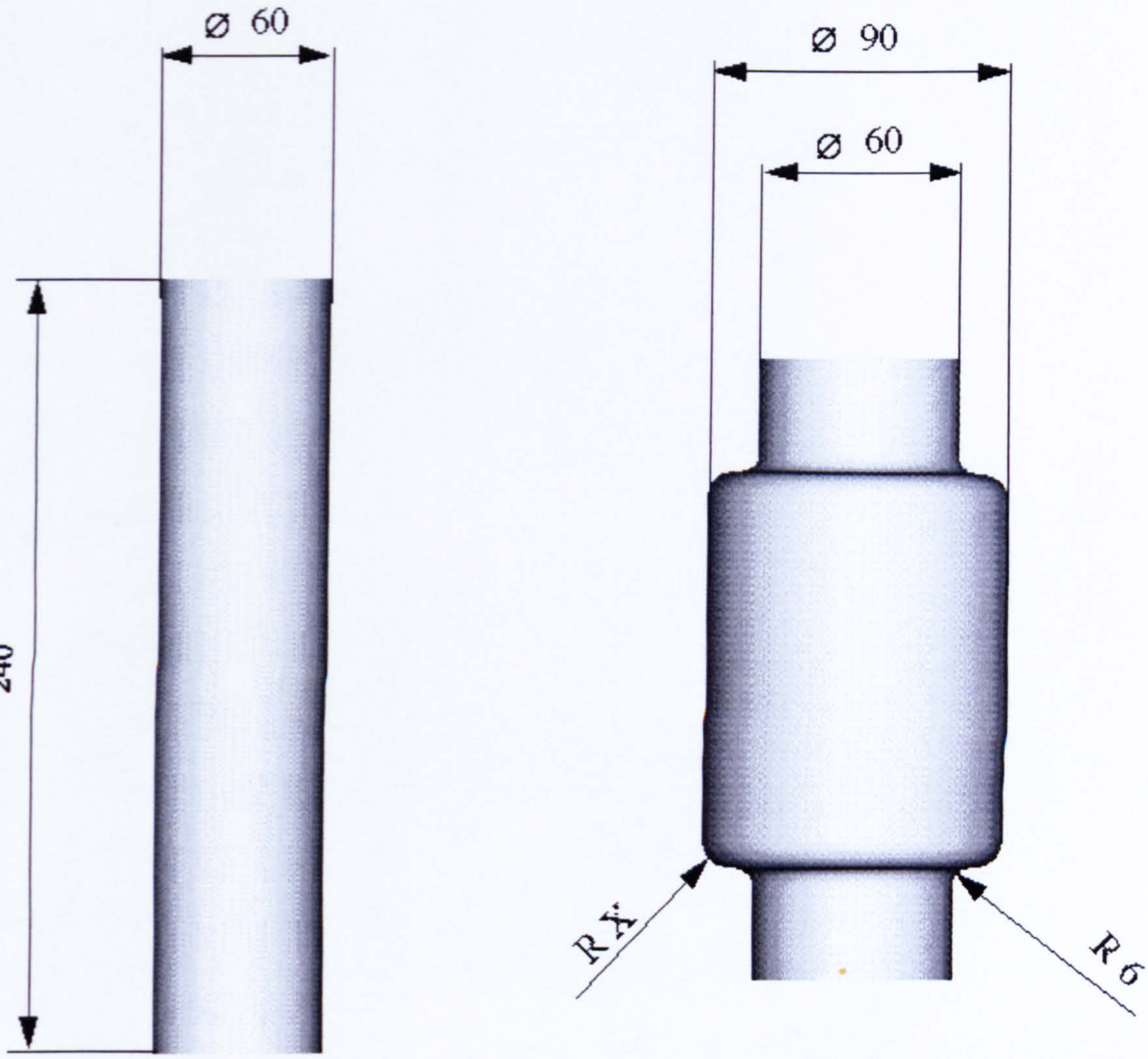

origin tube

tube after the forming process
starting wall-thickness : 4mm

Figure E-1 Work-Piece before and after the Forming Process

As the material is a steel Ck 45 is chosen. The material has the following properties :

tensile strength $R_m = 600 \frac{N}{mm^2}$

density $\delta = 7.8 \cdot 10^{-6} \frac{Ns}{mm^4}$

young's modulus $E = 2.1 \cdot 10^5 \frac{N}{mm^2}$

friction $\mu = 0.04$

poisons ratio $\upsilon = 0.3$

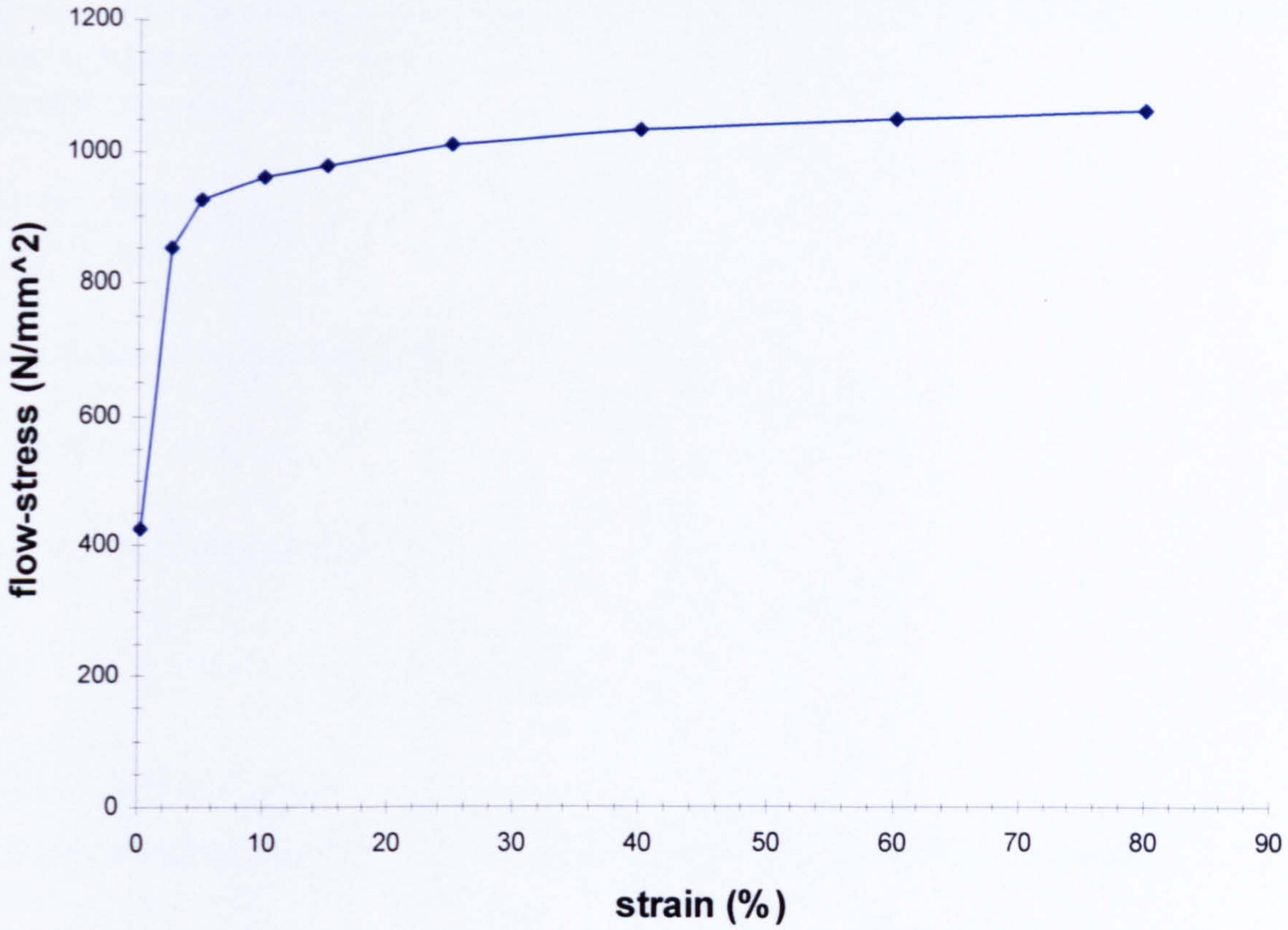

Figure E-2 Flow-Curve for Ck 45

Now the load-curves for axial force and interior pressure are calculated with the presented method.

E.2 Interior Pressure

The flow-pressure is calculated with the following formula :

$$p_f = \frac{2 \cdot s_0 \cdot R_m}{d_0 - s_0} = \frac{2 \cdot 4mm \cdot 600 \frac{N}{mm^2}}{60mm - 4mm} = 86 \frac{N}{mm^2} \Rightarrow 860 \text{ bar}$$

Point 1 on the load-curve for interior pressure must be approximately 10% lower than the calculated flow-pressure. The period between the points 1 and 2 are the main forming period, therefore the gradient of the curve should be low.

$p_{i1} =$ 0.9 * 860 bar = 774 bar

The interior pressure at point 2 is calculated with the equation . The presented configuration has only a small resistance against the axial force. The interior pressure must be responsible for most of the forming process. Therefore the geometric factor g_f is chosen to 0.4 in order to get a high value for the work va (equation 5-18).

$p_{i2} = p_f + g_f \cdot p_f =$ 860 bar + 0.4 * 860 bar = 1200 bar

For estimating the calibration pressure, the radius-curve (**Figure 4-51**) is used. The radius X adjusted after the calibration must be at least 8 mm. The wall-thickness after the expansion phase is estimated to be 3 mm.
Therefor the y-factor is :

$$y = \frac{r}{s'} = \frac{8mm}{3mm} = 2.66$$

The x-factor using the radius-curve is :

$$x = 0.45$$

Thus the calibration pressure is :

$$p_{i3} = x \cdot k_{f,20} = 0.45 \cdot 995 \frac{N}{mm^2} = 447 \frac{N}{mm^2}$$

E.3 Axial Force

First the area of the circular section of the tube before the expansion is required.

$$D_0 = 60_{\text{mm}} \quad s_0 = 4_{\text{mm}} \quad d_0 = 52_{\text{mm}}$$

$$A_{R0} = \left(D_0^2 - d_0^2\right) \cdot \frac{\pi}{4} = \left(60^2 - 52^2\right) \cdot \frac{\pi}{4} = 703.7mm^2$$

The axial force necessary to make the tube tight results to :

$$p_{a0} = 0.15 \cdot k_{f0} = 0.15 \cdot 425 \frac{N}{mm^2} = 63.75 \frac{N}{mm^2}$$

$$F_{a0} = p_{a0} \cdot A_{R0} = 44.8kN$$

The axial pre-load should be 45 kN.

Now the starting length of the tube is calculated. The wall-thickness at the end of the expansion phase is estimated to be 3 mm. The cross-section area after the expansion is calculated as follows:

$$s_1 = 3_{\text{mm}} \quad D_1 = 92_{\text{mm}} \quad d_1 = 86_{\text{mm}}$$

$$A_{R1} = 838.8mm^2$$

$$V = A_{R1} \cdot l_1 = 838.3mm^2 \cdot 120mm = 100596mm^3$$

$$l_0 = \frac{V}{A_{R0}} = \frac{100596mm^3}{703.7mm^2} = 142.9mm$$

The degree of deformation at the end of the expansion phase and the flow-stress belonging to it can be determined using of the cross-sections of the tube A_{R1} and A_{R0}.

$$\varphi_1 = \ln\frac{A_{R1}}{A_{R0}} = \ln\frac{838.8mm^2}{703.7mm^2} = 0.176$$

$$\varepsilon_1 = e^{\varphi_1} - 1 = 0.192$$

Further the middle flow-stress must be calculated. It is determined using the flow-stress at the begin of the expansion phase and at the end of this phase.

$$k_{fm} = \frac{k_{f0} + k_{f1}}{2} = \frac{425\frac{N}{mm^2} + 995\frac{N}{mm^2}}{2} = 710\frac{N}{mm^2}$$

The required forming work is :

$$W_{id} = V \cdot k_{fm} \cdot \varphi_1 = 100596mm^3 \cdot 710\frac{N}{mm^2} \cdot 0.176 = 12570000Nmm = 12.57kNm$$

The work done from the interior pressure is :

$$W_{pi} = p_{im} \cdot A_{proj} \cdot \left(\frac{d_1 - d_0}{2}\right)$$

$$A_{proj} = d_m \cdot l_m = \frac{d_0 + d_1}{2} \cdot \frac{l_0 + l_1}{2} = \frac{52mm + 86mm}{2} \cdot \frac{142.9mm + 120mm}{2} = 9070mm^2$$

$$p_{im} = \frac{p_{i0} + p_{i1}}{2} = \frac{p_{i1}}{2} = \frac{1200bar}{2} = 60\frac{N}{mm^2}$$

$$W_{pi} = 60\frac{N}{mm^2} \cdot 9070mm^2 \cdot 17mm = 9.25kNm$$

The work done from the axial force is :

$$W_{pa} = W_{id} - W_{pa} = 12.57kNm - 9.25kNm = 3.32kNm$$

A further criterion for the design of the load-curve for the axial force are the relationship between the work from the interior pressure and the work from the axial force.

$$va = \frac{W_{pi}}{W_{pa}} = \frac{9.25kNm}{3.32kNm} = 2.8$$

The relationship between both works depends on the configuration and it should be between 2 and 3.

For the presented example a great part of the work done is caused by the interior pressure. When the forming process increase the geometry can bring only a low resistance against the axial force. Therefore the part of the work done from the interior pressure must be great. The

relation from the work done should be near to 3. For this example they are refined to $g_f = 0.4$, so a large va is possible (see Chapter 5.1.2).

The axial force necessary at the end of the expansion phase is calculated over the interior pressure.

$$p_{a1} = \frac{2 \cdot W_{pa}}{A_{Rm} \cdot (l_0 - l_1)} - p_{a0}$$

$$A_{Rm} = \frac{A_{R0} + A_{R1}}{2} = \frac{703.7mm^2 + 838.8mm^2}{2} = 771.25mm$$

$$p_{a0} = 63.75 \frac{N}{mm^2}$$

$$p_{a1} = \frac{2 \cdot 3320000Nmm}{771.25mm^2 \cdot (142.9mm - 120m)} - 63.75 \frac{N}{mm^2} = 215.8 \frac{N}{mm^2}$$

From p_{a1} follows the axial force F_{a1}:

$$F_{a1} = p_{a1} \cdot A_{R0} = 219.7kN$$

Figures E-3 and **E-4** show the load-curves which are calculated.

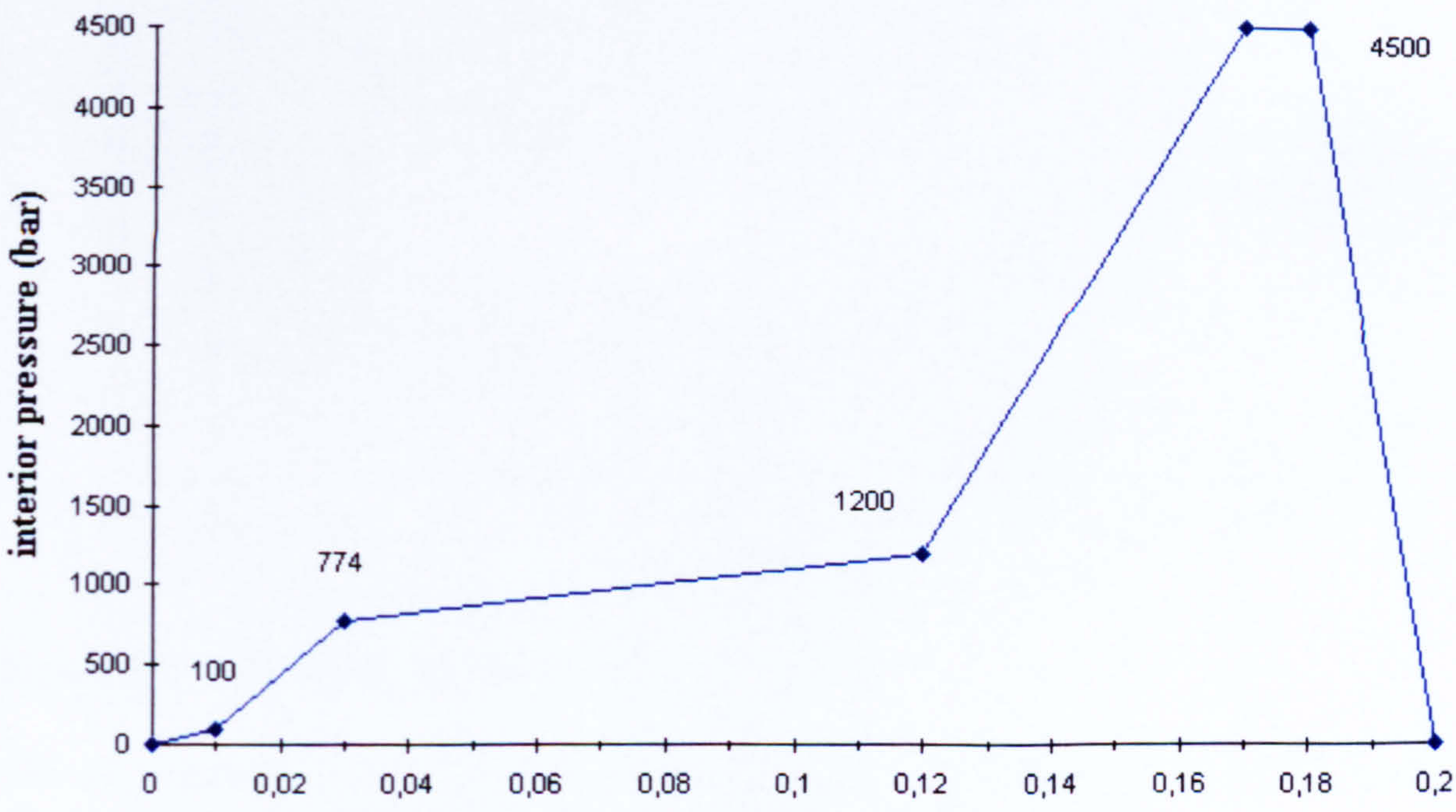

Figure E-3 Interior pressure vs. time

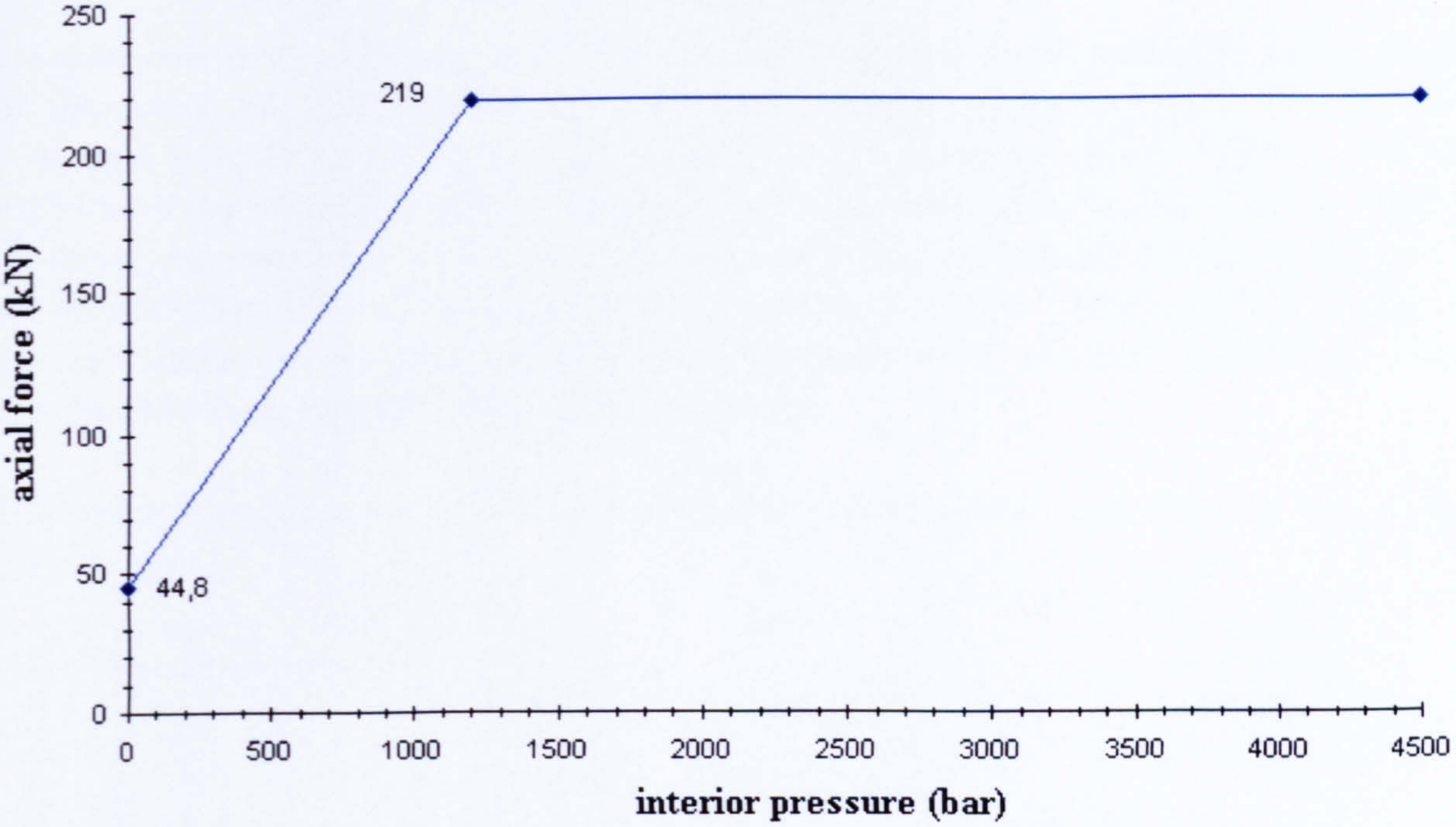

Figure E-4 Axial force vs. interior pressure

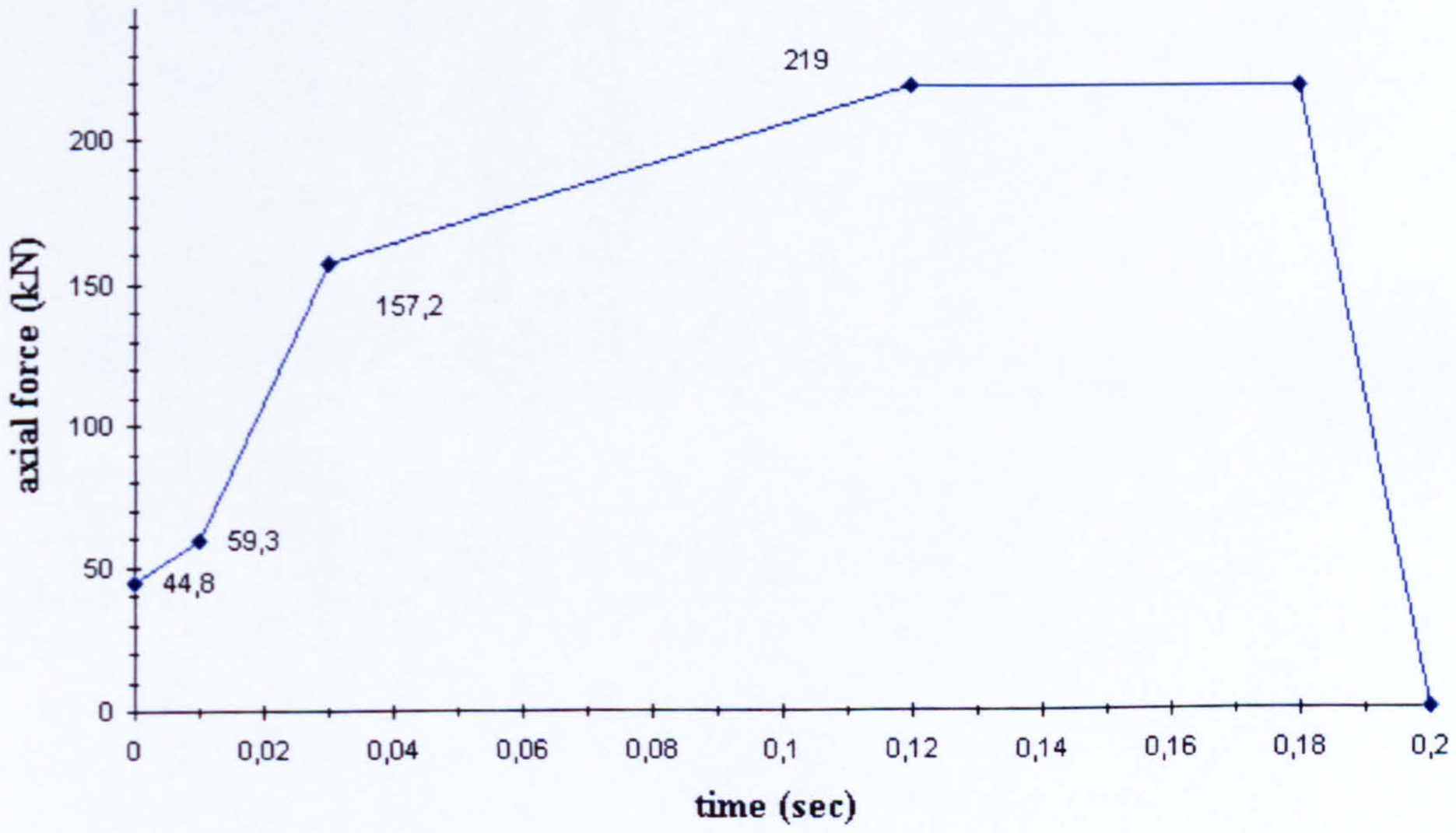

Figure E-5 Axial Force vs. Time

The FE simulation of the forming process is carried out using LS-DYNA. The tools and punches are modelled in Pro/ENGINEER and exported as VDA-surfaces.

E.4 The result of the FE-simulation

The most important goal of the simulation is the investigation of the developed radius-curve. For this reason the radius formed due to the interior pressure is not limited by the tool. The radius should result only from the interior pressure. The required radius is 8 mm. Out of the radius-curve the calibration pressure necessary to form a radius with 8 mm is 4500 bar. **Figure E-1** shows the work-piece after the forming process. Within the instigated section a radius of 7 mm originate from the calibration pressure. The geometric shape which comes into existence is not an exact arc of 90 degrees. If the tool has a forming radius of 8 mm the calibration pressure would be large enough to form a radius of 8 mm.

Therefore it is suitable to use the radius-curve for the design of the load-curve for the calibration pressure.

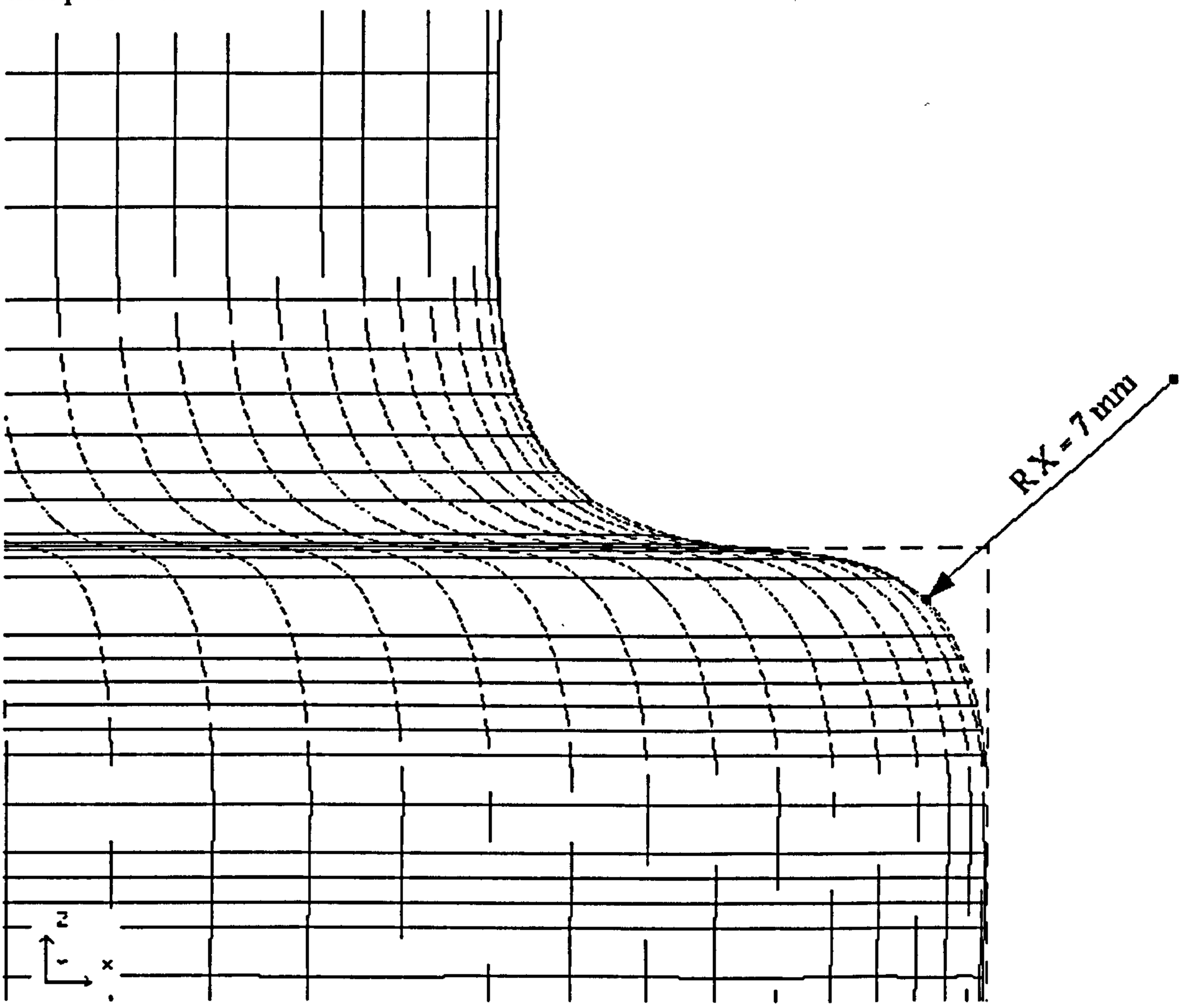

Figure E-6 Corner Radius due to the Calculated Interior Pressure

The next **Figures E-7** show the forming stages, Table E-1 lists the appropriate timescale.

stage 1	starting stage	0.00 sec
stage 2	expansion phase	0.10 sec
stage 3	end of the expansion phase	0.13 sec
stage 4	end of the forming process	0.20 sec

Table E-1 Forming Stages

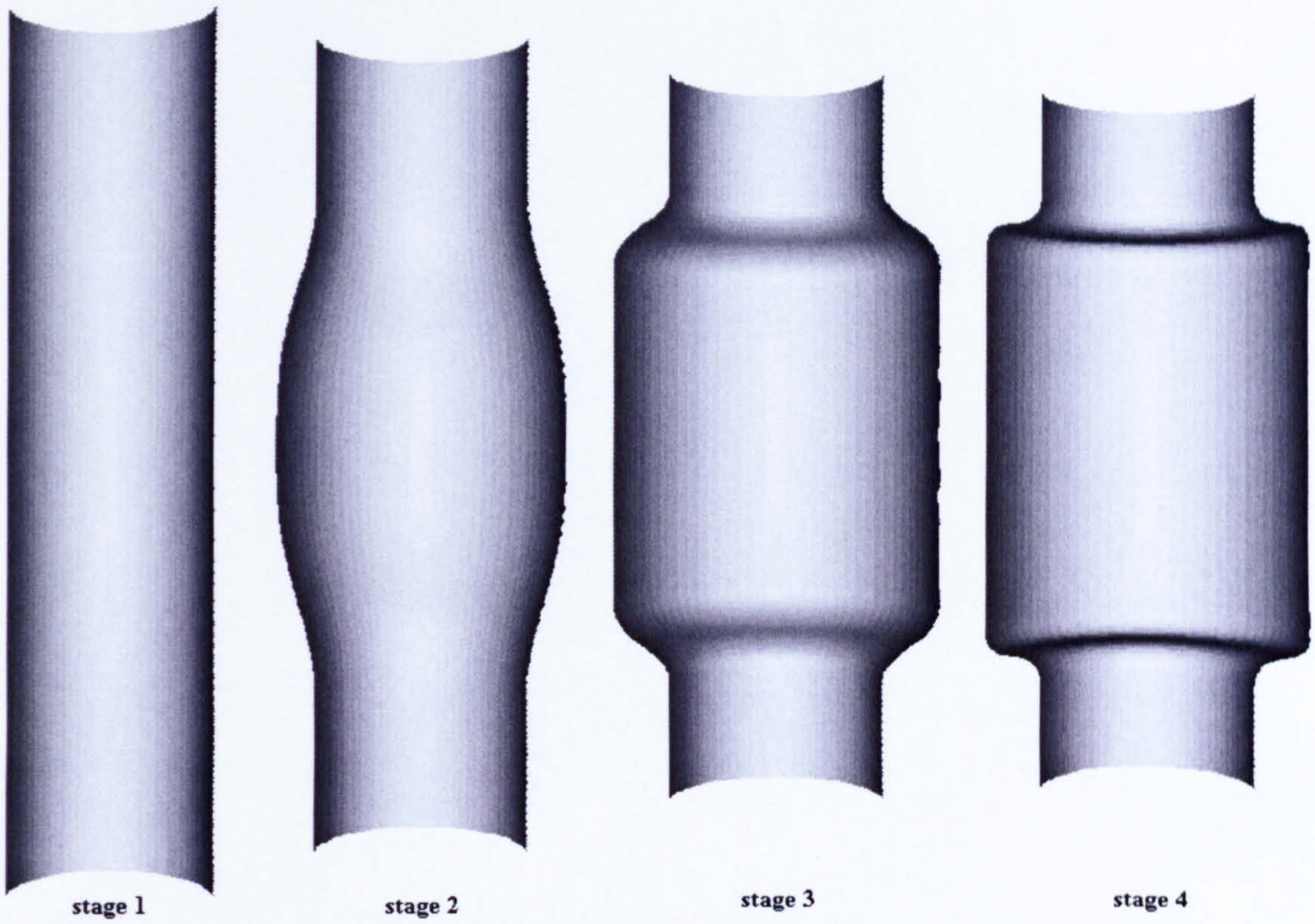

Figure E-7 Description of the Forming Stages

Appendix F

Appendix F shows some examples for the reconstruction of parts described in chapter 7.

F.1 Example : Expanded Tube

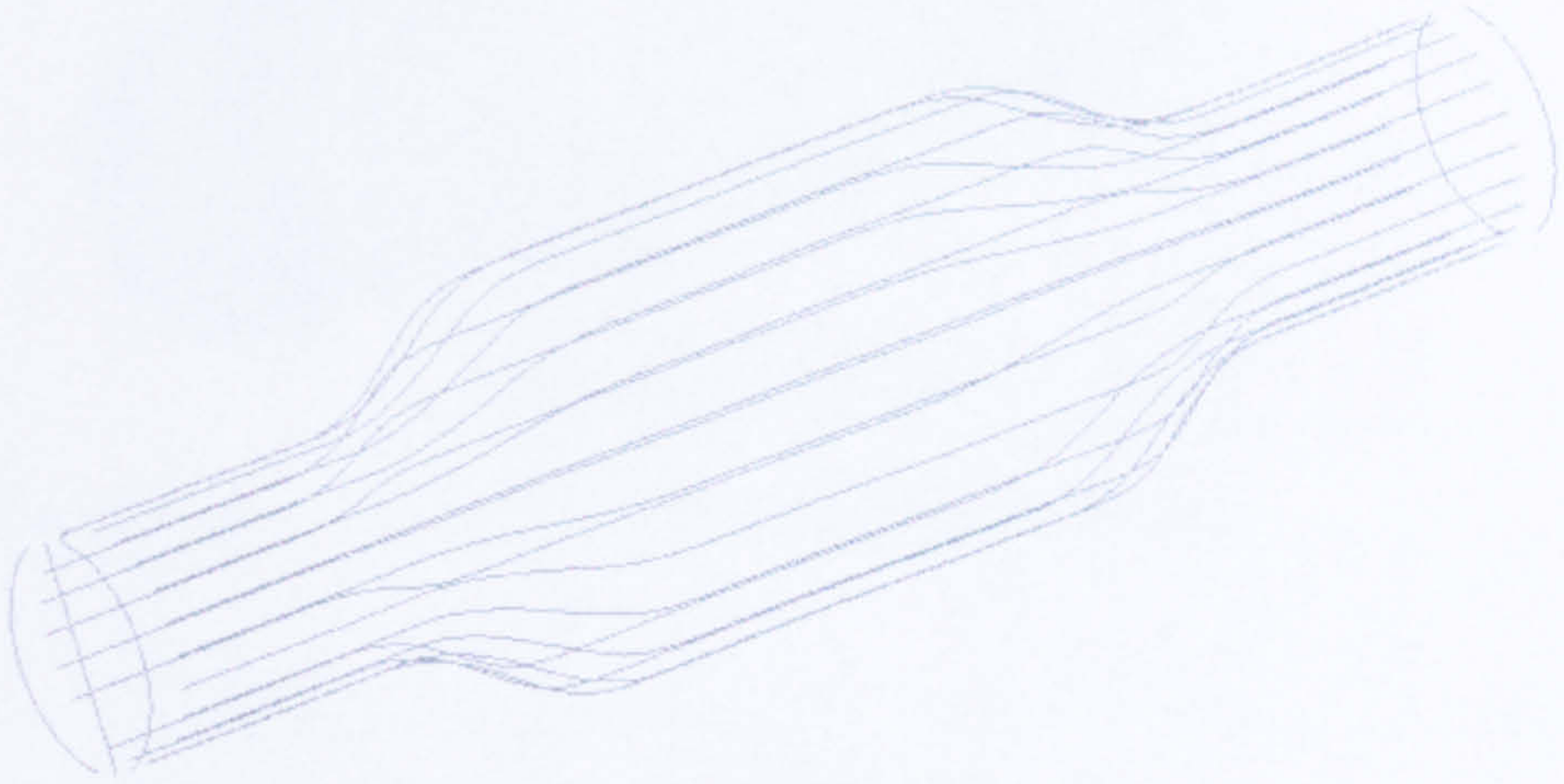

Figure F-1 Scan Curves (longitudinal)

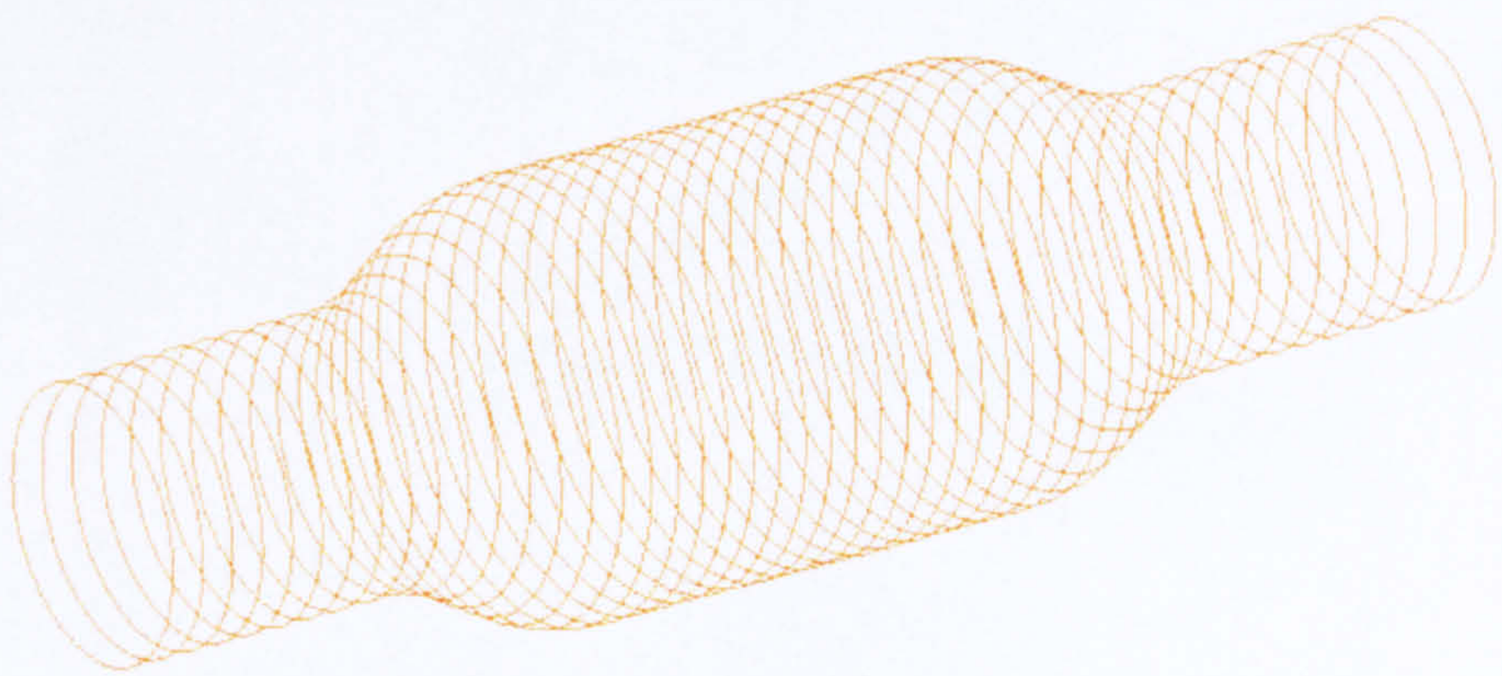

Figure F-2 Style Curves (out of Radial sorted Scan Curves)

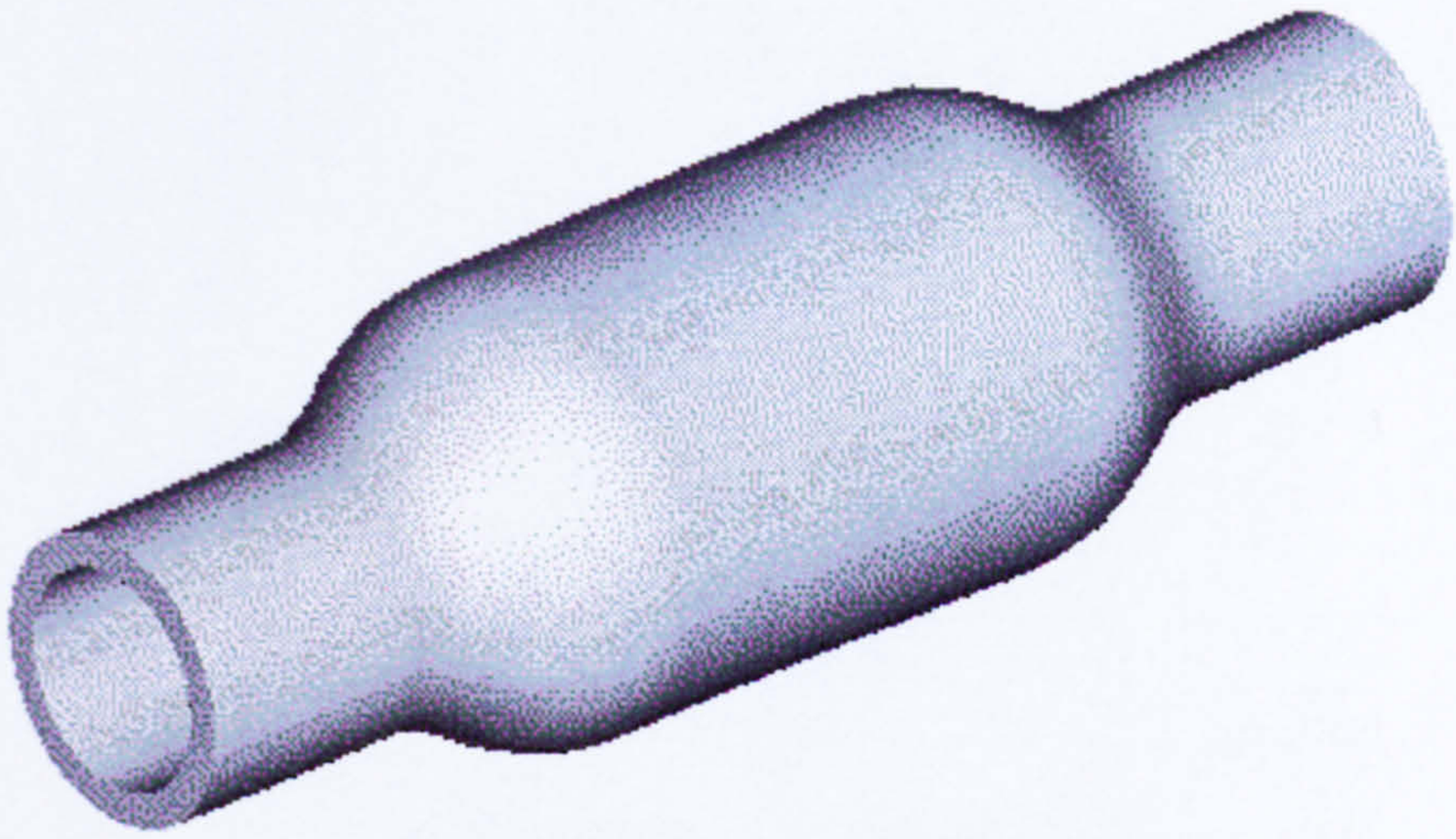

Figure F-3 Reconstructed Part

F.2 Example : T-Piece with a slanting Dome

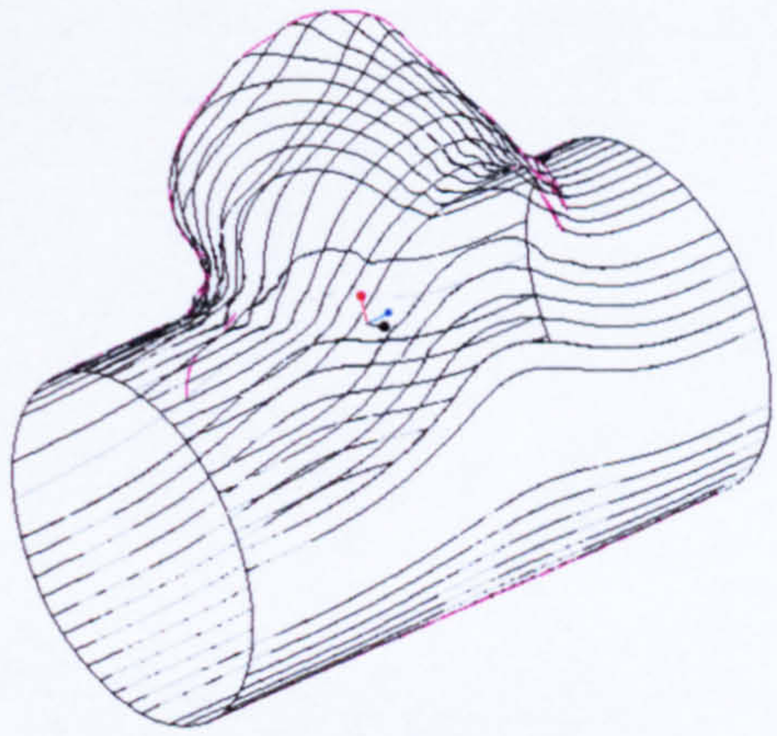

Figure F-4 Scan Curves

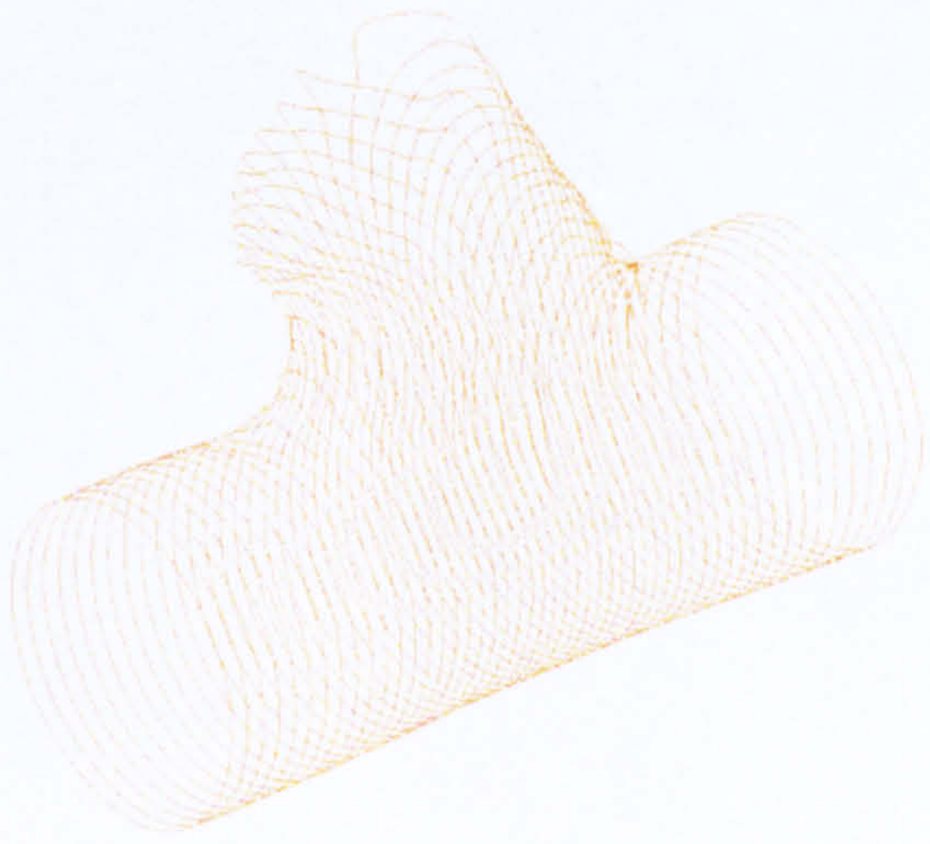

Figure F-5 Style Curves

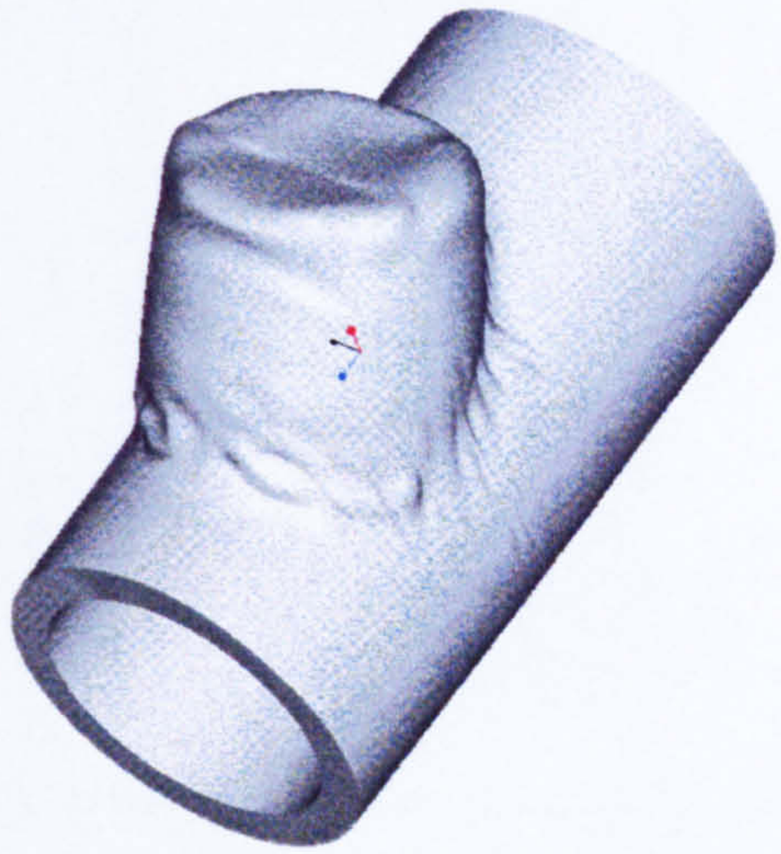

Figure F-6 Reconstructed Part

The folds in the part are not from the surface reconstruction but exist in reality.

F.3 Example : Rear Axle Cross Member

The geometric shape of the pre-formed rear axle component cross member will be used to optimise the IHP tool and to construct the punch geometry.

Figure F-7 Scan Curves

Figure 7-40 shows the scan curves before sorting them in radial direction. **Figure 7-41** shows the style curves created form the radial sorted points, **Figure 7-42** displays the part in Pro/ENGINEER.

Figure F-8 Style Curves (radial sorted)

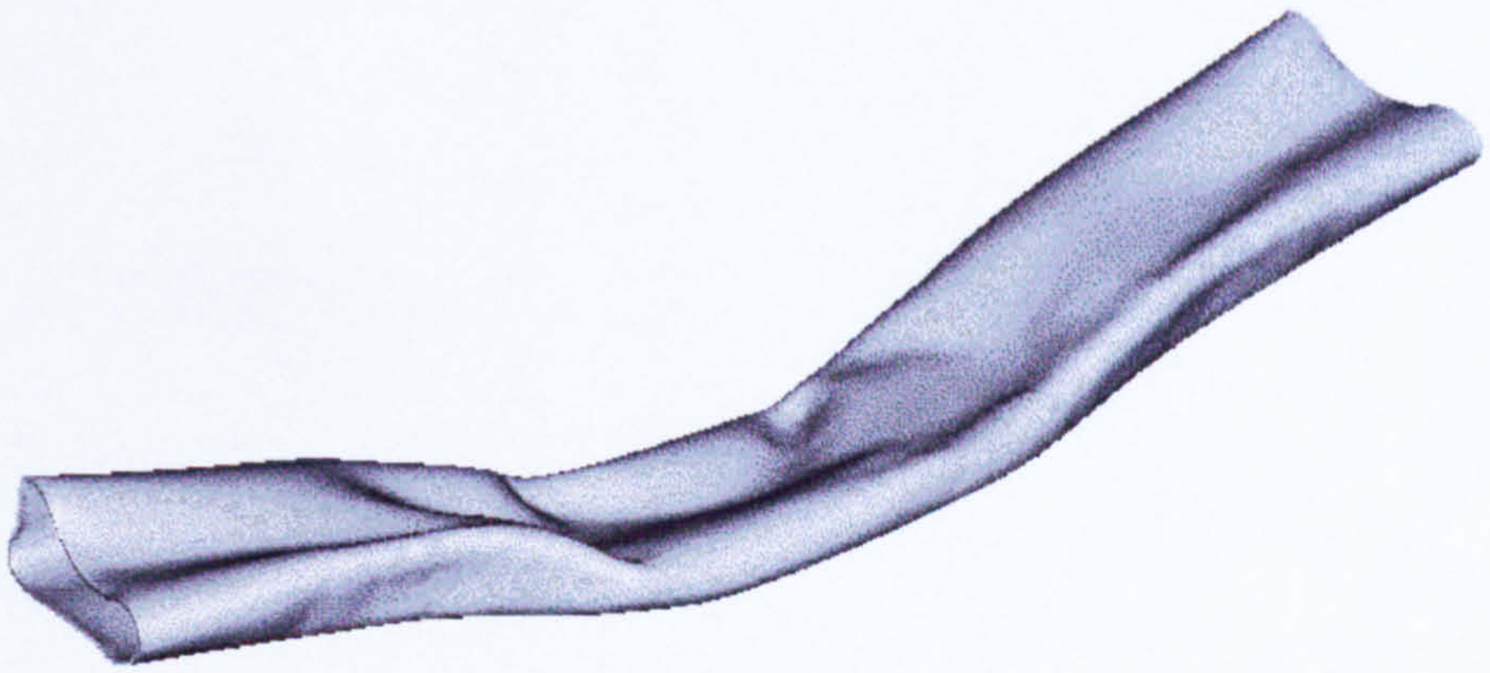

Figure F-9 Reconstructed Part

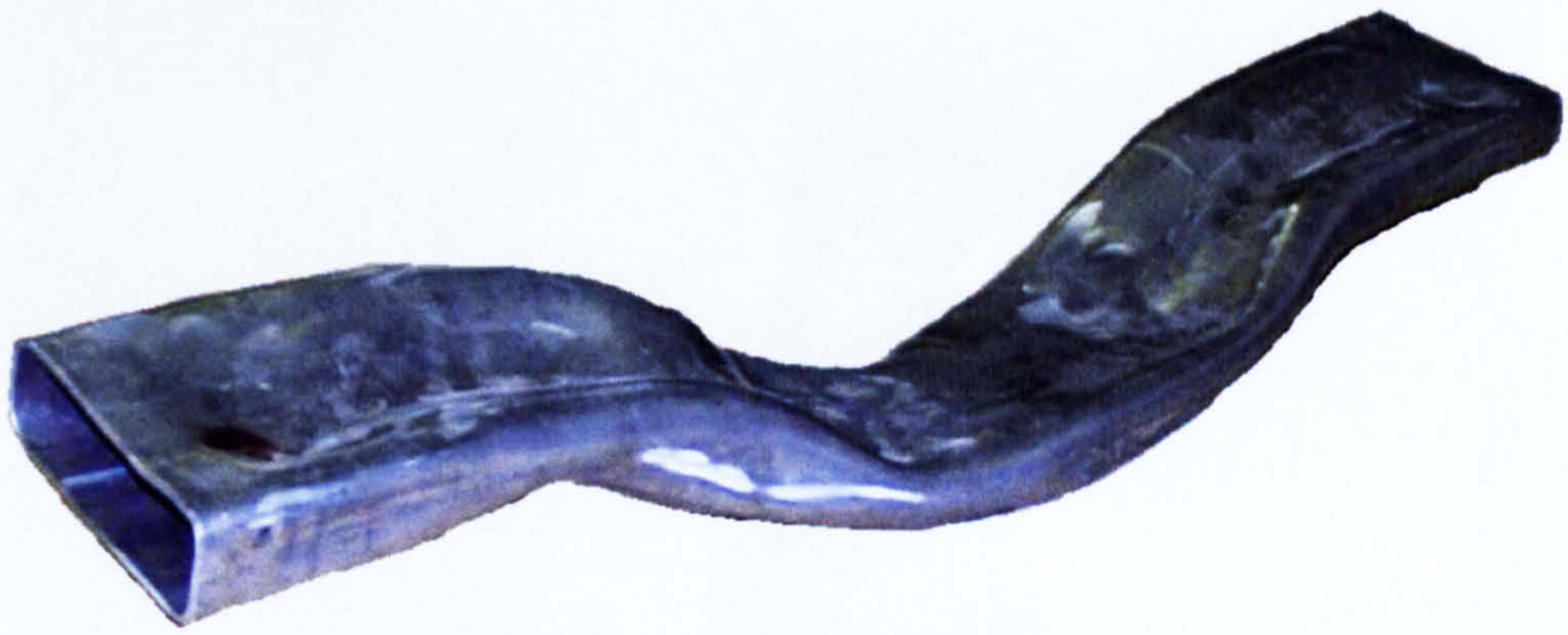

Figure F-10 Picture of a Similar Rear Axle Component

Figure 7-43 represents a real part. The surface reconstruction will be done with the points sorted in longitudinal and radial directions. Once again it can be noticed that the processing of the radial points is much more efficient than the use of the longitudinal points, because less manual labour is necessary.

THESIS CONTAINS CD